iClick reactions as a modular access to palladium(II) and platinum(II) triazolato complexes: Trends in kinetics and biological activity

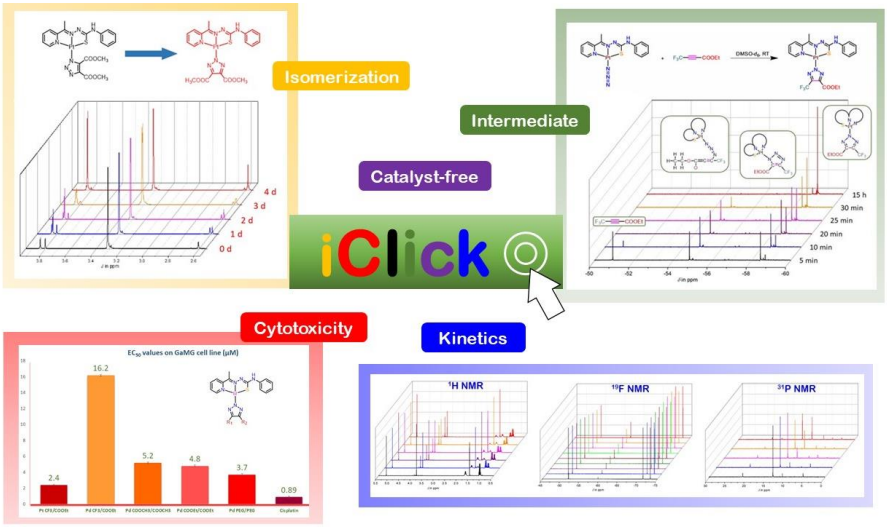

Dissertation zur Erlangung des naturwissenschaftlichen Doktorgrades der Julius-Maximilians-Universität Würzburg

vorgelegt von

Kun Peng

aus Zhengzhou, V.R. China

Würzburg, 2020

CC BY

Eingereicht bei der Fakultät für Chemie und Pharmazie am

_____

Gutachter der schriftlichen Arbeit

1. Gutachter: Prof. Dr. Ulrich Schatzschneider

2. Gutachter: Prof. Dr. Axel Klein

Prüfer des öffentlichen Promotionskolloquiums

1. Prüfer: Prof. Dr. Ulrich Schatzschneider

2. Prüfer: Prof. Dr. Axel Klein

3. Prüfer: Prof. Dr. Ann-Christin Pöppler

Datum des öffentlichen Promotionskolloquiums

_____

Doktorurkunde ausgehändigt am

_____

Try not to become a man of success but rather try to become a man of value.

--Albert Einstein

Die vorliegende Arbeit wurde von November 2015 bis Juli 2020
am Institut für Anorganische Chemie der Julius-Maximilians-Universität Würzburg
unter der Anleitung von Prof. Dr. Ulrich Schatzschneider angefertigt

Acknowledgements

First of all, I want to give my thanks to **Prof. Dr. Ulrich Schatzschneider** for providing me with the opportunity to be a part of his group. During my stay in Germany, he gave me a lot of help and guidance not only on scientific matters but also for my daily life. Most importantly, from him I learnt the real way to do scientific research. In addition, I would like to thank **Mersedeh Schatzschneider**, who has always been very kind and helped me to quickly adapt to life here.

I also want to express my deep gratitude to **Prof. Dr. Axel Klein** and **Prof. Dr. Ann-Christin Pöppler** for their willingness to review my thesis in spite of their busy schedule.

Thanks to **Marie-Luise Schäfer** and **Dr. Rüdiger Bertermann** for the NMR measurements, and to **Liselotte Michels** as well as **Sabine Timmroth** for the elemental analysis. I also want to show my gratitude to **Dr. Alexandra Friedrich** for the X-ray structure determination and **Ellina Schulz** as well as **Dr. Carsten Hagemann** for carrying out the biological assays. What is more, thanks to **Maria C. Eckhardt** and **Cornelia Walter** for helping me with administrative affairs in the institute.

I am also very grateful to the **China Scholarship Council** (**CSC**) for financially supporting me during my study in Germany. *Happy 70th birthday to China and I love my country.* Thanks to **Prof. Dr. Jin'an Zhao** for leading me to the field of inorganic chemistry.I would also like to thank my lovely colleagues, Viviane Mawamba, Patrick Roth, Dominic Graf, Paul Güntzel, Paul Schmid, Dr. Nilab Feizy, Jan Mößeler, Kevin Lüken, Lorena Rüger, Dr. Luisa Waag-Hiersch, Marvin Schock, Patrick Schuster, Nesrin Toptan, Janik Miekisch, Katinka Theis, Dr. Ahmed Mansour, Lisa Gourdon, Sofia Chueca, and Janina Gawehn for the help and company in the lab.

Many thanks to my parents, **Yanxia Li** and **Zhi Peng**, my grandparents, **Yulian Tang** and **Kailiang Peng**, and my aunt, **Mandi Peng**, who gave my life, raised me to grow up, and taught me how to be a person with good quality. *I have always been grateful and love you so much.* I also want to thank **Chushi** for giving your love to me. I really appreciate it.

Thanks to **Dr. Wenbo Ming**, **Dr. Xiaocui Liu** and **Dr. Xiaodong Duan** for spending a good time with me in Germany. Also thanks to Dr. Jing Zhou, Shouguang Huang, Shuai An, Zhen Zhou, Shitong Du, Dr. Mo Zhu, Dr. Siyuan Liu, Dr. Kang Du, Mingming Huang, Bolin Wang, Ruiqi Liu, Dr. Yuehui Tian, Dr. Shiqiang Gao, Dr. Hao Wu, Prof. Dr. Xiaoning Guo, Yaming Tian, Dr. DongLiang Peng, Dr. Fang Wu, Shang Yang, Prof. Dr. Qing Ye, Shenghua Qu, Linxiao Guo, Jinghua Zhou, Zhu Wu, Peipei Fei, Yang Zhou, Prof. Dr. Lei Ji, and Janis Mendic for making my life in Würzburg more colourful. I should also mention my best friends, **Xi Yu**, **Ting Zhang** and **Hanhua Zhong** for always standing by me. *Very glad to know you guys.*

Last but definitely not least, special thanks to **Dr. Meng Qu**, who accompanies me, cares about me, trusts me, encourages me, helps me and brings happiness to me all the time.

Publication list

The publications listed below are partly reproduced in this thesis. Some tables and figures are modified or adapted directly from the corresponding publications, and are noted in the respective captions.

Publication	Contributions
K. Peng, V. Mawamba, E. Schulz, M. Löhr, C. Hagemann, U. Schatzschneider*, iClick reactions of square-planar palladium(II) and platinum(II) azido complexes with electron-poor alkynes: Metal-dependent preference for N1 *vs.* N2 triazolate coordination and kinetic studies with ^{1}H and ^{19}F NMR spectroscopy. *Inorg. Chem.* **2019,** *58*, 11508 − 11521.	**K. Peng**: Syntheses, characterizations, kinetic measurements, manuscript writing **V. Mawamba**: Ligand synthesis **E. Schulz, M. Löhr, C. Hagemann**: Biological assays **U. Schatzschneider**: Project design, manuscript revision
K. Peng, A. Friedrich, U. Schatzschneider*, 2,2':6',2"-Terpyridine switches from tridentate to monodentate coordination in a gold(III) terpy complex upon reaction with sodium azide. *Chem. Commun.* **2019**, *55*, 8142 − 8145.	**K. Peng**: Syntheses, characterizations, manuscript writing **A. Friedrich**: X-ray crystal structure determination **U. Schatzschneider**: X-ray structure database searching, DFT calculations, manuscript revision
K. Peng, R. Einsele, P. Irmler, R. Winter*, U. Schatzschneider*, The iClick reaction of a BODIPY platinum(II) azido complex with electron-poor alkynes provides triazolate complexes with good $^{1}O_2$ sensitization efficiency. *Organometallics* **2020**, *39*, 1423 − 1430.	**K. Peng**: Syntheses of triazolate complexes, characterizations, kinetic measurements, manuscript writing **R. Einsele:** DFT calculations **P. Irmler**, **R. Winter**: Synthesis of azido complex, X-ray crystal structure analysis, photophysical measurements **U. Schatzschneider**: Project design, manuscript revision

Abbreviations

ADIBO	azadibenzocyclooctyne
APCl	atmospheric pressure chemical ionization
ASAP	atmospheric solid analysis probe
BCN	bicyclo-[6.1.0]-non-4-yne
BODIPY	4,4-difluoro-4-bora-3a,4a-diaza-*s*-indacene
bpcd	6-benzylpyrido[2,3-*a*]pyrrolo[3,4-*c*]carbazole-5,7(6*H*,12*H*)-dione
bpy	2,2'-bipyridine
COD	1,5-cyclooctadiene
COSY	correlation spectroscopy
Cp^*	1,2,3,4,5-pentamethylcyclopentadienyl
CT-DNA	calf thymus DNA
CuAAC	copper(I)-catalyzed azide-alkyne cycloaddition
cyclam	1,4,8,11-tetraazacyclotetradecane
DEAD	diethyl acetylenedicarboxylate
DFT	density functional theory
DMAD	dimethyl acetylenedicarboxylate
DMSO	dimethyl sulfoxide
dppe	bis(diphenylphosphino)ethane
dppm	bis(diphenylphosphino)methane
ESI	electrospray ionization
HMBC	heteronuclear multiple bond correlation
HOMO	highest occupied molecular obital
HPLC	high performance liquid chromatography
hptab	*N*,*N*,*N*',*N*',*N*'',*N*''-hexakis(2-pyridylmethyl)-1,3,5-tris(aminomethyl)benzene
HSQC	heteronuclear single quantum correlation
iClick	inorganic click
im	imidazole
NCL	native chemical ligation
NHC	*N*-heterocyclic carbene
NMR	nuclear magnetic resonance
NSCLC	non-small cell lung cancer

OTf	trifluoromethanesulfonate
phbpy	6-phenyl-2,2’-bipyridine
pht	*(E)-N*-phenyl-2-(1-(pyridin-2-yl)ethylidene)hydrazinecarbothioamide
py	pyridine
salen	*N,N’*-ethylenebis(salicylimine)
SCLC	small cell lung cancer
SPAAC	strain-promoted azide-alkyne cycloaddition
tandem crDA	tandem [3+2] cycloaddition-retro-Diels-Alder reaction
TE	Tris-HCl/EDTA buffer
terpy	2,2’:6’,2”-terpyridine
tt	1,4,7-trithionane

Table of contents

1 Introduction

1.1 Transition metal complexes as anticancer agents

Cancer is a leading cause of death in the developed world. At present, surgery, radiotherapy, and chemotherapy are the three main therapeutic approaches on cancer. In the field of chemotherapy, metal complexes are an important class of compounds with promising biological activity, since they bind to important biological entities, such as structural proteins and enzymes as well as nucleic acids.[1] In the 1960s, the serendipitous discovery of the antitumor drug cisplatin, *cis*-[$PtCl_2(NH_3)_2$], by Rosenberg greatly revolutionized cancer chemotherapy.[2] Today, cisplatin is used in more than 50% of all treatment regimes for cancer patients. Sales of platinum-based anticancer drugs are estimated at more than one billion US-$ per year.[3] Fueled by this widespread success of cisplatin in the clinical treatment of various types of malignancies, the chemistry of metal-based drugs has received enormous attention over the last few decades.[4]

1.1.1 Clinically approved platinum antitumor drugs

In 1965, during a study of the effect of an electronic field on the growth of bacteria, Rosenberg and coworkers serendipitously discovered that cisplatin, which was generated from the platinum electrodes by reaction with ammonium chloride in the buffer, has an inhibitiory effect on bacterial cell division.[2] Cisplatin was subsequently screened for biological activity on small solid sarcoma 180 tumors and leukemia L1210 cells in mice,[5] and entered phase I clinical trials in humans in 1971. Seven years later, it was approved for clinical treatment of testicular and bladder cancer. Since then, cisplatin has been one of the most widely used antitumor drugs, with demonstrated activity against testicular, bladder, ovarian, cervical, head and neck cancer as well as non-small cell lung cancer (NSCLC) and small cell lung cancer (SCLC).[6] However, besides its widespread success in the clinical treatment of various types of malignancies, the clinical effectiveness of cisplatin is often limited by high general toxicity, severe side effects, and the development of resistance.[4, 7]
To overcome these disadvantages, intensive efforts have been made by researchers all around the world to identify more effective derivatives of cisplatin. Consequently, several promising analogues of cisplatin have been developed (**Figure 1.1**). However, from the second generation of platin-based anticancer agents, only carboplatin and oxaliplatin have so far been approved from clinical application worldwide.[8-9] It is important to note that carboplatin has fewer side effects and thus is better tolerated by patients and can be used at

higher doses than cisplatin.[10] Oxaliplatin is known to overcome cisplatin resistance and also has considerably lower side effects than cisplatin. In addition, another second generation cisplatin analogue, nedaplatin, has been approved in the treatment of non-small cell lung cancer (NSCLC), small cell lung cancer (SCLC), esophageal cancer, and head and neck cancer in Japan.[11-12] Compared to cisplatin, nedaplatin has a ten-fold higher solubility in water and also shows less nephrotoxicity. The third generation of cisplatin analogues are represented by lobaplatin and heptaplatin, which have been approved for clinical cancer treatment in China and Korea, respectively. The advantage of lobaplatin is the absence of nephrotoxicity, neurotoxicity, and ototoxicity even after about two weeks of drug administration,[13-17] while heptaplatin shows high solution stability, no significant toxicity, and potent anticancer activity towards cisplatin resistant cells.[13, 18-19] The structure of the six platinum anticancer drugs clinically approved to date are shown in **Figure 1.2** while in **Table 1.1,** their biological properties are summarized.

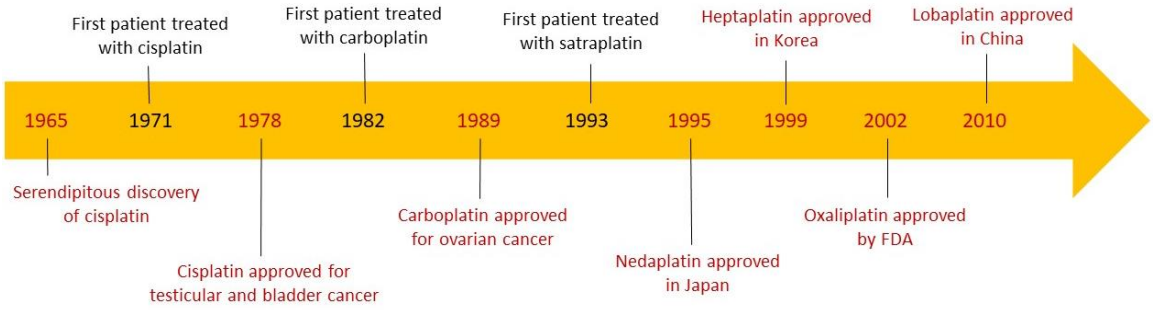

Figure 1.1: Chronology of platinum anticancer drug development.

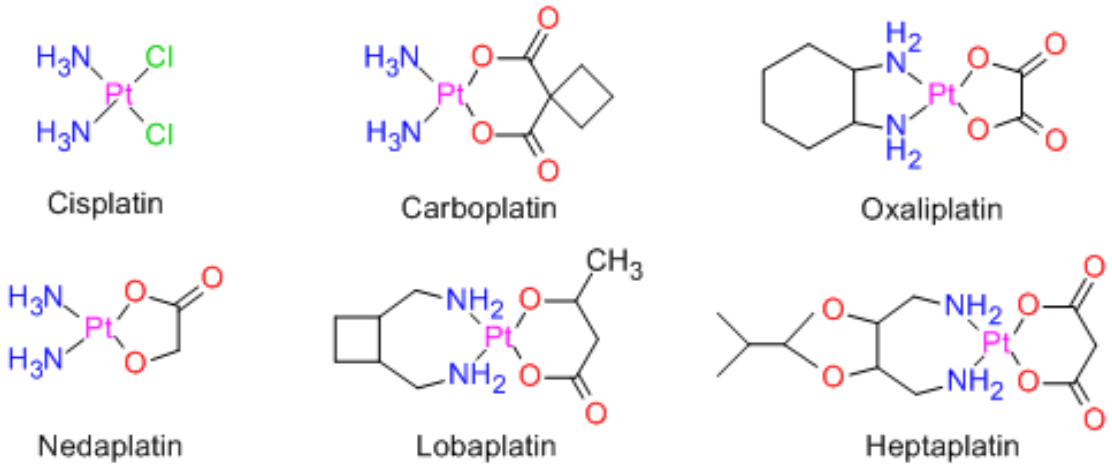

Figure 1.2: Structure of the platinum anticancer drugs approved for clinical use.

Table 1.1: Comparison of the platinum antitumor drugs approved for treatment of humans.

Drug	Application region	Cancers for treatment	Advantages	Disadvantanges
Cisplatin	Worldwide	Testicular, ovarian, bladder, cervical, head and neck, small-cell and non-small cell lung cancers	High cytotoxicity towards a great number of tumor cell lines	High general toxicity, severe side effects, development of resistance
Carboplatin	Worldwide	Ovarian carcinoma, lung, head and neck cancers	Fewer side effects than cisplatin, higher dose toleration	Myelo suppressive effect, nausea and vomiting
Oxaliplatin	Worldwide	Adjuvant and metastatic colorectal cancers when used in combination with 5-FU and folinic acid	Overcame cisplatin resistance and considerably lower side effects as compared to cisplatin	Neuropathy, fatigue, neutropenia, ototoxicity, hypoleukemia
Nedaplatin	Japan	Esophageal, head and neck, non-small cell and small cell lung cancers	Tenfold higher water solubility than cisplatin. Less nephrotoxicity than both cisplatin and carboplatin	Mild nausea, vomiting and nephrotoxicity
Lobaplatin	China	Chronic myelogenous leukemia, inoperable metastatic breast and single cell lung cancers	Much fewer side effects	Anaemia and leukopenia
Heptaplatin	Korea	Gastric cancer	High solution stability, no remarkable toxicity, potent anticancer activity towards cisplatin resistant cells	Hepatotoxicity, nephrotoxicity and myelosuppression

1.1.2 Experimental antitumor agents based on platinum complexes

Other than the six clinically approved platinum antitumor drugs discussed in the previous section, a large number of other platinum complexes have also been extensively evaluated for *in vitro* and *in vivo* anticancer activity. For example, Farrell and coworkers replaced the ammonia ligand in *trans*-$[PtCl_2(NH_3)_2]$ with a range of amines to produce a series of compounds with significantly improved cytotoxicity compared to transplatin and in many cases equivalent to that of cisplatin (**Figure 1.3a**).[20-22] Gautier *et al.* synthesized several triazolato ligands for platinum chelation *via* click reactions (**Figure 1.3b**). Among these

coordination compounds, one of the triazole-amine platinum(II) complexes exhibits a cytotoxic potency against the MCF7 breast carcinoma cell line comparable to that of cisplatin. Importantly, it is almost inactive against normal fibroblasts, an argument supporting a favourable therapeutic index *in vivo*.[23] In the group of Guo, a series of monofunctional platinum(II) complexes of the general formula [PtCl(L)] was synthesized (**Figure 1.3c**), in which the chlorido ligand is the only leaving group. These compounds were tested against a wide range of tumor cell lines and demonstrated promising cytotoxicity. It is worth noting that the most lipophilic complex is also the most cytotoxic one, showing a nearly six-time higher cytotoxicity against BEL-7402 than cisplatin.[24]

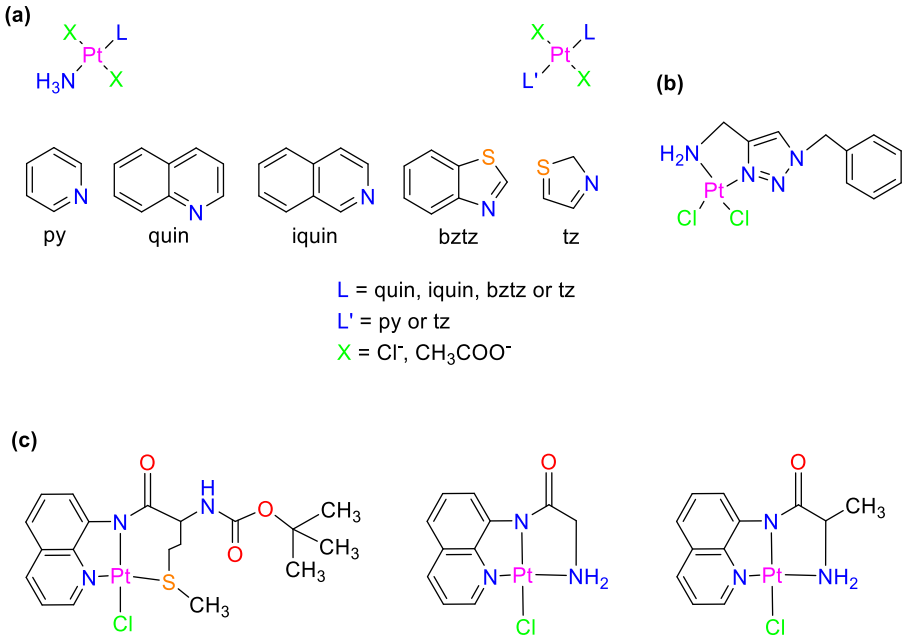

Figure 1.3: Selected examples of platinum(II) anticancer drug candidates: **(a)** a series of cytotoxic *trans*-amine Pt(II) complexes with different heteroaromatic ligands; **(b)** a Pt(II) complex with a triazolate ligand synthesized by copper catalyzed azide-alkyne cycloaddition (CuAAC) click reaction; **(c)** a series of monofunctional Pt(II) complexes based on 8-aminoquinoline.

Multinuclear platinum complexes containing two, three, or four metal centres are able to bind to DNA in a manner different from cisplatin and also show great potential for cancer chemotherapy.[25] One of the best studied examples of this class of compoundsis BBR3464 (**Figure 1.4a**), which is currently in phase II clinical trials. This trinuclear compound showed high activity against seven tested human tumor cell lines, and turned out to be extremely potent against tumor xenografts which are naturally resistant to cisplatin, with IC_{50} values at least 20-fold lower than that of cisplatin.[26] In addition, a trinuclear monofuctional platinum(II) complex $[Pt_3Cl_3(hptab)](ClO_4)_3$ with hptab = *N*,*N*,*N*',*N*',*N*'',*N*''-hexakis(2-

pyridylmethyl)-1,3,5-tris(aminomethyl)benzene **(Figure 1.4b)** also has a strong binding ability to DNA and shows promising cytotoxic effects on human and mouse tumor cells, including those resistant to cisplatin.[27] Two multinuclear platinum(II) complexes, a trinuclear complex bridged by the biogenic polyamine spermidine and a dinuclear complex linked by spermine (**Figure 1.4c**), also demonstrated high antiproliferative and cytotoxicity against the human cervical cancer cell line HeLa and HSC-3 epithelial-type cells. Importantly, their effect on healthy cells is reversible upon drug removal.[28]

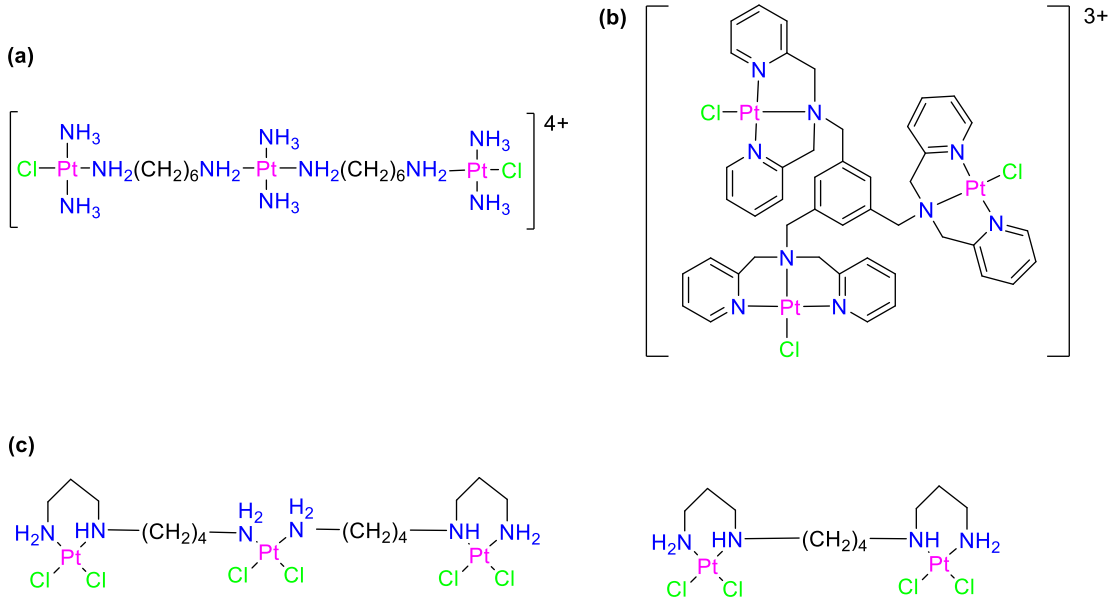

Figure 1.4: Selected examples of multinuclear platinum(II) anticancer compounds: **(a)** trinuclear compound BBR3464 which is in phase II clinical evaluation; **(b)** a trinuclear monofuctional platinum(II) compound with strong DNA binding ability; **(c)** two complexes contain the biogenic polyamines spermidine and spermine as bridging linkers.

In the 1990s, platinum(IV) complexes were for the first time explored as prodrugs by scientists at Johnson Matthey. Since then, the development of such compounds has gained significant attention.[29-32] The low-spin $5d^6$ electronic configuration and octahedral coordination geometry leads to slower ligand exchange rates of platinum(IV) complexes compared to platinum(II) compounds. However, it is generally assumed that upon reduction inside cancer cells, the two axial ligands are lost and the original platinum(II) drug is released (**Scheme 1.1**).

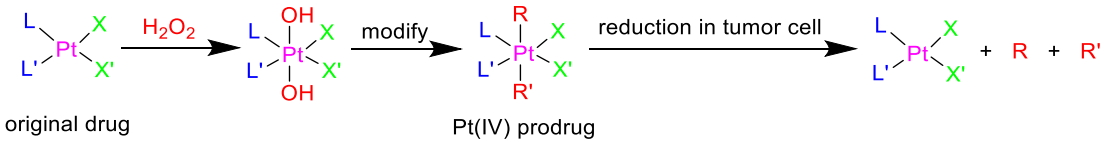

Scheme 1.1: Synthesis of platinum(IV) prodrugs by oxidation of a Pt(II) precursor with hydrogen peroxide followed by axial ligand exhange, and activation by reduction inside tumor cells.

Up to now, the four platinum(IV) compounds tetraplatin, iproplatin, satraplatin, and LA-12 have entered clinical trials (**Figure 1.5**). Tetraplatin is one of the first platinum(IV) antitumor agents to advance that far, and its advantage is due to the fact that it is rapidly reduced to release the original drug in both tissue culture medium and undiluted rat plasma. However, this comes along with severe neurotoxicity, which limited further clinical utilization.[33] Compared to tetraplatin, iproplatin has a higher water solubility and is less prone to reduction and deactivation by biological reducing agents. However, since it did not exhibit cytotoxicity better than cisplatin or carboplatin in a variety of phase I–III clinical trials, further evaluation was finally stopped.[34] Satraplatin was the first reported oral platinum agent[35] and demonstrated antitumor activity towards some cancers which are not responsive to cisplatin, but the overall survival rates of patients did not improve significantly.[36] A derivative of satraplatin, LA-12, in which the cyclohexylamine ligand is replaced by adamantylamine, has finished phase I clinical trials and further clinical studies are underway.[37]

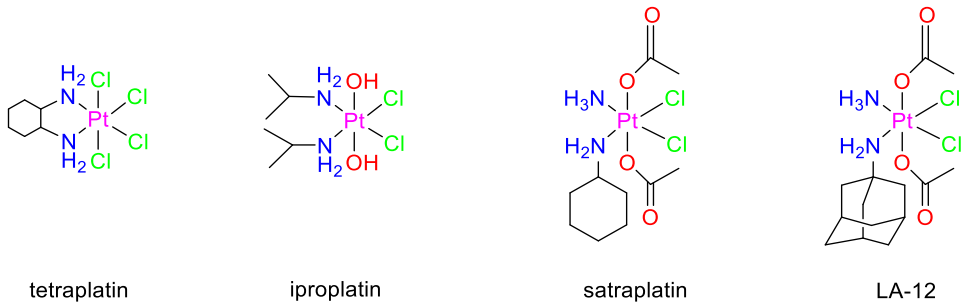

Figure 1.5: Platinum(IV) antitumor drug candidates currently undergoing clinical trials.

1.1.3 Antitumor agents based on non-platinum metal complexes

While most of the stuides on antitumor metal complexes are focused on cisplatin analogues, there is also a growing number of non-platinum compounds which display remarkable biological activity. The advantage of using transition metals other than platinum includes additional coordination sites, alterations in ligand affinity and substitution kinetics, changes in oxidation state, and photodynamic approaches to chemotherapy.[38] The most prominent place in the development of such new antitumor agents probably goes to ruthenium.[39] The compounds explored for such activity were Ru(III) chloro-ammine complexes such as *cis*-$[RuCl_2(NH_3)_4]Cl$, (HIm)*trans*-$[RuCl_4(im)_2]$ and *fac*-$[RuCl_3(NH_3)_3]$ (im = imidazole). The Keppler-type complex (Him)*trans*-$[RuCl_4(im)_2]$ (KP1019, **Figure 1.6a**) is more cytotoxic than cyclophosphamide, cisplatin, and 5-fluorouracil when examined against P388 leukemia and B16 melanoma cells as well as against platinum-resistant colorectal tumors.[40] It entered phase I clinical trials but due to solubility issues, the maximum-tolerated dose was not

reached. To overcome the solubility problem, the indazolium cation of KP1019 was replaced by sodium in a compound labelled KP1339. This sodium complex has better aqueous solubility and is currently in phase I clinical trials.[41] Another promising ruthenium antitumor agent is (Him)*trans*-[$RuCl_4$(dmso-*S*)(im)] also known as NAMI-A (**Figure 1.6b**), which is particularly useful for the treatment of metastatic or cisplatin-resistant tumors. NAMI-A is the first ruthenium complex to enter and complete phase I clinical trials.[38, 42]

In recent years, the use of gold complexes as an alternative to cisplatin treatment was proposed based on similarities of gold and platinum chemistry.[43] Already in the 1980s, screening efforts on different gold complexes led to the identification of the cationic tetrahedral gold(I) phosphine complex [$Au(dppe)_2$]Cl (**Figure 1.6c**).[44] It is worth noting that the bis(diphenylphosphino)ethane (dppe) ligand itself also displays antitumor activity, and the gold might serve to protect it from degradation. Furthermore, the antitumor activity demonstrated for [$Au(dppe)_2$]Cl was 20-fold higher than that of dppe alone,[44-45] which suggests that the effect of gold expands beyond simple protection against degradation. Other than gold(I) species, gold(III) complexes also have potential for anticancer chemotherapy as they are isostructural and isoelectronic to platinum(II) compounds. Consequently, gold(III) complexes are expected to have similar antitumor properties to those of cisplatin,[46] and DNA is among the most suspected target molecules for them.[47]

For instance, a series of gold(III) complexes based on terpyridine derivatives with high stability and solubility were synthesized, which displayed higher *in vitro* cytotoxicity than cisplatin against A-549, SGC-7901, HeLa, HCT-116, BEL-7402, P-388, and HL-60 cell lines (**Figure 1.6d**).[48] It is worth noting that a correlation between the DNA binding affinity and cytotoxicity was identified for these complexes, suggesting that both properties can be fine-tuned by the steric and electronic properties of the ligands.

Wee1 is a G2/M checkpoint protein from a family of tyrosine kinases and a key regulator of cell cycle progression.[49-50] Lipkowitz and coworkers showed that inhibition of Wee1 leads to accumulation of DNA, alteration in cell cycle regulation, and induction of apoptosis in breast cancer cells.[50] Very recently, a rhodium(III) complex was identified as a potent Wee1 inhibitor by *in vitro* and *in cellulo* studies (**Figure 1.6e**).[51] This complex inhibited Wee1 activity in MDA-MB-231 cells with an IC_{50} value of 11.2 ± 1.8 nM and showed higher activity than organic compound, 2-allyl-1-(6-(2-hydroxypropan-2-yl)pyridin-2-yl)-6-((4-(4-methylpiperazin-1-yl)phenyl)amino)-1H-pyrazolo-[3,4-d]pyri-midin-3(2H)-one, which is known as MK1775 and now in clinical trials as a Wee1 inhibitor. The rhodium(III) complex also induced cell damage and death in TP53-mutated triple-negative breast cancer cells and

has potential to become the first metal-based Wee1 antagonist. Other than the complexes mentioned above, there are more potential antitumor agents based on other transition metals such as palladium, silver, rhenium, iridium, vanadium, manganese, tin, iron, and copper, which are currently under development by researchers around the world. Although most of these studies are still at an early stage, complexes based on transition metals with multiple structural motifs are worth looking for to develop novel anticancer agents. Therefore, synthetic methodology that can quickly generate high molecular diversity and has great reaction efficiency is required to optimize compounds for specific biological properties and activities.

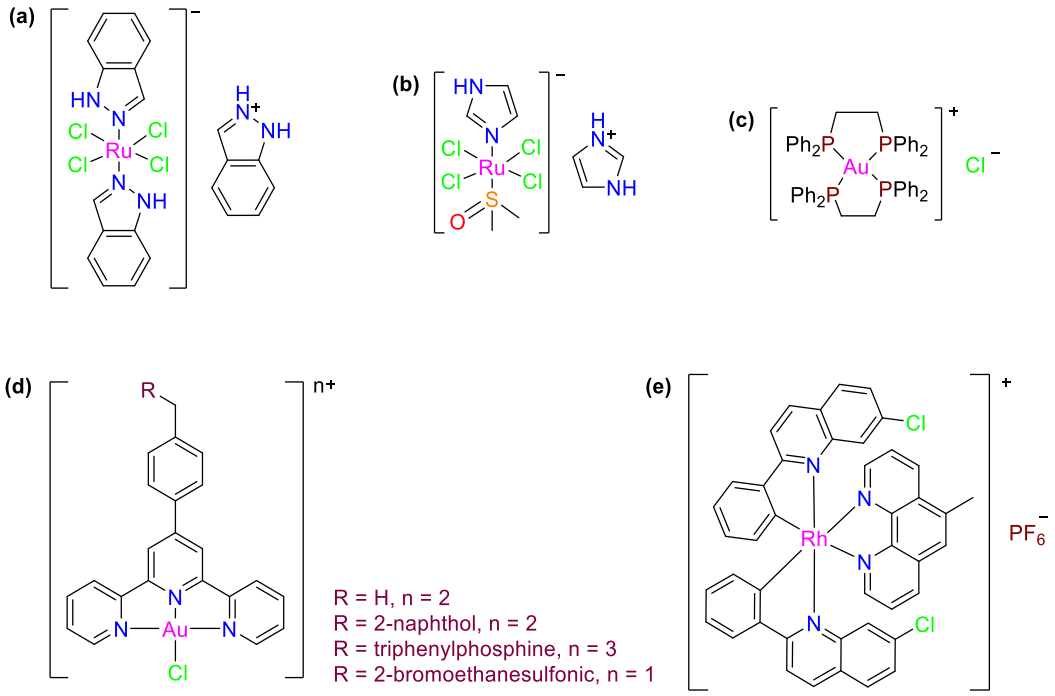

Figure 1.6: Selected examples of non-platinum anticancer drug candidates: **(a)** the Keppler-type compound KP1019; **(b)** NAMI-A, the first ruthenium complex to enter and complete phase I clinical trials; **(c)** cationic tetrahedral gold(I) phosphine complex $[Au(dppe)_2]Cl$; **(d)** series of gold(III) complexes based on terpyridine derivatives; **(e)** rhodium(III) cyclometalated complex as a potent Wee1 inhibitor.

1.2 Click reactions

In 2001, Sharpless and coworkers introduced the concept of "click chemistry" with the aim to develop an expanding set of powerful, selective, and modular building "blocks" that work reliably in both small- and large-scale applications,[52] which is ideal for selective and site-specific bio-orthogonal conjugations in chemical biology. According to their stringent criteria, "click reactions" should fulfill the following pre-requisites: i) modular and wide scope; ii) high yield, nearly quantitative conversion; iii) only inoffensive or no residual byproducts; iv) stereospecific product formation; v) simple reaction conditions; vi) readily available starting materials and reagents; vii) no or only benign solvent; viii) simple product isolation.[52] At present, several classes of conversions meet these criteria and can be classified as "click reactions".

The most iconic type of click reaction is probably the copper(I)-catalyzed azide-alkyne cycloaddition (CuAAC). As shown in **Scheme 1.2**, an alkyne reacts with an azide under formation of a five-membered triazole heterocycle in a [3+2] cycloaddition with copper(I) serving as a catalyst. The CuAAC is attractive due to its high yield and good tolerance towards a number of solvents. More importantly, this kind of reaction regioselectively gives 1,4-disubstituted 1,2,3-triazoles only and products usually have good stability under biological conditions.[53-57] However, the toxicity of copper is a concern for *in vitro* and *in vivo* applications and strict efforts have to be made to remove the copper catalyst to obtain a pure product. Therefore, catalyst-free variants are important for the further development of biodirected click reactions.

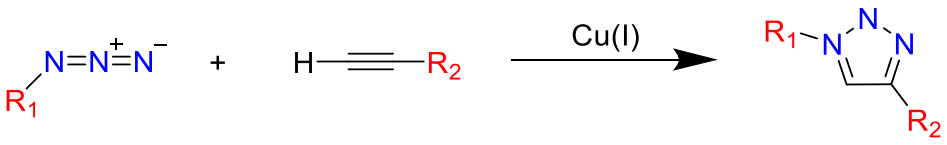

Scheme 1.2: The copper(I)-catalyzed azide-alkyne cycloaddition (CuAAC) of alkynes and azides leads to 1,4-disubstituted triazoles.

In 2004, Bertozzi reported on a [3+2] cycloaddition of azides with cyclooctyne derivatives which readily occurs under physiological conditions in the absence of catalyst.[58] Several strained cyclooctynes were explored in this reaction to replace the alkynes involved in the Huisgen 1,3-dipolar cycloaddition. The release of intramolecular ring strain is the driving force for the cyclooctyne to readily react with an azide to form the trizolate product at ambient temperature in high yield (**Scheme 1.3**). Therefore, this kind of reaction is termed

the "strain-promoted azide-alkyne cycloaddition" (SPAAC). It has been applied to label biomolecules *in vivo*[59-61] and it is of great significance for the synthesis of hybrid biomaterials and the labelling of bio(macro)molecules in living systems.[62] Although the SPAAC avoids issues related to the use of the copper catalyst in the CuAAC, the regioselectivity of this reaction is poor.[62] In addition, cyclooctynes are prone to react with thiols such as cysteine residues in proteins in a thiol-yne reaction, resulting in non-specific labelling.[63] Furthermore, the high cost and difficult synthesis of cyclooctynes also limit a broder utilization of this kind of reaction.

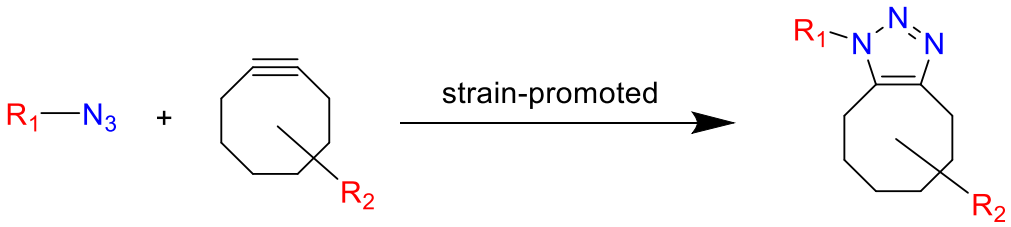

Scheme 1.3: The strain-promoted azide-alkyne cycloaddition (SPAAC).

In addition to the SPAAC, Ju and coworkers carried out 1,3-dipolar cycloadditions without catalyst using either elevated reaction temperatures[64] or electron-poor alkynes.[65] Furthermore, Rutjes showed that the combination of ring strain and electron deficiency in alkynes facilitates a spontaneous tandem [3+2] cycloaddition-retro-Diels-Alder (tandem crDA) ligation that results in a stable 1,2,3-triazole linkage.[66] This reaction involves a bicyclic oxanorbornadiene with either identical or different electron-deficient substituents such as trifluoromethyl or ester groups (also called a "masked alkyne") and an azide to give two triazolate isomers under release of furan (**Scheme 1.4**). The tandem crDA reaction proceeds much faster than those involving the corresponding alkynes, and this kind of reaction turned out to be an effective method for the preparation of PEGylated oligopeptides. It can be performed in aqueous medium and at ambient temperature, which makes it promising as a bioconjugation method for the labelling and functionalization of proteins.[66] Still, the poor regioselectivity may affect general applicability.

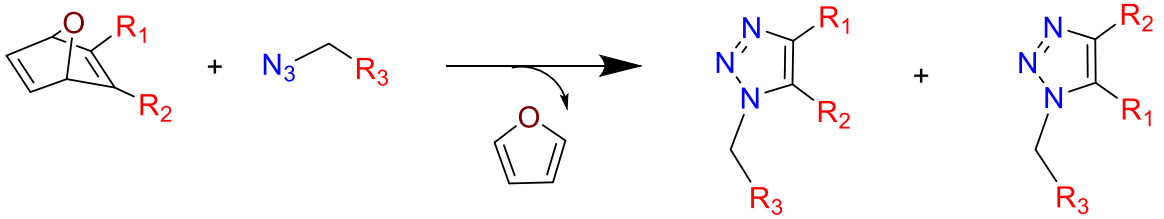

Scheme 1.4: Regioisomeric products of the tandem [3+2] cycloaddition-retro-Diels-Alder (tandem crDA).

In addition, some other "click" reactions such as the thiol-ene reaction,[67] thiol-Michael addition,[68] oxime ligation,[69] Staudinger ligation (**Scheme 1.5**),[70-71] and native chemical ligation (NCL)[72] are also of great importance in the field of bioconjugate chemistry. While each of these established "click" reactions has particular advantages and disadvantages, the further development for improved synthetic methods to give better yields and regioselectivity, and generate products with good stability, solubility, and biological activity is still very active.

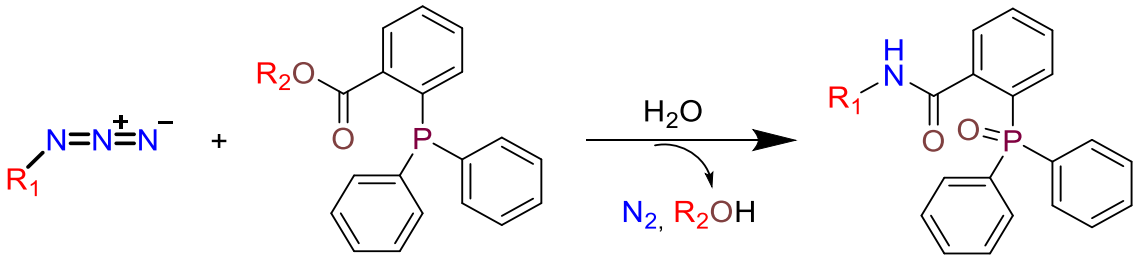

Scheme 1.5: The Staudinger ligation of an azide and a substituted triphenylphosphine leads to amide bond formation under mild and biocompatible conditions.

1.3 Inorganic Click (iClick) reactions

Inspired by the success of organic "click" reactions, Veige introduced the concept of "inorganic click reactions" (iClick reactions).[73] In contrast to the prominent CuAAC, iClick reactions take place directly in the inner metal coordination sphere and do not require use of a catalyst. As shown in **Scheme 1.6**, the reaction of a metal-azido complex and a dipolorphilic C≡X compound (X = C, N) leads to metal triazolato complexes. Alternatively, an "inverse" iClick reaction can also be envisioned, in which a metal-acetylide reacts with an organoazide or a metal-azido complex. The iClick reaction kinetics are controlled by the choice of metal and its oxidation state as well as steric and electronic properties of the coligands. Furthermore, the stereochemistry around the metal centre should be retained during iClick reactions, thus giving facile access to diastereomerically or enantiomerically pure products from a single precursor without the need for tedious isomer separation. So far, iClick reactions have been reported for a range of transition metals as well as main group metal compounds as summarized below.

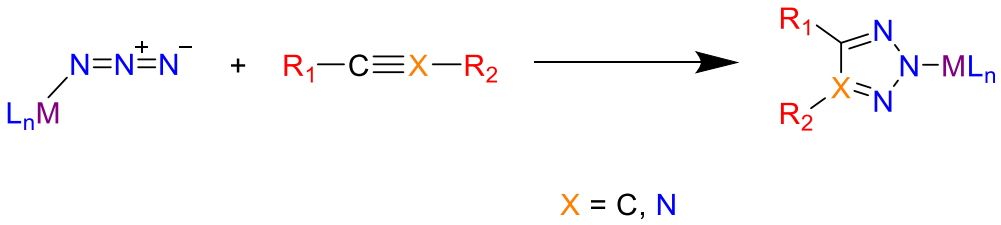

Scheme 1.6: Inorganic click (iClick) reaction of a metal-azido complex and a dipolorphilic C≡X (X = C, N) compound to give a metal-triazolato product. In addition to the N2-coordinated triazolate shown, N1- and N3-bound species may also form.

1.3.1 iClick reactions of main group metals

Main group compounds were the first to be applied in an iClick reaction, decades before the term was actually coined. In 1966, Birkofer and Wegner reacted trimethylsilyl azide with a series of alkynes to prepare the corresponding *N*-(trimethylsilyl)-1,2,3-triazoles in high yield in the absence of solvent.[74] According to NMR spectroscopy, all isolated triazolato products were "symmetrically" coordinated to the silicon atom *via* the N2 nitrogen atom, which requires a 1,2-shift from the terminal N1-coordinated azido ligand to the N2 triazolato product (**Figure 1.7a**). In the same year, Gorth and Henry studied the reaction of triphenyl lead azide with a number of olefinic and acetylenic compounds. However, the cycloaddition only takes place with strongly dipolarophilic dimethyl acetylenedicarboxylate (DMAD). In contrast, no formation of triazolates was observed for maleic anhydride, maleic

dimethylester, vinyl ethyl ether, morpholinocyclopentene, diphenylacetylene, phenylacetylene, propargyl alcohol, and 2-methyl-3-butyn-2-ol even at elevated temperatures, indicating the electronic properties of the dipolarphile have a great effect on the reaction. Two isomeric lead triazolates were identified as the products (**Figure 1.7b**).[75]

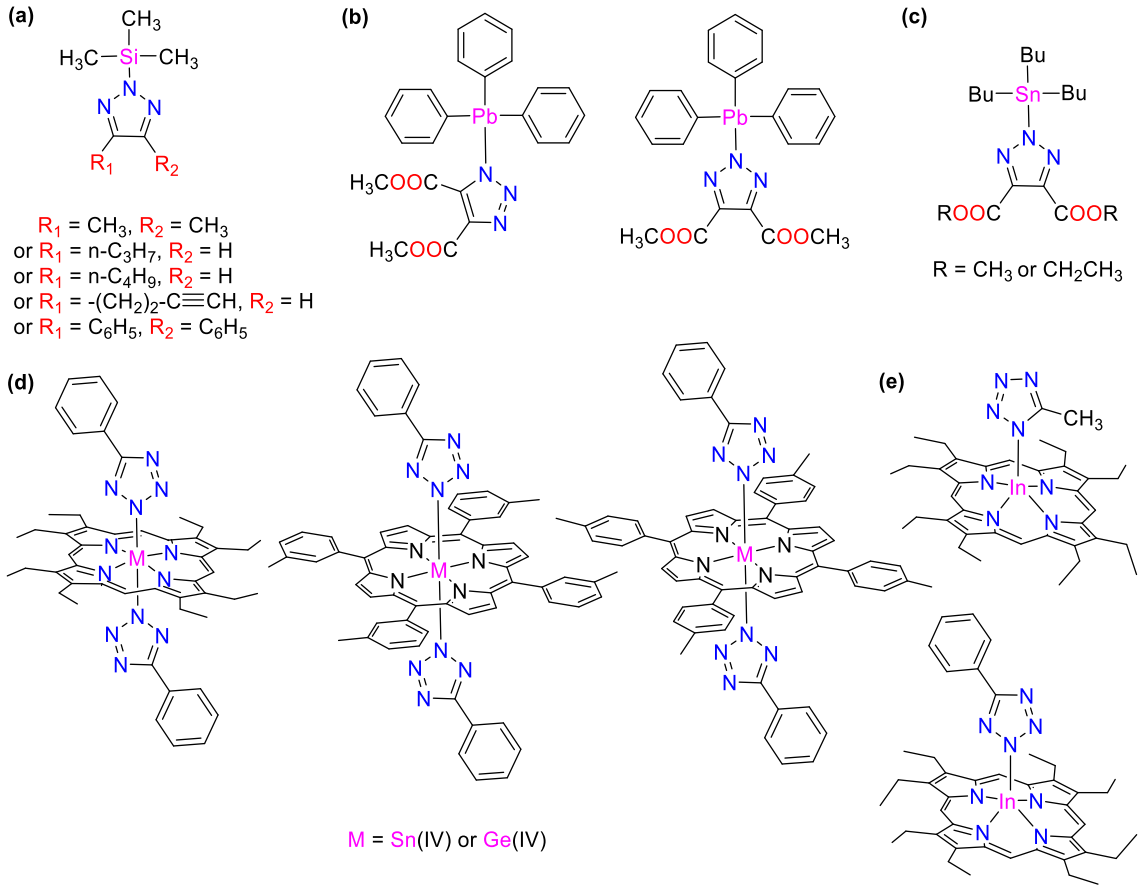

Figure 1.7: Examples of main group metal iClick products: **(a)** *N*-(trimethylsilyl)-1,2,3-triazoles; **(b)** mixture of N1 and N2 lead triazolate isomers resulting from the catalyst-free cycloaddition of triphenyl lead azide and DMAD; **(c)** *N*-(trialkylstannyl)-4,5-bis(alkoxycarbonyl)-1,2,3-triazoles identified by ^{13}C NMR as the N2 isomers; **(d)** bis(phenyltetrazolato)germanium(IV) and tin(IV) metalloporphyrins synthesized by iClick reaction of diazido-metal porphyrins and benzonitrile; **(e)** indium(III) phorphyrine iClick products show that the binding mode depends on thesteric demand of the nitrile substituent.

Among the group III elements, iClick reactions have been reported for germanium and tin azides. Using DMAD and DEAD, two *N*-(trialkylstannyl)-4,5-bis(alkoxycarbonyl)-1,2,3-triazoles were synthesized and in both cases the ^{13}C NMR spectroscopy showed that the *N*-trialkylstannyl group is attached to the N2 atom (**Figure 1.7c**).[76] In the group of Guilard, benzonitrile was also reacted with diazido-germanium(IV) and tin (IV) porphyrins. In the course of the reaction, the sharp signal of the antisymmetric azido stretching vibration at approx. 2070 cm^{-1} was monitored by IR spectroscopy and bis(phenyltetrazolato)-

germanium(IV) and tin(IV) metalloporphyrins obtained. The N2 isomer is expected to be the final product due to steric interactions between the phenyl ring of the phenyltetrazole and the porphyrin macrocycle (**Figure 1.7d**).[77] In the same group, several indium(III) triazolato and tetrazolato complexes were prepared by this method. The phenyl-substituted tetrazolato ligands are coordinated to the indium(III) center *via* the N2 atom, while the smaller methyl-substituted ligand leads to the N1 isomer (**Figure 1.7e**).[78-79] Beyond silicon, germanium, tin, lead, and indium, no other main group elements have been used in iClick reactions so far.

1.3.2 iClick reactions of group V metals

Among the group V elements, tantalum is the only one so far reported to undergo an iClick reaction. Using this method, Herberhold and coworkers synthesized two pentamethylcyclopentadienyl tantalum(V) triazolato complexes.[80] In the first case, an azido-bridged binuclear tantalum compound, $[Cp^*TaCl(N_3)_2(\mu\text{-}N_3)]_2$, was treated with DMAD to give a mononuclear complex (**Scheme 1.7a**), in which the tantalum centre is additionally coordinated by one oxygen atom from the ester substituent on the triazolate ligand to give a N3-methylated 1,2,3-triazolato chelate ligand bound to tantalum(V) through the N1 atom. Interestingly, the reaction also involves a methyl group transfer from the ester oxygen to the triazolate nitrogen atom. On the other hand, with $[Cp^*Ta(N_3)(C_6H_5)_3]$ as the precursor, a N2-coordinated tantalum(V) 1,2,3-triazolato product was obtained upon reaction with DMAD (**Scheme 1.7b**).[80]

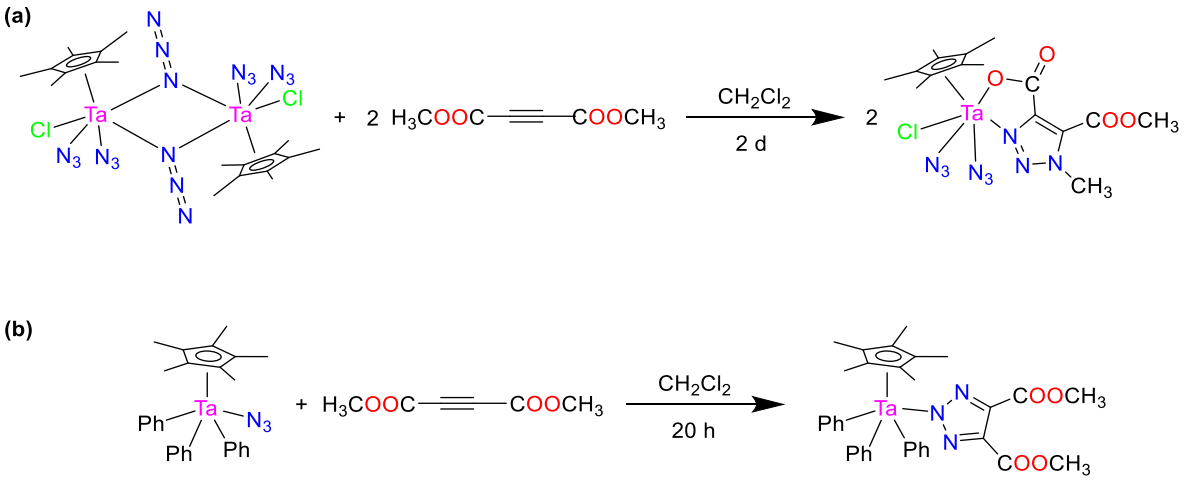

Scheme 1.7: iClick reactions of tantalum(V) azido complexes with DMAD lead to different triazolate coordination modes.

1.3.3 iClick reactions of group VI metals

In the last ten years, a number of iClick reactions of the group VI metals have been reported. The first such paper was by Liu *et al.*, who studied the reactions of molybdenum azido complexes with nitriles and DMAD.[81] The resulting triazolato and tetrazolato ligands are in the N1- or N2-binding mode (**Figure 1.8a**). The reactivity of these molybdenum(II) azido compounds was also investigated towards other dipolarophiles such as tetracyanoethylene, 4-nitrobenzonitrile, acrylonitrile and diethyl acetylenedicarboxylate (DEAD).[82] In all structures obtained, the ligand was N2-coordinated to the metal, as demonstrated by single crystal X-ray structure analysis.

Recently, our own group reported on the room-temperature iClick reaction of isoelectronic molybdenum(II) and tungsten(II) azido complexes with electron-poor alkynes. The resulting triazolates are coordinated *via* the N2 atom of the triazolate ring (**Figure 1.8b**).[83] A trifluoromethyl-substituted alkyne was employed in this work, which served as a sensitive ^{19}F NMR marker to monitor the progress of the reaction and determine the rate constant of the cycloaddition. Using this method, a N1-bound intermediate was detected in the course of the reaction and the second-order rate constant for the reaction of the tungsten(II) azido compound with 4,4,4-trifluoro-2-butynoic acid ethyl ester determined as $k_2 = (7.3 \pm 0.1) \times 10^{-2}$ M^{-1} s^{-1}, which is comparable to some strain-promoted azide-alkyne cycloadditions (SPAAC). In the case of the analogous molybdenum complex, the reaction proceeded too fast to be followed by NMR. However, using solution IR spectroscopy, rate constants could be determined in a range of 0.4 to 6.5 × 10^{-3} s^{-1} and were shown to increase in the order of Mo > W and $F_3C–C{\equiv}C–COOEt$ > DMAD.

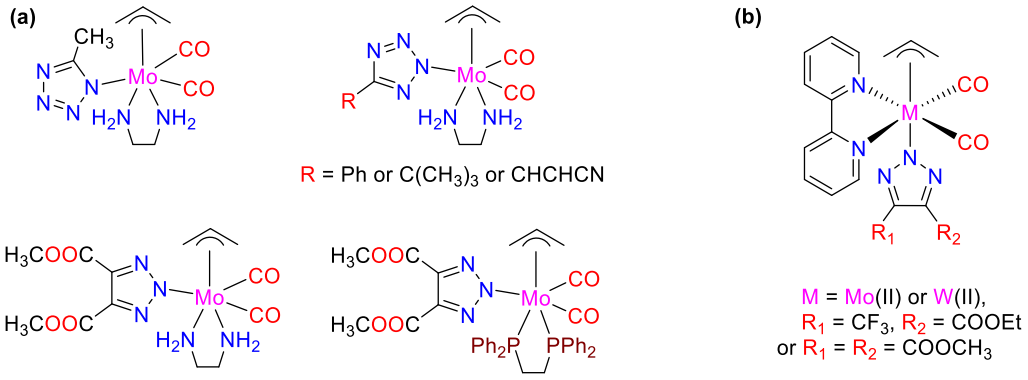

Figure 1.8: (a) N1 and N2 tetrazolato and triazolato complexes obtained by iClick reactions of molybdenum(II) azido compounds with nitriles or DMAD; **(b)** N2 triazolato complexes synthesized by iClick reactions of molybdenum(II) and tungsten(II) azido compounds with electron-deficient alkynes.

1.3.4 iClick reactions of group VII metals

In group VII, several manganese(I) tricarbonyl azido compounds with different coligands reacted with trifluoroacetonitrile or hexafluoro-2-butyne at room temperature to give the corresponding tetrazolato or triazolato complexes. Structural characterization confirmed a N2-coordination mode (**Figure 1.9**).[84-85] On the other hand, our own group utilized an nonsymmetrically 2,3-disubstituted oxanorbornadiene (OND) as a "masked" alkyne equivalent in the iClick reaction with [Mn(N_3)(bpy)($CO)_3$] (**Scheme 1.8**). A triazolate-linked phenyl alanine bioconjugate was obtained this way by simply stirring the two reactants at room temperature for an extended period of time.[86] In 2016, two rhenium(I)-NHC azido compounds were used in the iClick reaction with DMAD (**Scheme 1.9**). The X-ray structure of the resulting triazolato complexes showed that in both cases, the triazolato ligand is coordinated to the N2 nitrogen.[87] Furthermore, luminescence studies demonstrated that the triazolato complexes exhibit higher emission quantum yields and longer decay lifetimes than the corresponding azido compounds. In total, however, iClick reactions of group VII metals have been very limited, and no iClick reaction has been reported on technetium so far, which is possibly due to its radioactivity.

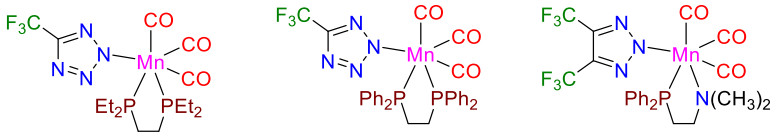

Figure 1.9: Manganese(I) tetrazolato and triazolato complexes synthesized by iClick reactions.

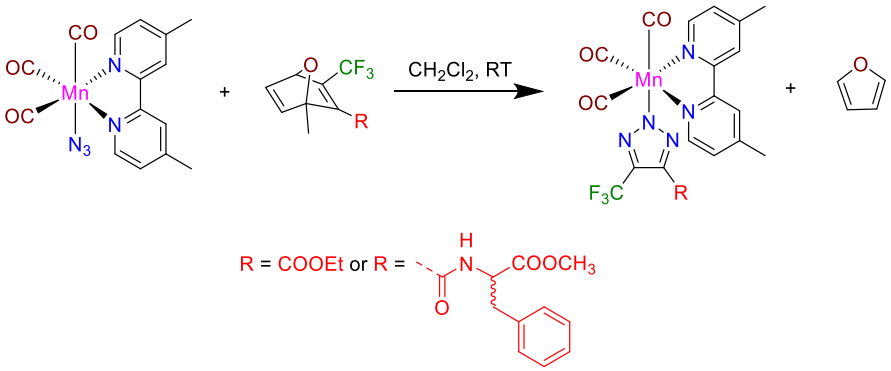

Scheme 1.8: iClick reaction of a manganese(I) azido complex with a "masked" alkyne.

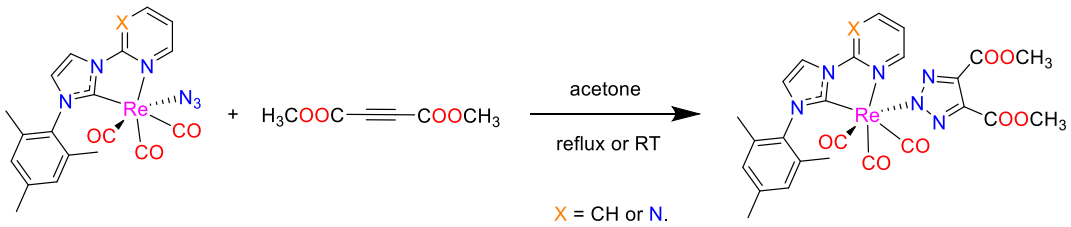

Scheme 1.9: iClick reactions of rhenium(I)-NHC azido complexes with DMAD.

1.3.5 iClick reactions of group VIII metals

Metal-centered [3+2] cycloadditions of group VIII complexes are possibly among the most studies ones so far. Already in 1991, a series of iron(III) porphyrins with σ-bonded tetrazolato or triazolato axial ligands were prepared by iClick reactions of [Fe(N_3)(porphyrinato)] with a series of nitriles (**Figure 1.10**), and an electrochemical study demonstrated that the electronic configuration of the corresponding compounds is not significantly altered by the cycloaddition.[88] Busetto and coworkers carried out iClick reactions of bimetallic (M = Fe, Ru) azido compounds and dipolarophiles to obtain triazolato products. Upon reaction with internal alkynes such as DMAD, the triazolato ligand was found to be N2-coordinated, while in the case of propiolic acid, which features a terminal alkyne group, a mixture of N1 and N2 isomers was obtained (**Scheme 1.10**).[89]

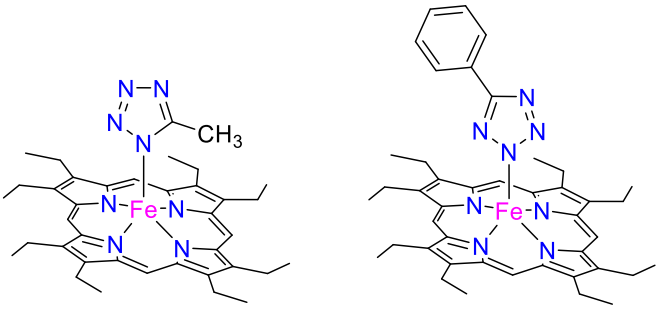

Figure 1.10: Two representative iron(III) tetrazolato complexes prepared by iClick reactions of [Fe(N_3)(porphyrinato)] with acetonitrile and benzonitrile, respectively.

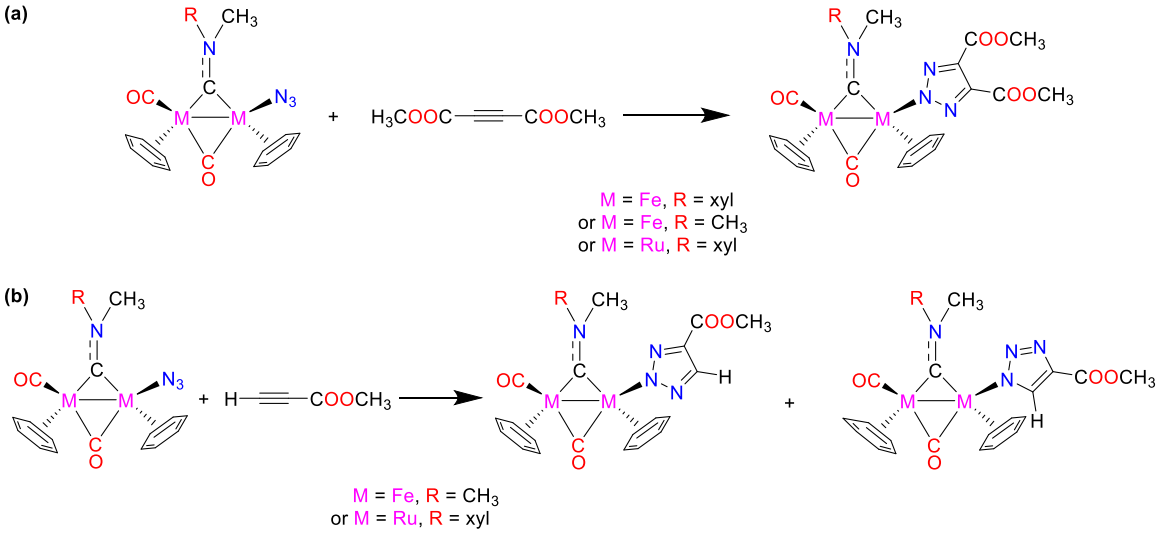

Scheme 1.10: (a) iClick reaction of bimetallic iron or ruthenium azido compounds with internal alkyne DMAD results in formation of the N2 triazolato product; **(b)** iClick reaction with methyl propiolate leads to the product as a mixture of the N1 and N2 isomers.

Different binding modes were also found by Rao, who explored the iClick reaction of neutral arene ruthenium azido complexes with DMAD, DEAD, and fumaronitrile, and found that use of DMAD exclusively lead to the N2-bound isomer while with DEAD, only the N1-coordinated compound was generated (**Scheme 1.11**).[90] Although this result was also confirmed in some follow-up work,[91] other metal azido fragments only lead to N2-coordinated ruthenium triazolato complexes in the case of both DMAD and DEAD.[92-95] Apparently, it is difficult to predict the binding mode of the triazolato ligand as it appears to be governed by synergistic electronic and steric factors.

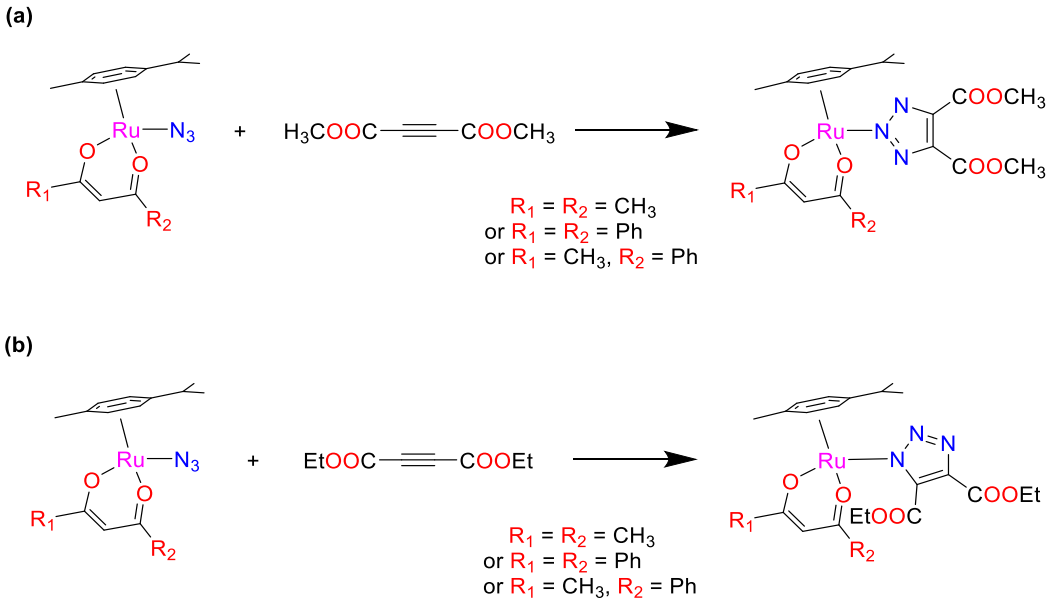

Scheme 1.11: (a) iClick reaction of arene ruthenium azido compounds with DMAD leads to the N2 triazolato product; **(b)** Alternatively, reaction with DEAD produces the N1 triazolato product.

Using a pyridocarbazole ruthenium(II) azido compound, Meggers *et al.* extended the concept of the strain-promoted azide-alkyne cycloaddition (SPAAC) from purely organic azides to metal-coordinated azido compounds. The reactivity was tested towards strain-activated, non-activated, and electron-poor alkynes. However, no cycloaddition was observed with less-strained cyclooctyne, while highly strained bicyclo-[6.1.0]-non-4-yne (BCN) and azadibenzocyclooctyne (ADIBO) smoothly underwent a [3+2] cycloaddition with the azido compound to form stable N2 triazolato complexes (**Figure 1.11**). The non-activated alkynes failed to react, but a fast cycloaddition took place with DMAD.[96] In addition, the kinetics of the iClick reactions were studied by HPLC. Second-order rate constants were in a range of 2.7×10^{-4} to 6.9×10^{-2} M^{-1} s^{-1}, which are generally slower than in the SPAAC, but the speed of the cycloaddition of ADIBO with the ruthenium(II) azido complex is comparable to that of ADIBO with organic benzyl azide.[96]

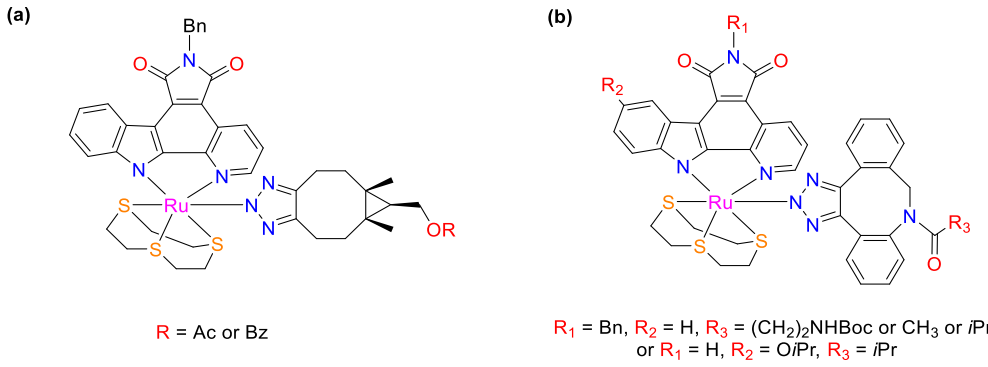

Figure 1.11: Structures of the iClick products from the strain-promoted cycloaddition of a pyridocarbazole ruthenium(II) azido compound with alkyne building blocks BCN **(a)** and ADIBO **(b)**.

Compared to ruthenium, iClick reactions based on osmium are much less studied. However, an osmium(II) bis(azido) compound underwent the cycloaddition reaction with DMAD in the absence of catalyst and the N1-coordinated triazolato complex initially isolated was further converted to the N2 isomer upon heating (**Scheme 1.12**).[97] Notably, only one of the two azido ligands reacts under these conditions.

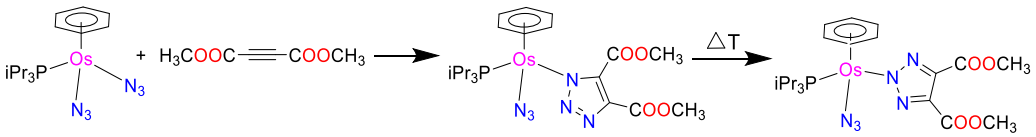

Scheme 1.12: iClick reaction of osmium(II) bis(azido) compound with DMAD.

Furthermore, an osmium azido compound bearing bulky triphenylphosphine groups also underwent the iClick reactions with activated alkynes and nitriles (**Figure 1.12**).[98] However, the analogous ruthenium azido complex did not react this way under similar conditions, implying that the size of the metal centre might play an important role in facilitating the iClick reaction.

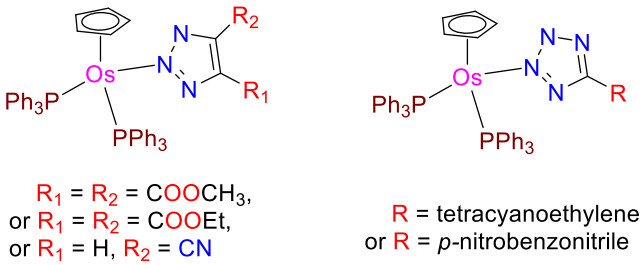

Figure 1.12: Triazolato and tetrazolato osmium(II) complexes obtained by iClick reaction of an osmium(II) azido compound with activated alkynes and nitriles.

1.3.6 iClick reactions of group IX metals

In 1982, Beck and coworkers reported on the catalyst-free 1,3-dipolar cycloaddition of cobalt azido complexes with electron-deficient alkynes, alkenes, and nitriles under mild conditions (**Figure 1.13**).[99] They realized that the N2 isomer is thermodynamically more stable, but the N1 isomer is the kinetic product of the reaction. The reactivity of the dipolarophile increased with a stronger electron-withdrawing ability of its substituents, and the reactivity of metal azido compounds is influenced by the nature of neutral *trans*-coordinated ligands (*trans* effect) as well as the anionic chelating system (*cis* effect).[99] However, a later study of the kinetics of cobalt-centered iClick reactions by IR spectroscopy showed that the reaction rates are not very sensitive to the nature of the ligand *trans* to the azide except in the case of *para*-substituted triaryl phosphines and tricylohexyl phosphine.[100]

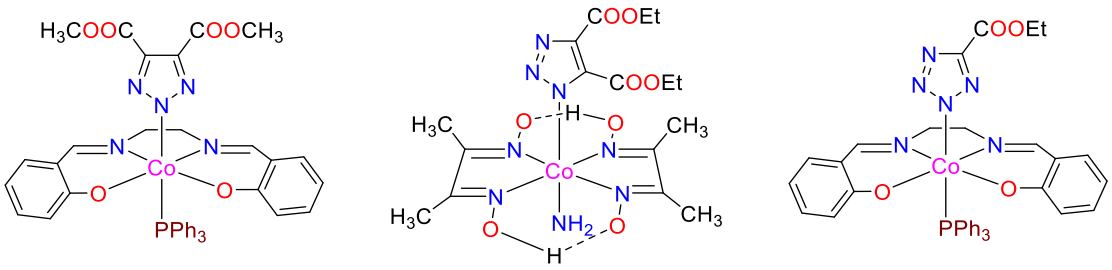

Figure 1.13: Selected examples of products from the iClick reactions of cobalt azido complexes with electron-deficient alkynes, alkenes, and nitriles, respectively.

In the group of Mirica, several first-row transition metal azido complexes including cobalt compounds with the biomimetic cyclam ligand were successfully employed in the cycloaddition reaction with DMAD (**Scheme 1.13**), while the use of azido compounds with salen ligands as well as less electron-deficient alkynes did not lead to the corresponding triazolato products. Furthermore, when the macrocyclic ligand Me_4cyclam was replaced by anionic cyclamAc, no product was isolated, suggesting that even subtle changes in the electronic properties of the metal centre and coligand control the reactivity.[101]

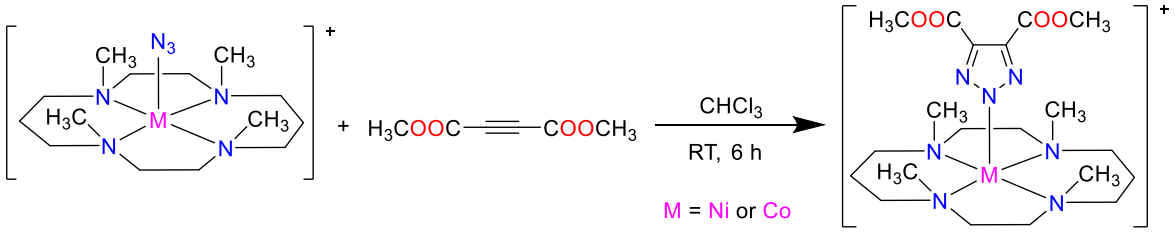

Scheme 1.13: iClick reaction of a cobalt azido compound with the macrocyclic cyclam coligand and DMAD.

Recently, the first example of a [3+2] cycloaddition between a metal azido compound and alkynyl Fischer carbenes were reported. In that context, $[Co(N_3)(Me_4cyclam)]ClO_4$ reacted with Cr(0) and W(0) alkynyl Fischer carbenes at room temperature to give the corresponding triazolate products in good yield (**Scheme 1.14**).[102] The first iClick reaction of a rhodium azido complex was described by Maitlis.[103] A dimeric rhodium diazido complexes reacted with the highly activated dipolarophiles CF_3CN and $CF_3C{\equiv}CCF_3$ *via* the terminal and bridging azido ligands (**Scheme 1.15**). However, the former turned out to be much more reactive than the bridging ones. Similarly, Lastra *et al.* recently reported on other rhodium(III) diazido complexes bearing alkenylphosphanes which reacted with alkynes and nitriles to give triazolato and tetrazolato complexes respectively.[104] They also noticed that the ancillary phosphine ligand greatly influences the reactivity and regioselectivity. As for the iClick reaction of fumaronitrile and rhodium azide, the cycloaddition took place *via* the C=C bond than the C≡N bond (**Scheme 1.15d**).[104] In our own group, a series of half-sandwich rhodium(III) azido complexes with 4,4'-disubstituted 2,2'-bipyridine coligands were used in the iClick reaction with ethyl 4,4,4-trifluoro-2-butynoate (**Scheme 1.16**). The stability of the azido compounds was strongly dependent on the substituents of the bipyridine, and increased in the order $COOCH_3 < H < OCH_3$.

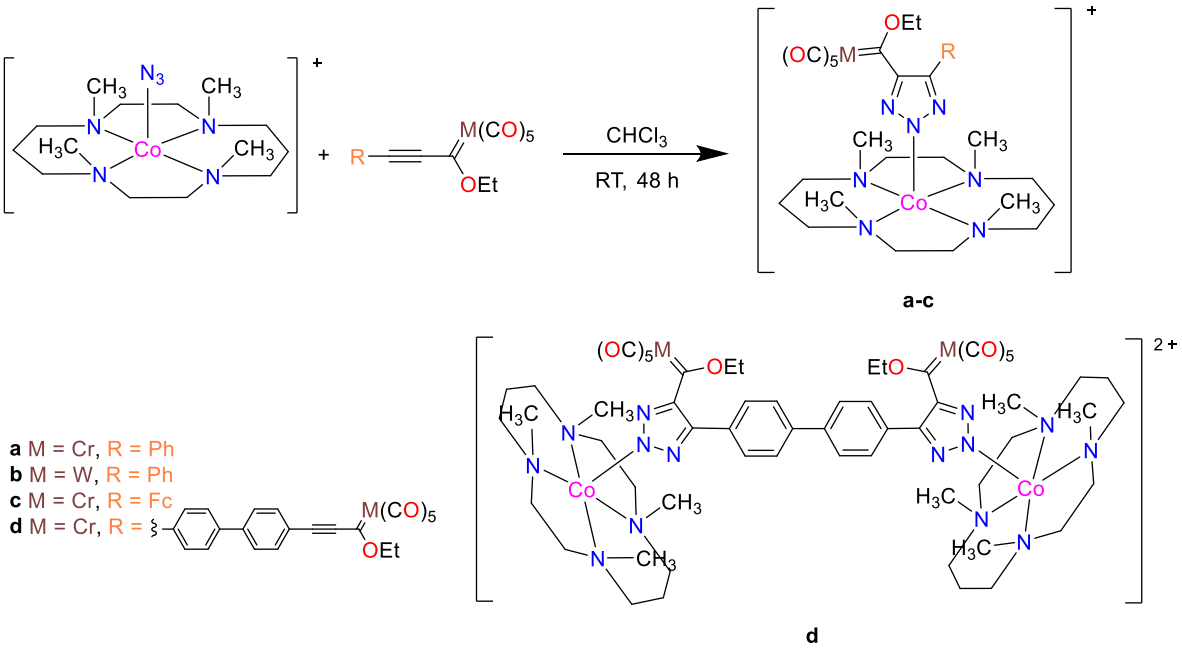

Scheme 1.14: iClick reactions of cobalt(II) azido compound with alkynyl Fischer carbene complexes.

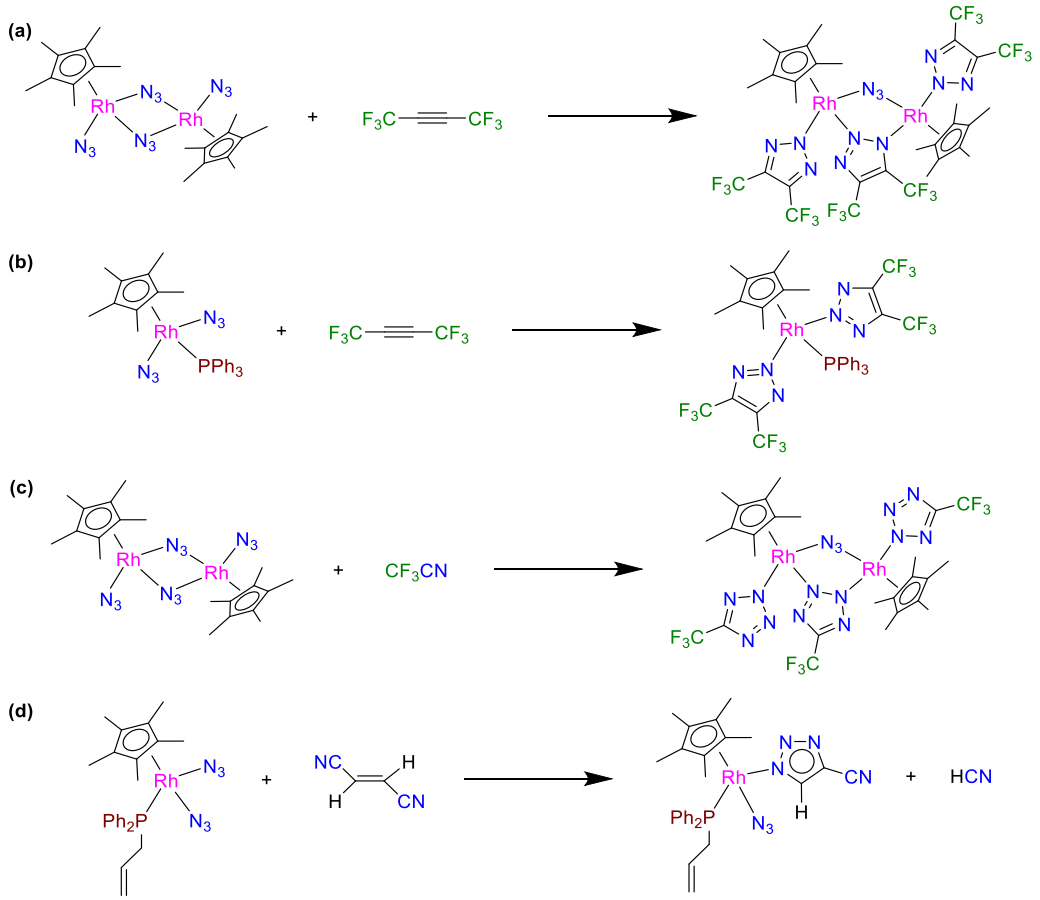

Scheme 1.15: iClick reaction of **(a)** a dimeric rhodium diazido compound with $CF_3C{\equiv}CCF_3$; **(b)** a rhodium diazido compound with $CF_3C{\equiv}CCF_3$; **(c)** a dimeric rhodium diazido compound reacting with CF_3CN; **(d)** a rhodium azido compound with fumaronitrile.

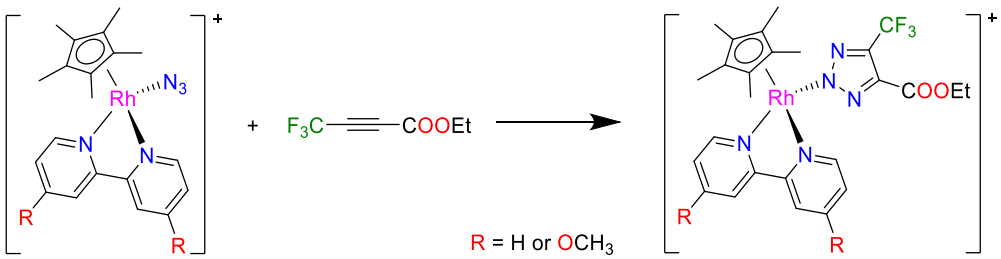

Scheme 1.16: iClick reaction of two Cp^* half-sandwich rhodium(III) azido compounds with ethyl 4,4,4-trifluoro-2-butynoate.

The electronic influence on the kinetic of iClick reactions was studied by solution IR spectroscopy. Electron-donating groups in the 4- and 4'-position of the bpy coligand accelerated the reaction. Pseudo-first order rate constants were all in the range of 10^{-3} s^{-1}, comparable to that of the Staudinger ligations.[105] As a rare example of a 5d element of group IX undergoing the iClick reaction, in 1983, Beck *et al.* successfully reacted *trans*-[Ir(N_3)(CO)(PPh_3)$_2$] with nitriles to give iridium tetrazolato complexes (**Scheme 1.17**).

A kinetic study revealed that the rate constant increases with the donor strength of the phosphine coligands and more electron-deficient nitriles.[106-107] Very recently, catalyst-free [3+2] cycloaddition reactions for semi-sandwich iridium(III) azido complexes with nitriles are reported.[108] These iridium diazido complexes react with tetracyanoethylene (TCNE) to give iridium(III) tetrazolato complexes through the azide-nitrile cycloaddition, in which both single azide-CN as well as double azide-nitrile cycloadditions take place, depending on the reaction conditions (**Scheme 1.18a**). In addition, the fumaronitrile reacted with some iridium(III) diazido complexes through the C=C double bond instead of the C≡N triple bond, to generate the corresponding triazolinato complexes, which further lose hydrogen cyanide upon treatment with alumina, resulting in aromatic triazolato complexes (**Scheme 1.18b**).

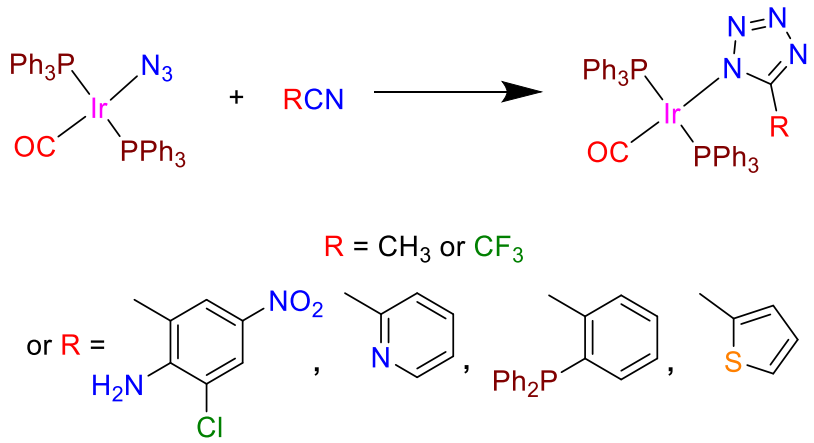

Scheme 1.17: iClick reaction of *trans*-[Ir(N_3)(CO)(PPh_3)$_2$] with different nitriles.

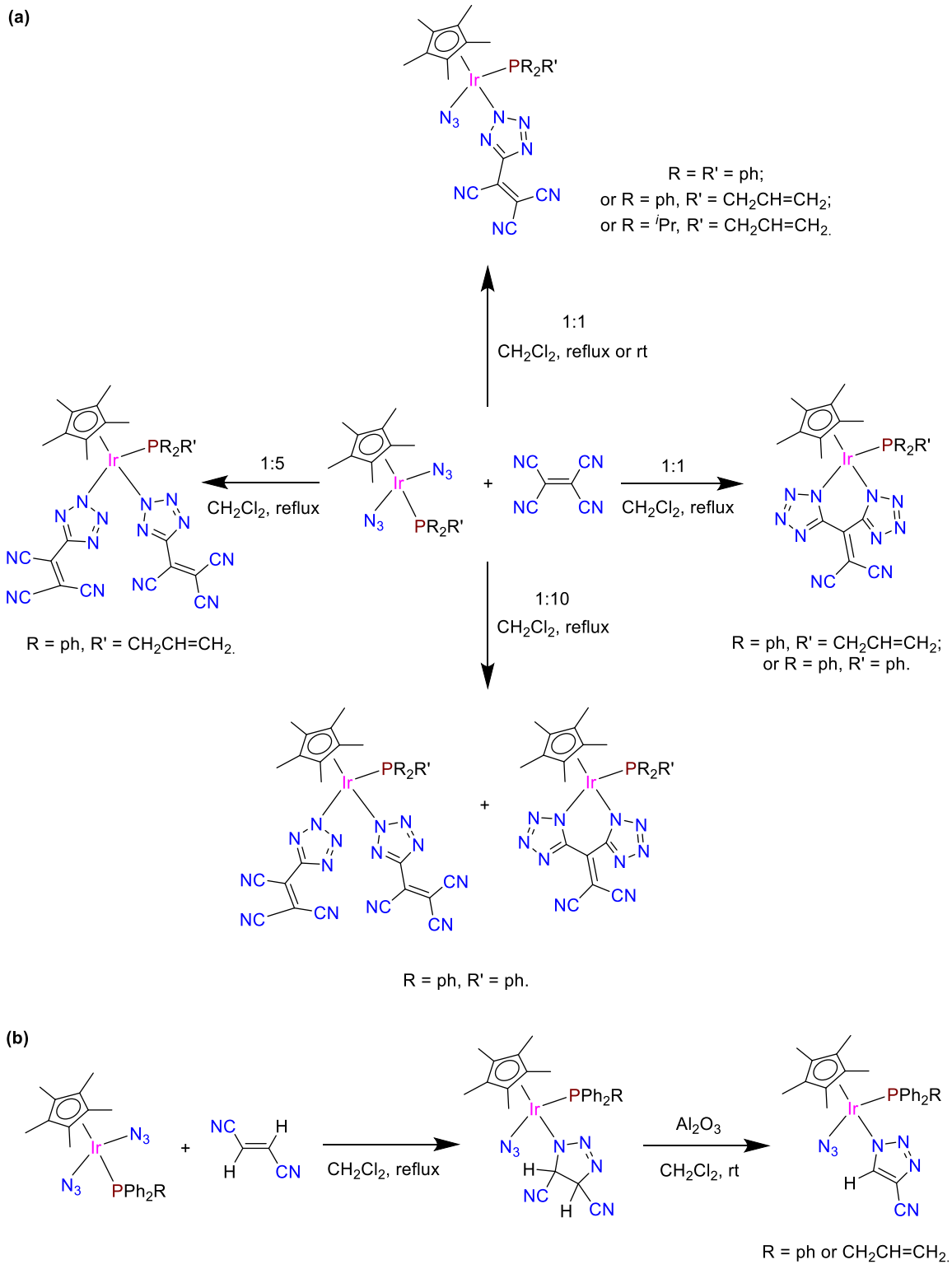

Scheme 1.18: iClick reactions of semisandwich iridium(III) diazido complexes with **(a)** tetracyanoethylene to give iridium(III) tetrazolato complexes at different conditions; **(b)** fumaronitrile through the C=C double bond to generate the corresponding triazolinato complexes which can further lose HCN upon treatment with aluminato give the aromatic triazolato complexes.

1.3.7 iClick reactions of group X metals

The first iClick reactions based on nickel(II) were reported by Nag and Paul, who tested mononuclear as well as binuclear 1,3-bridged nickel(II) azido complexes towards different dipolarophiles (**Figure 1.14**).[109] Furthermore, related nickel-coordinated tetrazolates were prepared from nitriles, triazolinates from alkenes, triazolates from alkynes, and tetrazolinethionates from phenylisothiocyanate. In all cycloaddition products obtained, either a mixture of N1 and N2 isomers or only the N2 isomer was obtained. With μ-azido complexes, either binuclear heterocycle-bridged compounds were generated, or mononuclear cycloaddition products formed. In addition, kinetic studies showed that the reactivity of the dipolarophiles increases with a stronger electron-withdrawing ability of the substituents. The reaction rate is also influenced by the electron-donating power of the terminal nitrogen atom of the parent compound.[109] Other nickel(II)-centered iClick reactions were studied together with the related iron and cobalt compounds by Mirica. A nickel(II) azido complex with the neutral Me_4cyclam ligand smoothly underwent the catalyst-free [3+2] cycloaddition with DMAD to generate the N2-bound triazolato product under very mild condition, but failed to react with less electron-deficient internal and terminal alkynes (**Scheme 1.13**).[101]

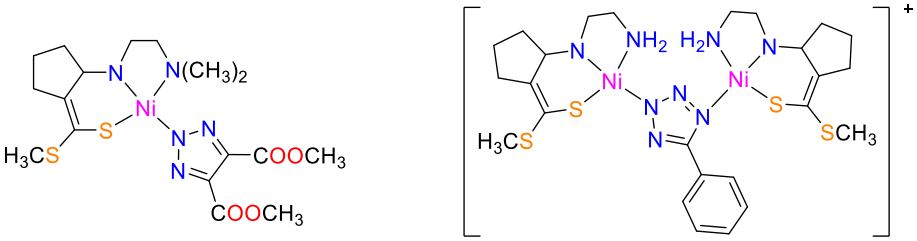

Figure 1.14: Selected examples of mononuclear cycloaddition product and binuclear heterocycle-bridged compound obtained by iClick reactions of nickel(II) azido compounds with different dipolarophiles.

Nag *et al.* also explored the iClick reactions of a series of palladium(II) azido complexes with methyl 2-((2-aminoethyl)amino)cyclopent-1-enedithiocarboxylate, methyl 2-((2-(dimethylamino)-ethyl)amino)cyclopent-1-enedithiocarboxylate, and methyl 2-((2-(diethylamino)ethyl)amino)-cyclopent-1-enedithiocarboxylate coligands, respectively (**Scheme 1.19**).[110] The resulting tetrazolates formed from nitriles were always obtained as a mixture of the N1- and N2-isomer. However, the amount of the N2 species increased with stronger electron-withdrawing substituents on the tetrazolates, while the triazolates and triazolinates obtained from alkynes and alkenes, respectively, turned out to be exclusively the N2 isomer. Kinetic studies with aromatic nitriles showed that the reaction rate strongly

depends on the Hammett parameter of the peripheral substituents, and increasing steric hindrances of the ligand decreases the rate constants of those iClick reactions.[110] Other iClick reactions based on palladium(II) are often compared to the isoelectronic platinum(II) complexes.[106-107, 111-112] For example, Busetto and Palazzi carried out iClick reactions of azido-bridged palladium(II) and platinum(II) complexes with carbon disulfide, trifluoroacetonitrile, and phenyl isothiocyanate to generate dinuclear complexes bridged by the resulting thiatriazolate or tetrazolate groups (**Scheme 1.20**).[112] In the Veige laboratory, two heterotrinuclear Pt^{II}/Au^{I}_2 complexes were synthesized by the iClick reactions of platinum(II) diazido complexes with gold(I) acetylides, indicating that the procedure is a facile way to connect multiple metal ions through triazolate bridges for building heterometallic structures (**Figure 1.15**).[113]

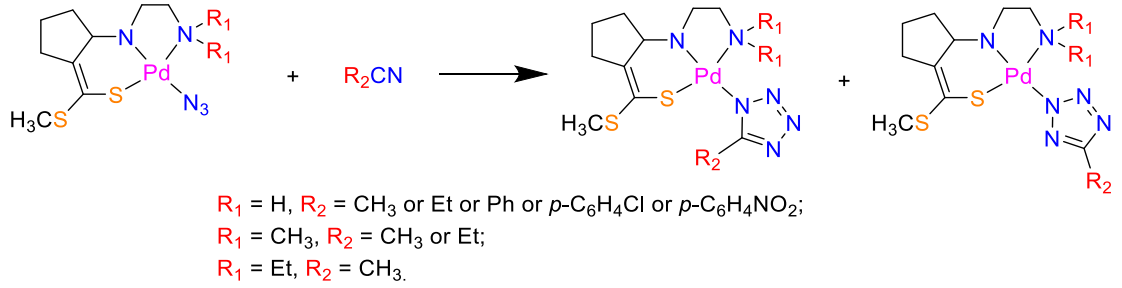

Scheme 1.19: iClick reactions of substituted palladium(II) azido compounds with different nitriles to give a mixture of N1 and N2 isomers.

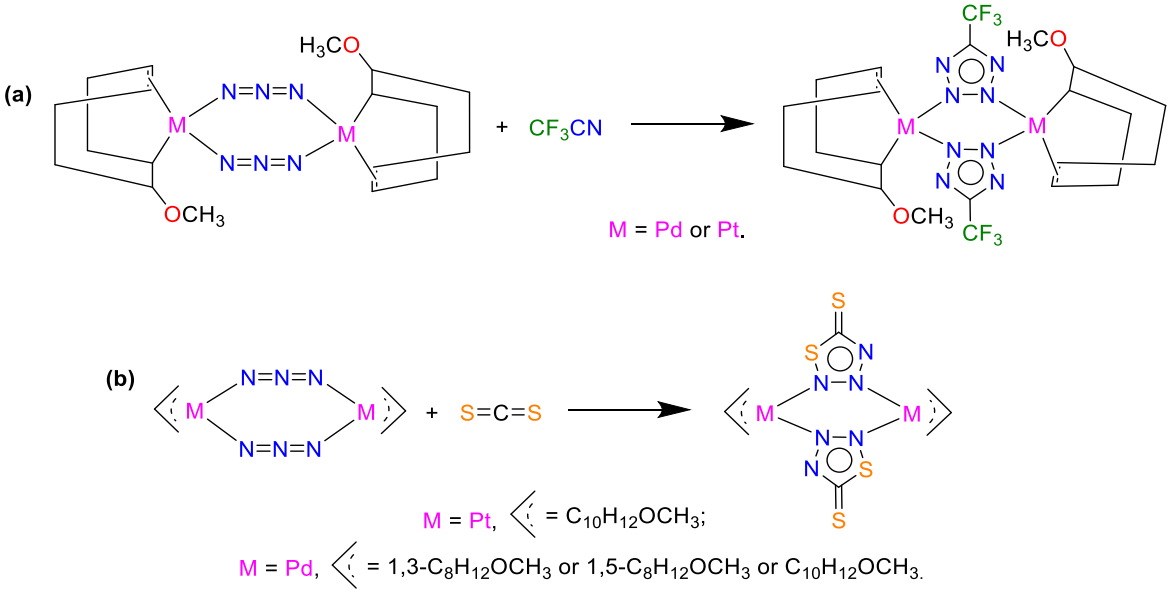

Scheme 1.20: Selected examples of iClick reactions of azido-bridged palladium(II) and platinum(II) compounds with **(a)** trifluoroacetonitrile to give tetrazolato complexes and **(b)** carbon disulfide to give thiotriazolato complexes.

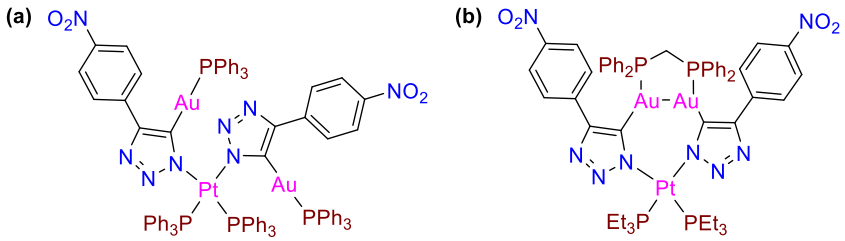

Figure 1.15: Structures of heterotrinuclear Pt^{II}/Au^{I}_2 complexes synthesized by the iClick reaction of **(a)** *cis*-$(PPh_3)_2Pt^{II}(N_3)_2$ with two equivalents of $PPh_3Au^{I}C{\equiv}CC_6H_4NO_2$ and **(b)** *cis*-$(PEt_3)_2Pt^{II}(N_3)_2$ with $[Au^{I}(C{\equiv}CC_6H_4NO_2)]_2(\mu$-dppm) (dppm = bis(diphenylphosphino)methane).

The first example of an iClick reaction involving an octahedral platinum(IV) complex was recently reported by Farrer and Sadler.[114] A platinum(IV) diazido complex with *trans,trans* pyridine and hydroxo ligands smoothly reacted with DMAD or DEAD under mild condition to form the corresponding mono- and bis-triazolato complexes. In an intramolecular process, one of the metal-coordinated hydroxo ligands then hydrolyses one of the ester groups, with the resulting free carboxylate group subsequently coordinating to the metal center (**Scheme 1.21**). The platinum(IV) diazido complex also reacted with some strained alkynes, but showed no reactivity towards less electron-deficient alkynes. Curiously, in this work, all triazolato ligands were found to be attached to the metal *via* the N1 nitrogen atom. The rate of the iClick reaction of the platinum(IV) species is slower than those reported for platinum(II) compounds, and the strained alkynes were converted significantly faster than the electron-poor ones.[114]

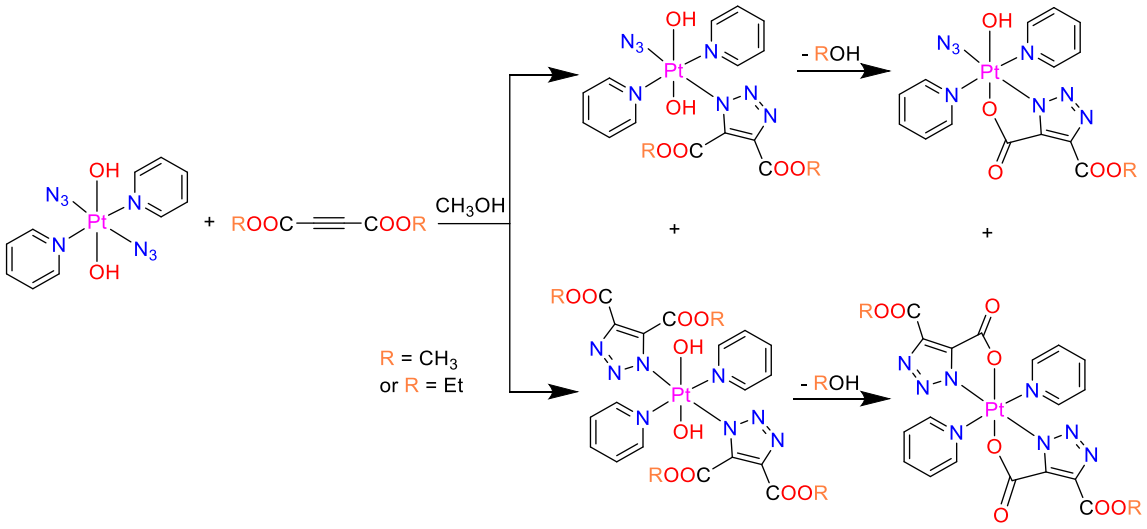

Scheme 1.21: iClick reaction of *trans,trans,trans*-$[Pt(N_3)_2(OH)_2(py)_2]$ with DMAD and DEAD leads to a mixture of mono- and bis-triazolato complexes. The coordinated hydroxo ligands also facilitate hydrolysis of the 4,5-ester substituents on the triazolate.

1.3.8 iClick reactions of group XI metals

In the early 1970s, Dori and coworkers explored some iClick reactions of group XI metals. For example, copper(I) and silver(I) tetrazolato complexes were obtained by the catalyst-free [3+2] cycloaddition of the corresponding azides with trifluoroacetonitrile (**Figure 1.16a**).[115-116] In the case of azidobis(triphenylphosphine) silver(I), an unexpected binuclear complex linked by the N2 and N3 atoms from two tetrazolate rings was obtained.[116] Very recently, the first example of a copper(I)-NHC azido compound was reported.[117] The reactivity of this compound was tested with a series of alkynes and nitriles. A conversion was only observed with activated alkynes and nitriles to generate the corresponding triazolate and tetrazolate complexes. It is worth noting that when reacted with the bulky 4-(triflurometyl)benzonitrile, a dimeric tetrazolato complex with two N2-N3 bridging tetrazoles was formed, while in the cases of DMAD and *p*-toluenesulfonyl cyanide, the catalyst-free cycloaddition reaction lead to the monomeric N1-bound triazolato and tetrazolato complexes (**Figure 1.16b**).[117] In contrast, iClick reactions of gold complexes are more common than those of copper and silver. In 1971, Beck *et al.* studied some cycloaddition reactions of gold(I) and gold(III) azido complexes with isonitriles and characterized the corresponding gold tetrazolates.[111] Their structures are quite peculiar, as all tetrazolato ligands are coordinated *via* the carbon instead of a nitrogen atom, which requires a shift of the metal moiety from the terminal N1-coordinated azide ligand to the tetrazolate carbon atom (**Figure 1.16c**).

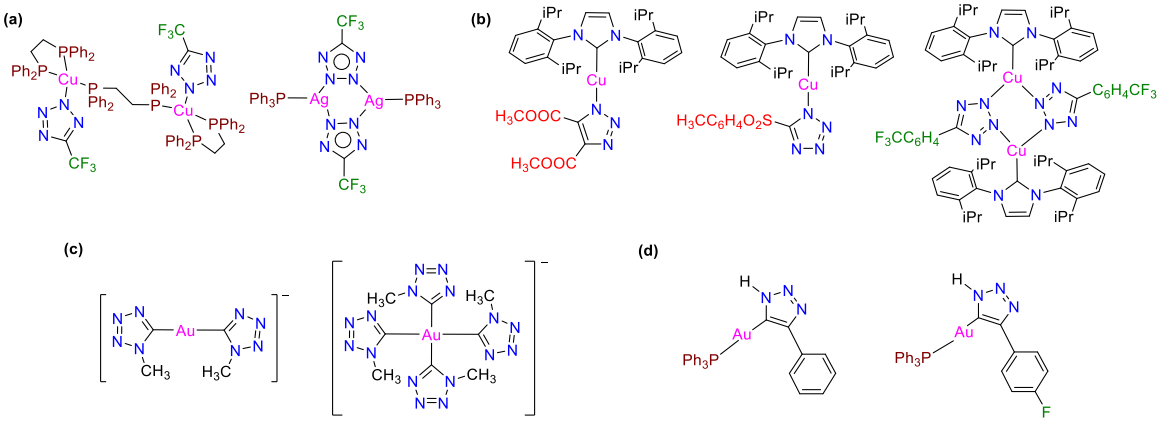

Figure 1.16: (a) Copper(I) tetrazolato complex and binuclear silver(I) compound linked by the tetrazolate N2 and N3 atoms obtained from the iClick reaction of $[Ag(N_3)(PPh_3)_2]$ and CF_3CN; **(b)** triazolato and tetrazolato complexes synthesized by iClick reactions of a copper(I)-NHC azido complex with DMAD and nitriles ; **(c)** selected examples of gold(I) iClick products in which the metal is coordinated *via* the carbon atom; **(d)** additional examples of gold(I) *C*-tetrazolato complexes obtained by iClick reactions.

In addition, Gray found that iClick reactions of phosphine and carbene gold(I) azido complexes with terminal alkynes unexpectedly gave gold(I) *C*-tetrazolato complexes as well (**Figure 1.16d**).[118-119] In the context of this work, Veige was the first to introduce the term "iClick" for the reaction of [Au(N_3)(PPh_3)] with [Au(C≡C-C_6H_5)(PPh_3)] to give a bimetallic triazolate-bridged product (**Scheme 1.22a**).[73] In addition, this iClick reaction mirrors the mechanism of the classic copper(I)-catalyzed azide-alkyne cycloaddition (CuAAC). A kinetic study gave a rate constant *k* of 7.6(5) × 10^{-3} M^{-1} s^{-1}.[120] Veige and coworkers also expanded the iClick reaction to rhodium and iridium, when they reacted [Au(C≡C-$C_6H_4NO_2$)(PPh_3)] with [M(N_3)(CO)(PPh_3)$_2$] with M = Rh, Ir to generate the corresponding Rh(I)/Au(I) and Ir(I)/Au(I) heterobimetallic triazolato complexes.[121] As already discussed above, the same group also synthesized heterotrimetallic Pt(II)/Au(I)/Au(I) triazolato complexes from platinum(II) diazido complexes and gold(I) acetylides,[113] and they have also worked on expanding the iClick reaction to access more complex gold(I) tetranuclear clusters and 1D oligomers involving aurophilic interactions (**Scheme 1.22**).[122]

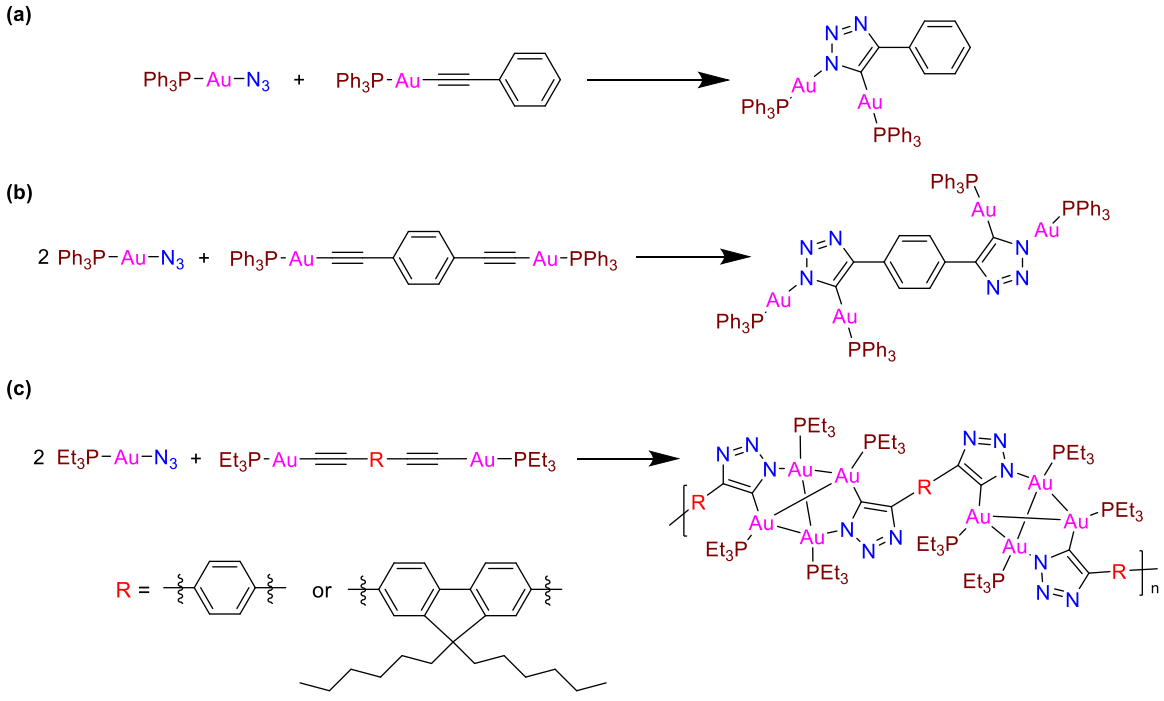

Scheme 1.22: (a) Prototypical "iClick" reaction as originally proposed by Veige;[73] **(b)** iClick reaction to synthesize a tetranuclear gold(I) complex; **(c)** iClick reactions for synthesis of gold(I)-based 1D oligomers.

1.3.9 iClick reactions of group XII metals

Only a single example of an iClick reaction involving a group XII metal was reported almost 50 years ago, when a bis(triphenylphosphine)mercury(II) diazido complex was reacted with acetonitrile at ambient temperature to give a mononuclear mercury(II) compound coordinated by two tetrazolato ligands (**Scheme 1.23**).[111]

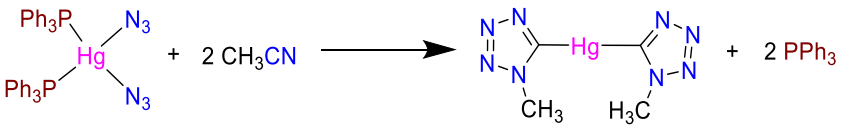

Scheme 1.23: The iClick reaction of diazidobis(triphenylphosphine)mercury(II) with two equivalents of acetonitrile leads to a linear mercury(II) complex *C*-coordinated by two tetrazolates.

1.3.10 General trends regarding the iClick reaction

To date, the catalyst-free iClick reaction of a metal-azido building block with a dipolarophile has been demonstrated for about 20 metallic elements from 10 different groups of the periodic (**Figure 1.17**). While the first iClick reactions were established for main group elements, most of them are now focused on electron-rich transition metals. Among those, elements from groups VIII to X feature particularly prominent, especially the 4d metals ruthenium, rhodium, and palladium.

	I	II	III	IV	V	VI	VII	VIII	IX	X	XI	XII	XIII	XIV	XV	XVI	XVII	XVIII
1	H																	He
2	Li	Be											B	C	N	O	F	Ne
3	Na	Mg											Al	**Si**	P	S	Cl	Ar
4	K	Ca	Sc	Ti	V	Cr	**Mn**	**Fe**	**Co**	**Ni**	**Cu**	Zn	Ga	**Ge**	As	Se	Br	Kr
5	Rb	Sr	Y	Zr	Nb	**Mo**	Tc	**Ru**	**Rh**	**Pd**	**Ag**	Cd	**In**	**Sn**	Sb	Te	I	Xe
6	Cs	Ba	†	Hf	**Ta**	**W**	**Re**	**Os**	**Ir**	**Pt**	**Au**	**Hg**	Tl	**Pb**	Bi	Po	At	Rn
7	Fr	Ra	‡	Rf	Db	Sg	Bh	Hs	Mt	Ds	Rg	Cn	113	Fl	115	Lv	117	118
	†	La	Ce	Pr	Nd	Pm	Sm	Eu	Gd	Tb	Dy	Ho	Er	Tm	Yb	Lu		
	‡	Ac	Th	Pa	U	Np	Pu	Am	Cm	Bk	Cf	Es	Fm	Md	No	Lr		

Figure 1.17: "iClick" periodic table: Elements with only one example of an iClick reaction reported to date are color-coded in green, those for which two to five iClick reactions known are highlighted in orange, and elements with more than five different iClick reactions published are marked in red.

So far, most of the triazolato and tetrazolato ligands resulting from the iClick reaction are coordinated to the metal center *via* the N2 nitrogen atom. Only in a few special cases, the N1 isomer or a mixture of the N1 and N2 isomers was isolated. Steric factors favour coordination *via* the central N2 nitrogen atom while electronic effects lead to preferential formation of the N1 isomer. Thus, the final structure of an iClick product is determined by a mix of electronic and steric influences. Furthermore, in some cases, a 1,2-shift of the metal-coligand fragment is observed and the final product features the metal C-coordinated to the triazolate, a binding mode that is particularly prevalent in gold triazolates. Kinetic studies of the iClick reaction have demonstrated that 4d metal azido compounds are generally more reactive than their 5d analogues. Furthermore, the reactivity of the dipolarophile increases with stronger electron-withdrawing substituents. In addition, steric hindrance and strongly electron-withdrawing coligands decrease the rate constants of the iClick reaction.

2 Motivation

Cancer is a leading cause of death around the world. The discovery of the antitumoral activity of cisplatin by Rosenberg in the 1960s has greatly revolutionized cancer chemotherapy. Since then, novel transition metal-based antitumor drugs have received enormous attention. While some metal-based drugs are successfully used on a variety of cancers, the clinical effectiveness is often hampered by poor solubility, low bioavailability, and lack of target specificity. Therefore, synthetic methods which can quickly generate high molecular diversity and have great reaction efficiency are required to optimize metal compounds for specific biological applications.

Inspired by the success of “Click reactions” such as the copper-catalyzed azide-alkyne cycloaddition (CuAAC), the concept was also extended to “inorganic click reactions”, for which the acronym “iClick” has been coined. These are emerging as a powerful tool to quickly synthesize transition metal complexes of great structural variability under very mild conditions and with only minimal work-up. Current iClick reactions usually involve a metal-azido building block and an electron-deficient alkyne directly in the inner coordination sphere of a metal centre, although also an "inverse" iClick reaction can be envisioned, in which a metal acetylide complex reacts with an organoazide compound. Importantly, also the reaction kinetics can be tuned by proper choice of the metal and its oxidation state as well as the steric and electronic properties of the coligands.

In this context, the aim of the present thesis was to apply the iClick reaction for a modular access to a diverse set of bio-relevant transition metal complexes and to determine trends in the reactivity and structure of the resulting triazolate products. As most current examples of iClick reactions were focused on octahedral mid-transition metals such as ruthenium and iron, this work was directed at square-planar palladium(II) and platinum(II) complexes with a range of tridentate coligands, to systematically compare the reactivity of 4d *vs*. 5d metals and the role of different chelating coligands such as 2,2’:6’,2”-terpyridine (terpy), 6’-phenyl-2,2’-bipyridine (phbpy), and *N*-phenyl-2-[1-(2-pyridinyl)ethylidene]hydrazine carbothioamide (pht). Selected metal triazolate products were also to be evaluated for their *in vitro* anticancer activity.

3 Results and discussion

3.1 iClick reactions of Pd(II) and Pt(II) terpy azido complexes

Platinum(II) and palladium(II) terpyridine complexes are well-known for their promising antitumor activity.[123-124] Initial studies of $[PtCl(terpy)]^+$ binding to calf-thymus DNA (CT-DNA) demonstrated a covalent interaction with the nucleobases, as well as indications of intercalative binding.[125] Thus, in order to prevent coordination to the nucleobases, several derivatives of $[PtCl(terpy)]^+$ with other donor ligands more tightly bound in the fourth coordination site of the square-planar metal centre were synthesized to replace the relatively labile chloride found in the original compound.[126-127] In this chapter, a series of palladium(II) and platinum(II) terpy triazolato complexes was to be synthesized in a modular fashion by the iClick reactions and their DNA binding ability studied.

3.1.1 Synthesis of 2,2':6',2"-terpyridine

2,2':6',2"-Terpyridine (terpy) was synthesized according to a published procedure (**Scheme 3.1**).[128] Briefly, the precursor *ß*-(dimethylamino)vinyl-2-pyridyl ketone **3** was prepared from 2-acetylpyridine and *N*,*N*-dimethylformamide dimethyl acetal and then further reacted with a mixture of potassium *tert*-butoxide and 2-acetylpyridine. The crude product was obtained as a dark brown oil, which was purified by column chromatography on alumina with a mixture of cyclohexane and ethyl acetate (20:1 *v/v*) as the eluent. The first light yellow fraction was collected and the final product obtained as a white powder in moderate yield after removal of the solvent.

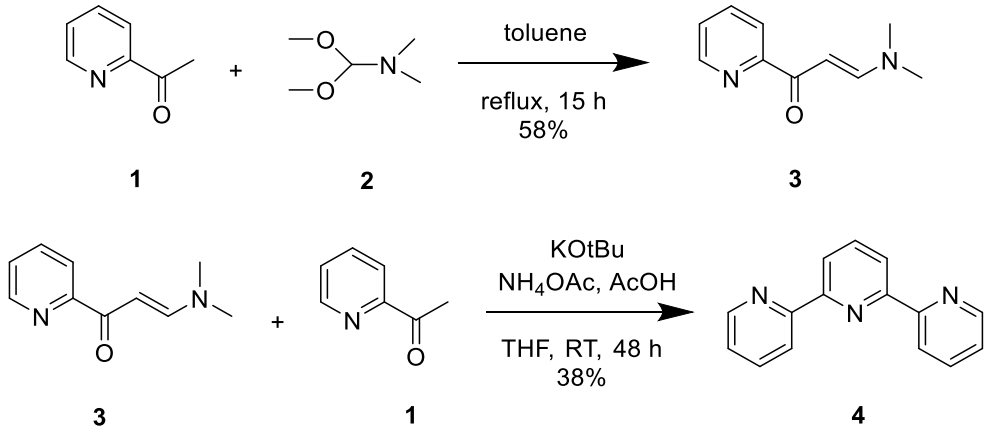

Scheme 3.1: Reaction of 2-acetylpyridine (**1**) and *N*,*N*-dimethylformamide dimethyl acetal (**2**) give *ß*-(dimethylamino)vinyl-2-pyridyl ketone (**3**) as an intermediate, which is further reacted with another equivalent of 2-acetylpyridine to give 2,2':6',2"-terpyridine (**4**).

The ^{1}H NMR spectrum of terpy **4** shows five signals with a total integral of 11H (**Figure 3.1**). The multiplet at 8.69 − 8.72 ppm results from the overlap of the H6/H6” and H3/H3” signals.[128] The triplet at 8.08 ppm is attributed to the centre pyridine proton H4’ based on a coupling constant $^{3}J_{H4',H3'/H5'}$ = 7.7 Hz and an integral of 1H. The doublet-of-a-triplet at 7.98 ppm is assigned to H4/H4”, as suggested by two distinct coupling constants of $^{3}J_{H4/H4",H5/H5"}$ = 7.7 Hz and $^{4}J_{H4/H4",H6/H6"}$ = 2.1 Hz. Finally, a doublet-of-a-doublet-of-a-doublet at 7.45 ppm is due to H5/H5”, based on $^{3}J_{H5/H5",H4/H4"}$ = 7.5 Hz, $^{3}J_{H5/H5",H6/H6"}$ = 4.6 Hz, and $^{4}J_{H5/H5",H3/H3"}$ = 1.4 Hz.

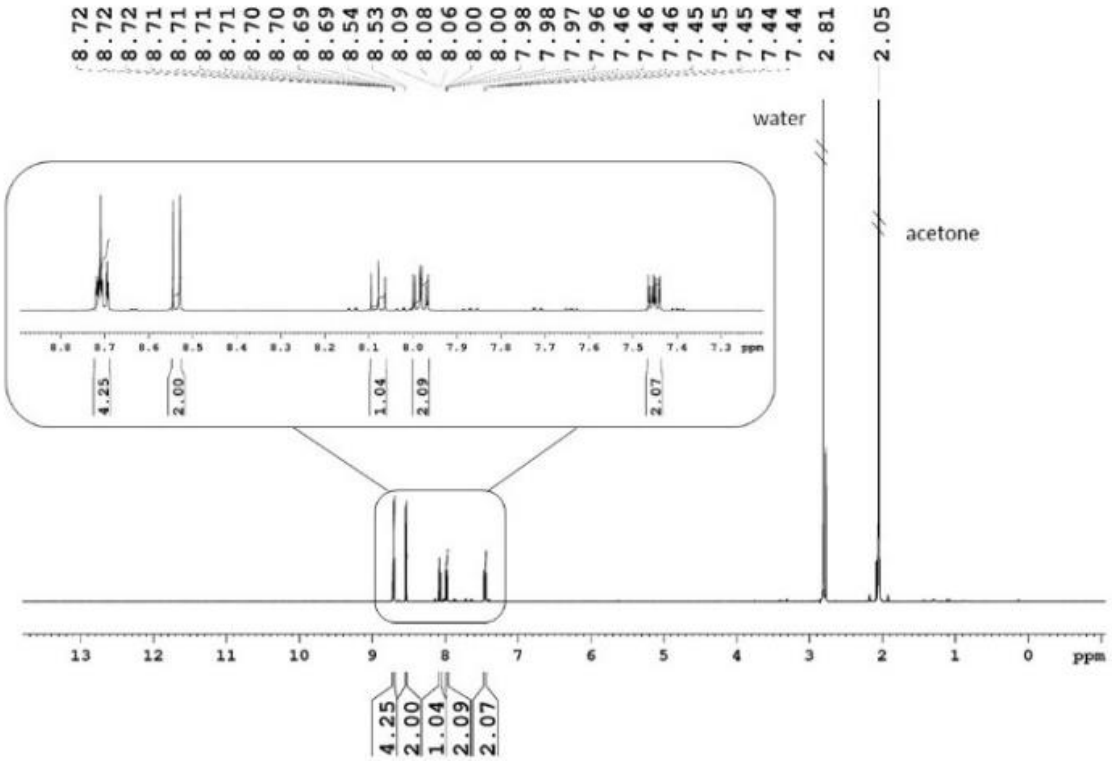

Figure 3.1: ^{1}H NMR spectrum of 2,2’:6’,2”-terpyridine **4** (500.13 MHz, acetone-d_6).

Due to the symmetry of **4**, the ^{13}C NMR spectrum shows only eight signals for 15 carbon atoms in the aromatic region at 121.66, 121.71, 125.02, 137.95, 138.96, 150.25, 156.40 and 156.85 ppm, respectively (**Figure 3.2**). Based on its relatively low intensity, the peak at 138.96 ppm is assigned to the central C4’ atom. The two closely positioned peaks at 121.66 and 121.71 ppm are assigned to C3’/C5’ and C3/C3”. Similarly, the signals at 125.02, 137.95, 150.25 ppm correspond to C5/C5”, C4/C4” and C6/C6”, respectively. At 156.40 and 156.85 ppm, the two signals for C2/C2” and C2’/C6’ are strongly shifted downfield due to the neighbouring nitrogen atoms.

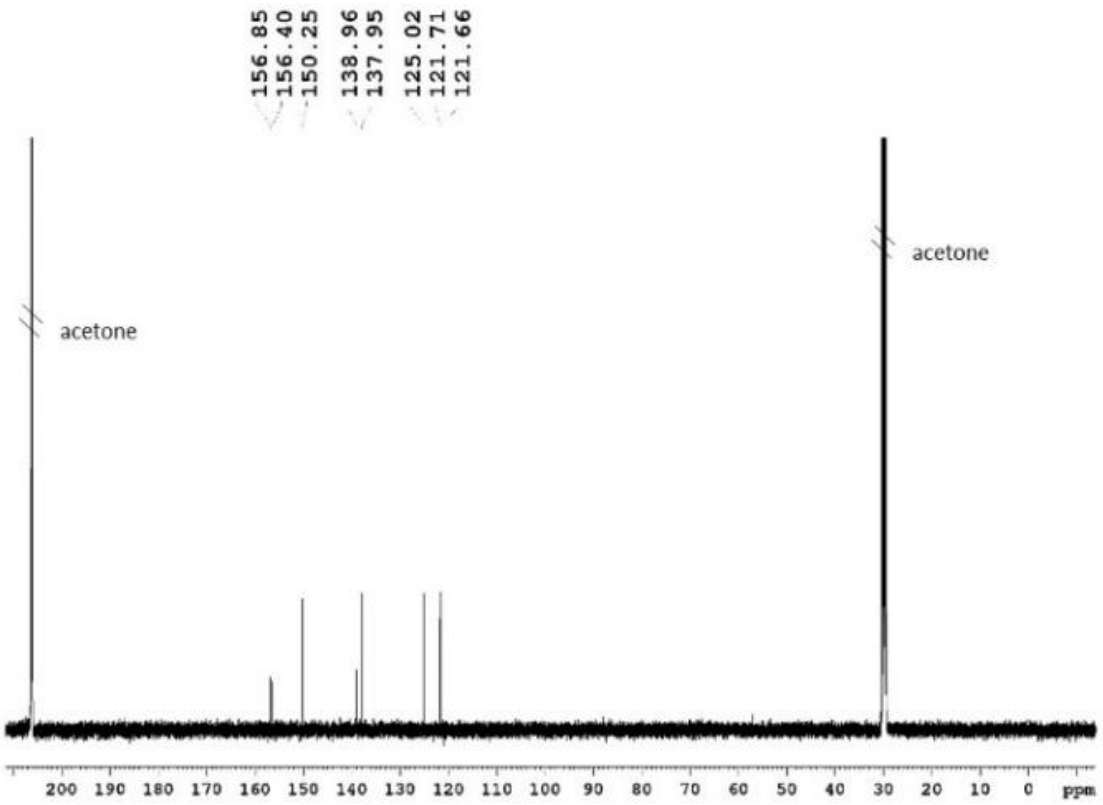

Figure 3.2: ^{13}C NMR spectrum of 2,2':6',2"-terpyridine **4** (125.76 MHz, acetone-d_6).

3.1.2 Synthesis of Pd(II) and Pt(II) terpy azido complexes

Palladium(II) and platinum(II) azido complexes are the key precursors for the iClick reaction and were prepared in three steps from the metal salts *via* their 1,5-cyclooctadiene complexes (**Scheme 3.2**). In the first step, palladium(II) chloride **5** was reacted with 1,5-cyclooctadiene (COD) **7** in methanol at room temperature for 2 d to give 1,5-cyclooctadiene palladium(II) dichloride **8** as a yellow powder.

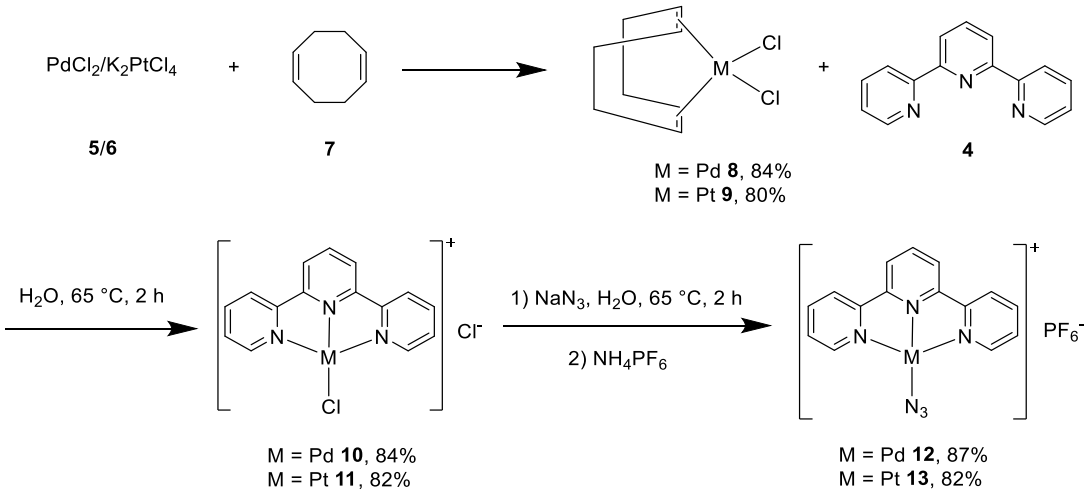

Scheme 3.2: Synthesis of $[M(N_3)(terpy)]PF_6$ with M = Pd **12** or Pt **13**.

This was further reacted in water with terpy **4** for 2 h to generate [PdCl(terpy)]Cl **10**, which was obtained as a yellow solid after removal of the solvent. In the last step, the chlorido complex **10** was dissolved in hot water and reacted with an excess of sodium azide for 2 h, followed by the addition of aqueous ammonium hexafluorophosphate solution. This lead to immediate precipitation of $[Pd(N_3)(terpy)]PF_6$ **12** as a pale yellow solid in very good yield. The orange platinum(II) anologue **13** was synthesized by three similar steps in equally good yield. However, the synthesis started from potassium tetrachloroplatinate(II) **6** and an ethanol/water mixture was used as the solvent instead of methanol.

The vibrational spectra of **12** and **13** are generally very similar. In the IR spectrum of **12**, a very strong peak at 2028 cm^{-1} is characteristic of the coordinated azido group (**Figure 3.3**). The medium intensity band at around 3095 cm^{-1} is due to the aromatic C-H stretches of the pyridine rings, whereas the peaks between 1400 and 1600 cm^{-1} are attributed to aromatic C=C and C=N stretches. The strong signals in the range of 700 to 850 cm^{-1} are assigned to aromatic C-H bending modes.

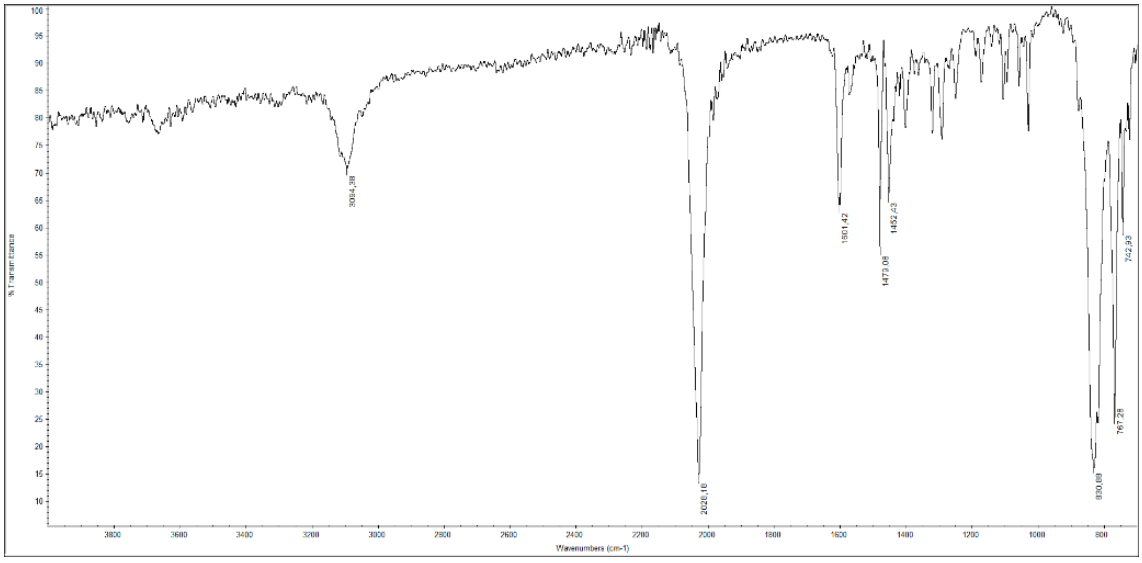

Figure 3.3: ATR IR spectrum of $[Pd(N_3)(terpy)]PF_6$ **12**.

Due to solubility issue in other solvents, NMR spectra of **12** were recorded in DMSO-d_6. Therefore, the chemical shifts cannot be directly compared to those of its chlorido precursor complex and the free terpy ligand. The ^{1}H NMR spectrum of **12** features five signals in the aromatic region with an overall integral of 11H (**Figure 3.4**). A doublet as the signal most strongly shifted downfield at 8.66 ppm with an integral of 2H corresponds to H3'/H5' due to the relatively large coupling constant $^3J_{H3'/H5',H4'}$ = 7.4 Hz. A multiplet with an integral of 3H (H6/H6" and H4') is present at 8.63 − 8.56 ppm, followed by a doublet-of-a-triplet at 8.49 ppm, which is assigned to H4/H4" based on $^3J_{H4/H4",H5/H5"}$ = 7.9 Hz and $^4J_{H4/H4",H6/H6"}$ =

1.6 Hz. A doublet-of-a-doublet-of-a-doublet at 8.39 ppm is due to H3/H3”, as suggested by coupling constants $^{3}J_{H3/H3”,H4/H4”}$ = 5.5 Hz, $^{4}J_{H3/H3”,H5/H5”}$ = 1.4 Hz, and $^{5}J_{H3/H3”,H6/H6”}$ = 0.6 Hz. Finally, the signal of H5/H5” shows up as a doublet-of-a-doublet-of-a-doublet at 7.97 ppm, featuring the coupling constants $^{3}J_{H5/H5”,H4/H4”}$ = 7.7 Hz, $^{3}J_{H5/H5”,H6/H6”}$ = 5.6 Hz, and $^{4}J_{H5/H5”,H3/H3”}$ = 1.4 Hz.

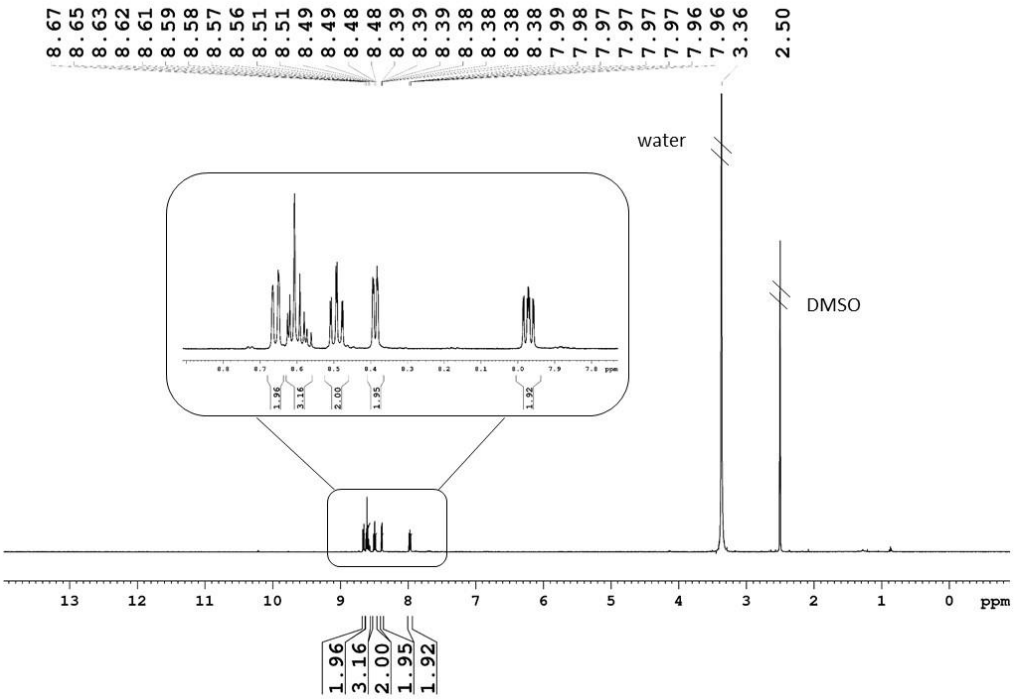

Figure 3.4: ^{1}H NMR spectrum of [Pd(N_3)(terpy)]PF_6 **12** (500.13 MHz, DMSO-d_6).

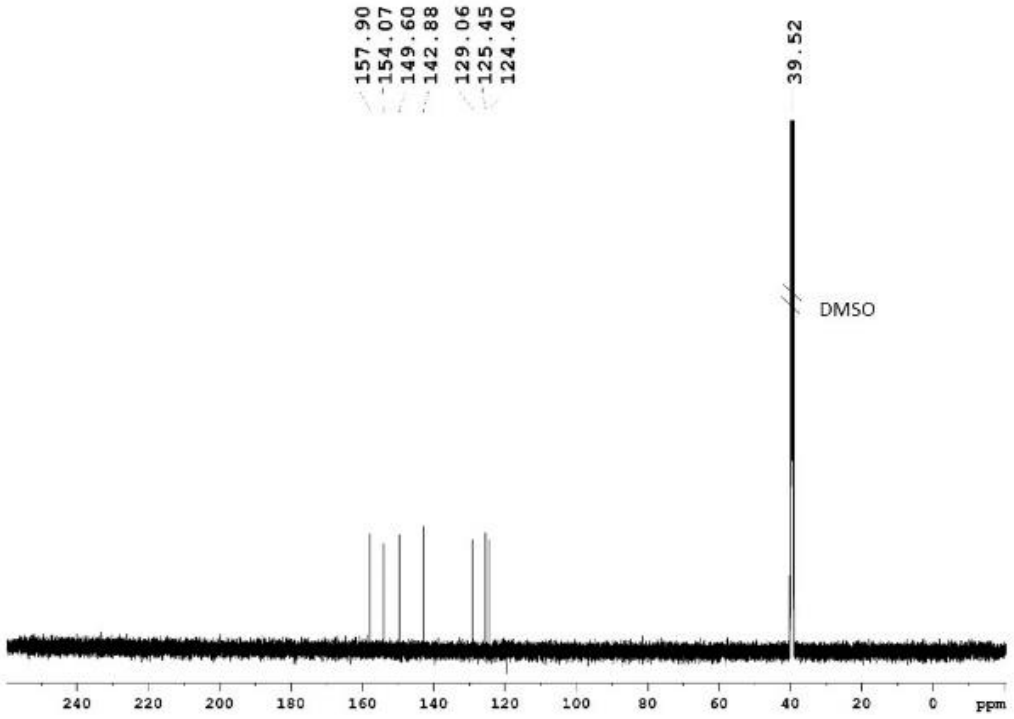

Figure 3.5: ^{13}C NMR spectrum of [Pd(N_3)(terpy)]PF_6 **12** (125.76 MHz, DMSO-d_6).

Seven signals are observed in the ^{13}C NMR spectrum of **12** (**Figure 3.5**). The signal most shifted upfield at 124.40 ppm is assigned to the two symmetry-equivalent carbon atoms C3/C3", followed by a neighbouring signal at 125.45 ppm resulting from C3'/C5'. The signal at 129.06 ppm is assigned to C5/C5". The signal at 142.88 ppm has a relative high intensity due to the overlap of two signals from C4/C4" and C4'. The remaining peaks at 149.60, 154.07, and 157.90 ppm correspond to C6/C6", C2/C2", and C2'/C6', respectively. The ^{1}H NMR spectrum of [Pt(N_3)(terpy)]PF_6 **13** is generally very similar to that of the palladium(II) analogue **12**. Only four peaks are observed in the region of 8.60 to 7.90 ppm due to overlap of the signals for H3'/H5', H6/H6" and H4'. The other peaks are only marginally shifted relative to those of **12**, with less than 0.1 ppm difference in chemical shift. Compared to the ^{13}C NMR spectrum of **12**, one additional signal is observed for **13**. This extra signal is located at 142.08 ppm and is due to the central C4', while in the palladium(II) case this signal overlaps with that of C4/C4". The remaining signals exhibit chemical shifts very similar to those of the palladium analogue, with a maximum difference of 0.5 ppm at most. In addition, the ^{195}Pt NMR spectrum of **13** was recorded in DMSO-d_6 (**Figure 3.6**). A single peak was observed at –2659 ppm. While the signal of the chlorido precursor **11** is located at –2704 ppm. However, this spectrum was recorded in D_2O due to the poor solubility of **11** in DMSO-d_6. Therefore, the moderate difference in chemical shift might be due to solvent effects.

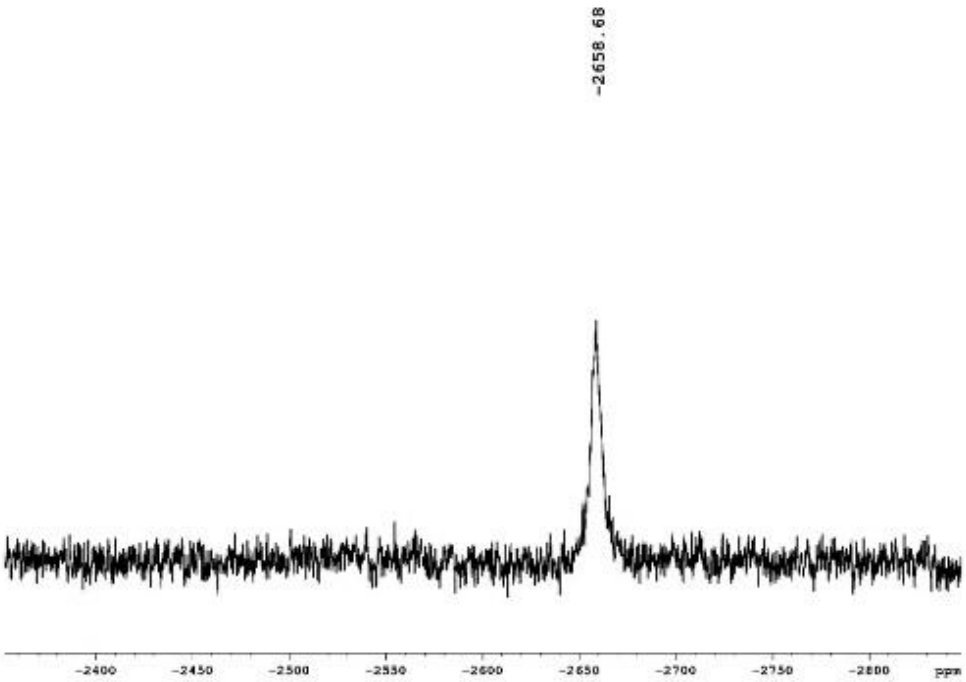

Figure 3.6: ^{195}Pt NMR spectrum of [Pt(N_3)(terpy)]PF_6 **13** (86.09 MHz, DMSO-d_6).

3.1.3 Triazolate coordination isomers formed in the iClick reaction

Normally, three different structural isomers can form in the iClick reaction, as the triazolate ligand can coordinate to the metal centre *via* its N1, N2, or N3 nitrogen atoms (**Figure 3.7A**). However, in the special case of identical C4- and C5-substituents, only two isomers are possible, the non-symmetrical N1 and the symmetrical N2 isomer (**Figure 3.7B**). Molecular orbital calculations demonstrated that these three structures are essentially isoenergetic.[129-131] In most systems studied in our group so far, the triazolato ligand was found to "symmetrically" coordinate *via* the N2 nitrogen atom.[83, 86, 105] As the azido group is always N1-coordinated to the metal centre, the initial formation of a N1-bound triazolate has to be followed by a 1,2-shift to the final N2-coordinated triazolate product. It is generally assumed that the N1 isomer is the kinetic product of the iClick reaction, but the formation of the N2-bound triazolate is driven by steric factors, although the N1 nitrogen atom is more nucleophilic than N2.[132-134]

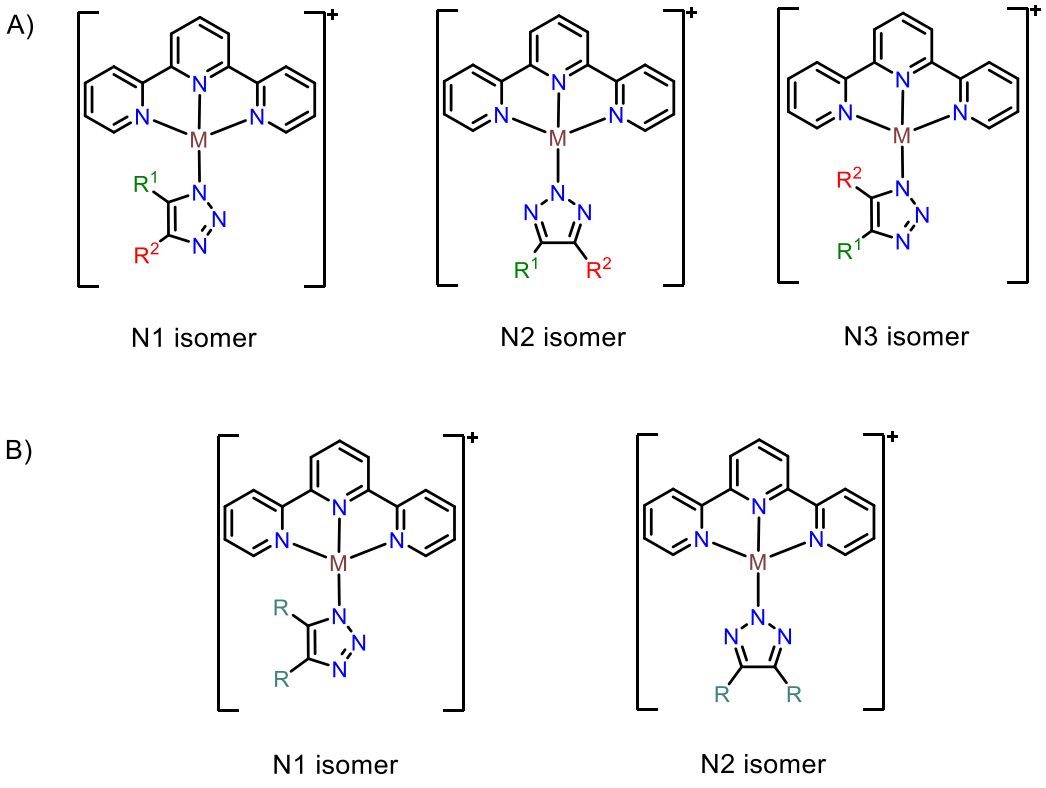

Figure 3.7: A) Structures of the three coordination isomers which can result from the iClick reaction if R^1 and R^2 are not identical; **B)** in the case of $R^1 = R^2$ only two isomeric products can form.

3.1.4 Synthesis of Pd(II) and Pt(II) terpy triazolato complexes

Four electron-deficient alkynes, namely dimethylacetylene dicarboxylate (DMAD, **14**), diethyl acetylenedicarboxylate (DEAD, **15**), 2-butynedioic acid 1,4-bis(2-methoxyethyl) ester **16**, and 4,4,4-trifluoro-2-butynoic acid ethyl ester **17** were used in the iClick reaction with $[M(N_3)(terpy)]PF_6$ (M = Pd **12**, or Pt **13**), respectively, which lead to eight triazolato complexes **18**–**25**. In general, the metal azido compound **12** or **13** and an excess of alkyne were dissolved in acetone and the reaction mixture then stirred at room temperature or heated to reflux, if required, with reaction times in the range of 4 h to 7 d (**Scheme 3.3**). The product usually precipitated upon cooling and was collected by filtration (or, in the case of **17**, obtained after removal of the solvent), washed with diethyl ether to remove unreacted alkyne, and dried under vacuum to obtain the final products in very good yield (60 − 91%).

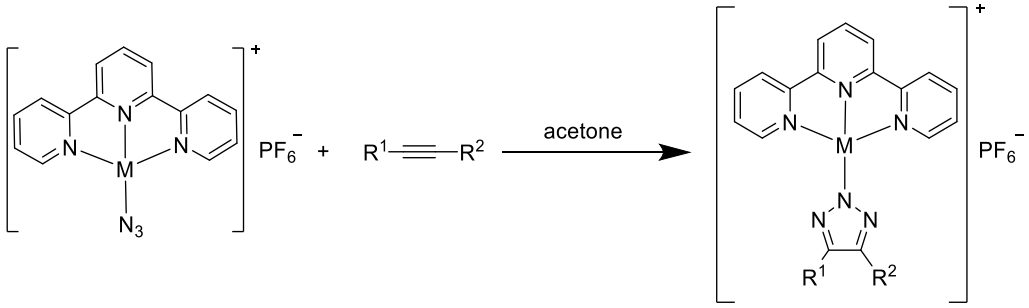

M = Pd, **12**
M = Pt, **13**

$R^1 = R^2 = COOCH_3$, **14**
$R^1 = R^2 = COOEt$, **15**
$R^1 = R^2 = COOCH_2CH_2OCH_3$, **16**
$R^1 = CF_3$, $R^2 = COOEt$, **17**

M = Pd, $R^1 = R^2 = COOCH_3$, **18** 64%
M = Pt, $R^1 = R^2 = COOCH_3$, **19** 73%
M = Pd, $R^1 = R^2 = COOEt$, **20** 60%
M = Pt, $R^1 = R^2 = COOEt$, **21** 91%
M = Pd, $R^1 = R^2 = COOCH_2CH_2OCH_3$, **22** 80%
M = Pt, $R^1 = R^2 = COOCH_2CH_2OCH_3$, **23** 80%
M = Pd, $R^1 = CF_3$, $R^2 = COOEt$, **24** 90%
M = Pt, $R^1 = CF_3$, $R^2 = COOEt$, **25** 80%

Scheme 3.3: Synthesis of palladium(II) and platinum(II) triazolate complexes $[M(triazolate^{R1,R2})(terpy)]PF_6$ **18**–**25** by iClick reaction of $[M(N_3)(terpy)]PF_6$ **12** (M = Pd) or **13** (M = Pt) and electron-poor alkynes **14**–**17**.

The IR spectra of the triazolato iClick products consistently lack the distinct band for coordinated azido group at around 2030 cm^{-1} as observed in their azido starting materials **12** and **13**. Instead, these spectra all feature a prominent signal at around 1740 cm^{-1}, which is due to the ester C=O stretching mode and provides a first hint on the success of the iClick reaction. The resulting triazolato complexes **18**–**25** were then further characterized by ^1H and ^{13}C NMR spectroscopy and, where appropriate, also by ^{19}F and ^{195}Pt NMR spectroscopy. In the aromatic region, the ^1H NMR spectra of these iClick products show signal patterns similar to the corresponding azido precursors, as these peaks are due to the invariant terpy

ligand backbone. The most distinctive difference is the position of the doublet-of-a-doublet-of-a-doublet corresponding to H5 and H5", which experiences a 0.07 − 0.21 ppm upfield shift relative to the starting material. In the aliphatic region, a varible number of new signals show up, depending on the alkyne reaction partner. In the case of triazolate complexes **18** and **19**, resulting from the reaction with DMAD **14**, a new singlet at approx. 3.90 ppm with an integral of 6H is due to the two chemically equivalent methyl ester groups in the 4- and 5-position of the triazolate, which indicates a symmetric coordination of the ligand. The ^{1}H NMR spectra of triazolates **20** and **21** show two new signals, a quartet at 4.34 ppm with an integral of 4H and a triplet at 1.35 ppm with an integral of 6H, which are due to protons from the chemically equivalent methylene and methyl groups of the ethyl ester moiety, respectively. In the case of **24** and **25**, such two signals are also observed at similar positions, corresponding to five ethyl ester protons from the triazolate C5-substituent. In the ^{1}H NMR spectra of the ethylene glycol-substituted triazolato complexes **22** and **23**, three new signals are found, two triplets at approx 4.40 and 3.70 ppm and a singlet at approx. 3.30 ppm, which are in accordance with symmetry-equivalent substituents in the 4- and 5-positions of the triazolate. Upon very close inspection, a number of additional minor signals are observed in the ^{1}H NMR spectra of [Pd(triazolate^{R1,R2})(terpy)]PF_6. These signals are assumed to be due to a minor N1 species, with the two isomers present in a ratio of approximately 8:1 ($R^1 = R^2 = COOCH_3$, **18**), 5:1 ($R^1 = R^2 =$ COOEt, **20**), 10:1 ($R^1 = R^2 = COOCH_2CH_2OCH_3$, **22**), and 8:1 ($R^1 = CF_3$, $R^2 =$ COOEt, **24**). Compared to these palladium(II) triazolato complexes, the N1 isomer is far less abundant in [Pt(triazolate^{R1,R2})(terpy)]PF_6, where it appears at a ratio of approximately 25:1 ($R^1 = R^2 = COOCH_3$, **19**) and 11:1 ($R^1 = R^2 =$ COOEt, **21**) relative to the major N2 species. In the case of **23** and **25**, no signal of the N1 isomer were observed.

The ^{13}C NMR spectra of these triazolato iClick products are also mostly identical to those of the azido starting materials **12** and **13**, although several additional signals are observed which are due to the triazolate ring and its substituents. The triazolate C4 and C5 carbon atoms give rise to only one single ^{13}C NMR peak at approx. 140 ppm for triazolates **18 − 23**, which further confirms the dominant formation of the symmetrical N2 isomer. In contrast, in the ^{13}C NMR spectra of the inherently non-symmetrically substituted complexes **24** and **25**, two signals at approx. 139 and 138 ppm are observed for the triazolate C4 and C5 carbons, respectively. Furthermore, the high-field signal is split into a quartet due to a $^{2}J_{C,F}$ coupling of 38 Hz with the three fluorine atoms of the CF_3 substituent. Similarly, another quartet is observed at approx. 122 ppm, resulting from the trifluoromethyl carbon atom,

which features a $^{1}J_{C,F}$ coupling of 269 Hz. In addition, for all triazolato complexes, a single peak at approx. 160 ppm is due to the ester C=O group(s) of the coordinated triazolato ligand. The other additional ^{13}C NMR signals in the aliphatic region are the resonances of the triazolato ester groups.

Apart from a doublet at approx. −71 ppm easily assigned to the hexafluorophosphate counter ion, complexes **24** and **25**, which feature a trifluoromethyl-substituted triazolate ligand, display an additional peak in the ^{19}F NMR spectrum at approx. −60 ppm for the CF_3 triazolate substituent, giving an approx. 8 ppm upfield shift relative to the alkyne starting material. In the ^{19}F NMR spectrum of **24**, an additional minor signal close to the major peak is also observed. This was present from the start of the reaction and gradually went down in intensity while the major signal grew in. Therefore, this minor peak is assumed to be due to the N1-coordinated triazolate. The ratio of the N2 and N1 isomers is approx. 11:1, roughly in line with the value determined from the corresponding ^{1}H NMR spectra. The ^{195}Pt NMR spectra of the platinum(II) triazolato complexes show a single peak in a small range of −2664 to −2690 ppm. As the signal of precursor $[PtN_3(terpy)]PF_6$ **13** is found at −2659 ppm, only a minor chemical shift difference of 5–31 ppm to the higher field is observed upon the iClick reaction.

3.1.5 Intermediate species in the iClick reaction

Since the trifluoromethyl group of 4,4,4-trifluoro-2-butynoic acid ethyl ester **17** is a sensitive ^{19}F NMR marker, the progress of the iClick reaction of [Pt(N_3)(terpy)]PF_6 **13** with **17** was followed by ^{19}F NMR spectroscopy. However, this method was restricted to the platinum compound **13**, as the iClick reaction of [Pd(N_3)(terpy)]PF_6 **12** and alkyne **17** was too fast to be monitored by standard NMR spectroscopy.

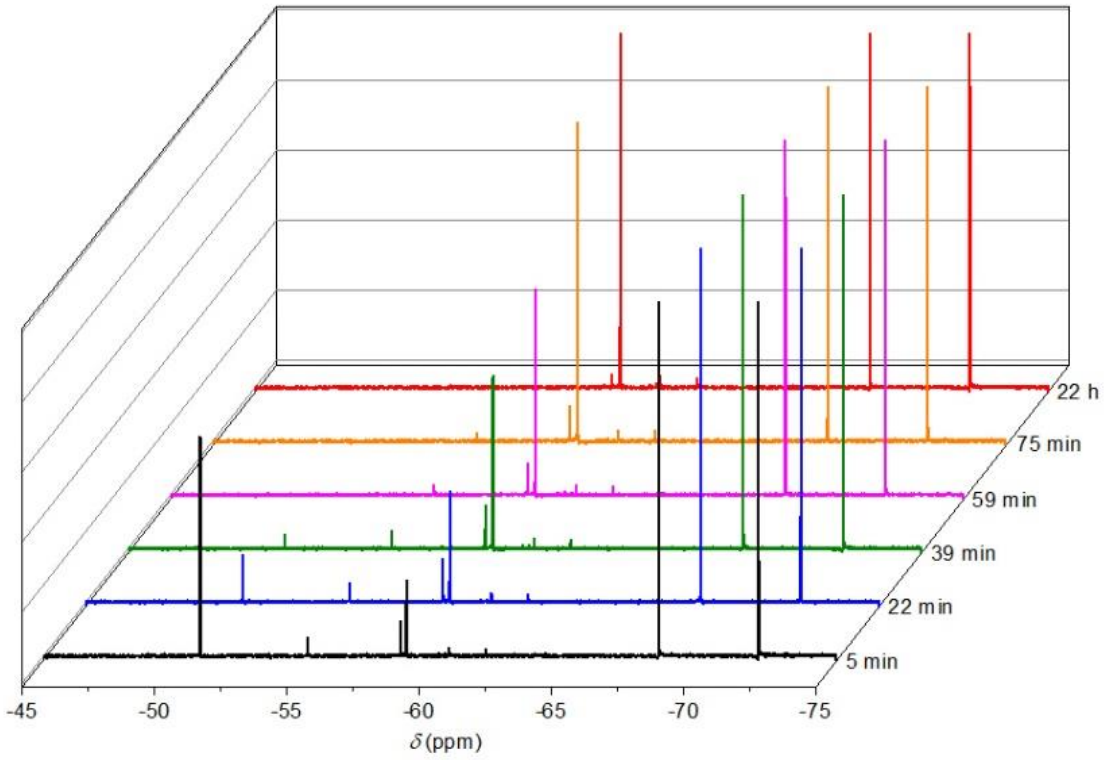

Figure 3.8: Changes in the ^{19}F NMR spectrum of a mixture of [Pt(N_3)(terpy)]PF_6 **13** and 4,4,4-trifluoro-2-butynoic acid ethyl ester **17** in DMSO-d_6 at room temperature followed over the course of 22 h (front to back). Major species observed are starting alkyne **17** at −52.77 ppm and N2 triazolate at −60.42 ppm. The doublet at −72.29 ppm is due to the hexafluorophosphate counter ion and minor signals at −55.00 and −60.29 ppm are assumed to be a linear intermediate and N1 isomer, respectively.

In a typical experiment, platinum(II) azido complex **13** was mixed with one equivalent of alkyne **17**. Five main signals were observed in the ^{19}F NMR spectrum at the early stages of the reaction (**Figure 3.8**, black trace). The singlet at −52.77 ppm is attributed to alkyne starting material **17**, while the peak at −55.00 ppm is assumed to be a yet unidentified intermediate, as it only appears at the beginning of the reaction and then gradually disappears later on. The signal at −60.29 ppm is thought to be the N1 isomer, while the other singlet at −60.42 ppm is due to the N2 isomer. Finally, the doublet at −72.29 ppm is clearly due to the

hexafluorophosphate counter ion, which remains unmodified during the course of the reaction and therefore serves as an internal standard. During the reaction, the alkyne signal at −52.77 ppm gradually decreases in intensity while the singlet of the N2 isomer at −60.42 ppm increases. After 2 h, the combined integral of the two singlets at −60.29 and −60.42 ppm has reached the intensity of the hexafluorophosphate counter ion and does not change much any further, indicating that the reaction is complete now. Afterwards, only a slow isomerization from the N1 to the N2 species is found. After 22 h, the peak of the N1 isomer has almost completely disappeared, and there are only two signals left in the final ^{19}F NMR spectrum (**Figure 3.8**, red trace), the singlet at −60.42 ppm for the N2-bound triazolato product and the doublet at −72.29 ppm of the hexafluorophosphate counter ion.

A potential mechanism for the iClick reaction, which also accounts for the early intermediate, is shown in **Scheme 3.4**. The azido group is thought to be initially attacked by the alkyne from the more electron-deficient side, which is the carbon atom bearing the CF_3 group, to form a linear intermediate, which give rise to the ^{19}F NMR signal at −55.00 ppm. Then, ring closure leads to initial formation of the N1 isomer with a peak at −60.29 ppm, which isomerizes to the more stable N2 species with a signal at −60.42 ppm. In this model, the initial attached and following cycloaddition are relatively fast processes, followed by slow isomerization. Therefore, after an initial build-up of the peak due to the N1 isomer, at later stages, both newly fromed N1 isomer as well as the final N2 species are observed in parallel. A similar effect was also reported by Purcell, who studied the progress of the "inverse iClick" reaction of a Co(III)-nitrile complex with sodium azide.[132]

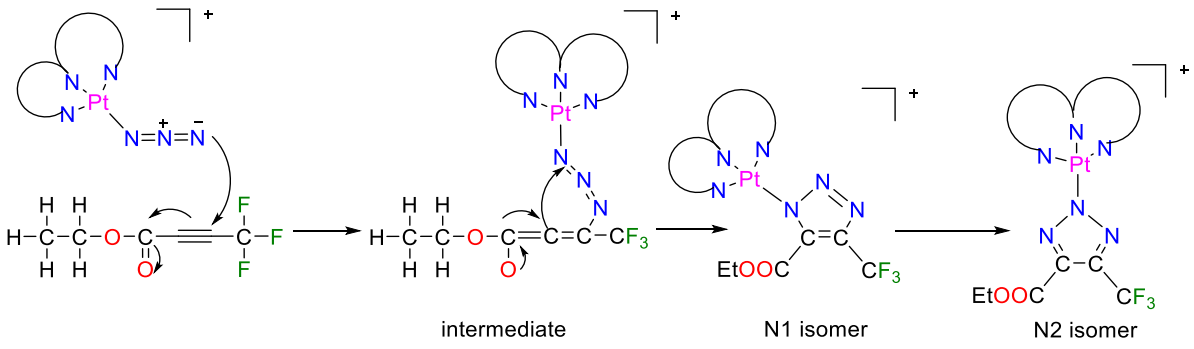

Scheme 3.4: Proposed mechanism of the iClick reaction as deduced from ^{19}F NMR spectroscopic study of the reaction of **13** and **17**. Initially, a linear intermediate is formed from attack of the more electron-deficient carbon atom of the C≡C triple bond on the terminal nitrogen atom of the metal azido moiety. This is followed by ring-closure to give the N1-coordinated isomer, which slowly isomerizes to the more stable N2 species.

3.1.6 DNA binding study by UV/Vis titration

DNA is an important intracellular target for antitumor drugs. Therefore, the investigation of metal complex-DNA interactions contributes to the understanding of the mechanism of action.[135] Transition metal complexes are known to bind to DNA either by covalent binding, mostly to the nitrogen donor atoms of the nucleobases, but in more rare cases also to the sugar-phosphate backbone, or non-covalent interactions, in the minor or major groove as well as the π system of the nucleobases.[136] The non-covalent interactions usually take place by either intercalation or insertion. Intercalation involves insertion of a planar polycyclic aromatic ligand between two adjacent base pairs of DNA, which is stabilised by π-π stacking between the base pairs and aromatic ring system to result in the lengthening, stiffening and unwinding of the DNA helix.[137] Insertion is closely related to intercalation, also involving incorporation of a ligand into the base pair stack. However, the main difference is that in insertion, one base pair is expelled from the double helix and replaced by the incoming ligand.[138] The group of Lippard was the first to report on a monocationic platinum(II) complex with the 2,2':6',2"-terpyridine (terpy) ligand to bind duplex DNA by intercalation. The planar structure of the metal complex allows it to gain access to the DNA base stack and interact with the DNA *via* π-stacking. A moderate binding constant of $K_b = 10^5$ M^{-1} was determined by UV/Vis titration.[125] Consequently, the DNA binding ability of triazolato complexes **18**, **19**, **24**, and **25** was also studied by this method. The assay was performed with a fixed concentration of complexes **18 (**30 μM), **19** (40 μM), **24** (50 μM) and **25** (50 μM) while gradually increasing the amount of CT-DNA from 0 to 12 μM. UV/Vis spectra were recorded in the range of 230–800 nm and the binding constant K_b determined from equation (**I**):[139]

$$c(\text{DNA}) \times (\varepsilon_a - \varepsilon_f)^{-1} = a \times 10^6 + b \times c(\text{DNA}) \quad \textbf{(I)}$$

$$\text{with } \varepsilon_a = A_{([\text{DNA}] = x)}/c(\text{complex}),$$

$$\varepsilon_f = A_{([\text{DNA}] = 0)}/c(\text{complex}).$$

Linear fit gives DNA binding constant $K_b = b/a$.

Upon the incremental addition of CT-DNA to a solution of **18** in TE buffer, the MLCT bands at 344 nm and 362 nm slight decrease in intensity with increasing amount of DNA, while the overall position of the two peaks remains unchanged (**Figure 3.9 A**).[140] The change in the absorbance at 362 nm was plotted against the concentration of the DNA (**Figure 3.9 B).** A linear fit to **equation I** gave an intrinsic binding constant of $K_b = 5.9 \times 10^5$ M^{-1} for **18**, which is of the same order of magnitude as that reported in the literature for $[PtCl(terpy)]^+$

and indicates a moderately strong DNA binding.[125] The DNA binding ability of triazolato complex **19**, **24**, and **25** was evaluated in a similar way as described in the previous section. The DNA binding constants determined are collected in **Table 3.1**. All values are in the range of 2–6 × 10^5 M^{-1}. Differences in the DNA bindung affinity between the isostructural palladium(II) and platinum(II) complexes **18** and **19** as well as **24** and **25** are only very minor, indicating that the nature of the metal center has essentially no influence on the DNA interaction. The symmetrically substituted triazolato complexes **18** and **19** with carboxymethyl groups exhibit a slightly higher DNA affinity than the CF_3,COOEt-functionalized compounds **24** and **25**, pointing to a possible stabilizing role of the triazolate C4- and C5-substituents, but even these variations do not lead to order-of-magnitude differences. The overall only moderate DNA affinity points against this biomacromolecule as a key cellular target. However, further mechanistic studies on the anticancer activity of compounds **18**, **19**, **24**, and **25** are still on-going.

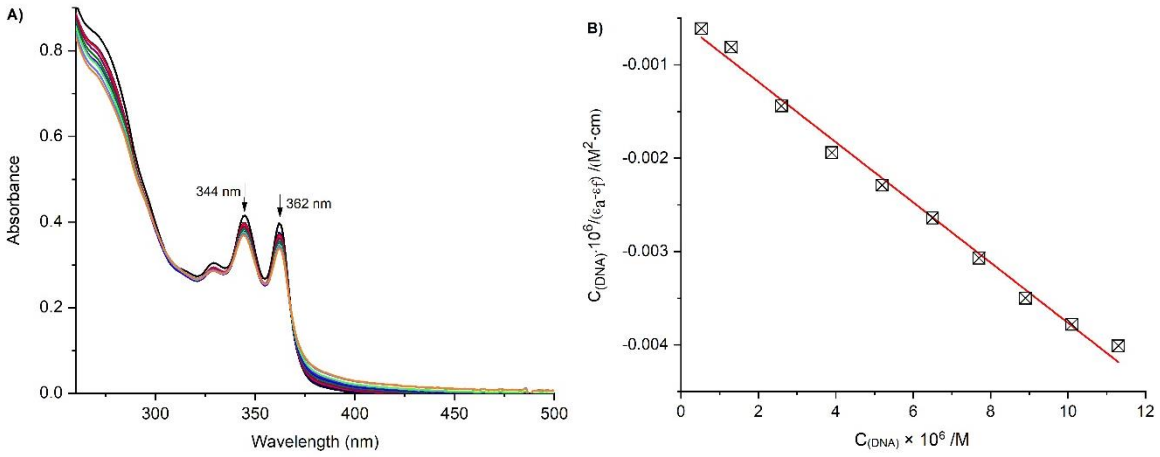

Figure 3.9: A) Changes in the UV/vis spectrum of **18** (30 µM) in the presence of increasing concentrations of CT-DNA; **B)** Linear fit of the change in the absorbance of the peak at 362 nm *vs*. increasing concentration of CT-DNA.

Table 3.1: DNA binding constants of triazolato complexes **18**, **19**, **24**, and **25** as determined by UV/Vis titration with CT-DNA.

Complex	Metal	Triazolate C4 and C5 substituents	Band analyzed	Change in absorbance	DNA binding constant (in 10^5 M^{-1})
18	Pd	$COOCH_3$,$COOCH_3$	362 nm	hypochromism	5.9
19	Pt	$COOCH_3$,$COOCH_3$	340 nm	hypochromism	3.9
24	Pd	CF_3,COOEt	270 nm	hypochromism	2.1
25	Pt	CF_3,COOEt	270 nm	hypochromism	3.4

3.2 iClick reactions of Pd(II) and Pt(II) phbpy azido complexes

In order to study the effect of the coligand on the product spectrum and kinetics of the iClick reaction, in this chapter, a series of palladium(II) and platinum(II) triazolato complexes with the C^N^N-chelating coligand 6'-phenyl-2,2'-bipyridine (phbpy, **28**) instead of 2,2':6',2"-terpyridine (terpy) was synthesized by room-temperature iClick reaction of the corresponding palladium(II) and platinum(II) azido compounds with electron-poor alkynes **14** and **17**. Since this tridentate ligand is nonsymmetrical, the NMR signals of the outer phenyl and pyridine rings are difficult to assign and analysis heavily relied on 2D ^{1}H-^{1}H COSY, ^{1}H-^{13}C HSQC and ^{13}C-^{13}C HMBC NMR spectra to solve this issue.

3.2.1 Synthesis of 6'-phenyl-2,2'-bipyridine

6'-Phenyl-2,2'-bipyridine (phbpy, **28**) was synthesized following a reported procedure (**Scheme 3.5**).[141] Briefly, to a solution of 2,2'-bipyridine (bpy) in anhydrous diethyl ether was added dropwise a 1.9 M solution of phenyl lithium in dibutyl ether at 0 °C under argon. After 2 h, the deep red mixture was quenched by addition of water. The aqueous layer was extracted with diethyl ether and then, the combined organic layers were dried over magnesium sulphate. After filtration, the solvent was removed and the remaining brown oil diluted with acetone. A saturated solution of potassium permanganate in acetone was added to re-oxidize the ring system. The resulting brown oil was then purified by column chromatography on silica using diethyl ether/*n*-hexane (2:7 *v/v*) as the eluent. The final product was obtained as a light yellow powder in moderate yield.

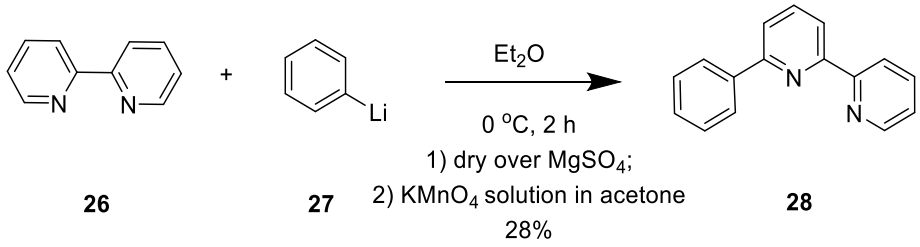

Scheme 3.5: Reaction of 2,2'-bipyridine **26** and phenyllithium **27** followed by re-aromatization of the final ring system with potassium permanganate gave 6'-phenyl-2,2'-bipyridine (phbpy, **28**).

The ^{1}H NMR spectrum of **28** shows nine signals in the aromatic region with a total integral of 12H (**Figure 3.10**). The most downfield shifted signal is a doublet-of-a-doublet-of-a-doublet (ddd) at 8.72 ppm, which is due to the peripheral pyridine H6 atom based on coupling constants of $^{3}J_{H6,H5}$ = 4.8 Hz, $^{4}J_{H6,H4}$ = 1.7 Hz, and $^{5}J_{H6,H3}$ = 0.8 Hz. A doublet at 8.67 ppm is assigned to the pyridine H3 atom from the same ring, in line with $^{3}J_{H3,H4}$ = 8.0 Hz. Another doublet at 8.42 ppm is attributed to the central ring pyridine H3' atom, due to the somewhat

different coupling constant $^{3}J_{H3',H4'}$ = 7.6 Hz. The multiplet at 8.17 − 8.14 ppm corresponds to H2" and H6" from the phenyl ring, followed by another multiplet at 7.93 − 7.86 ppm resulting from the overlap of the H4 and H4' signals. A doublet-of-a-doublet at 7.79 ppm is due to H5', as suggested by the two distinct coupling constants $^{3}J_{H5',H4'}$ = 7.8 Hz, and $^{4}J_{H5',H3'}$ = 0.9 Hz. The multiplet at 7.54 − 7.49 ppm with an integral of 2H is then due to the H3" and H5" atoms. Finally, another multiplet at 7.47 − 7.42 ppm is assigned to H4", while the doublet-of-a-doublet-of-a-doublet at 7.36 ppm is due to the H5 atom based on $^{3}J_{H5,H4}$ = 7.4 Hz, $^{3}J_{H5,H6}$ = 4.8 Hz, $^{4}J_{H5,H3}$ = 1.1 Hz.

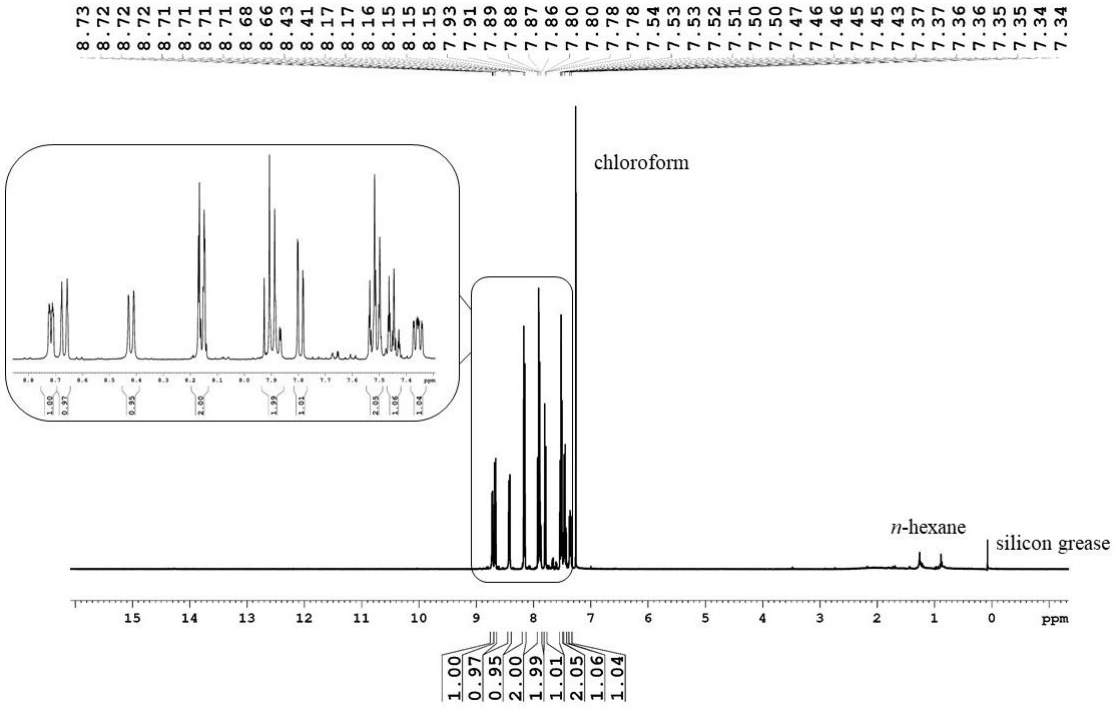

Figure 3.10: ^{1}H NMR spectrum of 6'-phenyl-2,2'-bipyridine **28** (400.40 MHz, $CDCl_3$).

The ^{13}C NMR spectrum of **28** shows a total of 13 signals for 16 carbon atoms at 156.70, 156.17, 148.75, 139.41, 137.95, 137.55, 129.22, 128.89, 127.10, 124.00, 121.72, 120.65 and 119.65 ppm (**Figure 3.11**). The reduced number of peaks is due to a combination of symmetry-equivalence of the phenyl ring C2 and C6 as well as C3 and C5 atoms plus an incidental overlap of two peaks. In the downfield area, the signal at 156.70 ppm is due to the overlap of the C2 and C2' signals, which are in a very similar chemical environment. The following signals at 156.17, 148.75, 139.41, 137.95, 137.55 and 129.22 ppm are attributed to C6', C6, C4', C4, C1" and C4", respectively. Two closely spaced signals with high intensity at 128.89 and 127.10 ppm correspond to the phenyl- C3"/C5" and C2"/C6" atoms, respectively. The remaining peaks at 124.00, 121.72, 120.65 and 119.65 ppm are assigned to C5, C3, C5' and C3', respectively.

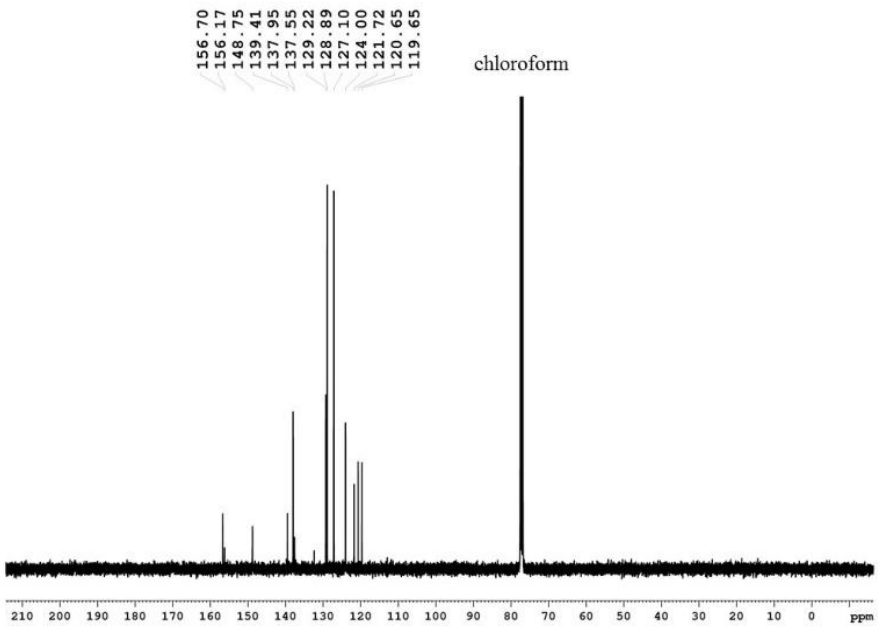

Figure 3.11: ^{13}C NMR spectrum of 6'-phenyl-2,2'-bipyridine **28** (100.68 MHz, $CDCl_3$).

3.2.2 Synthesis of Pd(II) and Pt(II) phbpy azido complexes

As principal reactants for the iClick reactions, the palladium(II) and platinum(II) azido complexes **31** and **32** were prepared in a standard procedure (**Scheme 3.6**). In the first step, 1,5-cyclooctadiene palladium(II) dichloride **8** and 6'-phenyl-2,2'-bipyridine **28** were reacted in chloroform at reflux for 18 h and [PdCl(phbpy)] **29** was obtained by filtration as a yellow solid. Then, chlorido compound **29** was heated to reflux in acetone together with an excess of sodium azide for 9 h. Patial removal of acetone and cooling to room temperature lead to the precipitation of [Pd(N_3)(phbpy)] **31** as a yellow solid in high yield. However, an attempt to synthesize [PtCl(phbpy)] **30** from 1,5-cyclooctadieneplatinum(II) dichloride **9** by a similar procedure failed. Therefore, potassium tetrachloroplatinate **6** was directly used as a starting material. The reaction of **6** with phbpy in a mixture of water and acetone at reflux for 18 h lead to [PtCl(phbpy)] **30** as an orange solid. The following ligand-exchange step was carried out exactly as in the case of the palladium analogue **29** and [Pt(N_3)(phbpy)] **32** was obtained as a dark red solid in excellent yield.

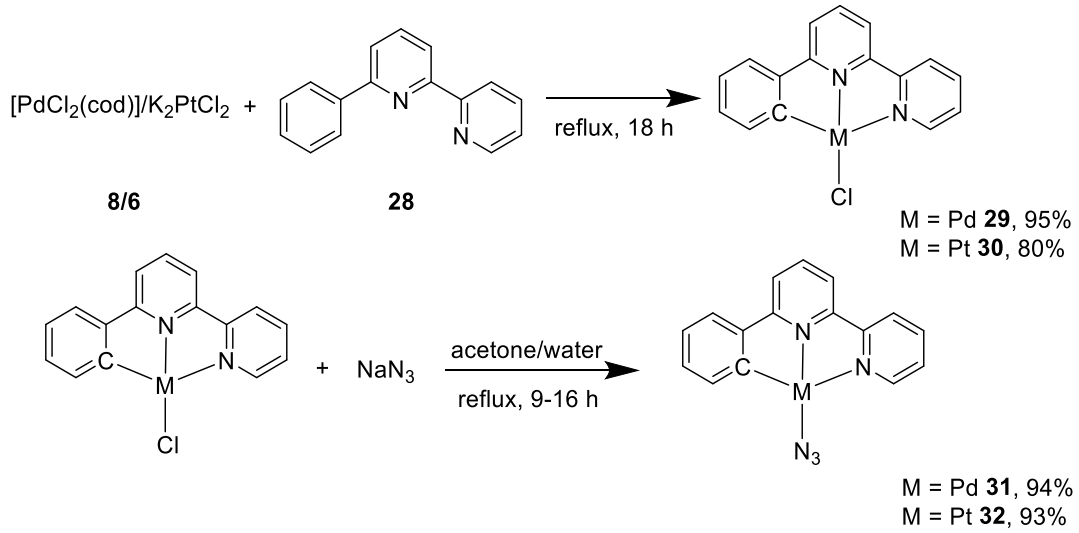

Scheme 3.6: Synthesis of [M(N_3)(phbpy)] with M = Pd **31** and Pt **32**.

The IR spectra of **31** and **32** are rather similar and therefore, only the spectrum of **31** is discussed in the following. The very strong peak at 2030 cm^{-1} is characteristic of a coordinated azido group and confirms the successful ligand exchange (**Figure 3.12**). The medium intensity band at 3060 cm^{-1} is due to the aromatic C-H stretches of the pyridine rings, whereas the peaks between 1400–1600 cm^{-1} are attributed to aromatic C=C and C=N stretches. Finally, the strong signal at 749 cm^{-1} is assigned to aromatic C-H bending modes.

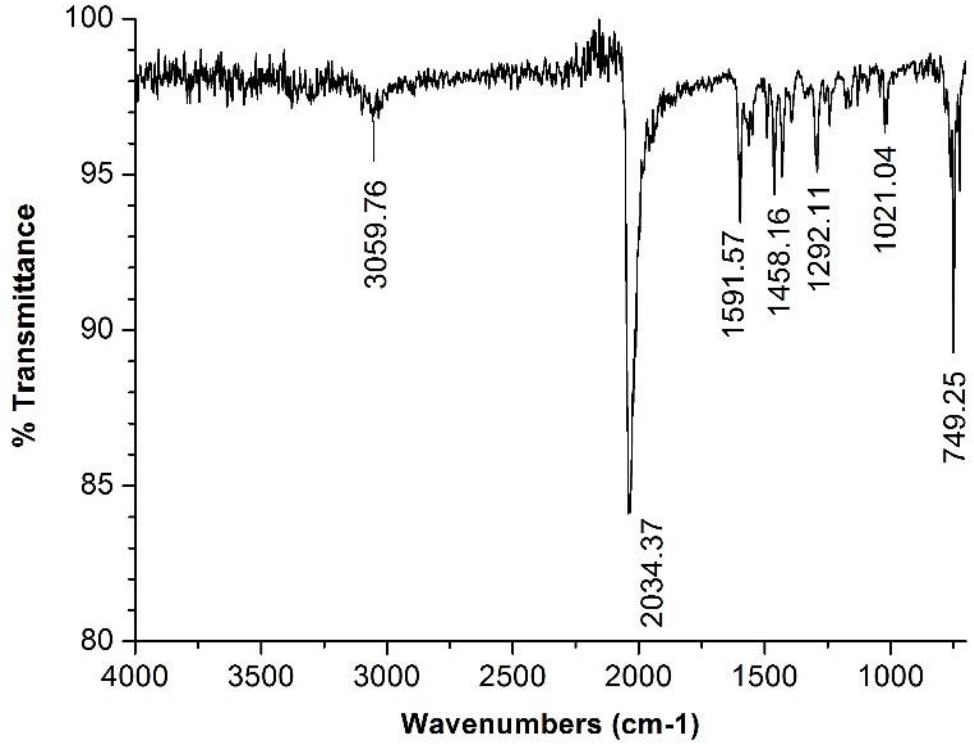

Figure 3.12: ATR IR spectrum of [Pd(N_3)(phbpy)] **31**.

The ^{1}H NMR spectrum of [Pd(N_3)(phbpy)] **31** shows 11 signals, as expected from the number of non-equivalent protons (**Figure 3.13**). Interestingly, the pyridine H3 signal is the most downfield shifted proton, which shows up as a doublet at 8.47 ppm with $^{3}J_{H3,H4}$ = 8.0 Hz. The doublet due to the H6 atom is located at 8.42 ppm, as evident from a smaller coupling constant $^{3}J_{H6,H5}$ = 5.0 Hz. A doublet-of-a-triplet at 8.25 ppm is attributed to H4 from the same pyridine ring, based on $^{3}J_{H4,H3/H5}$ = 7.8 Hz and $^{4}J_{H4,H6}$ = 1.6 Hz. A doublet at 8.19 ppm is attributed to H3', giving $^{3}J_{H3',H2'/H4'}$ = 7.9 Hz due to the roughly equivalent H2' and H4' coupling. Then, the signal for H4' is shown at 8.14 ppm as a triplet, which is caused by its surrounding H3' and H5' atoms with $^{3}J_{H4',H3'/H5'}$ = 7.9 Hz. A doublet at 8.00 ppm is assigned to H5', in line with the coupling constant of $^{3}J_{H5',H4'}$ = 7.8 Hz. A doublet-of-a-doublet-of-a-doublet shown at 7.77 ppm is assigned to H5, as suggested by three different coupling constants of $^{3}J_{H5,H4}$ = 7.6 Hz, $^{3}J_{H5,H6}$ = 5.1 Hz, and $^{4}J_{H5,H3}$ = 1.1 Hz, respectively. A doublet-of-a-doublet at 7.70 ppm corresponds to H2", followed with another doublet-of-a-doublet at 7.30 ppm for H5". Then, a doublet-of-a-triplet is located at 7.21 ppm, which is due to H4" featuring $^{3}J_{H4",H3"/H5"}$ = 7.4 Hz and $^{4}J_{H4",H2"}$ = 1.6 Hz. The most upfield shifted signal is also a doublet-of-a-triplet at 7.16 ppm, resulting from H3", based on $^{3}J_{H3",H2"/H4"}$ = 7.3 Hz and $^{4}J_{H3",H5"}$ = 1.3 Hz.

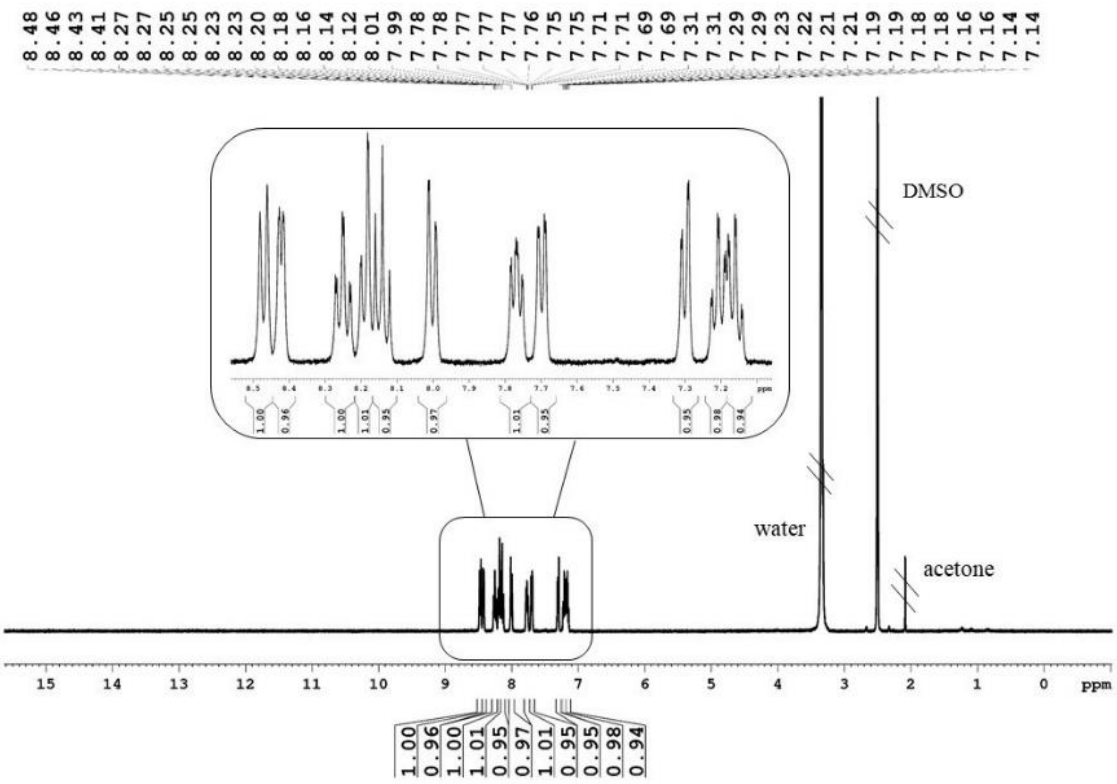

Figure 3.13: ^{1}H NMR spectrum of [Pd(N_3)(phbpy)] **31** (400.40 MHz, DMSO-d_6).

Compared to the chlorido precursor **29**, the py-H6 and phenyl-H5" signals of **31** experience the most significant shifts upon ligand exchange by more than 0.20 ppm to higher field. The other ^{1}H NMR signals, on the other hand, show very similar chemical shifts relative to those of the chlorido starting material **29**. On contrast to the free phbpy ligand, the ^{13}C NMR spectrum of palladium azido complex **31** shows 16 signals for 16 carbon atoms (**Figure 3.14**). From the downfield to highfield region, the signals at 162.91, 155.14, 153.69, 151.25, 148.77, 148.50, 140.68, 140.35, 130.93, 130.03, 127.56, 125.38, 124.97, 123.28, 119.98 and 119.91 ppm are assigned to C6', C2, C2', C1", C6", C6, C4, C4', C5", C4", C5, C3", C2", C3, C5' and C3', respectively. Interestingly, the most significant shifts are observed for the phenyl-C5" and C1", with 5.26 and 2.91 ppm upfield shifts relative to precursor **29**, respectively. On the other hand, the metal-coordinated phenyl-C6" carbon atom exhibits only a 0.68 ppm downfield shift, while the neighbouring carbon centers next to the coordinated nitrogen atoms py-C6, C2' and C6' only experience shift differences of 0.59, 0.10, and 0.71 ppm, respectively. The rest ^{13}C NMR signals show only marginal difference compared to those of its chlorido precursor **29**.

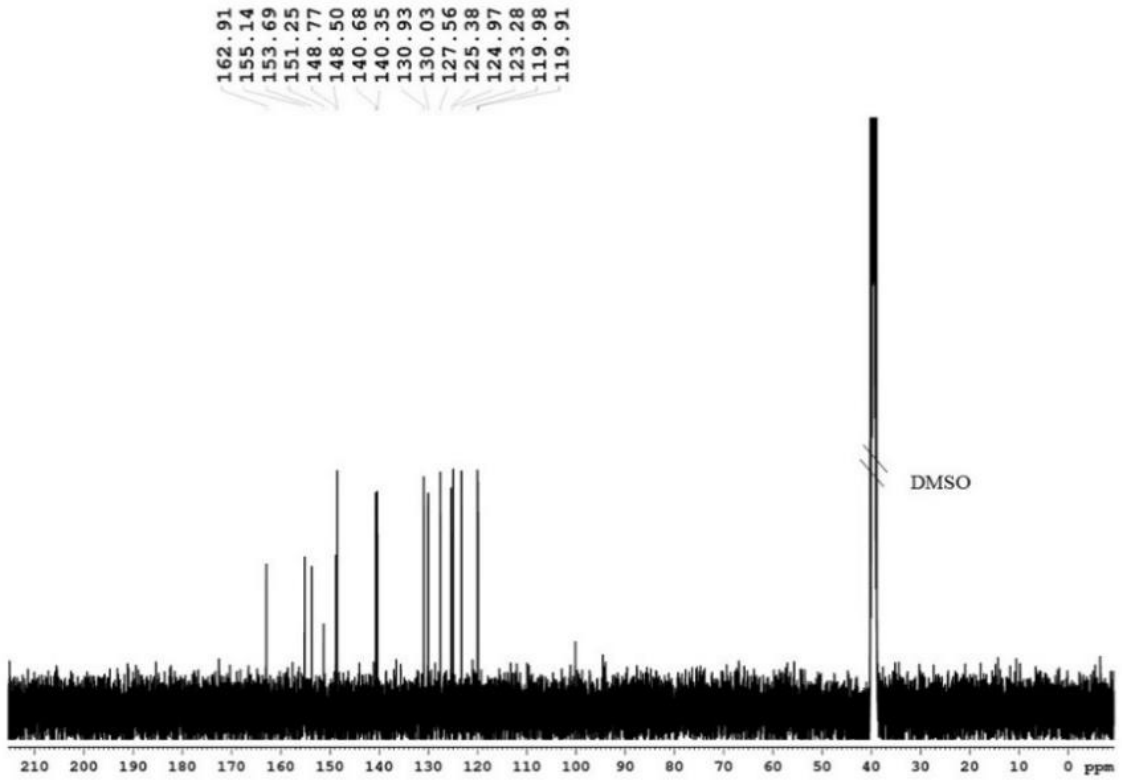

Figure 3.14: ^{13}C NMR spectrum of [Pd(N_3)(phbpy)] **31** (100.68 MHz, DMSO-d_6).

The ^{1}H NMR spectrum of [Pt(N_3)(phbpy)] **32** is generally very similar to that of the palladium analogue **31** The most pronounced difference is observed for the proton in the lowest field, which is py-H6 instead of py-H3, experiencing a difference of 0.20 ppm to lower field. All other ^{1}H NMR signals of **32** are located at essentially identical positions as those of **31**. The ^{13}C NMR spectra of **31** and **32** are also nearly superimposeable, with the notable exception of the metal-coordinated phenyl-C1" peak, for which a very upfield shift by 11.25 ppm is found. In addition, relative to the chlorido complex **30**, which has a ^{195}Pt NMR signal at −3471 ppm, the peak for **32** experiences a moderate 87 ppm downfield shift to −3384 ppm (**Figure 3.15**).

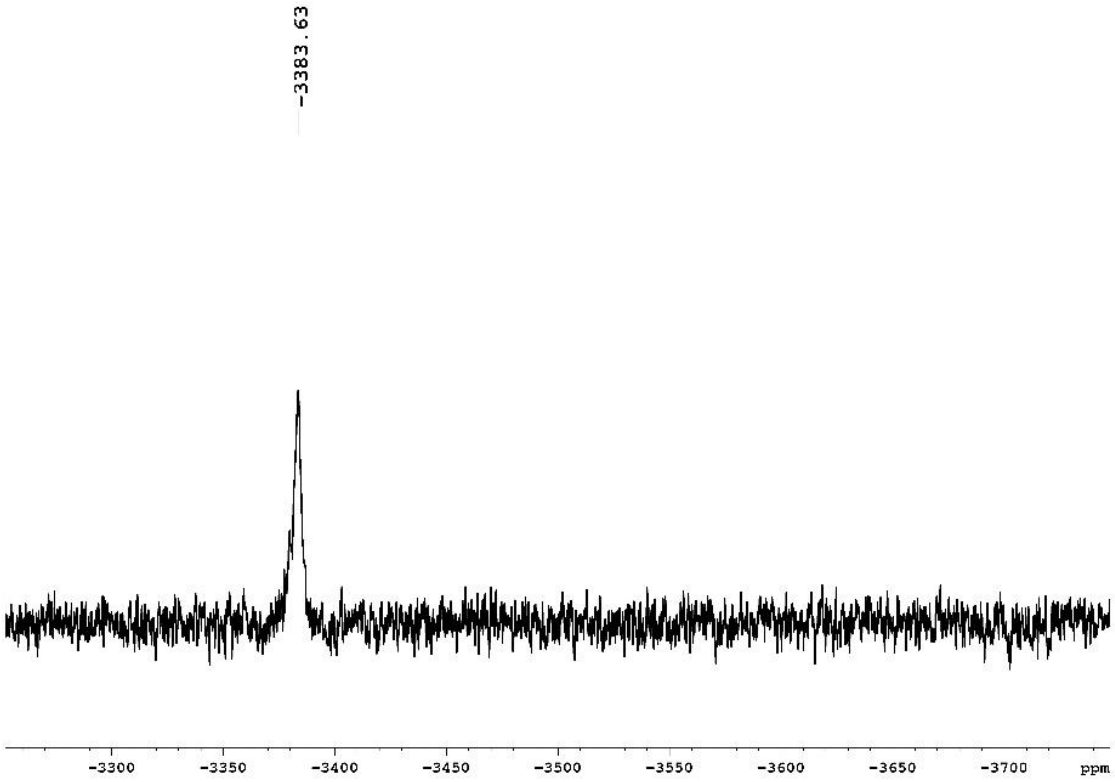

Figure 3.15: ^{195}Pt NMR spectrum of [Pt(N_3)(phbpy)] **32** (86.09 MHz, DMSO-d_6).

3.2.3 Synthesis of Pd(II) and Pt(II) phbpy triazolato complexes

The iClick reaction of [M(N_3)(phbpy)] (M = Pd **31** or Pt **32**) and electron-poor alkynes such as DMAD **14** and 4,4,4-trifluoro-2-butynoic acid ethyl ester **17**, gave four triazolato complexes **33**–**36** (**Scheme 3.7**). In general, a suspension of metal azido compound **31** or **32** in dichloromethane was reacted with a slight excess of alkyne **14** or **17** at room temperature for 4 − 24 h. Then, the solvent was partially removed and diethyl ether added to precipitate the product, which was filtered off and dried under vacuum.

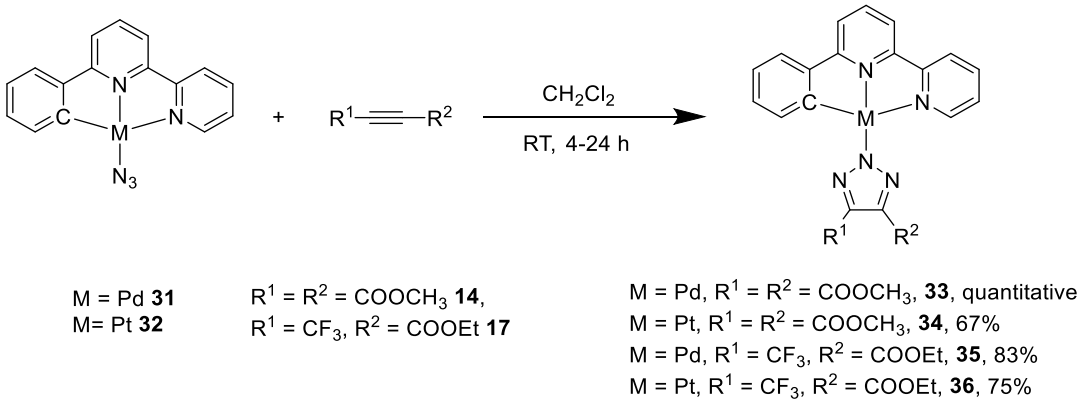

Scheme 3.7: iClick reaction of [M(N_3)(phbpy)]PF_6 with M = Pd **31** or Pt **32** with electron-poor alkynes **14** or **17** to give triazolato complexes **33**–**36** in good to excellent yield.

The IR spectra of the triazolato iClick products **33**–**36** are characterized by the absence of the coordinated azido group stretching vibration at approx. 2030 cm^{-1}, in contrast to the azido starting materials **31** and **32**. However, the spectra of **33**–**36** instead feature a prominent signal at approx. 1720 cm^{-1}, which is due to the ester C=O stretching mode, confirming the success of the iClick reaction.

The ^{1}H NMR spectrum of [Pd(phbpy)(triazolate^{COOCH3,COOCH3})] **33** was recorded in DMSO-d_6, but the signals were not very well-resolved due to poor solubility of the neutral complex. In general, signals in the aromatic region are in line with those of its azido precursor **31**. However, in the aliphatic region, a new singlet at 3.85 ppm with an integral of 6H is assigned to the two chemically equivalent methyl ester groups in the 4- and 5-position of the triazolate, indicating a symmetrical coordination of the ligand. In the ^{13}C NMR spectrum of **33**, 19 signals show up, three more than in that of the palladium azido compound **31**. Among these, the peak at 163.87 ppm is assigned to the two chemically equivalent ester C=O groups of the coordinated triazolato ligand. At higher field, the signal at 139.30 ppm is due to the symmetry-related triazolate C4 and C5 atoms. Finally, the signal in the aliphatic region at

51.91 ppm is attributed to the two methyl group carbons on the triazolate. The ^{13}C NMR signals of the phbpy backbone are generally located at positions similar to those of the azido precursor **31**, with phenyl-C1" and C6" featuring the most significant downfield shifts of 1.86 and 1.37 ppm, respectively. Taken together, the data confirms the symmetrical N2 coordination of the triazolate ligand. Due to the poor solubility of the triazolato complexes in DMSO-d_6, CD_2Cl_2 was used as the solvent for NMR measurement on **34** − **36** and therefore, the chemical shifts are not directly comparable to those of their azido precursor **31** and **32**. The ^{1}H and ^{13}C NMR spectra of platinum complex **34** are similar to those of the palladium(II) analogue **33**. Most importantly, a singlet at 3.97 ppm with an integral of 6H in the ^{1}H NMR spectrum as well as a single ^{13}C NMR peak at 52.36 ppm indicate that the two methyl esters in the 4- and 5-position of the triazolate ligand are chemically equivalent, as in complex **33**. The ^{1}H NMR spectra of **35** and **36** are also very similar, only the py-H6 signal of **35** is slightly more shifted upfield by 0.20 ppm compared to **36**. Due to the low solubility of **35** and **36**, some quaternary carbon atoms were not detected in the ^{13}C NMR spectra but otherwise there are not significant shift differences. Furthermore, both complexes **35** and **36** exhibit a single ^{19}F NMR peak at approx. −60 ppm from the CF_3 group on the triazolate substituent. The ^{195}Pt NMR spectra of **34** and **36** exhibit a single peak at −3455 and −3463 ppm, respectively, indicating only a very small shift difference between those two triazolato complexes.

3.3 iClick reactions of Pd(II) and Pt(II) semithiocarbazone azido complexes

3.3.1 Synthesis of *(E)-N*-phenyl-2-(1-(pyridin-2-yl)ethylidene)hydrazinecarbothioamide

The ligand *(E)-N*-phenyl-2-(1-(pyridin-2-yl)ethylidene)hydrazinecarbothioamide (pht, **38**) was synthesized according to a reported procedure (**Scheme 3.8**).[142] In the first step, *N*-phenyl hydrazine carbothioamide was prepared by reaction of phenyl isothiocyanate with hydrazine. Then, *N*-phenyl hydrazine carbothioamide was dissolved in hot ethanol and a slight excess of 2-acetylpyridine in acetic acid was added and the mixture heated to reflux for 4 h. After cooling to room temperature, the product was obtained as a light yellow solid in a good yield of 86%.

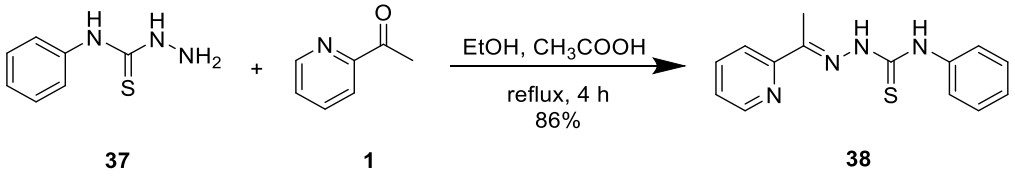

Scheme 3.8: Synthesis of *(E)-N*-phenyl-2-(1-(pyridin-2-yl)ethylidene)hydrazinecarbothioamide **38**.

The ^{1}H NMR spectrum of **38** shows nine signals with an integral of 14H (**Figure 3.16**). The signals at the lowest field, at 10.68 and 10.20 ppm, are due to the central amine NH and N*H*-phenyl protons, respectively.[142] The doublet-of-a-doublet-of-a-doublet at 8.60 ppm corresponds to py-H6, as it features coupling constants of $^{3}J_{H6,H5}$ = 4.8 Hz, $^{4}J_{H6,H4}$ = 1.6 Hz, and $^{5}J_{H6,H3}$ = 0.9 Hz. A doublet at 8.54 ppm is assigned to py-H3, based on $^{3}J_{H3,H4}$ = 8.1 Hz. A doublet-of-a-triplet at 7.81 ppm is due to py-H4, with coupling constants $^{3}J_{H4,H3/H5}$ = 7.8 Hz and $^{4}J_{H4,H6}$ = 1.6 Hz. A doublet at 7.58 ppm integrates to 2H and results from phenyl-H2'/H6', in line with a coupling constant $^{3}J_{H2'/H6',H3'/H5'}$ = 7.5 Hz. The multiplet at 7.41 − 7.37 ppm with an integral of 3H is ascribed to the overlapping signals of py-H5 and phenyl-H3'/H5'. The triplet at 7.23 ppm with an integral of 1H is attributed to the phenyl-H4' and features a coupling constant $^{3}J_{H4',H3'/H5'}$ = 7.4 Hz. In the aliphatic region, a singlet at 2.48 ppm is assigned to the three methyl group protons.

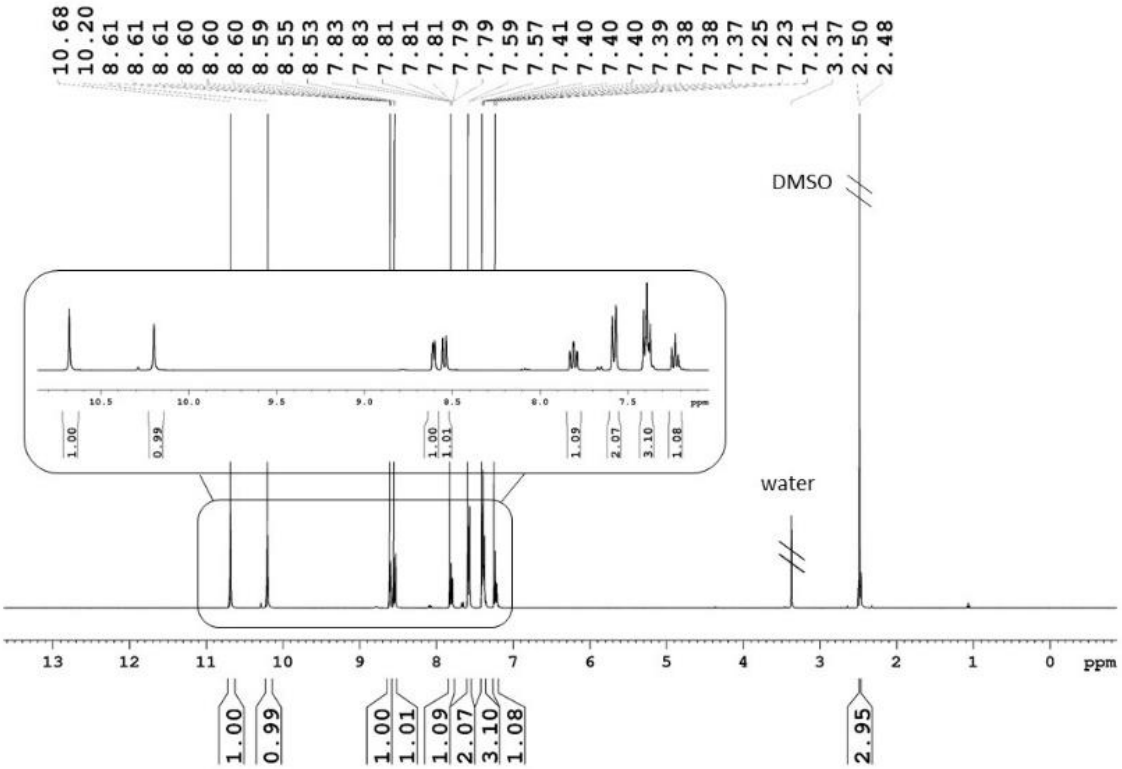

Figure 3.16: ^{1}H NMR spectrum of **38** (400.40 MHz, DMSO-d_6).

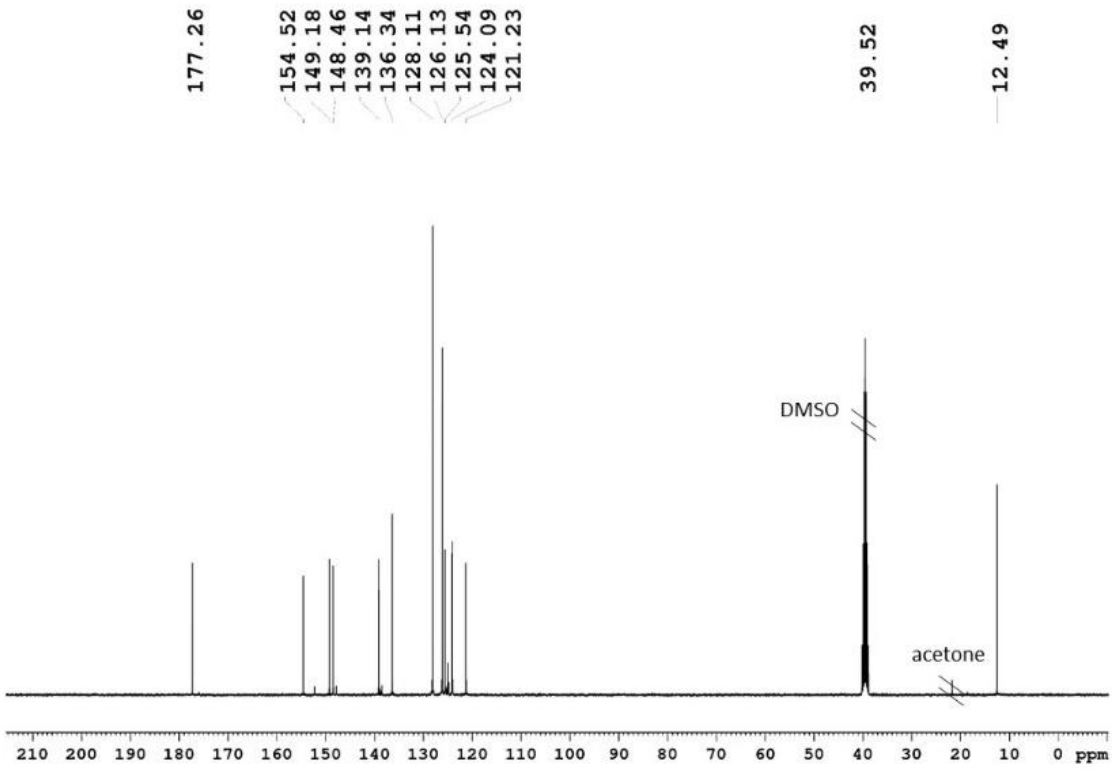

Figure 3.17: ^{13}C NMR spectrum of **38** (100.68 MHz, DMSO-d_6).

The ^{13}C NMR spectrum of **38** shows 12 signals for 14 carbon atoms at 177.26, 154.52, 149.18, 148.46, 139.14, 136.34, 128.11, 126.13, 125.54, 124.09, 121.23 and 12.49 ppm (**Figure 3.17**). The only peak located in the aliphatic region at 12.49 ppm is assigned to methyl carbon atom. In the aromatic region, signals at 121.23, 124.09 and 125.54 ppm correspond to phenyl-C4', py-C3, and C5, respectively. The signal at 126.13 ppm is due to the equivalent phenyl-C3' and C5' based on the symmetry of the freely rotating phenyl ring. Based on similar arguments, the neighbouring high intensity peak at 128.11 ppm is attributed to phenyl-C2' and C6'. The following peaks at 136.34, 139.14, 148.46 and 149.18 ppm are assigned to py-C4, phenyl-C1', py-C6, and C2, respectively. Lastly, the two peaks for the *C*=N and *C*=S carbon atoms are strongly shifted downfield and appear at 154.52 and 177.26 ppm, respectively.

3.3.2 Synthesis of Pd(II) and Pt(II) pht azido complexes

Following a standard procedures, the azido complexes **41** and **42** as the key precursors for the iClick reaction were prepared three steps as shown in **Scheme 3.9**. The COD complexes **8** and **9** were prepared as mentioned previously. They were then suspended in water and *(E)*-*N*-phenyl-2-(1-(pyridin-2-yl)ethylidene)hydrazinecarbothioamide **38** in acetone added. The mixture was heated to reflux for 3 h to generate the chlorido compound **39** or **40.** These were dissolved in acetone and reacted with an excess of sodium azide at reflux for 6 h. After partial removal of the solvent and cooling to room temperature, the azido compound **41** and **42** precipitated in high yield as yellow and red solids, respectivly.

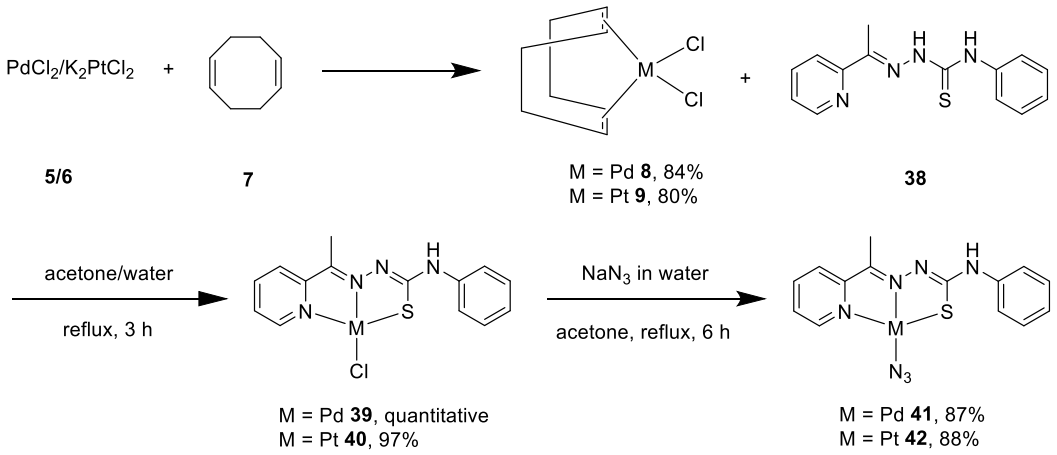

Scheme 3.9: Synthesis of [M(N_3)(pht)] with M = Pd **41** or Pt **42**.

The IR spectra of **41** and **42** are very similar and therefore, the discussion will be restricted to the IR spectrum of **41**, which shows a very strong peak at 2047 cm^{-1}, which is characteristic of the coordinated azido group (**Figure 3.18**). The medium intensity band at 3275 cm^{-1} is due to the N-H stretches, whereas peaks at approx. 1600 cm^{-1} are attributed to the N-H bending mode. The signals around 3100 cm^{-1} correspond to the aromatic C-H stretches of the pyridine rings, and the peaks between 1400 to 1600 cm^{-1} are attributed to aromatic C=C and C=N stretches. The signals between 700 to 800 cm^{-1} are assigned to aromatic C-H bending modes.

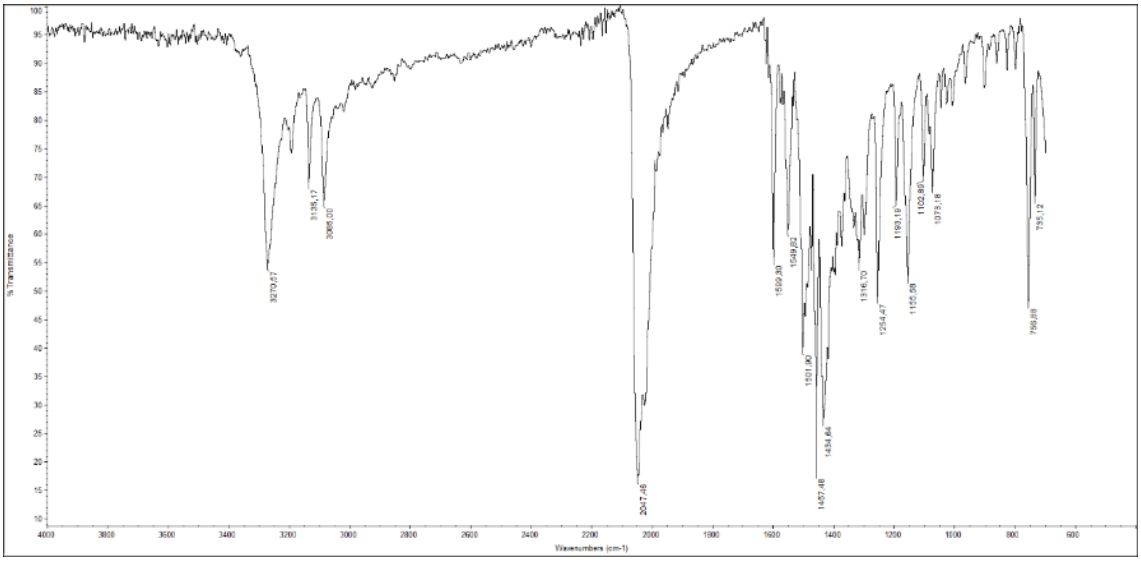

Figure 3.18: ATR IR spectrum of **41**.

The ^{1}H NMR spectrum of [Pd(N_3)(pht)] **41** shows nine signals with an overall integral of 13H (**Figure 3.19**). The most downfield shifted signal is a singlet at 10.20 ppm, which is attributed to the amide proton. A multiplet due to py-H6 is present at 8.23 − 8.21 ppm, followed by a doublet-of-a-doublet for py-H4 at 8.19 ppm, as suggesting by two different coupling constants of $^{3}J_{H4,H3/H5}$ = 7.9 Hz and $^{4}J_{H4,H6}$ = 1.7 Hz. A doublet at 7.93 ppm is assigned to py-H3, featuring $^{3}J_{H3,H4}$ = 7.9 Hz. A doublet-of-a-doublet-of-a-doublet at 7.66 ppm corresponds to py-H5, based on $^{3}J_{H5,H4}$ = 7.7 Hz, $^{3}J_{H5,H6}$ = 5.3 Hz, and $^{4}J_{H5,H3}$ = 1.2 Hz. A doublet at 7.61 ppm is due to phenyl- H3' and H5' with $^{3}J_{H3'/H5',H2'/H6'}$ = 7.7 Hz. A triplet at 7.33 ppm is assigned to phenyl- H2' and H6', in line with $^{3}J_{H2'/H6',H3'/H5'}$ = 8.0 Hz. Then, another triplet at 7.04 ppm resulting from phenyl-H4' with $^{3}J_{H4',H3'/H5'}$ = 7.4 Hz. Finally, the most upfield shifted signal is a singlet located at 2.45 ppm with an integral of 3H, which is clearly assigned to the methyl protons from pht ligand backbone. Compared to ^{1}H NMR peaks of the chlorido precursor **39**, the signal of py-H6 features a significant difference of 0.38 ppm upfield shift, while other peaks show marginal difference of 0.03 ppm at most.

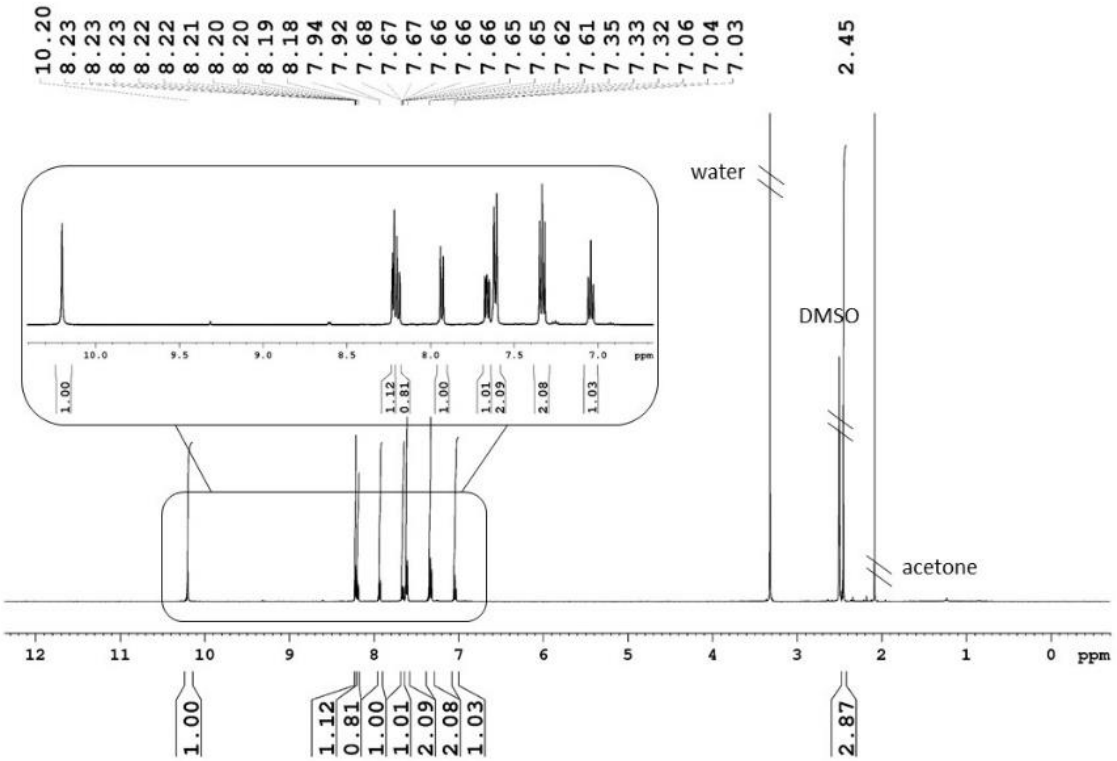

Figure 3.19: ^{1}H NMR spectrum of **41** (500.13 MHz, DMSO-d_6).

In the ^{13}C NMR spectrum of **41**, 12 signals are observed (**Figure 3.20**). The most downfield shifted signal at 172.68 ppm is assigned to the carbon atom attached to the sulphur, and the signal at 159.30 ppm is due to the carbon attached to methyl group. The following peaks at 157.57, 147.20, 141.09 and 140.21 ppm correspond to py-C2, py-C6, phenyl-C1' and py-C4, respectively. The signal with higher intensity at 128.72 ppm results from two equivalent carbon atoms, phenyl-C3' and C5', followed with a neighboring signal at 126.91 ppm for py-C5. The signal at 125.57 ppm is due to py-C3 atom, which is closely space to the peak at 123.21 ppm for phenyl-C4'. The last signal in the aromatic area at 119.89 ppm is assigned to phenyl-C2' and C6'. The only peak in the aliphatic region is located at 13.61 ppm, resulting from the pht backbone methyl carbon atom. Among these atoms, the sulphur attached carbon is the most sensitive to the chlorido to azido ligand exchange, featuring a 1.88 ppm upfield shift, while other peaks are located at very similar positions with those of the chlorido starting material **39**. The ^{1}H NMR spectrum of platinum complex **42** is very similar to that of its palladium(II) analogue **41**. However, the signal of the secondary amine proton at 10.30 ppm and a doublet-of-a-doublet-of-a-doublet at 8.44 ppm for py-H6 exhibit minor downfield shifts of 0.10 and 0.22 ppm, respectively. Most of the ^{13}C NMR signals of **42** also appear at positions identical to those found for **41**, with the only exception of the *C*-

S signal at 175.42 ppm, which experiences a 2.74 ppm downfield shift. The ^{195}Pt NMR spectrum of **42** exhibits a single peak at −3101 ppm, which corresponds to a 64 ppm downfield shift upon chlorido to azido ligand exchange (**Figure 3.21**).

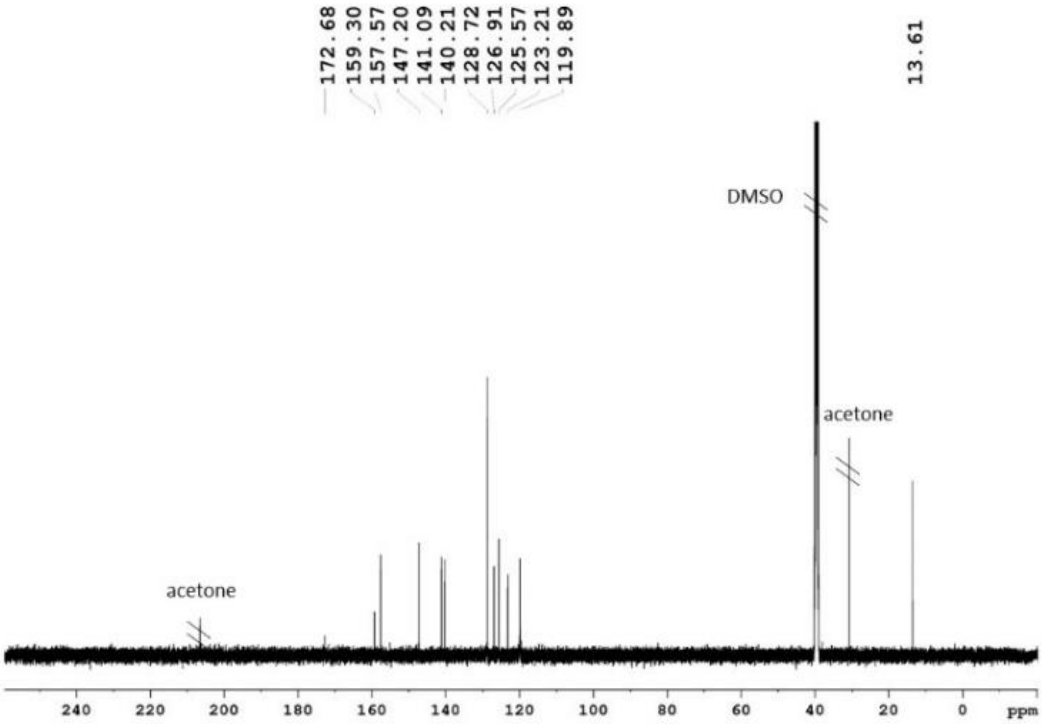

Figure 3.20: ^{13}C NMR spectrum of **41** (125.76 MHz, DMSO-d_6).

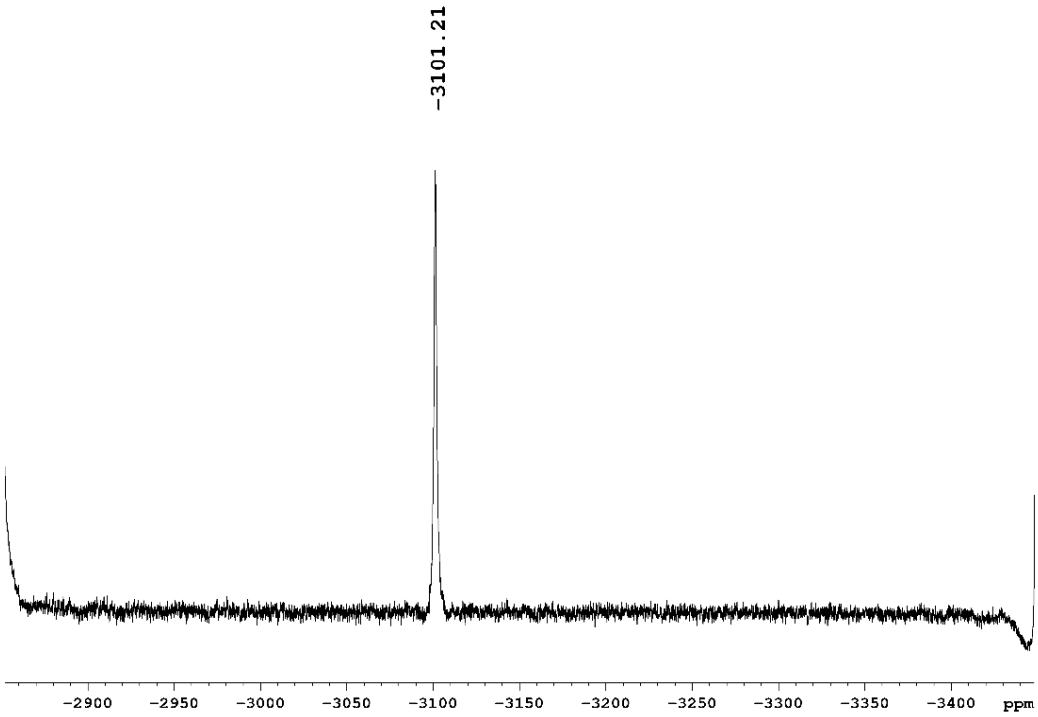

Figure 3.21: ^{195}Pt NMR spectrum of **42** (107.51 MHz, DMSO-d_6).

3.3.3 Synthesis of Pd(II) and Pt(II) pht triazolato complexes

The iClick reaction of [M(N_3)(pht)] (M = Pd **41** or Pt **42**) and electron-deficient alkynes **14** − **17**) was then examined. In the general procedure, an excess of alkyne was added to a suspension of the azido compound **41** or **42** in acetone, and the mixture was stirred at room temperature (**Scheme 3.10**). Depending on the different reagents, a reaction time of 3 h to 11 d had to be chosen. Then, the resulting precipitate was collected by filtration (although in the case of 2-butynedioic acid 1,4-bis(2-methoxyethyl) ester **16** and 4,4,4-trifluoro-2-butynoic acid ethyl ester **17** removal of the solvent was required to obtain a solid material), washed with *n*-hexane (or diethyl ether in the case of **16**) to remove unreacted alkyne, and dried under vacuum to obtain the final product in moderate to excellent yield (41 − 89%).

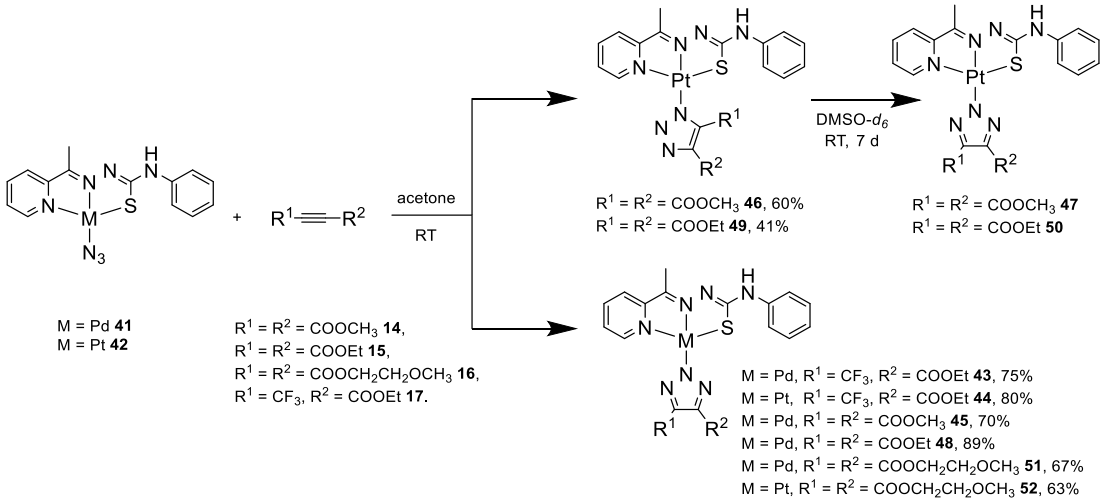

Scheme 3.10: iClick reaction of [M(N_3)(pht)] with M = Pd **41** or M = Pt **42** with electron-poor alkynes **14**–**17** leads to triazolate products **43**–**52**. Dependent on the solubility, N1 or N2 coordinated species are obtained and the N1 complexes **46** and **49** isomerize to the N2 compounds **47** and **50** in DMSO at room temperature.

The IR spectra of the resulting triazolato complexes consistently lack the distinct band for the coordinated azido group at approx. 2050 cm^{-1}, which is observed in the azido starting materials **41** and **42**. Instead, these spectra all feature a prominent signal at ~1720 cm^{-1}, which is due to the ester C=O stretching mode, confirming the success of the cycloaddition reaction. The iClick products were then further analyzed by ^{1}H and ^{13}C NMR spectroscopy and, if applicable, ^{19}F and ^{195}Pt NMR spectroscopy.

The ^{1}H NMR spectrum of [Pd(pht)(triazolate^{CF3,COOEt})] **43** includes 11 signals with an overall integral of 18H. Most notably, the ddd signal of py-H6 at 8.91 ppm is shifted downfield by 0.69 ppm relative to the starting material. On the other hand, most signals in the aromatic region appear at positions very similar to those of the azido precursor **41**. The aliphatic region

shows two new signals, a quartet at 4.31 ppm with an integral of 2H and a triplet at 1.30 ppm with an integral of 3H, which correspond to the methylene and methyl protons from the ester group in the 4-position of the triazolate ligand. Furthermore, the singlet of the methyl group in the pht ligand backbone experiences a downfield shift from 2.45 ppm in **41** to 2.53 ppm in **43**, which minor but still noticeable as it moves from the right side of the residual signal of the DMSO solvent to the left. In the ^{13}C NMR spectrum of **43**, five additional signals show up compared with that of **41**. The new peak at 159.70 ppm is due to the ester C=O group of the coordinated triazolato ligand. Two closely spaces signals at 137.88 and 136.64 ppm correspond to the triazolate C4 and C5 carbons, respectively. A quartet at 121.41 ppm is assigned to the trifluoromethyl carbon atom with a $^{1}J_{C,F}$ coupling of 268 Hz. In the aliphatic region, the two new signals at 60.74 and 13.99 ppm are attributed to the methylene and methyl carbons of the triazolate ethyl ester moiety. The ^{19}F NMR spectrum of **43** contains one major signal at −58.58 ppm as well as a minor peak at −58.42 ppm, indicating the presence of a mixture of the major N2 isomer and a minor N1 species in a ratio of approx. 13:1. The ^{1}H, ^{13}C, and ^{19}F NMR spectra of platinum analogue **44** are very similar to palladium(II) complex **43**. The ^{195}Pt NMR resonance of **44** appears at at −3108 ppm, which is only a 7 ppm upfield shift compared to its azido precursor **42**.

Reaction of palladium(II) azido compound **41** with the symmetrical alkynes **14** − **16** lead to triazolate N2 products **45**, **48**, and **51**, as demonstrated by their ^{1}H and ^{13}C NMR spectra. In particular, a major singlet at 3.81 ppm with an integral of 6H in the ^{1}H NMR spectrum of **45** as well as a single methyl ester carbon signal at 52.05 ppm in the ^{13}C NMR strongly support a symmetrical N2 coordination mode of the triazolate ligand. Similarly, in the aliphatic region of the ^{1}H and ^{13}C NMR spectra of complexes **48** and **51**, only two or three signals are observed for the triazolate C4 and C5 substituents, respectively, which confirms the chemical equivalence of the ester groups in the 4- and 5-position of the triazolate and thus the N2 coordination. This feature is also observed in the platinum(II) ethylene glycol-substituted triazolate **52**. Its ^{1}H NMR spectrum shows two triplets with an integral of 4H and a singlet with an integral of 6H in the range of 4.35 − 3.29 ppm. Furthermore, the ^{13}C NMR spectrum exhibits three peaks at 69.64, 63.81, and 58.12 ppm, which are due to chemically equivalent triazolate C4- and C5-substituents. Complex **52** also shows a single ^{195}Pt NMR signal at −3106 ppm, with only a neglegible shift (< 5 ppm) relative to its azido precursor **42** and CF_3-substituted triazolato complex **44**.

Surprisingly, the iClick reaction of platinum(II) azido compound **42** with DMAD or DEAD lead to the isolation of products with distinctly different NMR features. In the ^{1}H NMR spectrum of **46**, two singlets with equal intensity of 3H at 3.84 and 3.80 ppm indicate that the two methyl ester groups in the triazolate 4- and 5-position are chemically different. Along the same lines, complex **49** exhibits two overlapping quartets and triplets in the aliphatic region of the ^{1}H NMR spectrum with an intensity of 4H and 6H, respectively. More importantly, four ^{13}C NMR signals corresponding to two chemically distinct ethyl ester substituents are observed at 61.51, 60.31, 14.08, and 13.86 ppm. Taken together, this data indicates a non-symmetrical N1 coordination of the triazolate ligand. This is a surprising result, as most iClick products reported in the literature as well as the majority of complexes prepared in our own lab are more or less exclusively isolated as the N2 species only.

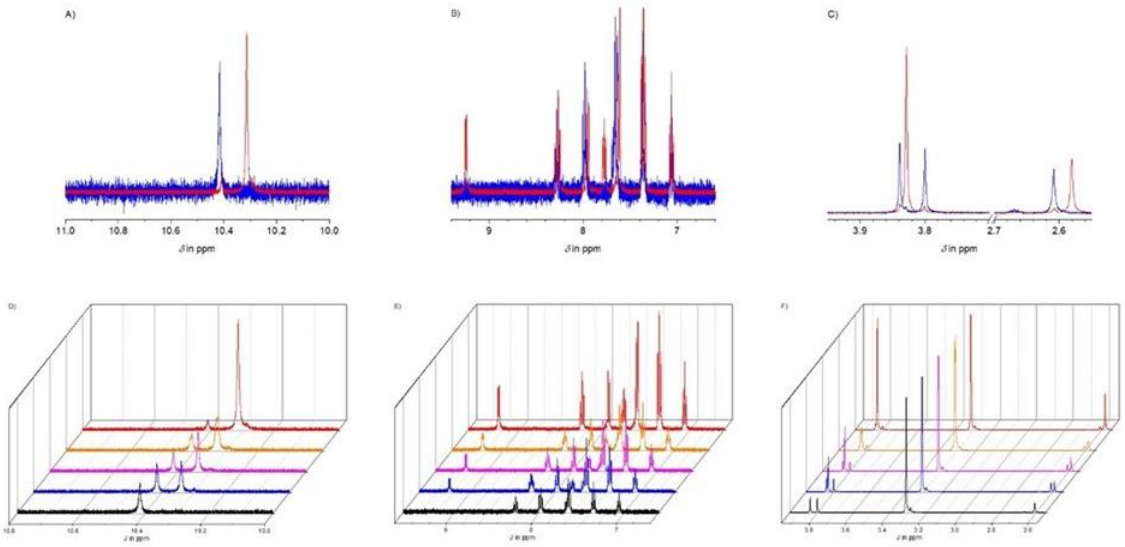

Figure 3.22: Spectral changes in the ^{1}H NMR spectrum of **46** suspended in DMSO-d_6 with increasing reaction time. Panels A-C: pht ligand backbone NH proton, aromatic, and aliphatic regions recorded immediately after suspension (blue trace) and after 4 d at room temperature (red trace); Panel D-F: Same spectral regions recorded at different time intervals (from front to back: 0 d, black trace; 1 d, blue trace; 2 d, magenta trace; 3 d, orange trace; 4 d, red trace).[143]

Interestingly, when N1 triazolate complex **46** was suspended in DMSO-d_6 and kept at room temperature in an NMR tube for several days, the solution became clear and the resulting NMR spectra changed to that of the N2 triazolate isomer **47**, as evident from only a single methyl ester signal at 3.83 ppm with an integral of 6H present. The N1 to N2 isomerization of **46** to **47** was monitored by ^{1}H NMR spectroscopy at room temperature in DMSO-d_6, and several prominent spectral changes were observed in the course of the reaction (**Figure 3.22 D − F**). In particular, the singlet of the secondary amine proton in the pht ligand backbone

experiences an upfield shift from 10.42 ppm in **46** to 10.30 ppm in **47**, and the signal of py-H6 moves downfield by 1.24 ppm (**Figure 3.22 A − B**). Furthermore, with increasing incubation time, the singlet of the pht backbone methyl group also gradually shifts from 2.61 to 2.58 ppm, and most notably, the two singlets of equal intensity at 3.84 and 3.80 ppm due to the non-symmetrical methyl ester groups in **46** gradually go down in intensity, while a peak between these two signals at 3.83 ppm grows in and became the dominant signal towards the end of the reaction time (**Figure 3.22 C**). After 4 d, the conversion reached an equilibrium state with a N2:N1 ratio of approx. 14:1.

The ethyl ester-substituted triazolate complexes **49** also underwent this N1 to N2 isomerization under the same conditions, as the resulting N2 triazolate **50** exhibits two clear ^{1}H NMR signals, a quartet at 4.29 ppm and a triplet at 1.29 ppm with a 4:6 intensity ratio, and only two ^{13}C NMR peaks at 60.75 and 14.02 ppm for the chemically equivalent ethyl ester groups in the triazolate. The ^{195}Pt NMR spectra of **47** and **50** are similar to those of **44** and **52**, showing a single peak at approx. −3105 ppm in each case.

The ^{195}Pt NMR signals of triazolato complexes **44**, **47**, **50**, and **52** are all located in a very narrow range of −3104 to −3108 ppm. This marginal difference in the ^{195}Pt NMR chemical shift also rules out a potential ligand substitution of the triazolato ligand by DMSO-d_6 solvent molecules upon extended incubation in this coordinating solvent. In particular, [Pt(pht)(dmso)]OTf **54** synthesized *in situ* by treatment of the platinum(II) chlorido compound **40** with silver triflate (**Scheme 3.11**) in the ^{195}Pt NMR spectrum shows a single peak at −3650 ppm. This significant shift difference of 485 and 545 ppm to higher field relative to the ^{195}Pt NMR signals of chlorido compound **40** and triazolate **47** rule out such a process (**Figure 3.23**). In addition, no signal was observed in the −3600 to −3700 ppm range in the ^{195}Pt NMR spectrum of **47**, confirming that no ligand replacement takes place in the DMSO-d_6 solvent.

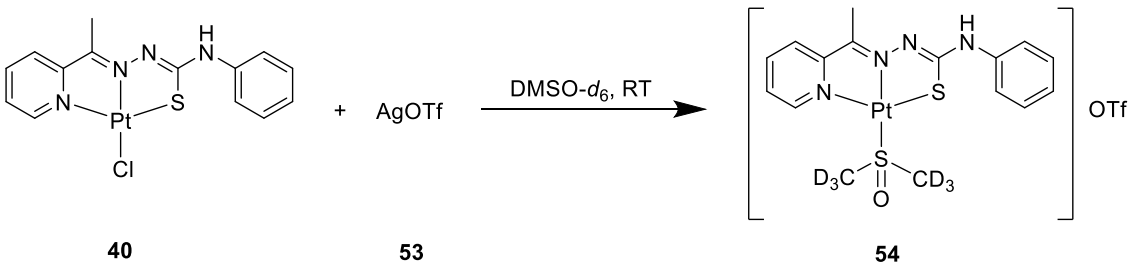

40 **53** **54**

Scheme 3.11: *In situ* synthesis of [Pt(pht)(dmso)]OTf **54** by halide abstraction from [PtCl(pht)] **40** with silver triflate.

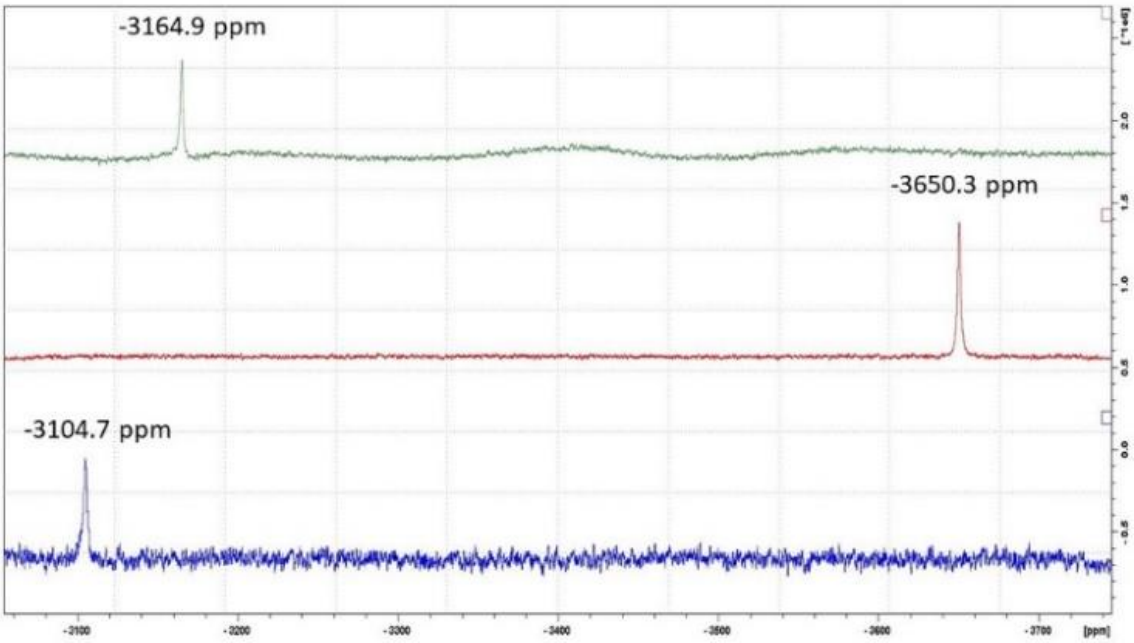

Figure 3.23: Comparison of ^{195}Pt NMR spectra (86.09 MHz, DMSO-d_6) of [PtCl(pht)] (**40**, green trace), [Pt(pht)(dmso)]OTf (**54**, red trace) and [Pt(pht)(triazolate$^{COOCH3,COOCH3\text{-}N2}$)] (**47**, blue trace).[143]

3.3.4 Intermediates in the iClick reaction

^{19}F NMR spectroscopy offers a good handle to explore the progress of the iClick reaction of platinum(II) azido compound **42** with trifluoromethyl-substituted alkyne **17**. Therefore, after mixing the two reactant in an NMR tube, a series of ^{19}F NMR spectra were recorded at room temperature during the course of the reaction (**Figure 3.24**). In the first spectrum, in addition to the signal of the alkyne starting material at −50.95 ppm, two additional peaks at −54.86 and −58.48 ppm show up, which are thought to be due to a linear intermediate and a N1-coordinated triazolate species as they appear at the beginning of the reaction and then gradually disappear towards the end. Upon further reaction, the intensity of these three peaks gradually goes down and they fully disappear at different stages of the reaction. Meanwhile, another signal at −58.73 ppm appears and gradually becomes the only major signal after 15 h, which leads to its assignment as the final N2 triazolate product. Notably, several additional minor peaks at higher field also intermittently show up, which may be due to additional unstable species. Beyond 15 h, no further changes are observed at longer incubation times.

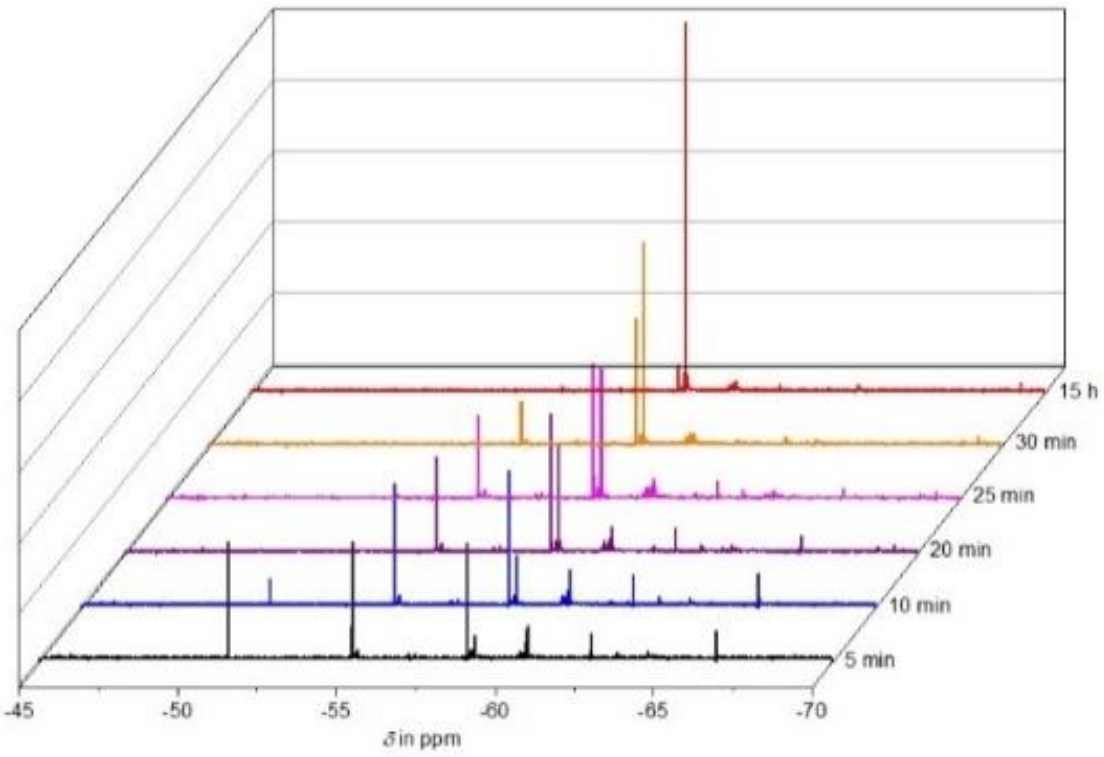

Figure 3.24: Changes in the ^{19}F NMR spectrum of a mixture of [Pt(N$_3$)(pht)] **42** and 4,4,4-trifluoro-2-butynoic acid ethyl ester **17** in DMSO-d_6 observed for 0–15 h.[143]

A possible mechanism for the iClick reaction which accounts for all assignable signals is presented in **Scheme 3.12**. In the first step, the azide is attacked by the alkyne with the more electron-deficient carbon atom of the C≡C triple bond to form a linear intermediate. This is followed by ring closure to initially lead to a N1-bound triazolate species. Finally, the N1 isomer is further converted to the more stable N2 product.

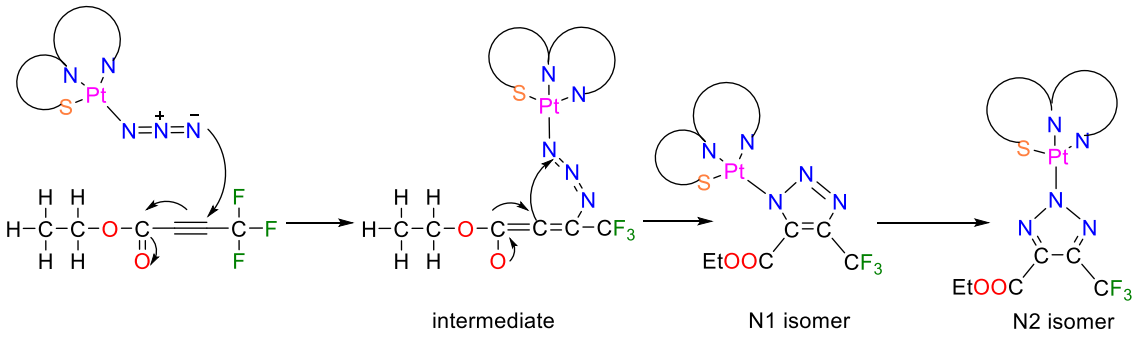

Scheme 3.12: Proposed step-wise mechanism of the iClick reaction of [Pt(N$_3$)(pht)] **42** and 4,4,4-trifluoro-2-butynoic acid ethyl ester **17** to account for the two intermediate species observed by ^{19}F NMR spectroscopy.

3.3.5 Cytotoxicity study

Since platinum(II) coordination compounds are well-established lead structures in the field of anticancer chemotherapy, selected triazolato complexes prepared were evaluated for their cytotoxic potential on the human GaMG glioblastoma cell line using the standard MTT assay.[6, 144] In general, the complexes studies exhibit low micromolar EC_{50} values in the range of 2 to 16 μM, indicating a moderate to strong cytotoxicity activity against human GaMG glioblastoma cells (**Table 3.2**). As most of the platinum(II) complexes reported in the previous section were not amenable for biological testing due to the slow N1 to N2 isomerization, only a limited comparison between the otherwise isostructural and isoelectronic palladium and platinum complexes was possible. It turned out that platinum(II) triazolato complex **44** is significantly more active than its palladium(II) congener **43** by a factor of seven. The former is also the most potent in the whole series with an EC_{50} value very close to that of cisplatin studied under similar conditions as a reference drug. Interestingly, among the palladium complexes, the substituents in the C4- and C5-position of the triazolate ligand modulate the biological activity in a systematic way, as the cytotoxic potential increases in the order CF_3/COOEt < $COOCH_3$ < COOEt < $COOCH_2CH_2OCH_3$, which suggests that the antitumor activity increases with increasing chain length of the substituents on the triazolate ligand.

Table 3.2: EC_{50} values of selected palladium(II) and platinum(II) triazolate complexes evaluated on the human GaMG glioblastoma cell line by the standard MTT assay.[143]

Complex	Metal	C4, C5 triazolate substituents	EC_{50} values (μM)
44	Pt	CF_3, COOEt	2.4 ± 0.1
43	Pd	CF_3, COOEt	16.2 ± 0.1
45	Pd	$COOCH_3$, $COOCH_3$	5.2 ± 0.1
48	Pd	COOEt, COOEt	4.8 ± 0.1
51	Pd	$COOCH_2CH_2OCH_3$, $COOCH_2CH_2OCH_3$	3.7 ± 0.1
Cisplatin			0.9 ± 0.1

Shown is the mean ± standard deviation of three independent experiment.

3.4 iClick reactions of a Pt(II) BODIPY azido complex

3.4.1 Synthesis of [Pt(bodipy)(triazolate^{R1,R2})(PEt$_3$)$_2$]

To further expand the scope of the iClick reaction and to study the effect of the conversion of the azido to a triazolato ligand on the photophysical properties of an emissive metal complex, a platinum(II) BODIPY azido compound (BODIPY = 4,4-difluoro-4-bora-3a,4a-diaza-s-indacen-8-yl) was prepared by the Winter group from the University of Konstanz which was used in the study presented herein. Thus, *trans*-[Pt(bodipy)(N$_3$)(PEt$_3$)$_2$] **55** and a slight excess of DMAD **14** or 4,4,4-trifluoro-2-butynoic acid ethyl ester **17** were dissolved in chloroform and stirred at room temperature for 3 − 5 d. After removal of the solvent, the resulting solid was dried under vacuum to get rid of unreacted alkyne and traces of solvent remaining. The corresponding triazolate complexes [Pt(bodipy)(triazolate^{R1,R2})(PEt$_3$)$_2$] with R^1 = R^2 = COOCH$_3$ **56** or R^1 = CF$_3$, R^2 = COOEt **57** were obtained in very good yield with only minimal work-up (**Scheme 3.13**).[145]

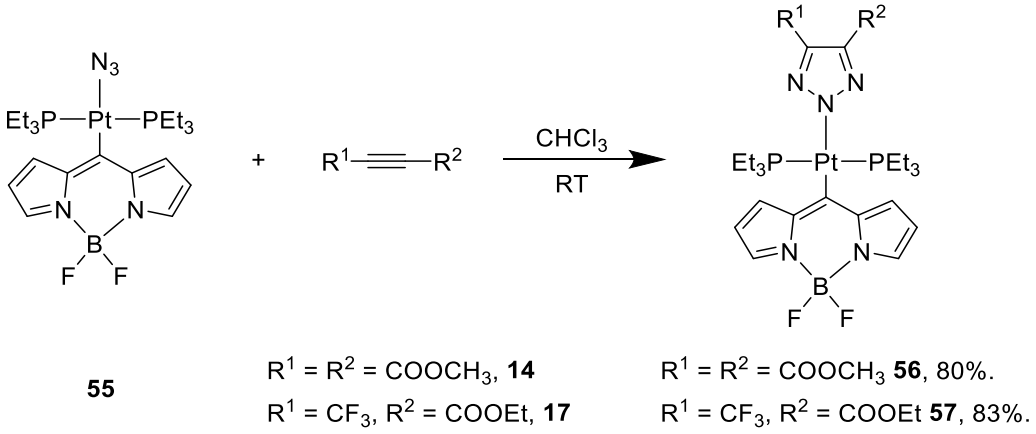

Scheme 3.13: iClick reaction of [Pt(bodipy)(N$_3$)(PEt$_3$)$_2$] **33** with DMAD **14** or 4,4,4-trifluoro-2-butynoic acid ethyl ester **17** leads to triazolate complexes [Pt(bodipy)(triazolate^{R1,R2})(PEt$_3$)$_2$] with R^1 = R^2 = COOCH$_3$ **56** or R^1 = CF$_3$, R^2 = COOEt **57**.

3.4.2 Characterization of [Pt(bodipy)(triazolate^{R1,R2})(PEt$_3$)$_2$]

The IR spectra of **56** and **57** consistently lack the distinct band of the coordinated azido group at around 2050 cm^{-1}. Instead, their spectra both feature a prominent signal at approx. 1725 cm^{-1}, which is due to the triazolate ester C=O stretching mode, confirming the success of the cycloaddition reaction. The ^{1}H NMR spectrum of the methyl ester triazolate **56** exhibits six signals with an overall integral of 42H (**Figure 3.25**). In the aromatic region, a singlet at 7.72 ppm corresponds to H3 and H5 from the BODIPY backbone. The doublet at 7.60 ppm is due to the H1 and H7 protons, followed with a multiplet at 6.48 − 6.47 ppm due to H2 and H6. Importantly, a singlet with an integral of 6H shows up at 3.94 ppm, which is assigned to the six chemically equivalent methyl ester protons in the 4- and 5-position of the triazolate ligand, indicating the formation of the symmetrical N2 isomer. The two multiplets at 1.46 − 1.42 and 1.04 − 0.96 ppm with an integral of 12H and 18H, respectively, are due to the methylene and methyl groups from the two *trans* triethylphosphine ligands. Similar ^{1}H NMR signals are also observed for the trifluoromethyl-substituted triazolato complex **57**, with the exception of the ethyl ester signals replacing the methyl ester ones. The methylene protons are present as a quartet at 4.43 ppm, while the signal of the terminal methyl groups overlaps with that of the methylene moiety of the triethylphosphine ligands, lead to an intense multiplet at 1.45 − 1.39 ppm. In addition, several minor signals are also observed in ^{1}H NMR spectra of **56** and **57**, indicating the presence of minor amounts of other isomers, which will be assigned below in the discussion of the ^{31}P and ^{195}Pt NMR spectra.

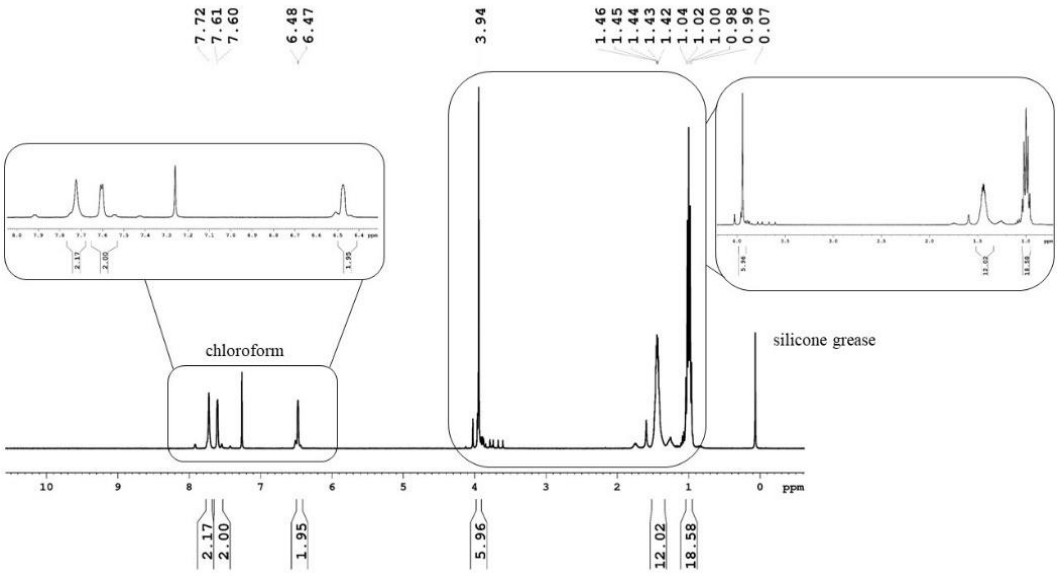

Figure 3.25: ^{1}H NMR spectrum of **56** (400.47 MHz, $CDCl_3$).

The ^{11}B NMR spectra of **56** and **57** show a triplet at approx. 0.10 ppm with a coupling constant $^{1}J_{B,F}$ = 30.1 Hz, which is typical for the BODIPY moiety. In the ^{13}C NMR spectrum of **56**, 10 signals are observed for 27 carbon atoms (**Figure 3.26**). The signal most shifted to lower field at 174.49 ppm is due to the BODIPY-C8 atom, as it is directly coordinated to the platinum centre. The four peaks at 142.75, 137.83, 133.45, and 116.51 ppm are assigned to the chemically equivalent C7a/C8a, C3/C5, C1/C7, and C2/C6 atoms from the BODIPY backbone, respectively. The *trans* triethylphosphine ligands gives rise to two signals. The *pseudo*-triplet at 14.08 ppm results from the overlap of a doublet due to a ^{1}J phosphorous coupling and a doublet resulting from a ^{2}J platinum coupling, with an averaged coupling constant of 16.8 Hz. This signal is therefore assigned to the phosphine ligand methylene groups. The peak at 7.75 ppm is then due to the methyl carbon atoms. Importantly, the triazolate ligand shows only three ^{13}C NMR signals at 162.93, 140.65, and 52.37 ppm, corresponding to the chemically equivalent carbonyl *C*=O atoms, triazolate C4 and C5, as well as methyl ester groups, respectively, which is in accordance with the formation of the N2 isomer. The ^{13}C NMR spectrum of **57** is more complicated as the trifluoromethyl substituent leads to further multiplet signals due to extensive C-F couplings. The triazolate C4 and C5 carbon signals are observed at 139.9 and 137.8 ppm, respectively, with the former signal splits into a quartet due to a coupling constant of $^{2}J_{C,F}$ = 38.2 Hz. In addition, the signal of CF_3 group is also visible as a quartet at 121.73 ppm with a coupling constant $^{1}J_{C,F}$ = 268.4 Hz. In the ^{19}F NMR spectrum of **56**, a quartet at −146.60 ppm with coupling constant $^{1}J_{F,B}$ = 30.1 Hz is due to the BODIPY unit. Complex **57** exhibits an additional peak at −59.83 ppm for the triazolate CF_3 substituent, as expected.

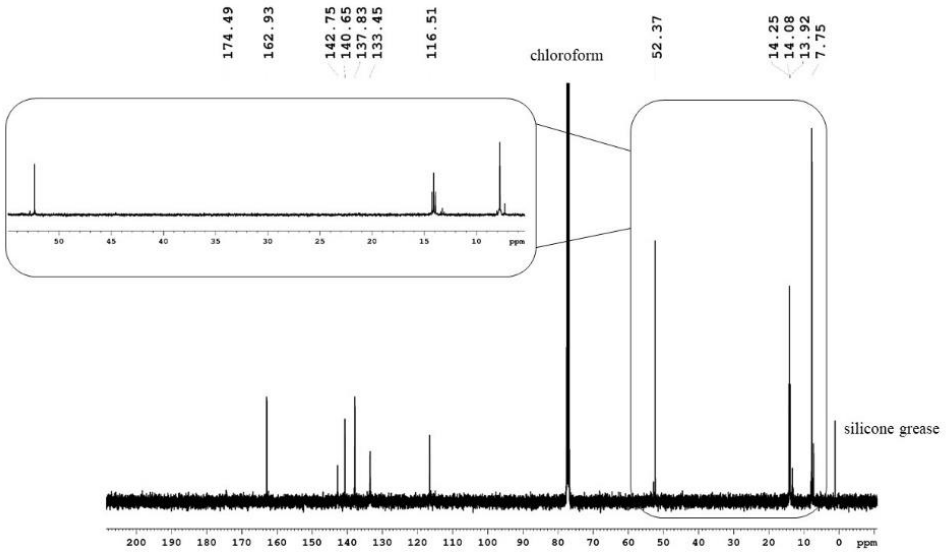

Figure 3.26: ^{13}C NMR spectrum of **56** (100.70 MHz, $CDCl_3$).

In the ^{31}P NMR spectrum of **56**, a major signal at 10.98 ppm is flanked by ^{195}Pt satellites with a coupling constant of $^{1}J_{P,Pt}$ = 2511 Hz (**Figure 3.27**). Furthermore, two additional minor signals at 11.72 and 7.93 ppm are also observed. The distinct $^{1}J_{P,Pt}$ coupling constants of 2503 and 2550 Hz, respectively, indicate of the formation of two other species, which are likely the N1-bound triazolate isomer and as well as further species arising from the *trans* to *cis* isomerization of the Pt(PEt_3)$_2$ moiety. The ratio of these three species is 83:3:14. Complex **57** also exhibits three different distinctive ^{31}P NMR signals at 11.26 ppm with coupling constants $^{1}J_{P,Pt}$ of 2511, 2502, and 2572 Hz, respectively. The intensity of the two minor components in **57** is reversed, as the overall ratio is 84:11:5.

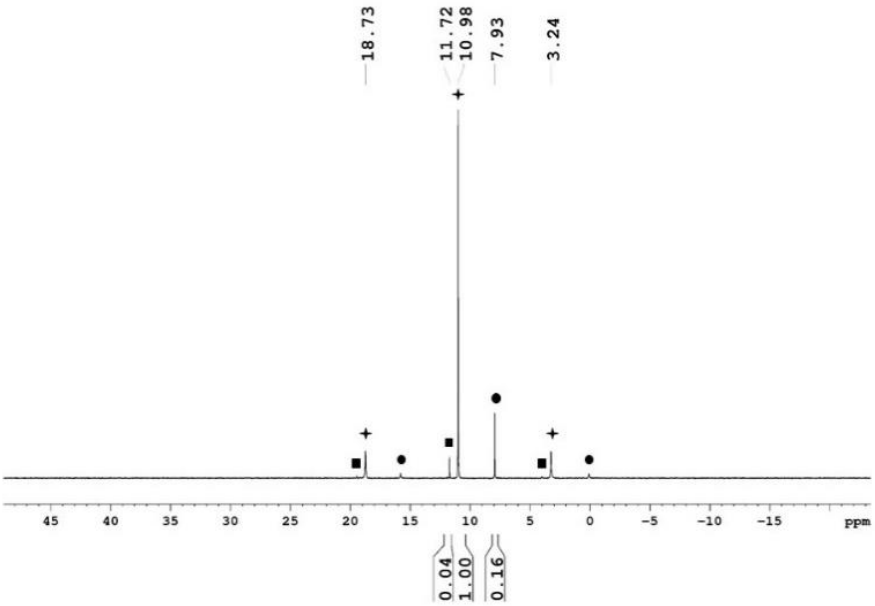

Figure 3.27: ^{31}P NMR spectrum of **56** (162.11 MHz, $CDCl_3$).

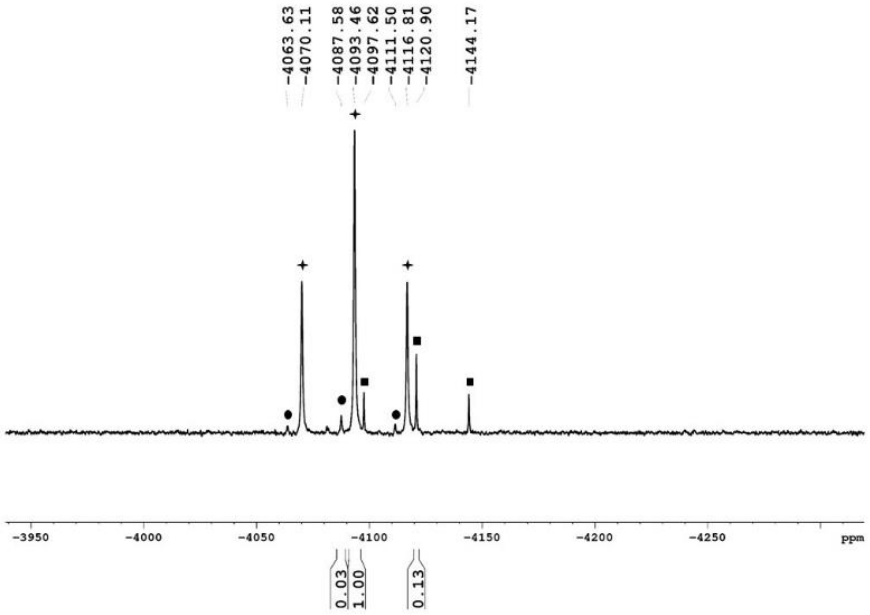

Figure 3.28: ^{195}Pt NMR spectrum of **57** (107.51 MHz, $CDCl_3$).

The ^{195}Pt NMR spectra of **56** and **57** both show a major triplet at −4093 ppm with coupling constants $^{1}J_{Pt,P}$ of 2516 or 2511 Hz. Notably, in the ^{195}Pt NMR spectrum of **57**, two additional triplets of two minor species are also clearly visible, which feature coupling constants $^{1}J_{Pt,P}$ of 2505 and 2580 Hz (**Figure 3.28**), respectively. The ratio of the three species is 85:11:4, in good accordance with that determined from the ^{31}P NMR spectrum.

3.5 Study of iClick reaction kinetics by NMR spectroscopy

The rate constant of the iClick reaction is an important parameter when this kind of cycloaddition reaction is to be applied for bioconjugation, since it has to be faster than the biological process to be studied. NMR spectroscopy is a facile way to follow the course of the reaction, as there are significant differences in NMR chemical shifts between starting materials and triazolate products. Thus, the iClick kinetics were extensively studied by monitoring the signal of the alkyne or metal azido reactants with ^{1}H, ^{19}F, and ^{31}P NMR spectroscopy. In the ^{1}H NMR experiments, 1,3,5-trioxane served as an internal standard, while in the case of reaction monitoring by ^{19}F and ^{31}P NMR, tetrabutyl ammonium hexafluorophosphate was added, against which the integration of the precursor is referenced in each NMR spectrum, allowing the concentration at different reaction times to be determined. In the case of the terpy complexes, the signal of the inherently present hexafluorophosphate counterion was used for referencing. For every kinetic measurement, the molar ratio between metal azido complex and alkyne was adjusted to 1:1 by proper dilution. Assuming a second-order rate law and equal concentrations of the two reagents as well as negligible side-reactions, the second-order rate constant *k* is obtained by eqn (**II**):

$$1/[A] = kt + 1/[A_o] \qquad (\mathbf{II})$$

where $[A_o]$ = initial concentration of alkyne or azide,

$[A]$ = concentration of alkyne or azide at t.

A series of ^{1}H, ^{19}F, or ^{31}P NMR spectra were recorded at 25 °C, and the intervals between each measurement are varied from 0 s to 10 h according to the expected rate for each iClick reaction. In all experiments, a time lag of about 1 min between mixing of the reactants and obtaining the first spectrum cannot be avoided due to experimental limitationsand was considered in the determination of the rate constants.

3.5.1 Study of the iClick kinetics of [M(N3)(terpy)]PF6 (M = Pd or Pt) with DMAD

In the iClick reaction of palladium(II) terpy azido compound **12** with DMAD, the alkyne methyl ester proton signal is a convenient handle for a determination of the rate constant by ^{1}H NMR spectroscopy (**Figure 3.29 A**). Over the course of the reaction, the singlet of the DMAD methyl protons at 3.81 ppm gradually decreases in intensity while a new signal at 3.88 ppm due to the symmetry-equivalent N2 triazolate methyl ester groups grows in.

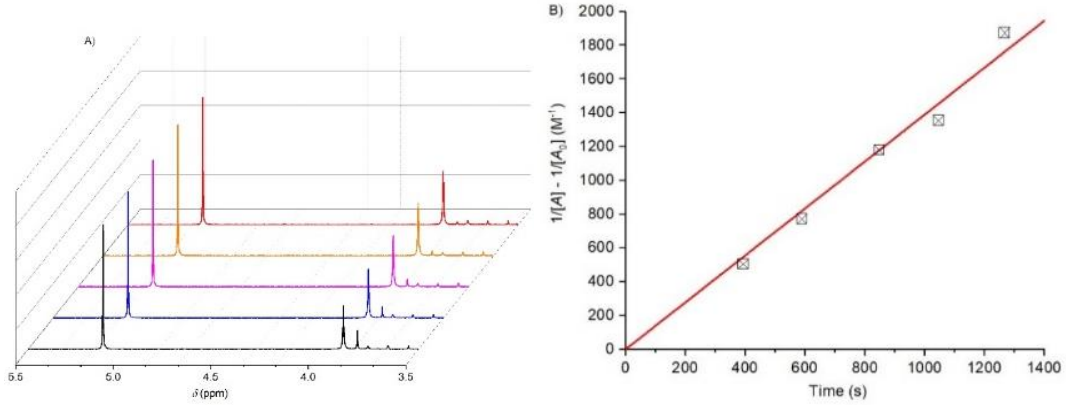

Figure 3.29: A) Changes in the 200 MHz ^{1}H NMR spectra of a mixture of palladium(II) azido complex **12** (6.7 mM), dimethyl acetylene dicarboxylate (DMAD, 6.7 mM), and 1,3,5-trioxane (6.7 mM) in DMSO-d_6 at room temperature with reaction time increasing from the black to the red trace for up to 21.5 min (front to back); **B)** linear fit of the change of the intensity of the DMAD methyl ester protons signal at 3.81 ppm to the second order rate law.

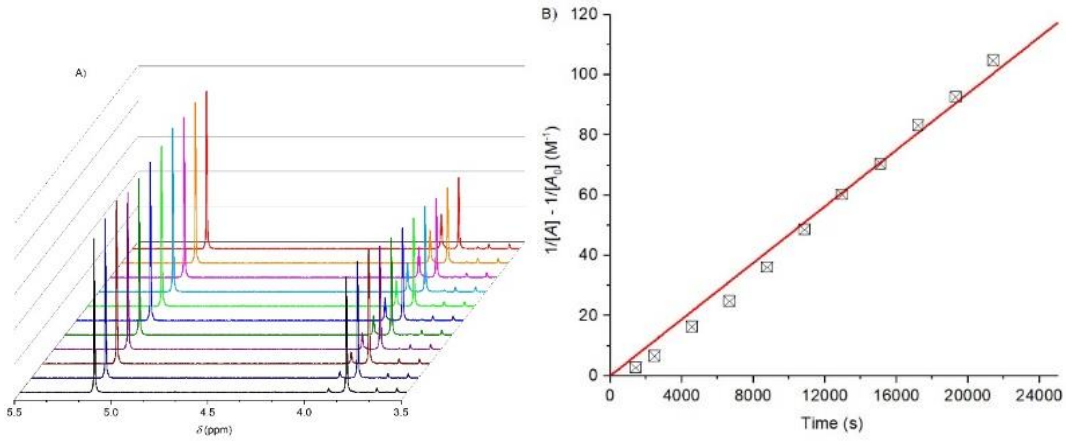

Figure 3.30: A) Changes in the 200 MHz ^{1}H NMR spectra of a mixture of platinum(II) azido complex **13** (6.7 mM), dimethyl acetylene dicarboxylate (DMAD, 6.7 mM), and 1,3,5-trioxane (6.7 mM) in DMSO-d_6 at room temperature with reaction time increasing from the black to the red trace for up to 6 h (front to back); **B)** linear fit of the change of the intensity of the DMAD methyl ester protons signal at 3.80 ppm to the second order rate law.

By relating the integral of the DMAD signal with that of the internal 1,3,5-trioxane standard at 5.12 ppm, the corresponding concentration of DMAD at different reaction time can be calculated. Then, upon linear fit of the change of the signal intensity *vs*. reaction time to the second-order rate law (**equation II**), a second-order rate constant of this reaction was determined as k_2 = (1.39 ± 0.04) M^{-1} s^{-1} (**Figure 3.29 B**). Similarly, the kinetics of the iClick reaction between platinum(II) terpy azido compound **13** and DMAD was studied by a similar method (**Figure 3.30 A**). This way, the second-order rate constant was obtained as k_2 = (4.7 ± 0.1) × 10^{-3} M^{-1} s^{-1} (**Figure 3.30 B**).

3.5.2 Study of the iClick kinetics of [M(N_3)(terpy)]PF_6 with F_3C-C≡C-COOEt

The iClick reaction of palladium(II) terpy azido compound **12** with the trifluoromethyl-substituted alkyne **17** is too fast to follow by NMR spectroscopy, as the alkyne signal had already completely disappeared in the first ^{19}F NMR spectrum recorded immediately after mixing of the two reactants. In the meantime, the combined integral of the two triazolate CF_3 group singlets at −58.51 and −58.65 ppm reached an intensity comparable to that of the hexafluorophosphate counter ion, which did not change any further upon extended incubation, indicating that the reaction is nearly complete on a very short timescale (**Figure 3.31**). An attempt was also made to slow down the reaction by decreasing the concentration of both precursors and minimizing the scan time of the NMR instrument, but still the alkyne signal was completely gone upon first measurement. However, from an estimate of the reaction half-time of the reaction of less than 3.5 min, a lower limit for the rate constant of k_2 > 1.41 M^{-1} s^{-1} can be estimated. Possibly, low-temperature NMR experiments will provide more accurate rates in the future.

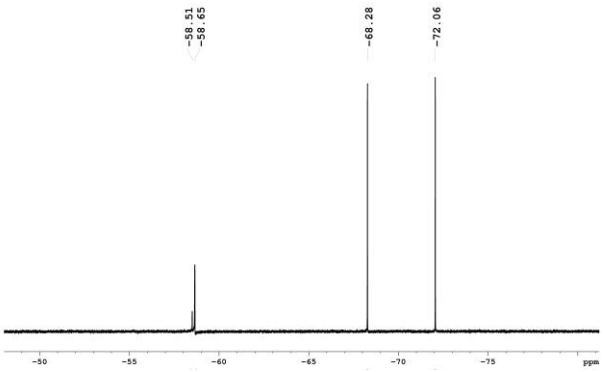

Figure 3.31: Initial ^{19}F NMR spectrum recorded immediately after mixing of palladium(II) azido complex **12** (6.7 mM) and F_3C-C≡C-COOEt (6.7 mM) in DMSO-d_6 at room temperature. Species observed are N1 triazolate at −58.51 ppm and N2 triazolate at −58.65 ppm. The doublet at −70.17 ppm is due to the hexafluorophosphate counter ion. Due to a lag time between mixing and recording of the first spectrum, this data was collected after 7 min.

In contrast, the iClick reaction of platinum(II) terpy azido compound **13** with the trifluoromethyl-substituted alkyne **17** proceeds much more slowly even at room temperature and therefore allowed determination of the rate constant by ^{19}F NMR spectroscopy. The intensity of the alkyne CF_3 peak at −50.94 ppm gradually decreased with increasing reaction time while two closely spaced singlets at −58.52 and −58.76 ppm appear, which are assigned to the N1 and N2 triazolates, respectively (**Figure 3.32 A**). By comparison of the integral of the CF_3 signal to that of the internal hexafluorophosphate standard, the concentration of the alkyne was calculated at different reaction times. The rate constant was obtained from the slope of the fit line as $k_2 = (6.2 \pm 0.4) \times 10^{-1}\ M^{-1}\ s^{-1}$ (**Figure 3.32 B**).

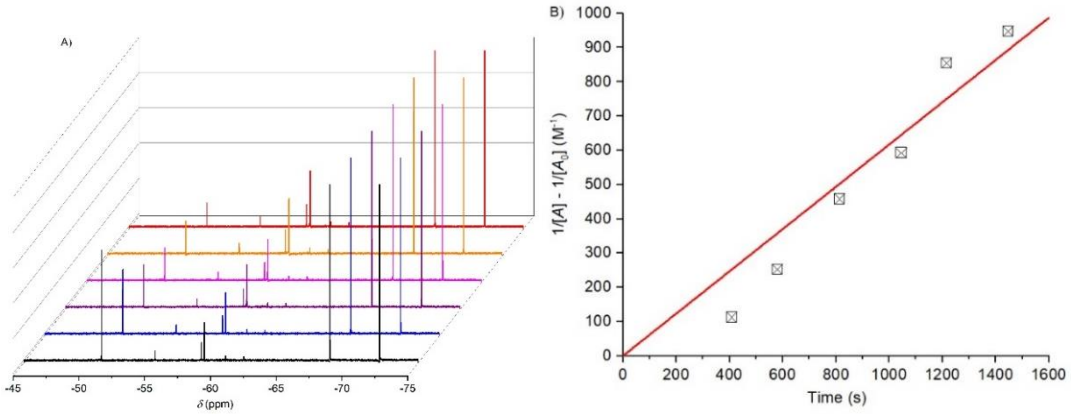

Figure 3.32: A) Changes in the 188 MHz ^{19}F NMR spectra of a mixture of platinum(II) azide complex **13** (6.7 mM) and F_3C-C≡C-COOEt (6.7 mM) in DMSO-d_6 at room temperature with reaction time increasing from 0–24 min (front to back); **B)** linear fit of the change of the intensity of the trifluoromethyl fluorine signal of alkyne at -50.94 ppm to the second order rate law. Due to a lag time between mixing of the reactants and recording of the first spectrum, no data was collected during the first 6 min.

3.5.3 Study of the iClick kinetics of [M(N3)(terpy)]PF6 with methyl propiolate

In all previous kinetic experiments as well as the preparative scale synthesis of triazolate complexes by iClick reaction, only internal alkynes R^1-C≡C-R^2 were utilized. However, for bioconjugation purposes, it would be beneficial to use terminal alkynes R-C≡C-H, as propiolic acid, propargyl alcohol, and proparglyamine are common building blocks in the CuAAC- or SPPAC-based modification of bio(macro)molecules. Therefore, in a small scale NMR tube experiment by mixing palladium(II) terpy azido complex **12** and methyl propiolate, slow but gradual decrease of methyl propiolate peaks together with some new signals are observed in the ^1H NMR spectrum, indicating azide **12** also shows reactivity with methyl propiolate. Therefore, the kinetics of this iClick reaction was studied by monitoring changes in the intensity of the alkyne methyl ester signal by ^1H NMR spectroscopy (**Figure**

3.33 A). During the reaction, the intensity of the methyl ester singlet at 3.73 ppm gradually decreased while two new peaks at 3.87 and 3.84 ppm grew in, which are assigned to the N1 and N2 triazolate products, respectively. The concentration of the terminal alkyne was determined for each time step by comparison of the integral of the alkyne methyl ester peak to that of the internal 1,3,5-trioxane standard at 5.12 ppm. By linear fit to the second-order rate law, the rate constant was obtained as $k_2 = (5.5 \pm 0.4) \times 10^{-4}$ M^{-1} s^{-1} (**Figure 3.33 B**).

The corresponding platinum(II) terpy azido complex **13** also showed reactivity towards methyl propiolate in a preliminary NMR experiment. Therefore, the kinetics of this reaction were studied by a procedure identical to that described in the preceeding section (**Figure 3.34 A**). From the slope of the linear fit, the second-order rate constant was determined as $k_2 = (6.6 \pm 0.2) \times 10^{-4}$ M^{-1} s^{-1} (**Figure 3.34 B**).

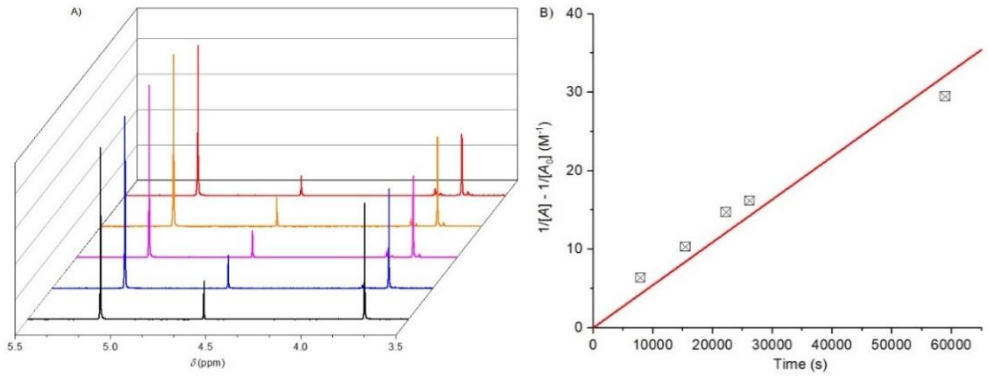

Figure 3.33: A) Changes in the 400 MHz ^{1}H NMR spectra of a mixture of palladium(II) azido complex **12** (6.7 mM), methyl propiolate (6.7 mM), and 1,3,5-trioxane (6.7 mM) in DMSO-d_6 at room temperature with reaction time increasing from the black to the red trace for up to 16.4 h (front to back); **B)** linear fit of the change of the intensity of the methyl ester protons signal at 3.73 ppm to the second order rate law.

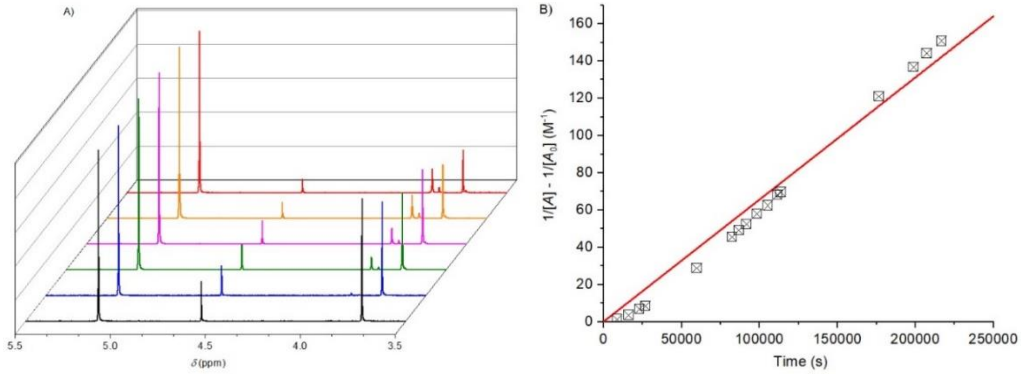

Figure 3.34: A) Changes in the 400 MHz ^{1}H NMR spectra of a mixture of platinum(II) azido complex **13** (6.7 mM), methyl propiolate (6.7 mM), and 1,3,5-trioxane (6.7 mM) in DMSO-d_6 at room temperature with reaction time increasing from the black to the red trace for up to 60.2 h (front to back); **B)** linear fit of the change of the intensity of the methyl ester protons signal at 3.73 ppm to the second order rate law.

3.5.4 Study of the iClick kinetics of [Pd(N3)(phbpy)] with internal alkynes

Palladium(II) azido compound **31** featuring the cyclometalating C^N^N coligand 6-phenyl-2,2'-bipyridine (phbpy) generally reacts too fast with internal alkynes such as DMAD **14** and 4,4,4-trifluoro-2-butynoic acid ethyl ester **17** to allow determination of the rate constant with NMR spectroscopy, as no signal of starting material was visible even in the very first ^{1}H or ^{19}F NMR spectra recorded. For example, in the first ^{19}F NMR spectrum recorded immediately after mixing azide **31**, trifluoromethyl-substituted alkyne **17**, and tetrabutyl ammonium hexafluorophosphate serving as an internal standard, only two main signals were observed (**Figure 3.35**). The singlet at −58.22 ppm is due to the N2 triazolate CF_3 group, while the doublet at −70.15 ppm arises from the hexafluorophosphate of the internal standard. No signal at around 52 ppm was observed, which is the spectral region in which the CF_3 alkyne signal should appear. Assuming a half-time of these reactions of less than 192.5 s, a lower limit for the rate constant of $k_2 > 4.0\ M^{-1}\ s^{-1}$ can be estimated for the iClick reaction of **31** with 4,4,4-trifluoro-2-butynoic acid ethyl ester **17**, while a similar approximation for the reaction of **31** with DMAD gave $k_2 > 4.2\ M^{-1}\ s^{-1}$.

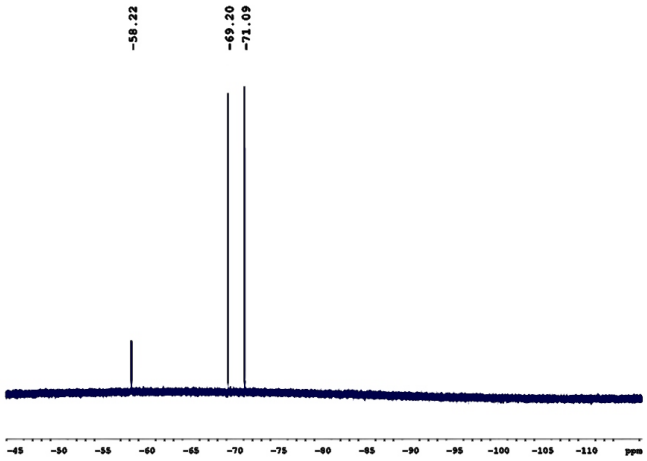

Figure 3.35: Initial ^{19}F NMR spectrum recorded immediately after mixing palladium(II) azido complex **31** (1.3 mM), 4,4,4-trifluoro-2-butynoic acid ethyl ester (1.3 mM), and tetrabutyl ammonium hexafluoro-phosphate (1.3 mM) in DMSO-d_6 at room temperature. Species observed are N2 triazolate at −58.22 ppm. The doublet at −70.15 ppm is due to the hexafluorophosphate internal standard. Due to a lag time between mixing of the reactants and recording of the first spectrum, this data was collected after 6 min.

3.5.5 Study of the iClick kinetics of [Pt(N3)(phbpy)] with internal alkynes

The iClick reaction of platinum(II) phbpy azido compound **32** with internal alkynes such as DMAD **14** and 4,4,4-trifluoro-2-butynoic acid ethyl ester **17** are also too fast to follow by NMR spectroscopy. For example, in a mixture of DMAD and 1,3,5-trioxane serving as the

internal standard in ^{1}H NMR experiments, two singlets are present at 5.11 and 3.81 ppm, due to the standard and the DMAD methyl ester groups (**Figure 3.36**). However, in the first ^{1}H NMR spectrum recorded immediately after mixing with metal azido complex **32**, the DMAD signal had already lost approx. 80% of its intensity. A new signal, which shows up at 3.86 ppm, is assigned to the resulting N2 triazolate, along with two singlets at 3.84 and 3.61 ppm, which would be expected for the additional presence of a non-symmetrically coordinated N1 isomer. Over the next 10–15 min, the DMAD signal fully disappeared. With the limited number of data points that can be recorded in this short time, due to the delay in recording consecutive NMR spectra, a valid linear fit is not possible. However, assuming a half-time of the reaction of less than 6.75 min, a lower limit for the rate constant is estimated, which gives $k_2 > 2.2\ M^{-1}\ s^{-1}$. Along the same lines, the rate constant of the iClick reaction of **32** with 4,4,4-trifluoro-2-butynoic acid ethyl ester **17** is estimated as $k_2 > 3.6\ M^{-1}\ s^{-1}$.

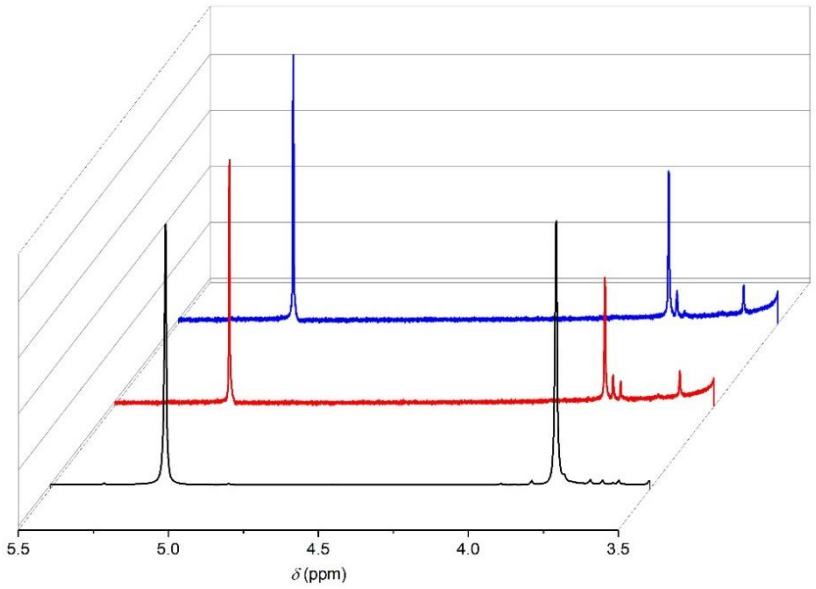

Figure 3.36: Changes in the 400 MHz ^{1}H NMR spectra of a mixture of platinum(II) azido complex **32** (1.2 mM), DMAD (1.2 mM), and 1,3,5-trioxane (1.2 mM) in DMSO-d_6 at room temperature. With increasing reaction time, the following spectra were recorded:black trace (0 min), red trace (8.5 min), and blue trace (13.5 min). For peak assignments, refer to the main text.

3.5.6 Study of the iClick kinetics of [M(N$_3$)(phbpy)] with methyl propiolate

Since palladium(II) phbpy azido complex **31** demonstrated high reactivity towards different internal alkynes, the kinetics of its reaction with methyl propiolate as one of the most simple terminal alkynes was also investigated. The terminal C≡C*H* proton signal was monitored by ^{1}H NMR spectroscopy, as this signal experiences a significant shift in the triazolate product. Over the course of the reaction, the intensity of the terminal C≡C*H* proton signal at 4.57 ppm

gradually decreased (**Figure 3.37 A**), while a new signal of the triazolate H5 gain intensity in the aromatic range, but overlaps with signals of the phbpy ligand backbone. By comparison of the C≡C*H* peak integral to that of the 1,3,5-trioxane reference at 5.12 ppm, the concentration of methyl propiolate was calculated at different reaction times. From a linear fit to the second-order rate law, the second-order rate constant was obtained as k_2 = (7.7 ± 0.3) × 10^{-3} M^{-1} s^{-1} (**Figure 3.37 B**). By a similar method, the rate constant for the iClick reaction of the corresponding platinum(II) phbpy azido complex **32** with methyl propiolate was obtained as k_2 = (5.6 ± 0.3) × 10^{-3} M^{-1} s^{-1} (**Figure 3.38**).

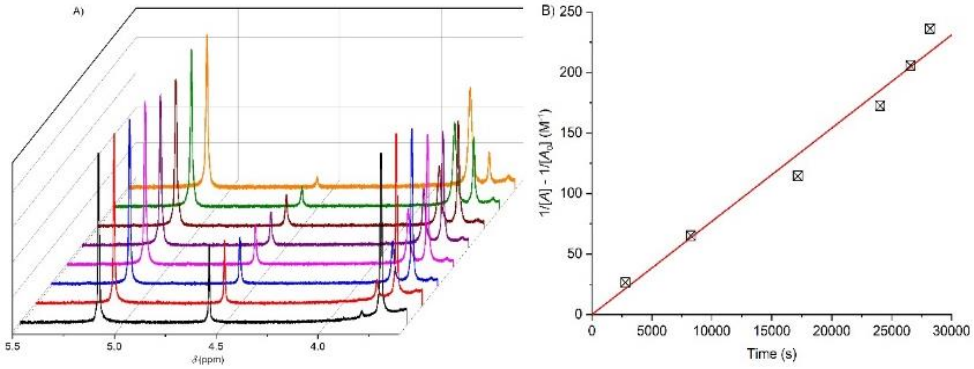

Figure 3.37: A) Changes in the 400 MHz ^{1}H NMR spectra of a mixture of palladium(II) azido complex **31** (4.2 mM), methyl propiolate (4.2 mM), and 1,3,5-trioxane (4.2 mM) in DMSO-d_6 at room temperature with reaction time increasing from the black to the orange trace over 8 h (front to back); **B)** linear fit of the change of the intensity of the terminal C≡C*H* proton signal at 4.57 ppm to the second order rate law.

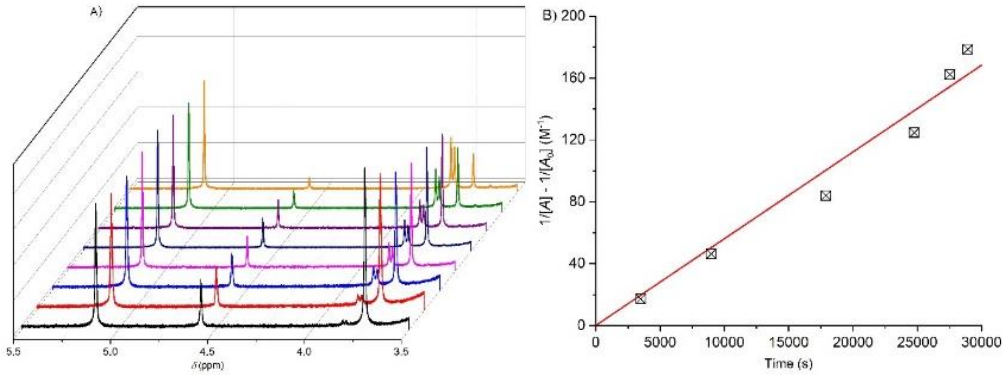

Figure 3.38: A) Changes in the 400 MHz ^{1}H NMR spectra of a mixture of platinum(II) azido complex **32** (3.8 mM), methyl propiolate (3.8 mM), and 1,3,5-trioxane (3.8 mM) in DMSO-d_6 at room temperature with reaction time increasing from the black to the orange trace over 8 h (front to back); **B)** Linear fit of the change of the intensity of the terminal C≡C*H* proton signal at 4.57 ppm to the second order rate law.

3.5.7 Study of the iClick kinetics of [Pd(N$_3$)(pht)] with internal alkynes

The iClick reaction of palladium(II) pht azido compound **41** with internal alkynes DMAD **14**, DEAD **15**, 2-butynedioic acid 1,4-bis(2-methoxyethyl) ester **16**, and 4,4,4-trifluoro-2-butynoic acid ethyl ester **17** were generally too fast to determine the rate constant by NMR

spectroscopy, as no signal of starting materials was observed already in the first ^{1}H or ^{19}F NMR spectrum recorded as soon as possible after mixing of the reactants. For example, in the first ^{19}F NMR spectrum obtained immediately after combination of metal azido complex **41**, 4,4,4-trifluoro-2-butynoic acid ethyl ester **17**, and tetrabutyl ammonium hexafluorophosphate as the internal standard, only two signals were observed which are due to the N2 triazolate product and the hexafluorophosphate anion from the standard added (**Figure 3.39**). In particular, no signal was found at around −52 ppm, indicating that the CF_3-substituted alkyne was already completely consumed at this time. Assuming a half-time for the reaction of less than 1.5 min, only a lower limit for the rate constant was estimated, which gave $k_2 > 3.7\ M^{-1}\ s^{-1}$ for the iClick reaction of **41** with CF_3-substituted alkyne **17**, and $k_2 > 0.8\ M^{-1}\ s^{-1}$ for the iClick reactions of **41** with the other ester-substituted alkynes **14**−**16**.

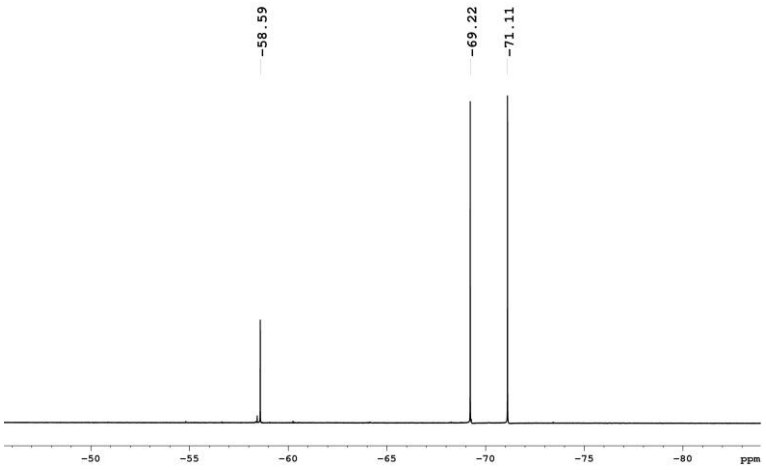

Figure 3.39: ^{19}F NMR spectrum recorded immediately after mixing palladium(II) azido complex **41** (3.0 mM), 4,4,4-trifluoro-2-butynoic acid ethyl ester (3.0 mM), and tetrabutyl ammonium hexafluorophosphate (3.0 mM) in DMSO-d_6 at room temperature. Species observed are N2 triazolate at −58.59 ppm. The doublet at −70.17 ppm is due to the hexafluorophosphate internal standard. Note a lag time of 3 min between mixing of the reactants and recording of the spectrum.

3.5.8 Study of the iClick kinetics of [Pt(N_3)(pht)] with internal alkynes

The reaction of platinum(II) pht azido compound **42** with CF_3-substituted alkyne **17** was studied by ^{19}F NMR spectroscopy, as it provides much less background signals (**Figure 3.40**). However, already in the first spectrum recorded immediately after mixing of the two reactants, the signal of the CF_3-substituted alkyne had already substiantially lost intensity and signals of intermediates as well as the expected triazolate products were observed. Upon further incubation, the alkyne signal fully disappeared. Due to the limited number of data points, no useful linear fit was possible. However, assuming a half-time of the reaction of less than 5.25 min, a lower limit for the rate constant was estimated as $k_2 > 0.6\ M^{-1}\ s^{-1}$.

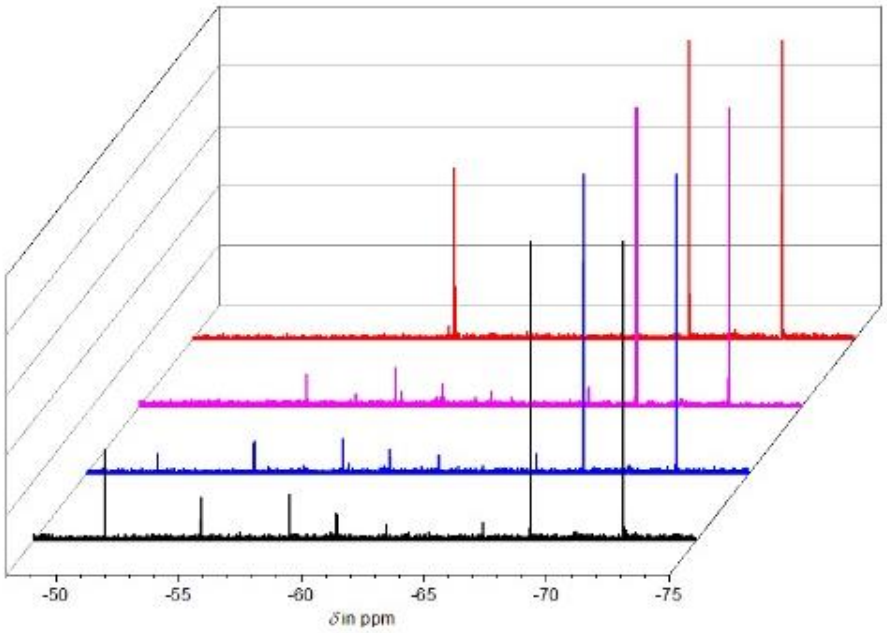

Figure 3.40: Changes in the 188 MHz ^{1}H NMR spectra of a mixture of platinum(II) azido complex **42** (5.0 mM), 4,4,4-trifluoro-2-butynoic acid ethyl ester (5.0 mM), and tetrabutyl ammonium hexafluorophosphate (5.0 mM) in DMSO-d_6 at room temperature with reaction time increasing from front to back: black trace (3.5 min), blue trace (7 min), magenta trace (10.5 min), red trace (20.5 h).

In the iClick reaction of platinum(II) pht azido compound **42** and DMAD, the signal of the DMAD methyl ester protons was monitored by ^{1}H NMR spectroscopy. With increasing reaction time, the intensity of the singlet at 3.81 ppm gradually decreased while a new peak appeared at 3.83 ppm, which is due to the N2 triazolate methyl ester groups (**Figure 3.41 A**). A comparison of the integral of the DMAD singlet to that of the internal 1,3,5-trioxane standard at 5.12 ppm, the concentration of DMAD at different reaction times was calculated. The second-order rate constant was obtained from a linear fit to the proper rate law as k_2 = (7.7 ± 0.1) × 10^{-2} M^{-1} s^{-1} (**Figure 3.41 B**). In the iClick reaction of platinum(II) pht azido compound **42** with DEAD, the singlet of the methyl group of azide pht ligand backbone at 2.45 ppm was monitored by ^{1}H NMR spectroscopy. With increasing reaction time, the intensity of this signal gradually decreased while a new singlet at 2.59 ppm assigned to the N2 triazolate grew in (**Figure 3.42 A**). Comparison of the integral of the singlet at 2.45 ppm to that of the internal 1,3,5-trioxane reference at 5.12 ppm allowed the concentration of the azido compound be calculated at different reaction times. From a linear fit to the second-order rate law, k_2 = (3.4 ± 0.1) × 10^{-2} M^{-1} s^{-1} was obtained (**Figure 3.42 B**). The iClick reaction of **42** with ethylene glycol-substituted alkyne **16** was studied by similar methodology and the rate constant determined as k_2 = (3.0 ± 0.2) × 10^{-2} M^{-1} s^{-1} (**Figure 3.43**).

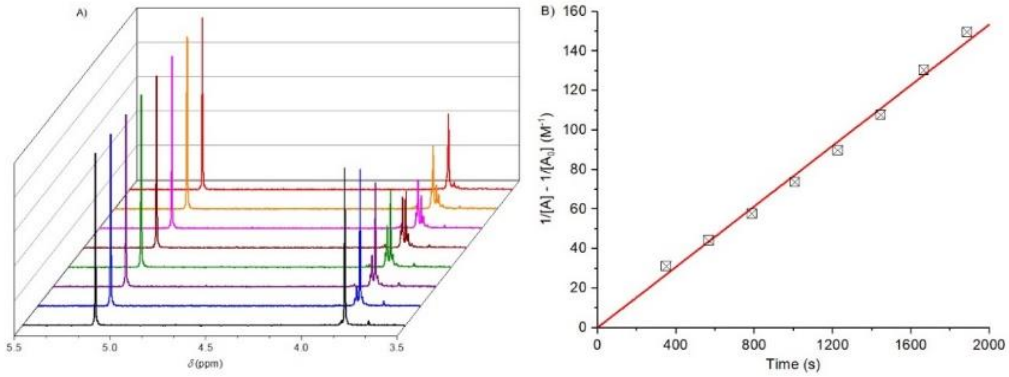

Figure 3.41: A) Changes in the 200 MHz ^{1}H NMR spectra of a mixture of platinum(II) azido complex **42** (6.0 mM), DMAD (6.0 mM), and 1,3,5-trioxane (6.0 mM) in DMSO-d_6 at room temperature with reaction time increasing from the black to the red trace over 20 h (front to back); **B)** Linear fit of the change of the intensity of the DMAD methyl ester protons signal at 3.81 ppm to the second order rate law.[143]

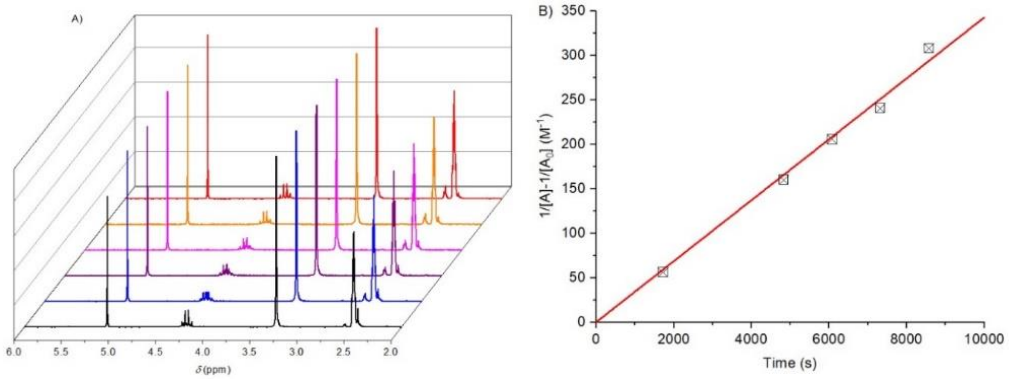

Figure 3.42: A) Changes in the 200 MHz ^{1}H NMR spectra of a mixture of platinum(II) azido complex **42** (6.7 mM), DEAD (6.7 mM), and 1,3,5-trioxane (6.7 mM) in DMSO-d_6 at room temperature with reaction time increasing from the black to the red trace over 2.4 h (from to back); **B)** Linear fit of the change of the intensity of the semithiocarbazone methyl group signal at 2.45 ppm to the second order rate law.[143]

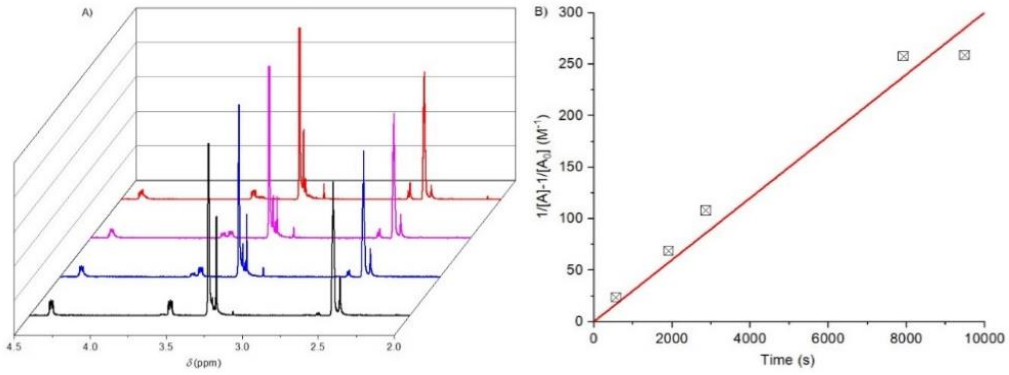

Figure 3.43: A) Changes in the 400 MHz ^{1}H NMR spectra of a mixture of platinum(II) azido complex **42** (6.7 mM), **2**-butynedioic acid 1,4-bis(2-methoxyethyl) ester (6.7 mM), and 1,3,5-trioxane (6.7 mM) in DMSO-d_6 at room temperature with reaction time increasing from the black to the red trace over 2.6 h (front to back); **B)** Linear fit of the change of the intensity of the semithiocarbazone methyl group signal at 2.45 ppm to the second order rate law.[143]

3.5.9 Study of the iClick kinetics of [M(N3)(pht)] with methyl propiolate

As the palladium(II) pht azido complex **41** exhibited a very high reactivity towards the internal alkynes tested, the kinetics of the reaction of this azido complex with methyl propiolate as a prototypical terminal alkyne was also studied by ^{1}H NMR spectroscopy (**Figure 3.44 A**). With increasing incubation time, the singlet of alkyne methyl ester protons at 3.73 ppm gradually decreased in intensity while two new peaks appeared at 3.79 ppm and 3.78 ppm which are assigned to the N1 and N2 triazolate methyl ester protons, respectively.

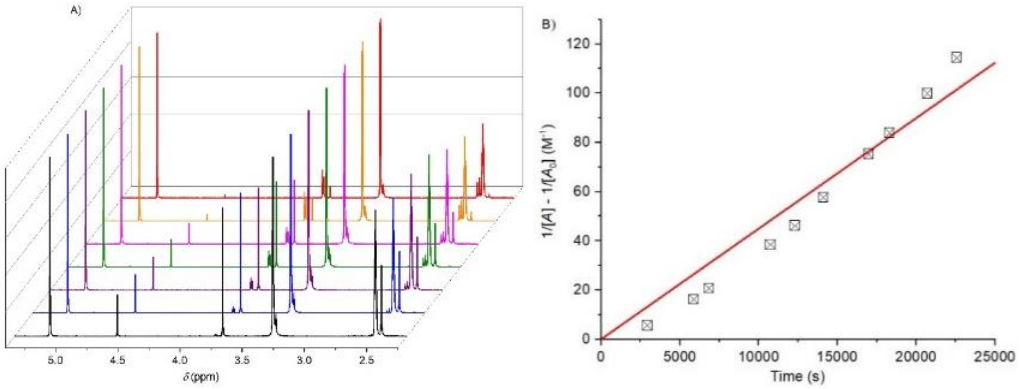

Figure 3.44: A) Changes in the 400 MHz ^{1}H NMR spectra of a mixture of palladium(II) azido complex **41** (6.7 mM), methyl propiolate (6.7 mM), and 1,3,5-trioxane (6.7 mM) in DMSO-d_6 at room temperature with reaction time increasing from the black to the red trace over 6.3 h (front to back); **B)** Linear fit of the change of the intensity of the methyl ester proton signal at 3.73 ppm with increasing reaction time.

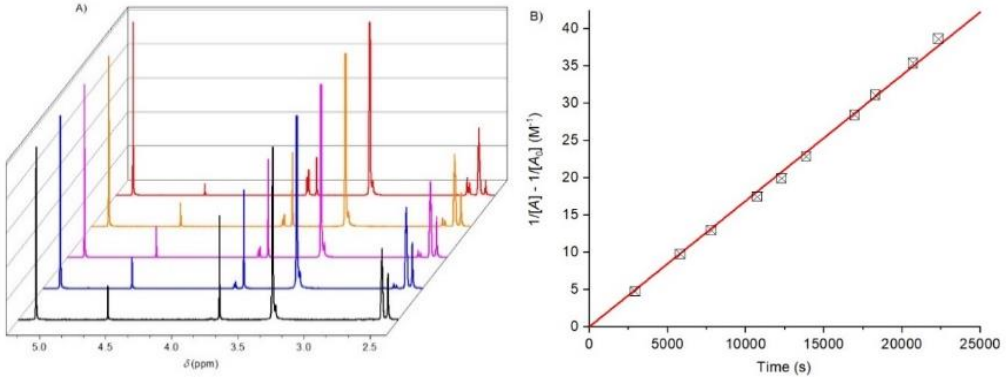

Figure 3.45: A) Changes in the 400 MHz ^{1}H NMR spectra of a mixture of platinum(II) azido complex **42** (10 mM), methyl propiolate (10 mM), and 1,3,5-trioxane (10 mM) in DMSO-d_6 at room temperature with reaction time increasing from the black to the red trace over 6.2 h (front to back); **B)** Linear fit of the change of the intensity of the methyl ester proton signal at 3.73 ppm with increasing reaction time.

Comparison of the integral of the alkyne methyl ester group peak to that of 1,3,5-trioxane serving as the internal standard at 5.12 ppm, the concentration of the terminal alkyne was calculated at different reaction times. The second-order rate constant of this reaction was then obtained as $k_2 = (4.5 \pm 0.2) \times 10^{-3}$ M^{-1} s^{-1} from a linear fit to the corresponding rate law (**Figure 3.44 B**). In a similar way, the second-order rate constant for the iClick reaction of platinum(II) pht azido complex **42** with methyl propiolate was determined as $k_2 = (1.69 \pm 0.01) \times 10^{-3}$ M^{-1} s^{-1} (**Figure 3.45**).

3.5.10 Study of the iClick kinetics of [Pt(bodipy)(N_3)(PEt_3)$_2$] with DMAD

The kinetics of the iClick reaction of platinum(II)-BODIPY azido compound **55** with DMAD was monitored from changes in the intensity of the signal of the DMAD methyl ester protons at 3.85 ppm by ^{1}H NMR spectroscopy (**Figure 3.46 A**). With increasing reaction time, the intensity of this signal gradually decreased while a new singlet at 3.94 ppm due to the N2 triazolate methyl ester groups slowly grew in. From the ratio of the integral of the DMAD singlet relative to that of the internal 1,3,5-trioxane reference at 5.16 ppm, the concentration of DMAD was calculated at different reaction times. The rate constant was obtained from the slope of the fit line as $k_2 = (2.46 \pm 0.02) \times 10^{-3}$ M^{-1} s^{-1} (**Figure 3.46 B**). The kinetic of its reaction with DMAD was also studied by ^{31}P NMR spectroscopy (**Figure 3.47 A**). The triethylphosphine signal shows up as a singlet with two Pt satellites at 13.45 ppm. During the reaction, the intensity of this peak gradually decreased while another singlet at 10.98 ppm resulting from the triazolate complex phosphine ligands gradually gained in intensity. The second order rate constant was obtained as $k_2 = (3.50 \pm 0.21) \times 10^{-3}$ M^{-1} s^{-1}, which is in line with the value determined by ^{1}H NMR spectroscopy (**Figure 3.47 B**).

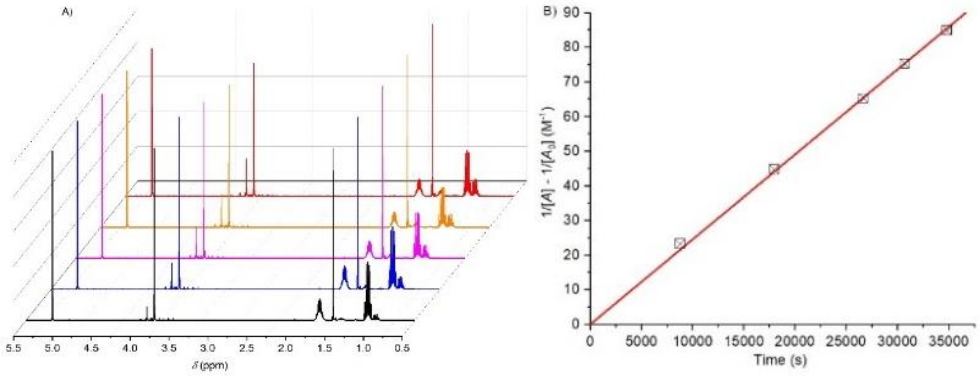

Figure 3.46: A) Changes in the 400 MHz ^{1}H NMR spectra of a mixture of platinum(II) azido complex **55** (5 mM), DMAD (5 mM), and 1,3,5-trioxane (5 mM) in $CDCl_3$ at room temperature with reaction time increasing from the black to the red trace over 9.7 h; **B)** Linear fit of the change of the intensity of the DMAD methyl ester protons signal at 3.85 ppm with increasing reaction time.

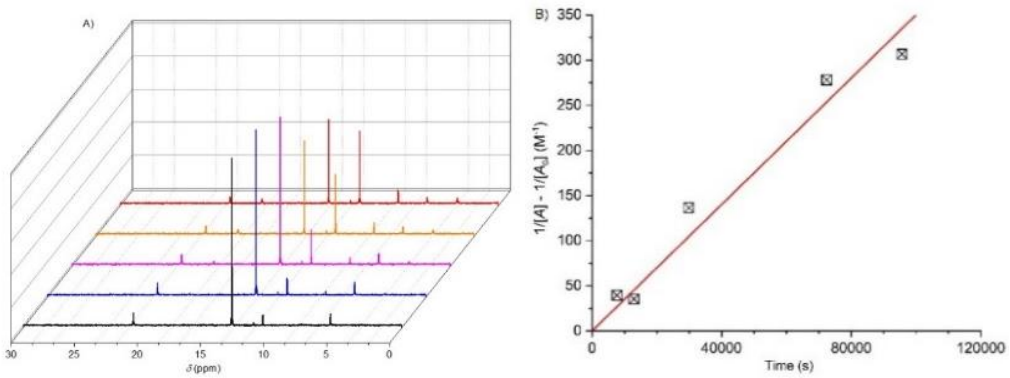

Figure 3.47: A) Changes in the 162 MHz ^{31}P NMR spectra of a mixture of platinum(II) azido complex **55** (4.8 mM), DMAD (4.8 mM), and tetrabutyl ammonium hexafluorophosphate (4.8 mM) in $CDCl_3$ at room temperature with reaction time increasing from the black to the red trace over 26.6 h; **B)** Linear fit of the change of the intensity of the triethylphosphine signal at 13.45 ppm with increasing reaction.

3.5.11 Study of the iClick kinetics of [Pt(bodipy)(N$_3$)(PEt$_3$)$_2$] with F$_3$C-C≡C-COOEt

In the iClick reaction of platinum(II) BODIPY azido compound **55** with trifluoromethyl-substituted alkyne **17**, the alkyne CF_3 group signal was monitored by ^{19}F NMR spectroscopy (**Figure 3.48 A**). During the reaction, the signal at −52.09 ppm gradually decreased in intensity while a new singlet at −59.80 ppm due to the triazolate CF_3 group grew in. From a comparison of the integral of the alkyne CF_3 signal to that of the doublet of hexafluorophosphate serving as an internal standard, the concentration of the alkyne was calculated at different reaction timesFrom a linear fit to the proper rate law, the second-order rate constant was obtained as $k_2 = (5.04 \pm 0.19) \times 10^{-3}$ M^{-1} s^{-1} (**Figure 3.48 B**).

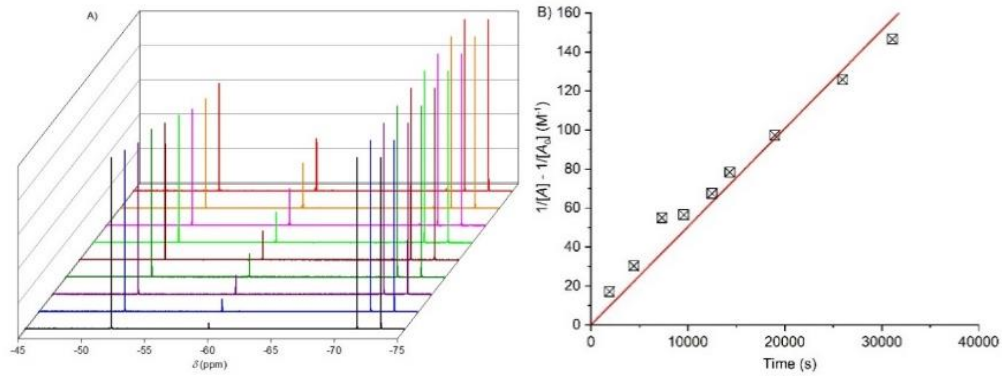

Figure 3.48: A) Changes in the 377 MHz ^{19}F NMR spectra of a mixture of platinum(II) azido complex **55** (5 mM), 4,4,4-trifluoro-2-butynoic acid ethyl ester (5 mM), and tetrabutyl ammonium hexafluorophosphate (5 mM) in $CDCl_3$ at room temperature with reaction time increasing from the black to the red trace over 8.6 h (front to back); **B)** Linear fit of the change of the intensity of the trifluoromethyl fluorine signal of the alkyne at -52.09 ppm with increasing reaction time to the second order rate law.[145]

The kinetics of this iClick reaction was also studied by ^{31}P NMR spectroscopy, as described above, with the rate constant determined as $k_2 = (6.01 \pm 0.64) \times 10^{-3}\ M^{-1}\ s^{-1}$, which is in good accordance with the value obtained by ^{19}F NMR spectroscopy (**Figure 3.49**).

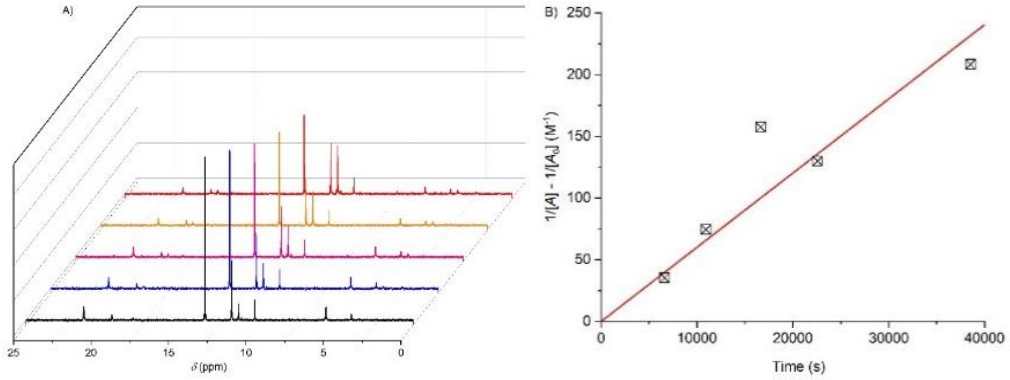

Figure 3.49: A) Changes in the 162 MHz ^{31}P NMR spectra of a mixture of platinum(II) azido complex **55** (4.8 mM), DMAD (4.8 mM), and tetrabutyl ammonium hexafluorophosphate (4.8 mM) in $CDCl_3$ at room temperature with reaction time increasing from the black to the red trace over 10.7 h (front to back); **B)** Linear fit of the change of the intensity of azide **55** triethylphosphine signal at 13.45 ppm with increasing reaction time to the second order rate law.[145]

3.5.12 Influences of the metal center, alkyne, and coligand on the rate constant of the iClick reaction

The extensive kinetic studies described in the previous sections allow general reactivity trends to be identified by correlation of the different rate constants to structural and electronic features (**Table 3.3**). First of all, palladium(II) azido complexes are generally much more reactive than their platinum(II) analogues in all systems studied. This is possibly due to the greater charge density on palladium(II) relative to platinum(II), which leads to the palladium-coordinated azido ligand to be more strongly polarized and thus facilitating attack of the alkyne.[146] A similar trend, with a higher reactivity of 4d metal complexes compared to their 5d analogues, was also previously described for molybdenum(II) *vs*. tungsten(II) allyl dicarbonyl compounds.[83] Furthermore, the CF_3-substituted alkyne **17** consistently reacts much faster than the ester-substituted alkynes **14 − 16**. This is due to the stronger electron-withdrawing nature of the trifluoromethyl group, which renders this alkyne more electron-deficient. In contrast to the internal alkynes of general structure R^1-C≡C-R^2, methyl propiolate as a prototypical terminal alkyne exhibited a significantly lower reactivity than all other dipolarophiles studied.

In addition, the rate constant also strongly depends on the nature of the tridentate coligand completing the coordination sphere of the metal center. Compounds with the cyclometalating 6'-phenyl-2,2'-bipyridine (phbpy) ligand, which provides a C^N^N donor set, consistently exhibited higher rate constants than complexes with a S^N^N or N^N^N ligand environment, as provided by *N*-phenyl-2-[1-(2-pyridinyl)ethylidene]hydrazine carbothioamide (pht) and 2,2':6',2"-terpyridine (terpy). Thus, the rate constant increases with the coligand donor set in the order N^N^N < S^N^N < C^N^N. For example, the iClick reaction of dimethyl acetylenedicarboxylate (DMAD) with [Pt(N_3)(phbpy)] proceeds about two orders of magnitude faster than the one with [Pt(N_3)(pht)] and three orders of magnitude faster than that of [Pt(N_3)(terpy)]$^+$. Since the pyridine groups increase the electrophilicity of the metal centre through π-back donation from the metal to the empty anti- or nonbonding π-orbitals of the heteroaromatic subunits, the terpy-coordinated metal centre is expected to be more electrophilic and thus the attached azido ligand has a weaker electron-releasing ability compared to the phbpy and pht coligands.[147]

To sum up, faster reaction kinetics are favored by a greater charge density on the metal centre (Pd(II) > Pt(II)), alkynes with strong electron-withdrawing substituents (CF_3 > COOR), and coligands with a strong electron-donating power (phbpy > pht > terpy). Although difficult

to compare to the other systems due to the presence of four monodentate ligands and a $Pt(C)(N)(P)_2$ coordination sphere, iClick reactions of the BODIPY complex revealed the slowest reaction kinetics among all compounds studied. Furthermore, in this system, the trifluoromethyl-substituted alkyne F_3C-C≡C-COOEt reacts "only" two times faster than DMAD, in contrast to the other compounds, in which at least one order of magnitude differences were observed between the "CF_3" alkyne and DMAD.

Table 3.3: Second order rate constants k_2 determined for the iClick reactions studied in this work.

Metal	Coligand	R_1-C≡C-R_2	Rate constant k_2 (M^{-1} s^{-1})
Pd	terpy	CF_3, COOEt	> 1.4
Pt	terpy	CF_3, COOEt	$(6.2 \pm 0.4) \times 10^{-1}$
Pd	terpy	$COOCH_3$, $COOCH_3$	1.39 ± 0.04
Pt	terpy	$COOCH_3$, $COOCH_3$	$(4.7 \pm 0.1) \times 10^{-3}$
Pd	terpy	H, $COOCH_3$	$(5.5 \pm 0.4) \times 10^{-4}$
Pt	terpy	H, $COOCH_3$	$(6.6 \pm 0.2) \times 10^{-4}$
Pd	phbpy	CF_3, COOEt	> 4.0
Pt	phbpy	CF_3, COOEt	> 3.6
Pd	phbpy	$COOCH_3$, $COOCH_3$	> 4.2
Pt	phbpy	$COOCH_3$, $COOCH_3$	> 2.2
Pd	phbpy	H, $COOCH_3$	$(7.7 \pm 0.3) \times 10^{-3}$
Pt	phbpy	H, $COOCH_3$	$(5.6 \pm 0.1) \times 10^{-3}$
Pd	pht	CF_3, COOEt	> 3.6
Pt	pht	CF_3, COOEt	$> 6.0 \times 10^{-1}$
Pd	pht	$COOCH_3$, $COOCH_3$	$> 8.0 \times 10^{-1}$
Pt	pht	$COOCH_3$, $COOCH_3$	$(7.7 \pm 0.1) \times 10^{-2}$
Pd	pht	COOEt, COOEt	$> 8.0 \times 10^{-1}$
Pt	pht	COOEt, COOEt	$(3.4 \pm 0.1) \times 10^{-2}$
Pd	pht	$COOCH_2CH_2OCH_3$, $COOCH_2CH_2OCH_3$	$> 8.0 \times 10^{-1}$
Pt	pht	$COOCH_2CH_2OCH_3$, $COOCH_2CH_2OCH_3$	$(3.0 \pm 0.2) \times 10^{-2}$
Pd	pht	H, $COOCH_3$	$(4.5 \pm 0.2) \times 10^{-3}$
Pt	pht	H, $COOCH_3$	$(1.69 \pm 0.01) \times 10^{-3}$
Pt	bodipy	CF_3, COOEt	$(5.0 \pm 0.2) \times 10^{-3}$
Pt	bodipy	$COOCH_3$, $COOCH_3$	$(2.46 \pm 0.02) \times 10^{-3}$

3.5.13 Comparison of iClick rate constants with those of established click reactions

Although the catalyst-free iClick reaction has been established for about 20 different metallic elements, to the best of our knowledge, only a few kinetic studies have been reported for these systems so far, which were mainly focused on molybdenum(II), tungsten(II), ruthenium(II), rhodium(III), and gold(I) complexes. The rate constants found in the literature after an extensive search are collected in **Table 3.4**. They cover a range of 10^{-4} to 10^{-2} M^{-1} (or M^{-1} s^{-1}). Thus, the palladium(II) iClick reactions reported in this work are significantly faster than all previously reported ones and even reactions of the analogous platinum(II) compounds, although slower than palladium(II) ones, are also faster than most other iClick reactions reported so far.

Table 3.4: Rate constants reported for iClick reactions in the literature.

Metal azido compound	Alkyne	Rate constant	Reference
$[Mo(\eta^3\text{-allyl})(N_3)(bpy)(CO)_2]$	$H_3COOC\text{-}C{\equiv}C\text{-}COOCH_3$	$(1.6 \pm 0.1) \times 10^{-3}\ s^{-1}$	[83]
$[Mo(\eta^3\text{-allyl})(N_3)(bpy)(CO)_2]$	$F_3C\text{-}C{\equiv}C\text{-}COOEt$	$(6.5 \pm 0.1) \times 10^{-3}\ s^{-1}$	[83]
$[W(\eta^3\text{-allyl})(N_3)(bpy)(CO)_2]$	$H_3COOC\text{-}C{\equiv}C\text{-}COOCH_3$	$(0.4 \pm 0.1) \times 10^{-3}\ s^{-1}$	[83]
$[W(\eta^3\text{-allyl})(N_3)(bpy)(CO)_2]$	$F_3C\text{-}C{\equiv}C\text{-}COOEt$	$(2.5 \pm 0.1) \times 10^{-3}\ s^{-1}$	[83]
$[Ru(N_3)(bpcd)(tt)]$	BCN	$2.7 \times 10^{-4}\ M^{-1}\ s^{-1}$	[96]
$[Ru(N_3)(bpcd)(tt)]$	ADIBO	$6.9 \times 10^{-2}\ M^{-1}\ s^{-1}$	[96]
$[Rh(Cp^*)(N_3)(bpy)]CF_3SO_3$	$F_3C\text{-}C{\equiv}C\text{-}COOEt$	$(2.44 \pm 0.01) \times 10^{-3}\ s^{-1}$	[105]
$[Rh(Cp^*)(N_3)(bpy^{OCH3,OCH3})]CF_3SO_3$	$F_3C\text{-}C{\equiv}C\text{-}COOEt$	$(3.75 \pm 0.01) \times 10^{-3}\ s^{-1}$	[105]
$[Au(N_3)(PPh_3)]$	$Ph_3P\text{-}Au\text{-}C{\equiv}C\text{-}C_6H_5NO_2$	$7.6 \times 10^{-3}\ M^{-1}\ s^{-1}$	[120]

The rate constants of most of the well-established click reactions reported so far are in the range of 10^{-4} to 10^{2} M^{-1} s^{-1}. The fastest coupling rates observed are those of photoclick reactions ($10 - 60$ M^{-1} s^{-1}) and the latest-generation copper-catalyzed azide-alkyne cycloadditions (CuAAC, $10 - 200$ M^{-1} s^{-1}). Somewhat slower kinetics are reported for the Staudinger ligation ($3.0 \times 10^{-4} - 8.0 \times 10^{-3}$ M^{-1} s^{-1}) and the strain-promoted azide-alkyne cycloaddition (SPAAC, $1.2 \times 10^{-3} - 4.0$ M^{-1} s^{-1}). Thus, the iClick reaction rate constants determined for the palladium(II) azido complexes in this work proceed on a timescale comparable to fast photoclick reactions and approach those of some advanced copper-catalyzed azide-alkyne cycloadditions (CuAAC). The rate constants of the corresponding

platinum(II) azido complexes cover a wider range ($10^{-3} - 10^{1}$ M^{-1} s^{-1}) which depend on the nature of the coligands as well as alkyne coupling partners, and therefore, general trends are more difficult to identify. In general, the iClick reaction kinetics determined for the palladium(II) and platinum(II) azido complexes studied in this project compare well with established literature procedures and hold great promise for applications in bioconjugation in the future (**Figure 3.50**).

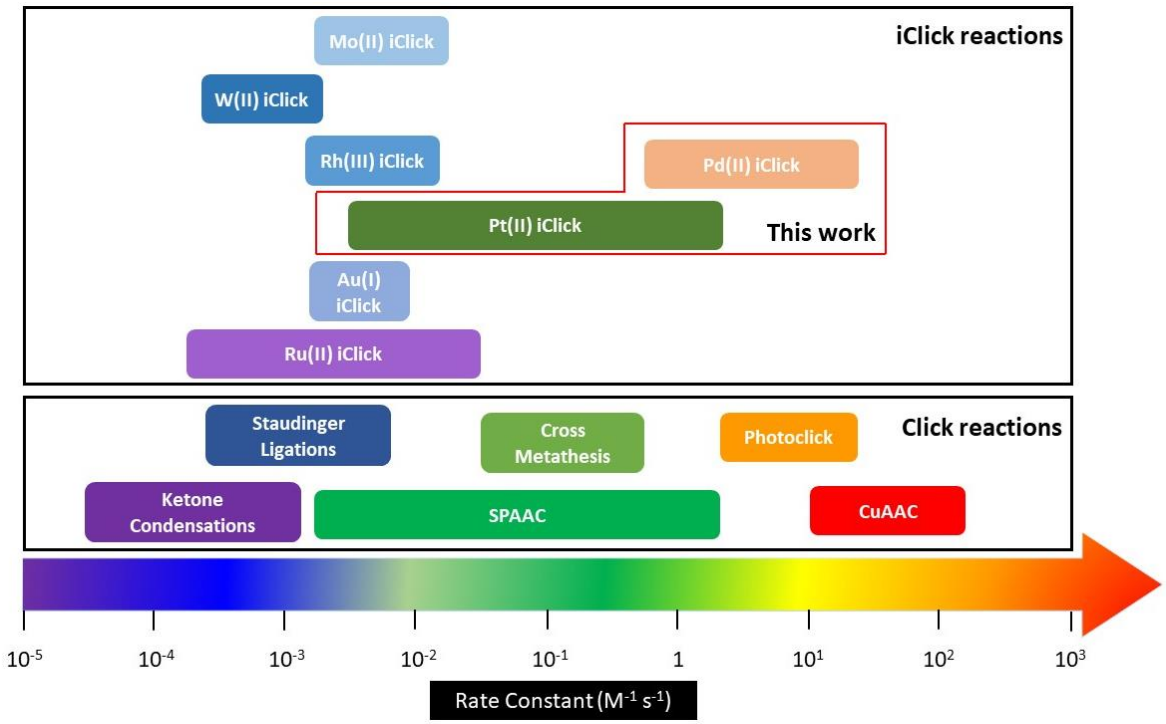

Figure 3.50: Comparison of the rate constants of the iClick reactions studied in this work to common reactions reported in the literature.

3.6 Synthesis and X-ray crystal structure of [Au(N3)3(terpy-κ^1-N^1)]

In order to compare the rate constants of iClick reactions based on palladium(II) and platinum(II), an attempt was also made to synthesize an isoelectronic gold(III) species, which should also feature a square planar coordination geometry and low-spin d^8 electronic configuration. As one of the most common tridentate ligands, 2,2':6',2"-terpyridine (terpy) was applied in this work. In the first step, the chlorido precursor [AuCl(terpy)]Cl_2 **59** was synthesized by reaction of potassium tetrachloroaurate(III) with terpy in a mixture of water and acetonitrile under reflux for 44 h. Then, following a standard procedure, an excess of sodium azide was added to the clear yellow solution of **59** in water and stirred at 60 °C for 4 h to give an orange precipitate. **(CAUTION) This material turned out to be rather unstable, as it exploded upon scratching with a metal spatula.** Still, recrystallization by slow diffusion of diethyl ether into a clear orange acetone solution of the product produced an orange block-like crystal which was suitable for single crystal X-ray diffraction. However, the X-ray crystal structure revealed that instead of the intended cproduct $[Au(N_3)(terpy)]^{2+}$, an unexpected gold(III) triazido compound [Au(N3)3(terpy-κ^1-N^1)] **60** was formed, in which the terpy ligand is in a highly unusual monodentate coordination mode (**Scheme 3.14**).

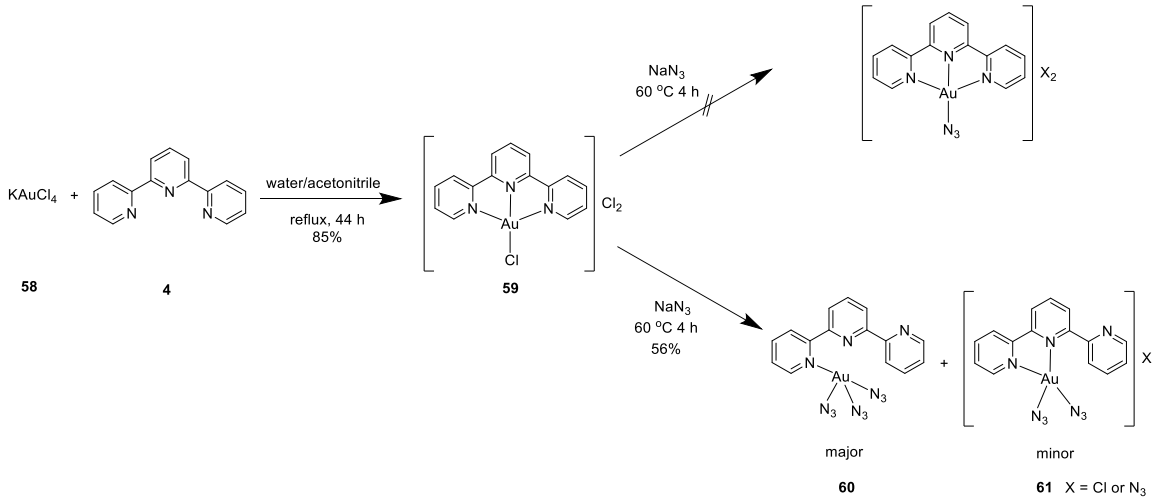

Scheme 3.14: Formation of the unexpected gold(III) triazido compound **60** with a monodentate terpy coligand instead of the intended product $[Au(N_3)(terpy)]^{2+}$.[148] In addition to the gold(III) triazido complex **60** characterized by X-ray diffraction, ^1H and ^{13}C NMR spectra also point to the presence of a minor species of bisazido complex **61** in solution.

3.6.1 IR spectroscopy

In the IR spectrum of **60**, a strong and broad signal at 2014 cm^{-1} is characteristic of a coordinated azido group (**Figure 3.51**). The weak intensity band around 3091 cm^{-1} is due to the aromatic C-H stretches of the pyridine rings, whereas the peaks between 1400 and 1600 cm^{-1} are attributed to aromatic C=C and C=N stretches. Two signals at 766 and 750 cm^{-1} are attributed to the aromatic C-H bending modes.

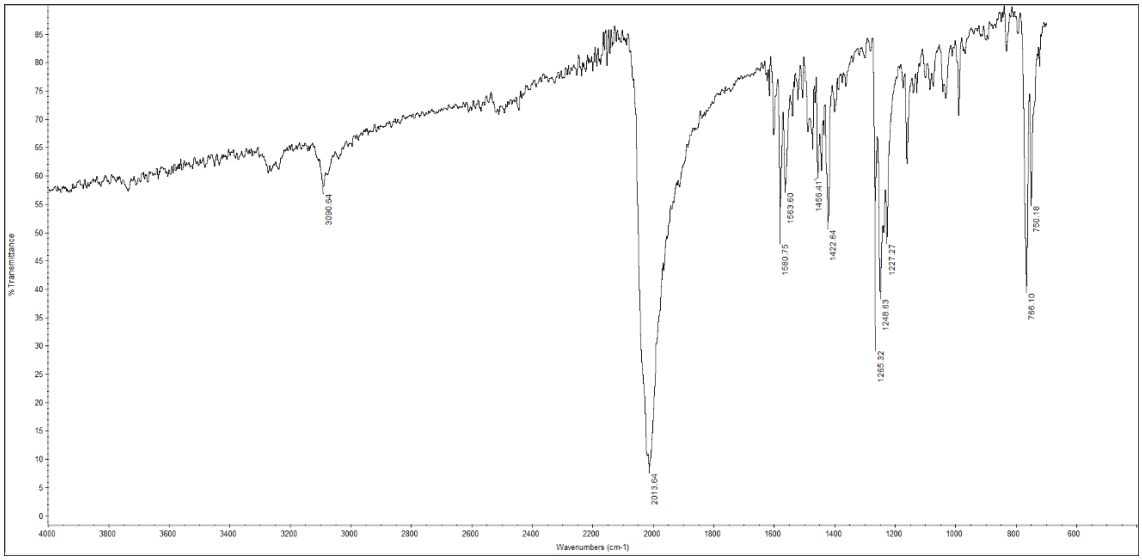

Figure 3.51: ATR IR spectrum of **60**.

3.6.2 ^{1}H and ^{13}C NMR spectroscopy

Due to spectral overlap, the ^{1}H NMR spectrum of **60** only exhibits seven major signals for 11H in the aromatic region (**Figure 3.52**). Notably, this is two peaks more than expected for a symmetrically coordinated terpy ligand, as in this coordination mode, the two outer pyridine rings are in an identical chemical environment and thus should give rise to only four peaks, plus two for the central pyridine ring, due to equivalence of the H3 and H4 protons. Therefore, the following assignment was made assuming a non-symmetrically bound terpyridine. The broad singlet at 9.08 ppm is assigned to the H6 atom. A multiplet at 8.75 − 8.70 ppm is due to overlapping signals from H3, H4, and H6". The doublet at 8.55 ppm is attributed to nearly identical H3' and H5', base on a common coupling constant of $^{3}J_{H3'/H5',H4'}$ = 7.8 Hz. Another multiplet at 8.32 − 8.26 ppm corresponds to H4' and H3". The doublet-of-a-triplet at 8.01 ppm is attributed to H4", as suggested by two characteristic coupling constants of $^{3}J_{H4",H3"/H5"}$ = 7.7 Hz, and $^{4}J_{H4",H6"}$ = 1.8 Hz. The multiplet at 7.82 ppm is then due to H5 and the ddd signal at 7.48 ppm is the H5" resonance, in line with the coupling constants $^{3}J_{H5",H4"}$ = 7.5 Hz, $^{3}J_{H5",H6"}$ = 4.7 Hz, and $^{4}J_{H5",H3"}$ = 1.2 Hz.

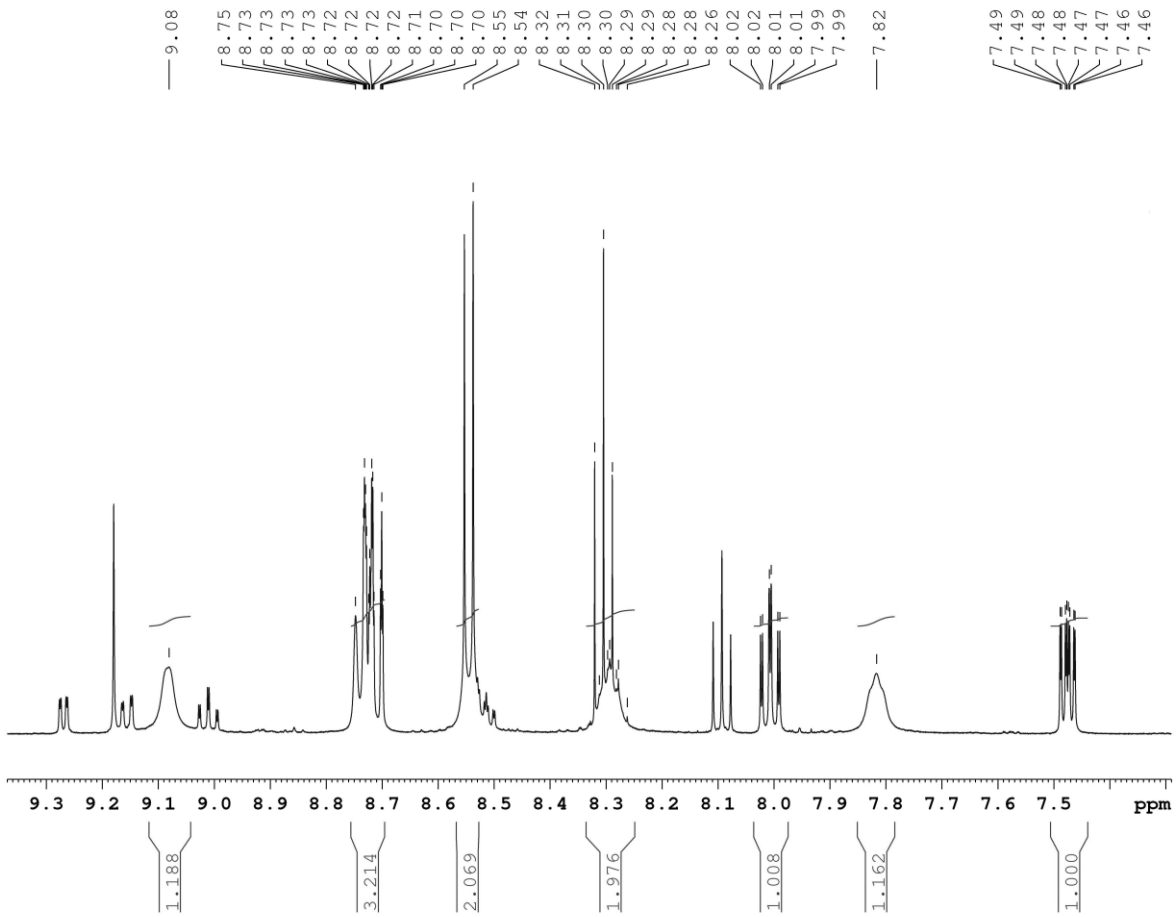

Figure 3.52: Major ^{1}H NMR signals of **60** (500.13 MHz, acetone-d_6).

Furthermore, another six minor signals of lower intensity are also observed in the ^{1}H NMR spectrum of **60** (**Figure 3.53**). These minor peaks can be explained by the presence of a minor species $[Au(N_3)_2(terpy\text{-}\kappa^2\text{-}N^{1,1'})]^+$ **61**, in which the terpy ligand is in a bidentate coordination mode (**Scheme 3.14 right bottom**). The doublet-of-a-doublet at 9.27 ppm is assigned to H6, as suggested by two distinct coupling constants of $^{3}J_{H6,H5}$ = 5.9 Hz and $^{4}J_{H6,H4}$ = 1.2 Hz. The signal of H6" shows up as a singlet at 9.18 ppm. The doublet-of-a-doublet at 9.16 ppm corresponds to H3", due to coupling constants $^{3}J_{H3",H4"}$ = 8.0 Hz and $^{4}J_{H3",H5"}$ = 1.4 Hz. A doublet-of-a-triplet at 9.01 ppm is attributed to H4", in line with $^{3}J_{H4",H3"/H5"}$ = 7.9 Hz and $^{4}J_{H4",H6"}$ = 1.4 Hz. A ddd signal at 8.51 ppm is partially overlapping with one of the major signals, but should correspond to nearly equivalent H4 and H4', based on coupling constants of $^{3}J_{H4/H4',H5/H5'}$ = 7.7 Hz, $^{3}J_{H4/H4',H3/H3'}$ = 6.0 Hz, and $^{4}J_{H4/H4',H6/H6'}$ = 1.6 Hz. The triplet at 8.09 ppm is assigned to H5 and H5', again due to very similar coupling constant of $^{3}J_{H5/H5',H4/H4'}$ = 7.8 Hz, very close to those of H4 and H4'. Finally, the signals of H3, H3' and H5" were not observed due to overlap with major species peaks. The ratio of the two compounds in acetone-d_6 solution is approx. 4:1.

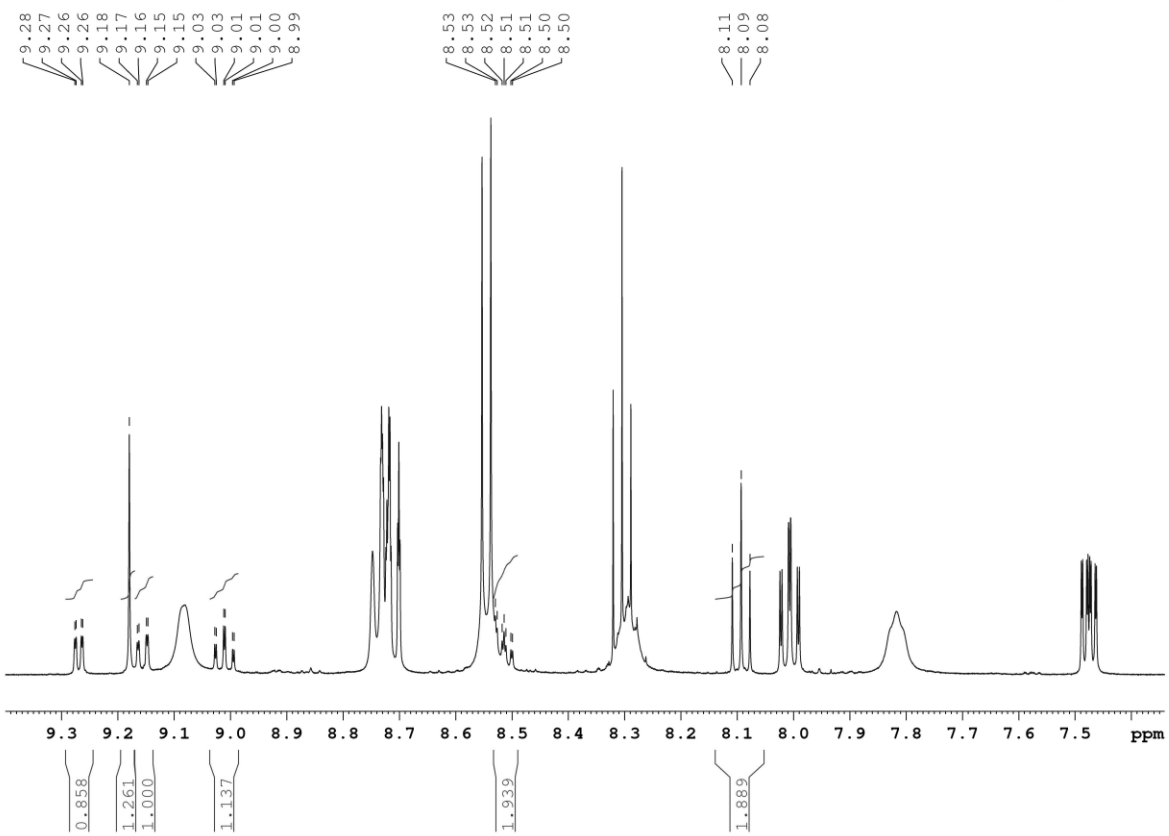

Figure 3.53: Minor ^{1}H NMR signals of **60** (500.13 MHz, acetone-d_6).

Interestingly, the ^{13}C NMR spectrum of **60** shows 15 distinct carbon signals, indicating that all three terpy pyridine rings are in a different chemical environment, thus giving rise to a very low symmetry (**Figure 3.54**). Based on this assumption, the signal at 156.50 ppm is assigned to C6', followed by a peak at 156.09 ppm due to C2'. The signal at 155.01 ppm is assigned to C2" while the following peaks at 151.16, 150.02, 140.33, 139.01, 138.15, 132.24, 130.02, 128.58, and 125.06 ppm correspond to C2, C6", C6, C4", C4', C4, C5", C5', and C5, respectively. Finally, the signals at 124.83, 121.78, and 121.70 ppm are resulting from C3", C3', and C3 atoms, respectively. Due to the lower sensitivity of the ^{13}C relative to the ^{1}H NMR, no signals clearly assignable to any minor species were detected.

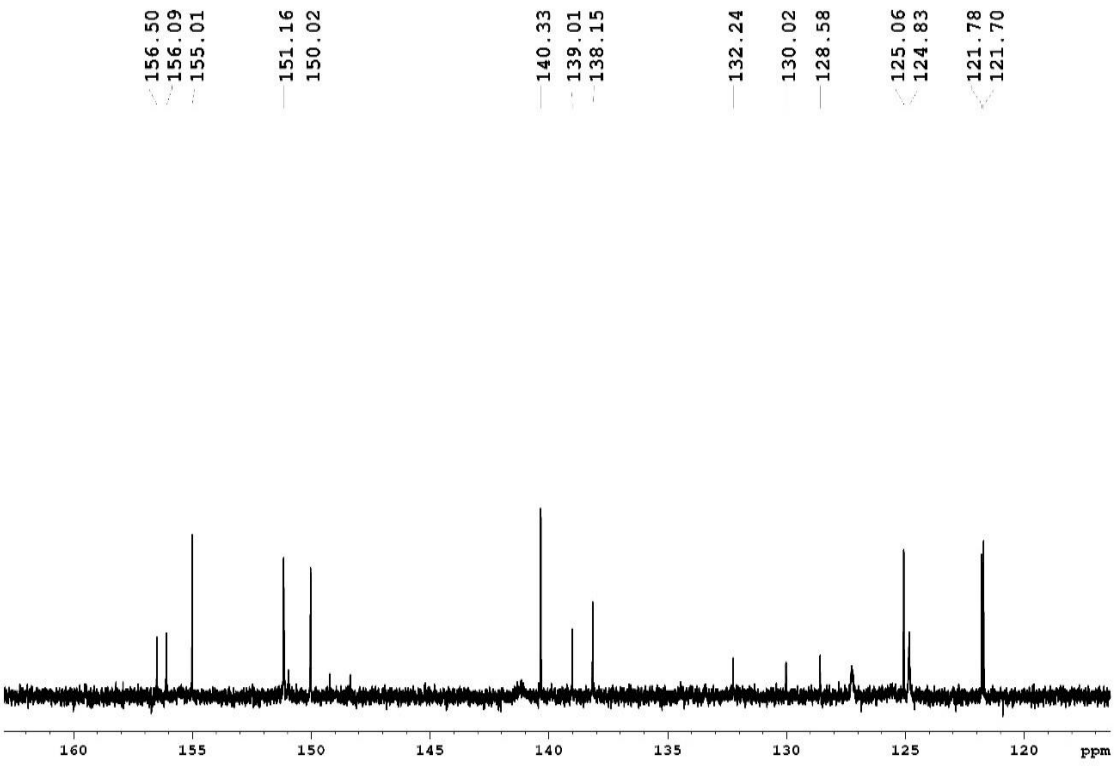

Figure 3.54: ^{13}C NMR spectrum of **60** (125.76 MHz, acetone-d_6).

3.6.3 Crystal structure of [Au(N$_3$)$_3$(terpy-κ^1-N^1)]

Orange block-like crystals of **60** suitable for X-ray diffraction were obtained by slow diffusion of diethyl ether into an acetone solution of the compound. The structure thus obtained shows the terpy ligand coordinated to a square-planar gold(III) centre *via* a single nitrogen donor atom from pyridine ring A, while the other coordination sites of the metal are fully occupied by three terminal azido ligands (**Figure 3.55**). The lengths of the Au1–N4 and Au1–N10 bonds of the azido ligands in *cis*-position relative to the terpy N1 are 2.043(4) and 2.049(4) Å, respectively, which is a bit shorter than the Au1–N1 bond length of 2.067(4) Å, while the *trans* Au1–N7 bond shows a much shorter distance of 2.009(4) Å. Bond lengths within the three azido ligands show consistently long N1–N2 and short N2–N3 distances. There is very overall little variation (< 0.02 Å) with an average of 1.209(6) Å for N1–N2 and 1.143(6) Å for N2–N3, which are in accordance with previously reported values.[149] The two *trans* N–Au–N angles are in line with a nearly linear arrangement, with average angles of 174.71(15)° and the three Au–N–N angles of 115.0(3)–116.8(3)° deviate only slightly from the expected bent azido coordination mode. The overall neutral charge of the crystal structure as well as the four-coordination square-planar metal centre strongly indicate that the gold centre is still in a +III oxidation state.

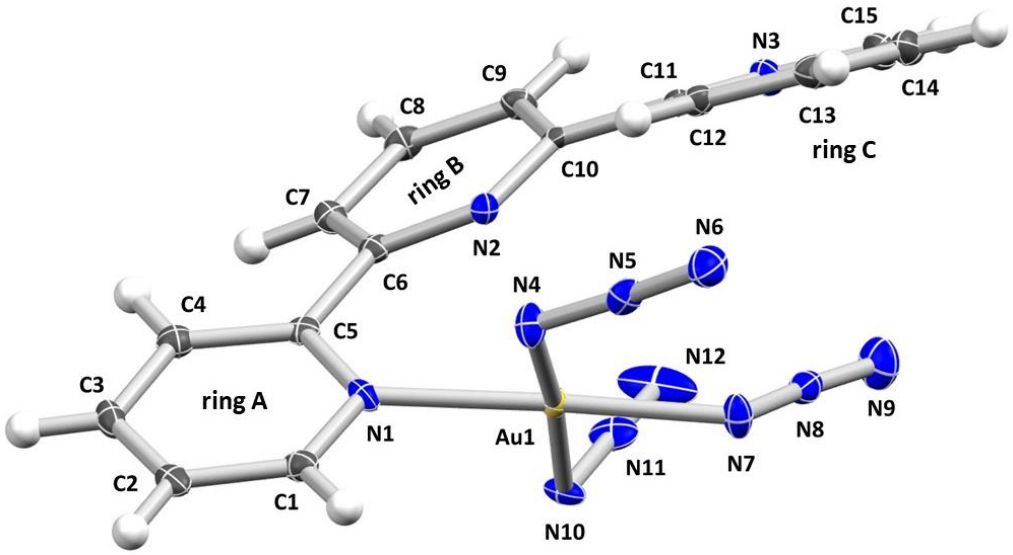

Figure 3.55: Single crystal structure of $[Au(N_3)_3(terpy\text{-}\kappa^1\text{-}N^1)]$ **60** with thermal ellipsoids displayed at the 50% probability level. Selected bond lengths [Å] and angles [°]: Au1–N1 2.067(4), Au1–N4 2.043(4), Au1–N7 2.009(4), Au1–N10 2.049(4), N4–N5 1.217(6), N5–N6 1.140(6), N7–N8 1.213(6), N8–N9 1.142(6), N10–N11 1.197(6), N11–N12 1.148(6), N1–Au1–N7 174.96(15), N4–Au1–N10 174.45(16), Au1–N4–N5 116.0(3), Au1–N7–N8 116.8(3), Au1–N10–N11 115.0(3), N4–N5–N6 175.0(5), N7–N8–N9 172.7(5), N10–N11–N12 174.8(5).[148]

In terpy ligand, pyridine rings A and B adopt a *cis* structure and are tilted relatively to each other by 23.25(12)°. In contrast, the two nitrogen atoms in rings B and C are located in a *trans* arrangement, with a twist angle of 24.79(12)° between these two heterocycles. The distance between N2 from terpy ring B and Au1 is 2.723(4) Å, which is beyond the normal N–Au bond length. The azido ligands N7–N8–N9 and N10–N11–N12 are oriented towards rings B and C, while the third azido ligand points away from the terpy coligand. The distance between the N9 atom of one of the azido ligand and the centroid of pyridine ring C is only 3.264(5) Å, which suggests that this terminal azide nitrogen atom significantly interacts with all six atoms from ring C. In addition, considering the distance between the terminal N12 atom from another azido ligand and C10 atom of ring B is only 3.150(6) Å, these strong lone-pair to π or π–π interactions are expected to also stabilize the observed conformation.

3.6.4 DFT calculations

In order to determine the relative energies of the different gold(III) azido complexes $[Au(N_3)_n(terpy\text{-}\kappa^n)_m]^{(3-n)}$ with $m = 0$, $n = 4$ and $m = 1$, $n = 1…3$, DFT calculations were carried out with the BP86 functional using a ZORA-def2-TZVP/SARC-ZORA-TZVP basis set. Since the calculation of the energies of ionic species is a considerable challenge for DFT, all results were carefully checked for negative HOMO energies, but calculations were found

to be generally well-behaved.[150] Furthermore, to further confirm the validity of the applied approach, the azide stretching vibrations at 2044, 2059, and 2067 cm^{-1} were calculated for [Au(N_3)$_3$(terpy-κ^1-N^1)], which were in reasonable agreement with the experimentally observed broad band at 2014 cm^{-1} from the ATR IR spectrum of **60**. Interestingly, from the results, the isolated [Au(N_3)$_3$(terpy-κ^1-N^1)] **60** turned out to be the most stable species, followed by the structure in which the terpy ligand assumes a bidentate coordination mode through pyridine rings A and B, which however is higher in energy by +100 kcal mol^{-1} (**Figure 3.56**). In addition, the initial target compound, [Au(N_3)$_3$(terpy-κ^3-$N^{1,1',1''}$)]$^{2+}$, was calculated to be much higher in energy by +197 kcal mol^{-1} relative to isolated complex **60**. Fortunately, the very likely unstable tetraazidoaurate(III) was found to be the most unfavorable species, at about +230 kcal mol^{-1} higher in energy relative to the reference state. In this case, the conformation of the terpy ligand (*cis* or *trans*) had very little effect on the calculated energy, with only 8 kcal mol^{-1} difference. Therefore, the DFT calculation results are in full accordance with the experimental findings, demonstrating that the isolated gold(III) complex [Au(N_3)$_3$(terpy-κ^1-N^1)] **60** is indeed the most stable species, followed by the species with a bidentate terpy, which is likely also present as a minor species in solution according to NMR spectroscopy.

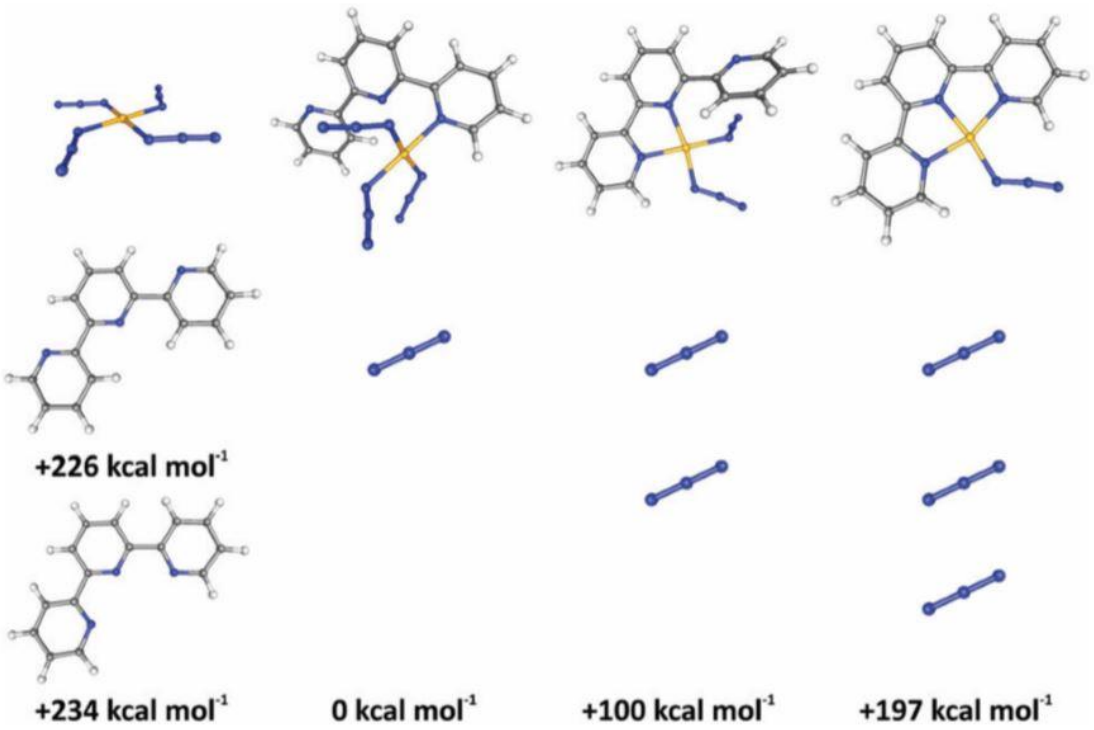

Figure 3.56: Relative energies of gold(III) azido species [Au(N_3)$_n$(terpy-κ^n)$_m$]$^{(3-n)}$ with m = 0, n = 4 and m = 1, n = 1…3, calculated with DFT using the BP86 functional and ZORA-def2-TZVP/SARC-ZORA-TZVP basis set in water using the CPCM solvent model.[148]

In conclusion, instead of the desired product [Au(N_3)(terpy-κ^3-$N^{1,1',1''}$)]$^{2+}$, an unexpected species identified as [Au(N_3)$_3$(terpy-κ^1-N^1)] was isolated upon reaction of [AuCl(terpy-κ^3-$N^{1,1',1''}$)]Cl_2 with an excess of sodium azide. Apparently, the neutral terpy ligand is unable to sufficiently stabilize the highly charged Au(III) center and thus the metal prefers the three monodentate azido ligands over the chelator when available. Such a decrease of the denticity of a chelating ligand is highly unusual and even extensive search in the CCDC single crystal X-ray structure database, [Au(N_3)$_3$(terpy-κ^1-N^1)] is the only one of so far sixth such motifs reported for the terpy ligand to date. In order to provide a gold(III) monoazido species for future comparison with the isoelectronic palladium(II) and platinum(II) compounds, the terpy ligand likely needs to be replaced by other more strongly electron-donating and possibly negatively charged ligands, for example with a C^N^N donor atom set.

4 Conclusion

4.1 English version

Metal complexes hold significant promise as potential drug candidates, in particular in the field of anticancer chemotherapy. To elaborate structure-activity relationships and speed up the coverage of substantial chemical space, a quick and modular access to molecular diversity is required. In recent years, click reactions such as the copper-catalyzed azide-alkyne cycloaddition (CuAAC) have gained substantial attention for such applications. To extend this approach from reactions in the ligand periphery of metal complexes to those which take place directly in the inner coordination sphere of a metal center, the inorganic click (iClick) reaction of metal-azido complexes with alkynes is an emerging alternative, which was to be explored in the context of this work. In order to study the influence of the metal center and the coligands on the kinetics and the structure of the resulting products, three different tridentate ligands with a N^N^N, C^N^N, and S^N^N donor atom set were studied, coordinated to isoelectronic palladium(II) and platinum(II) centers.

The first series of compounds was obtained by the iClick reaction of $[M(N_3)(terpy)]^+$ with M = Pd(II) or Pt(II) and terpy = 2,2':6',2"-terpyridine with different symmetrically or non-symmetrically functionalized internal alkynes R^1-C≡C-R^2 with R^1 = R^2 = COOR or R^1 = CF_3, R^2 = COOEt. The resulting triazolate products were easily accessible with only minimal work-up in good yield and purity. An unexpected linear intermediate and N1-coordinated triazolate species were detected by NMR spectroscopy, which puts into question the general assignment of this reaction as a [3+2] cycloaddition. The DNA binding affinity of some of the title triazolato products was determined by UV/Vis titration, but the binding constants were rather small and only in the range of 10^5 M^{-1} thus putting into question DNA as a cellular target for such compounds.

To study the effect of a more strongly electron-donating coligand on the kinetics, the series of terpy complexes was supplemented by a family of cyclometalated compounds based on $[M(N_3)(phbpy)]$ with M = Pd(II) or Pt(II) and phpby = 6'-phenyl-2,2'-bipyridine. The replacement of the N^N^N coligand by a C^N^N ligand system greatly enhanced the reactivity of the metal azido compounds towards different alkynes and also enabled for the first time the study of the reaction with terminal alkynes R-C≡CH.

A third group of compounds was based on S^N^N chelating semithiocarbazone ligand *(E)*-*N*-phenyl-2-[1-(2-pyridinyl)ethylidene]-hydrazinecarbothioamide (pht). Kinetic studies

revealed the same clear trend for the rate constants as in the other two series of compounds, with the palladium(II) azido complex consistently reacting significantly faster than their platinum(II) analogues, and alkynes with a strong electron-withdrawing substituent showing the highest reactivity. Surprisingly, however, among these compounds, a N1-coordinated triazolato complex was isolated for the first time and its isomerisation to the N2 isomer monitored by ^{1}H NMR spectroscopy in solution. Some of these complexes were also evaluated for their cytotoxicity on the GaMG human glioblastoma brain cancer cell line. The platinum(II) triazolato complex [Pt(triazolate^{CF3,COOEt})(pht)] was almost as potent as cisplatin tested under similar conditions as a reference drug and the analogous palladium(II) triazolato complexes also exhibited a surprisingly high activity against the cancer cell line in the panel, with low EC_{50} values in the range of 4–15 µM.

Additionally, the scope of the iClick reaction was further expanded to a BODIPY-functionalized platinum(II) azido compound. Upon reaction with two different electron-deficient alkynes, the corresponding platinum(II) triazolato complexes were easily generated at room temperature with minimal work-up. The kinetics of the iClick reaction were studied by multinuclear ^{1}H, ^{19}F, and ^{31}P NMR spectroscopy, but overall rate constants were slower than those of the other compounds investigated in the course of this work. Finally, an attempt was made to supplement the palladium(II) and platinum(II) terpy complexes discussed above with the isoelectronic gold(III) compounds. However, the reaction of [AuCl(terpy)]Cl_2 with an excess of sodium azide did not lead to the expected product [Au(N_3)(terpy)]$^{2+}$, but rather the totally unprecedented gold(III) tris-azido complex [Au(N_3)$_3$(terpy-κ^1-N^1)] with a hypodentate terpy ligand, which had switched from a chelating N^N^N binding mode in the precursor to monodentate coordination to the gold(III) center. DFT calculations were in good agreement with the experimental observations, as the gold(III) tris-azido complex turned out to be the most stable species among all other possible combinations of a gold(III) center, four azido groups, and one terpy ligand. In summary, in the context of this work, important trends in the influence of the metal center, coligand, and alkyne reaction partner on the iClick reaction of square-planar palladium(II) and platinum(II) complexes with a N^N^N, C^N^N, or S^N^N coordination sphere and a number of internal as well as terminal alkynes were elaborated. Preliminary bioactivity studies on a human cancer cell line gave low micromolar EC_{50} values, for the most promising compound comparable to cisplatin serving as a reference drug. The further application of the iClick reaction to bioconjugation will be explored in future work.

4.2 German version

Metallkomplexe finden heutzutage großes Interesse als neuartige Wirkstoffkandidaten, insbesondere in der Chemotherapie von Krebserkrankungen. Um Struktur-Wirksamkeits-Beziehungen ableiten und schnell vielversprechende Leitstrukturen variieren zu können ist ein schneller und modularer Zugang zu "molekularer Vielfalt" notwendig. In den letzten Jahren haben Click-Reaktionen wie die Kupfer-katalysierte Azid-Alkin-Cycloaddition (*copper-catalyzed azide-alkyne cycloaddition*, CuAAC) erhebliche Aufmerksamkeit aufsich gezogen. Bisher erfolgen diese bei Metallkomplexen vor allem in der Peripherie der Liganden. In einem aktuellen alternativen Ansatz werden dagegen Reaktionen direkt in der inneren Koordinationssphäre eines Metallzentrums untersucht. Derartige iClick-Reaktionen (*inorganic click*) von Metall-Azid-Komplexen mit Alkinen stellen eine vielversprechende Alternative dar, da sich die Reaktionsgeschwindigkeit durch eine geschickte Wahl des Metallzentrums und der Coliganden in einem breiten Rahmen gezielt einstellen lassen sollte. Ziel der vorliegenden Arbeit war es daher isoelektronische Palladium(II)- und Platin(II)-Azido-Komplexe mit drei verschiedenen Coliganden auf der Basis von N^N^N-, C^N^N- und S^N^N-Donorgruppen herzustellen und deren Einfluß auf die Kinetik der iClick-Reaktion zu untersuchen.

In der ersten Serie von Verbindungen mit der generellen Formel $[M(N_3)(terpy)]+$ mit M = Pd(II) oder Pt(II) und terpy = 2,2':6',2"-Terpyridin wurde die Reaktion mit verschiedenen symmetrisch oder nicht-symmetrisch funktionalisierten internen Alkinen R^1-C≡C-R^2 mit R^1 = R^2 = COOR oder R^1 = CF3, R^2 = COOEt untersucht. Die resultierenden Triazolat-Produkte wurden mit nur minimaler Aufarbeitung in guter Ausbeute und Reinheit erhalten. Mit Hilfe der NMR-Spektroskopie konnten außerdem im Verlauf der Reaktion zwei unerwartete lineare bzw. N1-koordinierte Intermediate identifiziert werden die die übliche Beschreibung dieser Reaktion als [3+2]-Cycloaddition in Frage stellen. Eine DNA-Titration der Metall-Triazolat-Komplexe ergab nur ein moderate Affinität mit Bindungskonstanten in der Größenordnung von 10^5 M^{-1}, was die DNA als zelluläre Zielstruktur dieser Verbindungen in Frage stellt.

Um den Einfluß eines stärker elektronenschiebenden Coliganden auf die Kinetik der iClick-Reaktion zu untersuchen wurde neben den terpy-Komplexen auch eine verwandte Serie von Verbindungen der allgemeinen Strukutr $[M(N_3)(phbpy)]$ mit M = Pd(II) oder Pt(II) und phbpy = 6'-Phenyl-2,2'bipyridin hergestellt. Der Ersatz des N^N^N-Chelators durch einen

C^N^N-Liganden führte zu einer deutlich gesteigerten Reaktivität der resultierenden Azido-Komplex in der iClick-Reaktion mit elektronenarmen Alkinen und ermöglichte erstmals auch eine Umsetzung mit terminalen Alkinen wie zum Beispiel Propiolsäuremethylester. Eine dritte Verbindungsklasse basierte auf dem S^N^N-chelatisierenden Semithiocarbazone-Liganden *(E)*-*N*-phenyl-2-[1-(2-pyridinyl)ethylidene]hydrazincarbothioamid (pht). Kinetische Untersuchungen zeigten einen Trend in der Geschwindigkeit der iClick-Reaktion vergleichbar den anderen Ligandensystemen, so daß auch in diesem Fall die Palladium(II)-Azido-Komplexe deutlich schneller umgesetzt wurden als die entsprechenden Platin(II)-Analoga. Auch führen elektronenärmere Alkine zu einer Beschleunigung der Reaktionsgeschwindigkeit. Unerwarteterweise konnten in dieser Serie erstmals auch N1-koordinierte Triazolate isoliert und ihre Umwandlung in die stabilieren N2-Isomere in Lösung mit Hilfe von NMR-Spektroskopie verfolgt werden. Einige ausgewählte Verbindungen zeigten zudem vielversprechende Antitumor-Aktivität gegen menschliche Glioblastom-Zellen, mit EC_{50}-Werten im Bereich von 4–15 µM. Die aktivste Verbindung [Pt(triazolat^{CF3,COOEt})(pht)] erwies sich als nahezu so potent wie Cisplatin und auch die analogen Palladium(II)-Komplexe waren überraschend aktiv.

Schließlich konnte die Bandbreite der iClick-Reaktion auch auf einen BODIPY-funktionalisierten Platin-Azid-Baustein ausgeweitet werden. Die Kinetik der iClick-Reaktion wurde mittels multinuklearer ^{1}H, ^{19}F, and ^{31}P NMR-Spektroskopie verfolgt, die bestimmten Geschwindigkeitskonstanten waren jedoch kleiner als für alle anderen Reaktionen in dieser Arbeit ermittelt.

Schlußendlich wurde auch noch ein Versuch unternommen die Palladium(II)- und Platin(II)-Komplexe durch eine isoelektronische Gold(III)-Verbindung zu ergänzen. Unerwarteterweise ergab die Reaktion von [AuCl(terpy)]Cl_2 mit einem Überschuß an Natriumazid jedoch nicht das erhoffte Produkt $[Au(N_3)(terpy)]^{2+}$. Stattdessen wurde der Gold(III)-Tris-Azidokomplex [$Au(N_3)_3$(terpy-κ^1-N^1)] mit einem hypodentaten terpy-Liganden erhalten, in dem dieser von einem N^N^N-Bindungsmodus in der Vorstufezu einer monodentaten Koordination an das Gold(III)-Zentrum wechselte. Diese Ergebnisse wurden auch durch DFT-Rechnungen bestätigt, in denen der Gold(III)-Tris-Azido-Komplex die stabilste Spezies unter allen möglichen Kombinationen eines Gold(III)-Zentrums, vierer Azid-Gruppen und eines terpy-Ligand war.

Conclusion

Insgesamt konnten im Rahmen dieser Arbeit systematische Einflüsse des Metallzentrums, des Coliganden und des Alkins auf die Geschwindigkeit der iClick-Reaktion von quadratisch-planaren Palladium(II)- und Platin(II)-Azid-Komplexen mit internen und terminalen Alkinen identifiziert werden. So reagiert auch in dieser Serie das 4d-Element schneller als das entsprechend 5d-Metall, interne Alkinen mit elektronenarmen Substituenten führen zu einer höheren Reaktionsgeschwindigkeit als terminale Alkine und Geschwindigkeitskonstante steigt für tridentate Chelatliganden in der Reihenfolge N^N^N < S^N^N < C^N^N an. Erste orientierende biologische Studien an menschlichen Tumorzellen ergaben vielversprechende EC_{50}-Werte im unteren mikromolaren Bereich. Das Potential dieser Verbindungen und der iClick-Reaktion allgemein für die Biokonjugation und tiefgehende Untersuchungen des Mechanismus der Antitumor-Wirkung sollte in zukünftigen Studien noch weiter ausgedehnt werden.

5 Experimental section

5.1 Gernal procedures

Palladium(II) chloride, potassium tetrachloroplatinate(II) and potassium tetrachloroaurate(III) hydrate were obtained from Strem. All other chemicals were purchased from commercial sources and used as received. The ligand precursor *N*-phenyl hydrazine carbothioamide was available from the Bachelor thesis of Lorena Rüger, 2-butynedioic acid 1,4-bis(2-methoxyethyl) ester was prepared in the context of the Master thesis of Jan Mößeler, 4,4,4-trifluoro-2-butynoic acid ethyl ester was provided by Marvin Schock and the platinum(II)-BODIPY azido compound [Pt(bodipy)(N_3)(PEt_3)$_2$] was synthesized by Peter Irmler in the group of Prof. Dr. Rainer Winter at the Universität Konstanz. *Caution! Azides and azido complexes are potentially explosive. Although no problems were encountered with the preparations in this work, synthesis should only be performed on a very small scale (< 200 mg) and in particular heating of the solid compounds avoided.*

5.2 Instrumentations

5.2.1 NMR spectroscopy

NMR spectra were recorded on Bruker Avanve 200 (^{1}H: 199.93 MHz, ^{19}F: 188.12 MHz), Avance 400 (^{1}H: 400.47 MHz, ^{13}C: 100.70 MHz, ^{19}F: 376.76 MHz, ^{31}P: 162.11 MHz, ^{195}Pt: 86.09 MHz), and Avance 500 (^{1}H: 500.13 MHz, ^{13}C: 125.76 MHz, ^{19}F: 470.59 MHz, ^{195}Pt: 107.51 MHz) spectrometers. Chemical shifts are reported downfield relative to tetramethylsilane (TMS) and are referenced relative to the residual signal of the solvent.[151] The ^{19}F and ^{195}Pt NMR shifts are reported relative to CCl_3F and 1.2 M $Na_2[PtCl_6]$ in D_2O, respectively. Peak multiplicities are marked as singlet (s), doublet (d), doublet of doublet (dd), doublet of doublet of doublet (ddd), doublet of triplet (dt), triplet (t), and multiplet (m), respectively, and coupling constants *J* are given in Hertz (Hz). Spectra were analyzed by the Bruker TopSpin (version 3.5) software.

5.2.2 CHN analysis

The elemental composition of the compounds was determined with an Elementar Vario MICRO cube CHN analyzer. Addition of V_2O_5 was usually required to obtain proper results in the case of the metal complexes.

5.2.3 IR spectroscopy

IR spectra of pure solid samples were obtained using a Nicolet 380 FT-IR spectrometer fitted with a smart iTR ATR accessory. The spectra of pure solid samples were recorded in the range from 4000 to 700 cm^{-1} with 128 scans per sample. Peak intensities are marked as strong (s), medium (m) and weak (w). Spectra were analyzed by EZ OMNIC software.

5.2.4 Mass spectrometry

All mass spectra were recorded by Dominic Graf or Prof. Dr. Ulrich Schatzschneider on a Thermo Fisher Exactive Plus Orbitrap mass spectrometer at a solvent flow rate of 25 µL min^{-1}. For ESI: resolution R = 70000, sheath gas flow rate 15 L min^{-1}, aux gas flow rate 5 L min^{-1}, spray voltage 3.80 kV, capillary temperature 320 °C, S-lens level 50.0, and aux gas heater temperature 50 °C. For APCl and ASAP: resolution R = 140000, sheath gas flow rate 2 L min^{-1}, aux gas flow rate 10 L min^{-1}, spray voltage 3.80 kV, capillary temperature 320 °C, S-lens level 50.0, and aux gas heater temperature 400 °C.

5.2.5 UV/Vis spectroscopy

UV/Vis spectra were collected on an Agilent 8453 UV/Vis diode array spectrophotometer in quartz cuvettes (d = 1 cm).

5.2.6 Single crystal X-ray structure determination

The crystal structure determination was carried out by Dr. Alexandra Friedrich. Briefly, a crystal of $[Au(N_3)_3(terpy)]$ suitable for X-ray diffraction was selected, coated in perfluoropolyether oil, and mounted on a MiTeGen sample holder. Diffraction data was collected on a Bruker X8-APEX II 4-circle diffractometer with a CCD area detector using multi-layer mirror monochromated $Mo_{K\alpha}$ radiation. The crystal was cooled using an Oxford Cryostreams low-temperature device. Data was collected at 100 K. The images were processed and corrected for Lorentz-polarization effects and absorption as implemented in the Bruker software packages. The structure was solved using the intrinsic phasing method (ShelXT)[152] and Fourier expansion techniques. All non-hydrogen atoms were refined in anisotropic approximation with hydrogen atoms "riding" in idealized positions, by full-matrix least squares against F2 of all data, using the ShelXL software.[153] Crystal data and experimental details are listed in **Table 5.1**.

5.2.7 DNA-binding assay

Calf thymus DNA (CT-DNA, Sigma Aldrich, product number: D4522) was dissolved in TE buffer at pH 7.4 and sitting in + 4 °C fridge overnight. The UV absorbance of the solution at 260 and 280 nm was checked and the ratio A_{260nm}/A_{280nm} found to be in the range of 1.8–1.9, indicating that the DNA was sufficiently free of protein. The DNA concentration per nucleotide was determined by absorption spectroscopy using a molar absorption coefficient of 6600 L mol^{-1} cm^{-1} at 260 nm. A concentrated stock solution was prepared by dissolving approximately 1.0 mg of each complex in DMSO (200 µL) in a small glass vial. Before titration, three solutions were prepared by diluting with an appropriate amount of TE buffer to the required concentration:

1. Solution **A** (800 µL): 30–50 µM of metal complex, dependent on the absorption coefficient of each complex so that the main absorption of complex is *approx.* 1.0;
2. Solution **B** (100 µL): same concentration (30–50 µM) of metal complex with solution **A** and 200 µM CT-DNA;
3. Solution **C** (100 µL): 200 µM CT-DNA.

Fill the reference cuvette with 750 µL of TE buffer and the sample cuvette with 750 µL of solution **A**. Record a UV/vis spectrum in the range of 230–800 nm. Add to the reference cuvette 5 µL of solution **C** and to the sample cuvette 5 µL of solution **B**. Mix with a small glass rod and let equilibrate for 5 min. Then record another UV/vis spectrum. Repeat the sequence of addition of solutions **B** and **C**, mixing, equilibration, and measurement of UV/vis spectra until the complete of 100 µL solutions **B** and **C** have been added. The binding constant K_b was then determined from a linear fit of the change of the main absorbance *vs*. the concentration of DNA added using equation (**I**):[137]

$$c(\text{DNA}) \times (\varepsilon_a - \varepsilon_f)^{-1} = a \times 10^6 + b \times c(\text{DNA}) \quad \textbf{(I)}$$

$$\text{with } \varepsilon_a = A_{(c\text{DNA}) = x)}/c(\text{complex}),$$

$$\varepsilon_f = A_{(c(\text{DNA}) = 0)}/c(\text{complex}).$$

The DNA binding constant is then calculated from the fit parameters as $K_b = b/a$.

5.2.8 Kinetic experiments

The kinetics of the iClick reaction was studied by ^{1}H, ^{19}F, and ^{31}P NMR spectroscopy. Depending on the nucleus, 1,3,5-trioxane or tetrabutyl ammonium hexafluorophosphate were applied as an internal standard for ^{1}H and $^{19}F/^{31}P$ NMR kinetic studies, respectively. In the case of the terpy complexes, addition of a standard was not required for the ^{19}F NMR measurements, as the compounds inherently feature as hexafluorophosphate counterion which does not change in concentration during the reaction and thus served as the standard. A representative and well-resolved signal of alkyne or azide starting material was referenced against the peak of the internal standard and the concentration of the tracked compound calculated at different reaction times. For sample preparation, in a small glass vial, similar molar amount of 1,3,5-trioxane or tetrabutyl ammonium hexafluorophosphate and alkyne or azide were initially dissolved in proper deuterated solvent as the stock solution. Then, a ^{1}H or ^{19}F or ^{31}P NMR spectrum was recorded and the precise molar amount of standard calculated from comparison of the interested signal intensities relative to the 1,3,5-trioxane or hexafluorophosphate peak integrals. In a second vial, a precisely weighed amount of an azido complex or alkyne was dissolved in the same deuterated solvent. Then, the NMR measurement was set up and, right next to the spectrometer, the stock solution of the alkyne (or azido complex)/standard mixture was added to that of the metal azido complex (or alkyne) directly in a NMR tube. For all measurements, the amount of both solutions was adjusted to give a final alkyne to azido complex ratio of 1:1. Under the assumption of a second-order reaction and equal concentrations of the two reactants as well as negligible side-reactions, the second order rate constant k is obtained from eqn (**II**):

$$1/c_t(\mathrm{A}) = k \cdot t + 1/c_{t=0}(\mathrm{A}) \qquad \textbf{(II)}$$

with $c_{t=0}(\mathrm{A})$ = initial concentration of alkyne or azido complex A,

$c_t(\mathrm{A})$ = concentration of alkyne or azido complex A at time t.

A series of ^{1}H, ^{19}F, or ^{31}P NMR spectra were recorded at 25 °C, with the intervals between the measurements varied from 0 to 10 h, dependent on the expected rate constant. For technical reasons, there was always a time lag of about 1 min between mixing of the reactants and recording of the first spectrum, which was included in the determination of the second-order rate constant.

5.2.9 DFT calculations

Density functional theory calculations were carried out by Prof. Dr. Ulrich Schatzschneider on the Linux cluster of the Leibniz-Rechenzentrum (LRZ) in Munich with ORCA version 4.0.0.25[154] using the BP86 functional, a ZORA-def2-TZVP basis set on the light atoms and SARC-ZORATZVP on gold[155] together with AutoAux, the tightscf, grid4, and DIISMaxEq 15 options, and the CPCM solvation model with water or acetone as the solvent for geometry optimizations and subsequent calculation of vibrational frequencies to characterize the structures obtained as minima by inspection for absence of imaginary modes. Graphics were created with gOpenmol.

5.2.10 Biological assays

The biological assays were carried out by Ellina Schulz in the Tumorbiology lab of the Universitätsklinikum Würzburg under the guidance of PD Dr. Carsten Hagemann. The human glioblastoma cell line GaMG (DSMZ) was cultured in 75 cm^2 cell culture flasks (Corning) in Dulbecco Modified Eagle Medium (DMEM) supplemented with 10% fetal bovine serum, 2% nonessential amino acids, and 0.4% penicillin/streptomycin (all from Gibco) in a cell culture incubator at 37 °C and 5% CO_2. For the MTT assay (Cell Proliferation KIT I (MTT) from Roche), 3000 cells resuspended in 100 µL of medium were plated into the wells of a 96-well plate (Sarstedt) each and incubated overnight so that the cells could adhere. The tested metal complexes were dissolved in dimethyl sulfoxide (Roth) and diluted in medium. The medium in the 96-well plates was replaced by 100 µL of medium containing the metal complexes in different concentrations ranging from 0.25 to 50 µM. After an incubation period of 72 h, the MTT assay was performed according to the manufacturer's manual and measured with an ELISA Reader (Tecan). EC_{50} values were calculated with Graph Pad Prism 6.

5.3 Synthesis and analytical data

5.3.1 Synthesis of ß-(dimethylamino)vinyl-2-pyridyl ketone

USC-KP001-01

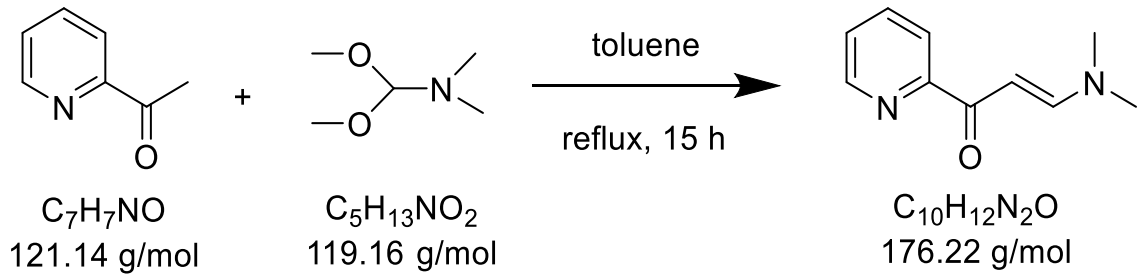

In a 250 mL single-neck flask, 2-acetylpyridine (20.0 g, 165 mmol) and *N*,*N*-dimethylformamide dimethyl acetal (24.0 g, 201 mmol) were dissolved in toluene (100 mL). The clear pale yellow solution was heated to reflux for 15 h in a Dean-Stark apparatus. Then, the now dark red solution was cooled to room temperature, upon which yellow crystals started to precipitate. These were filtered off and washed with toluene (2 × 10 mL). The volume of the solution was reduced to one-half and the mixture stored in a refrigerator overnight. This led to precipitation of additional yellow crystals, which were also collected by filtration and washed with toluene (2 × 10 mL). The combined material was dried under vacuum for 4 d to obtain the final product as yellow crystals. Yield: 58% (16.9 g, 96 mmol). **IR** (ATR): $\tilde{\nu}$ = 1632 (s), 1565 (m), 1531 (s), 1432 (m), 1360 (m), 1259 (s), 1063 (s), 767 (s) cm^{-1}; **^{1}H NMR** (500.13 MHz, acetone-d_6): δ = 8.61 (ddd, 1H, $^{3}J_{H6,H5}$ = 4.7 Hz, $^{4}J_{H6,H4}$ = 1.8 Hz, $^{5}J_{H6,H3}$ = 0.9 Hz, py-H6), 8.05 (td, 1H, $^{3}J_{H3,H4}$ = 7.8 Hz, $^{4/5}J_{H3,H5/H6}$ = 1.1 Hz, py-H3), 7.87 (ddd, 1H, $^{3}J_{H4,H3}$ = 7.9 Hz, $^{3}J_{H4,H5}$ = 7.5 Hz, $^{4}J_{H4,H6}$ = 1.8 Hz, py-H4), 7.77 (d, 1H, ^{3}J = 12.8 Hz, COC*H*), 7.45 (ddd, 1H, $^{3}J_{H5,H4}$ = 7.5 Hz, $^{3}J_{H5,H6}$ = 4.7 Hz, $^{4}J_{H5,H3}$ = 1.3 Hz, py-H5), 6.49 (d, 1H, ^{3}J = 12.6 Hz, C*H*N(CH_3)$_2$), 3.21 (s, 3H, NCH_3), 2.96 (s, 3H, NCH_3) ppm; **^{13}C NMR** (125.76 MHz, acetone-d_6): δ = 186.21 (*C*=O), 157.32 (py-C2), 154.71 (C=*C*N(CH_3)$_2$), 149.20 (py-C6), 137.39 (py-C4), 126.19 (py-C5), 122.07 (py-C3), 91.47 (C=*C*CO), 44.97 (N*C*H_3), 37.40 (N*C*H_3) ppm; **MS** (ASAP^{+}): *m*/*z* = 177.1020 $[M+H]^{+}$; **Elemental analysis** (%): calcd. for $C_{10}H_{12}N_2O$: C 68.16, H 6.86, N 15.90; found (%): C 68.02, H 6.86, N 15.96.

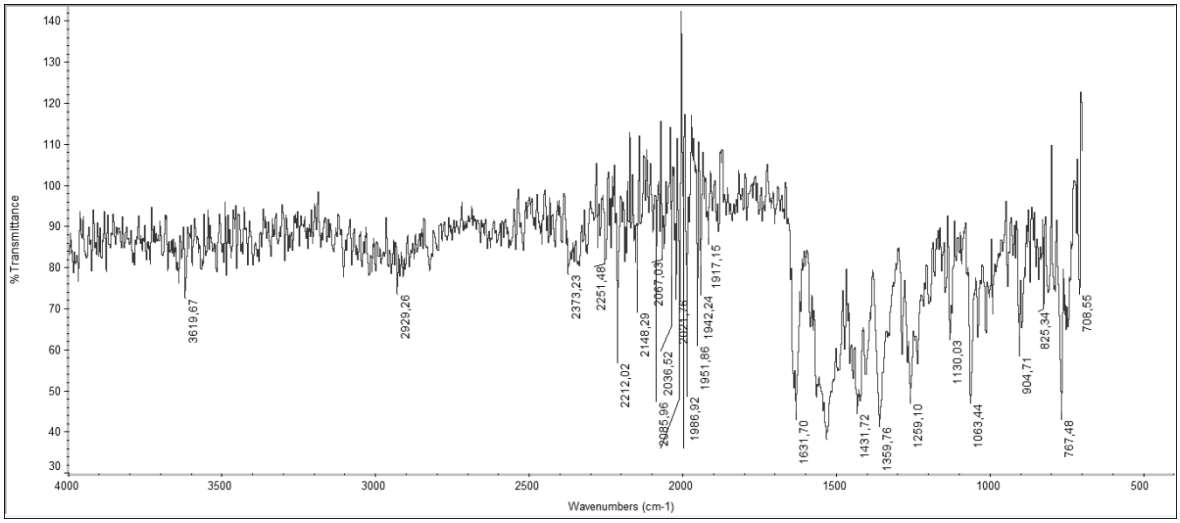
% Transmittance
Wavenumbers (cm-1)
3619,67
2929,26
2373,23
2251,48
2212,02
2148,29
2067,03
2036,52
1986,92
1951,86
1942,24
1917,15
1631,70
1431,72
1359,76
1259,10
1130,03
1063,44
904,71
825,34
767,48
708,55

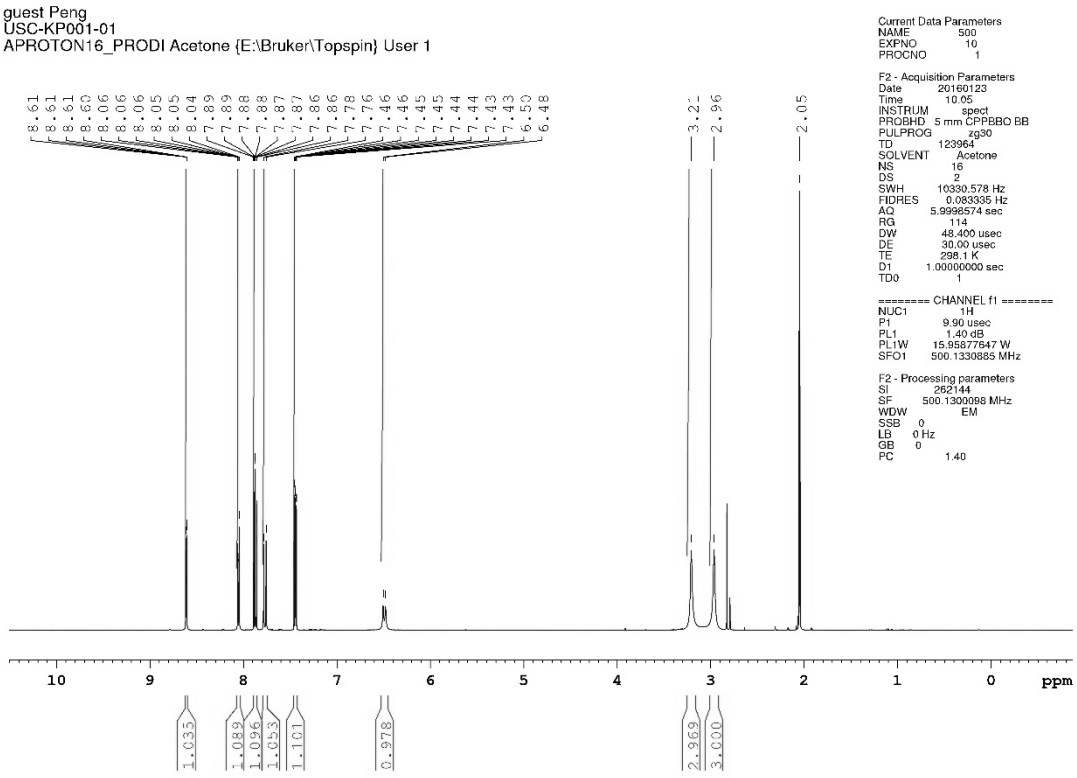
guest Peng
USC-KP001-01
APROTON16_PRODI Acetone {E:\Bruker\Topspin} User 1
Current Data Parameters
NAME 500
EXPNO 10
PROCNO 1
F2 - Acquisition Parameters
Date 20160123
Time 10.05
INSTRUM spect
PROBHD 5 mm CPPBBO BB
PULPROG zg30
TD 123964
SOLVENT Acetone
NS 16
DS 2
SWH 10330.578 Hz
FIDRES 0.083335 Hz
AQ 5.9998574 sec
RG 114
DW 48.400 usec
DE 30.00 usec
TE 298.1 K
D1 1.00000000 sec
TD0 1
======== CHANNEL f1 ========
NUC1 1H
P1 9.90 usec
PL1 1.40 dB
PL1W 15.95877547 W
SFO1 500.1330885 MHz
F2 - Processing parameters
SI 262144
SF 500.1300098 MHz
WDW EM
SSB 0
LB 0 Hz
GB 0
PC 1.40
8.61
8.61
8.61
8.60
8.06
8.06
8.06
8.05
8.05
8.04
7.89
7.89
7.88
7.88
7.87
7.87
7.86
7.86
7.78
7.76
7.46
7.46
7.45
7.45
7.44
7.44
7.43
7.43
6.50
6.48
3.2-
2.96
2.05
10
9
8
7
6
5
4
3
2
1
0
ppm
1.035
1.089
1.096
1.053
1.101
0.978
2.969
3.000

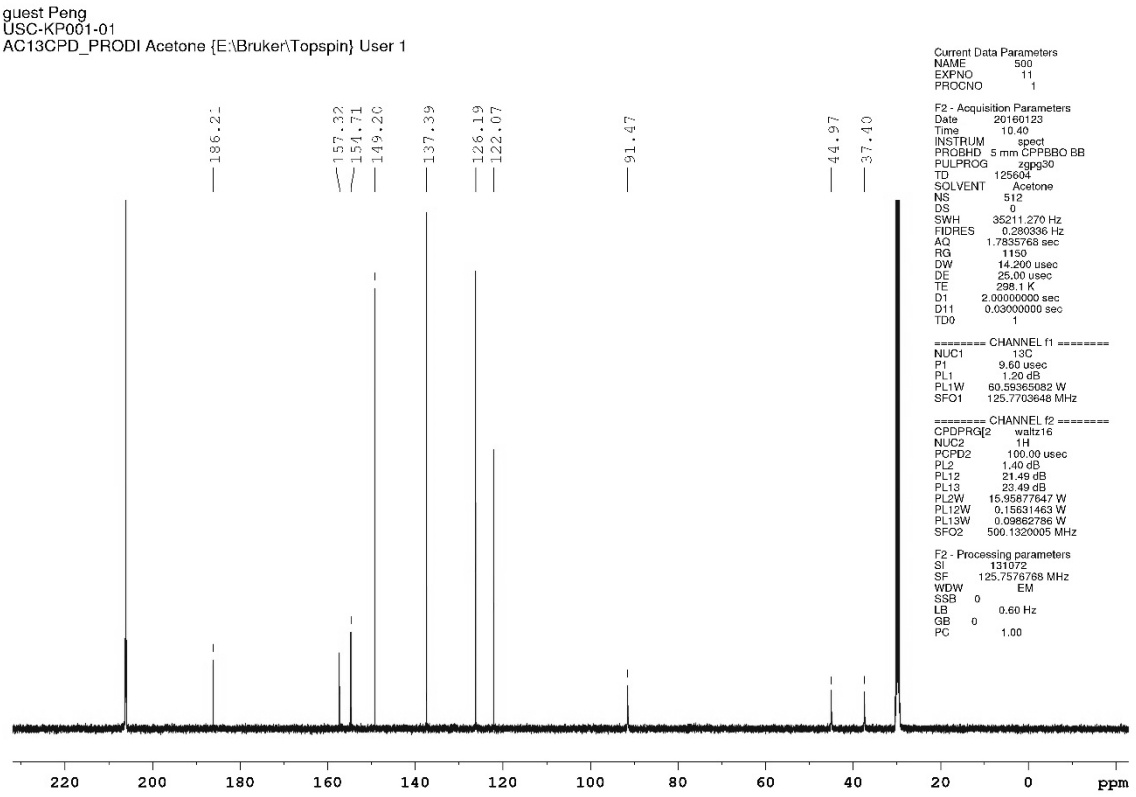
guest Peng
USC-KP001-01
AC13CPD_PRODI Acetone {E:\Bruker\Topspin} User 1
186.2
157.32
154.71
149.20
137.39
126.19
122.07
91.47
44.97
37.40
220
200
180
160
140
120
100
80
60
40
20
0
ppm
Current Data Parameters
NAME 500
EXPNO 11
PROCNO 1
F2 - Acquisition Parameters
Date 20160123
Time 10.40
INSTRUM spect
PROBHD 5 mm CPPBBO BB
PULPROG zgpg30
TD 125604
SOLVENT Acetone
NS 512
DS 0
SWH 35211.270 Hz
FIDRES 0.280336 Hz
AQ 1.7835768 sec
RG 1150
DW 14.200 usec
DE 25.00 usec
TE 298.1 K
D1 2.00000000 sec
D11 0.03000000 sec
TD0 1
======== CHANNEL f1 ========
NUC1 13C
P1 9.60 usec
PL1 1.20 dB
PL1W 60.59365082 W
SFO1 125.7703648 MHz
======== CHANNEL f2 ========
CPDPRG[2 waltz16
NUC2 1H
PCPD2 100.00 usec
PL2 1.40 dB
PL12 21.49 dB
PL13 23.49 dB
PL2W 15.95877647 W
PL12W 0.15631463 W
PL13W 0.09862786 W
SFO2 500.1320005 MHz
F2 - Processing parameters
SI 131072
SF 125.7576788 MHz
WDW EM
SSB 0
LB 0.60 Hz
GB 0
PC 1.00

5.3.2 Synthesis of 2,2':6',2"-terpyridine

USC-KP007-01

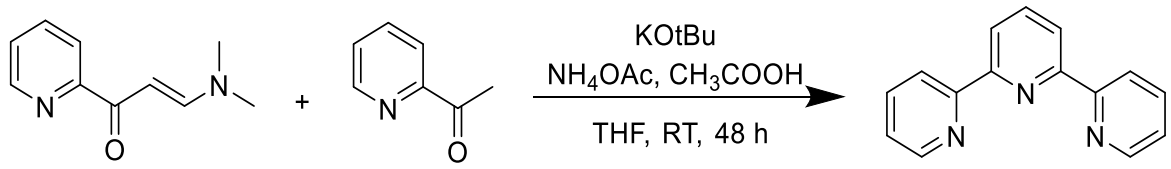

$C_{10}H_{12}N_2O$
176.22 g/mol

C_7H_7NO
121.14 g/mol

$C_{15}H_{11}N_3$
233.27 g/mol

A 500 mL three-neck flask was charged with anhydrous tetrahydrofuran (200 mL) under dinitrogen and then, solid potassium *tert*-butoxide (10.0 g, 89.1 mmol) was added. To this mixture, 2-acetylpyridine (4.84 g, 40.0 mmol) was added at once. The resulting light yellow solution was stirred at room temperature for about 2 h, during which a white solid formed. Then, solid 3-(dimethylamino)-1-(2-pyridinyl)-2-propen-1-one (7.04 g, 40.0 mmol) was added to the solution at once. The now dark red solution was stirred at room temperature for 48 h. Then, the mixture was cooled in an ice bath and a solution of ammonium acetate (30.0 g, 389 mmol) in acetic acid (100 mL) was added with stirring, whereupon the colour changed from deep red to dark brown. Next, methanol (25 mL) was added and the mixture immersed in an oil bath kept at 120 °C to completely distil off the tetrahydrofuran. The distillation was stopped when the head temperature had reached 115 °C (about 6 h). The resulting black solution was poured into water (200 mL) and neutralized with sodium carbonate (about 100 g) until the strong gas evolution had ceased. At this point, a black tarry material had formed, which was suspended in toluene (250 mL). The mixture was heated to 80 °C for 2 h to dissolve the material and then cooled to room temperature. The solution was filtered through Celite, which was washed with additional toluene (250 mL). The aqueous phase was separated from the organic one and activity I alumina (12 g) added to the latter with stirring. The solid material was filtered off and the filtrate evaporated to give a dark brown oil. This was dissolved in dichloromethane (20 mL), activity III alumina (20 g) added, and the solvent removed again. The resulting solid material was filled into a glass column and the product eluted with cyclohexane/ethyl acetate (20:1 v/v). Two main fractions separated, a first light yellow one and a second orange one. The light yellow fraction was collected, followed by another one, which was slightly contaminated by the orange material. The initial yellow fraction was evaporated to dryness and upon standing at room temperature, a white powder appeared. Recrystallization from *n*-hexane/cyclohexane (10:1 v/v, 100 mL) gave the product as a white powder, which was dried under vacuum for 3 d. Yield: 38% (3.56 g, 15.3 mmol).

IR (ATR): $\tilde{\nu}$ = 3049 (m), 1562 (s), 1501 (m), 1455 (m), 1421(s), 1257 (m), 1101 (m), 1079 (m), 989 (m), 759 (s) cm^{-1}; **^{1}H NMR** (500.13 MHz, acetone-d_6): δ = 8.72–8.69 (m, 4H, H3/H3”, H6/H6”), 8.54 (d, 2H, $^{3}J_{H3'/H5',H4'}$ = 7.8 Hz, H3’/H5’), 8.08 (t, 1H, $^{3}J_{H4',H3'/H5'}$ = 7.7 Hz, H4’), 7.98 (dt, 2H, $^{3}J_{H4,H3/H5;H4",H3"/H5"}$ = 7.7 Hz, $^{4}J_{H4,H6/H4",H6"}$ = 2.1 Hz, H4/H4”), 7.45 (ddd, 2H, $^{3}J_{H5,H4;H5",H4"}$ = 7.5 Hz, $^{3}J_{H5,H6;H5",H6"}$ = 4.6 Hz, $^{4}J_{H5,H3;H5",H3"}$ = 1.4 Hz, H5/H5”) ppm; **^{13}C NMR** (125.76 MHz, acetone-d_6): δ = 156.85 (C2’/C6’), 156.40 (C2/C2”), 150.25 (C6/C6”), 138.96 (C4’), 137.95 (C4/C4”), 125.02 (C5/C5”), 121.71 (C3/C3”), 121.66 (C3’/C5’) ppm; **Elemental analysis** (%) calcd. for $C_{15}H_{11}N_3$: C 77.23, H 4.75, N 18.01; found (%): C 77.16, H 4.81, N 18.33.

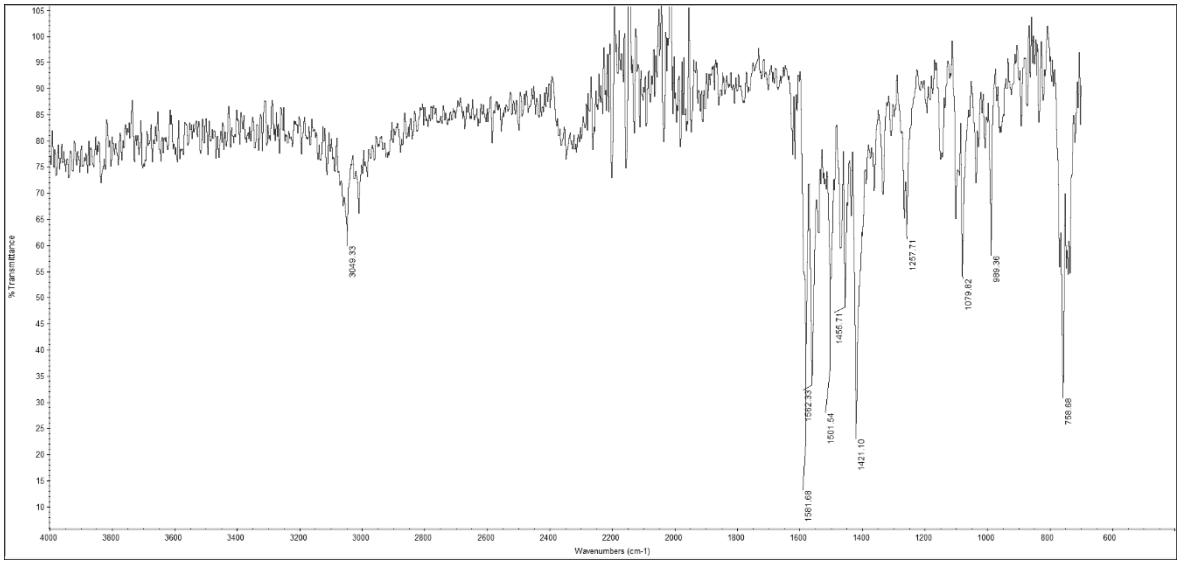

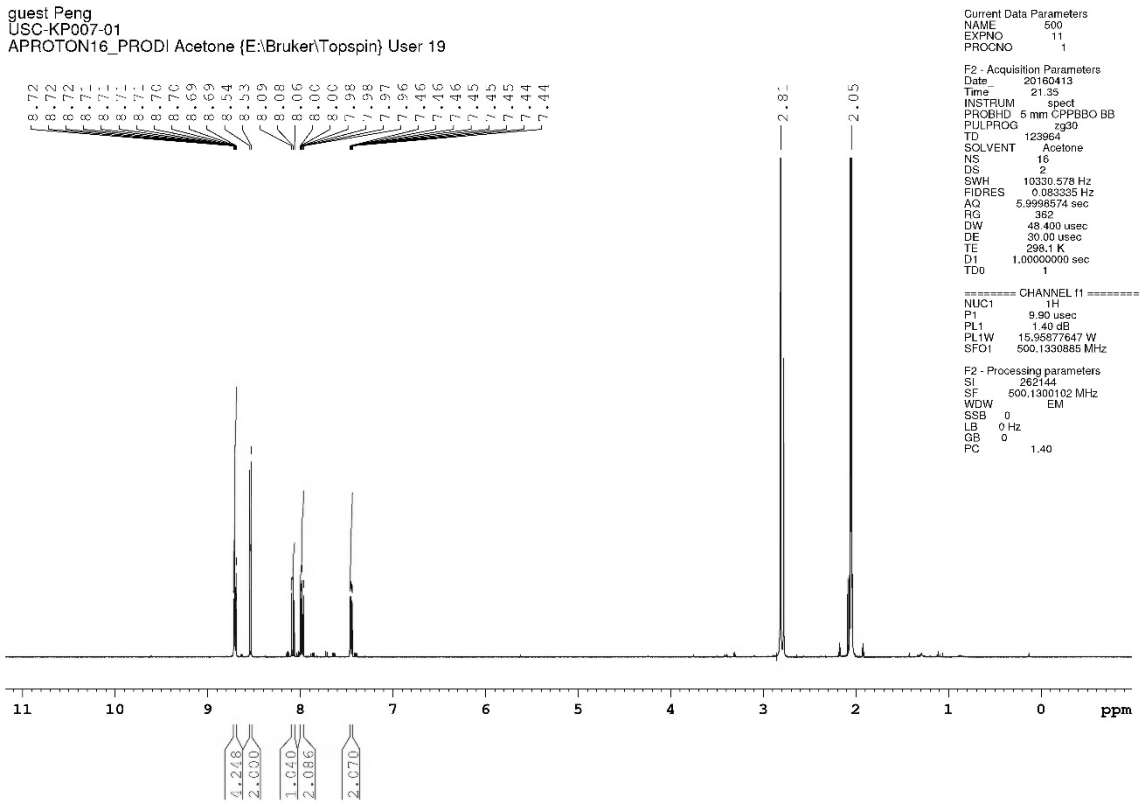
guest Peng
USC-KP007-01
APROTON16_PRODI Acetone {E:\Bruker\Topspin} User 19
8.72
8.72
8.72
8.71
8.71
8.71
8.71
8.70
8.69
8.69
8.54
8.53
8.09
8.08
8.06
8.05
8.05
7.98
7.98
7.97
7.96
7.46
7.46
7.46
7.45
7.45
7.45
7.44
7.44
2.83
2.05
4.248
2.000
1.640
2.086
2.070
11
10
9
8
7
6
5
4
3
2
1
0
ppm
Current Data Parameters
NAME 500
EXPNO 11
PROCNO 1
F2 - Acquisition Parameters
Date_ 20160413
Time 21.35
INSTRUM spect
PROBHD 5 mm CPPBBO BB
PULPROG zg30
TD 123964
SOLVENT Acetone
NS 16
DS 2
SWH 10330.578 Hz
FIDRES 0.083335 Hz
AQ 5.9998574 sec
RG 362
DW 48.400 usec
DE 30.00 usec
TE 298.1 K
D1 1.00000000 sec
TD0 1
======== CHANNEL f1 ========
NUC1 1H
P1 9.90 usec
PL1 1.40 dB
PL1W 15.95877647 W
SFO1 500.1330885 MHz
F2 - Processing parameters
SI 262144
SF 500.1300102 MHz
WDW EM
SSB 0
LB 0 Hz
GB 0
PC 1.40

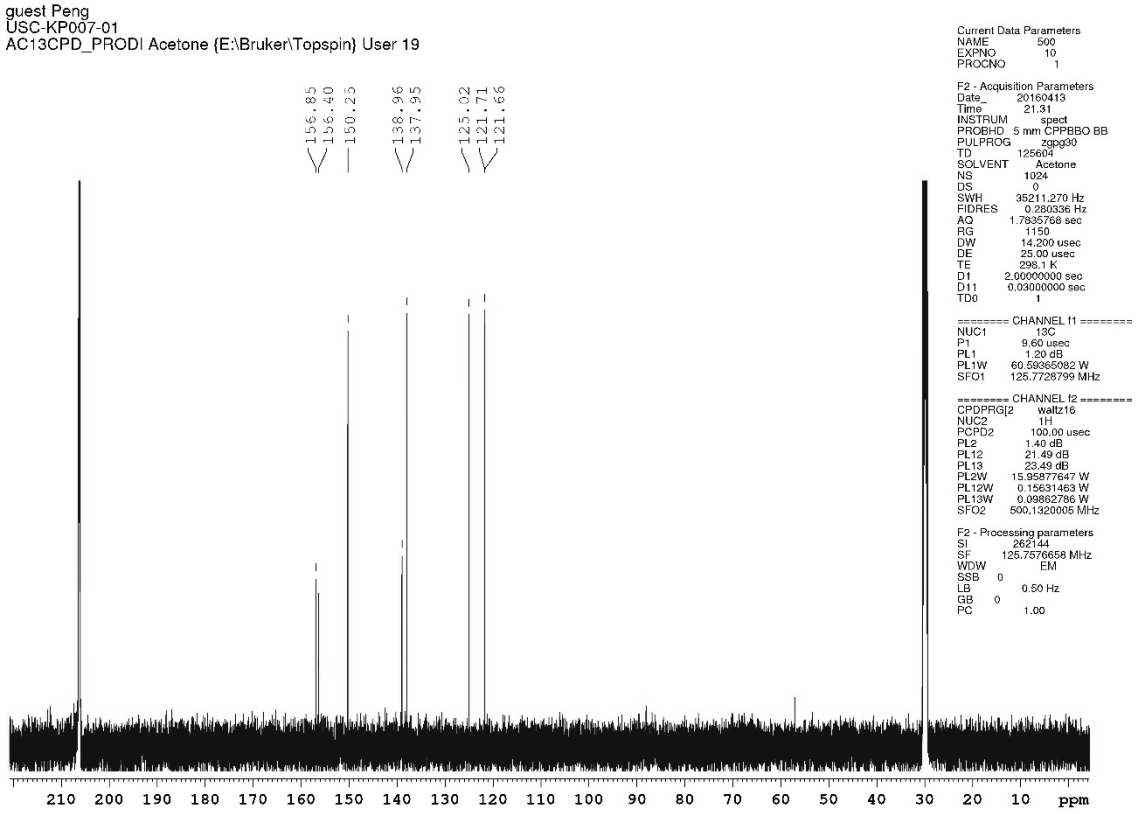
guest Peng
USC-KP007-01
AC13CPD_PRODI Acetone {E:\Bruker\Topspin} User 19
156.85
156.40
150.23
138.96
137.95
125.02
121.71
121.66
210
200
190
180
170
160
150
140
130
120
110
100
90
80
70
60
50
40
30
20
10
ppm
Current Data Parameters
NAME 500
EXPNO 10
PROCNO 1
F2 - Acquisition Parameters
Date_ 20160413
Time 21.31
INSTRUM spect
PROBHD 5 mm CPPBBO BB
PULPROG zgpg30
TD 125604
SOLVENT Acetone
NS 1024
DS 0
SWH 35211.270 Hz
FIDRES 0.280336 Hz
AQ 1.7835768 sec
RG 1150
DW 14.200 usec
DE 25.00 usec
TE 298.1 K
D1 2.00000000 sec
D11 0.03000000 sec
TD0 1
======== CHANNEL f1 ========
NUC1 13C
P1 9.60 usec
PL1 1.20 dB
PL1W 60.59365082 W
SFO1 125.7728799 MHz
======== CHANNEL f2 ========
CPDPRG[2 waltz16
NUC2 1H
PCPD2 100.00 usec
PL2 1.40 dB
PL12 21.49 dB
PL13 23.49 dB
PL2W 15.95877647 W
PL12W 0.15631463 W
PL13W 0.09862786 W
SFO2 500.1320005 MHz
F2 - Processing parameters
SI 262144
SF 125.7576658 MHz
WDW EM
SSB 0
LB 0.50 Hz
GB 0
PC 1.00

5.3.3 Synthesis of [PdCl₂(cod)]

USC-KP003-01

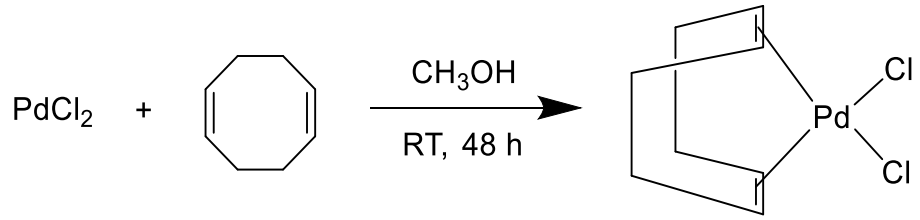

$PdCl_2$	C_8H_{12}	$C_8H_{12}Cl_2Pd$
177.32 g/mol	108.18 g/mol	285.51 g/mol

To a suspension of palladium(II) chloride (1.00 g, 5.6 mmol) in methanol (50 mL), 1,5-cyclooctadiene (2.1 mL, 1.85 g, 16.9 mmol) was added and the mixture stirred for 48 h at room temperature. During that time, the colour of the reaction mixture changed from dark red to yellow and a yellow precipitate formed. This was filtered off, washed with methanol (3 × 5 mL), and dried under vacuum for 1 d. Yield: 84% (1.35 g, 4.7 mmol). **IR** (ATR): $\tilde{\nu}$ = 2937 (m), 2889 (m), 1524 (w), 1510 (w), 1492 (w), 1453 (m), 1418 (m), 1348 (m), 1310 (m), 1247 (w), 1178 (w), 1082 (m), 1002 (m), 915 (m), 867 (m), 822 (w), 786 (s), 778 (m) cm^{-1}; **^{1}H NMR** (400.40 MHz, $CDCl_3$): δ = 6.34–6.29 (m, 4H, C*H*), 2.97–2.86 (m, 4H, CH_2), 2.60–2.54 (m, 4H, CH_2) ppm; **^{13}C NMR** (100.68 MHz, $CDCl_3$): δ = 116.81 (C*H*), 31.12 (CH_2) ppm; **Elemental analysis** (%) calcd. for $C_8H_{12}Cl_2Pd$: C 33.66, H 4.24; found (%): C 33.44, H 4.23.

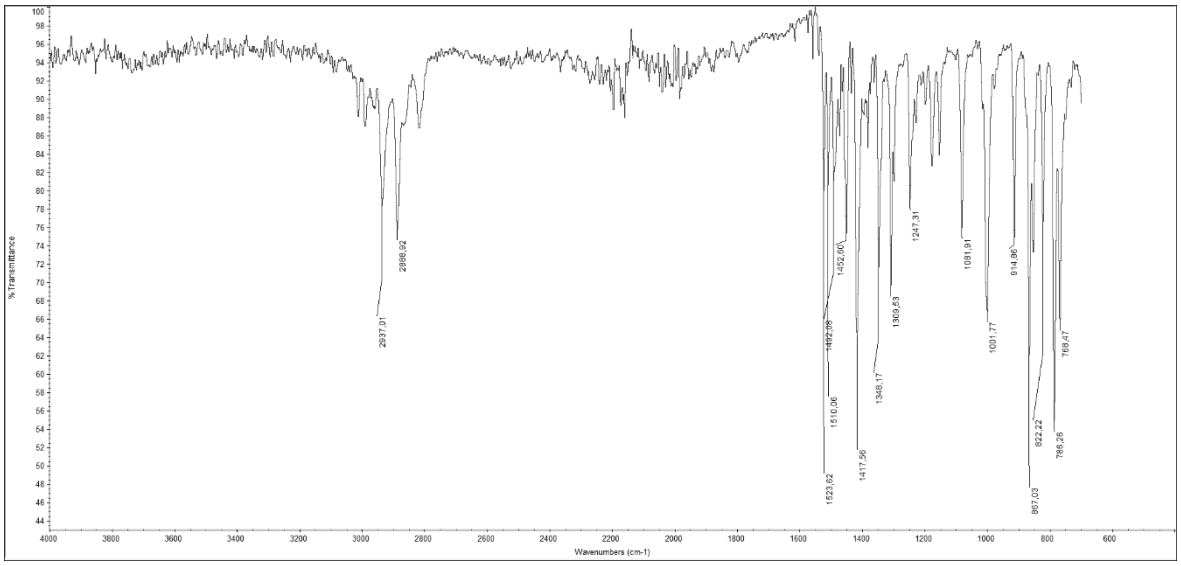

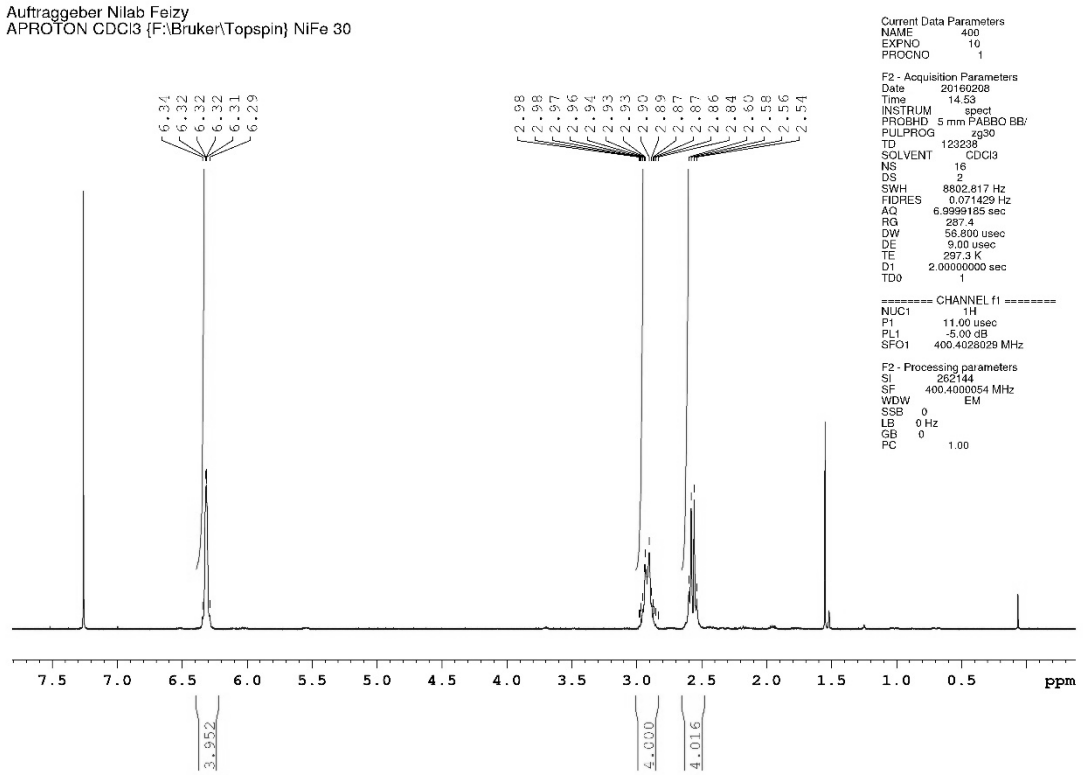
Auftraggeber Nilab Feizy
APROTON CDCl3 {F:\Bruker\Topspin} NiFe 30
6.34
6.32
6.32
6.32
6.31
6.29
2.98
2.98
2.97
2.96
2.94
2.93
2.93
2.90
2.89
2.87
2.87
2.86
2.84
2.60
2.58
2.56
2.54
Current Data Parameters
NAME 400
EXPNO 10
PROCNO 1
F2 - Acquisition Parameters
Date 20160208
Time 14.53
INSTRUM spect
PROBHD 5 mm PABBO BB/
PULPROG zg30
TD 123238
SOLVENT CDCl3
NS 16
DS 2
SWH 8802.817 Hz
FIDRES 0.071429 Hz
AQ 6.9999185 sec
RG 287.4
DW 56.800 usec
DE 9.00 usec
TE 297.3 K
D1 2.00000000 sec
TD0 1
======== CHANNEL f1 ========
NUC1 1H
P1 11.00 usec
PL1 -5.00 dB
SFO1 400.4028029 MHz
F2 - Processing parameters
SI 262144
SF 400.4000054 MHz
WDW EM
SSB 0
LB 0 Hz
GB 0
PC 1.00
7.5
7.0
6.5
6.0
5.5
5.0
4.5
4.0
3.5
3.0
2.5
2.0
1.5
1.0
0.5
ppm
3.952
4.000
4.016

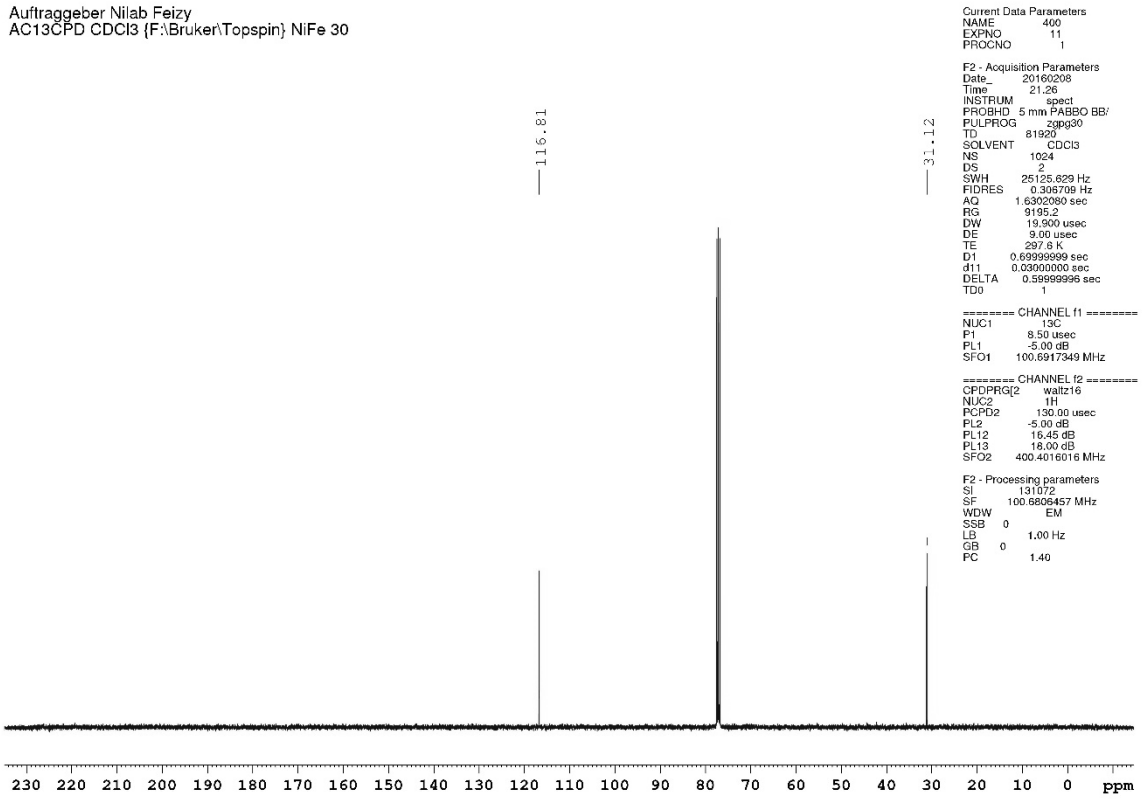
Auftraggeber Nilab Feizy
AC13CPD CDCl3 {F:\Bruker\Topspin} NiFe 30
116.81
31.12
Current Data Parameters
NAME 400
EXPNO 11
PROCNO 1
F2 - Acquisition Parameters
Date_ 20160208
Time 21.26
INSTRUM spect
PROBHD 5 mm PABBO BB/
PULPROG zgpg30
TD 81920
SOLVENT CDCl3
NS 1024
DS 2
SWH 25125.629 Hz
FIDRES 0.306709 Hz
AQ 1.6302080 sec
RG 9195.2
DW 19.900 usec
DE 9.00 usec
TE 297.6 K
D1 0.69999999 sec
d11 0.03000000 sec
DELTA 0.59999996 sec
TD0 1
======== CHANNEL f1 ========
NUC1 13C
P1 8.50 usec
PL1 -5.00 dB
SFO1 100.6917349 MHz
======== CHANNEL f2 ========
CPDPRG[2 waltz16
NUC2 1H
PCPD2 130.00 usec
PL2 -5.00 dB
PL12 16.45 dB
PL13 18.00 dB
SFO2 400.4016016 MHz
F2 - Processing parameters
SI 131072
SF 100.6806457 MHz
WDW EM
SSB 0
LB 1.00 Hz
GB 0
PC 1.40
230
220
210
200
190
180
170
160
150
140
130
120
110
100
90
80
70
60
50
40
30
20
10
0
ppm

5.3.4 Synthesis of [$PtCl_2$(cod)]

USC-KP004-01

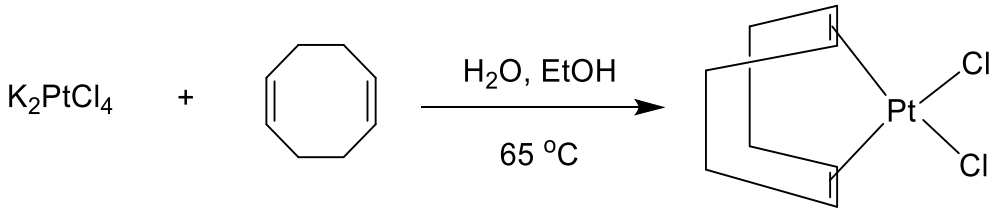

$PtCl_4K_2$	C_8H_{12}	$C_8H_{12}Cl_2Pt$
415.08 g/mol	108.18 g/mol	374.16 g/mol

A solution of potassium tetrachloroplatinate (0.5 g, 1.2 mmol) in water (30 mL) was heated to 65 °C with stirring for 15 min. Then, a solution of 1,5-cyclooctadiene (0.5 mL, 440 mg, 4.0 mmol) in ethanol (40 mL) was added to the clear light red solution. Stirring at 65 °C was continued until the colour of the solution turned from red to pale yellow, during which a white precipitate formed (about 30 min). The mixture was then cooled in ice and the white precipitate collected, washed with water (4 × 10 mL) and diethyl ether (4 × 10mL), and dried under vacuum for 3 d to obtain a white microcrystalline material. Yield: 80% (0.36 g, 0.96 mmol). **IR** (ATR): $\tilde{\nu}$ = 3009 (s), 2963 (m), 2896 (m), 2031 (w), 1972 (w), 1476 (m), 1451 (w), 1425 (w), 1339 (s), 1311 (m), 1179 (m), 1088 (w), 1009 (s), 911 (w), 872 (m), 832 (s), 812 (w), 781 (m), 778 (m) cm^{-1}; **^{1}H NMR** (400.40 MHz, $CDCl_3$): δ = 5.68–5.54 (m, 4H, C*H*), 2.75–2.68 (m, 4H, CH_2), 2.32–2.21 (m, 4H, CH_2) ppm; **^{13}C NMR** (125.76 MHz, $CDCl_3$): δ = 100.23 (d, $^1J_{C\text{-}Pt}$ = 152.2 Hz, *C*H), 31.05 (CH_2) ppm; **^{195}Pt NMR** (107.51 MHz, $CDCl_3$): δ = -3332 ppm; **Elemental analysis** (%) calcd. for $C_8H_{12}Cl_2Pt$: C 25.68, H 3.23; found (%): C 25.85, H 3.25.

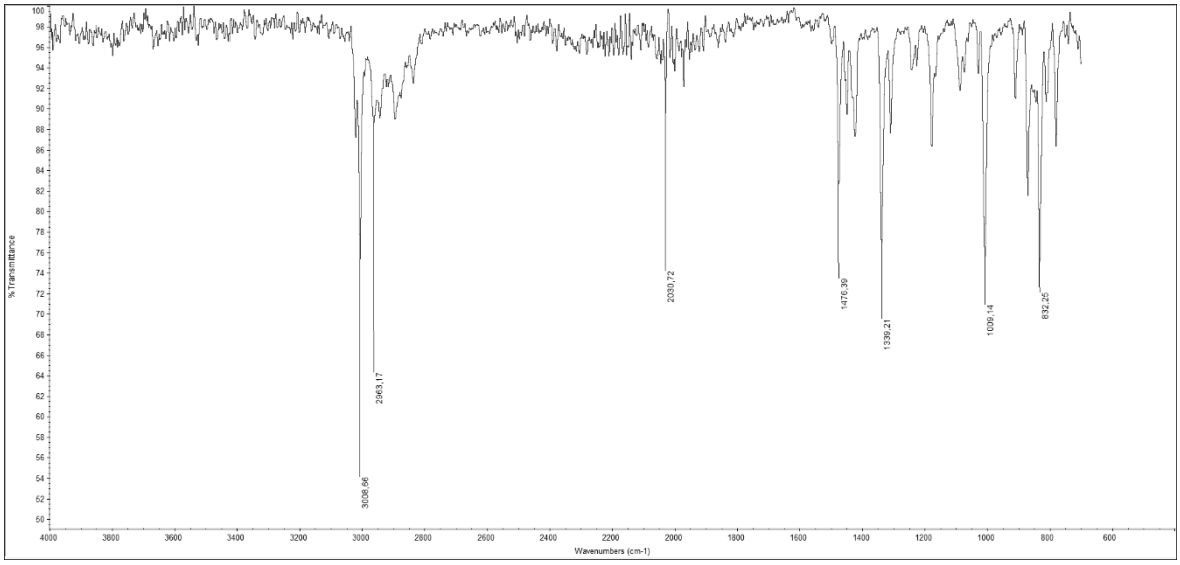
% Transmittance
Wavenumbers (cm-1)
3038.66
2963.17
2030.72
1476.39
1339.21
1099.14
832.25

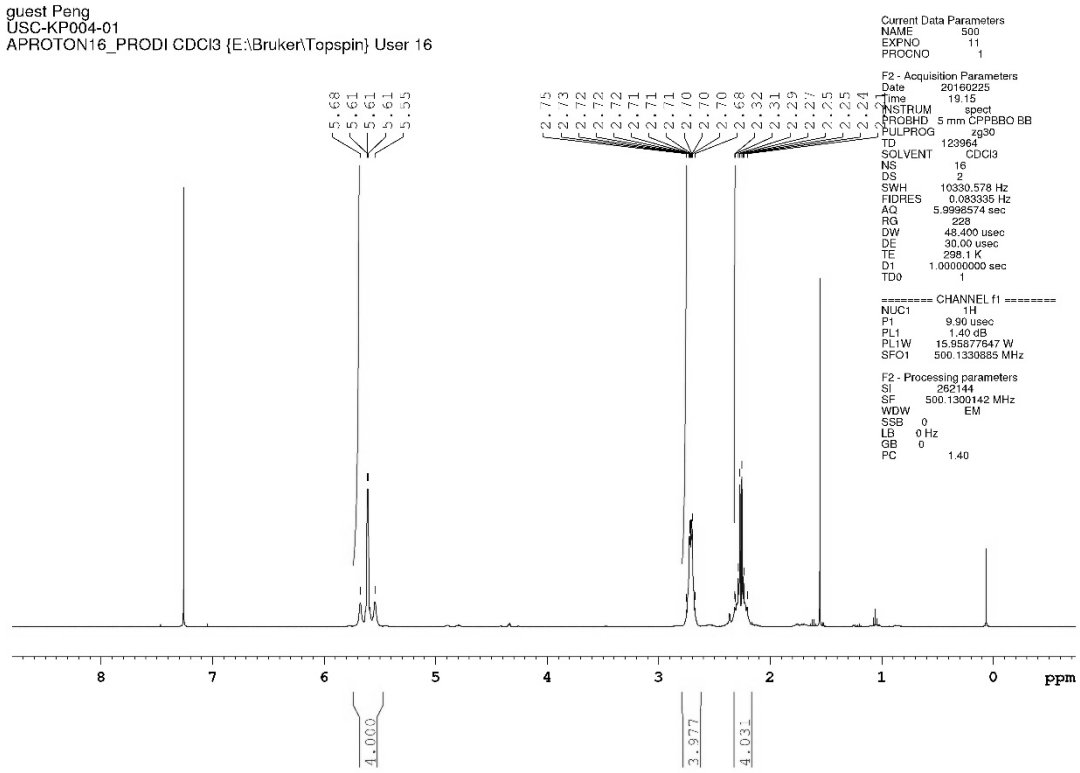
guest Peng
USC-KP004-01
APROTON16_PRODI CDCl3 {E:\Bruker\Topspin} User 16
Current Data Parameters
NAME 500
EXPNO 11
PROCNO 1
F2 - Acquisition Parameters
Date 20160225
Time 19.15
INSTRUM spect
PROBHD 5 mm CPPBBO BB
PULPROG zg30
TD 123964
SOLVENT CDCl3
NS 16
DS 2
SWH 10330.578 Hz
FIDRES 0.083335 Hz
AQ 5.9998574 sec
RG 228
DW 48.400 usec
DE 30.00 usec
TE 298.1 K
D1 1.00000000 sec
TD0 1
======== CHANNEL f1 ========
NUC1 1H
P1 9.90 usec
PL1 1.40 dB
PL1W 15.95877847 W
SFO1 500.1330885 MHz
F2 - Processing parameters
SI 262144
SF 500.1300142 MHz
WDW EM
SSB 0
LB 0 Hz
GB 0
PC 1.40
5.68
5.61
5.61
5.61
5.55
2.75
2.73
2.72
2.72
2.72
2.71
2.71
2.70
2.70
2.68
2.32
2.31
2.29
2.27
2.25
2.25
2.24
8
7
6
5
4
3
2
1
0
ppm
4.000
3.977
4.031

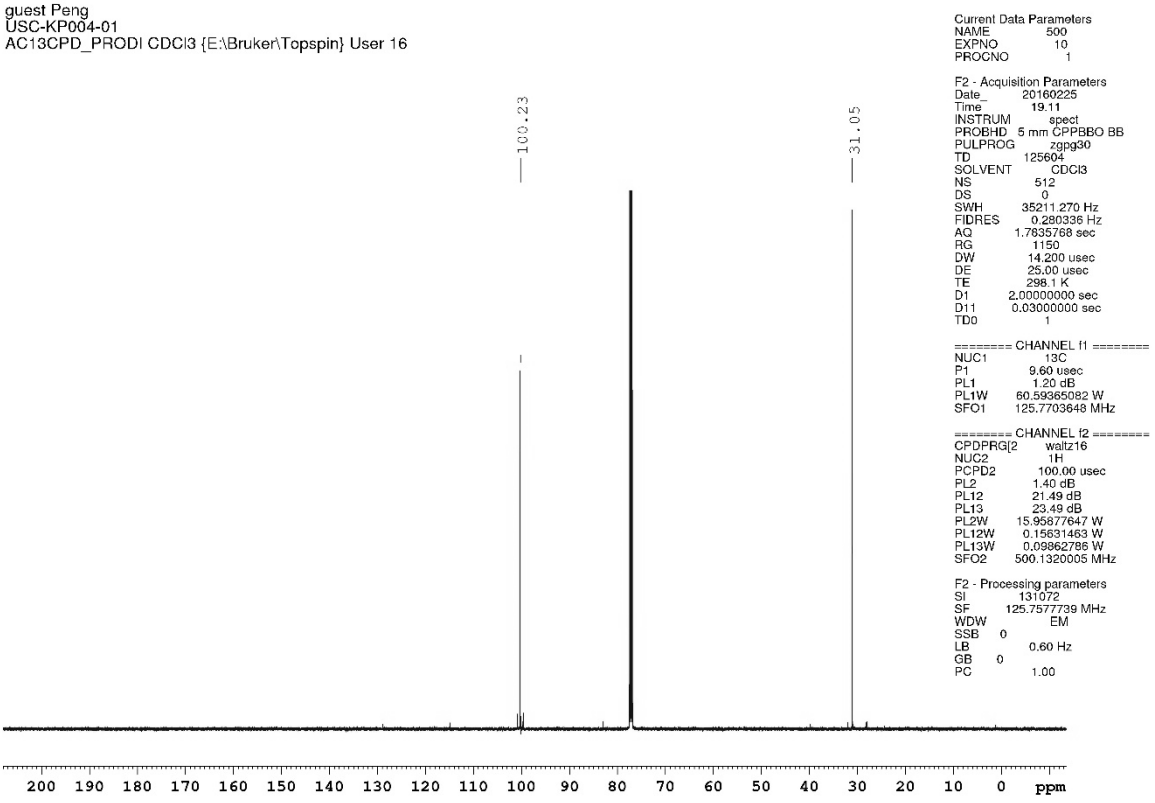
guest Peng
USC-KP004-01
AC13CPD_PRODI CDCl3 {E:\Bruker\Topspin} User 16
100.23
31.05
Current Data Parameters
NAME 500
EXPNO 10
PROCNO 1
F2 - Acquisition Parameters
Date_ 20160225
Time 19.11
INSTRUM spect
PROBHD 5 mm CPPBBO BB
PULPROG zgpg30
TD 125604
SOLVENT CDCl3
NS 512
DS 0
SWH 35211.270 Hz
FIDRES 0.280336 Hz
AQ 1.7835768 sec
RG 1150
DW 14.200 usec
DE 25.00 usec
TE 298.1 K
D1 2.00000000 sec
D11 0.03000000 sec
TD0 1
======== CHANNEL f1 ========
NUC1 13C
P1 9.60 usec
PL1 1.20 dB
PL1W 60.59365082 W
SFO1 125.7703648 MHz
======== CHANNEL f2 ========
CPDPRG[2 waltz16
NUC2 1H
PCPD2 100.00 usec
PL2 1.40 dB
PL12 21.49 dB
PL13 23.49 dB
PL2W 15.95877647 W
PL12W 0.15631463 W
PL13W 0.09862786 W
SFO2 500.1320005 MHz
F2 - Processing parameters
SI 131072
SF 125.7577739 MHz
WDW EM
SSB 0
LB 0.60 Hz
GB 0
PC 1.00
200 190 180 170 160 150 140 130 120 110 100 90 80 70 60 50 40 30 20 10 0 ppm

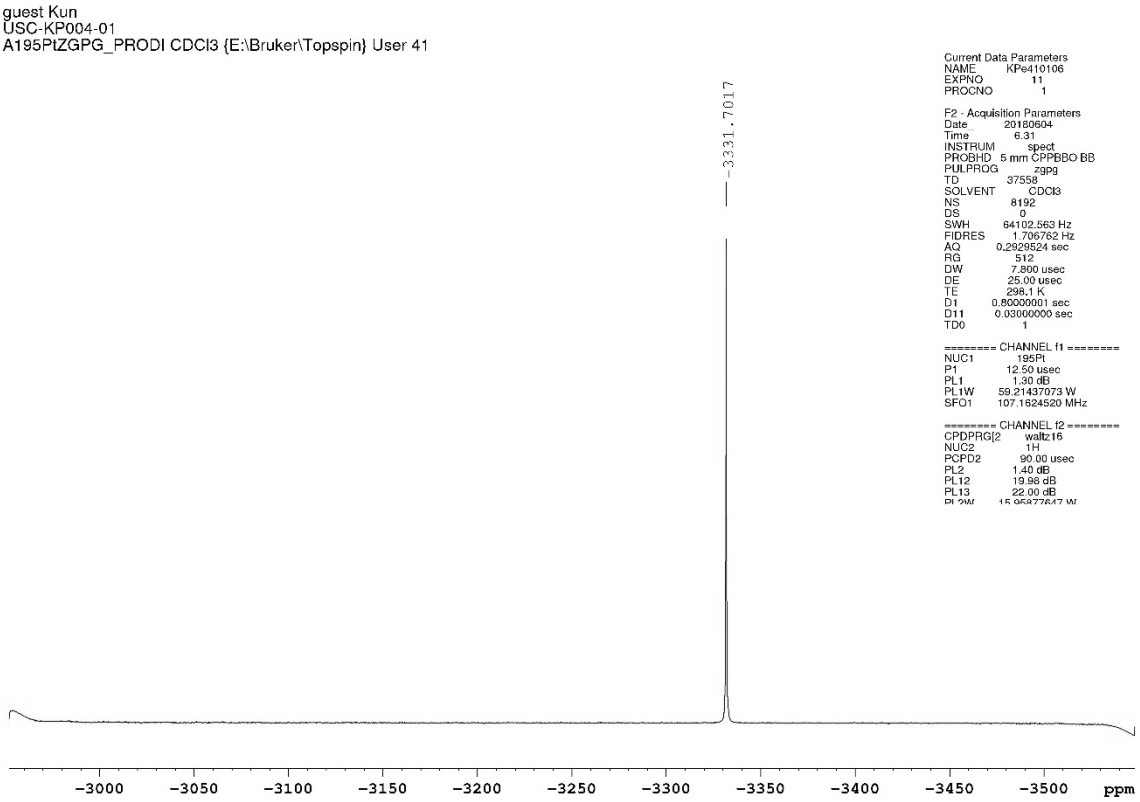
guest Kun
USC-KP004-01
A195PtZGPG_PRODI CDCl3 {E:\Bruker\Topspin} User 41
-3331.7017
Current Data Parameters
NAME KPe410106
EXPNO 11
PROCNO 1
F2 - Acquisition Parameters
Date 20180604
Time 6.31
INSTRUM spect
PROBHD 5 mm CPPBBO BB
PULPROG zgpg
TD 37558
SOLVENT CDCl3
NS 8192
DS 0
SWH 64102.563 Hz
FIDRES 1.706762 Hz
AQ 0.2929524 sec
RG 512
DW 7.800 usec
DE 25.00 usec
TE 298.1 K
D1 0.80000001 sec
D11 0.03000000 sec
TD0 1
======== CHANNEL f1 ========
NUC1 195Pt
P1 12.50 usec
PL1 1.30 dB
PL1W 59.21437073 W
SFO1 107.1524520 MHz
======== CHANNEL f2 ========
CPDPRG[2 waltz16
NUC2 1H
PCPD2 90.00 usec
PL2 1.40 dB
PL12 19.98 dB
PL13 22.00 dB
-3000 -3050 -3100 -3150 -3200 -3250 -3300 -3350 -3400 -3450 -3500 ppm

5.3.5 Synthesis of [PdCl(terpy)]Cl

USC-KP008-01

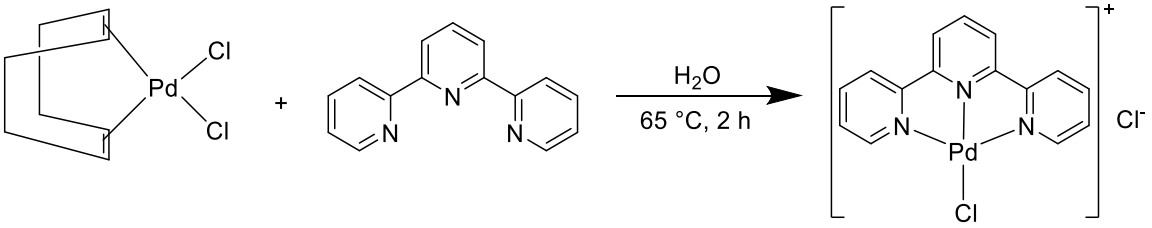

$C_8H_{12}Cl_2Pd$
285.51 g/mol

$C_{15}H_{11}N_3$
233.27 g/mol

$C_{15}H_{11}Cl_2N_3Pd$
410.59 g/mol

In a large vial, a suspension of [$PdCl_2$(cod)] (250 mg, 0.88 mmol) and 2,2':6',2"-terpyridine (208 mg, 0.89 mmol) in water (10 mL) was heated to 65 °C for 2 h with stirring. During that time, the colour of the solution gradually changed from orange to dark brown. The solution was then filtered through Celite and the solvent removed under vacuum. The resulting yellow solid was washed with diethyl ether (5 × 20 mL) and dried under vacuum for 6 d. Yield: 84% (303 mg, 0.74 mmol). **IR** (ATR): $\tilde{\nu}$ = 3342 (s), 3022 (m), 1601 (s), 1477 (s), 1449 (s), 1321 (m), 1028 (m), 768 (s), 721 (m) cm^{-1}; **^{1}H NMR** (500.13 MHz, D_2O): δ = 8.25 (t, 1H, $^3J_{H4',H3'/H5'}$ = 8.0 Hz, H4'), 8.13 (dt, 2H, $^3J_{H4,H3/H5;H4",H3"/H5"}$ = 7.8 Hz, $^4J_{H4,H6;/H4",H6"}$ = 1.5 Hz, H4/H4"), 8.04–8.00 (m, 4H, H3'/H5', H6/H6"), 7.86 (d, 2H, $^3J_{H3,H4;H3",H4"}$ = 5.5 Hz, H3/H3"), 7.42 (ddd, 2H, $^3J_{H5,H4;H5",H4"}$ = 7.5 Hz, $^3J_{H5,H6;H5",H6"}$ = 5.4 Hz, $^4J_{H5,H3;H5",H3"}$ = 1.4 Hz, H5/H5") ppm; **^{13}C NMR** (125.76 MHz, D_2O): δ = 157.08 (C2'/C6'), 154.28 (C2/C2"), 151.67 (C6/C6"), 143.46 (C4'), 142.88 (C4/C4"), 129.10 (C5/C5"), 125.21 (C3/C3"), 124.52 (C3'/C5') ppm; **MS** (ESI^+, CH_3OH): *m*/*z* = 375.9664 $[M\text{-}Cl]^+$; **Elemental analysis** (%) calcd. for $C_{15}H_{11}N_3Cl_2Pd$: C 43.88, H 2.70, N 10.23; found (%): C 43.29, H 3.09, N 10.34.

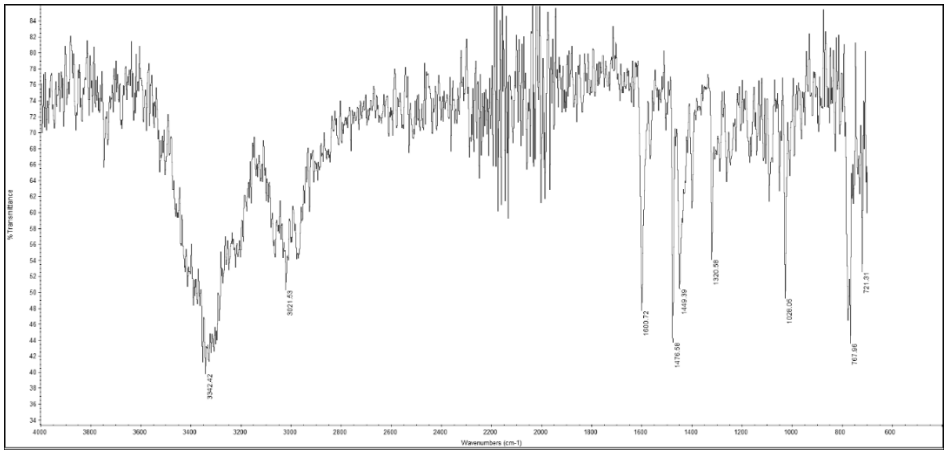
% Transmittance
Wavenumbers (cm-1)
3342.42
3021.83
1603.72
1476.98
1449.89
1320.56
1026.09
767.66
721.31

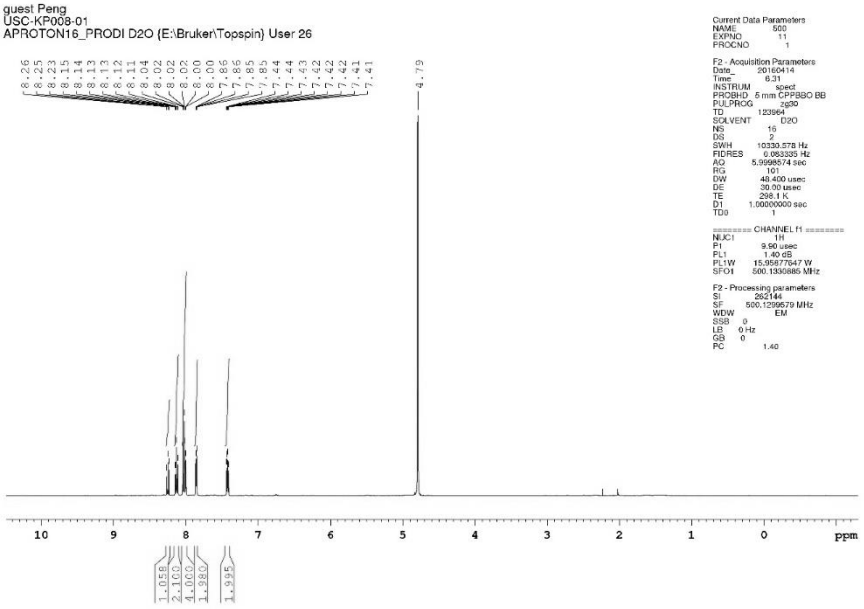
guest Peng
USC-KP008-01
APROTON16_PRODI D2O (E:\Bruker\Topspin) User 26
4.779
ppm
1.058
2.100
4.000
1.980
1.995

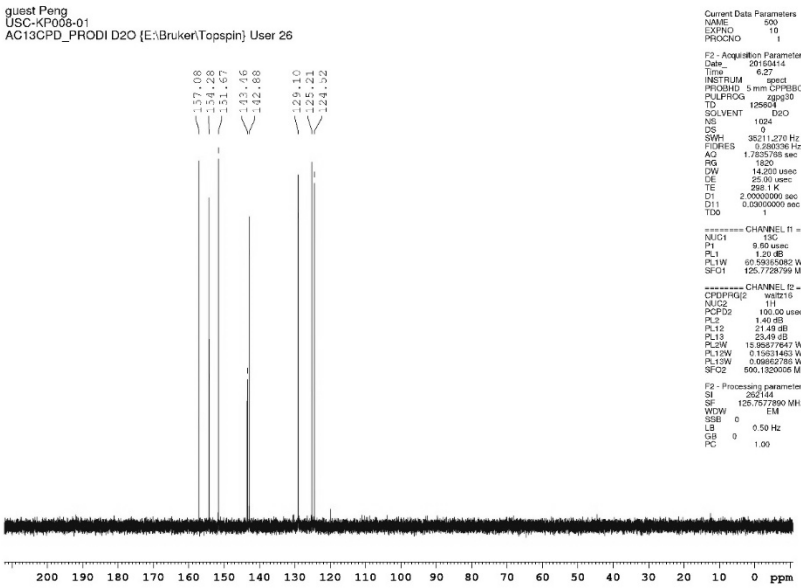
guest Peng
USC-KP008-01
AC13CPD_PRODI D2O {E:\Bruker\Topspin} User 26
157.08
134.28
131.67
143.46
142.88
129.10
125.21
124.92
ppm

5.3.6 Synthesis of [PtCl(terpy)]Cl

USC-KP009-01

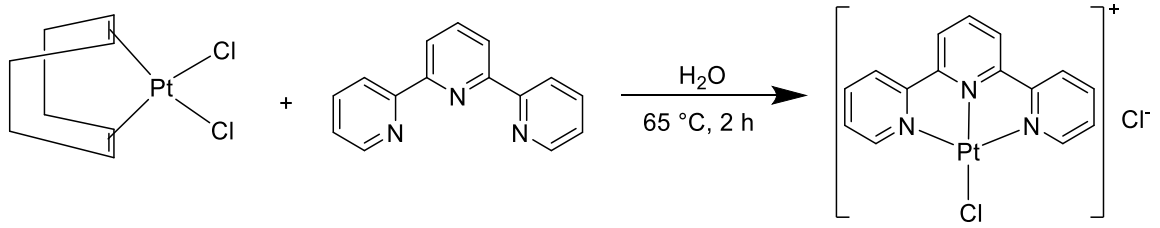

$C_8H_{12}Cl_2Pt$
374.16 g/mol

$C_{15}H_{11}N_3$
233.27 g/mol

$C_{15}H_{11}Cl_2N_3Pt$
499.25 g/mol

In a large vial, a suspension of [$PtCl_2$(cod)] (150 mg, 0.40 mmol) and 2,2':6',2"-terpyridine (96 mg, 0.41 mmol) in water (10 mL) was heated to 65 °C for 2 h with stirring. During that time, the colour of the solution gradually changed from orange to dark red. The solution was then filtered through Celite and the solvent removed under vacuum. The resulting red solid was washed with diethyl ether (5 × 20 mL) and dried under vacuum for 6 d. Yield: 83% (163 mg, 0.33 mmol). **IR** (ATR): $\tilde{\nu}$ = 3318 (s), 3024 (m), 1604 (m), 1476 (m), 1451 (m), 1437 (w), 1400 (w), 1317 (w), 1032 (w), 775 (m) cm^{-1}; **^{1}H NMR** (400.47 MHz, D_2O): δ = 8.18–8.10 (m, 3H, H6/H6", H4'), 7.92–7.87 (m, 6H, H3'/H5', H3/H3", H4/H4"), 7.42 (ddd, 2H, $^3J_{H5,H4;/H5",H4"}$ = 7.4 Hz, $^3J_{H5,H6;H5",H6"}$ = 5.4 Hz, $^4J_{H5,H3;H5",H3"}$ = 1.4 Hz, H5/H5") ppm; **^{13}C NMR** (100.70 MHz, D_2O): δ = 157.32 (C2'/C6'), 153.77 (C2/C2"), 150.70 (C6/C6"), 142.76 (C4/C4"), 142.38 (C4'), 129.16 (C5/C5"), 125.48 (C3/C3"), 124.23 (C3'/C5') ppm; **^{195}Pt NMR** (86.09 MHz, D_2O): δ = -2704 ppm; **MS** (ESI^+, CH_3OH): *m*/*z* = 464.0276 $[M\text{-}Cl]^+$; **Elemental analysis** (%) calcd. for $C_{15}H_{11}N_3Cl_2Pt$: C 36.09, H 2.22, N 8.42; found (%): C 35.54, H 2.44, N 8.27.

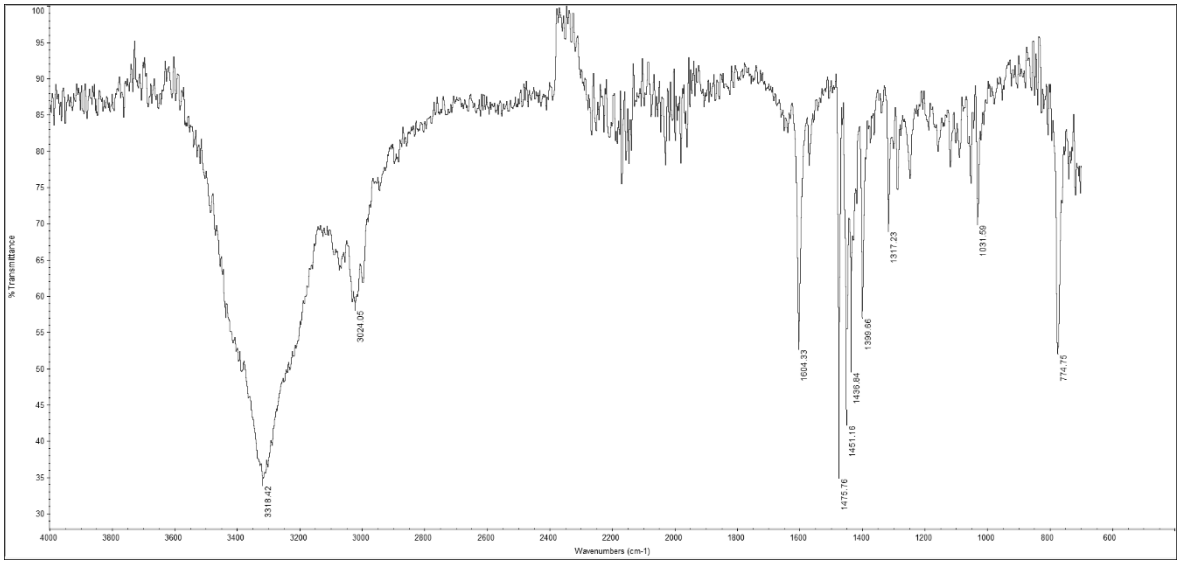
% Transmittance
Wavenumbers (cm-1)
3518.42
3024.05
1604.33
1475.76
1451.16
1439.84
1399.66
1317.23
1031.59
774.76

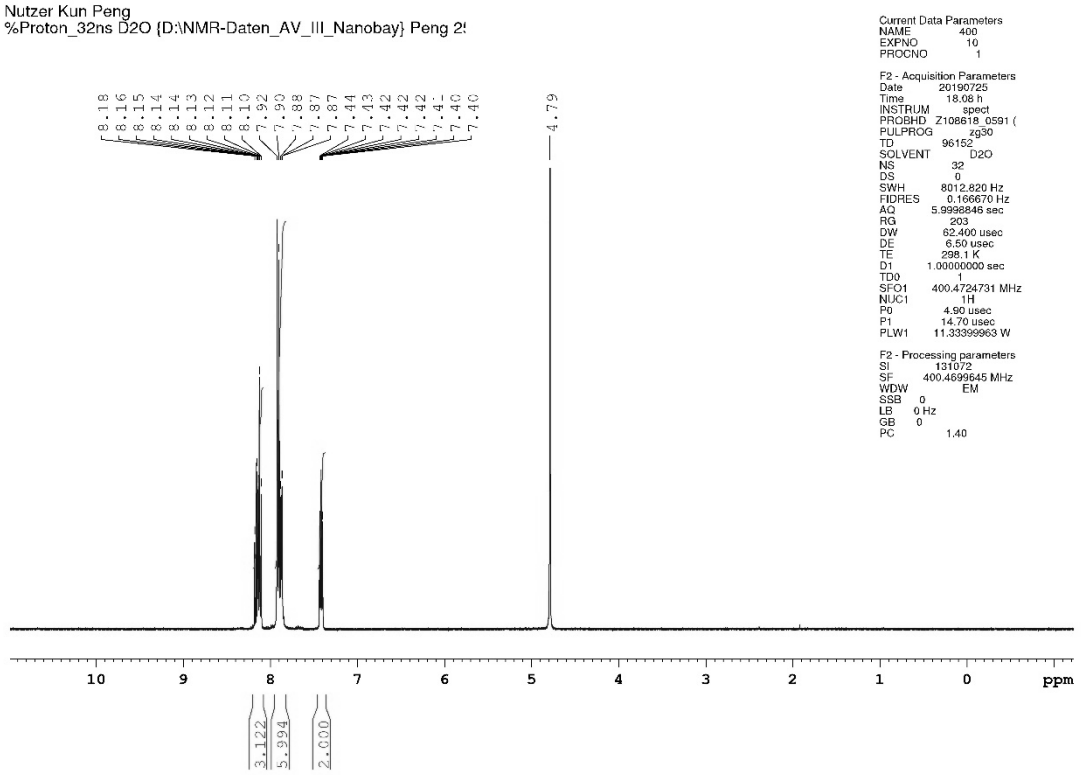
Nutzer Kun Peng
%Proton_32ns D2O {D:\NMR-Daten_AV_III_Nanobay} Peng 2
Current Data Parameters
NAME 400
EXPNO 10
PROCNO 1
F2 - Acquisition Parameters
Date 20190725
Time 18.08 h
INSTRUM spect
PROBHD Z108818_0591 (
PULPROG zg30
TD 96152
SOLVENT D2O
NS 32
DS 0
SWH 8012.820 Hz
FIDRES 0.166670 Hz
AQ 5.9998846 sec
RG 203
DW 62.400 usec
DE 6.50 usec
TE 298.1 K
D1 1.00000000 sec
TD0 1
SFO1 400.4724731 MHz
NUC1 1H
P0 4.90 usec
P1 14.70 usec
PLW1 11.33399963 W
F2 - Processing parameters
SI 131072
SF 400.4699645 MHz
WDW EM
SSB 0
LB 0 Hz
GB 0
PC 1.40
8.18
8.16
8.15
8.14
8.14
8.13
8.12
8.11
8.10
7.92
7.90
7.88
7.87
7.87
7.44
7.43
7.42
7.42
7.42
7.41
7.40
7.40
4.79
10
9
8
7
6
5
4
3
2
1
0
ppm
3.122
5.994
2.000

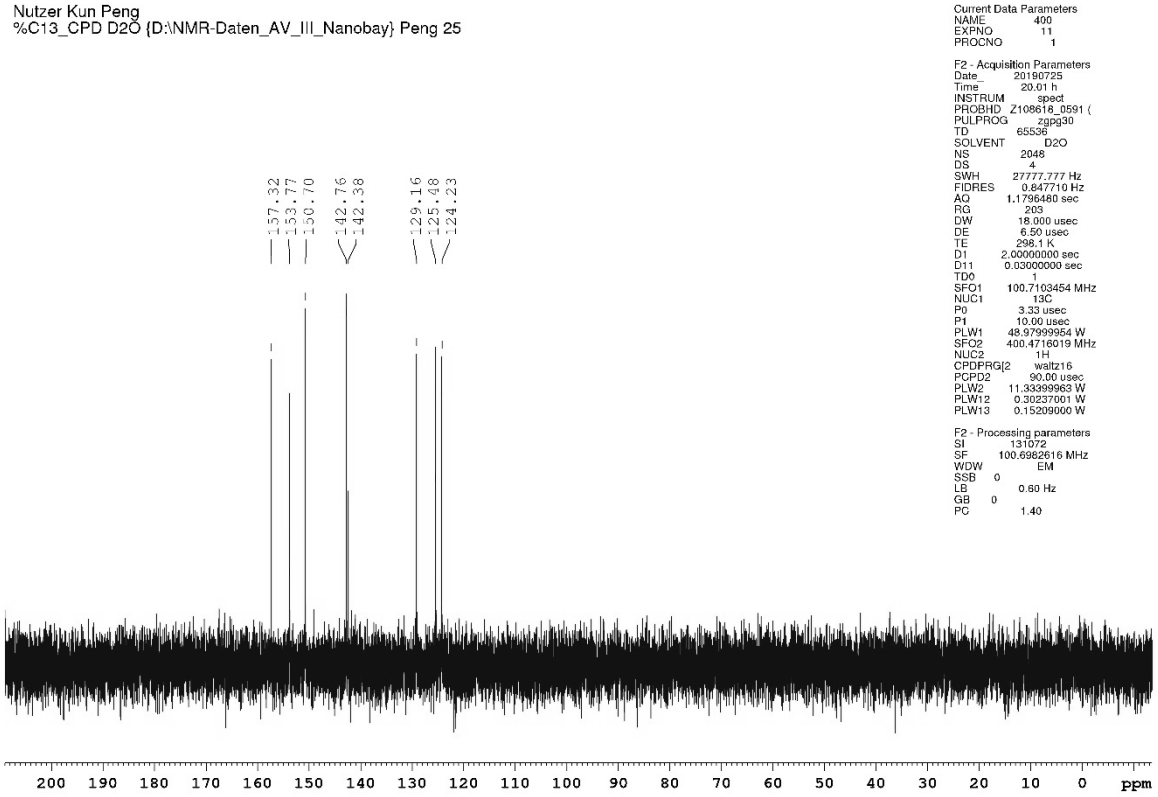
Nutzer Kun Peng
%C13_CPD D2O {D:\NMR-Daten_AV_III_Nanobay} Peng 25
157.32
153.77
150.70
142.76
142.38
129.16
125.48
124.23
Current Data Parameters
NAME 400
EXPNO 11
PROCNO 1
F2 - Acquisition Parameters
Date_ 20190725
Time 20.01 h
INSTRUM spect
PROBHD Z108618_0591 (
PULPROG zgpg30
TD 65536
SOLVENT D2O
NS 2048
DS 4
SWH 27777.777 Hz
FIDRES 0.847710 Hz
AQ 1.1796480 sec
RG 203
DW 18.000 usec
DE 6.50 usec
TE 298.1 K
D1 2.00000000 sec
D11 0.03000000 sec
TD0 1
SFO1 100.7103454 MHz
NUC1 13C
P0 3.33 usec
P1 10.00 usec
PLW1 48.97999954 W
SFO2 400.4716019 MHz
NUC2 1H
CPDPRG[2 waltz16
PCPD2 90.00 usec
PLW2 11.33999963 W
PLW12 0.30237001 W
PLW13 0.15209000 W
F2 - Processing parameters
SI 131072
SF 100.6982616 MHz
WDW EM
SSB 0
LB 0.60 Hz
GB 0
PC 1.40
200 190 180 170 160 150 140 130 120 110 100 90 80 70 60 50 40 30 20 10 0 ppm

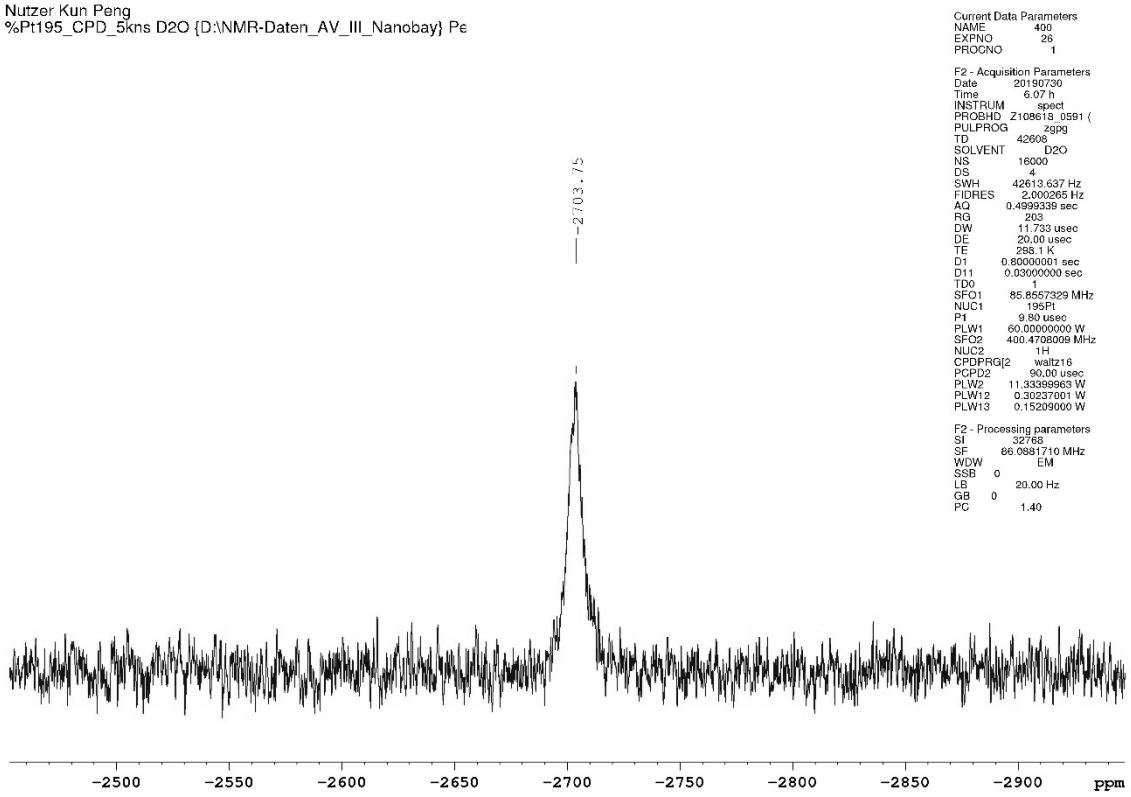
Nutzer Kun Peng
%Pt195_CPD_5kns D2O {D:\NMR-Daten_AV_III_Nanobay} Pe
-2703.75
Current Data Parameters
NAME 400
EXPNO 26
PROCNO 1
F2 - Acquisition Parameters
Date 20190730
Time 6.07 h
INSTRUM spect
PROBHD Z108618_0591 (
PULPROG zgpg
TD 42608
SOLVENT D2O
NS 16000
DS 4
SWH 42613.637 Hz
FIDRES 2.000265 Hz
AQ 0.4999339 sec
RG 203
DW 11.733 usec
DE 20.00 usec
TE 298.1 K
D1 0.80000001 sec
D11 0.03000000 sec
TD0 1
SFO1 85.8557329 MHz
NUC1 195Pt
P1 9.80 usec
PLW1 60.00000000 W
SFO2 400.4708009 MHz
NUC2 1H
CPDPRG[2 waltz16
PCPD2 90.00 usec
PLW2 11.33999963 W
PLW12 0.30237001 W
PLW13 0.15209000 W
F2 - Processing parameters
SI 32768
SF 86.0881710 MHz
WDW EM
SSB 0
LB 20.00 Hz
GB 0
PC 1.40
−2500 −2550 −2600 −2650 −2700 −2750 −2800 −2850 −2900 ppm

5.3.7 Synthesis of $[Pd(N_3)(terpy)]PF_6$

USC-KP010-01

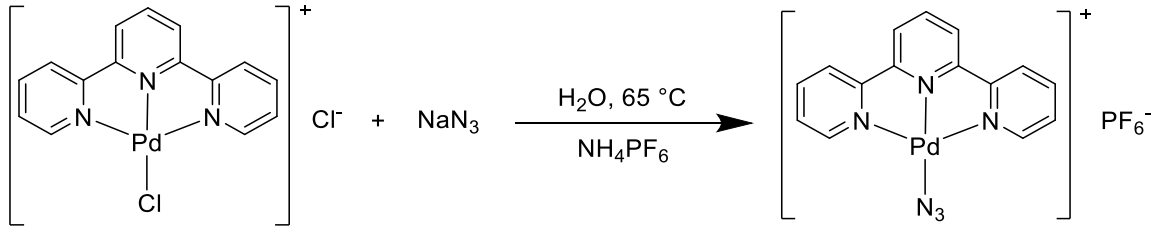

$C_{15}H_{11}Cl_2N_3Pd$
410.59 g/mol

NaN_3
65.01 g/mol

$C_{15}H_{11}N_6PF_6Pd$
526.67 g/mol

In a big glass vial, [PdCl(terpy)]Cl (150 mg, 0.37 mmol) was dissolved in water (10 mL) by heating to 65 °C. To the resulting orange solution, solid sodium azide (240 mg, 3.69 mmol) was added. The mixture was stirred at 65 °C for another 2 h. Then, ammonium hexafluorophosphate (1.20 g, 7.36 mmol) in water (approx. 2 mL) was added to immediately give a yellow precipitate. This was filtered off, washed with water (3 × 20 mL) and diethyl ether (3 × 30 mL), and then dried under vacuum for 3 d to obtain the product as a pale yellow solid. Yield: 87% (168 mg, 0.32 mmol). **IR** (ATR): $\tilde{\nu}$ = 3093 (w), 2158 (w), 2030 (s), 1953 (w), 1600 (w), 1453 (w), 825 (m), 767 (m) cm^{-1}; **^{1}H NMR** (500.13 MHz, DMSO-d_6): δ = 8.66 (d, 2H, $^3J_{H3'/H5',H4'}$ = 7.4 Hz, H3'/H5'), 8.63–8.56 (m, 3H, H6/H6", H4'), 8.49 (dt, 2H, $^3J_{H4,H3/H5;H4",H5"/H3"}$ = 7.9 Hz, $^4J_{H4,H6;H4",H6"}$ = 1.6 Hz, H4/H4"), 8.39 (ddd, 2H, $^3J_{H3,H4;H3",H4"}$ = 5.5 Hz, $^4J_{H3,H5;H3",H5"}$ = 1.4 Hz, $^5J_{H3,H6;H3",H6"}$ = 0.6 Hz, H3/H3"), 7.97 (ddd, 2H, $^3J_{H5,H4;H5",H4"}$ = 7.7 Hz, $^3J_{H5,H6;H5",H6"}$ = 5.6 Hz, $^4J_{H5,H3;H5",H3"}$ = 1.4 Hz, H5/ H5") ppm; **^{13}C NMR** (125.76 MHz, DMSO-d_6): δ = 157.90 (C2'/C6'), 154.07 (C2/C2"), 149.60 (C6/C6"), 142.88 (C4', C4/C4"), 129.06 (C5/C5"), 125.45 (C3'/C5'), 124.40 (C3/C3") ppm; **MS** (ESI^+, CH_3OH): *m*/*z* = 381.0071 $[M\text{-}PF_6]^+$; **Elemental analysis** (%) calcd. for $C_{15}H_{11}N_6PF_6Pd$: C 34.21, H 2.11, N 15.96; found (%): C 34.27, H 2.28, N 15.42.

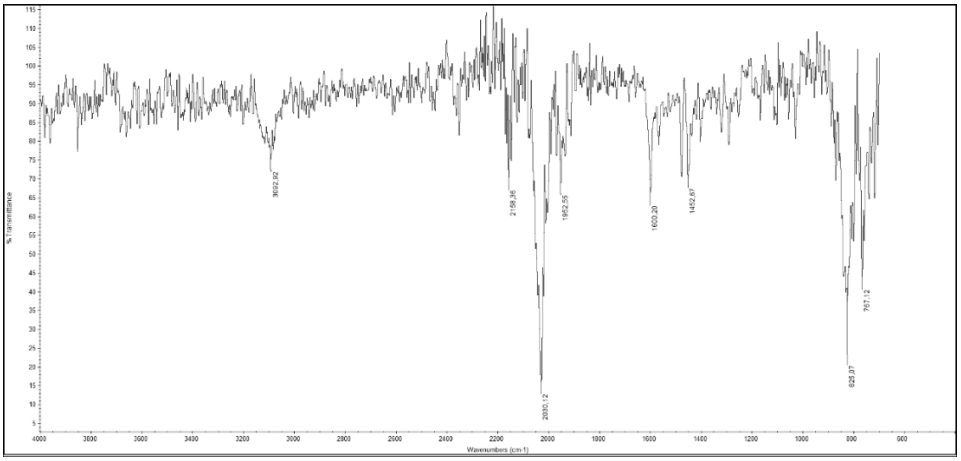
% Transmittance
Wavenumbers (cm-1)
3632.82
2156.35
2030.12
1852.55
1603.20
1452.87
757.12
628.97

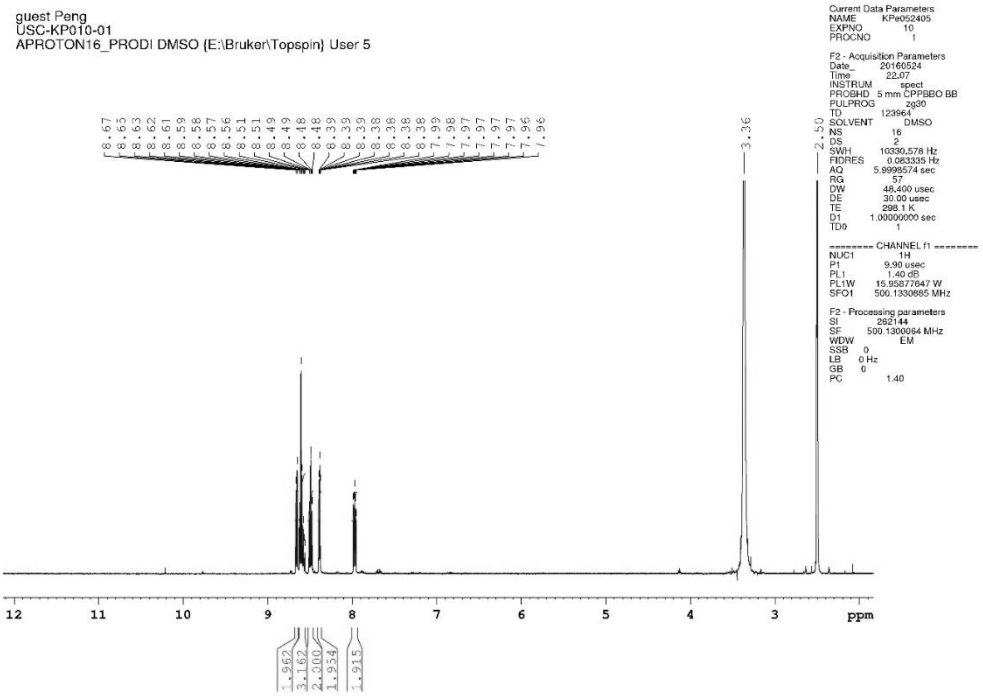
guest Peng
USC-KP010-01
APROTON16_PRODI DMSO {E:\Bruker\Topspin} User 5
Current Data Parameters
NAME KPe052405
EXPNO 10
PROCNO 1
F2 - Acquisition Parameters
Date_ 20160524
Time 22.07
INSTRUM spect
PROBHD 5 mm CPPBBO BB
PULPROG zg30
TD 123964
SOLVENT DMSO
NS 16
DS 2
SWH 10330.578 Hz
FIDRES 0.083335 Hz
AQ 5.9996574 sec
RG 57
DW 48.400 usec
DE 30.00 usec
TE 298.1 K
D1 1.00000000 sec
TD0 1
======== CHANNEL f1 ========
NUC1 1H
P1 9.90 usec
PL1 1.40 dB
PL1W 15.85877647 W
SFO1 500.1330885 MHz
F2 - Processing parameters
SI 262144
SF 500.1300064 MHz
WDW EM
SSB 0
LB 0 Hz
GB 0
PC 1.40
8.67
8.65
8.63
8.62
8.61
8.59
8.58
8.57
8.56
8.51
8.49
8.49
8.48
8.48
8.39
8.39
8.38
8.38
8.38
8.38
8.38
7.99
7.98
7.97
7.97
7.97
7.97
7.96
7.96
3.36
2.50
12
11
10
9
8
7
6
5
4
3
ppm
1.962
3.162
2.000
1.934
1.915

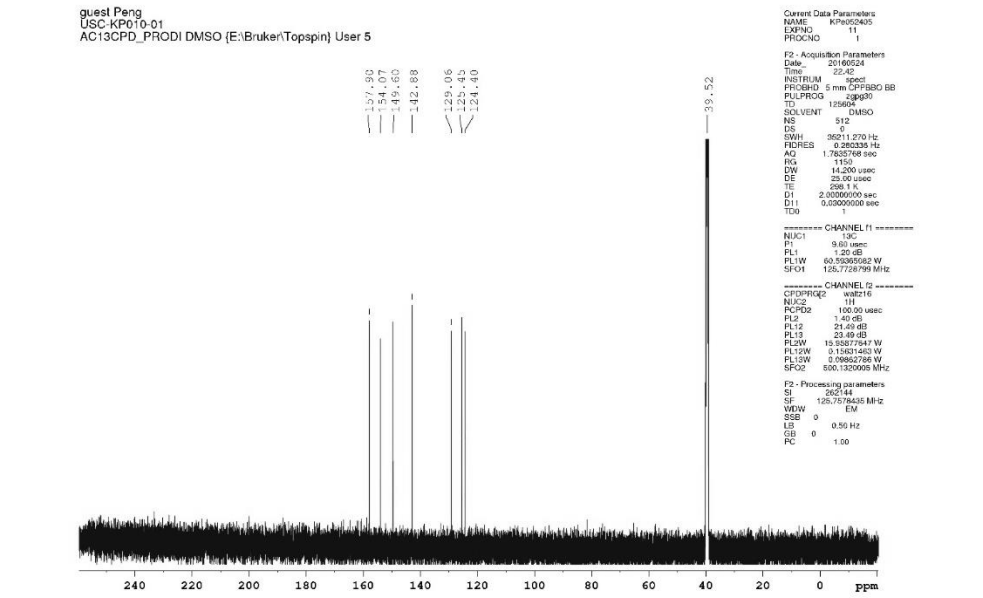
guest Peng
USC-KP010-01
AC13CPD_PRODI DMSO {E:\Bruker\Topspin} User 5
Current Data Parameters
NAME KPe052405
EXPNO 11
PROCNO 1
F2 - Acquisition Parameters
Date_ 20160524
Time 22.42
INSTRUM spect
PROBHD 5 mm CPPBBO BB
PULPROG zgpg30
TD 125604
SOLVENT DMSO
NS 512
DS 0
SWH 35211.270 Hz
FIDRES 0.280335 Hz
AQ 1.7835768 sec
RG 1150
DW 14.200 usec
DE 25.00 usec
TE 298.1 K
D1 2.00000000 sec
D11 0.03000000 sec
TD0 1
======== CHANNEL f1 ========
NUC1 13C
P1 9.60 usec
PL1 1.20 dB
PL1W 60.55365082 W
SFO1 125.7728799 MHz
======== CHANNEL f2 ========
CPDPRG2 waltz16
NUC2 1H
PCPD2 100.00 usec
PL2 1.40 dB
PL12 21.49 dB
PL13 23.49 dB
PL2W 15.85877547 W
PL12W 0.15631463 W
PL13W 0.09852796 W
SFO2 500.1320005 MHz
F2 - Processing parameters
SI 262144
SF 125.7578435 MHz
WDW EM
SSB 0
LB 0.50 Hz
GB 0
PC 1.00
157.93
154.07
149.60
142.68
129.06
125.43
124.80
39.52
240
220
200
180
160
140
120
100
80
60
40
20
0
ppm

5.3.8 Synthesis o [Pt(N$_3$)(terpy)]PF$_6$

USC-KP011-16

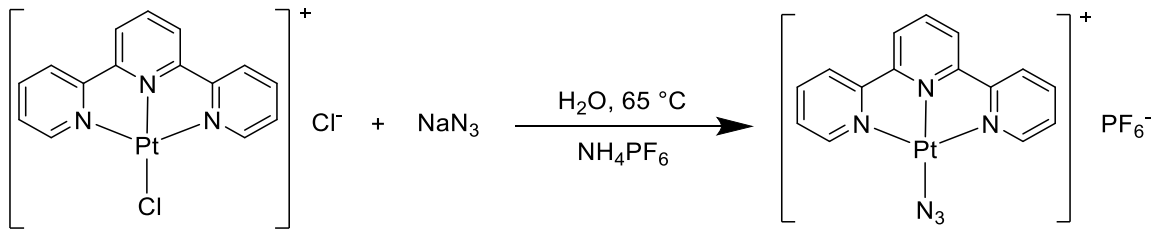

$C_{15}H_{11}Cl_2N_3Pt$ 499.25 g/mol

NaN_3 65.01 g/mol

$C_{15}H_{11}N_6PF_6Pt$ 615.33 g/mol

In a big glass vial, [PtCl(terpy)]Cl (200 mg, 0.40 mmol) was dissolved in water (10 mL) with heating to 65 °C. To the resulting red solution, solid sodium azide (260 mg, 4.0 mmol) was added. After stirring at 65 °C for 2 h, the dark red solution was filtered through Celite. Addition of a saturated solution of ammonium hexafluorophosphate (660 mg, 4.0 mmol) in water (2 mL) immediately led to formation of an orange precipitate, which was filtered of, washed with water (3 × 15 mL) and diethyl ether (3 × 30 mL), and then dried under vacuum for 6 d to obtain the product as an orange solid. Yield: 80% (197.8 mg, 0.32 mmol). **IR** (ATR): $\tilde{\nu}$ = 3088 (w), 2053 (s), 1603 (m), 1479 (w), 1453 (w), 1401 (m), 1298 (w), 1033 (w), 832 (s), 772 (s), 723 (m) cm^{-1}; **^{1}H NMR** (400.47 MHz, DMSO-d_6): δ = 8.59–8.54 (m, 5H, H6/H6”, H4’, H3’/H5’), 8.49 (dt, 2H, $^3J_{H4,H3/H5;H4”,H3”/H5”}$ = 7.8 Hz, $^4J_{H4,H6;H4”,H6”}$ = 1.4 Hz, H4/H4”), 8.32 (ddd, 2H, $^3J_{H3,H4;H3”,H4”}$ = 5.6 Hz, $^4J_{H3,H5;H3”,H5”}$ = 1.4 Hz, $^5J_{H3,H6;H3”,H6”}$ = 0.5 Hz, H3/H3”), 7.94 (ddd, 2H, $^3J_{H5,H4;H5”,H4”}$ = 7.5 Hz, $^3J_{H5,H6;H5”,H6”}$ = 5.8 Hz, $^4J_{H5,H3;H5”,H3”}$ = 1.4 Hz, H5/H5”) ppm; **^{13}C NMR** (100.70 MHz, DMSO-d_6): δ =157.98 (C2’/C6’), 153.75 (C2/C2”), 149.29 (C6/C6”), 142.93 (C4/C4”), 142.08 (C4’), 129.33 (C5/C5”), 125.95 (C3’/C5’), 124.36 (C3/C3”) ppm; **^{195}Pt NMR** (86.09 MHz, DMSO-d_6): δ = 2659 ppm; **MS** (ESI$^+$, CH_3OH): *m*/*z* = 470.0686 $[M\text{-}PF_6]^+$; **Elemental analysis** (%) calcd. for $C_{15}H_{11}N_6PF_6Pt$: C 29.28, H 1.80, N 13.66; found (%): C 29.35, H 1.89, N 13.11.

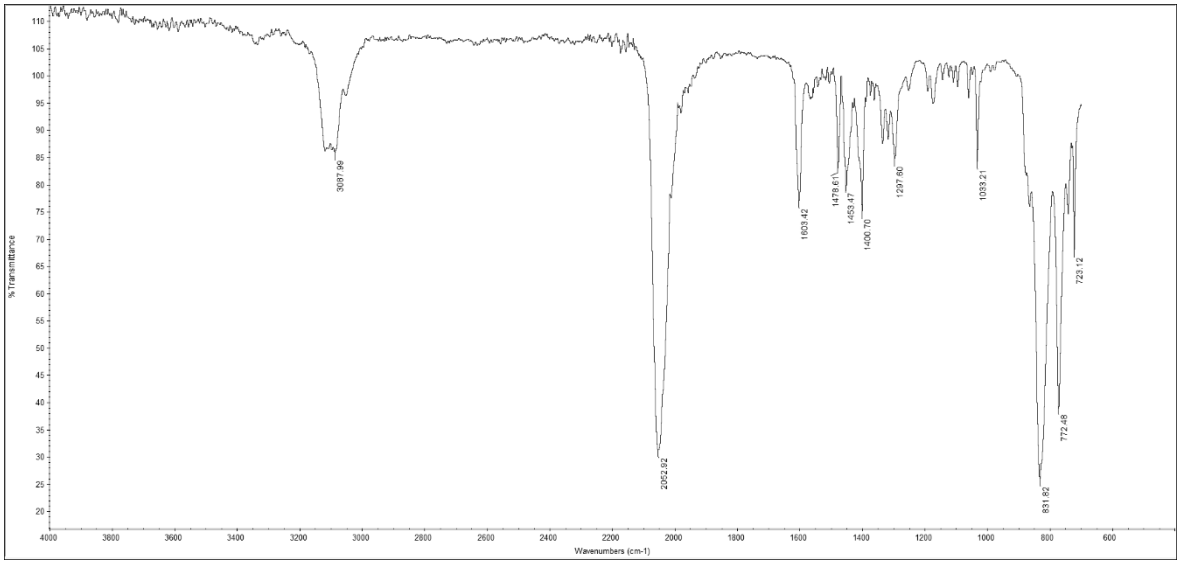
% Transmittance
Wavenumbers (cm-1)
3097.99
2952.62
1603.42
1478.61
1453.47
1400.70
1237.60
1033.21
831.82
772.48
726.12

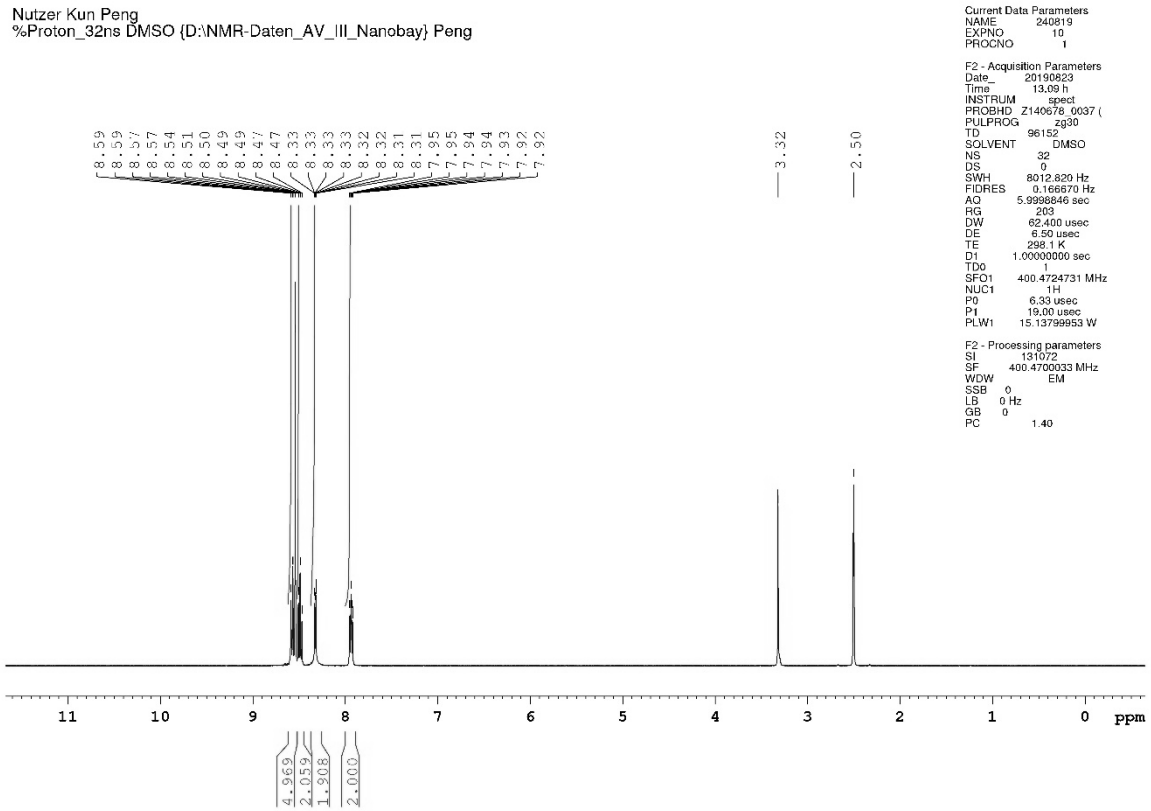
Nutzer Kun Peng
%Proton_32ns DMSO {D:\NMR-Daten_AV_III_Nanobay} Peng
Current Data Parameters
NAME 240819
EXPNO 10
PROCNO 1
F2 - Acquisition Parameters
Date_ 20190823
Time 13.09 h
INSTRUM spect
PROBHD Z140678_0037 (
PULPROG zg30
TD 96152
SOLVENT DMSO
NS 32
DS 0
SWH 8012.820 Hz
FIDRES 0.166670 Hz
AQ 5.9998846 sec
RG 203
DW 62.400 usec
DE 6.50 usec
TE 298.1 K
D1 1.00000000 sec
TD0 1
SFO1 400.4724731 MHz
NUC1 1H
P0 6.33 usec
P1 19.00 usec
PLW1 15.13799953 W
F2 - Processing parameters
SI 131072
SF 400.4700033 MHz
WDW EM
SSB 0
LB 0 Hz
GB 0
PC 1.40
8.59
8.59
8.57
8.57
8.54
8.51
8.50
8.49
8.49
8.47
8.47
8.33
8.33
8.33
8.32
8.32
8.31
8.31
7.95
7.95
7.94
7.94
7.93
7.92
7.92
3.32
2.50
ppm
4.969
2.059
1.908
2.000

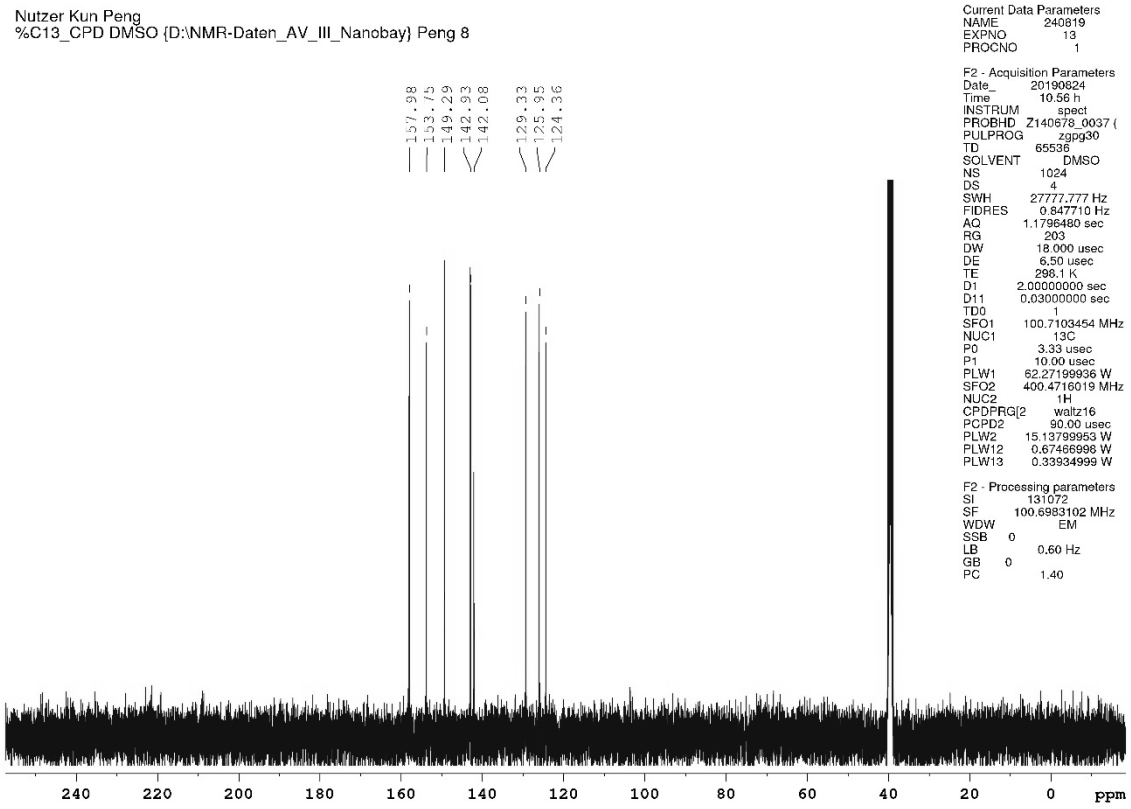
Nutzer Kun Peng
%C13_CPD DMSO {D:\NMR-Daten_AV_III_Nanobay} Peng 8
157.98
153.75
149.29
142.93
142.08
129.33
125.95
124.36
Current Data Parameters
NAME 240819
EXPNO 13
PROCNO 1
F2 - Acquisition Parameters
Date_ 20190824
Time 10.56 h
INSTRUM spect
PROBHD Z140678_0037 (
PULPROG zgpg30
TD 65536
SOLVENT DMSO
NS 1024
DS 4
SWH 27777.777 Hz
FIDRES 0.847710 Hz
AQ 1.1796480 sec
RG 203
DW 18.000 usec
DE 6.50 usec
TE 298.1 K
D1 2.00000000 sec
D11 0.03000000 sec
TD0 1
SFO1 100.7103454 MHz
NUC1 13C
P0 3.33 usec
P1 10.00 usec
PLW1 62.27199936 W
SFO2 400.4716019 MHz
NUC2 1H
CPDPRG[2 waltz16
PCPD2 90.00 usec
PLW2 15.13799953 W
PLW12 0.67466998 W
PLW13 0.33934999 W
F2 - Processing parameters
SI 131072
SF 100.6983102 MHz
WDW EM
SSB 0
LB 0.60 Hz
GB 0
PC 1.40
240
220
200
180
160
140
120
100
80
60
40
20
0
ppm

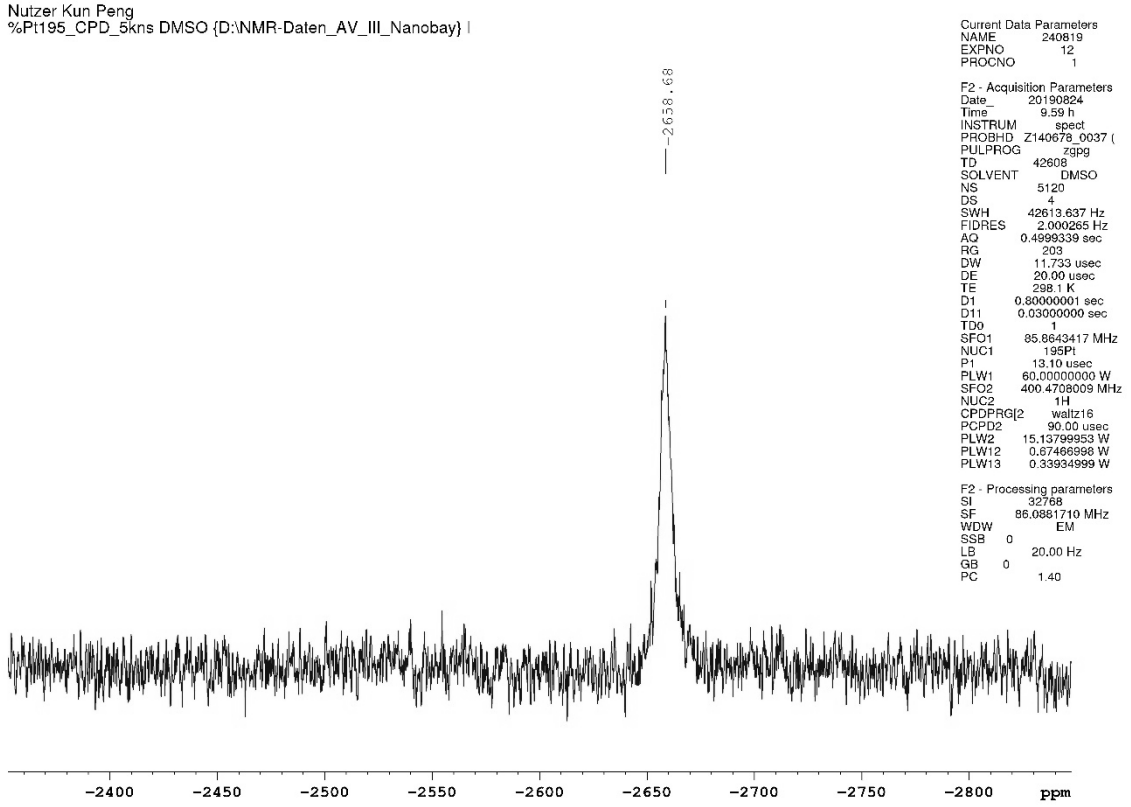
Nutzer Kun Peng
%Pt195_CPD_5kns DMSO {D:\NMR-Daten_AV_III_Nanobay} I
-2638.68
Current Data Parameters
NAME 240819
EXPNO 12
PROCNO 1
F2 - Acquisition Parameters
Date_ 20190824
Time 9.59 h
INSTRUM spect
PROBHD Z140678_0037 (
PULPROG zgpg
TD 42608
SOLVENT DMSO
NS 5120
DS 4
SWH 42613.637 Hz
FIDRES 2.000265 Hz
AQ 0.4999339 sec
RG 203
DW 11.733 usec
DE 20.00 usec
TE 298.1 K
D1 0.80000001 sec
D11 0.03000000 sec
TD0 1
SFO1 85.8643417 MHz
NUC1 195Pt
P1 13.10 usec
PLW1 60.00000000 W
SFO2 400.4708009 MHz
NUC2 1H
CPDPRG[2 waltz16
PCPD2 90.00 usec
PLW2 15.13799953 W
PLW12 0.67466998 W
PLW13 0.33934999 W
F2 - Processing parameters
SI 32768
SF 86.0861710 MHz
WDW EM
SSB 0
LB 20.00 Hz
GB 0
PC 1.40
-2400
-2450
-2500
-2550
-2600
-2650
-2700
-2750
-2800
ppm

5.3.9 Synthesis of [Pd(triazoate^{COOCH3,COOCH3})(terpy)]PF_6

USC-KP012-01

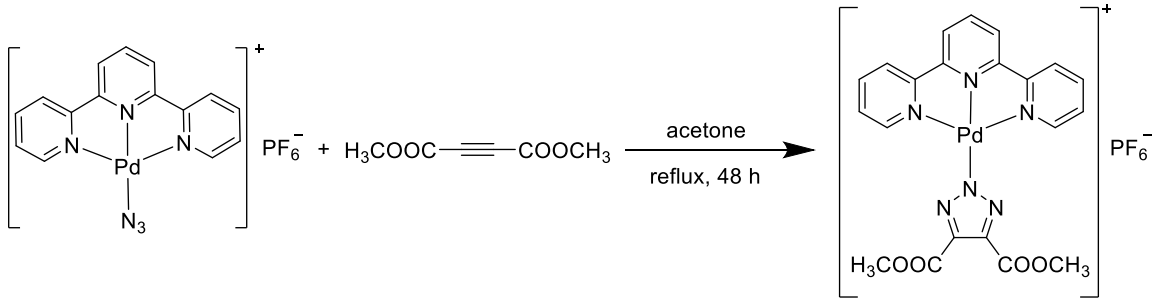

$C_{15}H_{11}F_6N_6PPd$
526.67 g/mol

$C_6H_6O_4$
142.11 g/mol

$C_{21}H_{17}F_6N_6O_4PPd$
668.78 g/mol

In a three-neck flask, $[Pd(N_3)(terpy)]PF_6$ (150 mg, 0.28 mmol) was dissolved in acetone (5 mL) under dinitrogen with heating. To the clear yellow solution, dimethyl acetylenedicarboxylate (52 µL, 60 mg, 0.42 mmol) was added and the reaction mixture then stirred under reflux for 48 h. After cooling to room temperature, the resulting yellow solid was filtered off, washed with acetone (4 × 3 mL) and diethyl ether (5 × 5 mL), and dried under vacuum for 7 d to obtain the product as a pale yellow solid. Yield: 64% (123 mg, 0.18 mmol). **IR** (ATR): $\tilde{\nu}$ = 3114 (w), 3041 (w), 1737 (m), 1721 (m), 1605 (w), 1442 (w), 1303 (m), 1092 (m), 834 (s), 800 (m), 777 (m) cm^{-1}; **^{1}H NMR** (500.13 MHz, DMSO-d_6): δ = 8.60–8.54 (m, 7H, H6/H6”, H3/H3”, H4’, H3’/H5’), 8.44 (dt, 2H, $^3J_{H4,H3/H5;\ H4”,\ H3”/H5”}$ = 7.9 Hz, $^4J_{H4,H6;H4”,H6”}$ = 1.5 Hz, H4/H4”), 7.84 (ddd, 2H, $^3J_{H5,H4;H5”,H4”}$ = 7.7 Hz, $^3J_{H5,H6;H5”,H6”}$ = 5.8 Hz, $^4J_{H5,H3;H5”,H3”}$ = 1.4 Hz, H5/H5”), 3.88 (s, 6H, COOCH_3) ppm; **^{13}C NMR** (125.76 MHz, DMSO-d_6): δ = 161.52 (*C*=O), 157.39 (C2’/C6’), 154.53 (C2/C2”), 151.95 (C6/C6”), 143.61 (C4’), 142.91 (C4/C4”), 140.22 (triazolate-C4/C5), 128.87 (C5/C5”), 125.39 (C3’/C5’), 124.48 (C3/C3”), 52.26 (COO*C*H_3) ppm; MS (ESI^+, CH_3OH): *m*/*z* = 523.0341 $[M\text{-}PF_6]^+$; **Elemental analysis** (%) calcd. for $C_{21}H_{17}N_6PF_6O_4Pd$: C 37.71, H 2.56, N 12.57; found (%): C 37.51, H 2.41, N 12.10.

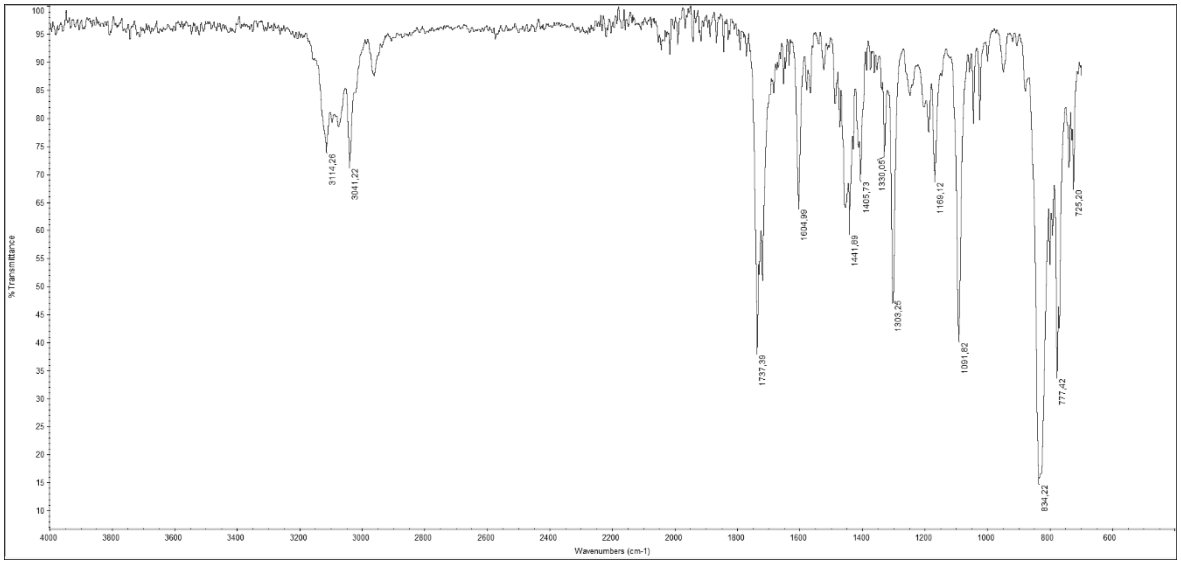

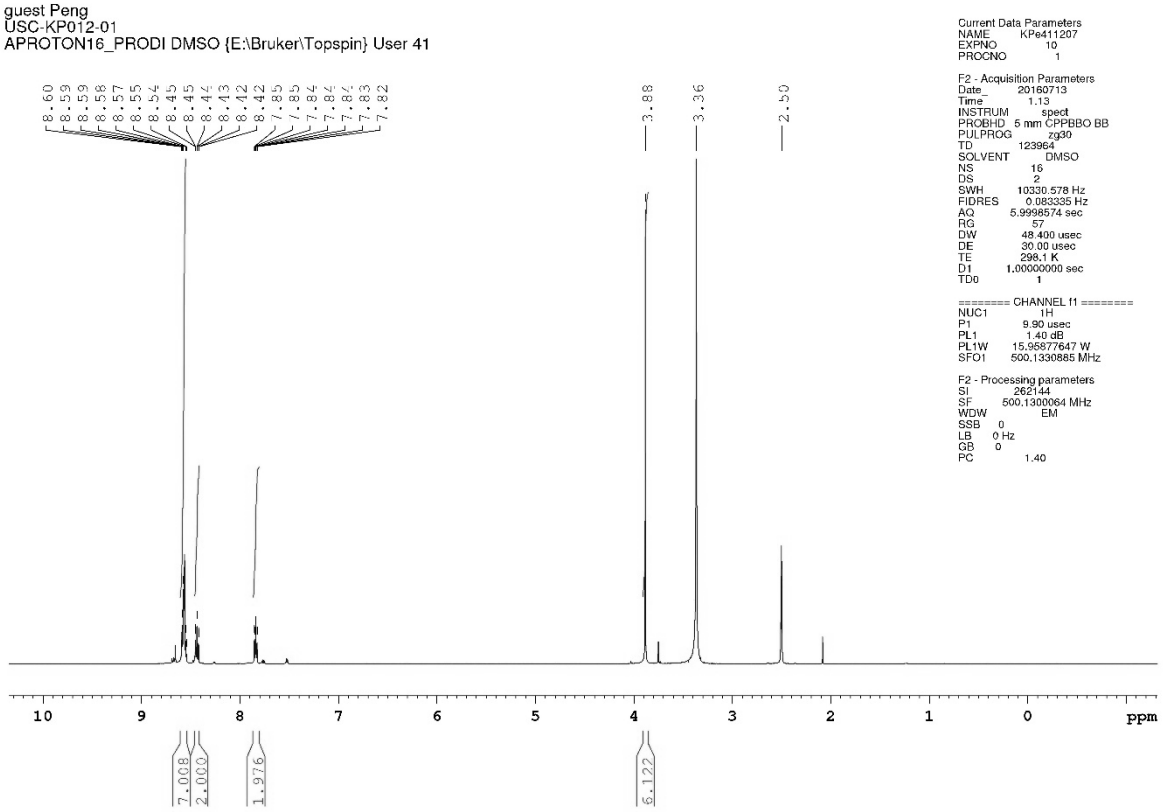

Current Data Parameters
NAME KPe411207
EXPNO 10
PROCNO 1

F2 - Acquisition Parameters
Date_ 20160713
Time 1.13
INSTRUM spect
PROBHD 5 mm CPPBBO BB
PULPROG zg30
TD 123964
SOLVENT DMSO
NS 16
DS 2
SWH 10330.578 Hz
FIDRES 0.083335 Hz
AQ 5.9998574 sec
RG 57
DW 48.400 usec
DE 30.00 usec
TE 298.1 K
D1 1.00000000 sec
TD0 1

======== CHANNEL f1 ========
NUC1 1H
P1 9.90 usec
PL1 1.40 dB
PL1W 15.95877647 W
SFO1 500.1330885 MHz

F2 - Processing parameters
SI 262144
SF 500.1300064 MHz
WDW EM
SSB 0
LB 0 Hz
GB 0
PC 1.40

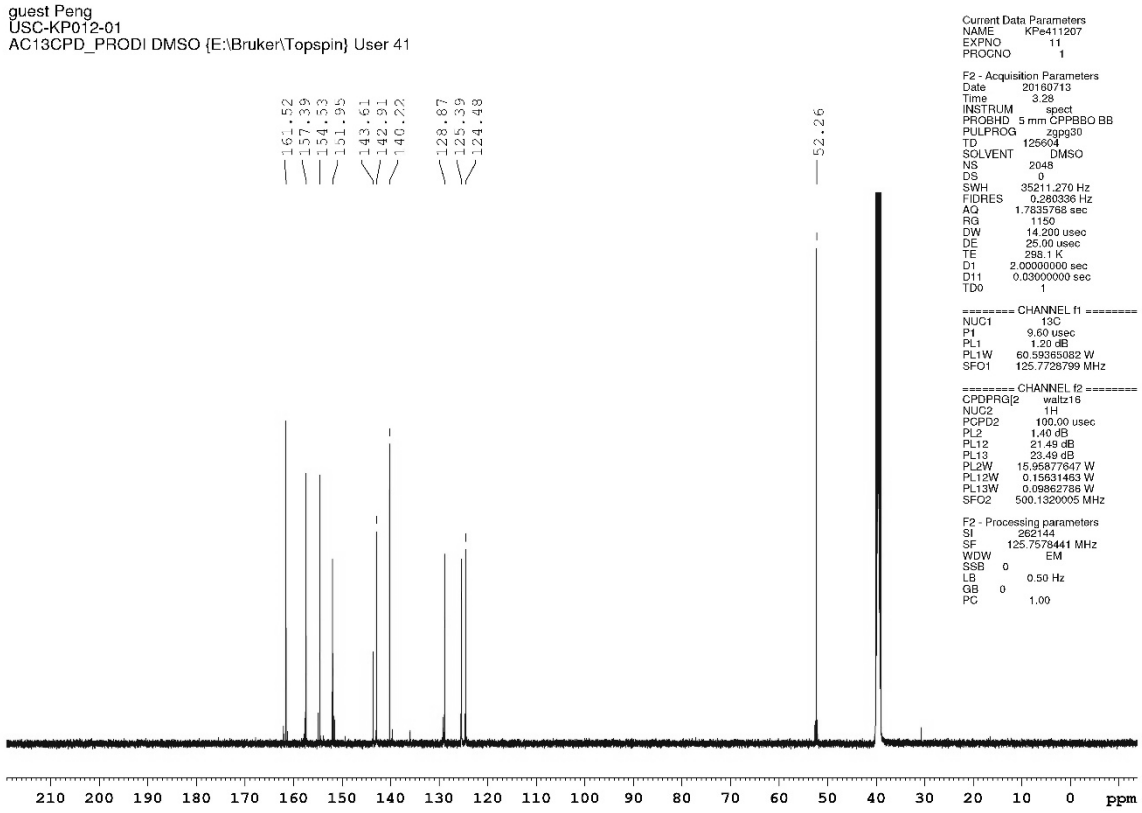
guest Peng
USC-KP012-01
AC13CPD_PRODI DMSO {E:\Bruker\Topspin} User 41
161.52
157.39
154.53
151.95
143.61
142.91
140.22
128.87
125.39
124.48
52.26
Current Data Parameters
NAME KPe411207
EXPNO 11
PROCNO 1
F2 - Acquisition Parameters
Date 20160713
Time 3.28
INSTRUM spect
PROBHD 5 mm CPPBBO BB
PULPROG zgpg30
TD 125604
SOLVENT DMSO
NS 2048
DS 0
SWH 35211.270 Hz
FIDRES 0.280336 Hz
AQ 1.7835768 sec
RG 1150
DW 14.200 usec
DE 25.00 usec
TE 298.1 K
D1 2.00000000 sec
D11 0.03000000 sec
TD0 1
======== CHANNEL f1 ========
NUC1 13C
P1 9.60 usec
PL1 1.20 dB
PL1W 60.59365082 W
SFO1 125.7728799 MHz
======== CHANNEL f2 ========
CPDPRG[2 waltz16
NUC2 1H
PCPD2 100.00 usec
PL2 1.40 dB
PL12 21.49 dB
PL13 23.49 dB
PL2W 15.95877647 W
PL12W 0.15631463 W
PL13W 0.09862786 W
SFO2 500.1320005 MHz
F2 - Processing parameters
SI 262144
SF 125.7578441 MHz
WDW EM
SSB 0
LB 0.50 Hz
GB 0
PC 1.00
210 200 190 180 170 160 150 140 130 120 110 100 90 80 70 60 50 40 30 20 10 0 ppm

5.3.10 Sythesis of [Pt(triazolate^{COOCH3,COOCH3})(terpy)]PF_6

USC-KP013-06

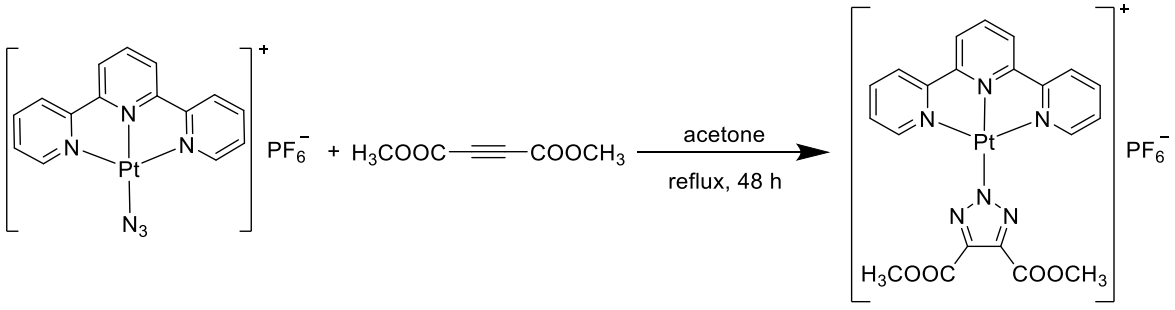

$C_{15}H_{11}F_6N_6PPt$
615.33 g/mol

$C_6H_6O_4$
142.11 g/mol

$C_{21}H_{17}F_6N_6O_4PPt$
757.44 g/mol

In a three-neck flask, [Pt(N_3)(terpy)]PF_6 (200 mg, 0.33 mmol) was dissolved in acetone (6 mL) with heating under dinitrogen. To the clear orange solution, dimethyl acetylenedicarboxylate (60 µL, 69 mg, 0.49 mmol) was added and the reaction mixture heated to reflux for 48 h. After cooling to room temperature, the resulting yellow solid was filtered off, washed with acetone (5 × 3 mL) and diethyl ether (6 × 5 mL), and dried under vacuum for 7 d to obtain the product as an orange solid. Yield: 73% (178 mg, 0.24 mmol). **IR** (ATR): $\tilde{\nu}$ = 3043 (w), 1737 (s), 1608 (w), 1442 (w), 1405 (w), 1303 (m), 1171 (w), 1095 (m), 833 (s), 776 (s), 741 (w), 725 (w) cm^{-1}; **^{1}H NMR** (400.17 MHz, DMSO-d_6): δ = 8.68 (d, 2H, $^3J_{H6,H5;H6",H5"}$ = 5.8 Hz, H6/H6"), 8.57–8.49 (m, 5H, H3/H3", H3'/H5', H4'), 8.44 (dt, 2H, $^3J_{H4,H3/H5;H4",H3"/H5"}$ = 7.8 Hz, $^4J_{H4,H6;H4",H6"}$ = 1.3 Hz, H4/H4"), 7.83 (ddd, 2H, $^3J_{H5,H4;H5",H4"}$ = 7.4 Hz, $^3J_{H5,H6;H5",H6"}$ = 5.8 Hz, $^4J_{H5,H3;H5",H3"}$ = 1.6 Hz, H5/H5"), 3.89 (s, 6H, COOCH_3) ppm; **^{13}C NMR** (100.70 MHz, DMSO-d_6): δ = 161.20 (*C*=O), 157.22 (C2'/C6'), 154.21 (C2/C2"), 152.21 (C6/C6"), 143.25 (C4'), 142.90 (C4/C4"), 140.02 (triazolate-C4/C5), 128.96 (C5/C5"), 125.85 (C3'/C5'), 124.32 (C3/C3"), 52.22 (COO*C*H_3) ppm; **^{195}Pt NMR** (86.09 MHz, DMSO-d_6): δ = -2680 ppm; **MS** (ESI$^+$, CH_3OH): *m*/*z* = 612.0947 [M-PF_6]$^+$; **Elemental analysis** (%) calcd. for $C_{21}H_{17}N_6PF_6O_4Pt$: C 33.30, H 2.26, N 11.10; found (%): C 33.17, H 2.22, N 10.83.

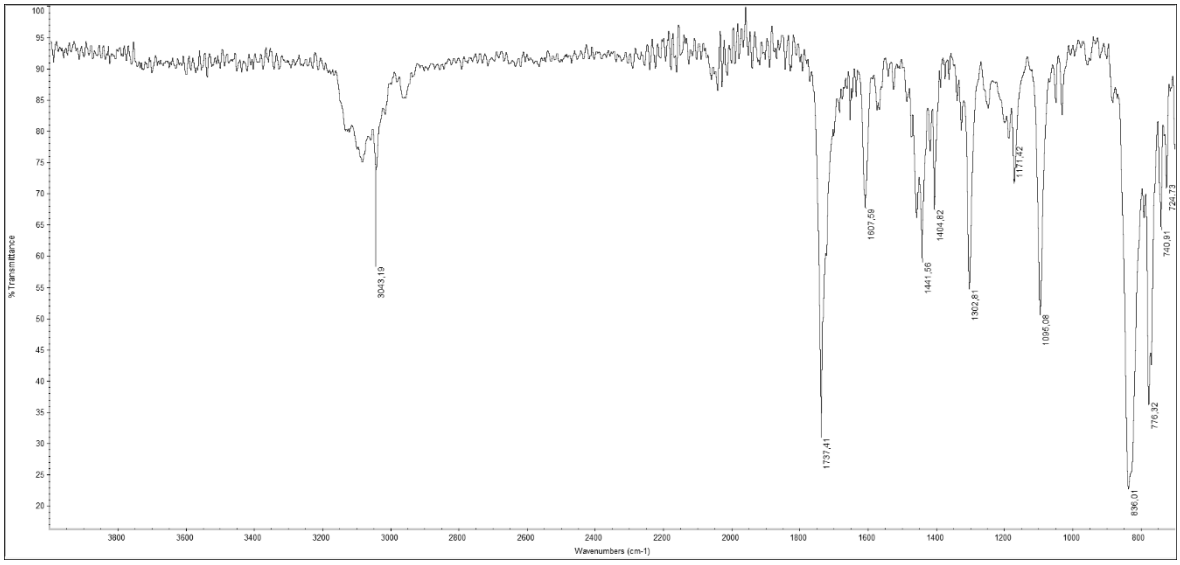
%Transmittance
Wavenumbers (cm-1)
3043.19
1737.41
1607.59
1464.82
1441.56
1302.81
1171.42
1095.08
896.01
776.32
740.81
724.73

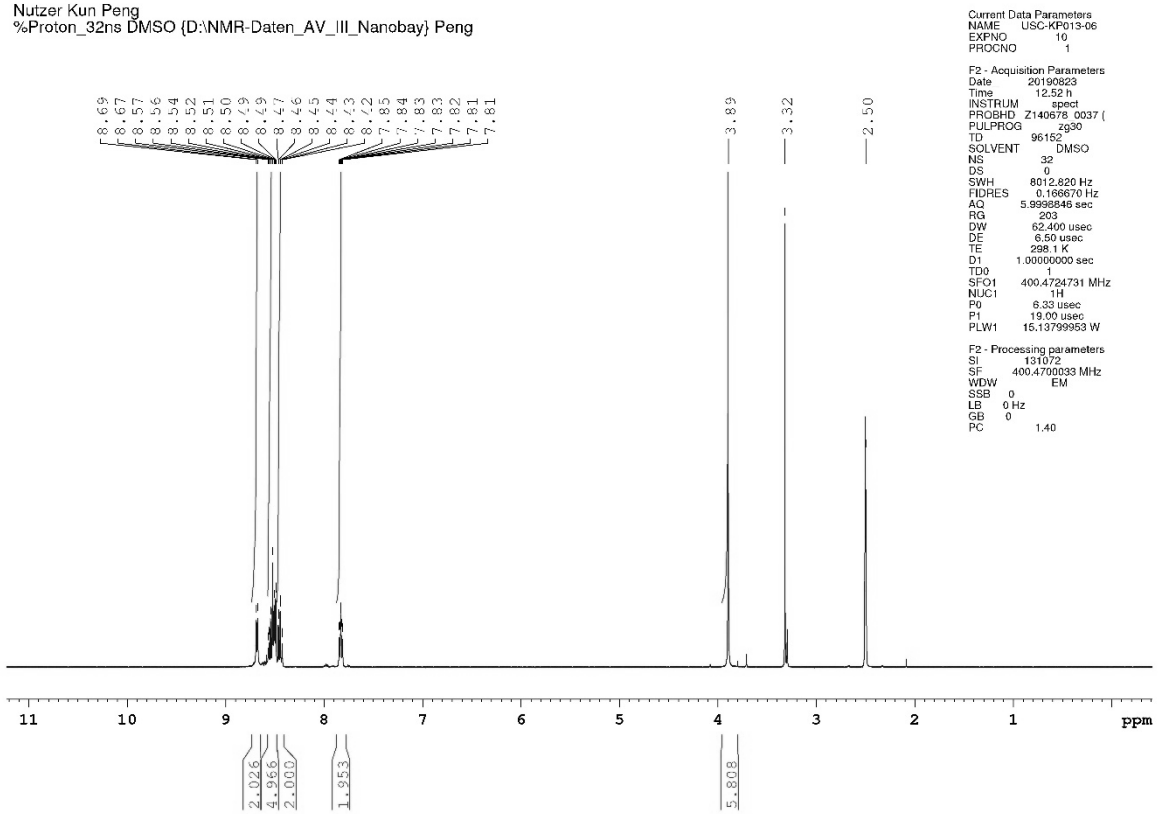
Nutzer Kun Peng
%Proton_32ns DMSO {D:\NMR-Daten_AV_III_Nanobay} Peng
8.69
8.67
8.57
8.56
8.54
8.52
8.51
8.50
8.49
8.49
8.47
8.46
8.45
8.44
8.43
8.42
7.85
7.84
7.83
7.82
7.81
7.81
3.89
3.32
2.50
Current Data Parameters
NAME USC-KP013-06
EXPNO 10
PROCNO 1
F2 - Acquisition Parameters
Date 20190823
Time 12.52 h
INSTRUM spect
PROBHD Z140678 0037 (
PULPROG zg30
TD 96152
SOLVENT DMSO
NS 32
DS 0
SWH 8012.820 Hz
FIDRES 0.166670 Hz
AQ 5.9998846 sec
RG 203
DW 62.400 usec
DE 6.50 usec
TE 298.1 K
D1 1.00000000 sec
TD0 1
SFO1 400.4724731 MHz
NUC1 1H
P0 6.33 usec
P1 19.00 usec
PLW1 15.13799953 W
F2 - Processing parameters
SI 131072
SF 400.4700033 MHz
WDW EM
SSB 0
LB 0 Hz
GB 0
PC 1.40
11
10
9
8
7
6
5
4
3
2
1
ppm
2.026
4.966
2.000
1.953
5.808

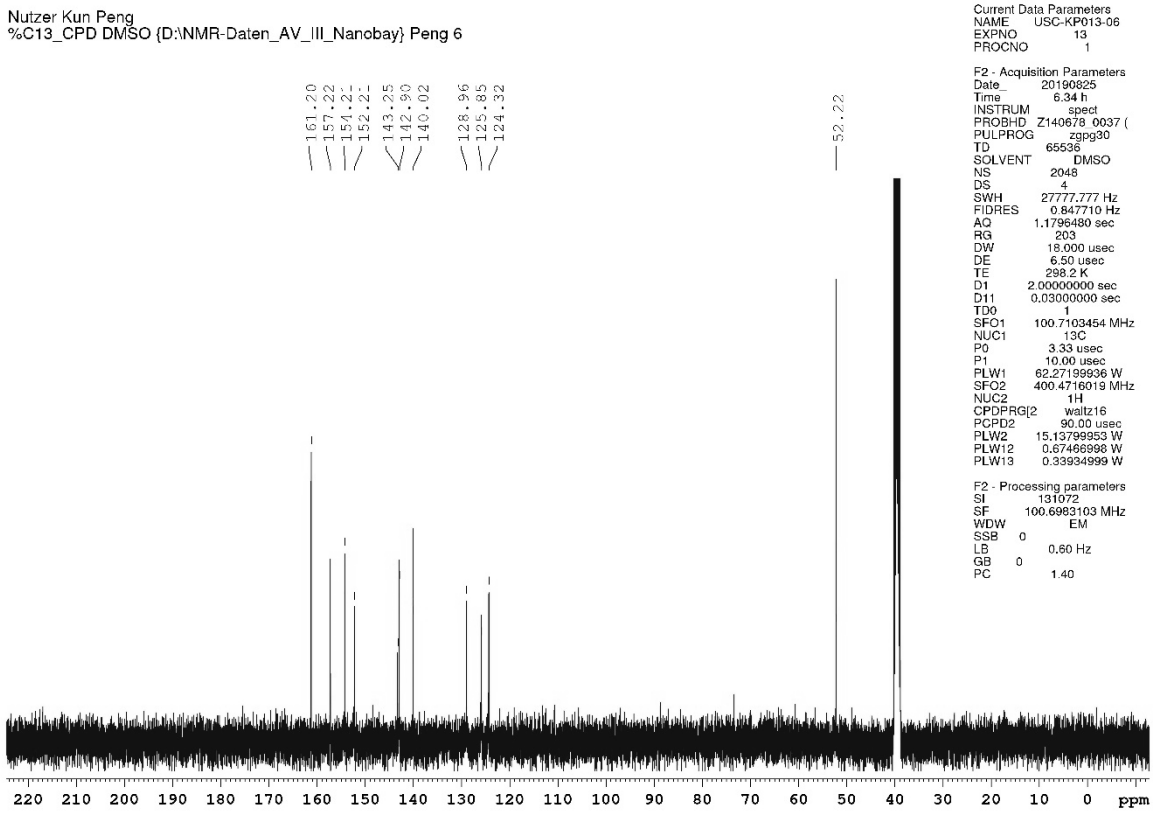
Nutzer Kun Peng
%C13_CPD DMSO {D:\NMR-Daten_AV_III_Nanobay} Peng 6
161.20
157.22
154.2-
152.2-
143.25
142.90
140.02
128.96
125.85
124.32
52.22
Current Data Parameters
NAME USC-KP013-06
EXPNO 13
PROCNO 1
F2 - Acquisition Parameters
Date_ 20190825
Time 6.34 h
INSTRUM spect
PROBHD Z140678_0037 (
PULPROG zgpg30
TD 65536
SOLVENT DMSO
NS 2048
DS 4
SWH 27777.777 Hz
FIDRES 0.847710 Hz
AQ 1.1796480 sec
RG 203
DW 18.000 usec
DE 6.50 usec
TE 298.2 K
D1 2.00000000 sec
D11 0.03000000 sec
TD0 1
SFO1 100.7103454 MHz
NUC1 13C
P0 3.33 usec
P1 10.00 usec
PLW1 62.27199936 W
SFO2 400.4716019 MHz
NUC2 1H
CPDPRG[2 waltz16
PCPD2 90.00 usec
PLW2 15.13799953 W
PLW12 0.67466998 W
PLW13 0.33934999 W
F2 - Processing parameters
SI 131072
SF 100.6983103 MHz
WDW EM
SSB 0
LB 0.60 Hz
GB 0
PC 1.40
220 210 200 190 180 170 160 150 140 130 120 110 100 90 80 70 60 50 40 30 20 10 0 ppm

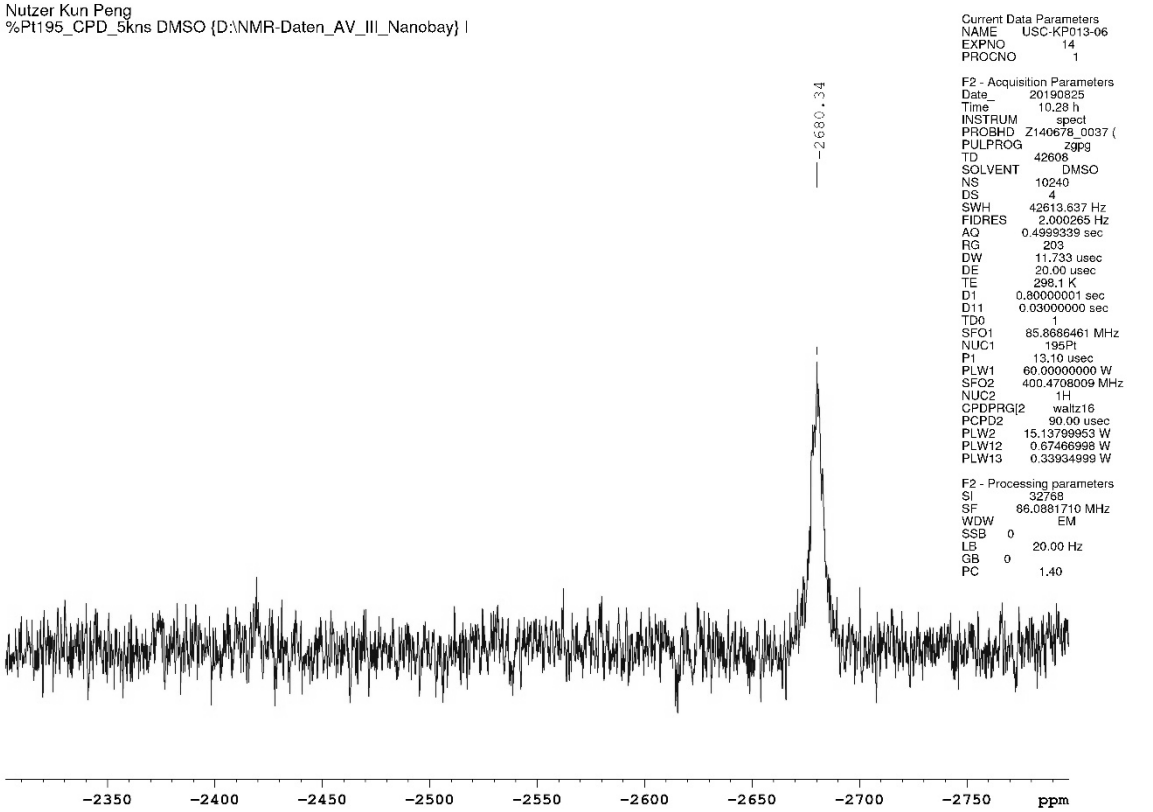
Nutzer Kun Peng
%Pt195_CPD_5kns DMSO {D:\NMR-Daten_AV_III_Nanobay} I
-2680.34
Current Data Parameters
NAME USC-KP013-06
EXPNO 14
PROCNO 1
F2 - Acquisition Parameters
Date_ 20190825
Time 10.28 h
INSTRUM spect
PROBHD Z140678_0037 (
PULPROG zgpg
TD 42608
SOLVENT DMSO
NS 10240
DS 4
SWH 42613.637 Hz
FIDRES 2.000265 Hz
AQ 0.4999339 sec
RG 203
DW 11.733 usec
DE 20.00 usec
TE 298.1 K
D1 0.80000001 sec
D11 0.03000000 sec
TD0 1
SFO1 85.8686461 MHz
NUC1 195Pt
P1 13.10 usec
PLW1 60.00000000 W
SFO2 400.4708009 MHz
NUC2 1H
CPDPRG[2 waltz16
PCPD2 90.00 usec
PLW2 15.13799953 W
PLW12 0.67466998 W
PLW13 0.33934999 W
F2 - Processing parameters
SI 32768
SF 86.0881710 MHz
WDW EM
SSB 0
LB 20.00 Hz
GB 0
PC 1.40
-2350 -2400 -2450 -2500 -2550 -2600 -2650 -2700 -2750 ppm

5.3.11 Synthesis of [Pd(triazolate^{COOEt,COOEt})(terpy)]PF_6

USC-KP048-04

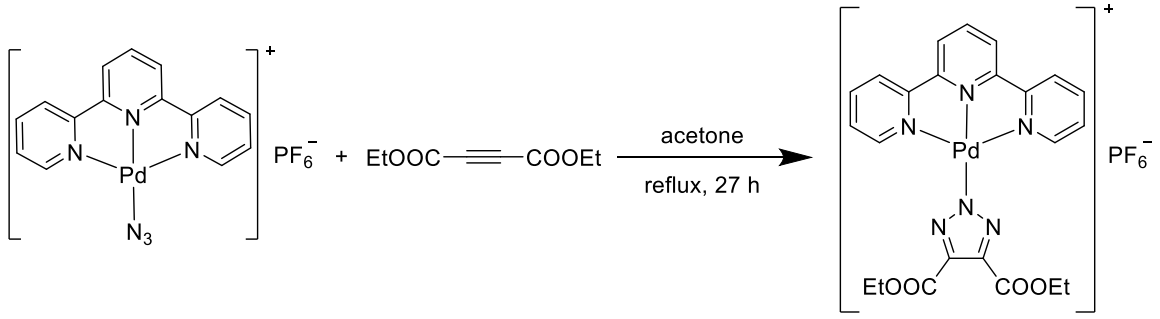

$C_{15}H_{11}F_6N_6PPd$
526.67 g/mol

$C_8H_{10}O_4$
170.16 g/mol

$C_{23}H_{21}F_6N_6O_4PPd$
696.83 g/mol

[Pd(N_3)(terpy)]PF_6 (28.5 mg, 0.05 mmol) was dissolved in acetone (6 mL) at 60 °C. Then, diethyl acetylenedicarboxylate (18 µL, 19 mg, 0.11 mmol) was added and heating continued for 27 h. Upon cooling to room temperature, a pale yellow solid formed, which was filtered off, washed with acetone (3 × 3 mL) and diethyl ether (3 × 20 mL), and dried under vacuum for 2 d to obtain the product as a pale yellow solid. Yield: 60% (22 mg, 0.03 mmol). **IR** (ATR): $\tilde{\nu}$ = 3078 (w), 3038 (w), 1730 (s), 1601 (w), 1460 (w), 1404 (w), 1328 (w), 1298 (m), 1188 (w), 1093 (m), 1027 (w), 834 (s), 778 (s), 744 (w), 724 (w) cm^{-1}; **^{1}H NMR** (400.40 MHz, DMSO-d_6): δ = 8.71–8.63 (m, 5H, H3/H3”, H3’/H5’, H4’), 8.56 (d, 2H, $^3J_{H6,H5;H6”,H5”}$ = 5.7 Hz, H6/H6”), 8.49 (dt, 2H, $^3J_{H4,H3/H5;H4”,H3”/H5”}$ = 7.9 Hz, $^4J_{H4,H6;H4”,H6”}$ = 1.3 Hz, H4/H4”), 7.90 (ddd, 2H, $^3J_{H5,H4;H5”,H4”}$ = 7.5 Hz, $^3J_{H5,H6;H5”,H6”}$ = 5.9 Hz, $^4J_{H5,H3;H5”,H3”}$ = 1.3 Hz, H5/H5”), 4.34 (q, 4H, ^3J = 7.1 Hz, COOCH_2CH$_3$), 1.33 (t, 6H, ^3J = 7.1 Hz, COOCH$_2$CH_3) ppm; **^{13}C NMR** (100.68 MHz, DMSO-d_6): δ = 161.23 (*C*=O), 157.65 (C2’/C6’), 154.68 (C2/C2”), 151.77 (C6/C6”), 143.50 (C4’), 142.86 (C4/C4”), 140.50 (triazolate-C4/C5), 128.85 (C5/C5”), 125.38 (C3’/C5’), 124.41 (C3/C3”), 60.96 (COO*C*H$_2$CH$_3$), 14.01 (COOCH$_2$*C*H$_3$) ppm; **MS** (ESI$^+$, CH$_3$OH): *m*/*z* = 551.0651 [M-PF_6]$^+$; **Elemental analysis** (%) calcd. for $C_{23}H_{21}N_6PF_6O_4Pd$: C 39.64, H 3.04, N 12.06; found (%): C 39.19, H 3.03, N 12.05.

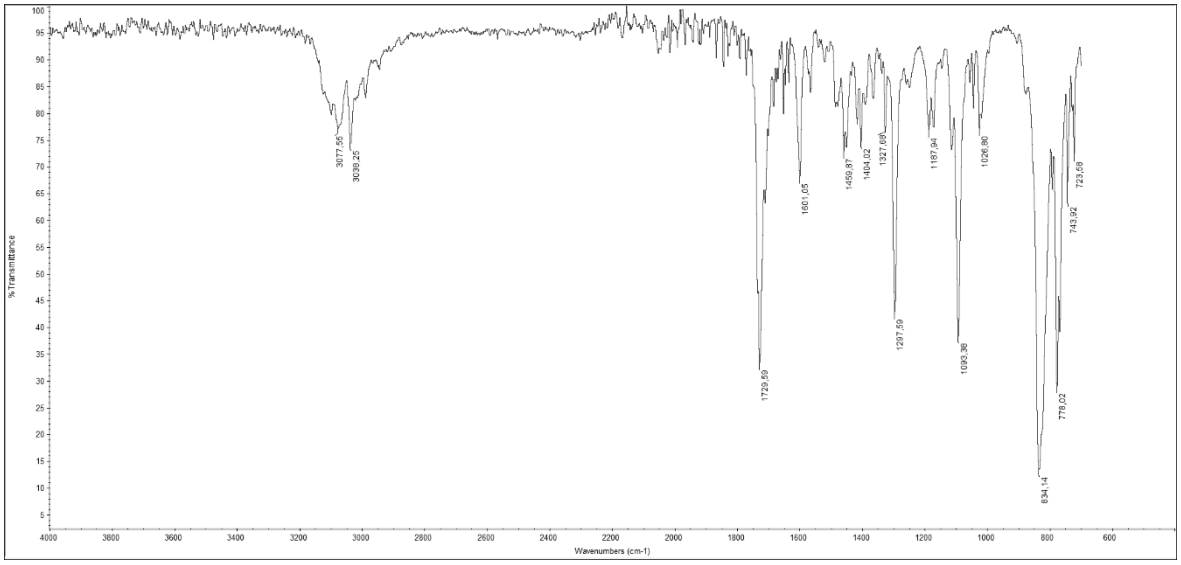
% Transmittance
Wavenumbers (cm-1)
3077.55
3038.25
1661.05
1459.87
1404.02
1327.69
1297.59
1187.94
1093.36
1026.80
834.14
778.02
743.92
723.69
1729.59

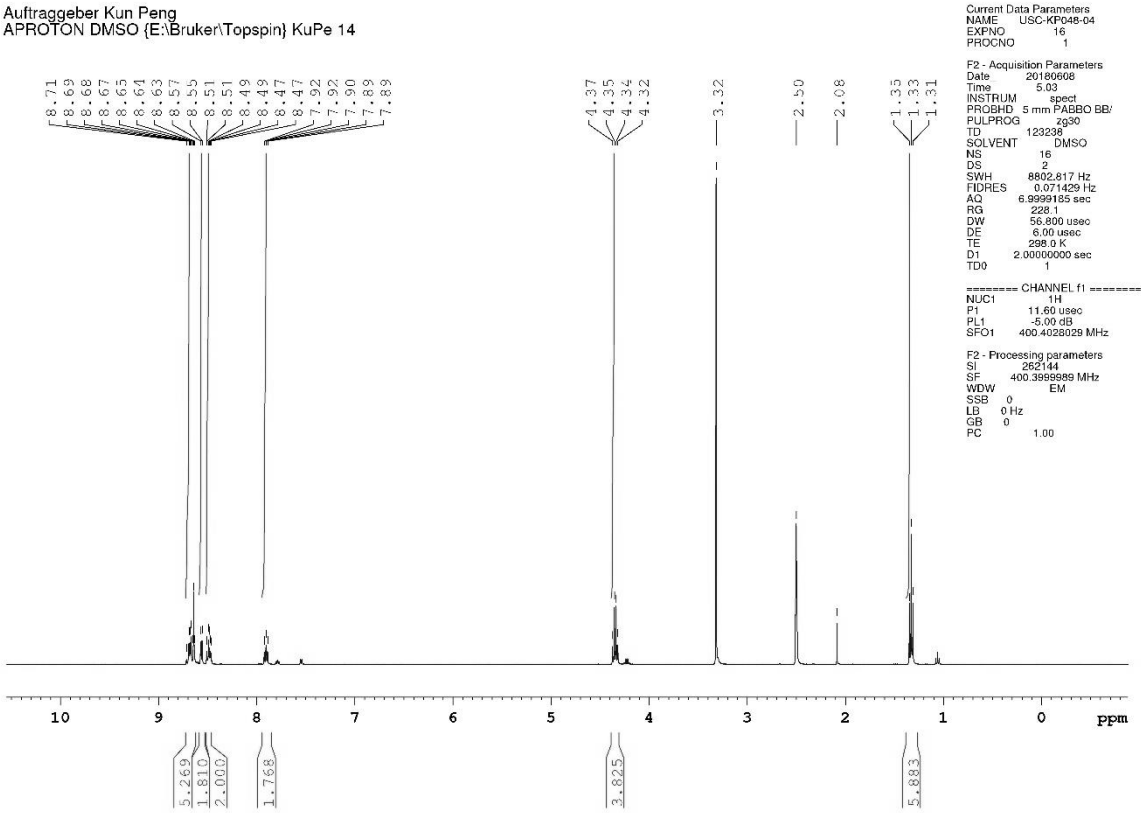
Auftraggeber Kun Peng
APROTON DMSO {E:\Bruker\Topspin} KuPe 14
8.71
8.69
8.68
8.67
8.65
8.64
8.63
8.57
8.55
8.51
8.51
8.49
8.49
8.47
8.47
7.92
7.92
7.90
7.89
7.89
4.37
4.35
4.34
4.32
3.32
2.50
2.08
1.35
1.33
1.31
10
9
8
7
6
5
4
3
2
1
0
ppm
5.269
1.810
2.000
1.768
3.825
5.883
Current Data Parameters
NAME USC-KP048-04
EXPNO 16
PROCNO 1
F2 - Acquisition Parameters
Date 20180608
Time 5.03
INSTRUM spect
PROBHD 5 mm PABBO BB/
PULPROG zg30
TD 123238
SOLVENT DMSO
NS 16
DS 2
SWH 8802.817 Hz
FIDRES 0.071429 Hz
AQ 6.9999185 sec
RG 228.1
DW 56.800 usec
DE 6.00 usec
TE 298.0 K
D1 2.00000000 sec
TD0 1
======== CHANNEL f1 ========
NUC1 1H
P1 11.60 usec
PL1 -5.00 dB
SFO1 400.4028029 MHz
F2 - Processing parameters
SI 262144
SF 400.3999989 MHz
WDW EM
SSB 0
LB 0 Hz
GB 0
PC 1.00

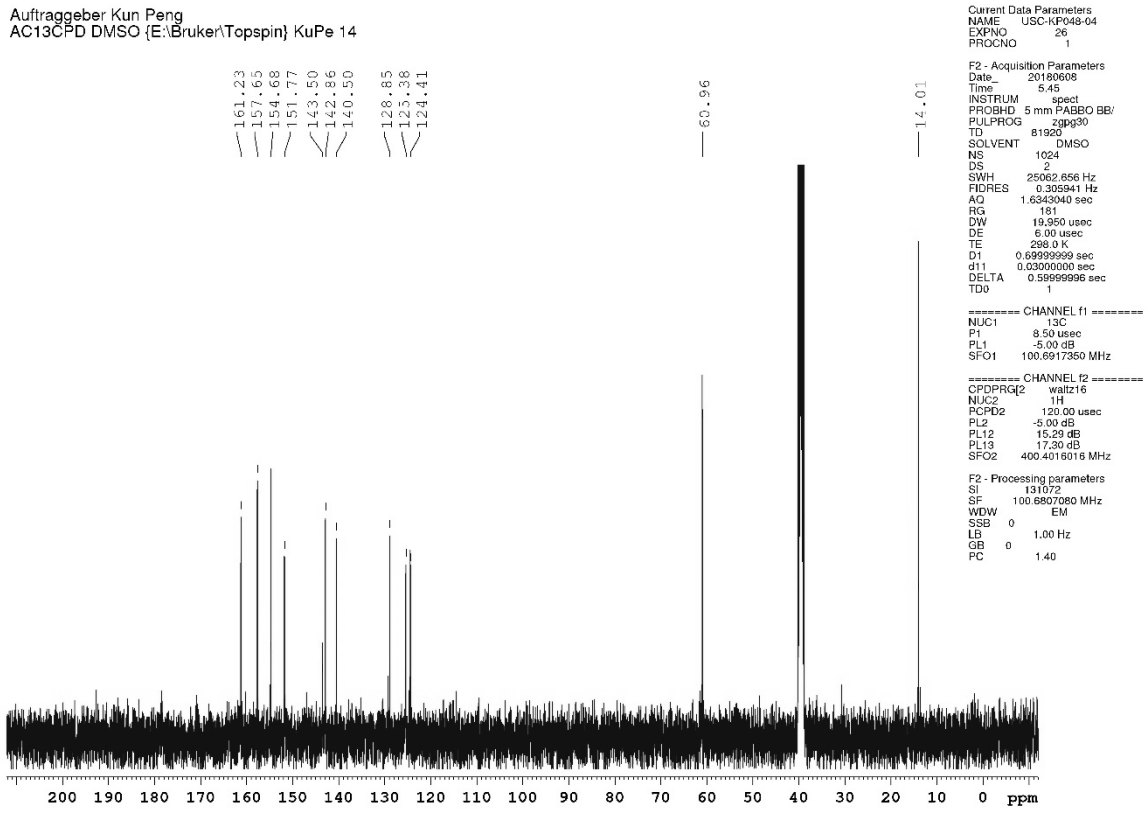
Auftraggeber Kun Peng
AC13CPD DMSO {E:\Bruker\Topspin} KuPe 14
161.23
157.65
154.68
151.77
143.50
142.86
140.50
128.85
125.38
124.41
60.96
14.01
200 190 180 170 160 150 140 130 120 110 100 90 80 70 60 50 40 30 20 10 0 ppm
Current Data Parameters
NAME USC-KP048-04
EXPNO 26
PROCNO 1
F2 - Acquisition Parameters
Date_ 20180608
Time 5.45
INSTRUM spect
PROBHD 5 mm PABBO BB/
PULPROG zgpg30
TD 81920
SOLVENT DMSO
NS 1024
DS 2
SWH 25062.656 Hz
FIDRES 0.305941 Hz
AQ 1.6343040 sec
RG 181
DW 19.950 usec
DE 6.00 usec
TE 298.0 K
D1 0.69999999 sec
d11 0.03000000 sec
DELTA 0.59999996 sec
TD0 1
======== CHANNEL f1 ========
NUC1 13C
P1 8.50 usec
PL1 -5.00 dB
SFO1 100.6917350 MHz
======== CHANNEL f2 ========
CPDPRG[2 waltz16
NUC2 1H
PCPD2 120.00 usec
PL2 -5.00 dB
PL12 15.29 dB
PL13 17.30 dB
SFO2 400.4016016 MHz
F2 - Processing parameters
SI 131072
SF 100.6807080 MHz
WDW EM
SSB 0
LB 1.00 Hz
GB 0
PC 1.40

5.3.12 Synthesis of [Pt(triazolate^{COOEt,COOEt})(terpy)]PF_6

USC-KP050-01

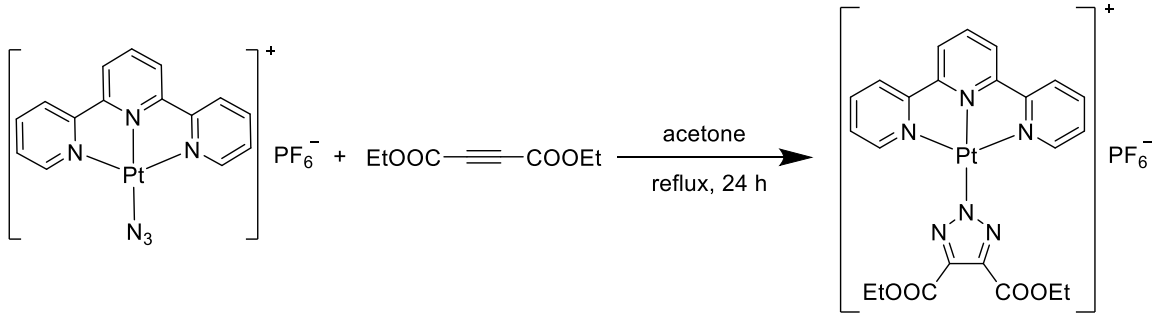

$C_{15}H_{11}F_6N_6PPt$
615.33 g/mol

$C_8H_{10}O_4$
170.16 g/mol

$C_{23}H_{21}F_6N_6O_4PPt$
785.49 g/mol

[Pt(N_3)(terpy)]PF_6 (66 mg, 0.11 mmol) was dissolved in acetone (20 mL) at 60 °C. To the clear orange solution, diethyl acetylenedicarboxylate (50 µL, 53 mg, 0.31 mmol) was added and heating continued for 24 h. Upon cooling to room temperature, an orange solid precipitated, which was collected by filtration, washed with acetone (3 × 3 mL) and diethyl ether (3 × 20 mL), and dried under vacuum for 2 d to obtain the product as an orange solid. Yield: 91% (76 mg, 0.10 mmol). **IR** (ATR): $\tilde{\nu}$ = 3080 (w), 1733 (m), 1607 (w), 1458 (w), 1404 (w), 1299 (m), 1176 (w), 1094 (m), 1019 (w), 839 (s), 777 (m) cm^{-1}; **^{1}H NMR** (400.47 MHz, DMSO-d_6): δ = 8.65 (d, 2H, $^3J_{H6,H5;H6",H5"}$ = 5.5 Hz, H6/H6"), 8.49–8.37 (m, 7H, H3/H3", H4', H3'/H5', H4/H4"), 7.75–7.71 (m, 2H, H5/H5"), 4.34 (q, 4H, ^3J = 7.1 Hz, COOC*H*$_2$CH$_3$), 1.35 (t, 6H, ^3J = 7.1 Hz, COOCH$_2$C*H*$_3$) ppm; **^{13}C NMR** (100.70 MHz, DMSO-d_6): δ = 160.78 (*C*=O), 157.03 (C2'/C6'), 154.01 (C2/C2"), 152.22 (C6/C6"), 143.22 (C4'), 142.89 (C4/C4"), 140.01 (triazolate-C4/C5), 128.91 (C5/C5"), 125.84 (C3'/C5'), 124.33 (C3/C3"), 61.00 (COO*C*H$_2$CH$_3$), 13.99 (COOCH$_2$*C*H$_3$) ppm; **^{195}Pt NMR** (86.09 MHz, DMSO-d_6): δ = -2664 ppm; **MS** (ESI$^+$, CH_3OH): *m*/*z* = 640.1264 [M-PF_6]$^+$; **Elemental analysis** (%) calcd. for $C_{23}H_{21}N_6PF_6O_4Pt$: C 35.17, H 2.69, N 10.70; found (%): C 34.67, H 2.66, N 10.11.

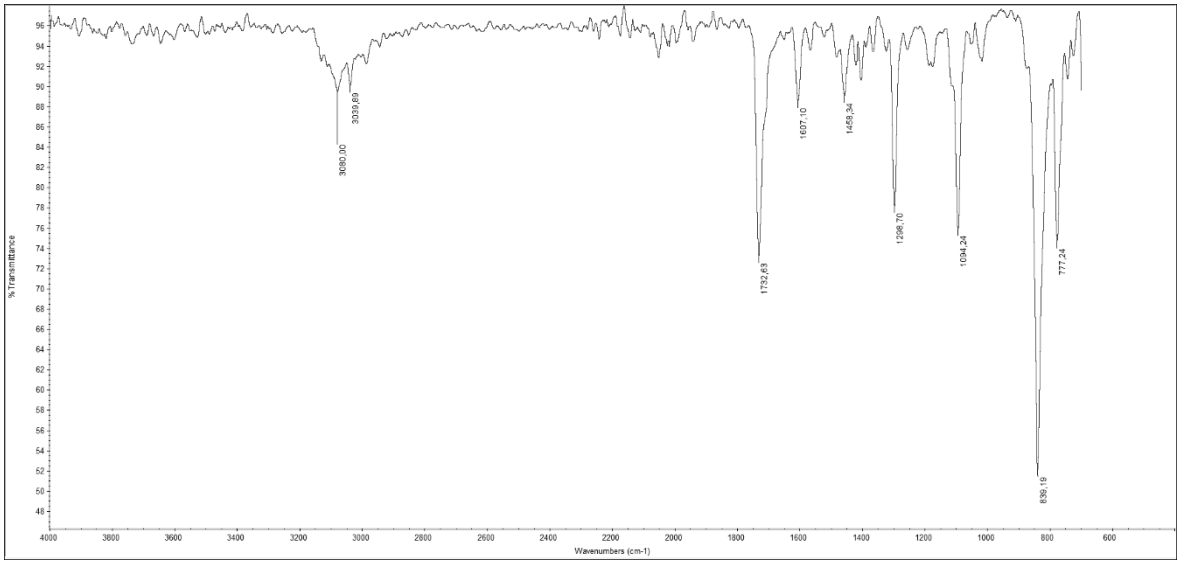
%Transmittance
Wavenumbers (cm-1)
3060.00
3039.69
1732.63
1607.10
1458.34
1298.70
1094.24
899.19
777.24

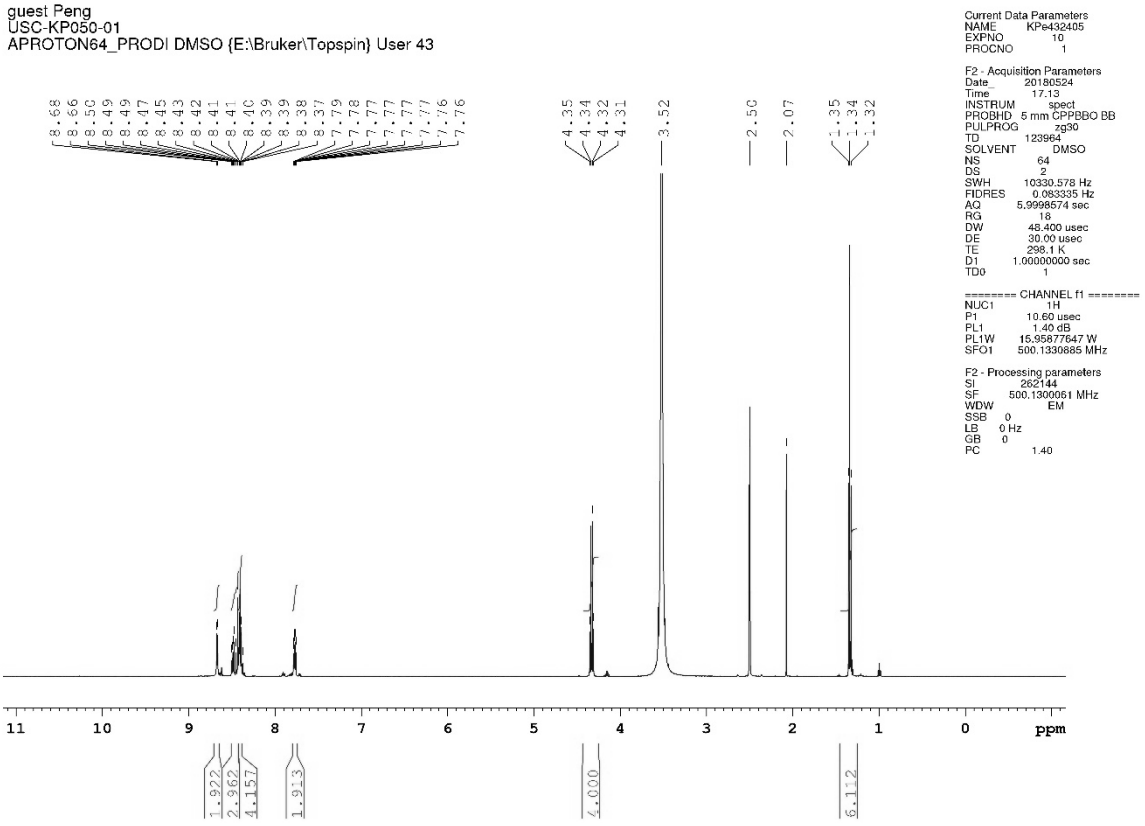
guest Peng
USC-KP050-01
APROTON64_PRODI DMSO {E:\Bruker\Topspin} User 43
Current Data Parameters
NAME KPe432405
EXPNO 10
PROCNO 1
F2 - Acquisition Parameters
Date 20180524
Time 17.13
INSTRUM spect
PROBHD 5 mm CPPBBO BB
PULPROG zg30
TD 123964
SOLVENT DMSO
NS 64
DS 2
SWH 10330.578 Hz
FIDRES 0.083335 Hz
AQ 5.9998574 sec
RG 18
DW 48.400 usec
DE 30.00 usec
TE 298.1 K
D1 1.00000000 sec
TD0 1
======== CHANNEL f1 ========
NUC1 1H
P1 10.60 usec
PL1 1.40 dB
PL1W 15.95877647 W
SFO1 500.1330885 MHz
F2 - Processing parameters
SI 262144
SF 500.1300061 MHz
WDW EM
SSB 0
LB 0 Hz
GB 0
PC 1.40
8.68
8.66
8.50
8.49
8.49
8.47
8.45
8.43
8.42
8.41
8.41
8.40
8.39
8.39
8.38
8.37
7.79
7.78
7.77
7.77
7.77
7.77
7.76
7.76
4.35
4.34
4.32
4.31
3.52
2.50
2.07
1.35
1.34
1.32
11
10
9
8
7
6
5
4
3
2
1
0
ppm
1.922
2.962
4.157
1.913
4.000
6.112

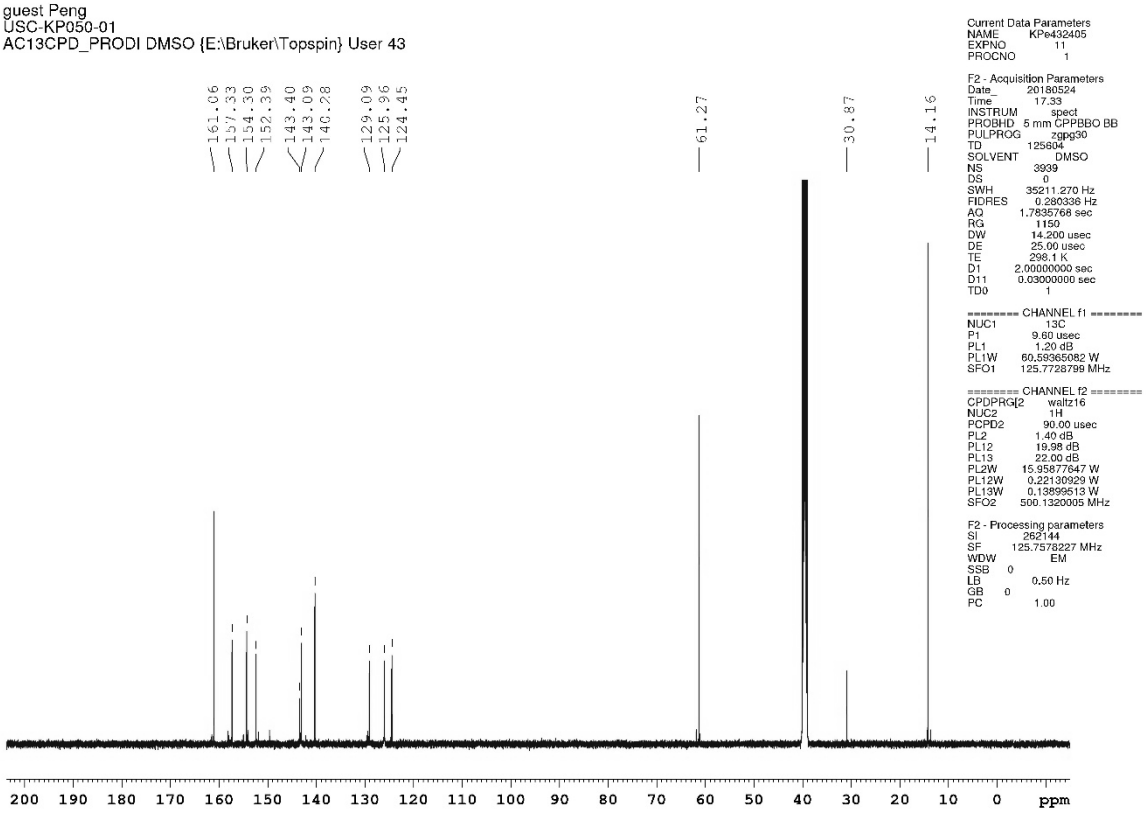
guest Peng
USC-KP050-01
AC13CPD_PRODI DMSO {E:\Bruker\Topspin} User 43
161.06
157.33
154.30
152.39
143.40
143.09
140.28
129.09
125.96
124.45
61.27
30.87
14.16
Current Data Parameters
NAME KPe432405
EXPNO 11
PROCNO 1
F2 - Acquisition Parameters
Date_ 20180524
Time 17.33
INSTRUM spect
PROBHD 5 mm CPPBBO BB
PULPROG zgpg30
TD 125604
SOLVENT DMSO
NS 3939
DS 0
SWH 35211.270 Hz
FIDRES 0.280338 Hz
AQ 1.7835768 sec
RG 1150
DW 14.200 usec
DE 25.00 usec
TE 298.1 K
D1 2.00000000 sec
D11 0.03000000 sec
TD0 1
======== CHANNEL f1 ========
NUC1 13C
P1 9.60 usec
PL1 1.20 dB
PL1W 60.59365082 W
SFO1 125.7728799 MHz
======== CHANNEL f2 ========
CPDPRG[2 waltz16
NUC2 1H
PCPD2 90.00 usec
PL2 1.40 dB
PL12 19.98 dB
PL13 22.00 dB
PL2W 15.95877647 W
PL12W 0.22130929 W
PL13W 0.13899513 W
SFO2 500.1320005 MHz
F2 - Processing parameters
SI 262144
SF 125.7578227 MHz
WDW EM
SSB 0
LB 0.50 Hz
GB 0
PC 1.00
200 190 180 170 160 150 140 130 120 110 100 90 80 70 60 50 40 30 20 10 0 ppm

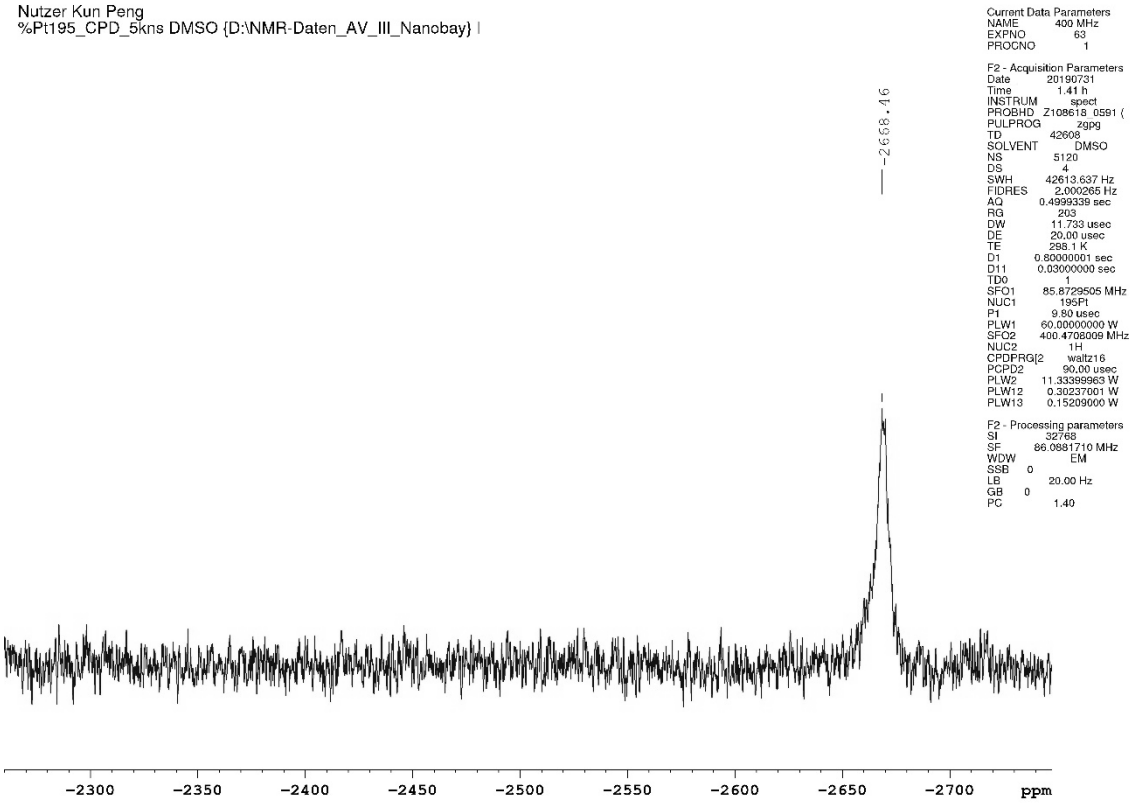
Nutzer Kun Peng
%Pt195_CPD_5kns DMSO {D:\NMR-Daten_AV_III_Nanobay} I
-2668.46
Current Data Parameters
NAME 400 MHz
EXPNO 63
PROCNO 1
F2 - Acquisition Parameters
Date 20190731
Time 1.41 h
INSTRUM spect
PROBHD Z108618_0591 (
PULPROG zgpg
TD 42608
SOLVENT DMSO
NS 5120
DS 4
SWH 42613.637 Hz
FIDRES 2.000265 Hz
AQ 0.4999339 sec
RG 203
DW 11.733 usec
DE 20.00 usec
TE 298.1 K
D1 0.80000001 sec
D11 0.03000000 sec
TD0 1
SFO1 85.8729505 MHz
NUC1 195Pt
P1 9.80 usec
PLW1 60.00000000 W
SFO2 400.4708009 MHz
NUC2 1H
CPDPRG[2 waltz16
PCPD2 90.00 usec
PLW2 11.33399963 W
PLW12 0.30237001 W
PLW13 0.15209000 W
F2 - Processing parameters
SI 32768
SF 86.0881710 MHz
WDW EM
SSB 0
LB 20.00 Hz
GB 0
PC 1.40
-2300 -2350 -2400 -2450 -2500 -2550 -2600 -2650 -2700 ppm

5.3.13 Synthesis o [Pd(triazolate^{COOCH2CH2OCH3,COOCH2CH2OCH3})(terpy)]PF_6

USC-KP123-01

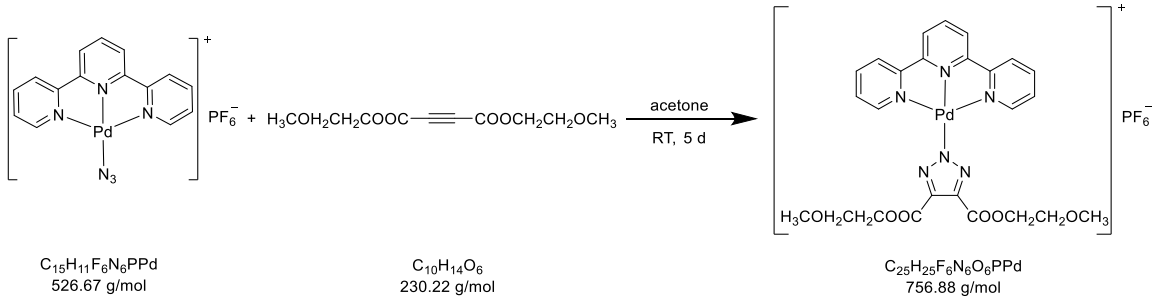

$C_{15}H_{11}F_6N_6PPd$ 526.67 g/mol

$C_{10}H_{14}O_6$ 230.22 g/mol

$C_{25}H_{25}F_6N_6O_6PPd$ 756.88 g/mol

$[Pd(N_3)(terpy)]PF_6$ (28.9 mg, 0.05 mmol) was dissolved in acetone (10 mL) at room temperature to give a clear yellow solution. Then, bis(2-methoxyethyl)-but-2-ynedioate (29.5 µL, 34.5 mg, 0.15 mmol) was added and stirring continued at room temperature for 5 d. The resulting pale yellow precipitate was filtered off, washed with diethyl ether (3 × 3 mL), and dried under vacuum for 2 d to obtain the product as a pale yellow solid. Yield: 80% (27.6 mg, 0.04 mmol). **IR** (ATR): $\tilde{\nu}$ = 3738 (w), 3089 (w), 1737 (m), 1601 (w), 1454 (w), 1425 (w), 1301 (m), 1192 (w), 1091 (m), 1025 (m), 838 (s), 782 (m), 723 (w) cm^{-1}; **^{1}H NMR** (400.47 MHz, DMSO-d_6): δ = 8.70–8.62 (m, 5H, H6/H6”, H4’, H3’/H5’), 8.56 (d, 2H, $^3J_{H3,H4;H3”,H4”}$ = 5.7 Hz, H3/H3”), 8.48 (dt, 2H, $^3J_{H4,H3/H5;H4”,\ H5”/H3”}$ = 7.7 Hz, $^4J_{H6,H4;H6”,H4”}$ = 1.4 Hz, H4/H4”), 7.88 (ddd, 2H, $^3J_{H5,H4;H5”,H4”}$ = 7.5 Hz, $^3J_{H5,H6;H5”,H6”}$ = 5.9 Hz, $^4J_{H5,H3;H5”,H3”}$ = 1.3 Hz, H5/H5”), 4.42 (t, 4H, ^3J = 4.6 Hz, OCH_2CH$_2$OCH$_3$), 3.66 (t, 4H, ^3J = 4.6 Hz, OCH$_2$CH_2OCH$_3$), 3.31 (s, 6H, OCH_3) ppm; **^{13}C NMR** (100.70 MHz, DMSO-d_6): δ = 161.11 (*C*=O), 157.67 (C2’/C6’), 154.69 (C2/C2”), 151.76 (C6/C6”), 143.51 (C4’), 142.90 (C4/C4”), 140.37 (triazolate-C4/C5), 128.83 (C5/C5”), 125.41 (C3’/C5’), 124.44 (C3/C3”), 69.61 (O*C*H$_2$CH$_2$OCH$_3$), 64.09 (OCH$_2$*C*H$_2$OCH$_3$), 58.12 (O*C*H$_3$) ppm; **MS** (ESI$^+$, CH$_3$OH): *m*/*z* = 611.0859 $[M\text{-}PF_6]^+$; **Elemental analysis** (%) calcd. for $C_{25}H_{25}N_6PF_6O_6Pd$: C 39.67, H 3.33, N 11.10; found (%): C 39.12, H 3.38, N 10.82.

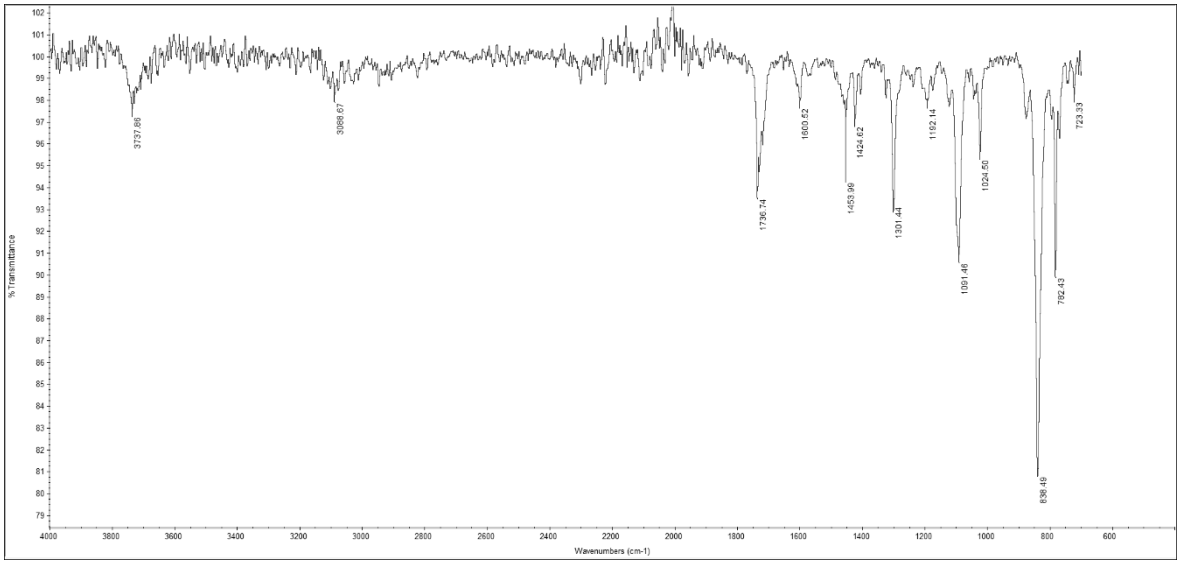
% Transmittance
Wavenumbers (cm-1)
3737.86
3088.67
1736.74
1600.62
1453.96
1424.62
1301.44
1162.14
1091.46
1024.55
792.43
639.49
723.33

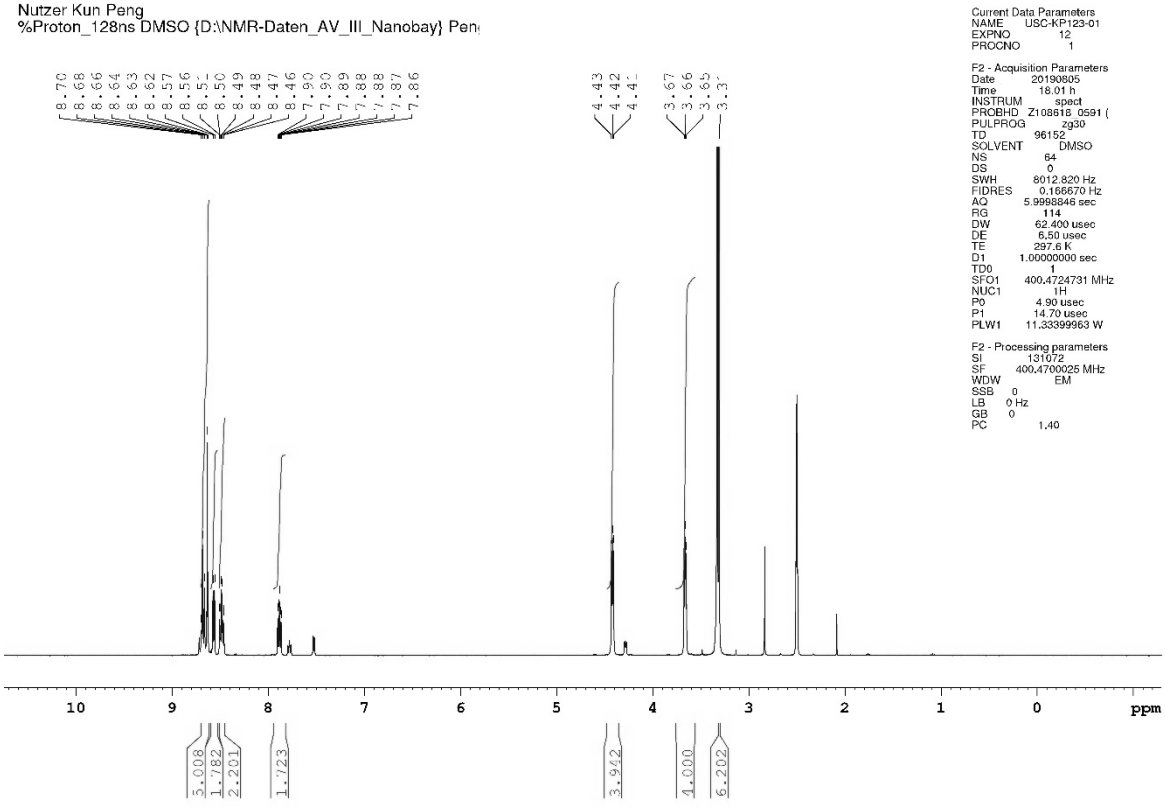
Nutzer Kun Peng
%Proton_128ns DMSO {D:\NMR-Daten_AV_III_Nanobay} Pen
Current Data Parameters
NAME USC-KP123-01
EXPNO 12
PROCNO 1
F2 - Acquisition Parameters
Date 20190805
Time 18.01 h
INSTRUM spect
PULPROG zg30
TD 96152
SOLVENT DMSO
NS 64
DS 0
SWH 8012.820 Hz
FIDRES 0.166670 Hz
AQ 5.9998846 sec
RG 114
DW 62.400 usec
DE 6.50 usec
TE 297.6 K
D1 1.00000000 sec
TD0 1
SFO1 400.4724731 MHz
NUC1 1H
P0 4.90 usec
P1 14.70 usec
PLW1 11.33399963 W
F2 - Processing parameters
SI 131072
SF 400.4700025 MHz
WDW EM
SSB 0
LB 0 Hz
GB 0
PC 1.40
ppm
3.008
1.782
2.201
1.723
3.942
4.000
6.202

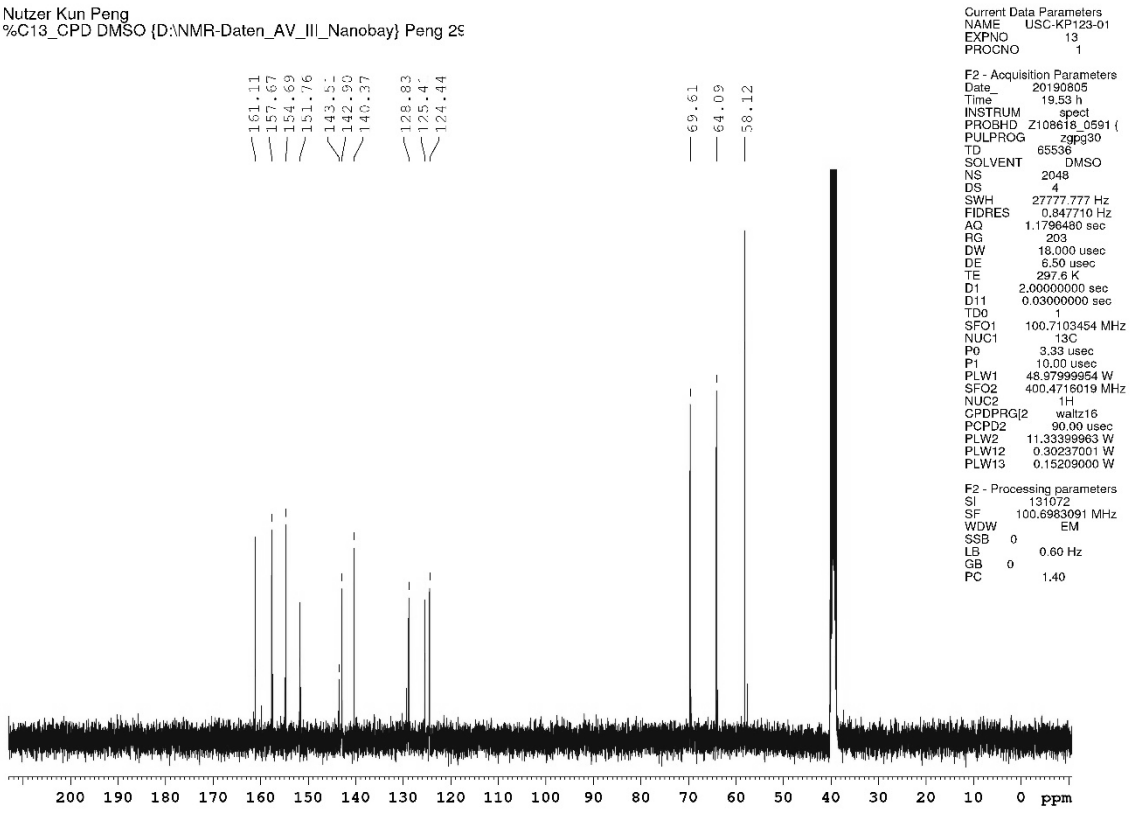
Nutzer Kun Peng
%C13_CPD DMSO {D:\NMR-Daten_AV_III_Nanobay} Peng 29
161.11
157.67
154.69
151.76
143.5
142.90
140.37
128.83
125.47
124.44
69.61
64.09
58.12
Current Data Parameters
NAME USC-KP123-01
EXPNO 13
PROCNO 1
F2 - Acquisition Parameters
Date_ 20190805
Time 19.53 h
INSTRUM spect
PROBHD Z108618_0591 (
PULPROG zgpg30
TD 65536
SOLVENT DMSO
NS 2048
DS 4
SWH 27777.777 Hz
FIDRES 0.847710 Hz
AQ 1.1796480 sec
RG 203
DW 18.000 usec
DE 6.50 usec
TE 297.6 K
D1 2.00000000 sec
D11 0.03000000 sec
TD0 1
SFO1 100.7103454 MHz
NUC1 13C
P0 3.33 usec
P1 10.00 usec
PLW1 48.97999954 W
SFO2 400.4716019 MHz
NUC2 1H
CPDPRG[2 waltz16
PCPD2 90.00 usec
PLW2 11.33399963 W
PLW12 0.30237001 W
PLW13 0.15209000 W
F2 - Processing parameters
SI 131072
SF 100.6983091 MHz
WDW EM
SSB 0
LB 0.60 Hz
GB 0
PC 1.40
200 190 180 170 160 150 140 130 120 110 100 90 80 70 60 50 40 30 20 10 0 ppm

5.3.14 Synthsis of [Pt(triazolate^{COOCH2CH2OCH3,COOCH2CH2OCH3})(terpy)]PF_6

USC-KP124-01

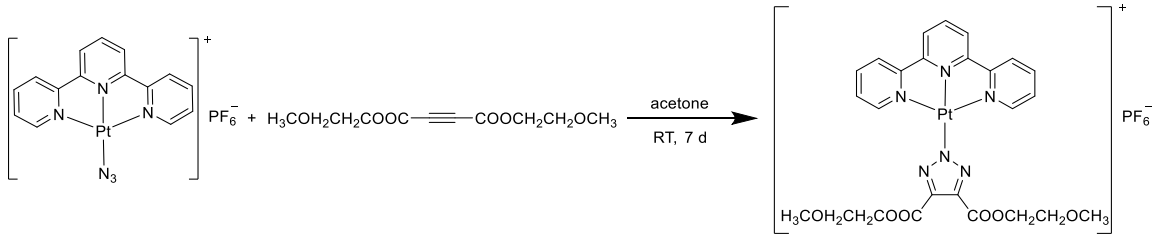

$C_{15}H_{11}F_6N_6PPt$ 615.33 g/mol

$C_{10}H_{14}O_6$ 230.22 g/mol

$C_{25}H_{25}F_6N_6O_6PPt$ 845.55 g/mol

$[Pt(N_3)(terpy)]PF_6$ (32.8 mg, 0.05 mmol) was dissolved in acetone (12 mL) at room temperature. To the resulting clear light orange solution, was add bis(2-methoxyethyl)-but-2-ynedioate (29.5 µL, 34.5 mg, 0.15 mmol) and stirring continued at room temperature for 7 d. The resulting yellow precipitate was filtered off, washed with diethyl ether (3 × 3 mL), and dried under vacuum for 2 d to obtain the product as a yellow solid. Yield: 80% (33.8 mg, 0.04 mmol). **IR** (ATR): $\tilde{\nu}$ = 3086 (w), 1731 (m), 1457 (m), 1427 (w), 1405 (w), 1302 (m), 1194 (w), 1092 (m), 1026 (m), 837 (s), 782 (m) cm^{-1}; **^{1}H NMR** (400.47 MHz, DMSO-d_6): δ = 8.68 (d, 2H, $^3J_{H6,H5;H6",H5"}$ = 5.6 Hz, H6/H6"), 8.57–8.55 (m, 5H, H3/H3", H4', H3'/H5'), 8.47 (dt, 2H, $^3J_{H4,H3/H5;H4",H3"/H5"}$ = 7.8 Hz, $^4J_{H4,H6;H4",H6"}$ = 1.4 Hz, H4/H4"), 7.85 (ddd, 2H, $^3J_{H5,H4;H5",H4"}$ = 7.5 Hz, $^3J_{H5,H6;H5",H6"}$ = 5.9 Hz, $^4J_{H5,H3;H5",H3"}$ = 1.4 Hz, H5/H5"), 4.44 (t, 4H, ^3J = 4.6 Hz, OCH_2CH$_2$OCH$_3$), 3.68 (t, 4H, ^3J = 4.6 Hz, OCH$_2$CH_2OCH$_3$), 3.33 (s, 6H, OCH_3) ppm; **^{13}C NMR** (100.70 MHz, DMSO-d_6): δ = 160.79 (*C*=O), 157.58 (C2'/C6'), 154.38 (C2/C2"), 151.97 (C6/C6"), 143.22 (C4'), 142.99 (C4/C4"), 140.14 (triazolate-C4/C5), 128.98 (C5/C5"), 125.92 (C3'/C5'), 124.31 (C3/C3"), 69.62 (O*C*H$_2$CH$_2$OCH$_3$), 64.17 (OCH$_2$*C*H$_2$OCH$_3$), 58.14 (O*C*H$_3$) ppm; **^{195}Pt NMR** (86.09 MHz, DMSO-d_6): δ = -2683 ppm; **MS** (ESI$^+$, CH_3OH): *m*/*z* = 700.1469 $[M\text{-}PF_6]^+$; **Elemental analysis** (%) calcd. for $C_{25}H_{25}N_6PF_6O_6Pt$: C 35.53, H 2.98, N 9.94; found (%): C 35.32, H 3.09, N 9.78.

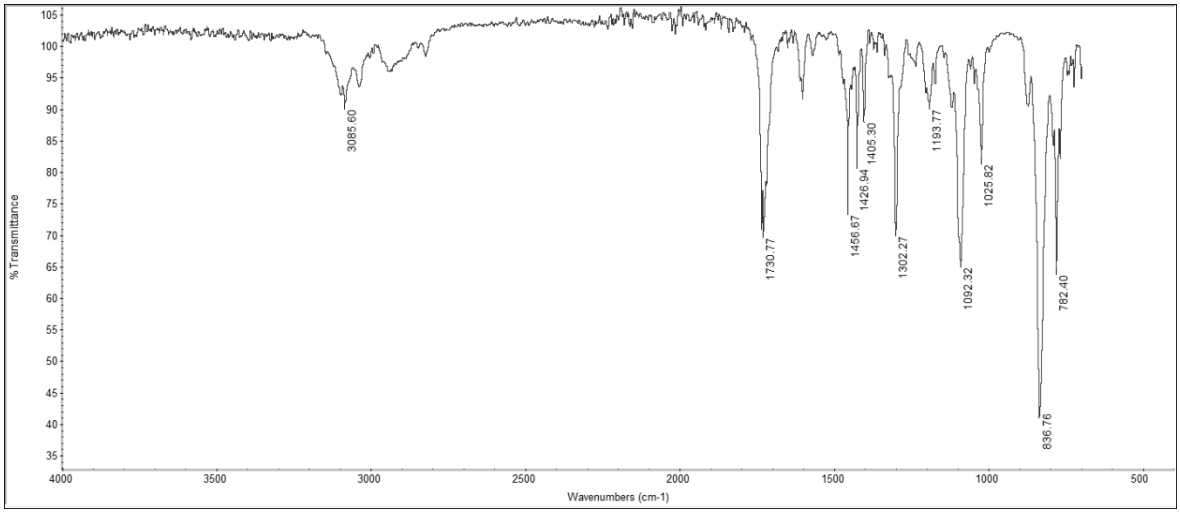
% Transmittance
Wavenumbers (cm-1)
3085.60
1730.77
1456.67
1426.94
1405.30
1302.27
1193.77
1092.32
1025.82
836.76
782.40

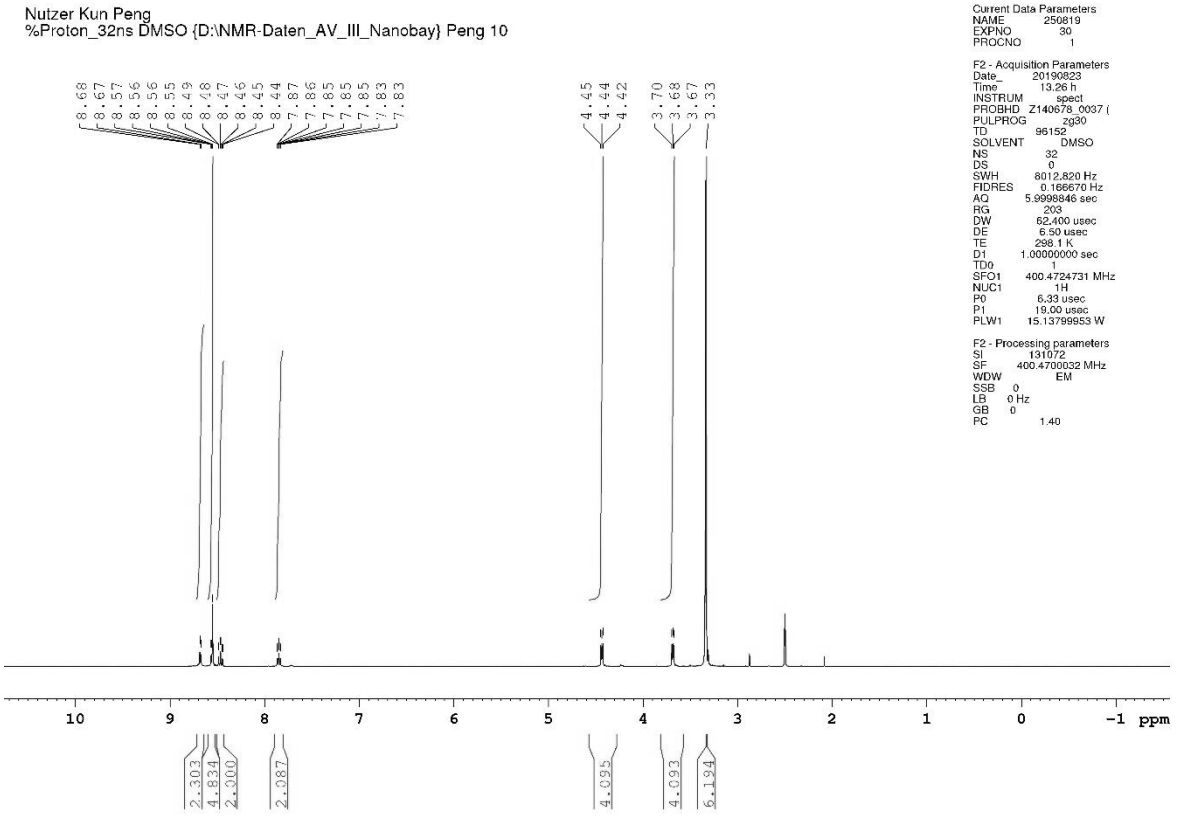
Nutzer Kun Peng
%Proton_32ns DMSO {D:\NMR-Daten_AV_III_Nanobay} Peng 10
8.68
8.67
8.57
8.56
8.55
8.49
8.48
8.47
8.46
8.45
8.44
7.87
7.86
7.85
7.85
7.85
7.83
7.83
4.45
4.44
4.42
3.70
3.68
3.67
3.33
Current Data Parameters
NAME 250819
EXPNO 30
PROCNO 1
F2 - Acquisition Parameters
Date_ 20190823
Time 13.26 h
INSTRUM spect
PROBHD Z140678_0037 (
PULPROG zg30
TD 96152
SOLVENT DMSO
NS 32
DS 0
SWH 8012.820 Hz
FIDRES 0.166670 Hz
AQ 5.9998846 sec
RG 203
DW 62.400 usec
DE 6.50 usec
TE 298.1 K
D1 1.00000000 sec
TD0 1
SFO1 400.4724731 MHz
NUC1 1H
P0 6.33 usec
P1 19.00 usec
PLW1 15.13799953 W
F2 - Processing parameters
SI 131072
SF 400.4700032 MHz
WDW EM
SSB 0
LB 0 Hz
GB 0
PC 1.40
10
9
8
7
6
5
4
3
2
1
0
-1 ppm
2.303
4.834
4.000
2.087
4.095
4.093
6.194

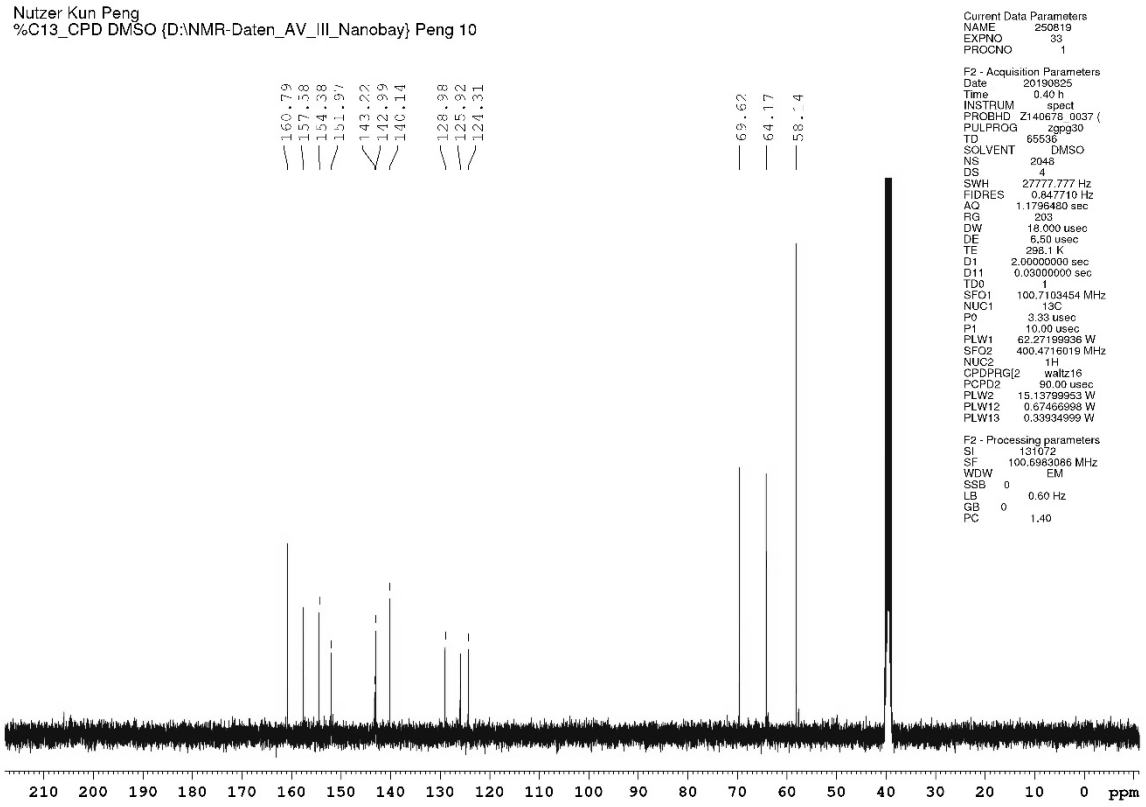
Nutzer Kun Peng
%C13_CPD DMSO {D:\NMR-Daten_AV_III_Nanobay} Peng 10
160.79
157.38
154.38
151.97
143.22
142.99
140.14
128.98
125.92
124.31
69.62
64.17
58.14
Current Data Parameters
NAME 250819
EXPNO 33
PROCNO 1
F2 - Acquisition Parameters
Date 20190825
Time 0.40 h
INSTRUM spect
PROBHD Z140678_0037 (
PULPROG zgpg30
TD 65536
SOLVENT DMSO
NS 2048
DS 4
SWH 27777.777 Hz
FIDRES 0.847710 Hz
AQ 1.1796480 sec
RG 203
DW 18.000 usec
DE 6.50 usec
TE 298.1 K
D1 2.00000000 sec
D11 0.03000000 sec
TD0 1
SFO1 100.7103454 MHz
NUC1 13C
P0 3.33 usec
P1 10.00 usec
PLW1 62.27199936 W
SFO2 400.4716019 MHz
NUC2 1H
CPDPRG[2 waltz16
PCPD2 90.00 usec
PLW2 15.13799953 W
PLW12 0.67466998 W
PLW13 0.33934999 W
F2 - Processing parameters
SI 131072
SF 100.6983086 MHz
WDW EM
SSB 0
LB 0.60 Hz
GB 0
PC 1.40
210 200 190 180 170 160 150 140 130 120 110 100 90 80 70 60 50 40 30 20 10 0 ppm

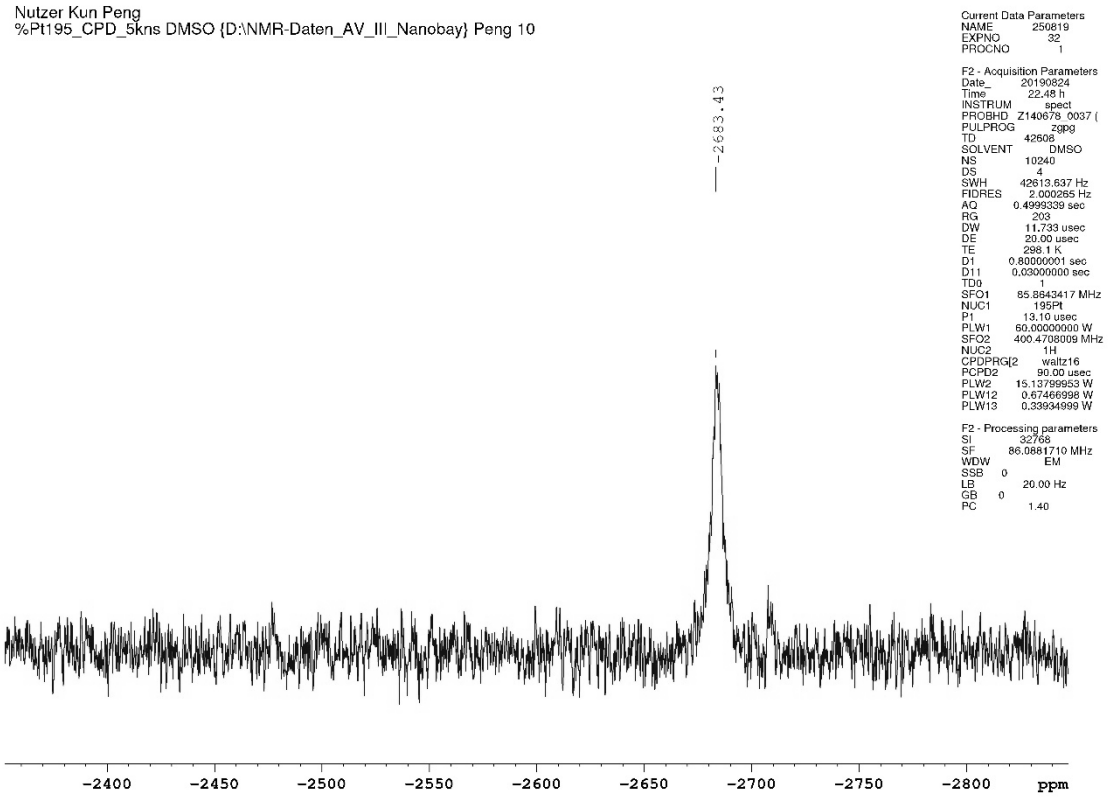
Nutzer Kun Peng
%Pt195_CPD_5kns DMSO {D:\NMR-Daten_AV_III_Nanobay} Peng 10
-2683.43
Current Data Parameters
NAME 250819
EXPNO 32
PROCNO 1
F2 - Acquisition Parameters
Date_ 20190824
Time 22.48 h
INSTRUM spect
PROBHD Z140678_0037 (
PULPROG zgpg
TD 42606
SOLVENT DMSO
NS 10240
DS 4
SWH 42613.637 Hz
FIDRES 2.000285 Hz
AQ 0.4999339 sec
RG 203
DW 11.733 usec
DE 20.00 usec
TE 298.1 K
D1 0.80000001 sec
D11 0.03000000 sec
TD0 1
SFO1 85.8843417 MHz
NUC1 195Pt
P1 13.10 usec
PLW1 60.00000000 W
SFO2 400.4708009 MHz
NUC2 1H
CPDPRG[2 waltz16
PCPD2 90.00 usec
PLW2 15.13799953 W
PLW12 0.67466998 W
PLW13 0.33934999 W
F2 - Processing parameters
SI 32768
SF 86.0881710 MHz
WDW EM
SSB 0
LB 20.00 Hz
GB 0
PC 1.40
-2400 -2450 -2500 -2550 -2600 -2650 -2700 -2750 -2800 ppm

5.3.15 Synthesis of [Pd(triazlate^{CF3,COOEt})(terpy)]PF_6

USC-KP036-05

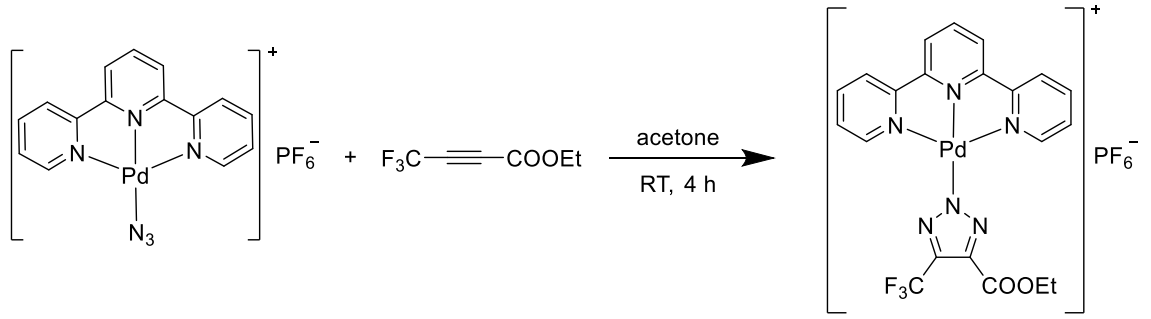

$C_{15}H_{11}F_6N_6PPd$
526.67 g/mol

$C_6H_5F_3O_2$
166.10 g/mol

$C_{21}H_{16}F_9N_6O_2PPd$
692.77 g/mol

[Pd(N_3)(terpy)]PF_6 (53 mg, 0.10 mmol) was dissolved in acetone (7 mL). Then, 4,4,4-trifluoro-2-butynoic acid ethyl ester (36 µL, 42 mg, 0.25 mmol) was added and stirring at room temperature continued for 4 h. The resulting clear yellow solution was then evaporated to dryness. The resulting yellow solid was washed with diethyl ether (5 × 5 mL) and dried under vacuum for 2 d to obtain the product as a pale yellow solid. Yield: 90% (60 mg, 0.09 mmol). **IR** (ATR): $\tilde{\nu}$ = 3099 (w), 1725 (m), 1604 (w), 1452 (m), 1315 (m), 1191 (m), 1138 (m), 1061 (m), 835 (s), 773 (m), 749 (w), 725 (w) cm^{-1}; **^{1}H NMR** (400.40 MHz, acetone-d_6): δ = 8.96 (ddd, 2H, $^3J_{H6,H5;H6",H5"}$ = 5.7 Hz, $^4J_{H6,H4;H6",H4"}$ = 1.5 Hz, $^5J_{H6,H3;H6",H3"}$ = 0.5 Hz, H6/H6"), 8.71–8.63 (m, 5H, H3/H3", H4', H3'/H5'), 8.55 (dt, 2H, $^3J_{H4,H3/H5;H4",H3"/H5"}$ = 7.8 Hz, $^4J_{H4,H6;H4",H6"}$ = 1.5 Hz, H4/H4"), 7.97 (ddd, 2H, $^3J_{H5,H4;H5",H4"}$ = 7.6 Hz, $^3J_{H5,H6;H5",H6"}$ = 5.7 Hz, $^4J_{H5,H3;H5",H3"}$ = 1.5 Hz, H5/H5"), 4.43 (q, 2H, ^3J = 7.1 Hz, COOCH_2CH$_3$), 1.41 (t, 3H, ^3J = 7.1 Hz, COOCH$_2$CH_3) ppm; **^{13}C NMR** (100.68 MHz, acetone-d_6): δ = 160.54 (*C*=O), 158.78 (C2'/C6'), 156.20 (C2/C2"), 153.71 (C6/C6"), 144.93 (C4'), 144.04 (C4/C4"), 140.03 (q, $^2J_{C,F}$ = 38.2 Hz, triazolate-C4), 139.17 (triazolate-C5), 129.85 (C5/C5"), 126.28 (C3'/C5'), 125.45 (C3/C3"), 122.37 (q, $^1J_{C,F}$= 268.8 Hz, *C*F$_3$), 61.84 (COO*C*H$_2$CH$_3$), 14.42 (COOCH$_2$*C*H$_3$) ppm; **^{19}F NMR** (376.75 MHz, acetone-d_6): δ = −60.37 (C*F*$_3$), −72.50 (d, $^1J_{F,P}$= 707.7 Hz, P*F*$_6$) ppm; MS (ESI$^+$, CH$_3$CN): *m*/*z* = 547.0310 [M-PF_6]$^+$; **Elemental analysis** (%) calcd. for $C_{21}H_{16}N_6PF_9O_2Pd$: C 36.41, H 2.33, N 12.13; found (%): C 36.62, H 2.38, N 11.76.

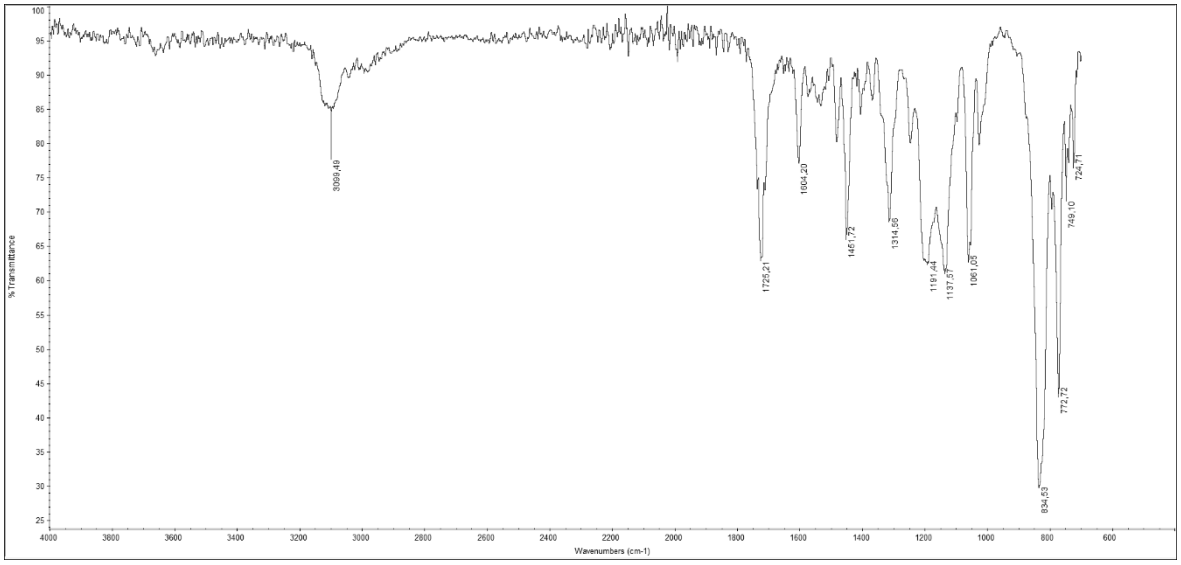
% Transmittance
Wavenumbers (cm-1)
3099.49
1725.21
1604.20
1461.72
1314.66
1191.44
1137.57
1061.05
834.63
772.72
749.10
724.71

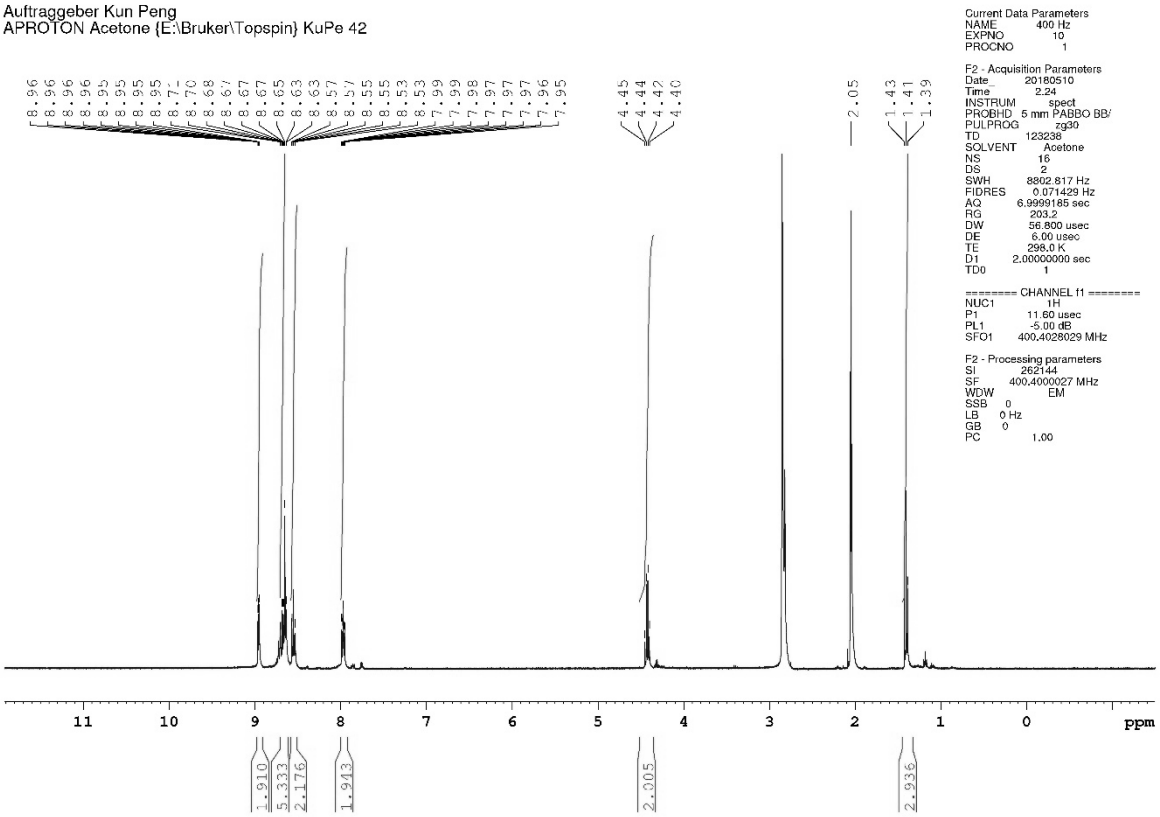
Auftraggeber Kun Peng
APROTON Acetone {E:\Bruker\Topspin} KuPe 42
Current Data Parameters
NAME 400 Hz
EXPNO 10
PROCNO 1
F2 - Acquisition Parameters
Date 20180510
Time 2.24
INSTRUM spect
PROBHD 5 mm PABBO BB/
PULPROG zg30
TD 123236
SOLVENT Acetone
NS 16
DS 2
SWH 8802.817 Hz
FIDRES 0.071429 Hz
AQ 6.9999185 sec
RG 203.2
DW 56.800 usec
DE 6.00 usec
TE 298.0 K
D1 2.00000000 sec
TD0 1
======== CHANNEL f1 ========
NUC1 1H
P1 11.60 usec
PL1 -5.00 dB
SFO1 400.4028029 MHz
F2 - Processing parameters
SI 262144
SF 400.4000027 MHz
WDW EM
SSB 0
LB 0 Hz
GB 0
PC 1.00
ppm
1.910
5.333
2.176
1.943
2.005
2.936

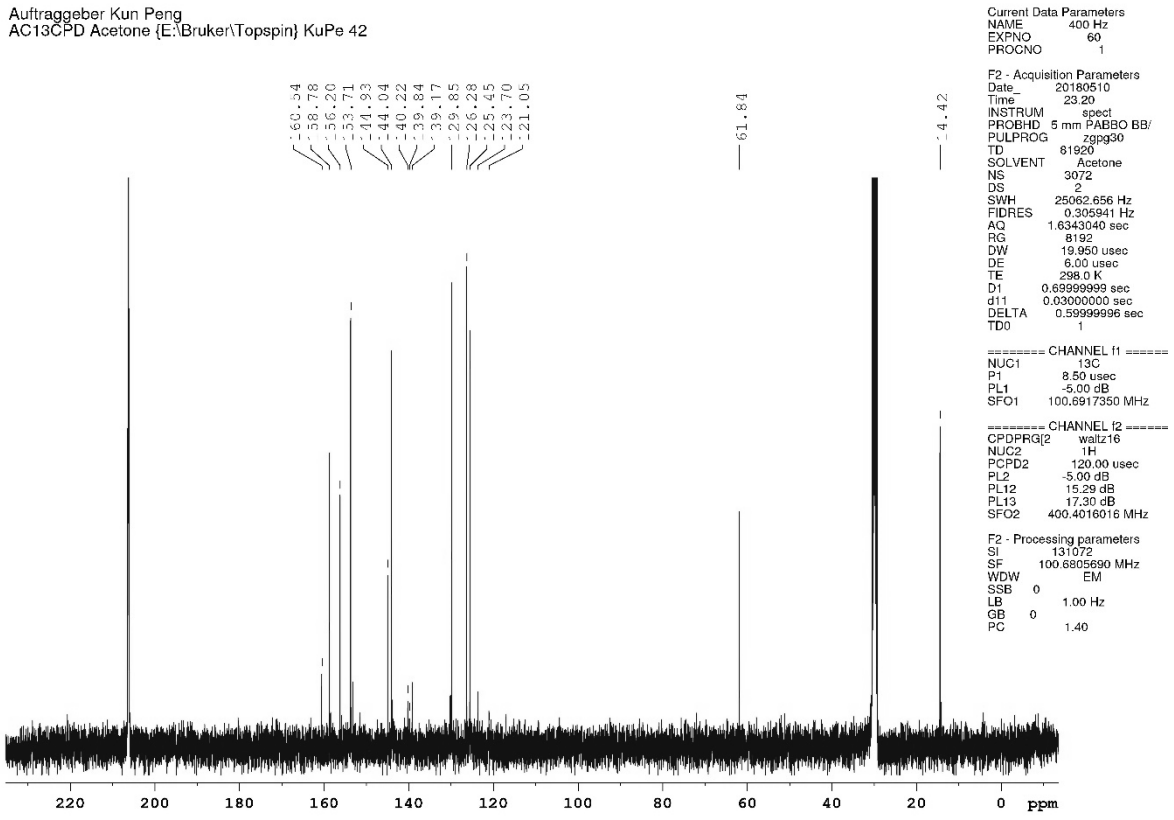
Auftraggeber Kun Peng
AC13CPD Acetone {E:\Bruker\Topspin} KuPe 42
60.54
58.78
56.20
53.71
44.93
44.04
40.22
39.84
39.17
29.85
26.28
25.45
23.70
21.05
61.84
14.42
Current Data Parameters
NAME 400 Hz
EXPNO 60
PROCNO 1
F2 - Acquisition Parameters
Date_ 20180510
Time 23.20
INSTRUM spect
PROBHD 5 mm PABBO BB/
PULPROG zgpg30
TD 81920
SOLVENT Acetone
NS 3072
DS 2
SWH 25062.656 Hz
FIDRES 0.305941 Hz
AQ 1.6343040 sec
RG 8192
DW 19.950 usec
DE 6.00 usec
TE 298.0 K
D1 0.69999999 sec
d11 0.03000000 sec
DELTA 0.59999996 sec
TD0 1
======== CHANNEL f1 ======
NUC1 13C
P1 8.50 usec
PL1 -5.00 dB
SFO1 100.6917350 MHz
======== CHANNEL f2 ======
CPDPRG[2 waltz16
NUC2 1H
PCPD2 120.00 usec
PL2 -5.00 dB
PL12 15.29 dB
PL13 17.30 dB
SFO2 400.4016016 MHz
F2 - Processing parameters
SI 131072
SF 100.6805690 MHz
WDW EM
SSB 0
LB 1.00 Hz
GB 0
PC 1.40
220
200
180
160
140
120
100
80
60
40
20
0
ppm

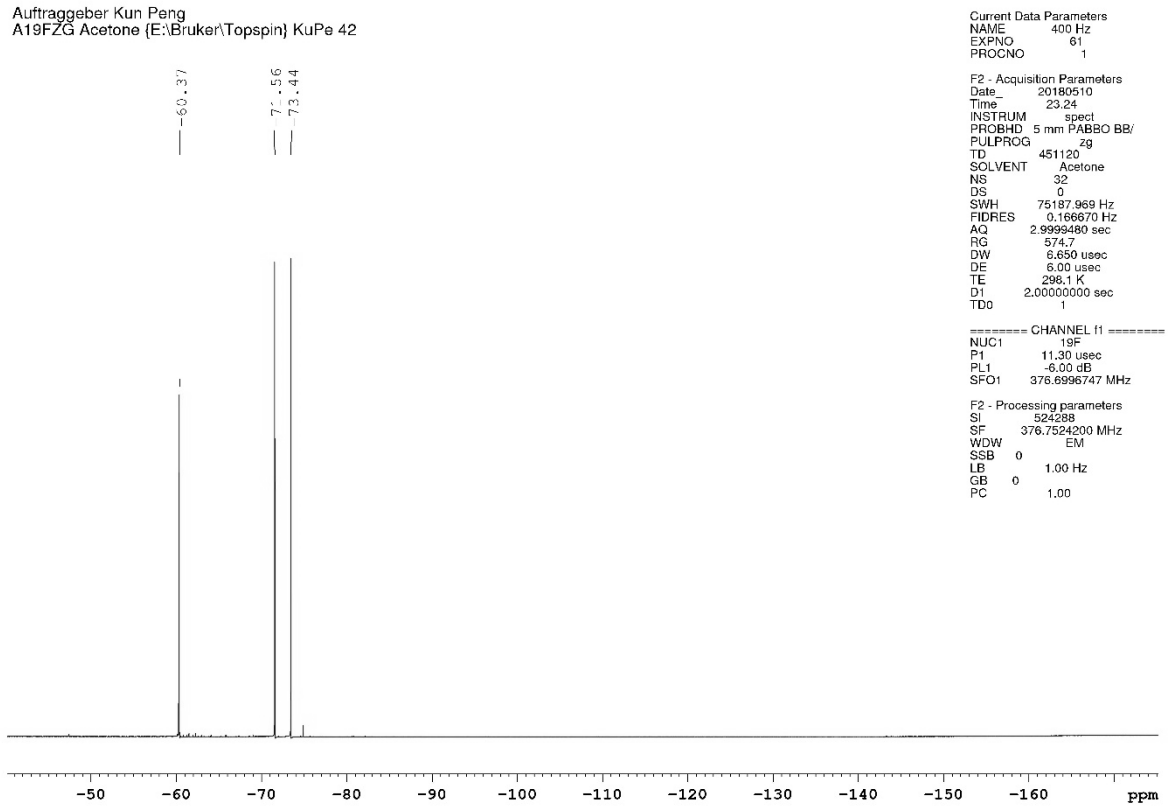
Auftraggeber Kun Peng
A19FZG Acetone {E:\Bruker\Topspin} KuPe 42
60.37
71.56
73.44
Current Data Parameters
NAME 400 Hz
EXPNO 61
PROCNO 1
F2 - Acquisition Parameters
Date_ 20180510
Time 23.24
INSTRUM spect
PROBHD 5 mm PABBO BB/
PULPROG zg
TD 451120
SOLVENT Acetone
NS 32
DS 0
SWH 75187.969 Hz
FIDRES 0.166670 Hz
AQ 2.9999480 sec
RG 574.7
DW 6.650 usec
DE 6.00 usec
TE 298.1 K
D1 2.00000000 sec
TD0 1
======== CHANNEL f1 ========
NUC1 19F
P1 11.30 usec
PL1 -6.00 dB
SFO1 376.6996747 MHz
F2 - Processing parameters
SI 524288
SF 376.7524200 MHz
WDW EM
SSB 0
LB 1.00 Hz
GB 0
PC 1.00
-50
-60
-70
-80
-90
-100
-110
-120
-130
-140
-150
-160
ppm

5.3.16 Synthesis of [Pt(triazolate^{CF3,COOEt})(terpy)]PF_6

USC-KP037-06

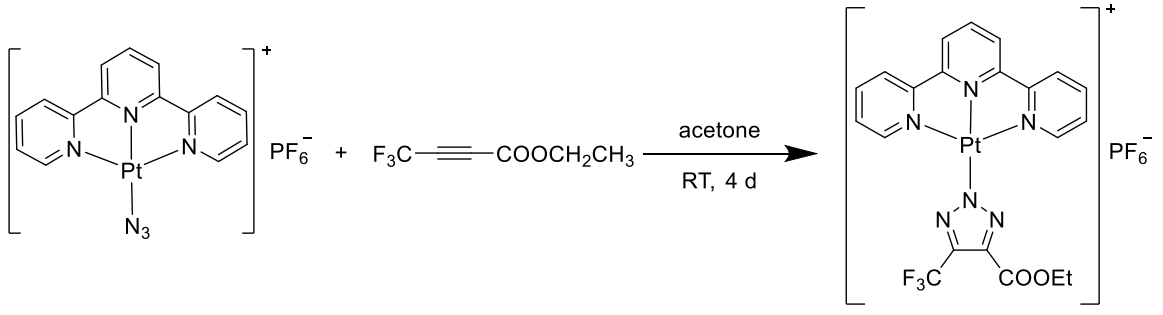

$C_{15}H_{11}F_6N_6PPt$
615.33 g/mol

$C_6H_5F_3O_2$
166.10 g/mol

$C_{21}H_{16}F_9N_6O_2PPt$
781.43 g/mol

$[Pt(N_3)(terpy)]PF_6$ (32 mg, 0.05 mmol) was dissolved in acetone (5 mL). Then, 4,4,4-trifluoro-2-butynoic acid ethyl ester (25 µL, 29 mg, 0.17 mmol) was added and stirring continued at room temperature for 4 d. The resulting clear orange solution was evaporated to dryness and the resulting orange solid washed with diethyl ether (5 × 5 mL) and dried under vacuum for 2 d to obtain the product as an orange solid. Yield: 80% (32 mg, 0.04 mmol). **IR** (ATR): $\tilde{\nu}$ = 3095 (w), 1727 (m), 1606 (w), 1452 (m), 1315 (m), 1196 (m), 1064 (m), 836 (s), 775 (s), 750 (w) cm^{-1}; **^{1}H NMR** (400.47 MHz, DMSO-d_6): δ = 8.61–8.55 (m, 7H, H6/H6”, H3/H3”, H4’, H3’/H5’), 8.48 (dt, 2H, $^3J_{H4,H3/H5;H4”,H3”/H5”}$ = 7.8 Hz, $^4J_{H4,H6;H4”,H6”}$ = 1.2 Hz, H4/H4’’), 7.86 (ddd, 2H, $^3J_{H5,H4;H5”,H4”}$ = 7.5 Hz, $^3J_{H5,H6;H5”,H6”}$ = 5.9 Hz, $^4J_{H5,H3;H5”,H3”}$ = 1.2 Hz, H5/H5”), 4.38 (q, 2H, ^3J = 7.1 Hz, COOCH_2CH$_3$), 1.36 (t, 3H, ^3J = 7.1 Hz, COOCH$_2$CH_3) ppm; **^{13}C NMR** (100.70 MHz, DMSO-d_6): δ = 159.21 (*C*=O), 157.37 (C2’/C6’), 154.40 (C2/C2”), 152.06 (C6/C6”), 143.42 (C4’), 143.05 (C4/C4”), 138.80 (q, $^2J_{C,F}$ = 37.7 Hz, triazolate-C4), 137.64 (triazolate-C5), 129.06 (C5/C5”), 125.94 (C3’/C5’), 124.36 (C3/C3”), 121.02 (q, $^1J_{C,F}$= 268.3 Hz, *C*F$_3$), 61.10 (COO*C*H$_2$CH$_3$), 13.91 (COOCH$_2$*C*H$_3$) ppm; **^{19}F NMR** (376.82 MHz, DMSO-d_6): δ = −58.87 (C*F*$_3$), −70.14 (d, $^1J_{F,P}$= 711.3 Hz, P*F*$_6$) ppm; **^{195}Pt NMR** (86.09 MHz, DMSO-d_6): δ = -2690 ppm; **MS** (ESI$^+$, CH$_3$CN): *m*/*z* = 636.0921 $[M\text{-}PF_6]^+$; **Elemental analysis** (%) calcd. for $C_{21}H_{16}N_6PF_9O_2Pt$: C 32.28, H 2.06, N 10.75; found (%): C 32.08, H 2.16, N 10.41.

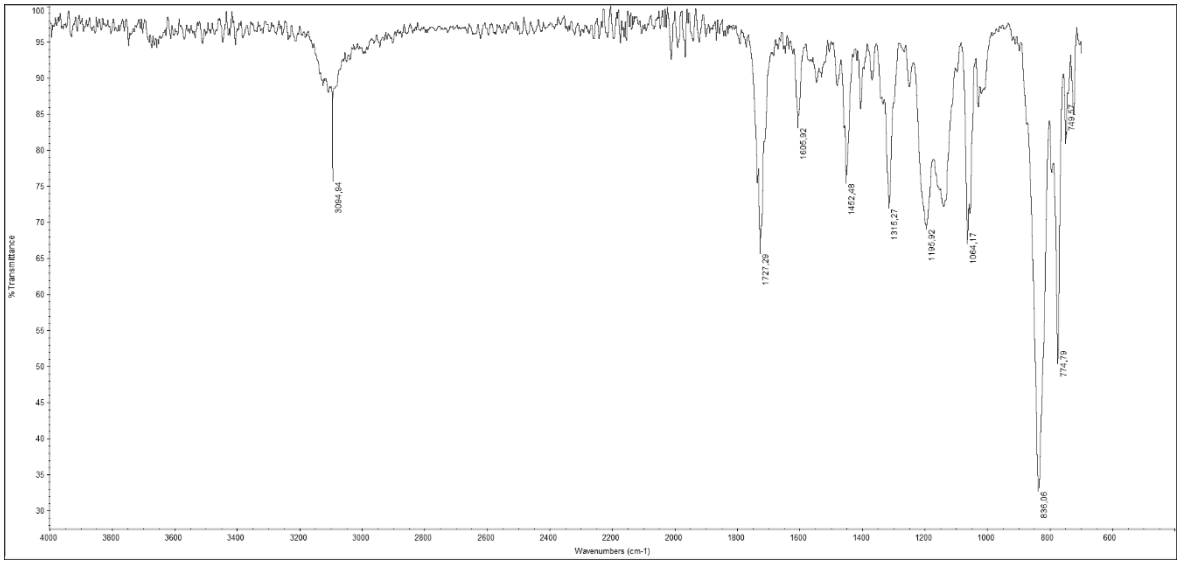
% Transmittance
Wavenumbers (cm-1)
3064.84
1727.29
1605.92
1452.48
1315.27
1195.92
1064.17
749.32
774.79
696.06

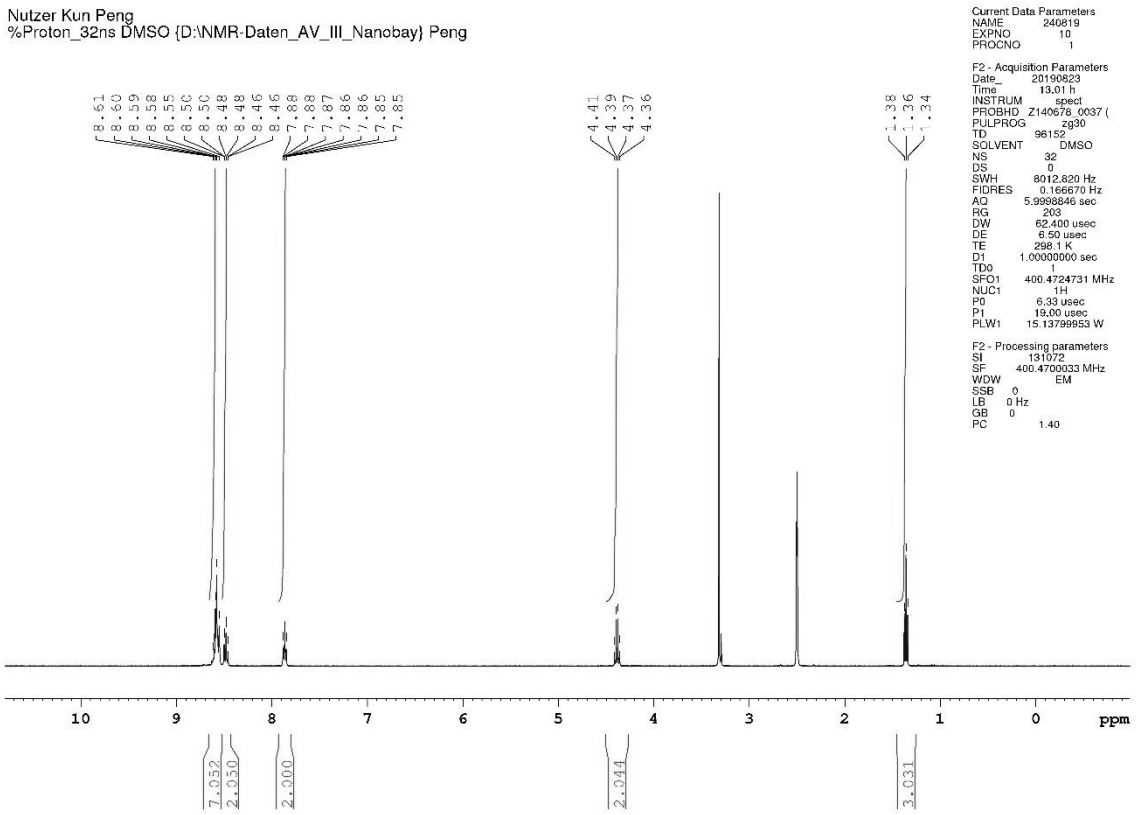
Nutzer Kun Peng
%Proton_32ns DMSO {D:\NMR-Daten_AV_III_Nanobay} Peng
8.61
8.60
8.59
8.58
8.55
8.50
8.48
8.46
7.88
7.87
7.86
7.86
7.85
7.85
4.41
4.39
4.37
4.36
1.38
1.36
1.34
Current Data Parameters
NAME 240819
EXPNO 10
PROCNO 1
F2 - Acquisition Parameters
Date_ 20190823
Time 13.01 h
INSTRUM spect
PROBHD Z140678_0037 (
PULPROG zg30
TD 96152
SOLVENT DMSO
NS 32
DS 0
SWH 8012.820 Hz
FIDRES 0.166670 Hz
AQ 5.9998846 sec
RG 203
DW 62.400 usec
DE 6.50 usec
TE 298.1 K
D1 1.00000000 sec
TD0 1
SFO1 400.4724731 MHz
NUC1 1H
P0 6.33 usec
P1 19.00 usec
PLW1 15.13799953 W
F2 - Processing parameters
SI 131072
SF 400.4700033 MHz
WDW EM
SSB 0
LB 0 Hz
GB 0
PC 1.40
10
9
8
7
6
5
4
3
2
1
0
ppm
2.052
2.030
2.000
2.044
3.031

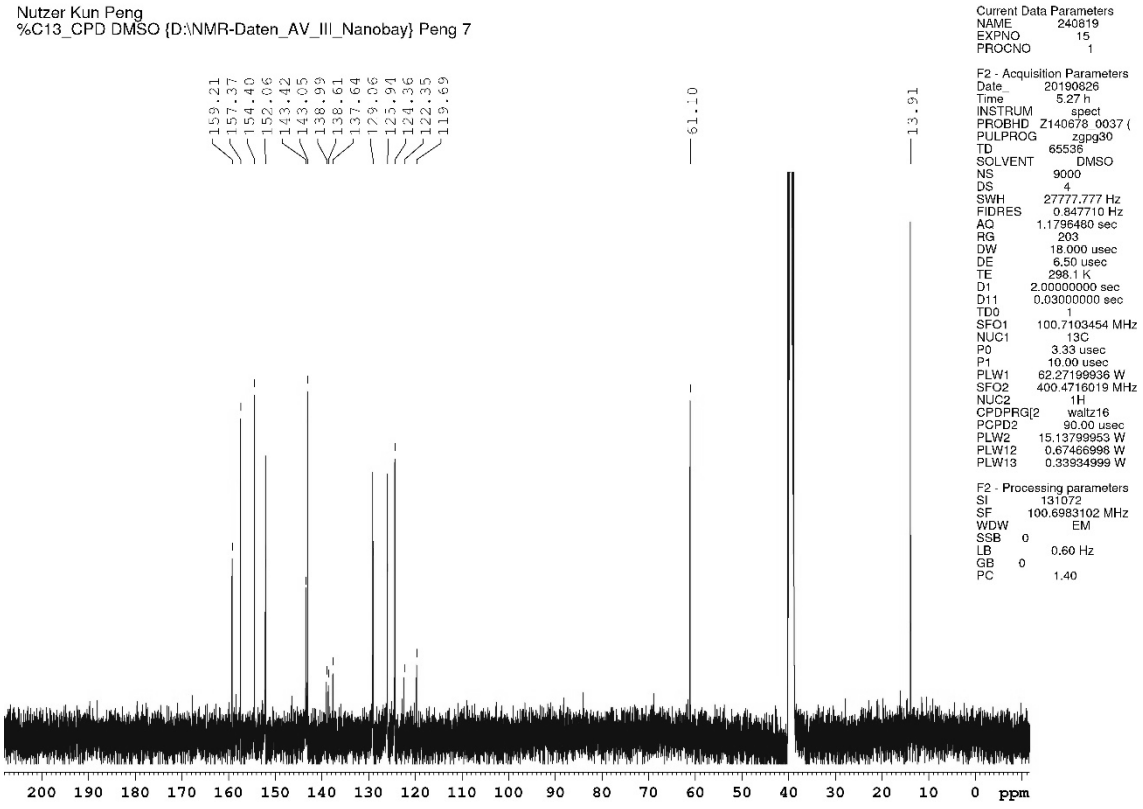
Nutzer Kun Peng
%C13_CPD DMSO {D:\NMR-Daten_AV_III_Nanobay} Peng 7
159.21
157.37
154.40
152.06
143.42
143.05
138.99
138.61
137.64
129.06
125.94
124.36
122.35
119.69
61.10
13.91
Current Data Parameters
NAME 240819
EXPNO 15
PROCNO 1
F2 - Acquisition Parameters
Date_ 20190826
Time 5.27 h
INSTRUM spect
PROBHD Z140678_0037 (
PULPROG zgpg30
TD 65536
SOLVENT DMSO
NS 9000
DS 4
SWH 27777.777 Hz
FIDRES 0.847710 Hz
AQ 1.1796480 sec
RG 203
DW 18.000 usec
DE 6.50 usec
TE 298.1 K
D1 2.00000000 sec
D11 0.03000000 sec
TD0 1
SFO1 100.7103454 MHz
NUC1 13C
P0 3.33 usec
P1 10.00 usec
PLW1 62.27199936 W
SFO2 400.4716019 MHz
NUC2 1H
CPDPRG[2 waltz16
PCPD2 90.00 usec
PLW2 15.13799953 W
PLW12 0.67466998 W
PLW13 0.33934999 W
F2 - Processing parameters
SI 131072
SF 100.6983102 MHz
WDW EM
SSB 0
LB 0.60 Hz
GB 0
PC 1.40
200 190 180 170 160 150 140 130 120 110 100 90 80 70 60 50 40 30 20 10 0 ppm

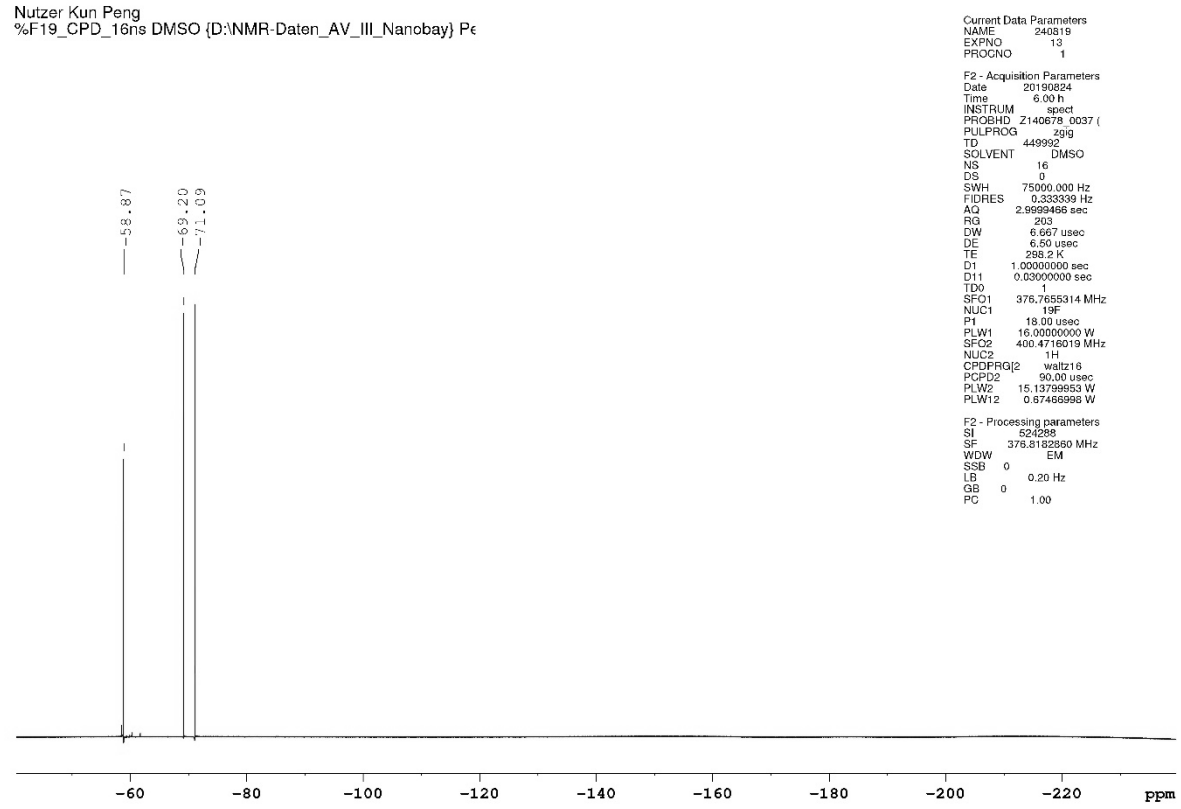
Nutzer Kun Peng
%F19_CPD_16ns DMSO {D:\NMR-Daten_AV_III_Nanobay} Pe
-58.87
-69.20
-71.09
Current Data Parameters
NAME 240819
EXPNO 13
PROCNO 1
F2 - Acquisition Parameters
Date 20190824
Time 6.00 h
INSTRUM spect
PROBHD Z140678_0037 (
PULPROG zgig
TD 449992
SOLVENT DMSO
NS 16
DS 0
SWH 75000.000 Hz
FIDRES 0.333339 Hz
AQ 2.9999486 sec
RG 203
DW 6.667 usec
DE 6.50 usec
TE 298.2 K
D1 1.00000000 sec
D11 0.03000000 sec
TD0 1
SFO1 376.7655314 MHz
NUC1 19F
P1 18.00 usec
PLW1 16.00000000 W
SFO2 400.4716019 MHz
NUC2 1H
CPDPRG[2 waltz16
PCPD2 90.00 usec
PLW2 15.13799953 W
PLW12 0.67466998 W
F2 - Processing parameters
SI 524288
SF 376.8182960 MHz
WDW EM
SSB 0
LB 0.20 Hz
GB 0
PC 1.00
-60 -80 -100 -120 -140 -160 -180 -200 -220 ppm

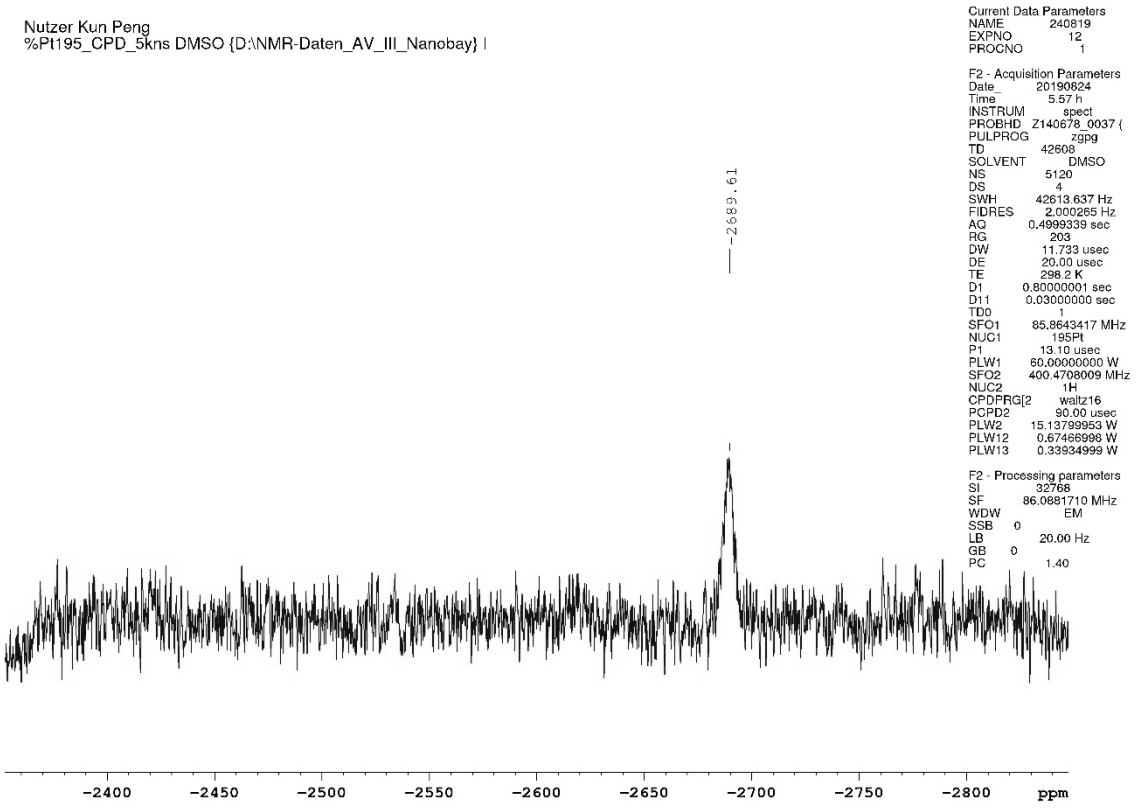
Nutzer Kun Peng
%Pt195_CPD_5kns DMSO {D:\NMR-Daten_AV_III_Nanobay} I
Current Data Parameters
NAME 240819
EXPNO 12
PROCNO 1
F2 - Acquisition Parameters
Date_ 20190824
Time 5.57 h
INSTRUM spect
PROBHD Z140678_0037 (
PULPROG zgpg
TD 42608
SOLVENT DMSO
NS 5120
DS 4
SWH 42613.637 Hz
FIDRES 2.000265 Hz
AQ 0.4999339 sec
RG 203
DW 11.733 usec
DE 20.00 usec
TE 298.2 K
D1 0.80000001 sec
D11 0.03000000 sec
TD0 1
SFO1 85.8643417 MHz
NUC1 195Pt
P1 13.10 usec
PLW1 60.00000000 W
SFO2 400.4708009 MHz
NUC2 1H
CPDPRG[2 waltz16
PCPD2 90.00 usec
PLW2 15.13799953 W
PLW12 0.67466998 W
PLW13 0.33934999 W
F2 - Processing parameters
SI 32768
SF 86.0881710 MHz
WDW EM
SSB 0
LB 20.00 Hz
GB 0
PC 1.40
-2689.61
-2400
-2450
-2500
-2550
-2600
-2650
-2700
-2750
-2800
ppm

5.3.17 Synthesis of [Pt(terpy)(dmso)](OTf)$_2$

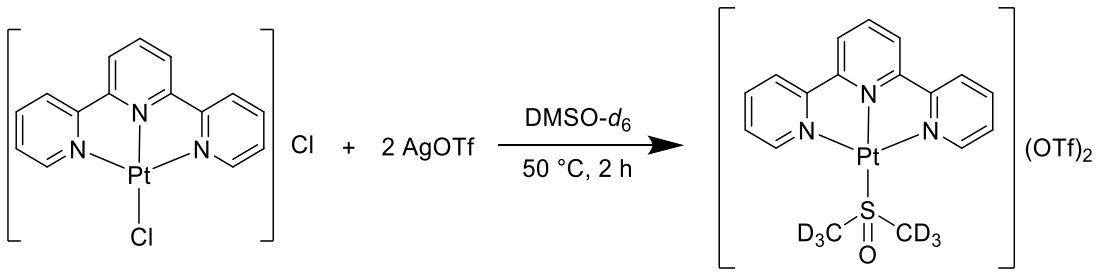

$C_{15}H_{11}Cl_2N_3Pt$ — 499.25 g/mol

$CAgF_3O_3S$ — 256.94 g/mol

$C_{19}H_{11}D_6F_6N_3O_7PtS_3$ — 810.65 g/mol

[PtCl(terpy)]Cl (5 mg, 10 µmol) was mixed with DMSO-d_6 (600 µL) in an NMR tube to give a light red suspension. After recording a NMR spectrum. solid silver triflate (5.7 mg, 22 µmol) was added and the suspension heated to 50 °C for 2 h. During that time, the red solid material fully dissolved and a white precipitate formed, which was filtered off. The resulting yellow filtrate was analysed by NMR spectroscopy again. **^{1}H NMR** (400.47 MHz, DMSO-d_6): δ = 8.77 (d, 2H, $^3J_{H6,H5;H6",H5"}$ = 4.9 Hz, H6/H6"), 8.60–8.58 (m, 5H, H3/H3", H4', H3'/H5'), 8.48 (dt, 2H, $^3J_{H4,H3/H5;H4",H3"/H5"}$ = 7.9 Hz, $^4J_{H4,H6;H4",H6"}$ = 1.3 Hz, H4/H4"), 7.90 (t, 2H, $^3J_{H5,H3/H4;H5",H3"/H4"}$ = 6.1 Hz, H5/H5") ppm; **^{19}F NMR** (376.82 MHz, DMSO-d_6): δ = −77.74 ($CF_3SO_3^-$) ppm; **^{195}Pt NMR** (86.09 MHz, DMSO-d_6): δ = -2725 ppm. Identical NMR spectra were also obtained when the procedure described above was repeated using silver tetrafluoroborate instead of silver triflate.

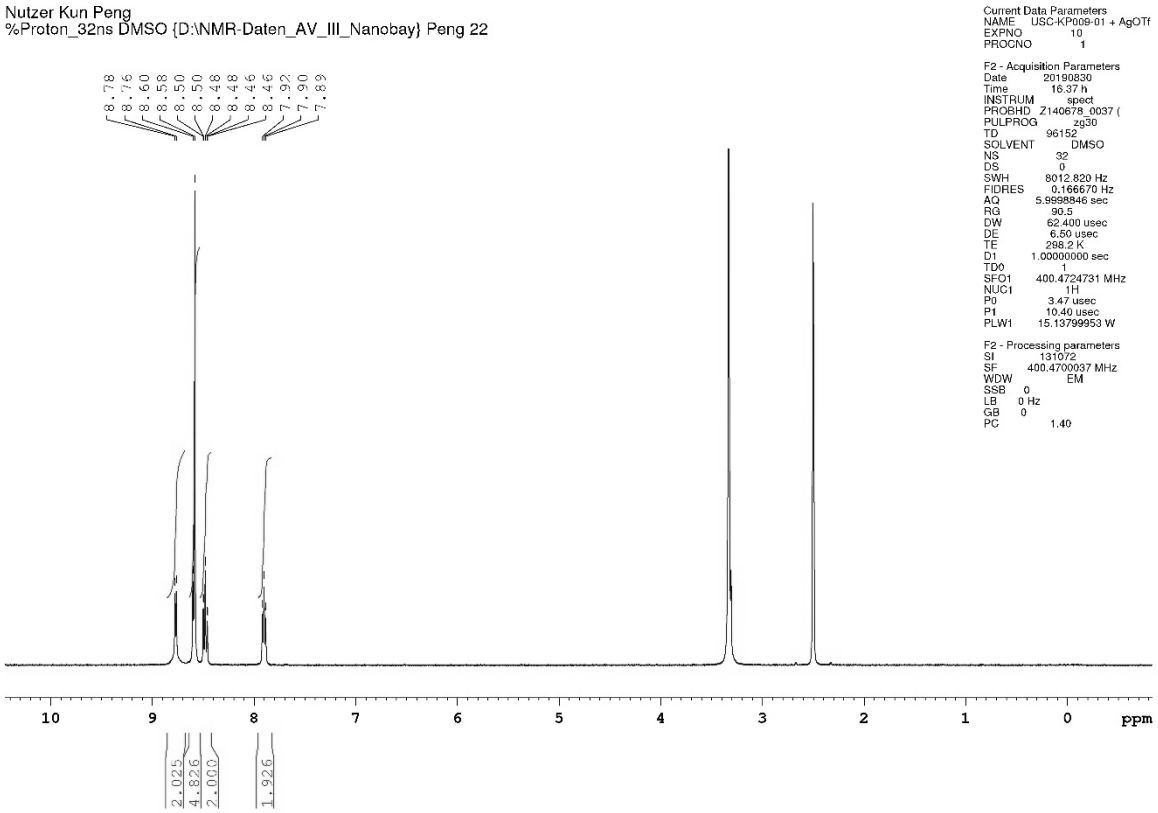
Nutzer Kun Peng
%Proton_32ns DMSO {D:\NMR-Daten_AV_III_Nanobay} Peng 22
8.78
8.76
8.60
8.58
8.50
8.50
8.48
8.48
8.46
8.46
7.92
7.90
7.89
Current Data Parameters
NAME USC-KP009-01 + AgOTf
EXPNO 10
PROCNO 1
F2 - Acquisition Parameters
Date 20190830
Time 16.37 h
INSTRUM spect
PROBHD Z140678_0037 (
PULPROG zg30
TD 96152
SOLVENT DMSO
NS 32
DS 0
SWH 8012.820 Hz
FIDRES 0.166670 Hz
AQ 5.9998846 sec
RG 90.5
DW 62.400 usec
DE 6.50 usec
TE 298.2 K
D1 1.00000000 sec
TD0 1
SFO1 400.4724731 MHz
NUC1 1H
P0 3.47 usec
P1 10.40 usec
PLW1 15.13799953 W
F2 - Processing parameters
SI 131072
SF 400.4700037 MHz
WDW EM
SSB 0
LB 0 Hz
GB 0
PC 1.40
10
9
8
7
6
5
4
3
2
1
0
ppm
2.025
4.826
2.000
1.926

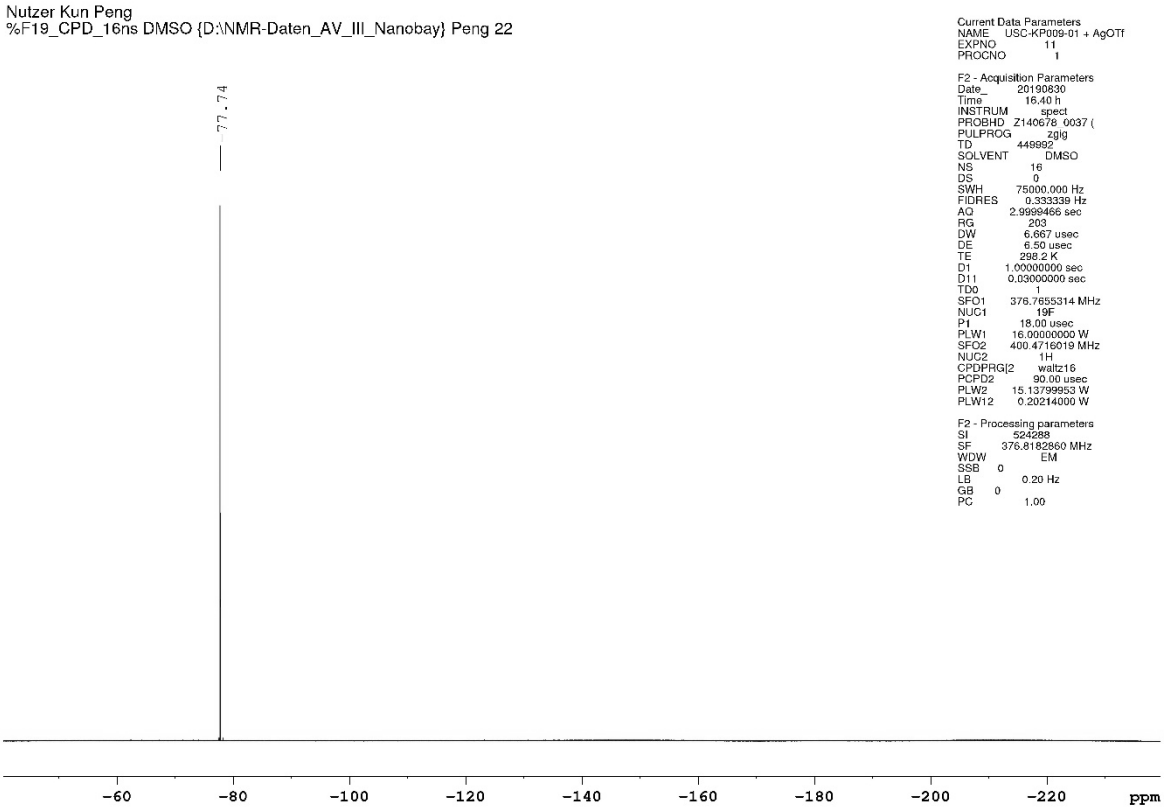
Nutzer Kun Peng
%F19_CPD_16ns DMSO {D:\NMR-Daten_AV_III_Nanobay} Peng 22
-77.74
Current Data Parameters
NAME USC-KP009-01 + AgOTf
EXPNO 11
PROCNO 1
F2 - Acquisition Parameters
Date_ 20190830
Time 16.40 h
INSTRUM spect
PROBHD Z140678 0037 (
PULPROG zgig
TD 449892
SOLVENT DMSO
NS 16
DS 0
SWH 75000.000 Hz
FIDRES 0.333339 Hz
AQ 2.9999466 sec
RG 203
DW 6.667 usec
DE 6.50 usec
TE 298.2 K
D1 1.00000000 sec
D11 0.03000000 sec
TD0 1
SFO1 376.7655314 MHz
NUC1 19F
P1 18.00 usec
PLW1 16.00000000 W
SFO2 400.4716019 MHz
NUC2 1H
CPDPRG[2 waltz16
PCPD2 90.00 usec
PLW2 15.13799953 W
PLW12 0.20214000 W
F2 - Processing parameters
SI 524288
SF 376.8182860 MHz
WDW EM
SSB 0
LB 0.20 Hz
GB 0
PC 1.00
-60
-80
-100
-120
-140
-160
-180
-200
-220
ppm

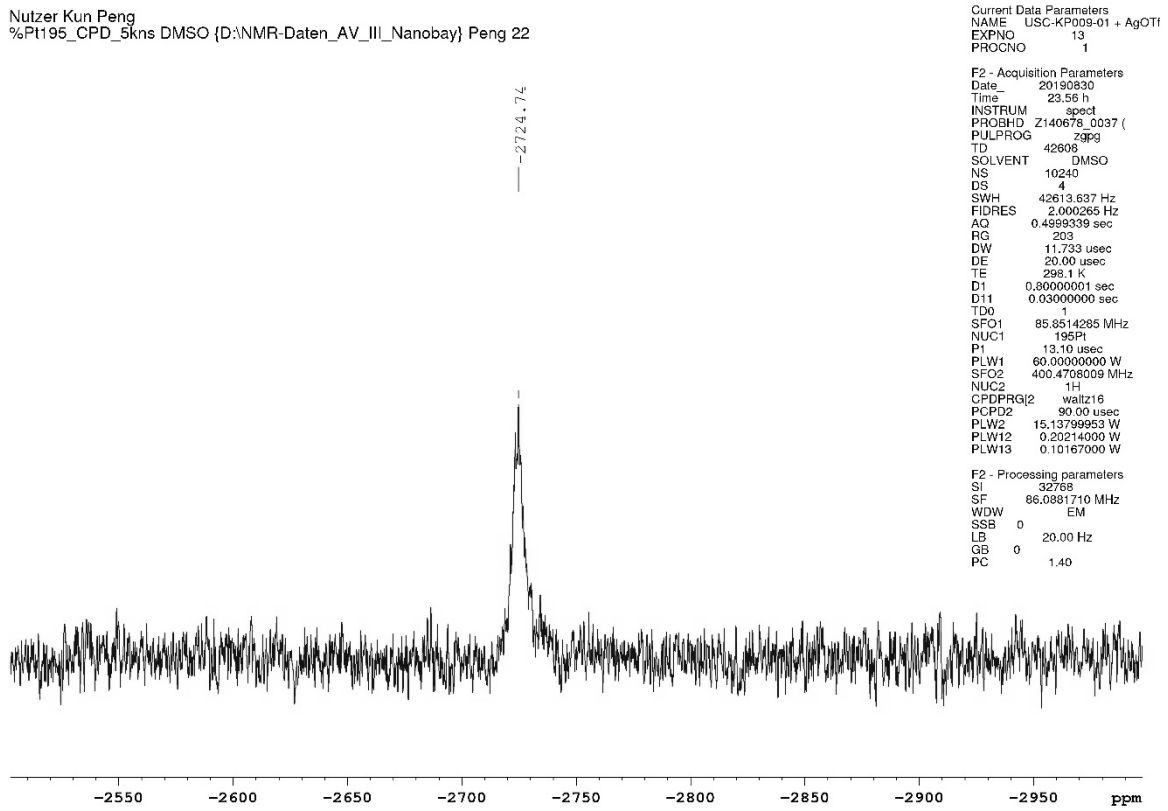

^{195}Pt NMR in DMSO-d_6

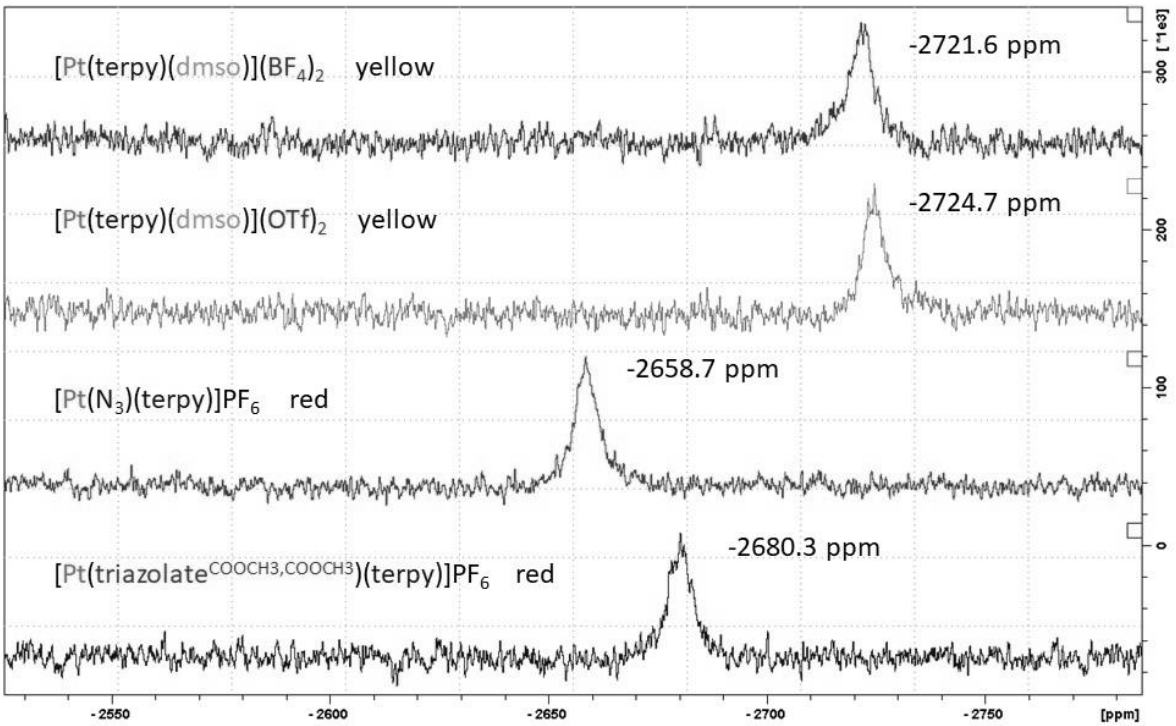

5.3.18 Systhesis of 6'-phenyl-2,2'-bipyridine (phbpy)

USC-KP130-12

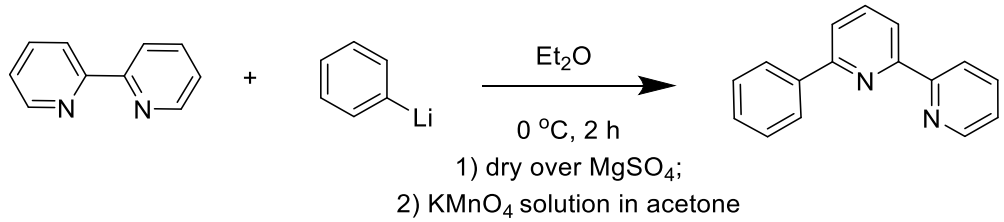

$C_{10}H_8N_2$ 156.19 g/mol

C_6H_5Li 84.05 g/mol

$C_{16}H_{12}N_2$ 232.29 g/mol

To a solution of 2,2'-bipyridine (1.56 g, 10 mmol) in anhydrous diethyl ether (15 mL) was added dropwise a 1.9 M solution of phenyl lithium (6 mL, 11.4 mmol) in dibutyl ether at 0 °C under argon. After 2 h, the deep red mixture was quenched by addition of water (30 mL). Then, the aqueous layer was extracted with diethyl ether (60 mL) and the combined orange organic phases were dried over magnesium sulphate. After filtration, the solvent was evaporated under reduced pressure and the remaining brown oil diluted with acetone (25 mL). A saturated solution of potassium permanganate in acetone (~2 mL) was added dropwise until the colour became dark brown. The resulting solution was filtered and the solvent evaporated. The resulting brown oil was purified by column chromatography on silica using diethyl ether/n-hexane (2:7 v/v) to obtain the product as a light yellow powder. Yield: 28% (653 mg, 28.1 mmol). **IR** (ATR): $\tilde{\nu}$ = 3066 (w), 1580 (m), 1563 (m), 1475 (m), 1453 (m), 1423 (s), 1155 (w), 1084 (w), 1022 (w), 755 (s) cm^{-1}; **^{1}H NMR** (400.47 MHz, $CDCl_3$): δ = 8.72 (ddd, 1H, $^3J_{H6,H5}$ = 4.8 Hz, $^4J_{H6,H4}$ = 1.7 Hz, $^5J_{H6,H3}$ = 0.8 Hz, H6), 8.67 (d, 1H, $^3J_{H3,H4}$ = 8.0 Hz, H3), 8.42 (d, 1H, $^3J_{H3',H4'}$ = 7.6 Hz, H3'), 8.17−8.14 (m, 2H, H2"/H6"), 7.93−7.86 (m, 2H, H4/H4'), 7.79 (dd, 1H, $^3J_{H5',H4'}$ = 7.8 Hz, $^4J_{H5',H3'}$ = 0.9 Hz, H5'), 7.54−7.49 (m, 2H, H3"/H5"), 7.47−7.42 (m, 1H, H4"), 7.36 (ddd, 1H, $^3J_{H5,H4}$ = 7.4 Hz, $^3J_{H5,H6}$ = 4.8 Hz, $^4J_{H5,H3}$ = 1.1 Hz, H5) ppm; **^{13}C NMR** (100.70 MHz, $CDCl_3$): δ = 156.70 (C2/C2'), 156.17 (C6'), 148.75 (C6), 139.41 (C4'), 137.95 (C4), 137.55 (C1"), 129.22 (C4"), 128.89 (C3"/C5"), 127.10 (C2"/C6"), 124.00 (C5), 121.72 (C3), 120.65 (C5'), 119.65 (C3') ppm; **MS** (ESI^+, CH_3OH): *m*/*z* = 233.1072 $[M+H]^+$; **Elemental analysis** (%) calcd. for $C_{16}H_{12}N_2$: C 82.73, H 5.21, N 12.06; found (%): C 82.43, H 5.29, N 11.90.

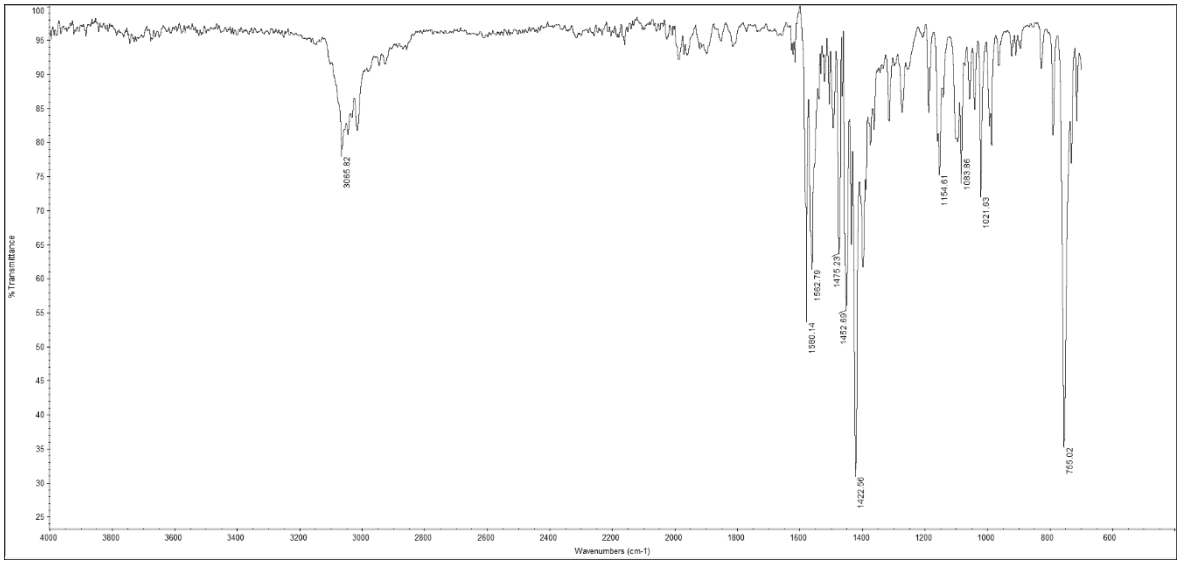
% Transmittance
Wavenumbers (cm-1)
3065.82
1580.14
1552.76
1475.23
1452.89
1422.96
1154.61
1083.86
1021.83
755.02

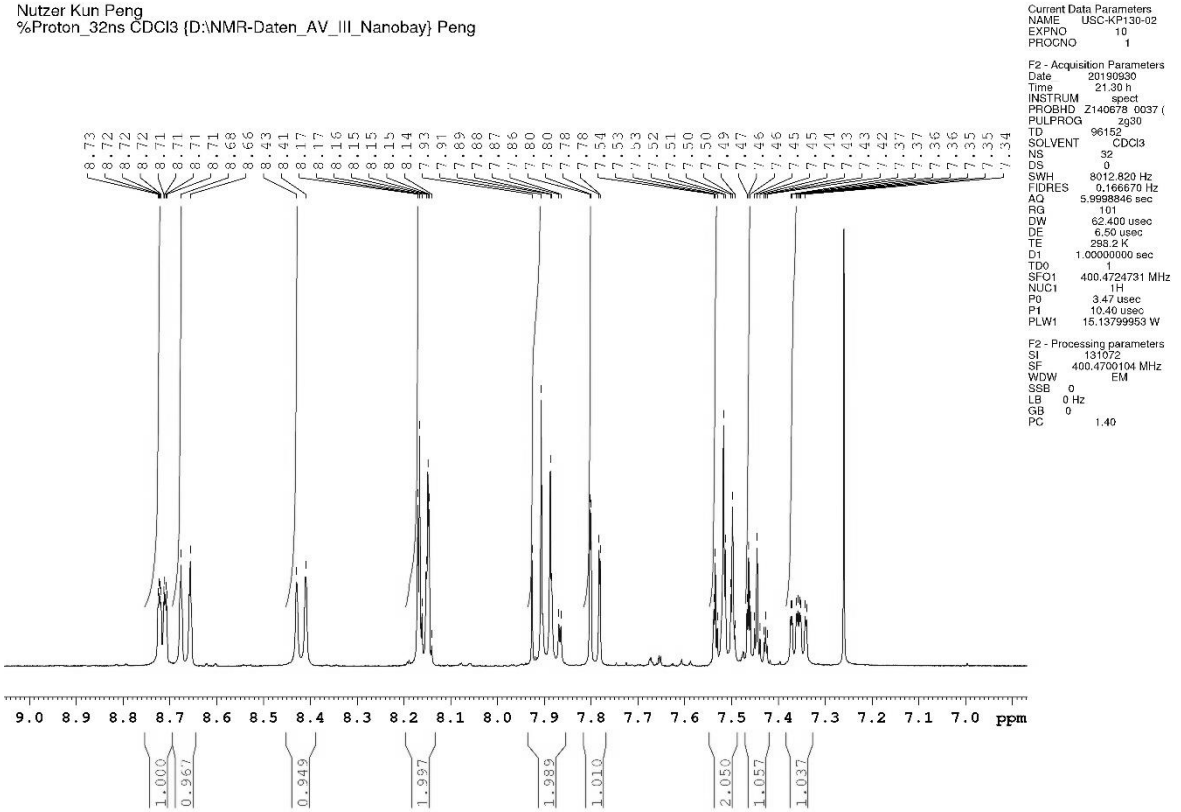
Nutzer Kun Peng
%Proton_32ns CDCl3 {D:\NMR-Daten_AV_III_Nanobay} Peng
Current Data Parameters
NAME USC-KP130-02
EXPNO 10
PROCNO 1
F2 - Acquisition Parameters
Date 20190530
Time 21.30 h
INSTRUM spect
PULPROG zg30
TD 96152
SOLVENT CDCl3
NS 32
DS 0
SWH 8012.820 Hz
FIDRES 0.166670 Hz
AQ 5.9998846 sec
RG 101
DW 62.400 usec
DE 6.50 usec
TE 298.2 K
D1 1.00000000 sec
TD0 1
SFO1 400.4724731 MHz
NUC1 1H
P0 3.47 usec
P1 10.40 usec
PLW1 15.13799953 W
F2 - Processing parameters
SI 131072
SF 400.4700104 MHz
WDW EM
SSB 0
LB 0 Hz
GB 0
PC 1.40
8.73 8.72 8.72 8.72 8.71 8.71 8.71 8.71 8.68 8.66 8.43 8.41 8.17 8.17 8.16 8.15 8.15 8.15 8.14 7.93 7.91 7.89 7.88 7.87 7.86 7.80 7.80 7.78 7.78 7.54 7.53 7.52 7.51 7.50 7.50 7.49 7.47 7.46 7.46 7.45 7.45 7.44 7.43 7.43 7.42 7.37 7.37 7.36 7.36 7.35 7.35 7.34
9.0 8.9 8.8 8.7 8.6 8.5 8.4 8.3 8.2 8.1 8.0 7.9 7.8 7.7 7.6 7.5 7.4 7.3 7.2 7.1 7.0 ppm
1.000 0.967 0.949 1.997 1.989 1.010 2.050 1.057 1.037

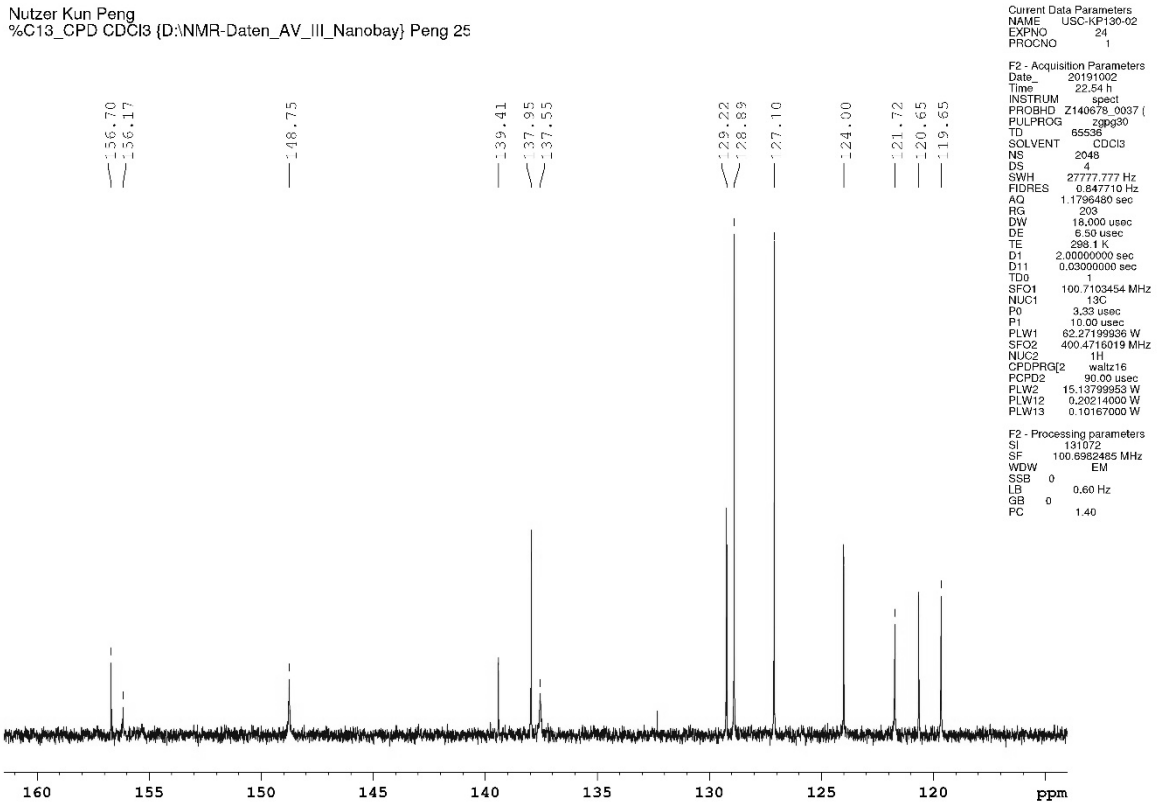
Nutzer Kun Peng
%C13_CPD CDCl3 {D:\NMR-Daten_AV_III_Nanobay} Peng 25
156.70
156.17
148.75
139.41
137.95
137.55
129.22
128.89
127.10
124.00
121.72
120.65
119.65
Current Data Parameters
NAME USC-KP130-02
EXPNO 24
PROCNO 1
F2 - Acquisition Parameters
Date_ 20191002
Time 22.54 h
INSTRUM spect
PROBHD Z140678_0037 (
PULPROG zgpg30
TD 65536
SOLVENT CDCl3
NS 2048
DS 4
SWH 27777.777 Hz
FIDRES 0.847710 Hz
AQ 1.1796480 sec
RG 203
DW 18.000 usec
DE 6.50 usec
TE 298.1 K
D1 2.00000000 sec
D11 0.03000000 sec
TD0 1
SFO1 100.7103454 MHz
NUC1 13C
P0 3.33 usec
P1 10.00 usec
PLW1 62.27199936 W
SFO2 400.4716019 MHz
NUC2 1H
CPDPRG[2 waltz16
PCPD2 90.00 usec
PLW2 15.13799953 W
PLW12 0.20214000 W
PLW13 0.10167000 W
F2 - Processing parameters
SI 131072
SF 100.6982485 MHz
WDW EM
SSB 0
LB 0.60 Hz
GB 0
PC 1.40
160
155
150
145
140
135
130
125
120
ppm

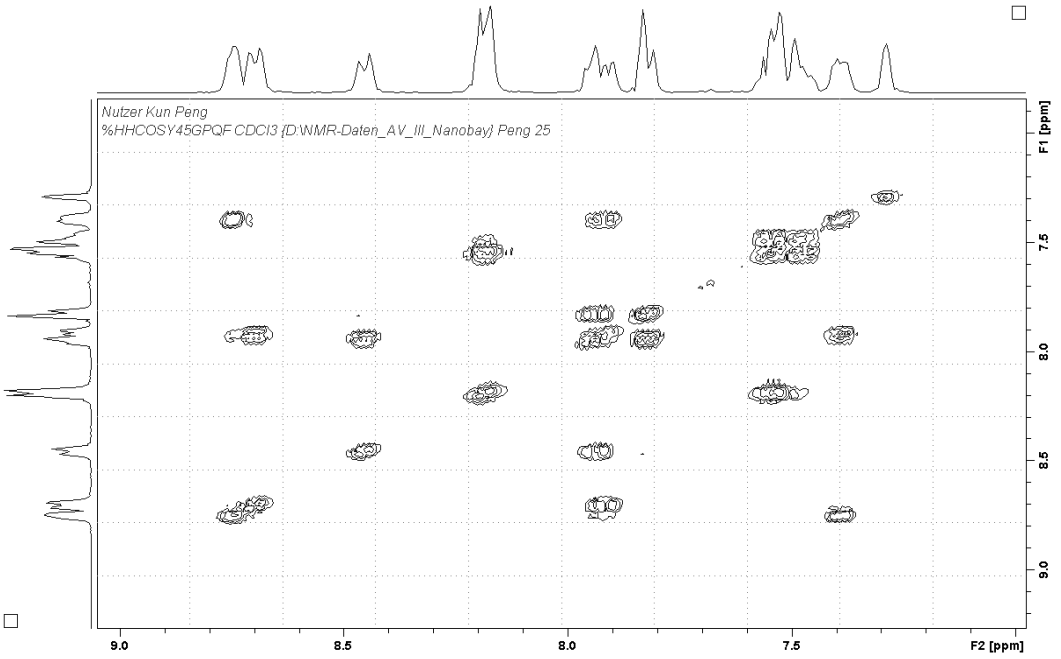
Nutzer Kun Peng
%HHCOSY45GPQF CDCl3 {D:\NMR-Daten_AV_III_Nanobay} Peng 25
F1 [ppm]
9.0
8.5
8.0
7.5
F2 [ppm]

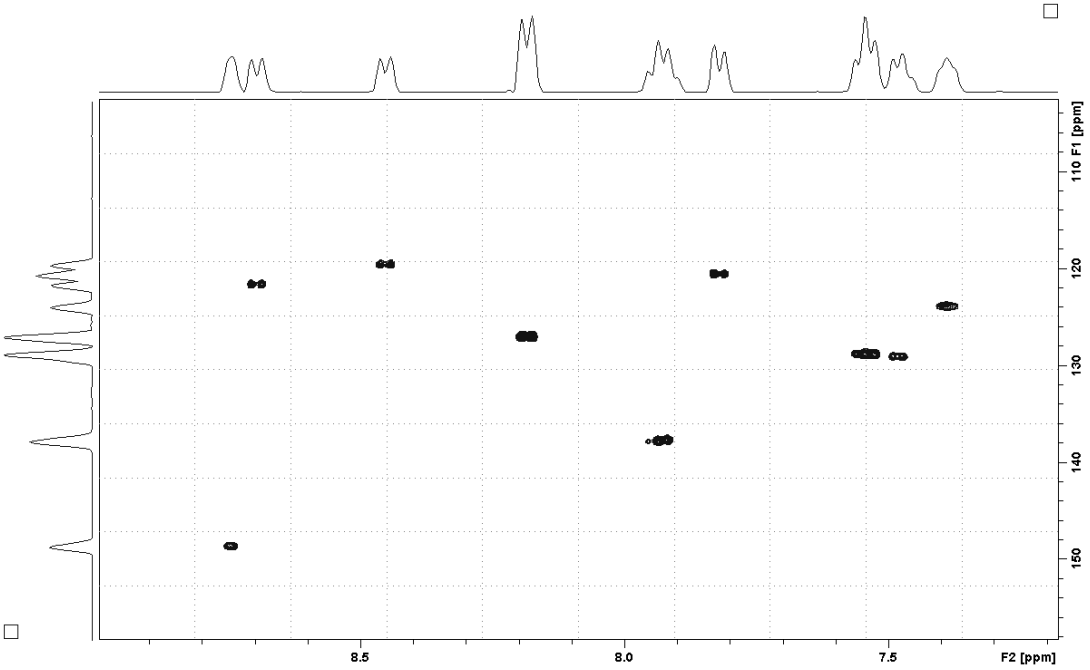
110 F1 [ppm]
120
130
140
150
8.5
8.0
7.5
F2 [ppm]

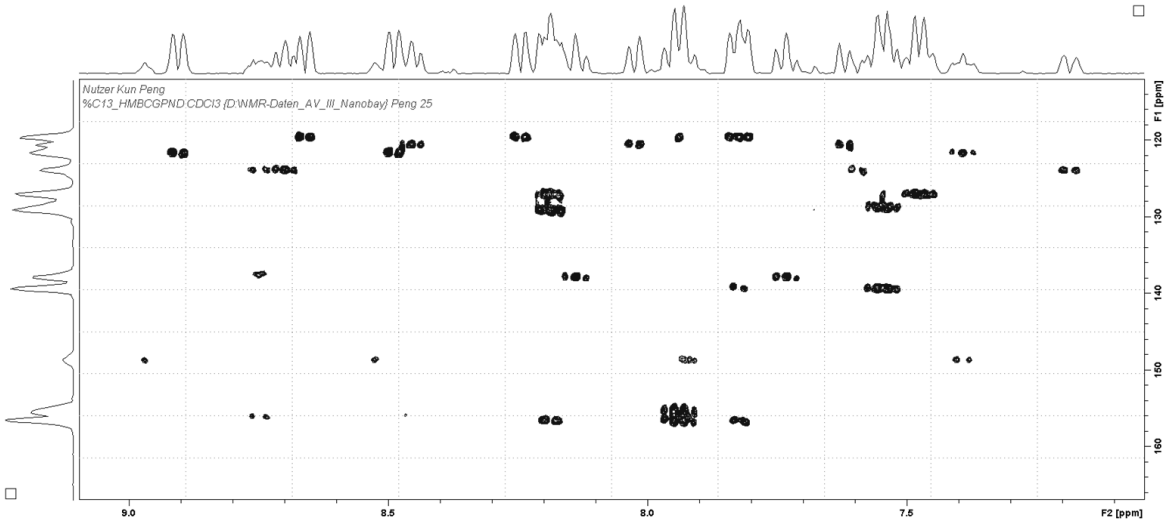
Nutzer Kun Peng
%C13_HMBCGPND CDCl3 {D:\NMR-Daten_AV_III_Nanobay} Peng 25
F1 [ppm]
120
130
140
150
160
9.0
8.5
8.0
7.5
F2 [ppm]

5.3.19 Synthesis of [PdCl(phbpy)]

USC-KP131-02

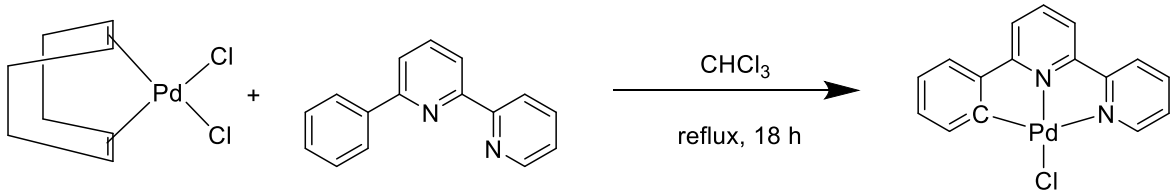

$C_8H_{12}Cl_2Pd$
285.51 g/mol

$C_{16}H_{12}N_2$
232.29 g/mol

$C_{16}H_{11}ClN_2Pd$
373.14 g/mol

In a round bottom flask, [PdCl(cod)]Cl (116.0 mg, 0.41 mmol) and 6'-phenyl-2,2'-bipyridine (98.1 mg, 0,42 mmol) were dissolved in chloroform (40 mL). The clear yellow solution was heated to reflux for 18 h to give a yellow suspension. Then, the solvent was removed to give a light yellow solid, which was washed with diethyl ether (2 × 20 mL) and dried under vacuum for 3 d. Yield: 95% (144.5 mg, 0.39 mmol). **IR** (ATR): $\tilde{\nu}$ = 3050 (w), 1598 (s), 1493 (m), 1462 (m), 1427 (m), 1304 (m), 1012 (w), 751 (s) cm^{-1}; **^{1}H NMR** (400.47 MHz, DMSO-d_6): δ = 8.63 (d, 1H, $^3J_{H6,H5}$ = 5.0 Hz, H6), 8.49 (d, 1H, $^3J_{H3,H4}$ = 8.0 Hz, H3), 8.27−8.21 (m, 2H, H3'/H4), 8.15 (t, 1H, $^3J_{H4',H3'/H5'}$ = 7.9 Hz, H4'), 8.00 (d, 1H, $^3J_{H5',H4'}$ = 8.0 Hz, H5'), 7.78 (ddd, 1H, $^3J_{H5,H4}$ = 7.6 Hz, $^3J_{H5,H6}$ = 5.3 Hz, $^4J_{H5,H3}$ = 0.9 Hz, H5), 7.64−7.62 (m, 1H, H2"), 7.53−7.51 (m, 1H, H5"), 7.12−7.05 (m, 2H, H3"/H4") ppm; **^{13}C NMR** (100.70 MHz, DMSO-d_6): δ = 163.62 (C6'), 155.22 (C2), 154.16 (C1"), 153.59 (C2'), 149.09 (C6), 148.09 (C6"), 140.50 (C4), 140.24 (C4'), 136.19 (C5"), 129.68 (C4"), 127.53 (C5), 124.77 (C3"), 124.67 (C2"), 123.23 (C3), 119.96 (C5'), 119.87 (C3') ppm; **Elemental analysis** (%) calcd. for $C_{16}H_{11}ClN_2Pd$: C 51.50, H 2.97, N 7.51; found (%): C 51.30, H 3.04, N 7.38.

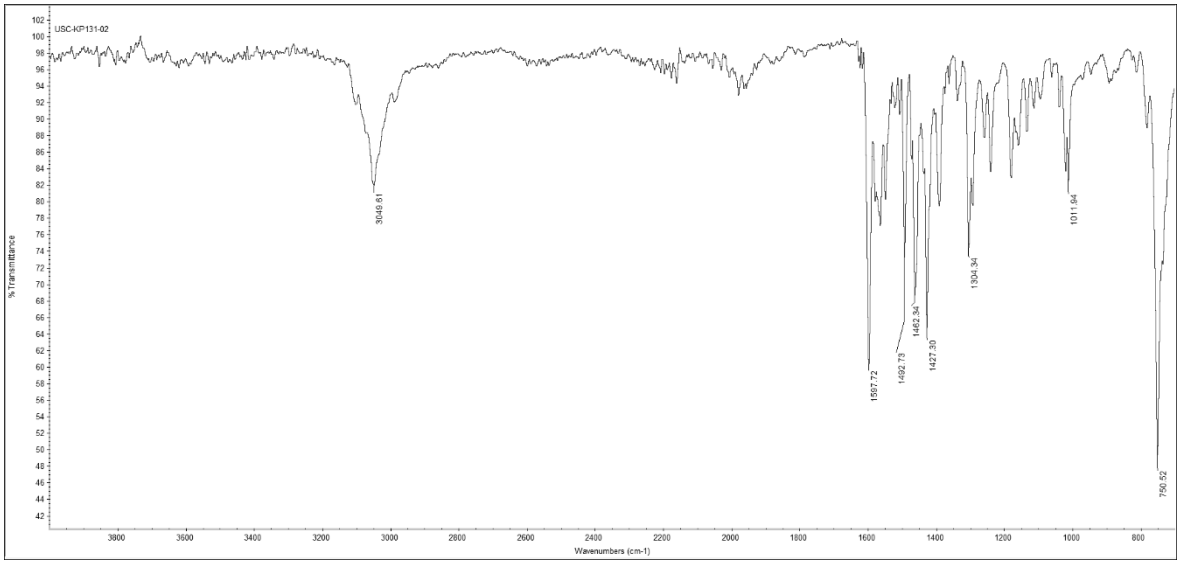
USC-KP131-02
% Transmittance
Wavenumbers (cm-1)
3049.61
1597.72
1492.73
1462.34
1427.30
1304.34
1011.94
750.52

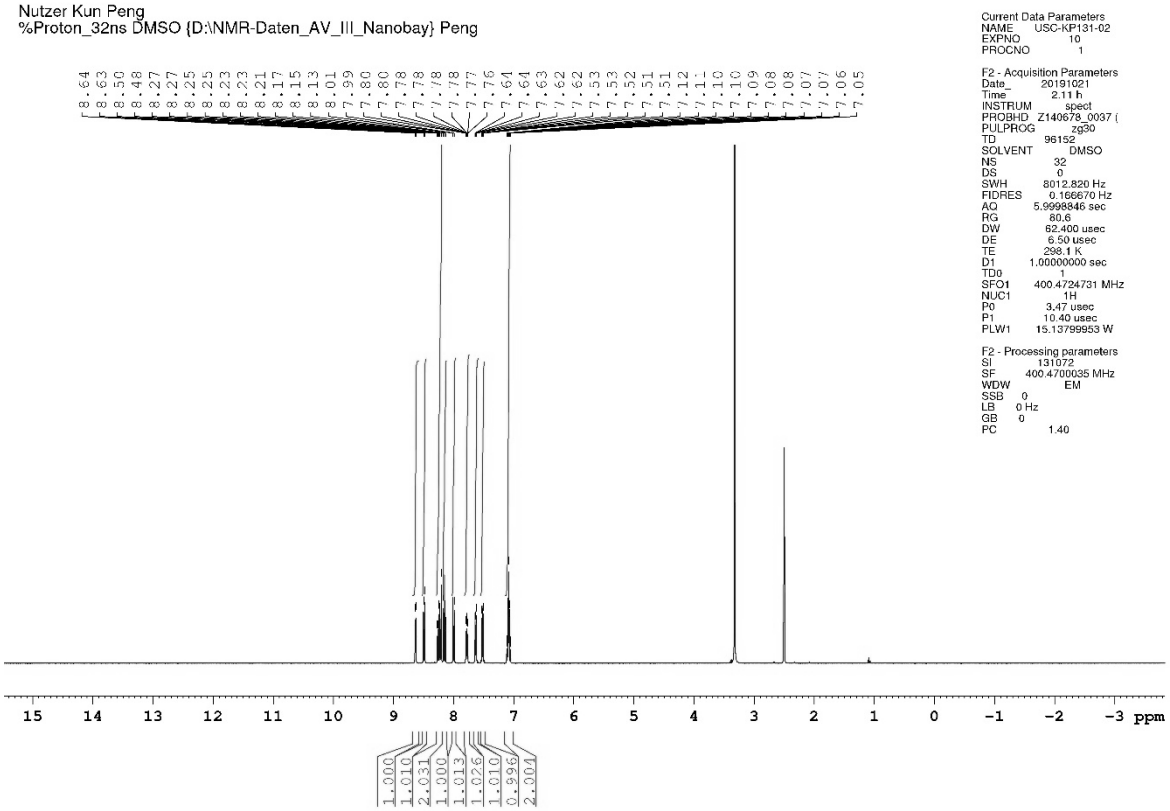
Nutzer Kun Peng
%Proton_32ns DMSO {D:\NMR-Daten_AV_III_Nanobay} Peng
Current Data Parameters
NAME USC-KP131-02
EXPNO 10
PROCNO 1
F2 - Acquisition Parameters
Date_ 20191021
Time 2.11 h
INSTRUM spect
PROBHD Z140679_0037 (
PULPROG zg30
TD 96152
SOLVENT DMSO
NS 32
DS 0
SWH 8012.820 Hz
FIDRES 0.166670 Hz
AQ 5.9998846 sec
RG 80.6
DW 62.400 usec
DE 6.50 usec
TE 298.1 K
D1 1.00000000 sec
TD0 1
SFO1 400.4724731 MHz
NUC1 1H
P0 3.47 usec
P1 10.40 usec
PLW1 15.13799953 W
F2 - Processing parameters
SI 131072
SF 400.4700035 MHz
WDW EM
SSB 0
LB 0 Hz
GB 0
PC 1.40
ppm

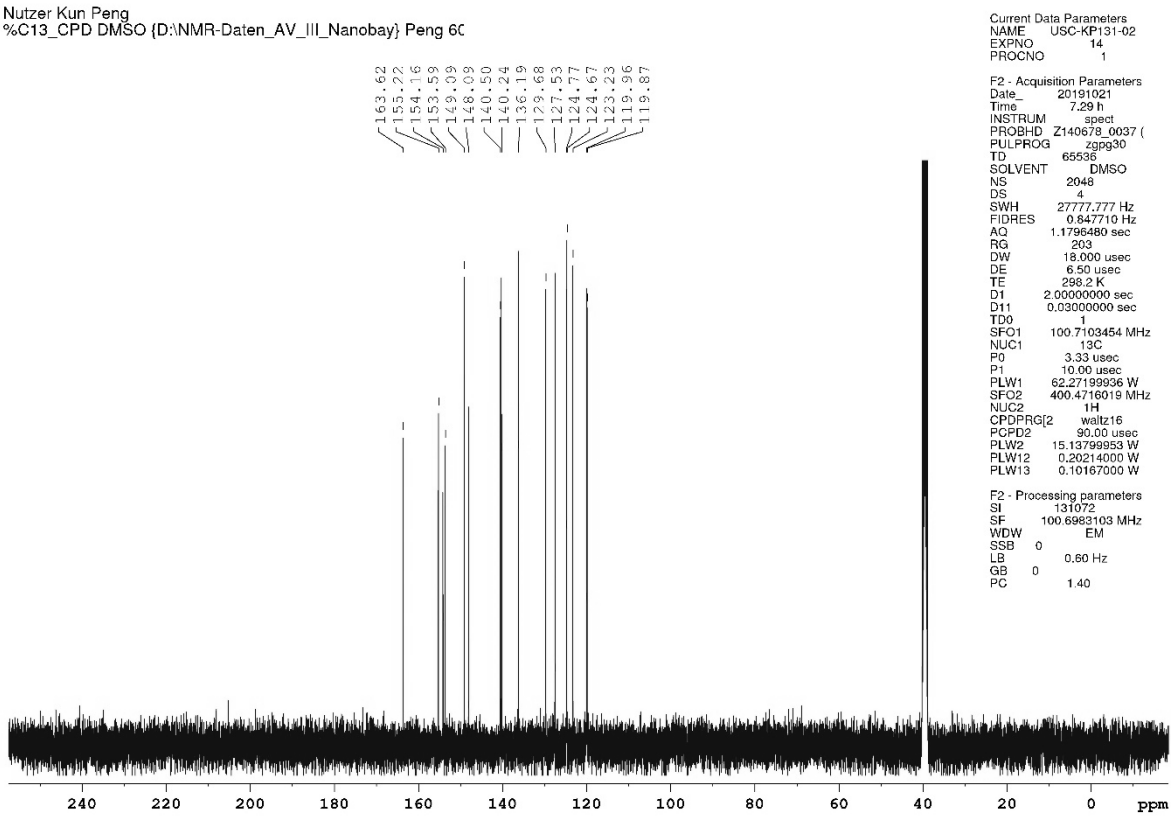
Nutzer Kun Peng
%C13_CPD DMSO {D:\NMR-Daten_AV_III_Nanobay} Peng 60
163.62
155.22
154.16
153.59
149.09
148.09
140.50
140.24
136.19
123.68
127.53
124.77
124.67
123.23
119.96
119.87
Current Data Parameters
NAME USC-KP131-02
EXPNO 14
PROCNO 1
F2 - Acquisition Parameters
Date_ 20191021
Time 7.29 h
INSTRUM spect
PROBHD Z140678_0037 (
PULPROG zgpg30
TD 65536
SOLVENT DMSO
NS 2048
DS 4
SWH 27777.777 Hz
FIDRES 0.847710 Hz
AQ 1.1796480 sec
RG 203
DW 18.000 usec
DE 6.50 usec
TE 298.2 K
D1 2.00000000 sec
D11 0.03000000 sec
TD0 1
SFO1 100.7103454 MHz
NUC1 13C
P0 3.33 usec
P1 10.00 usec
PLW1 62.27199936 W
SFO2 400.4716019 MHz
NUC2 1H
CPDPRG[2 waltz16
PCPD2 90.00 usec
PLW2 15.13799953 W
PLW12 0.20214000 W
PLW13 0.10167000 W
F2 - Processing parameters
SI 131072
SF 100.6983103 MHz
WDW EM
SSB 0
LB 0.60 Hz
GB 0
PC 1.40
240
220
200
180
160
140
120
100
80
60
40
20
0
ppm

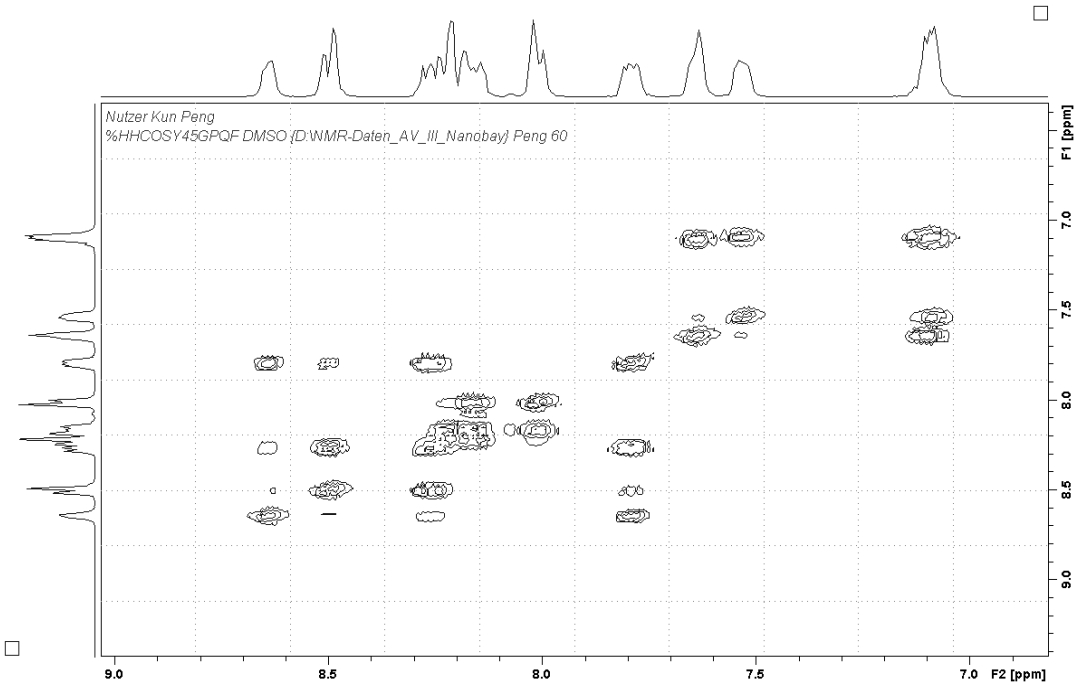
Nutzer Kun Peng
%HHCOSY45GPQF DMSO {D:\NMR-Daten_AV_III_Nanobay} Peng 60
F1 [ppm]
7.0
7.5
8.0
8.5
9.0
9.0
8.5
8.0
7.5
7.0 F2 [ppm]

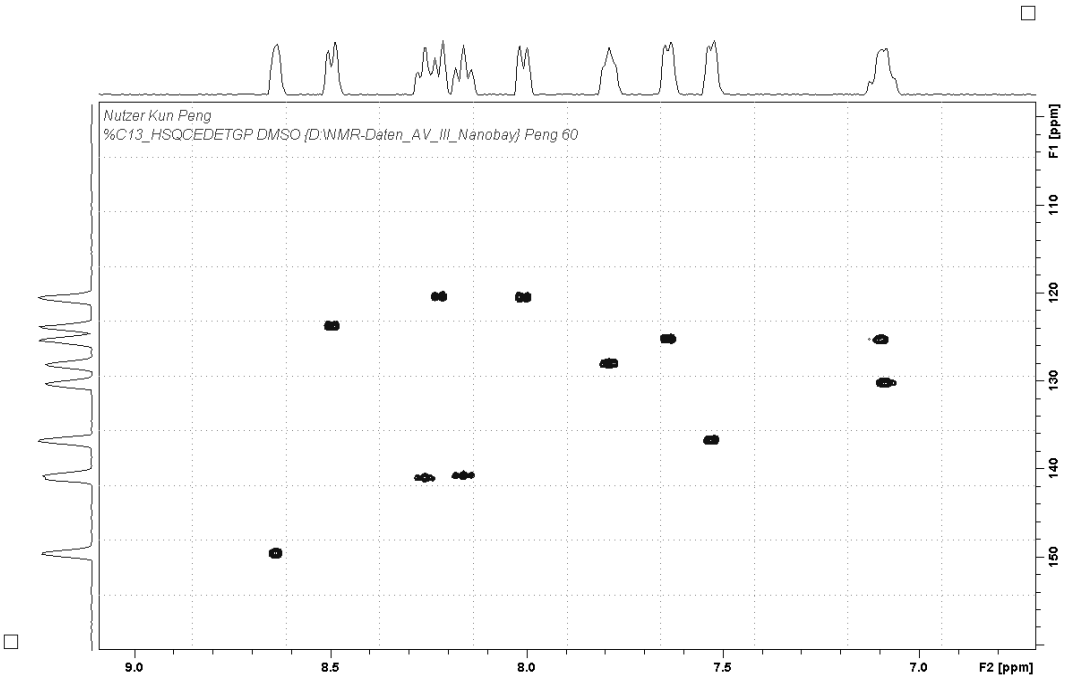
Nutzer Kun Peng
%C13_HSQCEDETGP DMSO {D:\NMR-Daten_AV_III_Nanobay} Peng 60
F1 [ppm]
110
120
130
140
150
9.0
8.5
8.0
7.5
7.0
F2 [ppm]

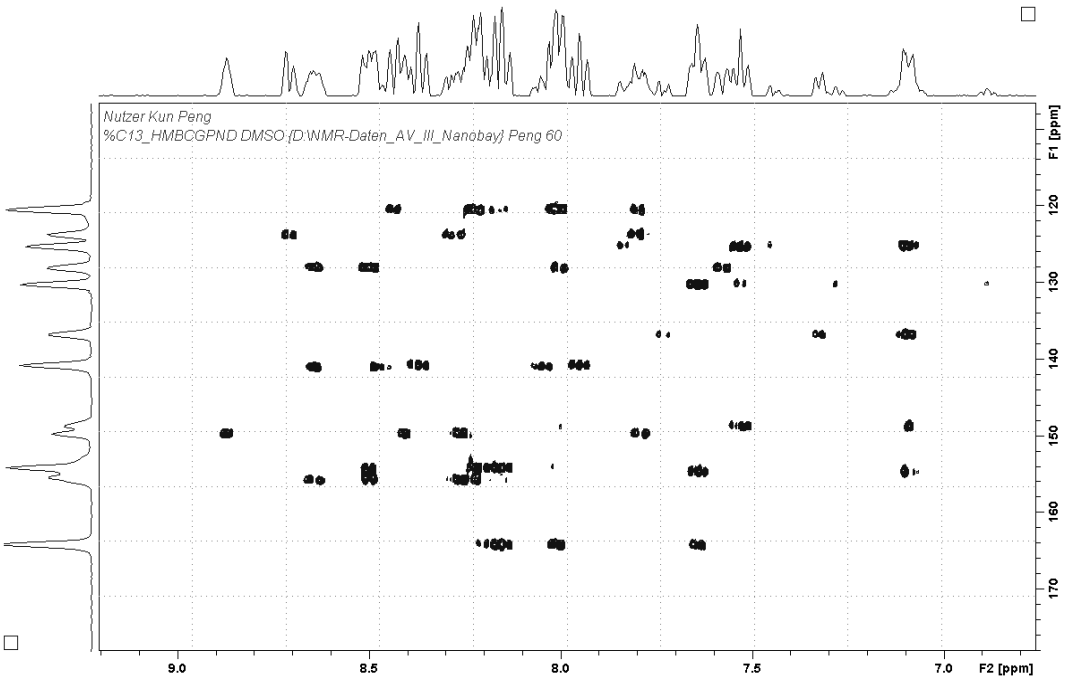
Nutzer Kun Peng
%C13_HMBCGPND DMSO {D:\NMR-Daten_AV_III_Nanobay} Peng 60
F1 [ppm]
120
130
140
150
160
170
9.0
8.5
8.0
7.5
7.0
F2 [ppm]

5.3.20 Synthesis of [PtCl(phbpy)]

USC-KP133-02

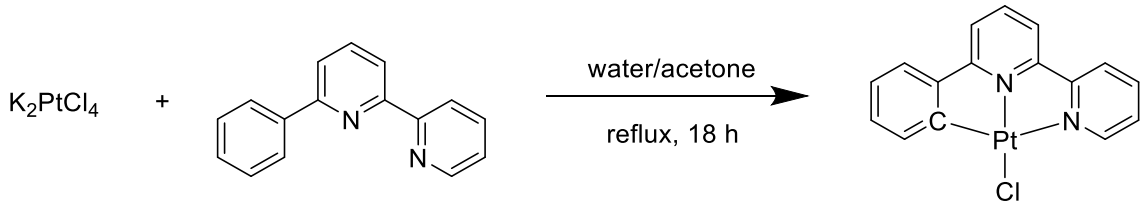

Cl_4K_2Pt	$C_{16}H_{12}N_2$	$C_{16}H_{11}ClN_2Pt$
415.08 g/mol	232.29 g/mol	461.80 g/mol

In a round bottom flask, potassium tetrachloroplatinate(II) (103.4 mg, 0.25 mmol) was dissolved in water (10 mL). Then, 6'-phenyl-2,2'-bipyridine (60.2 mg, 0.26 mmol) in acetone (10 mL) was added to the clear red solution. The mixture was heated to reflux for 18 h, during which an orange solid precipitated out. Then, the solvent was partially removed under reduced pressure and the resulting orange solid filtered off, washed with water (2 × 5 mL) and diethyl ether (3 × 8 mL), and dried under vacuum for 5 d. Yield: 80% (93.1 mg, 0.20 mmol). **IR** (ATR): $\tilde{\nu}$ = 3051 (w), 1601 (m), 1581 (w), 1492 (w), 1458 (w), 1430 (m), 1389 (m), 1300 (w), 1181 (w), 750 (s) cm^{-1}; **^{1}H NMR** (400.47 MHz, DMSO-d_6): δ = 8.89 (d, 1H, $^3J_{H6,H5}$ = 4.5 Hz, H6), 8.49 (d, 1H, $^3J_{H3,H4}$ = 8.0 Hz, H3), 8.33 (t, 1H, $^3J_{H4,H3/H5}$ = 7.4 Hz, H4), 8.17−8.09 (m, 2H, H3'/H4'), 7.94−7.89 (m, 2H, H5/H5'), 7.59 (d, 1H, $^3J_{H2",H3"}$ = 7.4 Hz, H2"), 7.49 (d, 1H, $^3J_{H5",H4"}$ = 7.1 Hz, H5"), 7.15 (t, 1H, $^3J_{H4",H3"/H5"}$ = 7.1 Hz, H4"), 7.07 (t, 1H, $^3J_{H3",H2"/H4"}$ = 7.4 Hz, H3") ppm; **^{13}C NMR** (100.70 MHz, DMSO-d_6): δ = 165.29 (C6'), 156.70 (C1), 154.32 (C2'), 148.17 (C6), 146.91 (C6"), 142.43 (C1"), 140.58 (C4), 139.69 (C4'), 134.27 (C5"), 130.32 (C4"), 128.31 (C5), 124.91 (C2"), 123.91 (C3/C3"), 119.49 (C5'), 119.41 (C3') ppm; ^{195}Pt NMR (86.09 MHz, DMSO-d_6): δ = -3471 ppm; **Elemental analysis** (%) calcd. for $C_{16}H_{11}ClN_2Pt$: C 41.61, H 2.40, N 6.07; found (%): C 41.33, H 2.50, N 5.98.

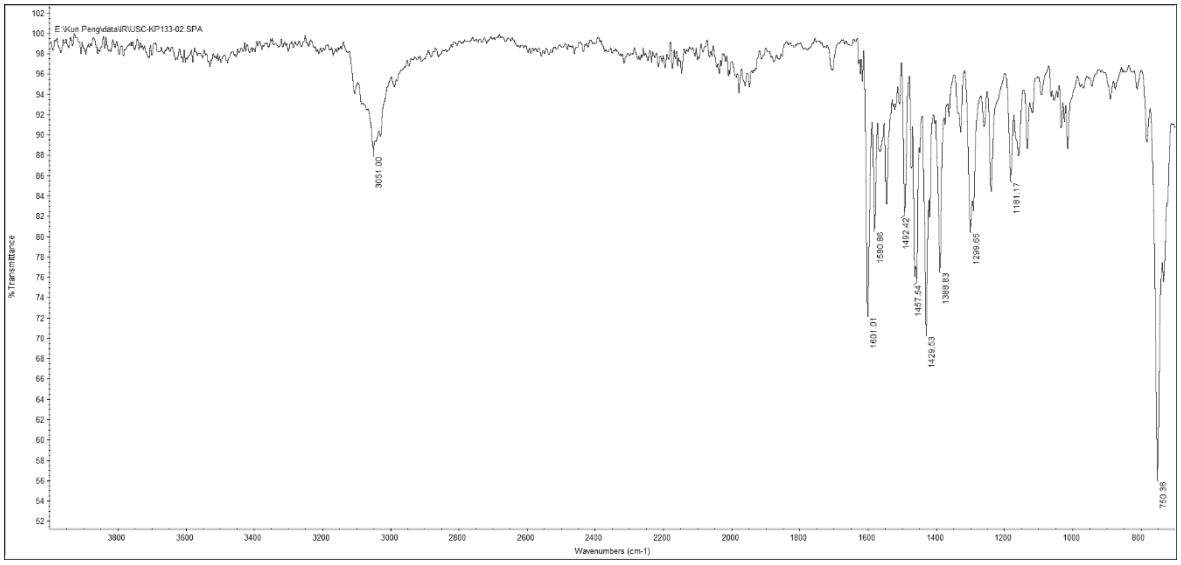
E:\Kun Peng\data\IR\USC-KP133-02.SPA
% Transmittance
Wavenumbers (cm-1)
3051.00
1631.01
1580.86
1492.42
1457.54
1429.53
1389.83
1299.65
1181.17
750.96

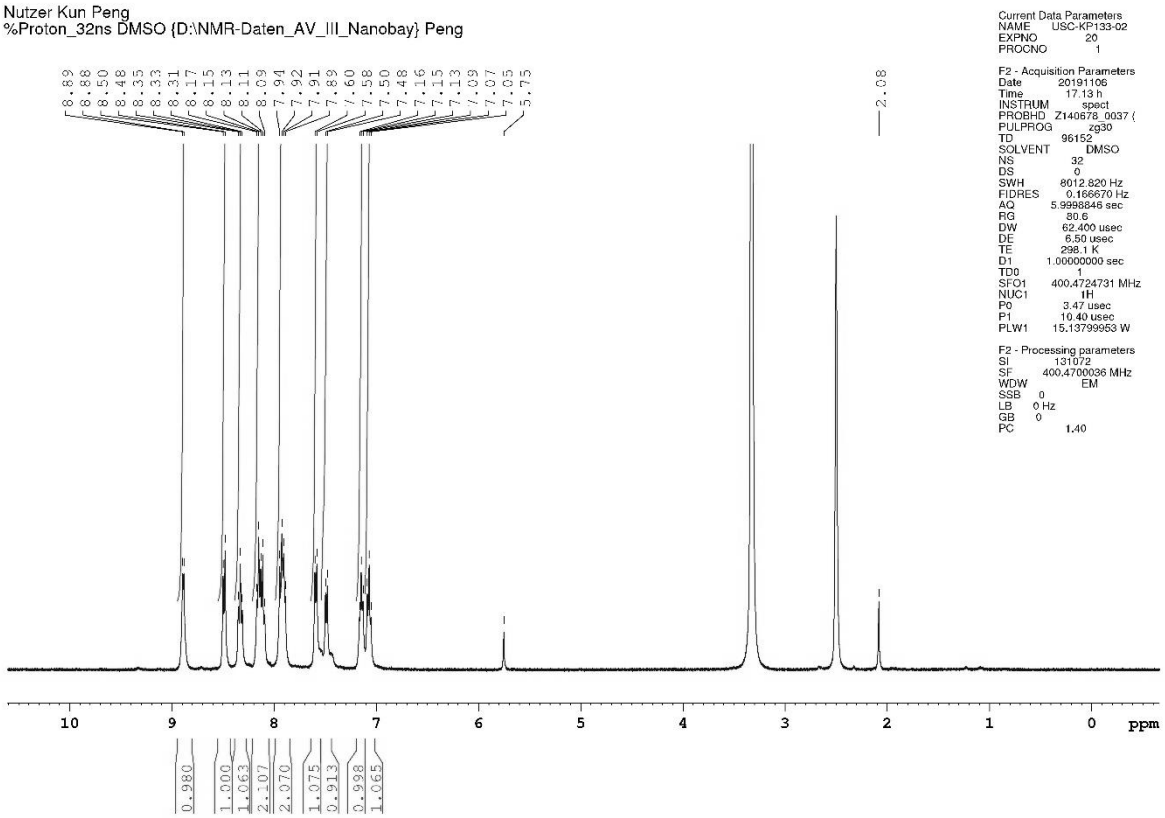
Nutzer Kun Peng
%Proton_32ns DMSO {D:\NMR-Daten_AV_III_Nanobay} Peng
8.89
8.88
8.50
8.48
8.35
8.33
8.31
8.17
8.15
8.13
8.11
8.09
7.94
7.92
7.91
7.89
7.60
7.58
7.50
7.48
7.16
7.15
7.13
7.09
7.07
7.05
5.75
2.08
Current Data Parameters
NAME USC-KP133-02
EXPNO 20
PROCNO 1
F2 - Acquisition Parameters
Date 20191106
Time 17.13 h
INSTRUM spect
PROBHD Z140678_0037 (
PULPROG zg30
TD 96152
SOLVENT DMSO
NS 32
DS 0
SWH 8012.820 Hz
FIDRES 0.166670 Hz
AQ 5.9998846 sec
RG 80.6
DW 62.400 usec
DE 6.50 usec
TE 298.1 K
D1 1.00000000 sec
TD0 1
SFO1 400.4724731 MHz
NUC1 1H
P0 3.47 usec
P1 10.40 usec
PLW1 15.13799953 W
F2 - Processing parameters
SI 131072
SF 400.4700036 MHz
WDW EM
SSB 0
LB 0 Hz
GB 0
PC 1.40
10
9
8
7
6
5
4
3
2
1
0
ppm
0.980
1.000
1.063
2.107
2.070
1.075
0.913
0.998
1.065

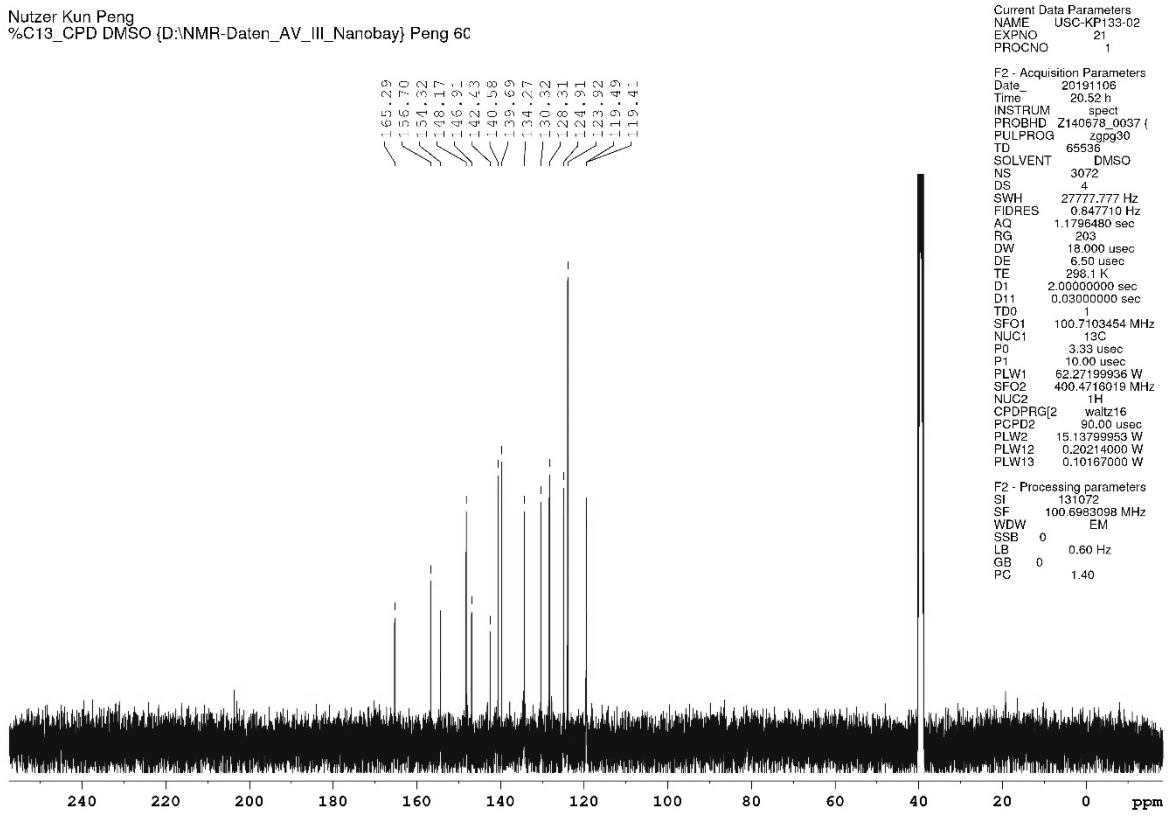
Nutzer Kun Peng
%C13_CPD DMSO {D:\NMR-Daten_AV_III_Nanobay} Peng 60
165.29
156.70
154.32
148.17
146.91
142.43
140.58
139.69
134.27
130.32
128.31
124.91
123.92
119.49
Current Data Parameters
NAME USC-KP133-02
EXPNO 21
PROCNO 1
F2 - Acquisition Parameters
Date_ 20191106
Time 20.52 h
INSTRUM spect
PROBHD Z140678_0037 (
PULPROG zgpg30
TD 65536
SOLVENT DMSO
NS 3072
DS 4
SWH 27777.777 Hz
FIDRES 0.847710 Hz
AQ 1.1796480 sec
RG 203
DW 18.000 usec
DE 6.50 usec
TE 298.1 K
D1 2.00000000 sec
D11 0.03000000 sec
TD0 1
SFO1 100.7103454 MHz
NUC1 13C
P0 3.33 usec
P1 10.00 usec
PLW1 62.27199936 W
SFO2 400.4716019 MHz
NUC2 1H
CPDPRG[2 waltz16
PCPD2 90.00 usec
PLW2 15.13799953 W
PLW12 0.20214000 W
PLW13 0.10167000 W
F2 - Processing parameters
SI 131072
SF 100.6983098 MHz
WDW EM
SSB 0
LB 0.60 Hz
GB 0
PC 1.40
240
220
200
180
160
140
120
100
80
60
40
20
0
ppm

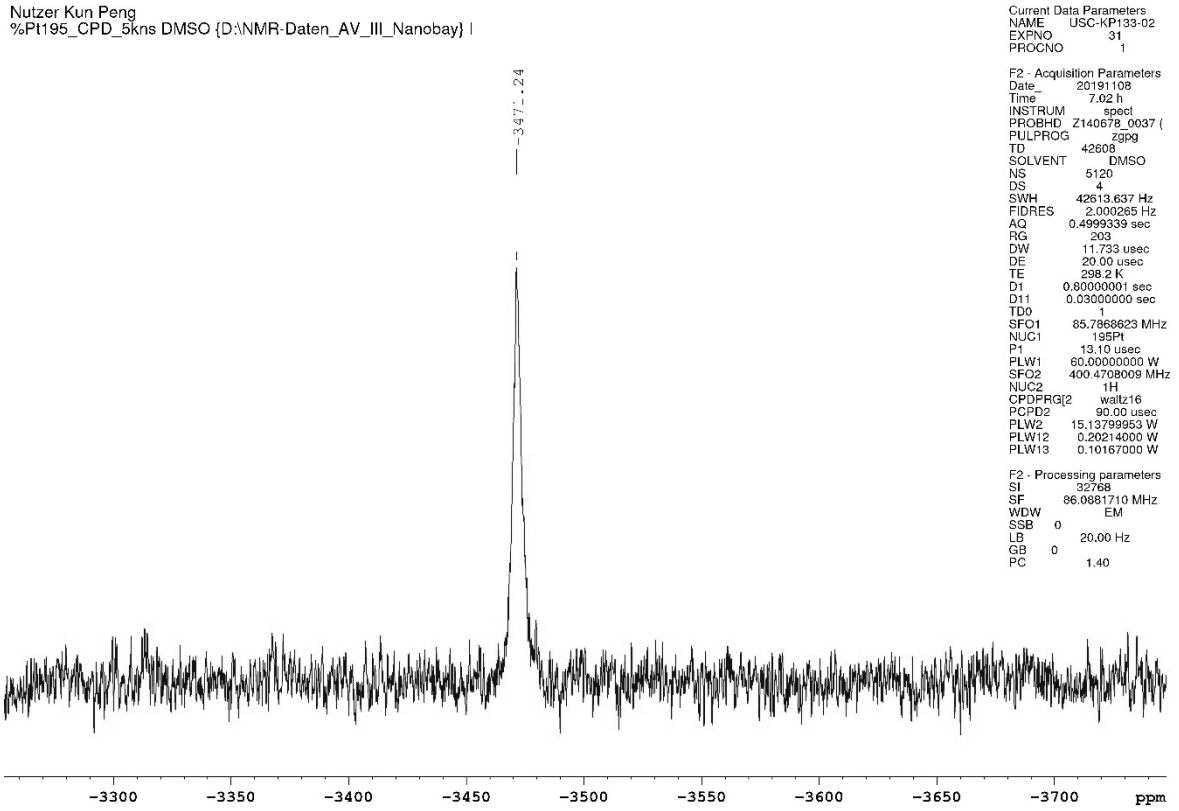
Nutzer Kun Peng
%Pt195_CPD_5kns DMSO {D:\NMR-Daten_AV_III_Nanobay} I
-3477.24
Current Data Parameters
NAME USC-KP133-02
EXPNO 31
PROCNO 1
F2 - Acquisition Parameters
Date_ 20191108
Time 7.02 h
INSTRUM spect
PROBHD Z140678_0037 (
PULPROG zgpg
TD 42608
SOLVENT DMSO
NS 5120
DS 4
SWH 42613.637 Hz
FIDRES 2.000265 Hz
AQ 0.4999339 sec
RG 203
DW 11.733 usec
DE 20.00 usec
TE 298.2 K
D1 0.80000001 sec
D11 0.03000000 sec
TD0 1
SFO1 85.7868623 MHz
NUC1 195Pt
P1 13.10 usec
PLW1 60.00000000 W
SFO2 400.4708009 MHz
NUC2 1H
CPDPRG[2 waltz16
PCPD2 90.00 usec
PLW2 15.13799953 W
PLW12 0.20214000 W
PLW13 0.10167000 W
F2 - Processing parameters
SI 32768
SF 86.0881710 MHz
WDW EM
SSB 0
LB 20.00 Hz
GB 0
PC 1.40
-3300
-3350
-3400
-3450
-3500
-3550
-3600
-3650
-3700
ppm

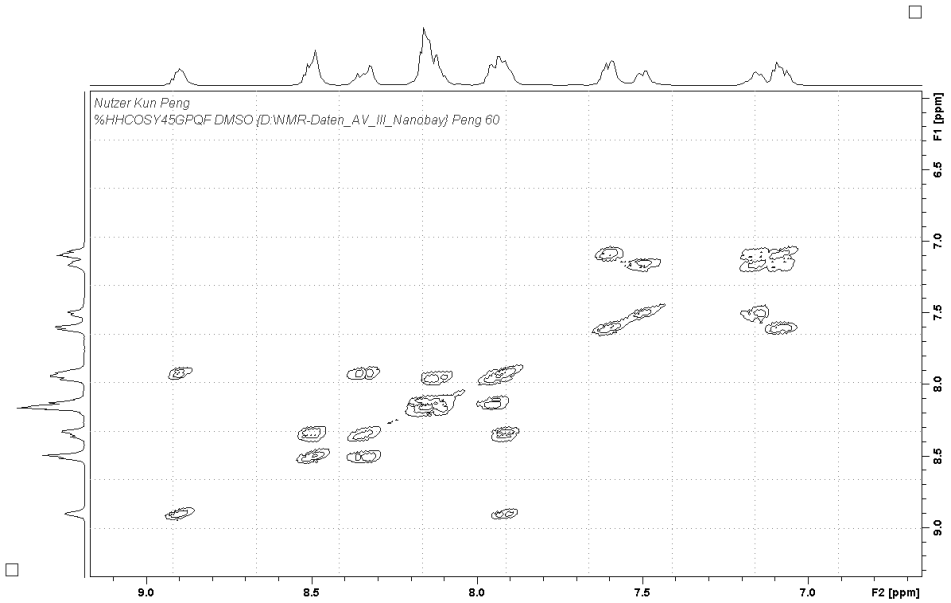
Nutzer Kun Peng
%HHCOSY45GPQF DMSO {D:\NMR-Daten_AV_III_Nanobay} Peng 60
F1 [ppm]
F2 [ppm]

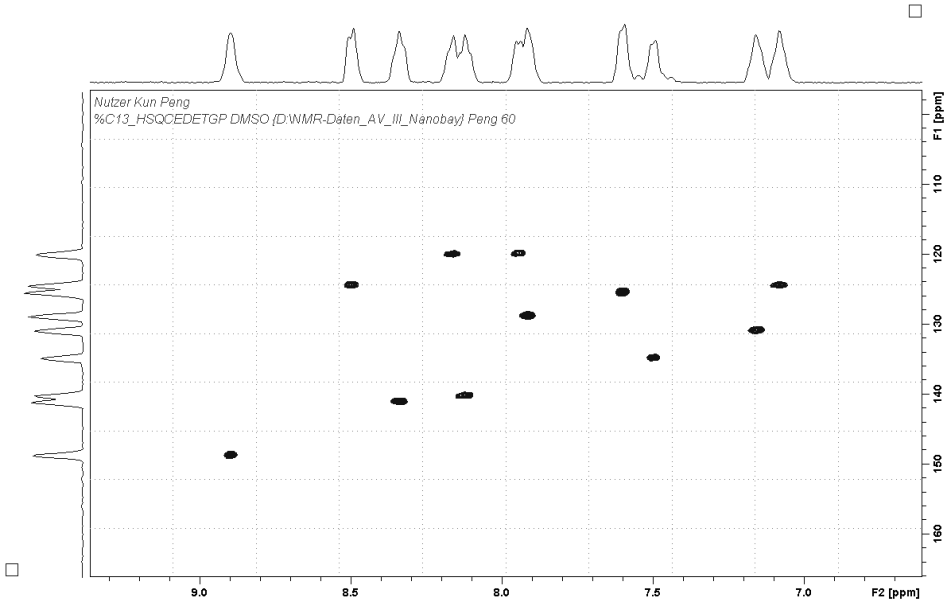
Nutzer Kun Peng
%C13_HSQCEDETGP DMSO {D:\NMR-Daten_AV_III_Nanobay} Peng 60
F1 [ppm]
F2 [ppm]

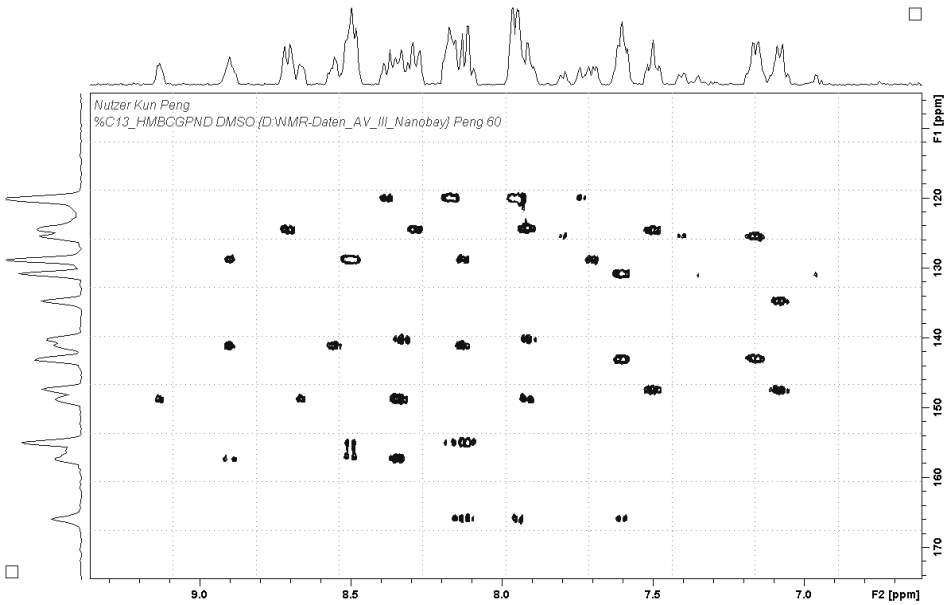
Nutzer Kun Peng
%C13_HMBCGPND DMSO {D:\NMR-Daten_AV_III_Nanobay} Peng 60
F1 [ppm]
F2 [ppm]

5.3.21 Synthesis of [Pd(N$_3$)(phbpy)]

USC-KP132-02

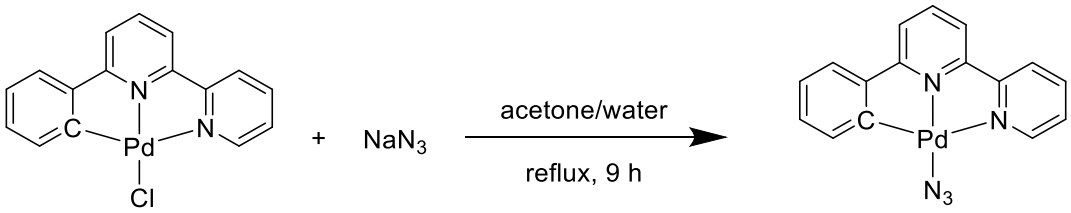

$C_{16}H_{11}ClN_2Pd$ 373.15 g/mol

NaN_3 65.01 g/mol

$C_{16}H_{11}N_5Pd$ 379.72 g/mol

In a round bottom flask, [PdCl(phbpy)] (68.2 mg, 0.18 mmol) was dissolved in acetone (70 mL) at 75 °C, and sodium azide (190.2 mg, 2.93 mmol) in water (8 mL) was added to the clear light yellow solution. The mixture was heated to reflux for 9 h. After cooling to room temperature, a yellow solid precipitat formed. The solvent was partially removed under reduced and the resulting yellow solid filtered off, washed with water (6 × 10 mL), and dried under vacuum for 4 d. Yield: 94% (63.5 mg, 0.17 mmol). **IR** (ATR): $\tilde{\nu}$ = 3060 (w), 2034 (s), 1592 (m), 1458 (w), 1292 (w), 1021 (w), 749 (m) cm^{-1}; **^{1}H NMR** (400.47 MHz, DMSO-d_6): δ = 8.47 (d, 1H, $^3J_{H3,H4}$ = 8.0 Hz, H3), 8.42 (d, 1H, $^3J_{H6,H5}$ = 5.0 Hz, H6), 8.25 (dt, 1H, $^3J_{H4,H3/H5}$ = 7.8 Hz, $^4J_{H4,H6}$ = 1.6 Hz, H4), 8.19 (d, 1H, $^3J_{H3',H2'/H4'}$ = 7.9 Hz, H3'), 8.14 (t, 1H, $^3J_{H4',H3'/H5'}$ = 7.9 Hz, H4'), 8.00 (d, 1H, $^3J_{H5',H4'}$ = 7.8 Hz, H5'), 7.77 (ddd, 1H, $^3J_{H5,H4}$ = 7.6 Hz, $^3J_{H5,H6}$ = 5.1 Hz, $^4J_{H5,H3}$ = 1.1 Hz, H5), 7.70 (dd, 1H, $^3J_{H2'',H3''}$ = 7.4 Hz, $^4J_{H2'',H4''}$ = 1.5 Hz, H2''), 7.30 (dd, 1H, $^3J_{H5'',H4''}$ = 7.4 Hz, $^4J_{H5'',H3''}$ = 1.1 Hz, H5''), 7.21 (dt, 1H, $^3J_{H4'',H3''/H5''}$ = 7.4 Hz, $^4J_{H4'',H2''}$ = 1.6 Hz, H4''), 7.16 (dt, 1H, $^3J_{H3'',H2''/H4''}$ = 7.3 Hz, $^4J_{H3'',H5''}$ = 1.3 Hz, H3'') ppm; **^{13}C NMR** (100.70 MHz, DMSO-d_6): δ = 162.91 (C6'), 155.14 (C2), 153.69 (C2'), 151.25 (C1''), 148.77 (C6''), 148.50 (C6), 140.68 (C4), 140.35 (C4'), 130.93 (C5''), 130.03 (C4''), 127.56 (C5), 125.38 (C3''), 124.97 (C2''), 123.28 (C3), 119.98 (C5'), 119.91 (C3') ppm; **Elemental analysis** (%) calcd. for $C_{16}H_{11}N_5Pd$: C 50.61, H 2.92, N 18.44; found (%): C 50.70, H 3.00, N 18.66.

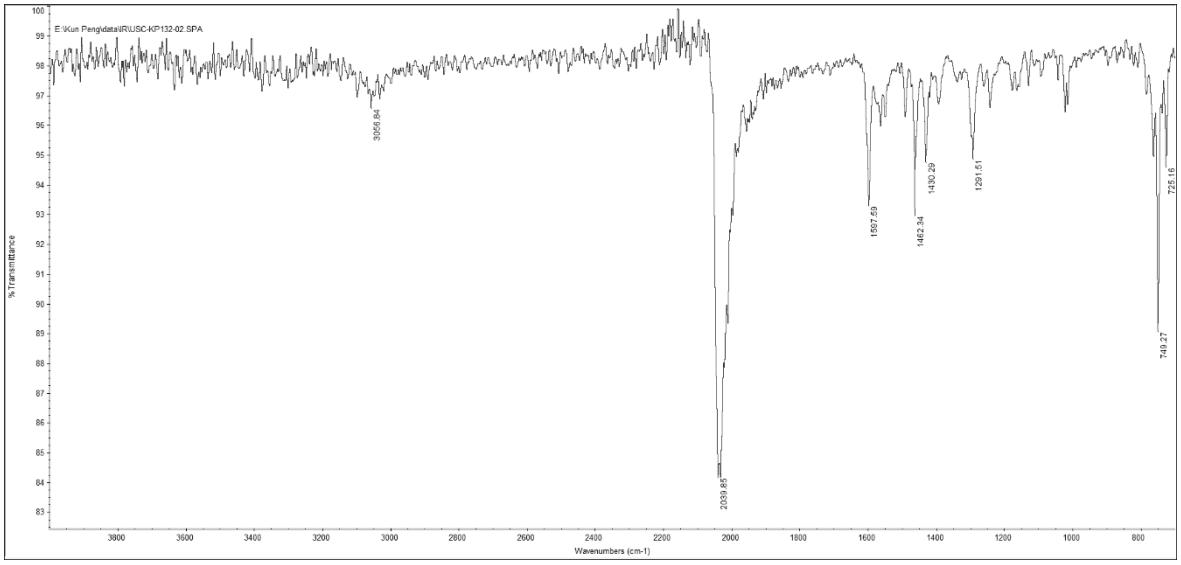
E:\Kun Peng\data\IR\USC-KP132-02.SPA
% Transmittance
Wavenumbers (cm-1)
3056.84
2039.85
1597.59
1462.34
1430.29
1291.51
749.27
725.16

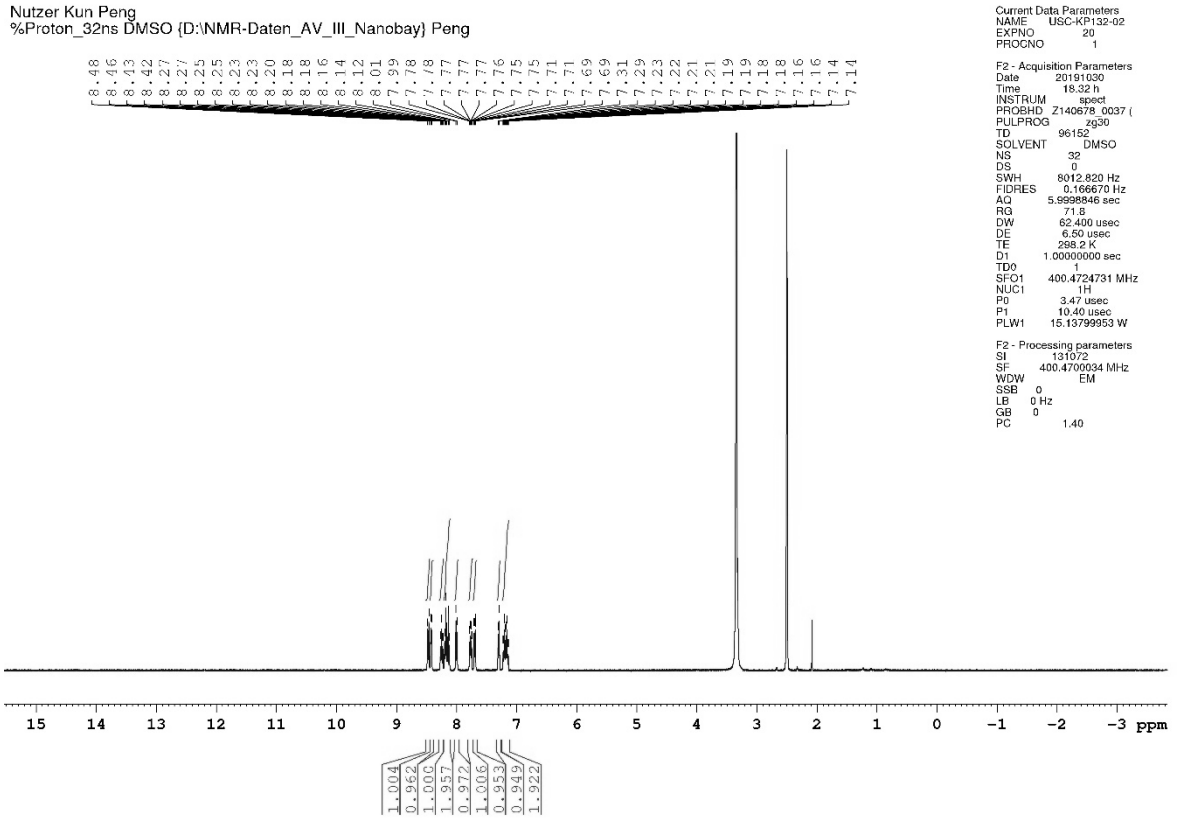
Nutzer Kun Peng
%Proton_32ns DMSO {D:\NMR-Daten_AV_III_Nanobay} Peng
Current Data Parameters
NAME USC-KP132-02
EXPNO 20
PROCNO 1
F2 - Acquisition Parameters
Date 20191030
Time 18.32 h
INSTRUM spect
PROBHD Z140678_0037 (
PULPROG zg30
TD 96152
SOLVENT DMSO
NS 32
DS 0
SWH 8012.820 Hz
FIDRES 0.166670 Hz
AQ 5.9998846 sec
RG 71.8
DW 62.400 usec
DE 6.50 usec
TE 298.2 K
D1 1.00000000 sec
TD0 1
SFO1 400.4724731 MHz
NUC1 1H
P0 3.47 usec
P1 10.40 usec
PLW1 15.13799953 W
F2 - Processing parameters
SI 131072
SF 400.4700034 MHz
WDW EM
SSB 0
LB 0 Hz
GB 0
PC 1.40
8.48 8.46 8.43 8.42 8.27 8.27 8.25 8.25 8.23 8.23 8.20 8.18 8.18 8.16 8.14 8.12 8.01 7.99 7.78 7.78 7.77 7.77 7.77 7.76 7.75 7.75 7.71 7.71 7.69 7.69 7.31 7.29 7.23 7.22 7.21 7.21 7.19 7.19 7.18 7.18 7.16 7.16 7.14 7.14
15 14 13 12 11 10 9 8 7 6 5 4 3 2 1 0 -1 -2 -3 ppm
1.004 0.962 1.000 1.957 0.972 1.006 0.953 0.949 1.922

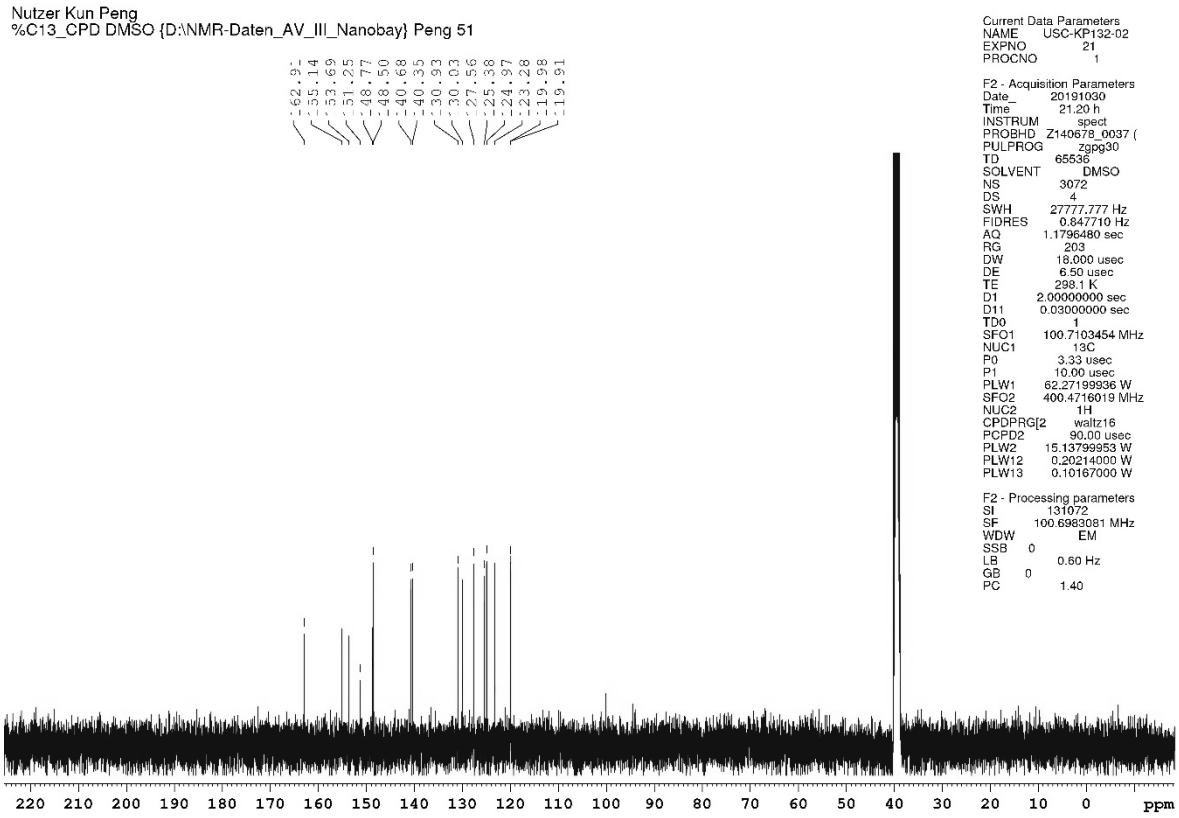
Nutzer Kun Peng
%C13_CPD DMSO {D:\NMR-Daten_AV_III_Nanobay} Peng 51
162.9
155.14
153.69
151.25
148.77
148.50
140.68
140.35
130.93
130.03
127.56
125.38
124.97
123.28
119.98
119.91
Current Data Parameters
NAME USC-KP132-02
EXPNO 21
PROCNO 1
F2 - Acquisition Parameters
Date_ 20191030
Time 21.20 h
INSTRUM spect
PROBHD Z140678_0037 (
PULPROG zgpg30
TD 65536
SOLVENT DMSO
NS 3072
DS 4
SWH 27777.777 Hz
FIDRES 0.847710 Hz
AQ 1.1796480 sec
RG 203
DW 18.000 usec
DE 6.50 usec
TE 298.1 K
D1 2.00000000 sec
D11 0.03000000 sec
TD0 1
SFO1 100.7103454 MHz
NUC1 13C
P0 3.33 usec
P1 10.00 usec
PLW1 62.27199936 W
SFO2 400.4716019 MHz
NUC2 1H
CPDPRG[2 waltz16
PCPD2 90.00 usec
PLW2 15.13799953 W
PLW12 0.20214000 W
PLW13 0.10167000 W
F2 - Processing parameters
SI 131072
SF 100.6983081 MHz
WDW EM
SSB 0
LB 0.60 Hz
GB 0
PC 1.40
220 210 200 190 180 170 160 150 140 130 120 110 100 90 80 70 60 50 40 30 20 10 0 ppm

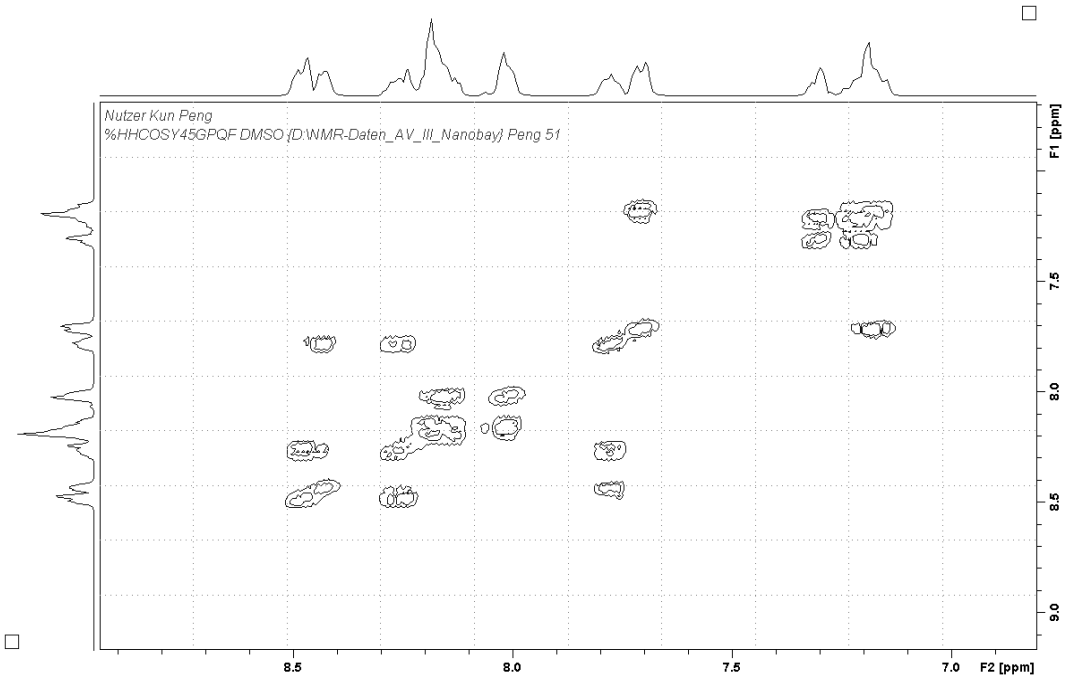
Nutzer Kun Peng
%HHCOSY45GPQF DMSO {D:\NMR-Daten_AV_III_Nanobay} Peng 51
F1 [ppm]
7.5
8.0
8.5
9.0
8.5
8.0
7.5
7.0 F2 [ppm]

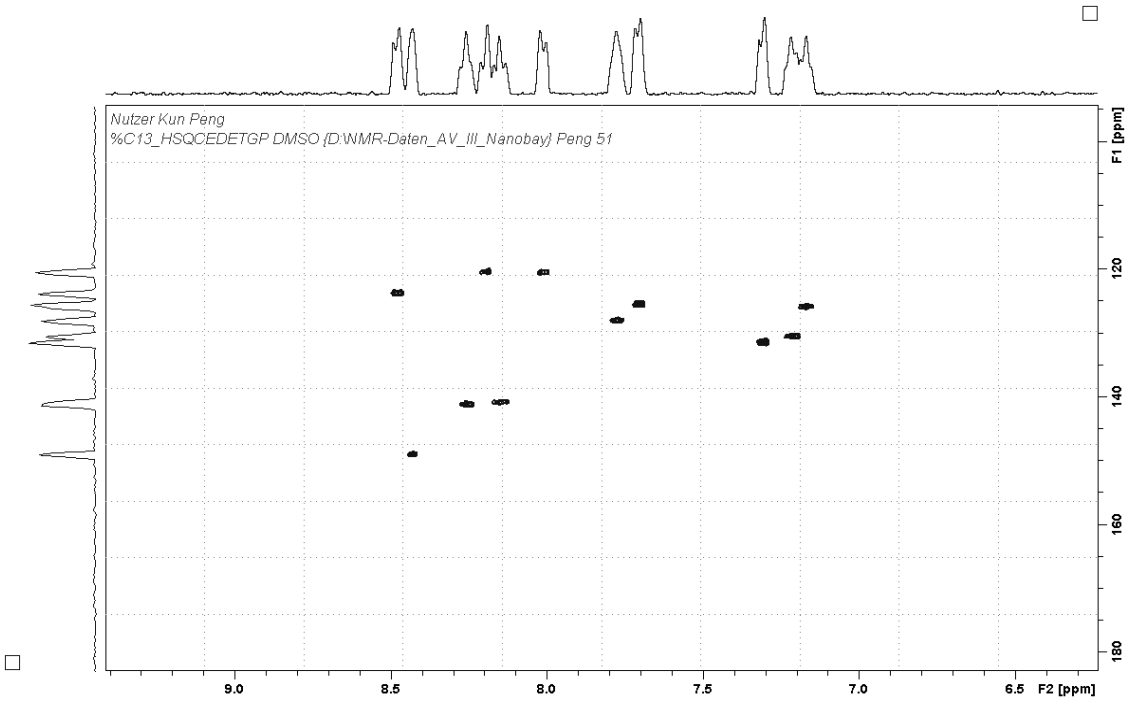
Nutzer Kun Peng
%C13_HSQCEDETGP DMSO {D:\NMR-Daten_AV_III_Nanobay} Peng 51
F1 [ppm]
120
140
160
180
9.0
8.5
8.0
7.5
7.0
6.5
F2 [ppm]

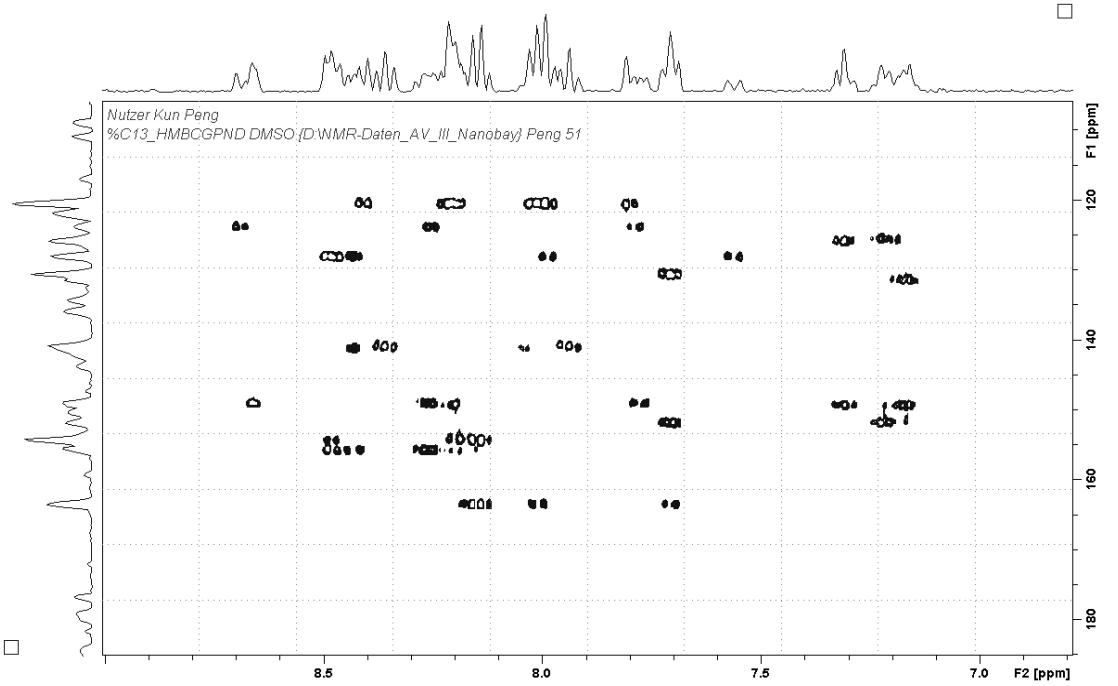
Nutzer Kun Peng
%C13_HMBCGPND DMSO {D:\NMR-Daten_AV_III_Nanobay} Peng 51
F1 [ppm]
120
140
160
180
8.5
8.0
7.5
7.0
F2 [ppm]

5.3.22 Synthesis of [Pt(N$_3$)(phbpy)]

USC-KP138-01

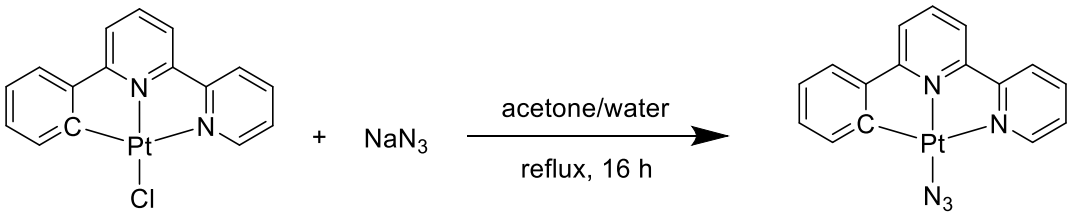

$C_{16}H_{11}ClN_2Pt$ 461.81 g/mol

NaN_3 65.01 g/mol

$C_{16}H_{11}N_5Pt$ 468.37 g/mol

In a round bottom flask, [PtCl(phbpy)] (68.2 mg, 0.15 mmol) was dissolved in acetone (80 mL) at 75 °C and sodium azide (159.3 mg, 2.45 mmol) in water (7 mL) was added to the clear orange solution. The mixture was heated to reflux for 16 h. Then, the solvent was partially removed under reduced pressure and the resulting dark red solid filtered off, washed with water (4 × 10 mL), and dried under vacuum for 5 d. Yield: 93% (66.2 mg, 0.14 mmol). **IR** (ATR): $\tilde{\nu}$ = 2920 (w), 2032 (s), 1604 (m), 1298 (m), 751 (s), 727 (m) cm^{-1}; **^{1}H NMR** (400.47 MHz, DMSO-d_6): δ = 8.62 (d, 1H, $^3J_{H6,H5}$ = 5.2 Hz, H6), 8.46 (d, 1H, $^3J_{H3,H4}$ = 8.1 Hz, H3), 8.32 (dt, 1H, $^3J_{H4,H3/H5}$ = 7.8 Hz, $^4J_{H4,H6}$ = 1.5 Hz, H4), 8.13 (d, 1H, $^3J_{H4',H3'/H5'}$ = 8.0 Hz, H3'), 8.07 (t, 1H, $^3J_{H4',H3'/H5'}$ = 7.9 Hz, H4'), 7.92 (d, 1H, $^3J_{H5',H4'}$ = 7.9 Hz, H5'), 7.86 (t, 1H, $^3J_{H5,H4/H6}$ = 6.4 Hz, H5), 7.66 (d, 1H, $^3J_{H2",H3"}$ = 7.6 Hz, H2"), 7.33 (d, 1H, $^3J_{H5",H4"}$ = 7.6 Hz, H5"), 7.23 (dt, 1H, $^3J_{H4",H3"/H5"}$ = 7.4 Hz, $^4J_{H4",H2"}$ = 1.1 Hz, H4"), 7.12 (t, 1H, $^3J_{H3",H2"/H4"}$ = 7.3 Hz, H3") ppm; **^{13}C NMR** (100.70 MHz, DMSO-d_6): δ = 164.35 (C6'), 156.55 (C2), 154.51 (C2'), 147.96 (C6"), 147.67 (C6), 140.66 (C4), 139.90 (C1"), 139.66 (C4'), 131.03 (C5"), 130.47 (C4"), 128.16 (C5), 125.16 (C2"), 124.26 (C3"), 123.94 (C3), 119.48 (C3'), 119.30 (C5') ppm; **^{195}Pt NMR** (86.09 MHz, DMSO-d_6): δ = -3384 ppm; **Elemental analysis** (%) calcd. for $C_{16}H_{11}N_5Pt$: C 41.03, H 2.37, N 14.95; found (%): C 41.58, H 2.51, N 14.80.

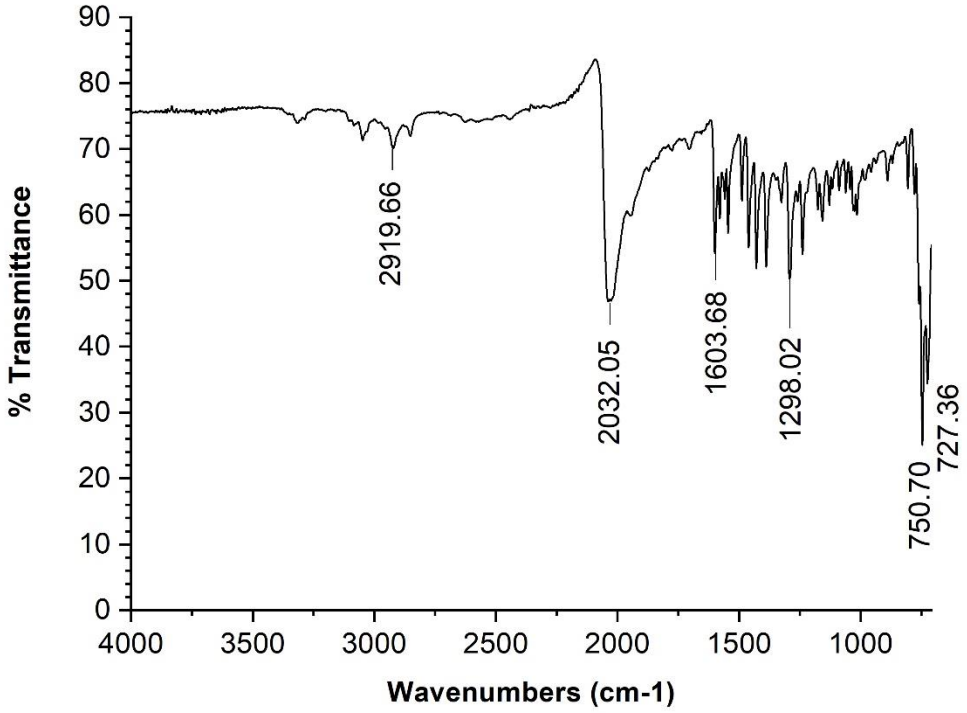
% Transmittance
Wavenumbers (cm-1)
2919.66
2032.05
1603.68
1298.02
750.70
727.36

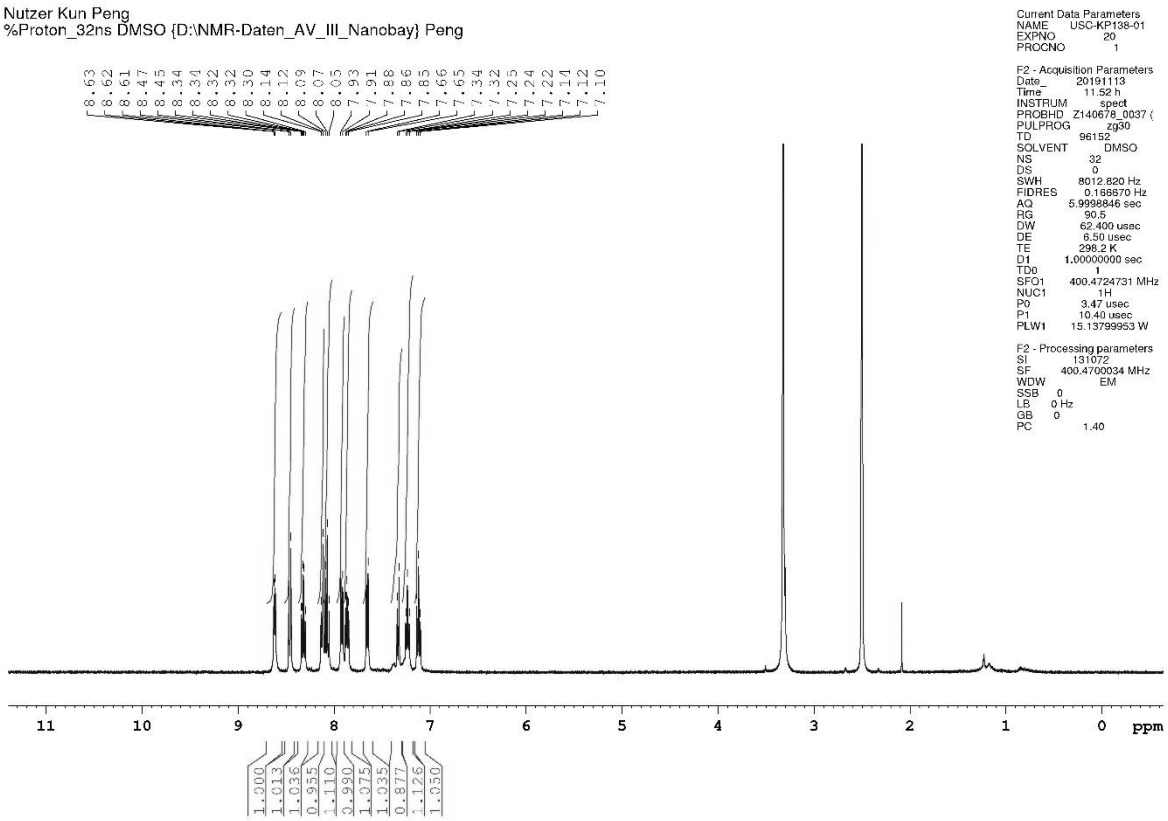
Nutzer Kun Peng
%Proton_32ns DMSO {D:\NMR-Daten_AV_III_Nanobay} Peng
Current Data Parameters
NAME USC-KP138-01
EXPNO 20
PROCNO 1
F2 - Acquisition Parameters
Date_ 20191113
Time 11.52 h
INSTRUM spect
PROBHD Z140678_0037 (
PULPROG zg30
TD 96152
SOLVENT DMSO
NS 32
DS 0
SWH 8012.820 Hz
FIDRES 0.166670 Hz
AQ 5.9998846 sec
RG 90.5
DW 62.400 usec
DE 6.50 usec
TE 298.2 K
D1 1.00000000 sec
TD0 1
SFO1 400.4724731 MHz
NUC1 1H
P0 3.47 usec
P1 10.40 usec
PLW1 15.13799953 W
F2 - Processing parameters
SI 131072
SF 400.4700034 MHz
WDW EM
SSB 0
LB 0 Hz
GB 0
PC 1.40
ppm

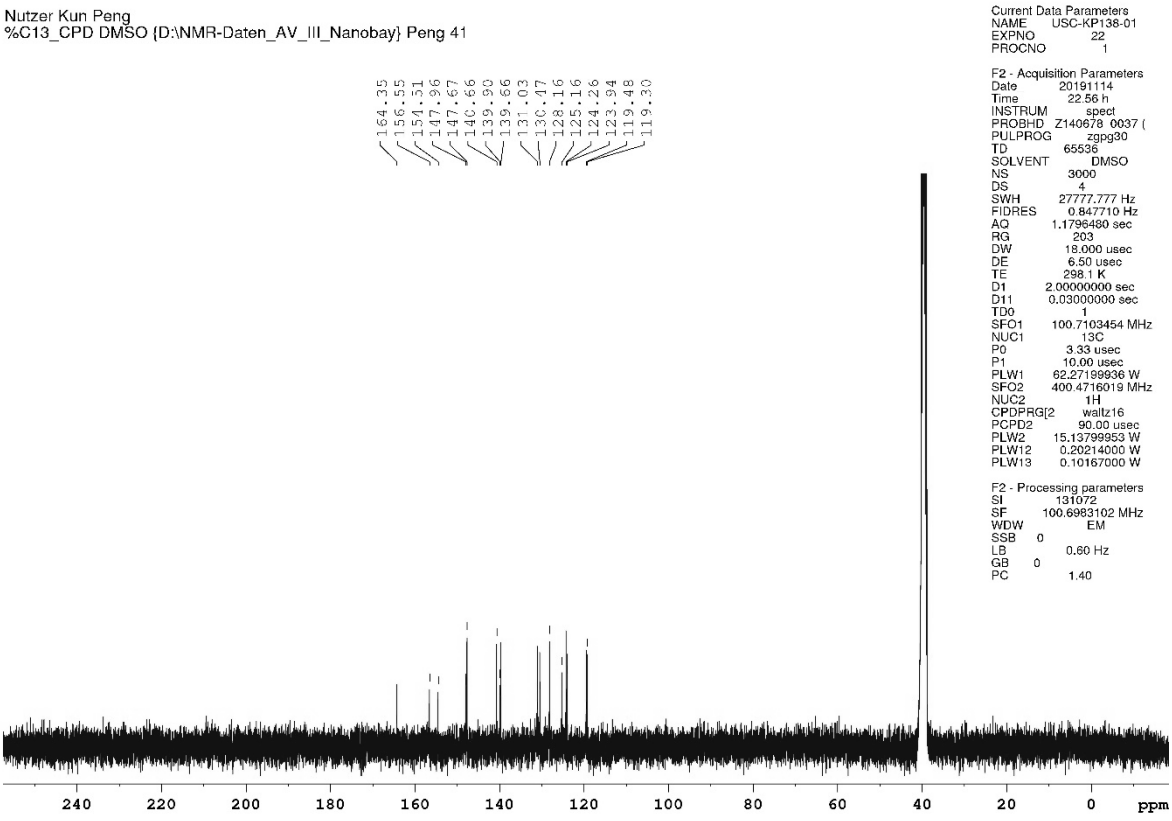
Nutzer Kun Peng
%C13_CPD DMSO {D:\NMR-Daten_AV_III_Nanobay} Peng 41
164.35
156.55
154.51
147.96
147.67
140.66
139.90
139.66
131.03
130.17
128.16
125.16
124.26
123.94
119.48
119.30
Current Data Parameters
NAME USC-KP138-01
EXPNO 22
PROCNO 1
F2 - Acquisition Parameters
Date 20191114
Time 22.56 h
INSTRUM spect
PROBHD Z140678 0037 (
PULPROG zgpg30
TD 65536
SOLVENT DMSO
NS 3000
DS 4
SWH 27777.777 Hz
FIDRES 0.847710 Hz
AQ 1.1796480 sec
RG 203
DW 18.000 usec
DE 6.50 usec
TE 298.1 K
D1 2.00000000 sec
D11 0.03000000 sec
TD0 1
SFO1 100.7103454 MHz
NUC1 13C
P0 3.33 usec
P1 10.00 usec
PLW1 62.27199936 W
SFO2 400.4716019 MHz
NUC2 1H
CPDPRG[2 waltz16
PCPD2 90.00 usec
PLW2 15.13799953 W
PLW12 0.20214000 W
PLW13 0.10167000 W
F2 - Processing parameters
SI 131072
SF 100.6983102 MHz
WDW EM
SSB 0
LB 0.60 Hz
GB 0
PC 1.40
240
220
200
180
160
140
120
100
80
60
40
20
0
ppm

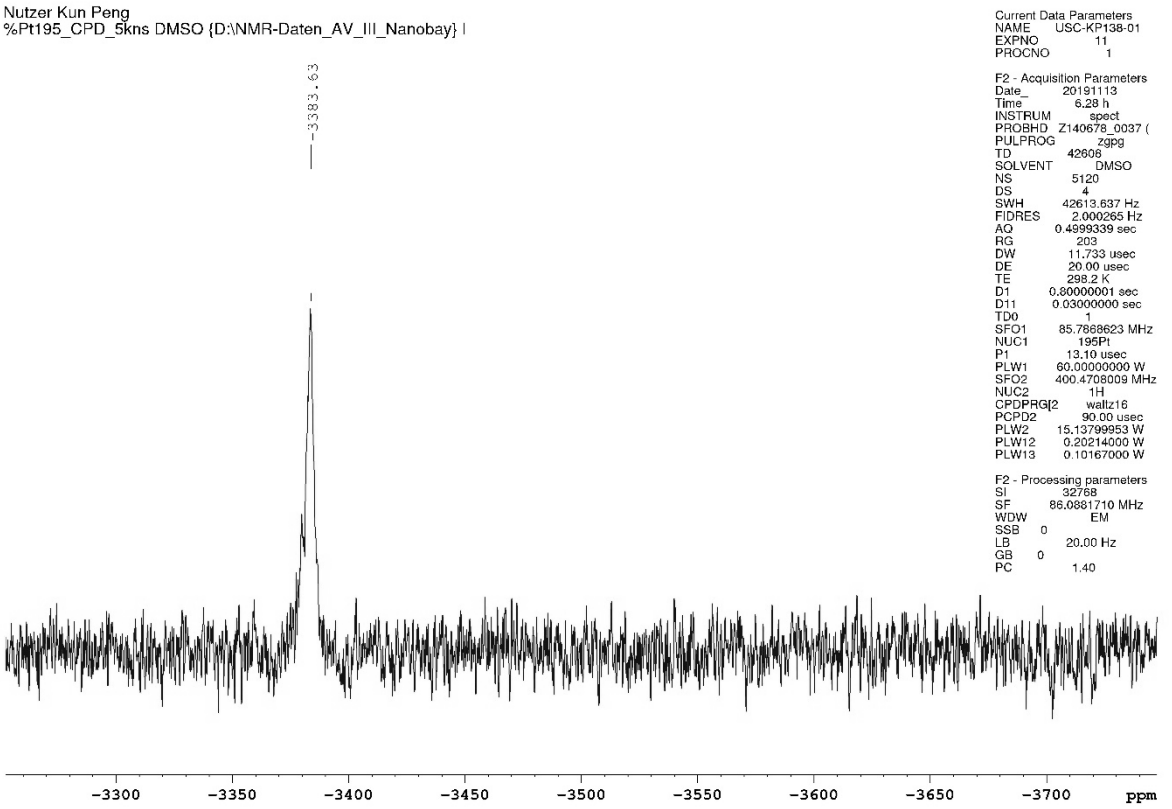
Nutzer Kun Peng
%Pt195_CPD_5kns DMSO {D:\NMR-Daten_AV_III_Nanobay} I
-3383.63
Current Data Parameters
NAME USC-KP138-01
EXPNO 11
PROCNO 1
F2 - Acquisition Parameters
Date_ 20191113
Time 6.28 h
INSTRUM spect
PROBHD Z140678_0037 (
PULPROG zgpg
TD 42608
SOLVENT DMSO
NS 5120
DS 4
SWH 42613.637 Hz
FIDRES 2.000265 Hz
AQ 0.4999339 sec
RG 203
DW 11.733 usec
DE 20.00 usec
TE 298.2 K
D1 0.80000001 sec
D11 0.03000000 sec
TD0 1
SFO1 85.7868623 MHz
NUC1 195Pt
P1 13.10 usec
PLW1 60.00000000 W
SFO2 400.4708009 MHz
NUC2 1H
CPDPRG[2 waltz16
PCPD2 90.00 usec
PLW2 15.13799953 W
PLW12 0.20214000 W
PLW13 0.10167000 W
F2 - Processing parameters
SI 32768
SF 86.0881710 MHz
WDW EM
SSB 0
LB 20.00 Hz
GB 0
PC 1.40
-3300
-3350
-3400
-3450
-3500
-3550
-3600
-3650
-3700
ppm

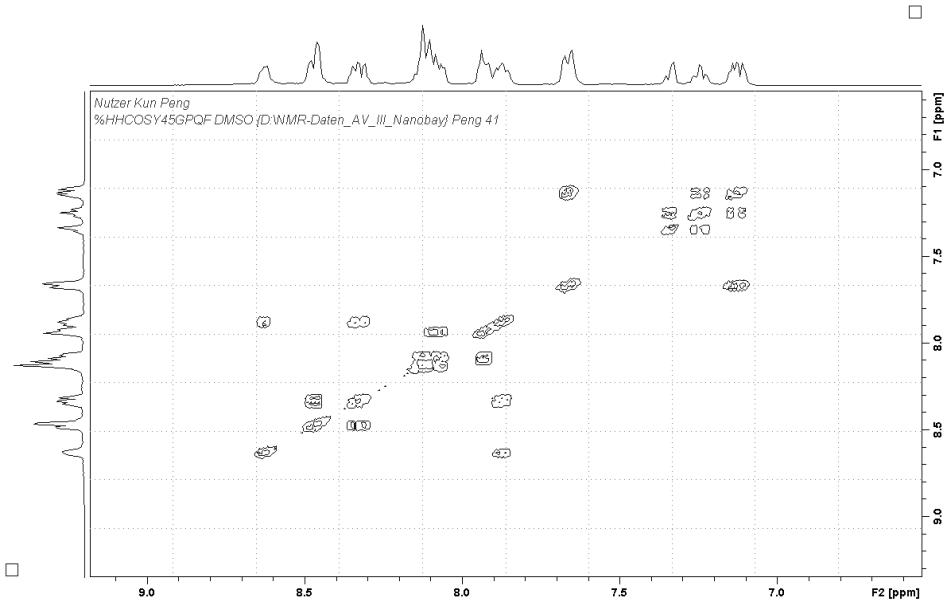
Nutzer Kun Peng
%HHCOSY45GPQF DMSO {D:\NMR-Daten_AV_III_Nanobay} Peng 41
F1 [ppm]
7.0
7.5
8.0
8.5
9.0
F2 [ppm]
9.0
8.5
8.0
7.5
7.0

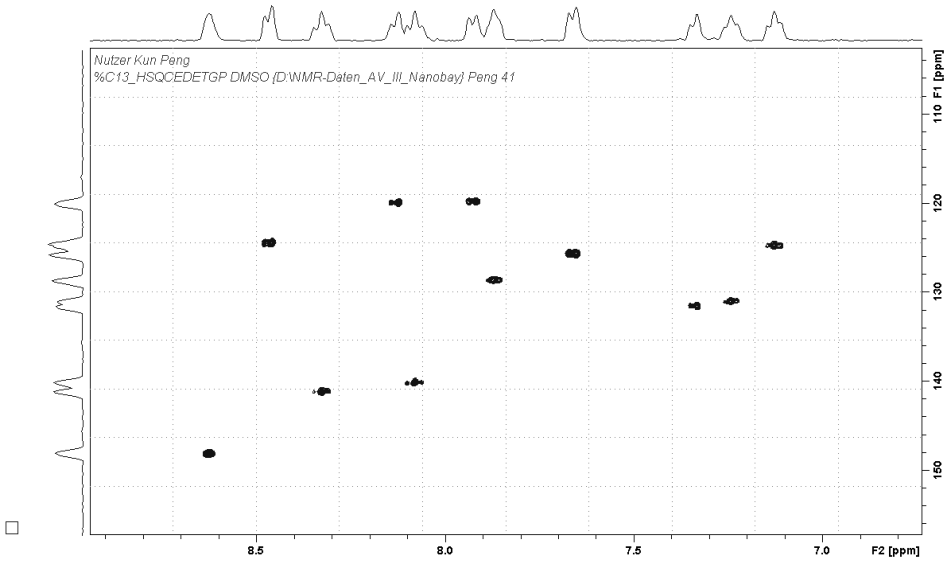
Nutzer Kun Peng
%C13_HSQCEDETGP DMSO {D:\NMR-Daten_AV_III_Nanobay} Peng 41
F1 [ppm]
110
120
130
140
150
F2 [ppm]
8.5
8.0
7.5
7.0

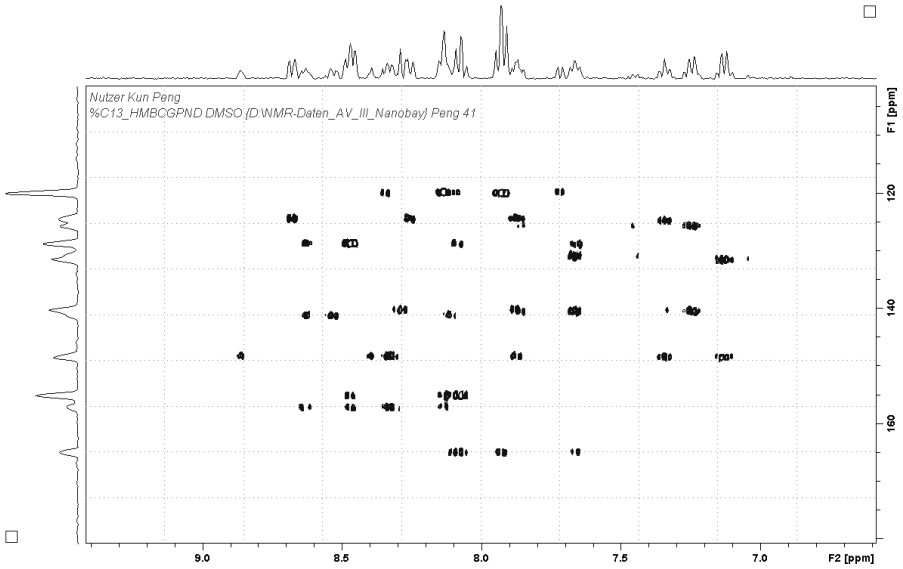
Nutzer Kun Peng
%C13_HMBCGPND DMSO {D:\NMR-Daten_AV_III_Nanobay} Peng 41
F1 [ppm]
120
140
160
F2 [ppm]
9.0
8.5
8.0
7.5
7.0

5.3.23 Synthesis of [Pd(phbpy)(triazolate^{COOCH3,COOCH3})]

USC-KP134-04

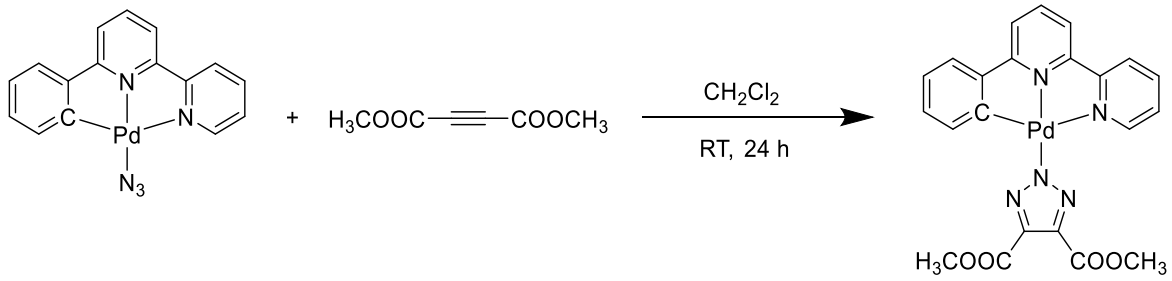

$C_{16}H_{11}N_5Pd$ 379.71 g/mol

$C_6H_6O_4$ 142.11 g/mol

$C_{22}H_{17}N_5O_4Pd$ 521.82 g/mol

[Pd(N_3)(phbpy)] (19.0 mg, 0.05 mmol) was suspended in dichloromethane (10 mL), and dimethyl acetylenedicarboxylate (16 µL, 18.5 mg, 0.13 mmol) was added. The mixture was stirred at room temperature for 1 d, during which the solution became clear yellow. It was then concentrated to approx. 3 mL and diethyl ether (25 mL) added to obtain a yellow solid, which was filtered off and dried under vacuum for 3 d. Yield: quantitative (25.3 mg, 0.05 mmol). **IR** (ATR): $\tilde{\nu}$ = 2950 (w), 1722 (s), 1601 (w), 1510 (w), 1431 (m), 1403 (w), 1282 (m), 1208 (m), 1086 (s), 774 (w), 754 (m) cm^{-1}; **^{1}H NMR** (400.47 MHz, DMSO-d_6): δ = 8.60−8.54 (m, 2H, H6/H3), 8.29−8.25 (m, 2H, H4/H3'), 8.20 (t, 1H, $^3J_{H4',H3'/H5'}$ = 7.9 Hz, H4'), 8.05 (d, 1H, $^3J_{H5',H4'}$ = 7.8 Hz, H5'), 7.76 (m, 1H, H5), 7.70 (d, 1H, $^3J_{H2'',H3''}$ = 8.0 Hz, H2"), 7.31 (m, 1H, H5"), 7.13−7.11 (m, 2H, H3"/H4"), 3.85 (s, 6H, COOCH_3) ppm; **^{13}C NMR** (100.70 MHz, DMSO-d_6): δ = 163.87 (COOCH$_3$), 162.41 (C6'), 155.20 (C2), 153.89 (C2'), 153.11 (C1"), 150.14 (C6"), 147.92 (C6), 141.20 (C4'), 140.78 (C4), 139.30 (triazolate-C4/C5), 135.11 (C5"), 129.98 (C4"), 127.58 (C5), 125.38 (C3"), 124.81 (C2"), 123.50 (C3), 120.13 (C5'), 120.06 (C3'), 51.91 (COOCH$_3$) ppm; **Elemental analysis** (%) calcd. for $C_{22}H_{17}N_5O_4Pd$: C 50.64, H 3.28, N 13.42; found (%): C 50.56, H 3.33, N 12.75.

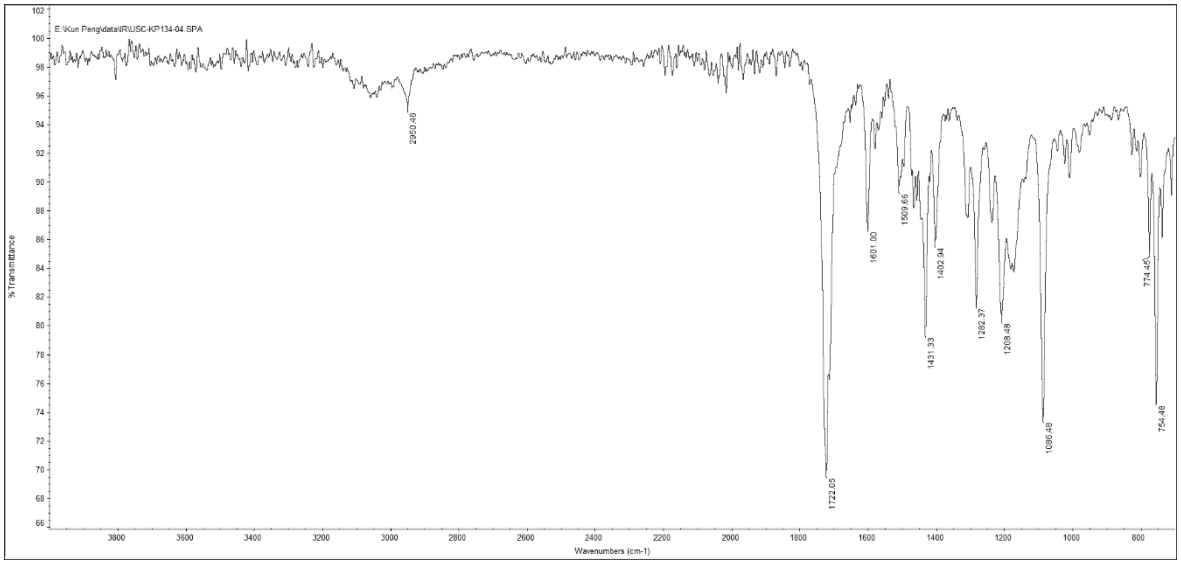
E:\Kun Peng\data\IR\USC-KP134-04.SPA
% Transmittance
Wavenumbers (cm-1)
2959.46
1722.05
1601.00
1509.66
1431.33
1402.94
1262.37
1208.48
1086.46
754.48
774.45

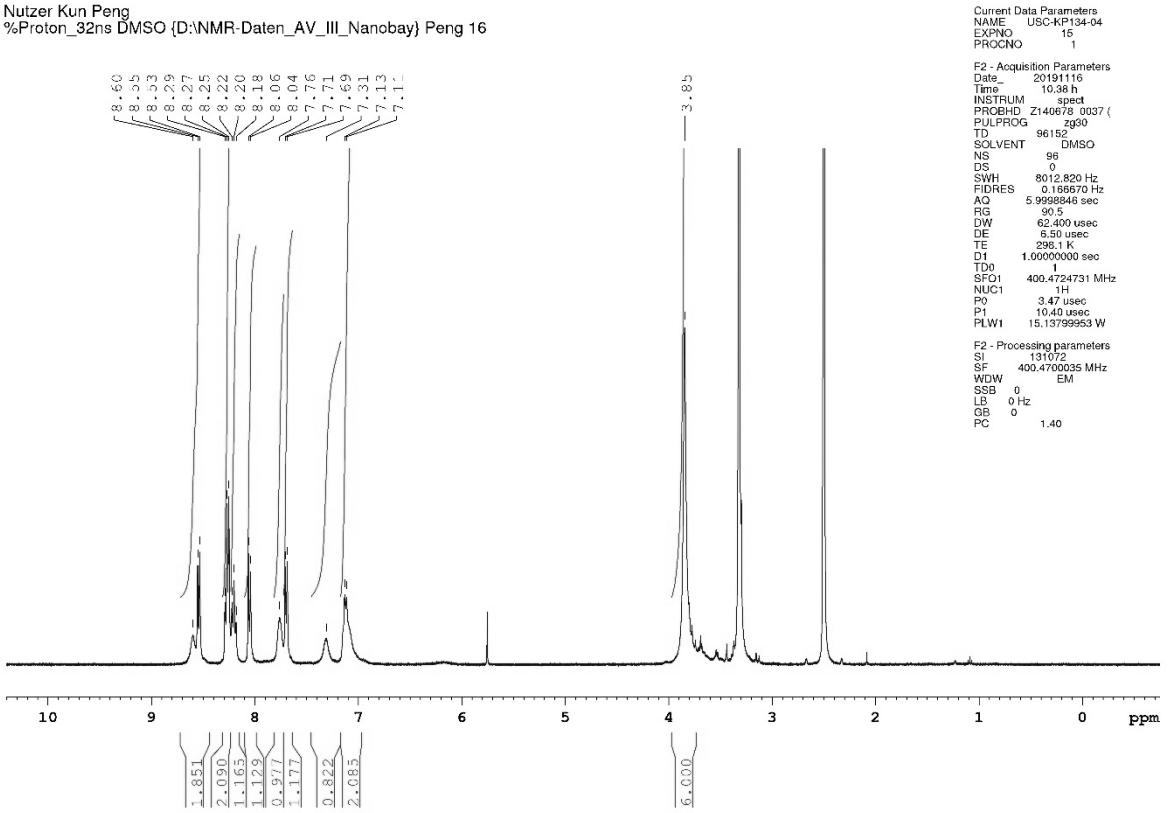
Nutzer Kun Peng
%Proton_32ns DMSO {D:\NMR-Daten_AV_III_Nanobay} Peng 16
8.60
8.35
8.33
8.29
8.27
8.25
8.22
8.20
8.18
8.06
8.04
7.76
7.71
7.69
7.31
7.13
3.85
Current Data Parameters
NAME USC-KP134-04
EXPNO 15
PROCNO 1
F2 - Acquisition Parameters
Date_ 20191116
Time 10.38 h
INSTRUM spect
PROBHD Z140678 0037 (
PULPROG zg30
TD 96152
SOLVENT DMSO
NS 96
DS 0
SWH 8012.820 Hz
FIDRES 0.166670 Hz
AQ 5.9998846 sec
RG 90.5
DW 62.400 usec
DE 6.50 usec
TE 298.1 K
D1 1.00000000 sec
TD0 1
SFO1 400.4724731 MHz
NUC1 1H
P0 3.47 usec
P1 10.40 usec
PLW1 15.13799953 W
F2 - Processing parameters
SI 131072
SF 400.4700035 MHz
WDW EM
SSB 0
LB 0 Hz
GB 0
PC 1.40
10
9
8
7
6
5
4
3
2
1
0
ppm
1.851
2.090
1.165
1.129
0.977
1.177
0.822
2.085
6.000

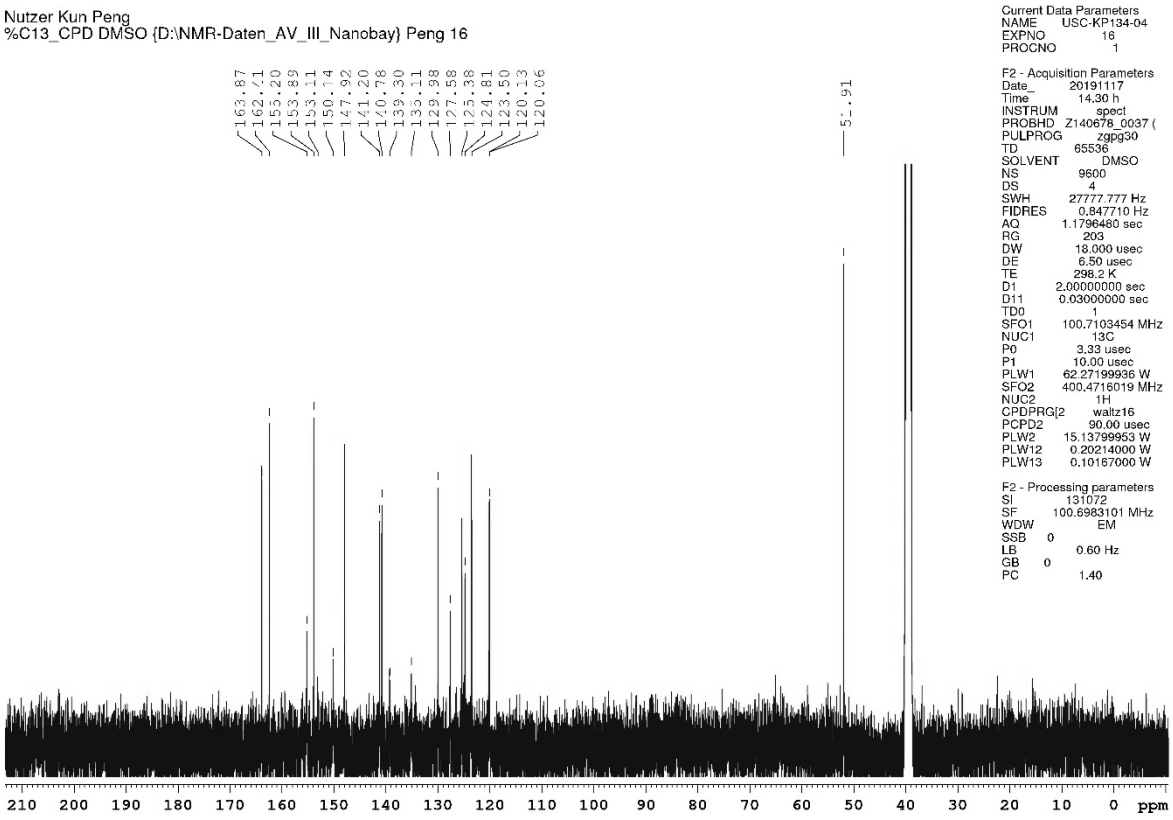
Nutzer Kun Peng
%C13_CPD DMSO {D:\NMR-Daten_AV_III_Nanobay} Peng 16
163.87
162.71
155.20
153.89
153.11
150.14
147.92
141.20
140.78
139.30
135.11
129.98
127.58
125.38
124.81
123.50
120.13
120.06
51.91
Current Data Parameters
NAME USC-KP134-04
EXPNO 16
PROCNO 1
F2 - Acquisition Parameters
Date_ 20191117
Time 14.30 h
INSTRUM spect
PROBHD Z140678_0037 (
PULPROG zgpg30
TD 65536
SOLVENT DMSO
NS 9600
DS 4
SWH 27777.777 Hz
FIDRES 0.847710 Hz
AQ 1.1796480 sec
RG 203
DW 18.000 usec
DE 6.50 usec
TE 298.2 K
D1 2.00000000 sec
D11 0.03000000 sec
TD0 1
SFO1 100.7103454 MHz
NUC1 13C
P0 3.33 usec
P1 10.00 usec
PLW1 62.27199936 W
SFO2 400.4716019 MHz
NUC2 1H
CPDPRG[2 waltz16
PCPD2 90.00 usec
PLW2 15.13799953 W
PLW12 0.20214000 W
PLW13 0.10167000 W
F2 - Processing parameters
SI 131072
SF 100.6983101 MHz
WDW EM
SSB 0
LB 0.60 Hz
GB 0
PC 1.40
210 200 190 180 170 160 150 140 130 120 110 100 90 80 70 60 50 40 30 20 10 0 ppm

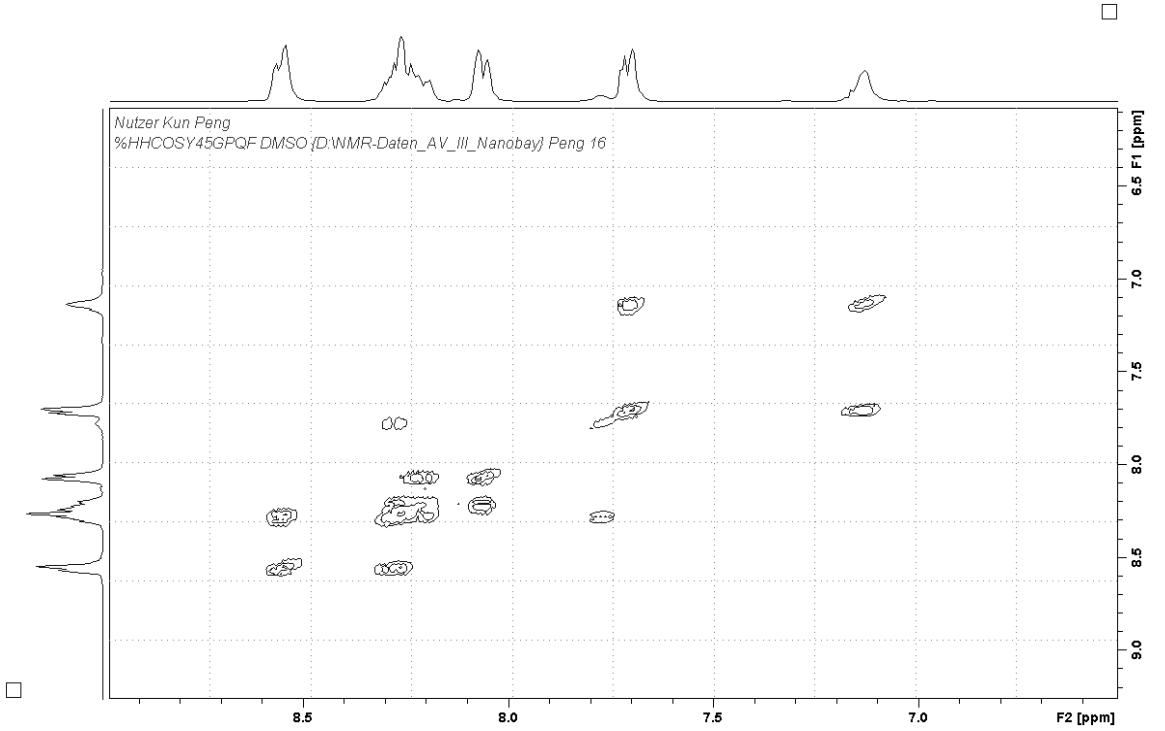
Nutzer Kun Peng
%HHCOSY45GPQF DMSO {D:\NMR-Daten_AV_III_Nanobay} Peng 16
6.5 F1 [ppm]
7.0
7.5
8.0
8.5
9.0
8.5 8.0 7.5 7.0 F2 [ppm]

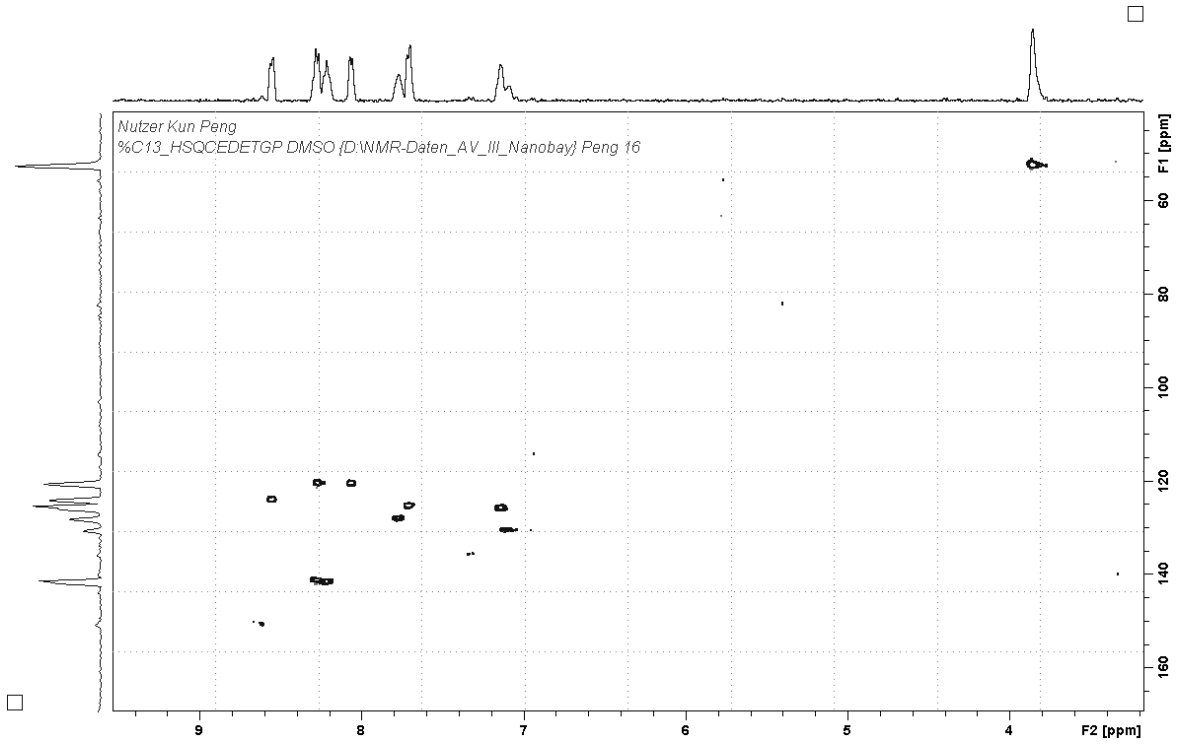
Nutzer Kun Peng
%C13_HSQCEDETGP DMSO {D:\NMR-Daten_AV_III_Nanobay} Peng 16
F1 [ppm]
60
80
100
120
140
160
9
8
7
6
5
4
F2 [ppm]

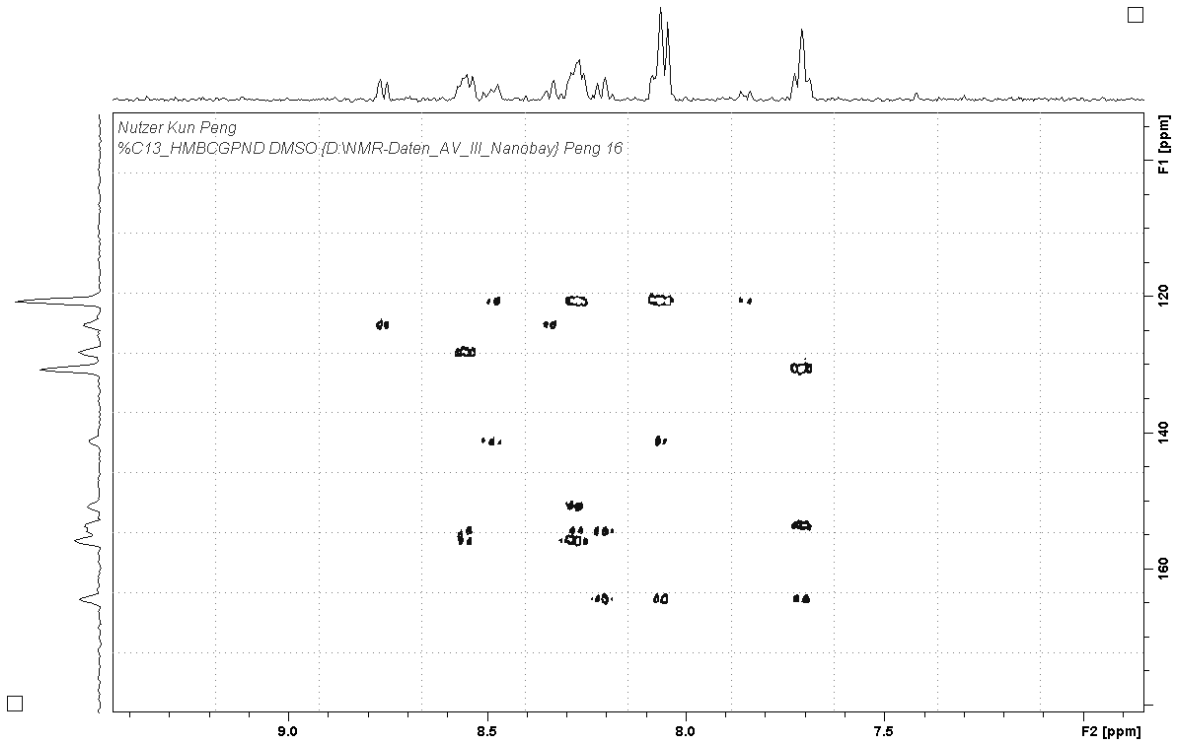
Nutzer Kun Peng
%C13_HMBCGPND DMSO {D:\NMR-Daten_AV_III_Nanobay} Peng 16
F1 [ppm]
120
140
160
9.0
8.5
8.0
7.5
F2 [ppm]

5.3.24 Synthesis of [Pt(phbpy)(triazolate^{COOCH3,COOCH3})]

USC-KP139-01

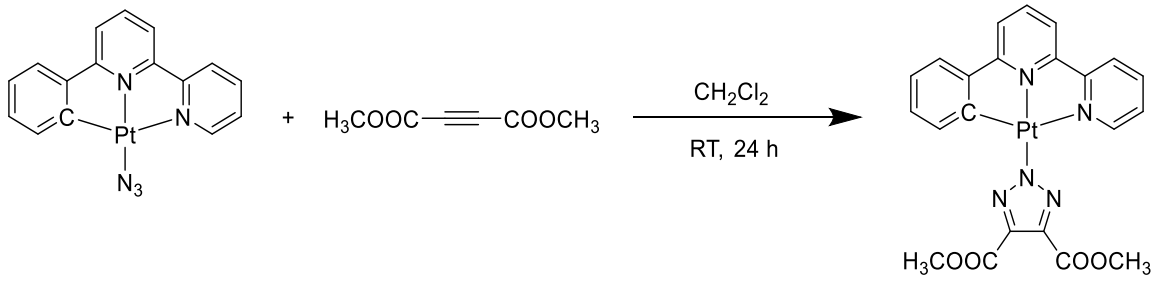

$C_{16}H_{11}N_5Pt$ 468.37 g/mol

$C_6H_6O_4$ 142.11 g/mol

$C_{22}H_{17}N_5O_4Pt$ 610.48 g/mol

[Pt(N_3)(phbpy)] (16.2 mg, 0.03 mmol) was suspended in dichloromethane (10 mL), and dimethyl acetylenedicarboxylate (8.2 µL, 9.5 mg, 0.07 mmol) was added. The mixture was stirred at room temperature for 24 h. It was then concentrated to approx. 4 mL and diethyl ether (25 mL) was added to give an orange precipitate, which was filtered off, washed with diethyl ether (5 mL), and dried under vacuum for 5 d. Yield: 67% (14.8 mg, 0.02 mmol). **IR** (ATR): $\tilde{\nu}$ = 2955 (w), 1726 (s), 1439 (m), 1198 (m), 1086 (s), 751 (s) cm^{-1}; **^{1}H NMR** (400.47 MHz, CD_2Cl_2): δ = 8.54 (d, 1H, $^3J_{H6,H5}$ = 5.4 Hz, H6), 7.96 (d, 1H, $^3J_{H3,H4}$ = 7.8 Hz, H3), 7.89 (dt, 1H, $^3J_{H4,H3/H5}$ = 7.9 Hz, $^4J_{H4,H6}$ = 1.6 Hz, H4), 7.58−7.57 (m, 2H, H3'/H4'), 7.38 (ddd, 1H, $^3J_{H5,H4}$ = 7.4 Hz, $^3J_{H5,H6}$ = 5.4 Hz, $^4J_{H5,H3}$ = 1.2 Hz, H5), 7.27−7.21 (m, 3H, $^3J_{H5,H4/H6}$ = 6.5 Hz, H5'/H2"/H5"), 7.11 (dt, 1H, $^3J_{H4",H3"/H5"}$ = 7.4 Hz, $^4J_{H4",H2"}$ = 1.5 Hz, H4"), 7.05 (dt,1H, $^3J_{H3",H2"/H4"}$ = 7.4 Hz, $^4J_{H3",H5"}$ = 1.2 Hz, H3"), 3.97 (s, 6H, COOCH_3) ppm; **^{13}C NMR** (100.70 MHz, CD_2Cl_2): δ = 166.44 (*C*OOCH$_3$), 163.07 (C6'), 157.32 (C2), 155.22 (C2'), 150.42 (C6), 147.19 (C6"), 141.46 (C1"), 140.35 (C4'), 140.06 (C4), 139.70 (triazolate-C4/C5), 135.23 (C5"), 131.02 (C4"), 127.46 (C5), 124.69 (C3"), 124.66 (C2"), 123.95 (C3), 119.18 (C3'), 118.85 (C5'), 52.36 (COO*C*H$_3$) ppm; **^{195}Pt NMR** (86.09 MHz, CD_2Cl_2): δ = -3455 ppm; **Elemental analysis** (%) calcd. for $C_{22}H_{17}N_5O_4Pt$: C 43.28, H 2.81, N 11.47; found (%): C 42.85, H 2.82, N 11.03.

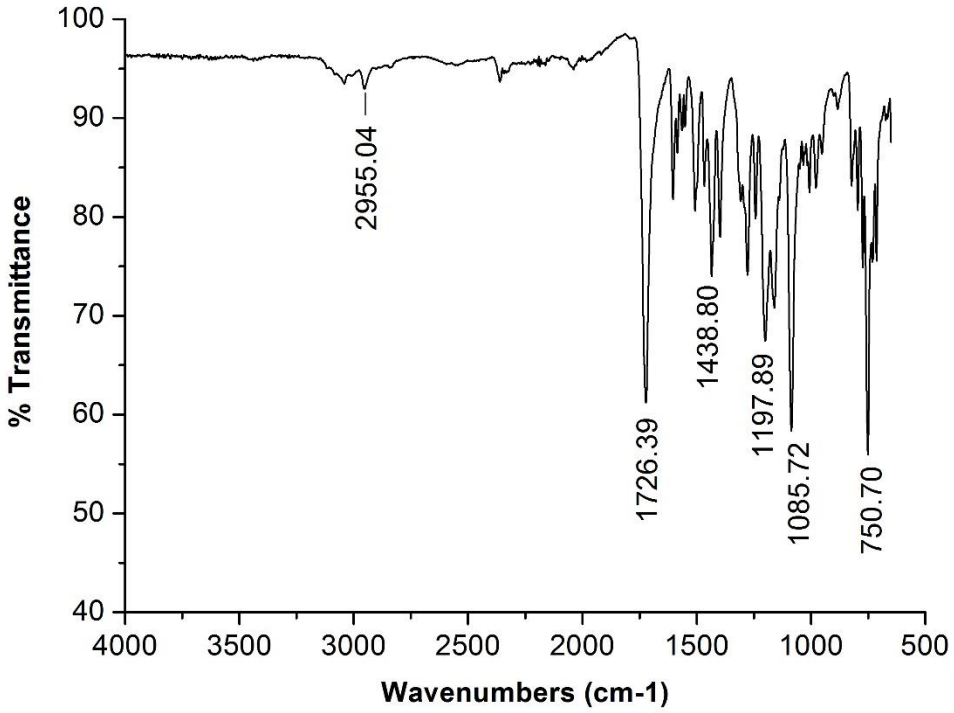
100
90
80
70
60
50
40
% Transmittance
2955.04
1726.39
1438.80
1197.89
1085.72
750.70
4000
3500
3000
2500
2000
1500
1000
500
Wavenumbers (cm-1)

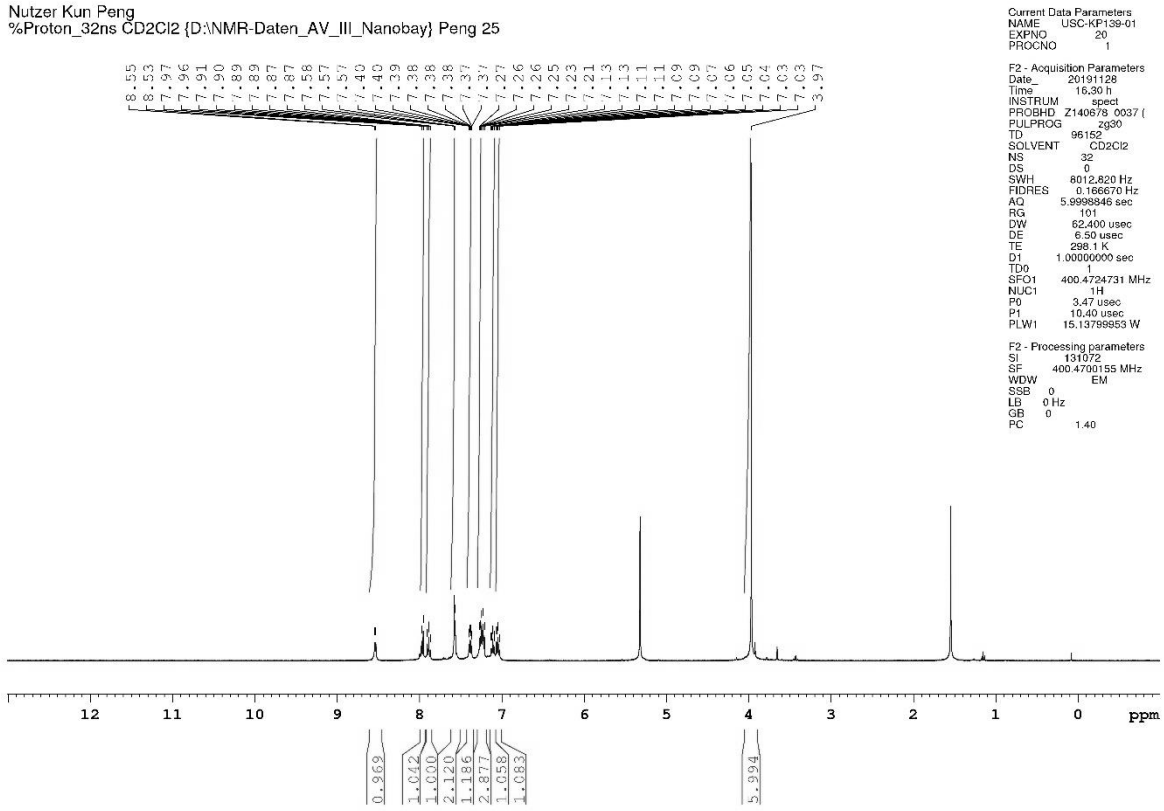
Nutzer Kun Peng
%Proton_32ns CD2Cl2 {D:\NMR-Daten_AV_III_Nanobay} Peng 25
Current Data Parameters
NAME USC-KP139-01
EXPNO 20
PROCNO 1
F2 - Acquisition Parameters
Date_ 20191128
Time 16.30 h
INSTRUM spect
PROBHD Z140678_0037 (
PULPROG zg30
TD 96152
SOLVENT CD2Cl2
NS 32
DS 0
SWH 8012.820 Hz
FIDRES 0.166670 Hz
AQ 5.9998846 sec
RG 101
DW 62.400 usec
DE 6.50 usec
TE 298.1 K
D1 1.00000000 sec
TD0 1
SFO1 400.4724731 MHz
NUC1 1H
P0 3.47 usec
P1 10.40 usec
PLW1 15.13799953 W
F2 - Processing parameters
SI 131072
SF 400.4700155 MHz
WDW EM
SSB 0
LB 0 Hz
GB 0
PC 1.40
8.55
8.53
7.97
7.96
7.91
7.90
7.89
7.89
7.87
7.87
7.58
7.57
7.57
7.40
7.40
7.39
7.38
7.38
7.38
7.37
7.37
7.27
7.26
7.26
7.25
7.23
7.21
7.13
7.13
7.11
7.11
7.09
7.09
7.07
7.06
7.05
7.04
7.03
7.03
3.97
12
11
10
9
8
7
6
5
4
3
2
1
0
ppm
0.969
1.042
1.000
2.120
1.186
2.877
1.058
1.083
5.994

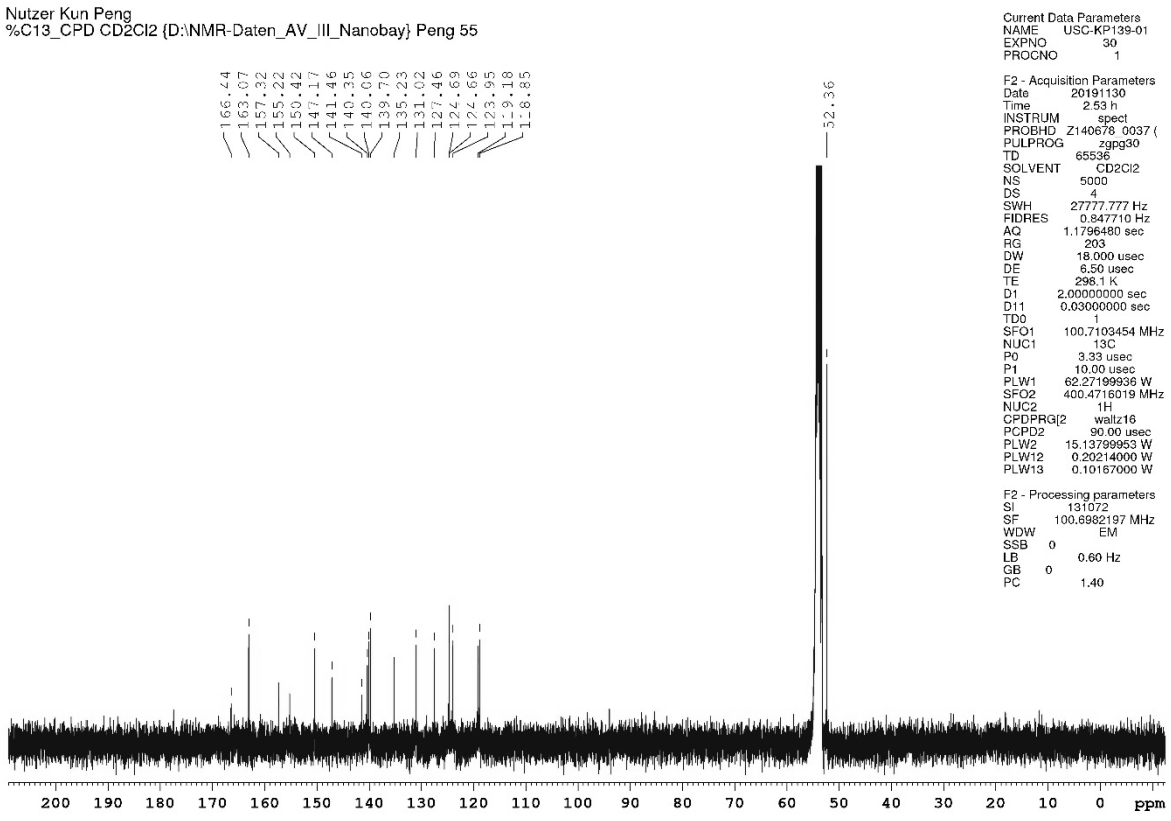
Nutzer Kun Peng
%C13_CPD CD2Cl2 {D:\NMR-Daten_AV_III_Nanobay} Peng 55
166.44
163.07
157.32
155.22
150.42
147.17
141.46
140.35
140.06
139.70
135.23
131.02
127.46
124.69
124.66
123.95
119.18
118.85
52.36
Current Data Parameters
NAME USC-KP139-01
EXPNO 30
PROCNO 1
F2 - Acquisition Parameters
Date 20191130
Time 2.53 h
INSTRUM spect
PROBHD Z140678_0037 (
PULPROG zgpg30
TD 65536
SOLVENT CD2Cl2
NS 5000
DS 4
SWH 27777.777 Hz
FIDRES 0.847710 Hz
AQ 1.1796480 sec
RG 203
DW 18.000 usec
DE 6.50 usec
TE 298.1 K
D1 2.00000000 sec
D11 0.03000000 sec
TD0 1
SFO1 100.7103454 MHz
NUC1 13C
P0 3.33 usec
P1 10.00 usec
PLW1 62.27199936 W
SFO2 400.4716019 MHz
NUC2 1H
CPDPRG[2 waltz16
PCPD2 90.00 usec
PLW2 15.13799953 W
PLW12 0.20214000 W
PLW13 0.10167000 W
F2 - Processing parameters
SI 131072
SF 100.6982197 MHz
WDW EM
SSB 0
LB 0.60 Hz
GB 0
PC 1.40
200 190 180 170 160 150 140 130 120 110 100 90 80 70 60 50 40 30 20 10 0 ppm

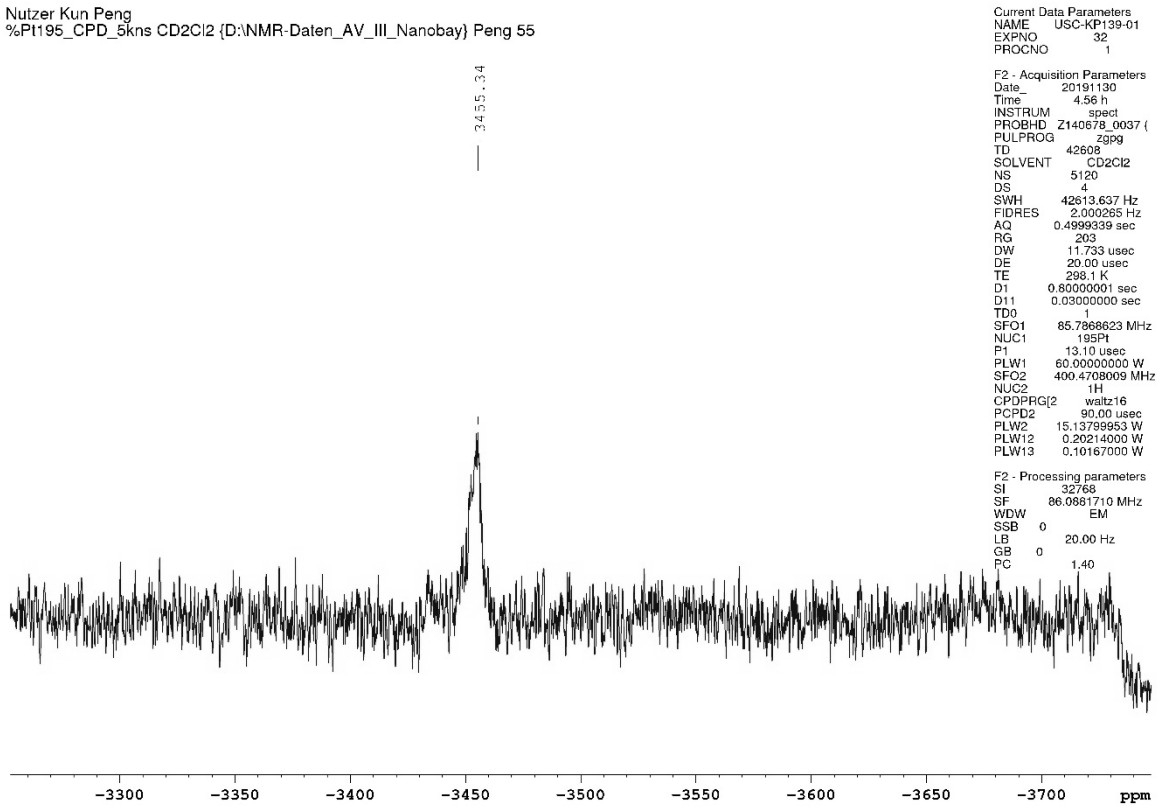
Nutzer Kun Peng
%Pt195_CPD_5kns CD2Cl2 {D:\NMR-Daten_AV_III_Nanobay} Peng 55
3455.34
Current Data Parameters
NAME USC-KP139-01
EXPNO 32
PROCNO 1
F2 - Acquisition Parameters
Date_ 20191130
Time 4.56 h
INSTRUM spect
PROBHD Z140678_0037 (
PULPROG zgpg
TD 42608
SOLVENT CD2Cl2
NS 5120
DS 4
SWH 42613.637 Hz
FIDRES 2.000265 Hz
AQ 0.4999339 sec
RG 203
DW 11.733 usec
DE 20.00 usec
TE 298.1 K
D1 0.60000001 sec
D11 0.03000000 sec
TD0 1
SFO1 85.7868623 MHz
NUC1 195Pt
P1 13.10 usec
PLW1 60.00000000 W
SFO2 400.4708009 MHz
NUC2 1H
CPDPRG[2 waltz16
PCPD2 90.00 usec
PLW2 15.13799953 W
PLW12 0.20214000 W
PLW13 0.10167000 W
F2 - Processing parameters
SI 32768
SF 86.0861710 MHz
WDW EM
SSB 0
LB 20.00 Hz
GB 0
PC 1.40
-3300 -3350 -3400 -3450 -3500 -3550 -3600 -3650 -3700 ppm

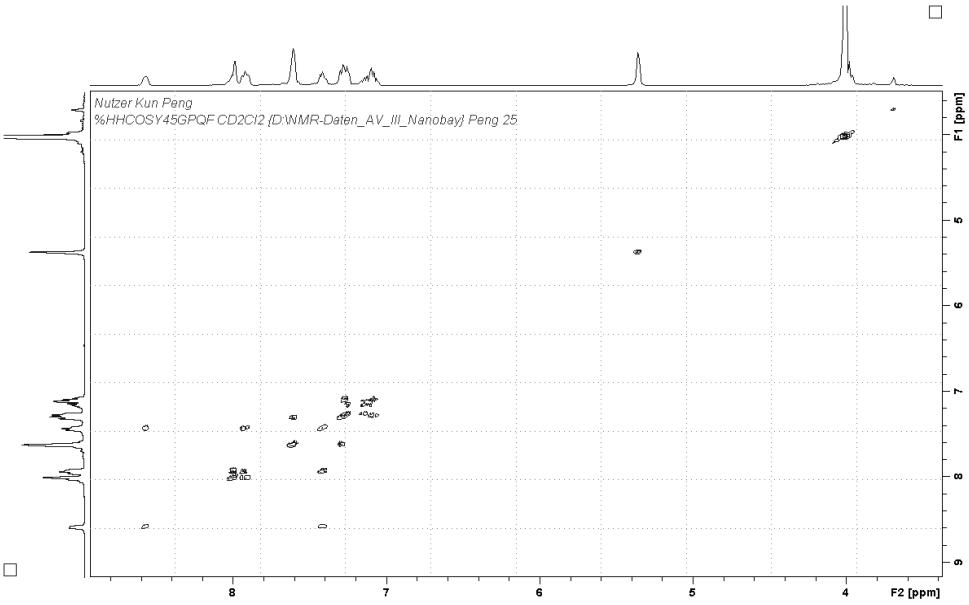
Nutzer Kun Peng
%HHCOSY45GPQF CD2Cl2 {D:\NMR-Daten_AV_III_Nanobay} Peng 25
F1 [ppm]
F2 [ppm]

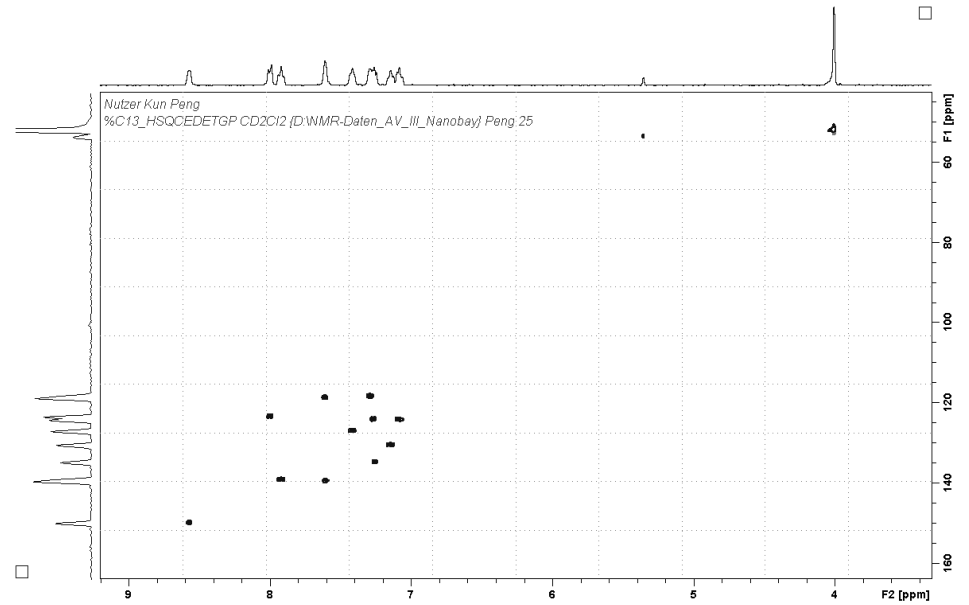
Nutzer Kun Peng
%C13_HSQCEDETGP CD2Cl2 {D:\NMR-Daten_AV_III_Nanobay} Peng 25
F1 [ppm]
F2 [ppm]

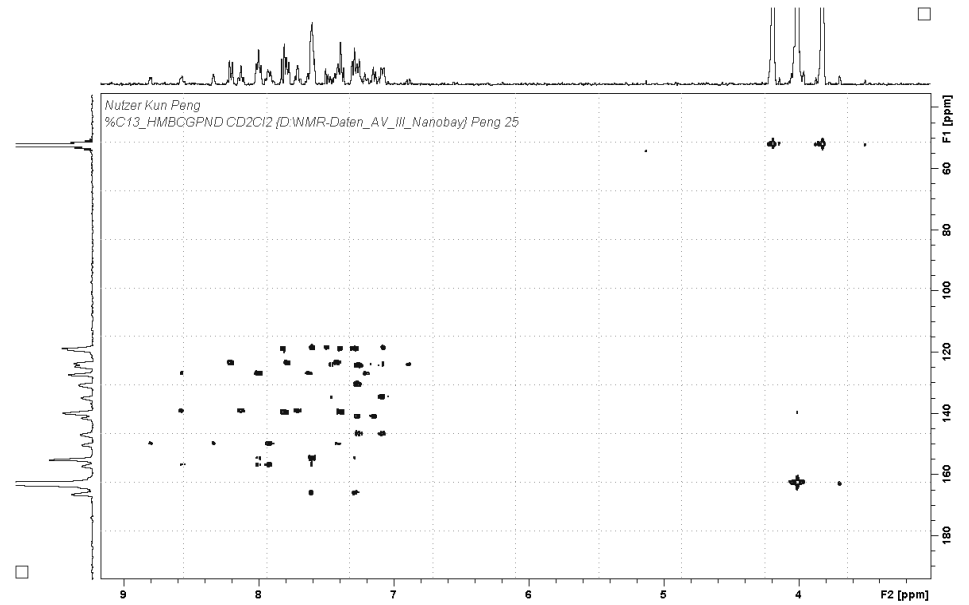
Nutzer Kun Peng
%C13_HMBCGPND CD2Cl2 {D:\NMR-Daten_AV_III_Nanobay} Peng 25
F1 [ppm]
F2 [ppm]

5.3.25 Synthesis of [Pd(phbpy)(triazolate^{CF3,COOEt})]

USC-KP136-03

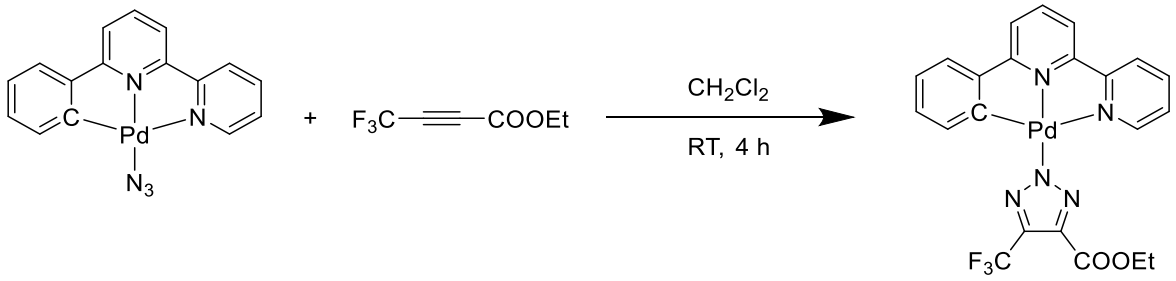

$C_{16}H_{11}N_5Pd$ 379.71 g/mol

$C_6H_5F_3O_2$ 166.10 g/mol

$C_{22}H_{16}F_3N_5O_2Pd$ 545.81 g/mol

[Pd(N_3)(phbpy)] (21.6 mg, 0.06 mmol) was suspended in dichloromethane (10 mL), and 4,4,4-trifluoro-2-butynoic acid ethyl ester (15 µL, 19.1 mg, 0.11 mmol) was added. The mixture was stirred at room temperature for 4 h. It was then concentrated to approx. 5 mL and diethyl ether (15 mL) was added to give a yellow solid, which was filtered off and dried under vacuum for 4 d. Yield: 83% (27.1 mg, 0.05 mmol). **IR** (ATR): $\tilde{\nu}$ = 3078 (w), 1710 (s), 1600 (w), 1465 (w), 1434 (m), 1310 (s), 1188 (m), 1125 (m), 1053 (s), 758 (s) cm^{-1}; **^{1}H NMR** (400.47 MHz, CD_2Cl_2): δ = 8.58 (d, 1H, $^3J_{H6,H5}$ = 5.2 Hz, H6), 8.02 (d, 1H, $^3J_{H3,H4}$ = 7.9 Hz, H3), 7.94 (dt, 1H, $^3J_{H4,H3/H5}$ = 7.9 Hz, $^4J_{H4,H6}$ = 1.3 Hz, H4), 7.80 (t, 1H, $^3J_{H4',H3'/H5'}$ = 7.9 Hz, H4'), 7.69 (d, 1H, $^3J_{H4',H3'/H5'}$ = 7.6 Hz, H3'), 7.48 (d, 1H, $^3J_{H5',H4'}$ = 8.2 Hz, H5'), 7.44 (t, 1H, $^3J_{H5,H4/H6}$ = 6.5 Hz, H5), 7.37−7.34 (m, 2H, H2"/H5"), 7.12−7.09 (m, 2H, H3"/H4"), 4.43 (q, 2H, ^3J = 7.1 Hz, COOCH_2CH$_3$), 1.43 (t, 3H, ^3J = 7.1 Hz, COOCH$_2$CH_3) ppm; **^{13}C NMR** (100.70 MHz, CD_2Cl_2): δ = 161.42 (*C*OOEt), 155.85 (C2), 153.71 (C2'), 151.25 (C6"), 148.08 (C6), 140.33 (C4'), 139.98 (C4), 136.05 (C5"), 130.86 (C4"), 127.21 (C5), 125.72 (C3"), 124.49 (C2"), 122.80 (C3), 119.68 (C5'), 119.27 (C3'), 61.24 (*C*H$_2$CH$_3$), 14.43 (CH$_2$*C*H$_3$) ppm (other carbon atoms were not observed due to low solubility of this complex); **^{19}F NMR** (376.82 MHz, CD_2Cl_2): δ = -59.84 (C*F*$_3$) ppm; **Elemental analysis** (%) calcd. for $C_{22}H_{16}F_3N_5O_2Pd$: C 48.41, H 2.96, N 12.83; found (%): C 48.59, H 3.16, N 12.82.

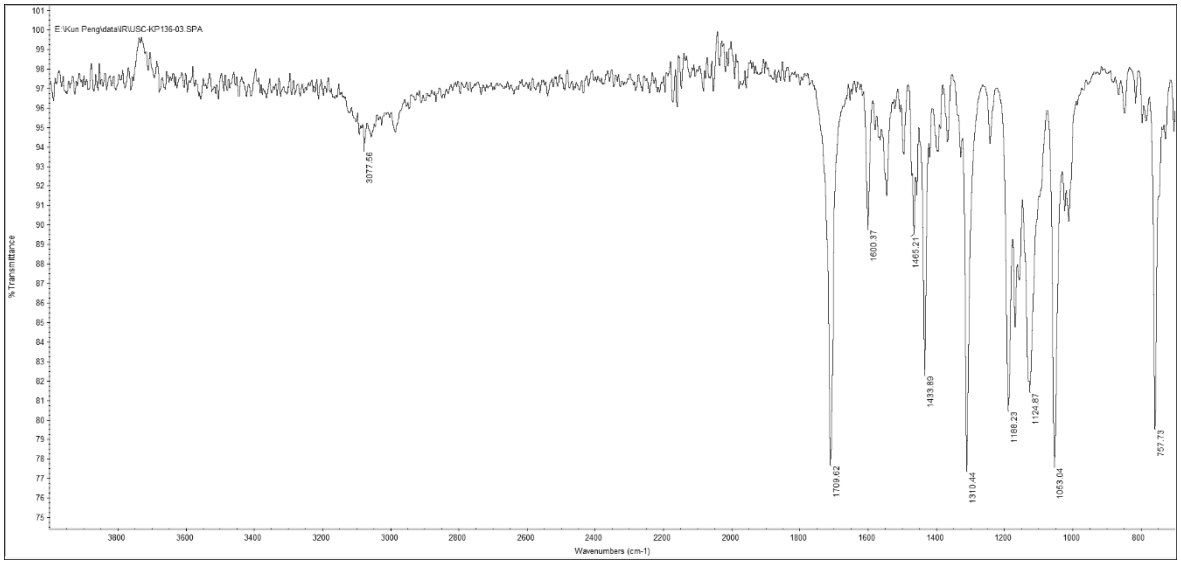
E:\Kun Peng\data\IR\USC-KP136-03.SPA
% Transmittance
Wavenumbers (cm-1)
3077.56
1709.62
1600.37
1465.21
1433.89
1310.44
1188.23
1124.87
1055.04
757.73

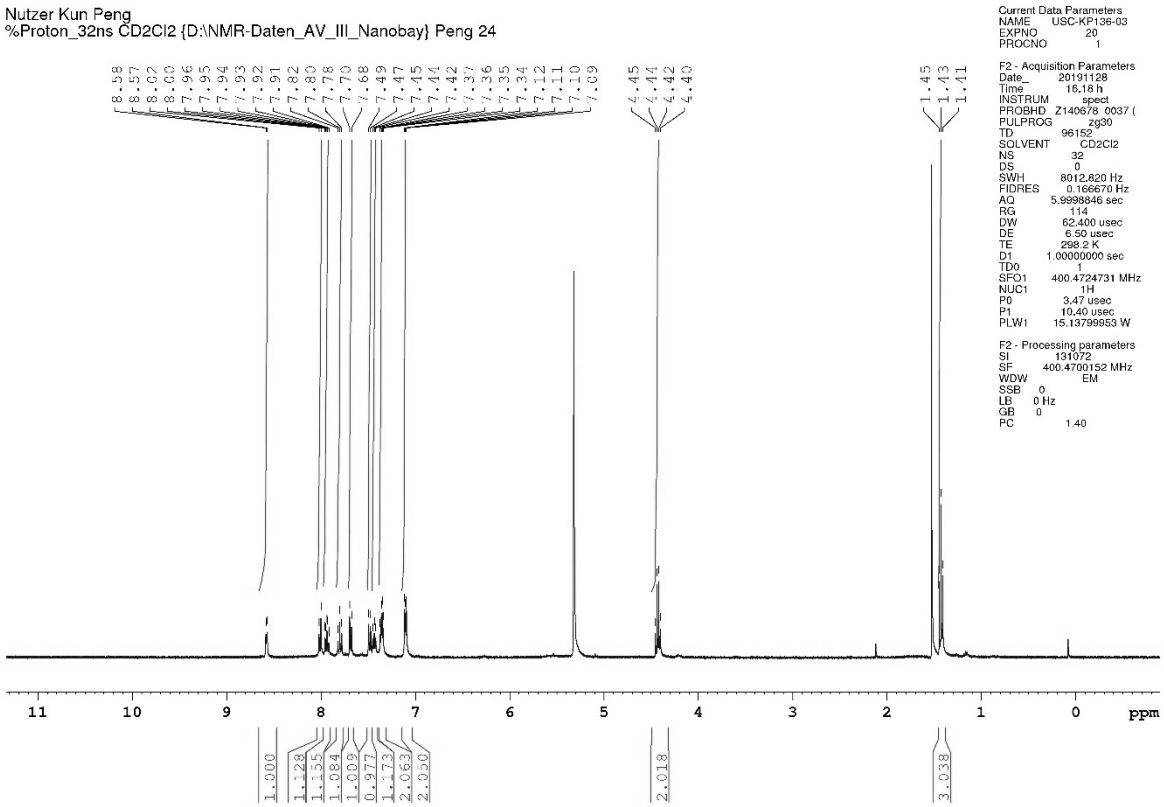
Nutzer Kun Peng
%Proton_32ns CD2Cl2 {D:\NMR-Daten_AV_III_Nanobay} Peng 24
Current Data Parameters
NAME USC-KP136-03
EXPNO 20
PROCNO 1
F2 - Acquisition Parameters
Date_ 20191128
Time 16.18 h
INSTRUM spect
PROBHD Z140678 0037 (
PULPROG zg30
TD 96152
SOLVENT CD2Cl2
NS 32
DS 0
SWH 8012.820 Hz
FIDRES 0.166670 Hz
AQ 5.9998846 sec
RG 114
DW 62.400 usec
DE 6.50 usec
TE 298.2 K
D1 1.00000000 sec
TD0 1
SFO1 400.4724731 MHz
NUC1 1H
P0 3.47 usec
P1 10.40 usec
PLW1 15.13799953 W
F2 - Processing parameters
SI 131072
SF 400.4700152 MHz
WDW EM
SSB 0
LB 0 Hz
GB 0
PC 1.40
8.58
8.57
8.02
8.00
7.96
7.95
7.94
7.93
7.92
7.91
7.82
7.80
7.78
7.70
7.68
7.49
7.47
7.45
7.44
7.42
7.37
7.36
7.35
7.34
7.12
7.11
7.10
7.09
4.45
4.44
4.42
4.40
1.45
1.43
1.41
11
10
9
8
7
6
5
4
3
2
1
0
ppm
1.000
1.128
1.155
1.084
1.009
0.977
1.173
2.063
2.050
2.018
3.038

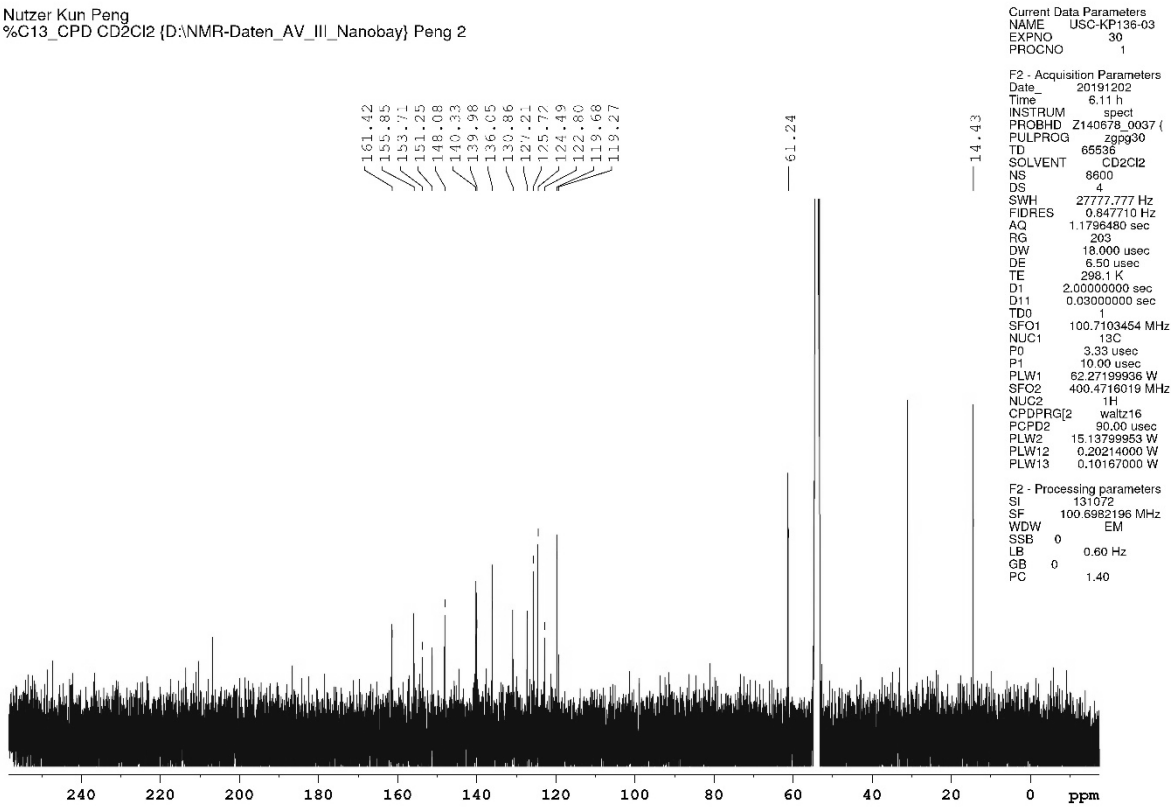
Nutzer Kun Peng
%C13_CPD CD2Cl2 {D:\NMR-Daten_AV_III_Nanobay} Peng 2
161.42
155.85
153.71
151.25
148.08
140.33
139.98
136.05
130.86
125.72
124.49
122.80
119.68
119.27
61.24
14.43
Current Data Parameters
NAME USC-KP136-03
EXPNO 30
PROCNO 1
F2 - Acquisition Parameters
Date 20191202
Time 6.11 h
INSTRUM spect
PROBHD Z140678_0037 (
PULPROG zgpg30
TD 65536
SOLVENT CD2Cl2
NS 8600
DS 4
SWH 27777.777 Hz
FIDRES 0.847710 Hz
AQ 1.1796480 sec
RG 203
DW 18.000 usec
DE 6.50 usec
TE 298.1 K
D1 2.00000000 sec
D11 0.03000000 sec
TD0 1
SFO1 100.7103454 MHz
NUC1 13C
P0 3.33 usec
P1 10.00 usec
PLW1 62.27199936 W
SFO2 400.4716019 MHz
NUC2 1H
CPDPRG[2 waltz16
PCPD2 90.00 usec
PLW2 15.13799953 W
PLW12 0.20214000 W
PLW13 0.10167000 W
F2 - Processing parameters
SI 131072
SF 100.6982196 MHz
WDW EM
SSB 0
LB 0.60 Hz
GB 0
PC 1.40
240
220
200
180
160
140
120
100
80
60
40
20
0
ppm

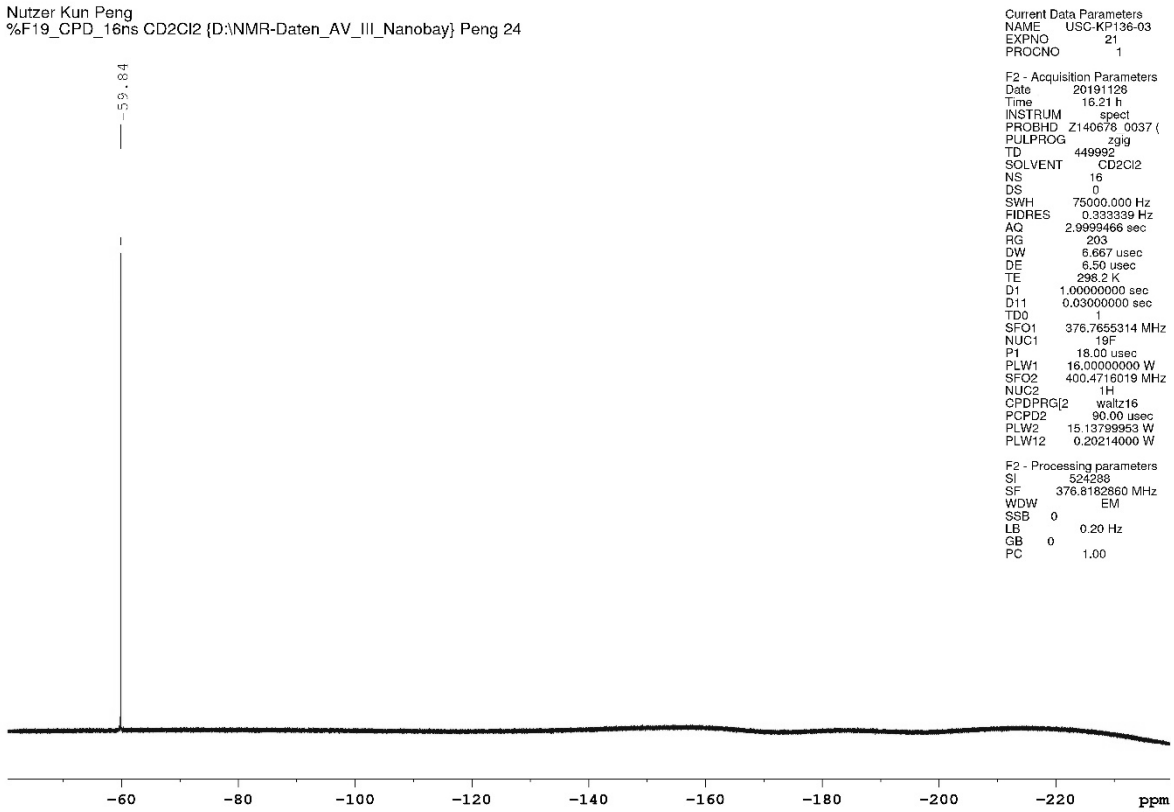
Nutzer Kun Peng
%F19_CPD_16ns CD2Cl2 {D:\NMR-Daten_AV_III_Nanobay} Peng 24
-59.84
Current Data Parameters
NAME USC-KP136-03
EXPNO 21
PROCNO 1
F2 - Acquisition Parameters
Date 20191126
Time 16.21 h
INSTRUM spect
PROBHD Z140678_0037 (
PULPROG zgig
TD 449992
SOLVENT CD2Cl2
NS 16
DS 0
SWH 75000.000 Hz
FIDRES 0.333339 Hz
AQ 2.9999466 sec
RG 203
DW 6.667 usec
DE 6.50 usec
TE 298.2 K
D1 1.00000000 sec
D11 0.03000000 sec
TD0 1
SFO1 376.7655314 MHz
NUC1 19F
P1 18.00 usec
PLW1 16.00000000 W
SFO2 400.4716019 MHz
NUC2 1H
CPDPRG[2 waltz16
PCPD2 90.00 usec
PLW2 15.13799953 W
PLW12 0.20214000 W
F2 - Processing parameters
SI 524288
SF 376.8182860 MHz
WDW EM
SSB 0
LB 0.20 Hz
GB 0
PC 1.00
-60
-80
-100
-120
-140
-160
-180
-200
-220
ppm

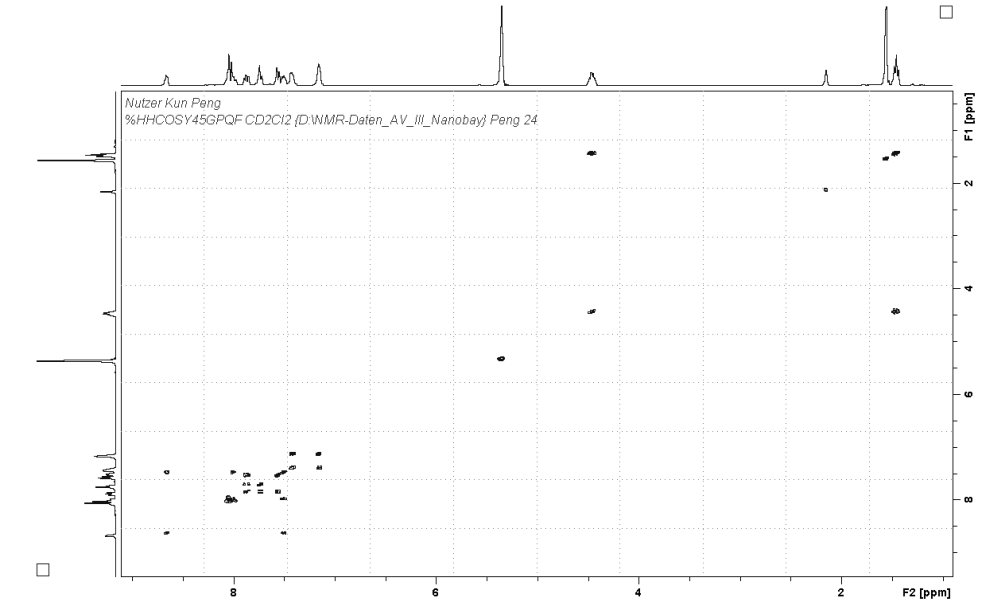
Nutzer Kun Peng
%HHCOSY45GPQF CD2Cl2 {D:\NMR-Daten_AV_III_Nanobay} Peng 24
F1 [ppm]
F2 [ppm]

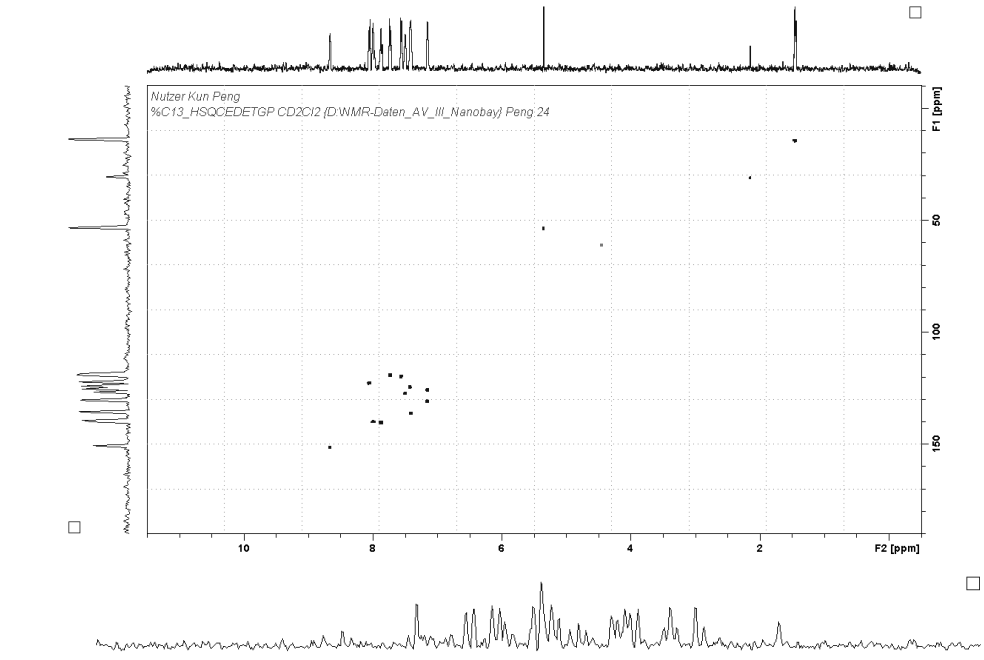
Nutzer Kun Peng
%C13_HSQCEDETGP CD2Cl2 {D:\NMR-Daten_AV_III_Nanobay} Peng 24
F1 [ppm]
F2 [ppm]

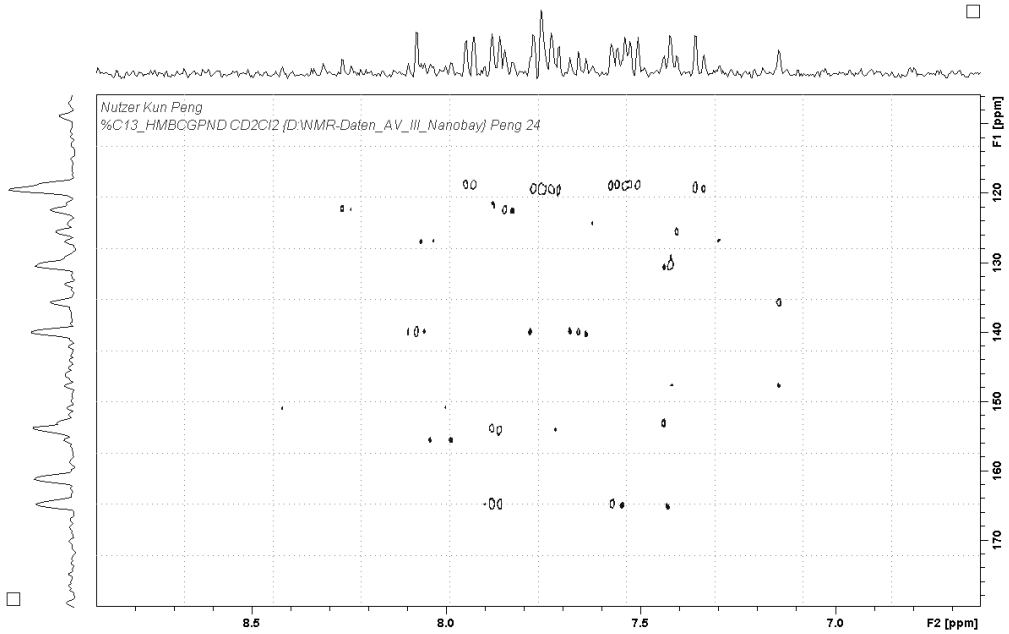
Nutzer Kun Peng
%C13_HMBCGPND CD2Cl2 {D:\NMR-Daten_AV_III_Nanobay} Peng 24
F1 [ppm]
F2 [ppm]

5.3.26 Synthesis of [Pt(phbpy)(triazolate^{CF3,COOEt})]

USC-KP140-02

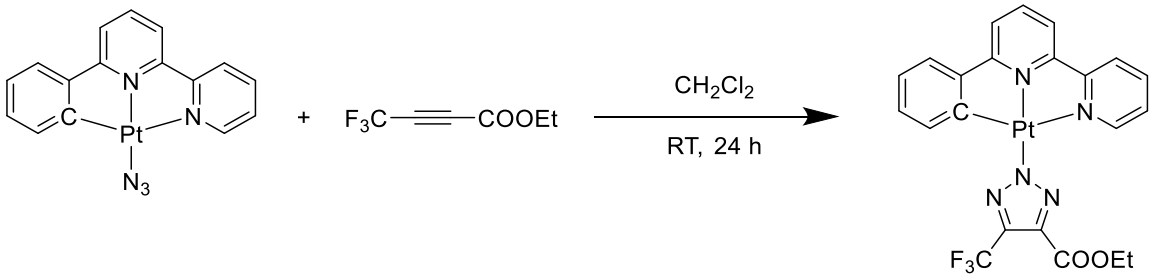

$C_{16}H_{11}N_5Pt$
468.37 g/mol

$C_6H_5F_3O_2$
166.10 g/mol

$C_{22}H_{16}F_3N_5O_2Pt$
634.47 g/mol

[Pt(N_3)(phbpy)] (17.1 mg, 0.04 mmol) was suspended in dichloromethane (10 mL), and 4,4,4-trifluoro-2-butynoic acid ethyl ester (6.6 µL, 8.4 mg, 0.05 mmol) was added. The mixture was stirred at room temperature for 24 h. It was then concentrated to approx. 4 mL and diethyl ether (25 mL) was added to give an orange precipitate, which was filtered off, washed with diethyl ether (5 mL), and dried under vacuum for 5 d. Yield: 75% (18.2 mg, 0.03 mmol). **IR** (ATR): $\tilde{\nu}$ = 3061 (w), 1709 (m), 1439 (m), 1309 (m), 1186 (m), 1127 (m), 1045 (s), 751 (s) cm^{-1}; **^{1}H NMR** (400.47 MHz, CD_2Cl_2): δ = 8.78 (d, 1H, $^3J_{H6,H5}$ = 5.4 Hz, H6), 8.02−7.94 (m, 2H, H3/H4), 7.72 (t, 1H, $^3J_{H4',H3'/H5'}$ = 8.0 Hz, H4'), 7.59 (d, 1H, $^3J_{H4',H3'/H5'}$ = 7.8 Hz, H3'), 7.53 (t, 1H, $^3J_{H5,H4/H6}$ = 6.4 Hz, H5), 7.41 (d, 1H, $^3J_{H5',H4'}$ = 8.2 Hz, H5'), 7.33−7.30 (m, 2H, H2"/H5"), 7.15 (t, 1H, $^3J_{H4",H3"/H5"}$ = 7.4 Hz, H4"), 7.09 (t,1H, $^3J_{H3",H2"/H4"}$ = 7.3 Hz, H3"), 4.44 (q, 2H, ^3J = 7.1 Hz, COOCH_2CH$_3$), 1.44 (t, 3H, ^3J = 7.2 Hz, COOCH$_2$CH_3) ppm; **^{13}C NMR** (100.70 MHz, CD_2Cl_2): δ = 150.87 (C6), 140.26 (C4'), 139.95 (C4), 135.29 (C5"), 131.29 (C4"), 127.80 (C5), 124.92 (C3"), 124.82 (C2"), 123.49 (C3), 119.05 (C5'), 118.66 (C3'), 61.36 (COOCH$_2$CH$_3$), 14.40 (COOCH$_2$$CH_3$) ppm (all quaternary carbon atoms were not observed due to low solubility of this complex); **^{19}F NMR** (376.82 MHz, CD_2Cl_2): δ = -59.97 (CF_3) ppm; **^{195}Pt NMR** (86.09 MHz, CD_2Cl_2): δ = -3463 ppm; **Elemental analysis** (%) calcd. for $C_{22}H_{16}F_3N_5O_2Pt$: C 41.65, H 2.54, N 11.04; found (%): C 41.50, H 2.52, N 10.54.

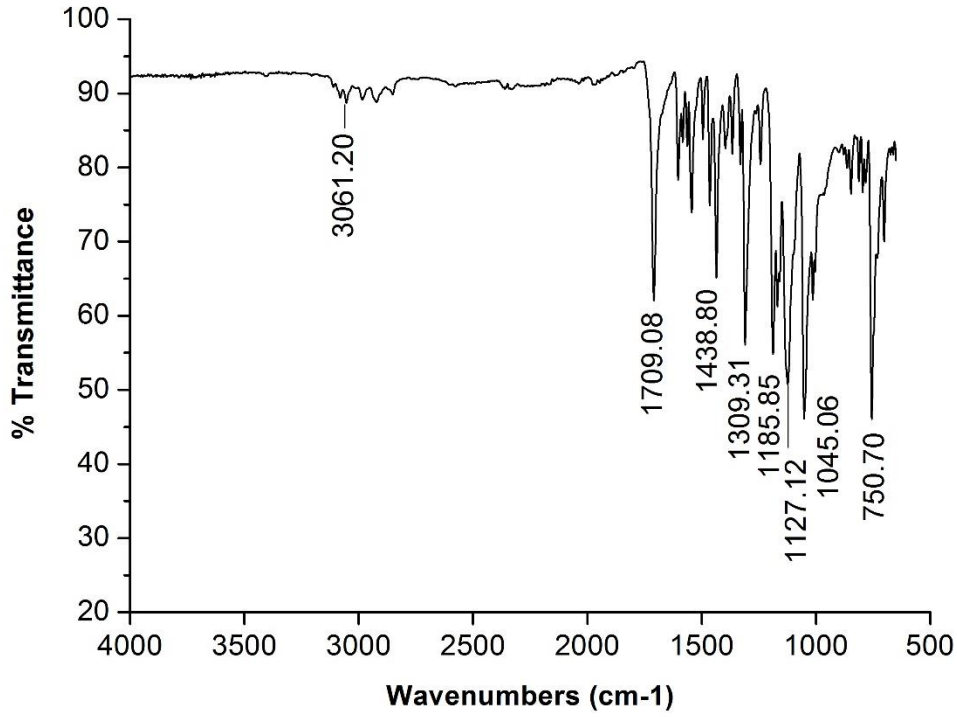
% Transmittance
Wavenumbers (cm-1)
3061.20
1709.08
1438.80
1309.31
1185.85
1127.12
1045.06
750.70

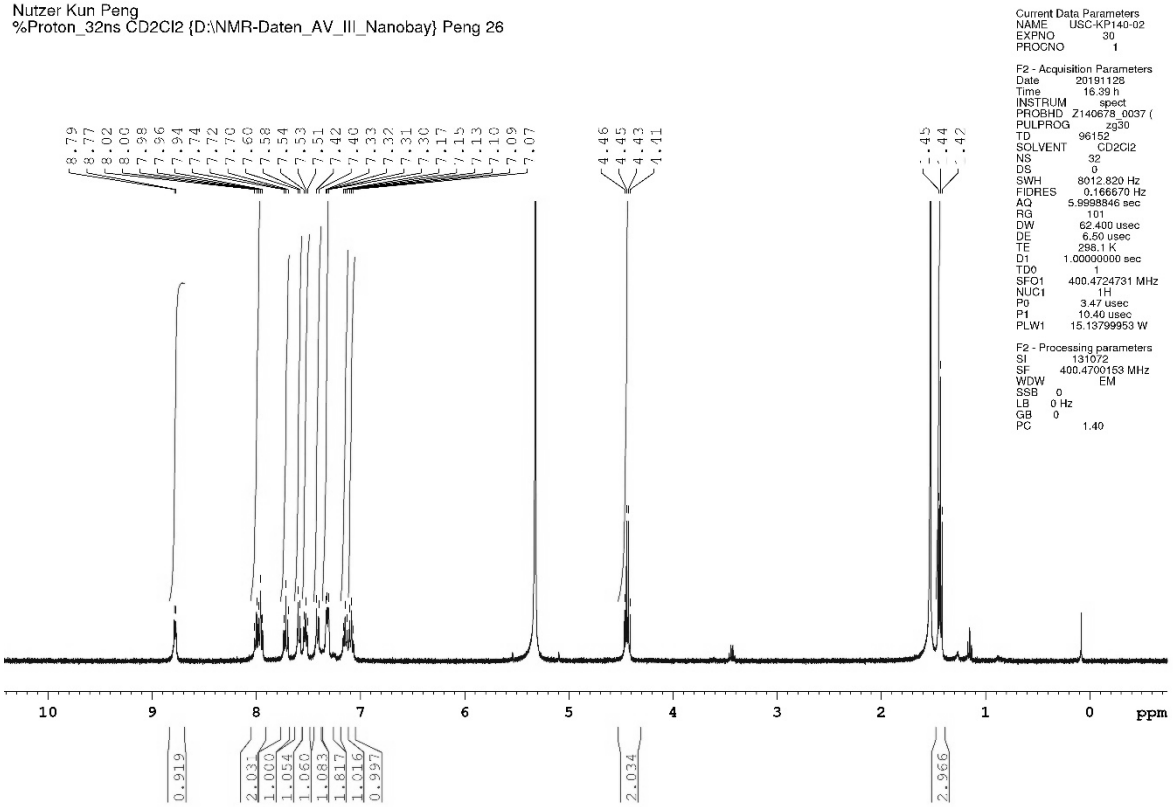
Nutzer Kun Peng
%Proton_32ns CD2Cl2 {D:\NMR-Daten_AV_III_Nanobay} Peng 26
Current Data Parameters
NAME USC-KP140-02
EXPNO 30
PROCNO 1
F2 - Acquisition Parameters
Date 20191126
Time 16.39 h
INSTRUM spect
PROBHD Z140678_0037 (
PULPROG zg30
TD 96152
SOLVENT CD2Cl2
NS 32
DS 0
SWH 8012.820 Hz
FIDRES 0.166670 Hz
AQ 5.9998846 sec
RG 101
DW 62.400 usec
DE 6.50 usec
TE 298.1 K
D1 1.00000000 sec
TD0 1
SFO1 400.4724731 MHz
NUC1 1H
P0 3.47 usec
P1 10.40 usec
PLW1 15.13799953 W
F2 - Processing parameters
SI 131072
SF 400.4700153 MHz
WDW EM
SSB 0
LB 0 Hz
GB 0
PC 1.40
8.79
8.77
8.02
8.00
7.98
7.96
7.94
7.74
7.72
7.70
7.60
7.58
7.54
7.53
7.51
7.42
7.40
7.33
7.32
7.31
7.30
7.17
7.15
7.13
7.10
7.09
7.07
4.46
4.45
4.43
4.41
10
9
8
7
6
5
4
3
2
1
0
ppm
0.919
2.03
1.000
1.054
1.060
1.083
1.817
1.016
0.997
2.034
2.966

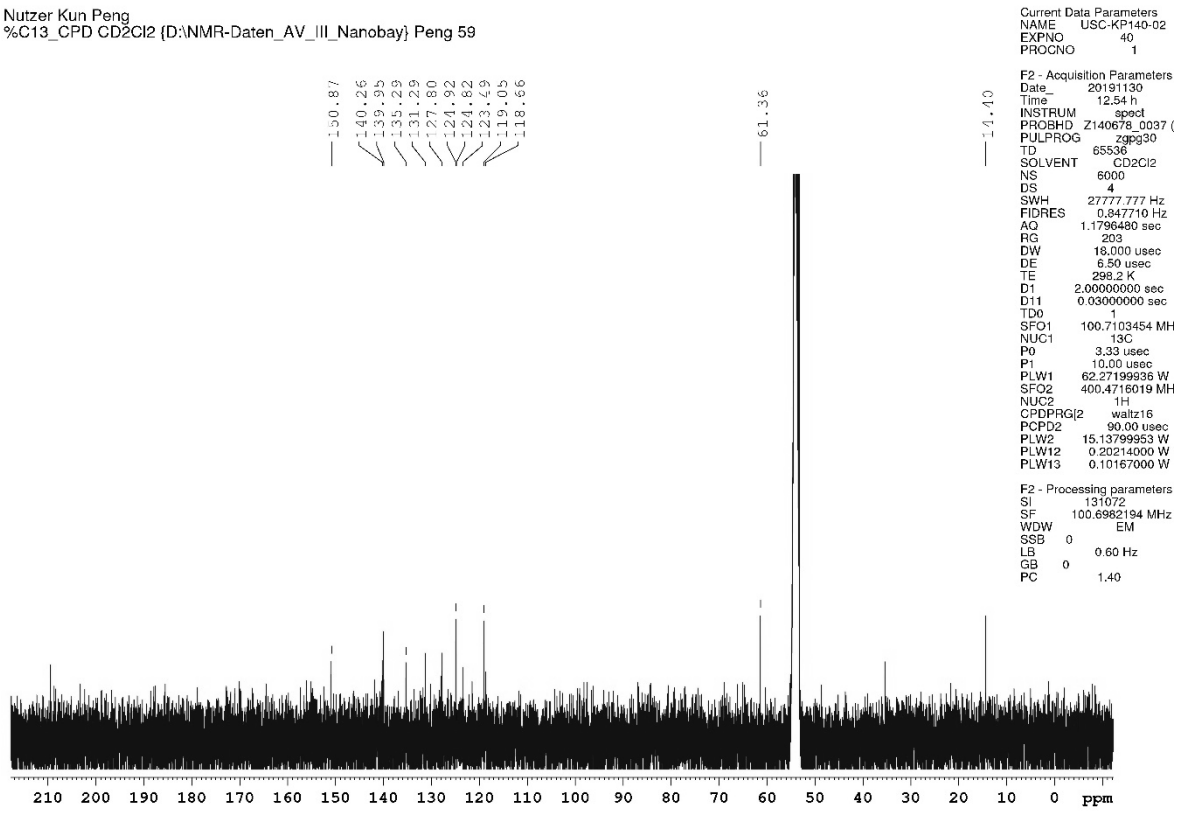
Nutzer Kun Peng
%C13_CPD CD2Cl2 {D:\NMR-Daten_AV_III_Nanobay} Peng 59
150.87
140.26
139.95
135.29
131.29
127.80
124.92
124.82
123.49
119.05
118.66
61.36
14.19
Current Data Parameters
NAME USC-KP140-02
EXPNO 40
PROCNO 1
F2 - Acquisition Parameters
Date_ 20191130
Time 12.54 h
INSTRUM spect
PROBHD Z140678_0037 (
PULPROG zgpg30
TD 65536
SOLVENT CD2Cl2
NS 6000
DS 4
SWH 27777.777 Hz
FIDRES 0.847710 Hz
AQ 1.1796480 sec
RG 203
DW 18.000 usec
DE 6.50 usec
TE 298.2 K
D1 2.00000000 sec
D11 0.03000000 sec
TD0 1
SFO1 100.7103454 MH
NUC1 13C
P0 3.33 usec
P1 10.00 usec
PLW1 62.27199936 W
SFO2 400.4716019 MH
NUC2 1H
CPDPRG[2 waltz16
PCPD2 90.00 usec
PLW2 15.13799953 W
PLW12 0.20214000 W
PLW13 0.10167000 W
F2 - Processing parameters
SI 131072
SF 100.6982194 MHz
WDW EM
SSB 0
LB 0.60 Hz
GB 0
PC 1.40
210 200 190 180 170 160 150 140 130 120 110 100 90 80 70 60 50 40 30 20 10 0 ppm

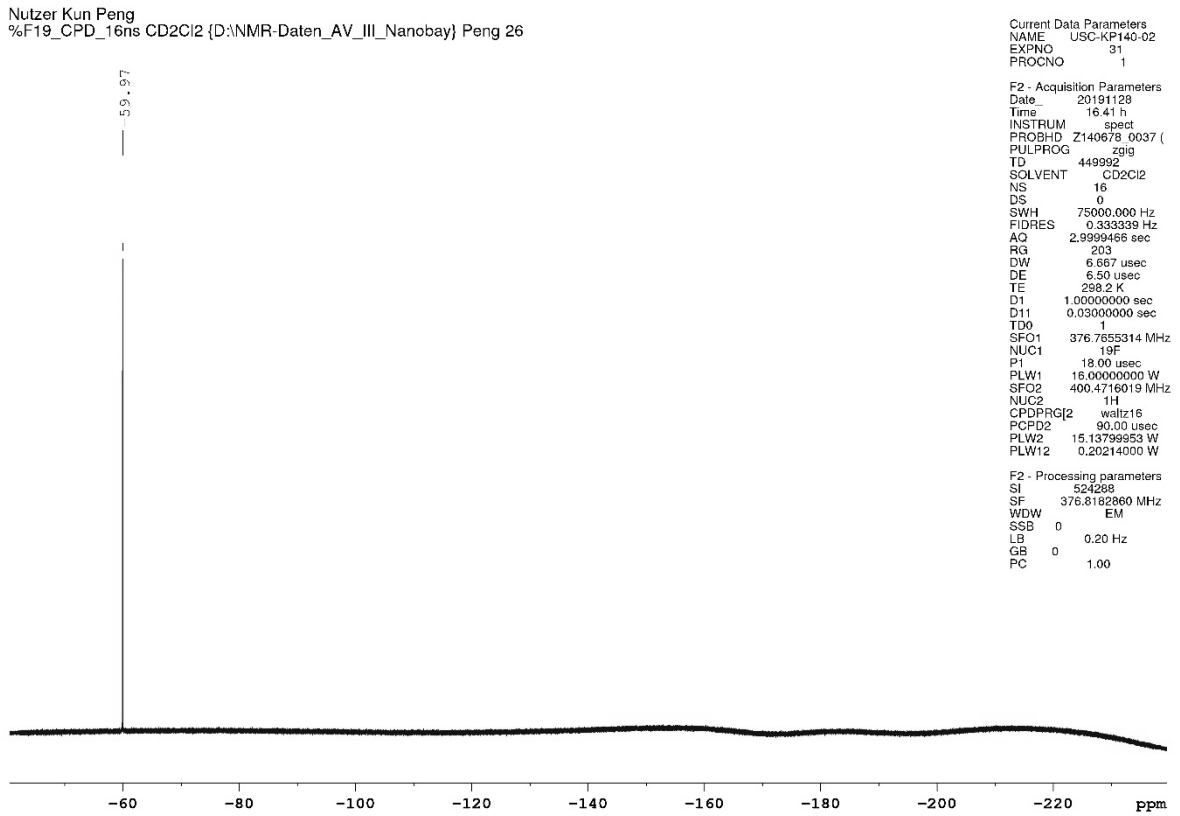
Nutzer Kun Peng
%F19_CPD_16ns CD2Cl2 {D:\NMR-Daten_AV_III_Nanobay} Peng 26
59.97
Current Data Parameters
NAME USC-KP140-02
EXPNO 31
PROCNO 1
F2 - Acquisition Parameters
Date_ 20191128
Time 16.41 h
INSTRUM spect
PROBHD Z140678_0037 (
PULPROG zgig
TD 449992
SOLVENT CD2Cl2
NS 16
DS 0
SWH 75000.000 Hz
FIDRES 0.333339 Hz
AQ 2.9999466 sec
RG 203
DW 6.667 usec
DE 6.50 usec
TE 298.2 K
D1 1.00000000 sec
D11 0.03000000 sec
TD0 1
SFO1 376.7655314 MHz
NUC1 19F
P1 18.00 usec
PLW1 16.00000000 W
SFO2 400.4716019 MHz
NUC2 1H
CPDPRG[2 waltz16
PCPD2 90.00 usec
PLW2 15.13799953 W
PLW12 0.20214000 W
F2 - Processing parameters
SI 524288
SF 376.8182860 MHz
WDW EM
SSB 0
LB 0.20 Hz
GB 0
PC 1.00
-60 -80 -100 -120 -140 -160 -180 -200 -220 ppm

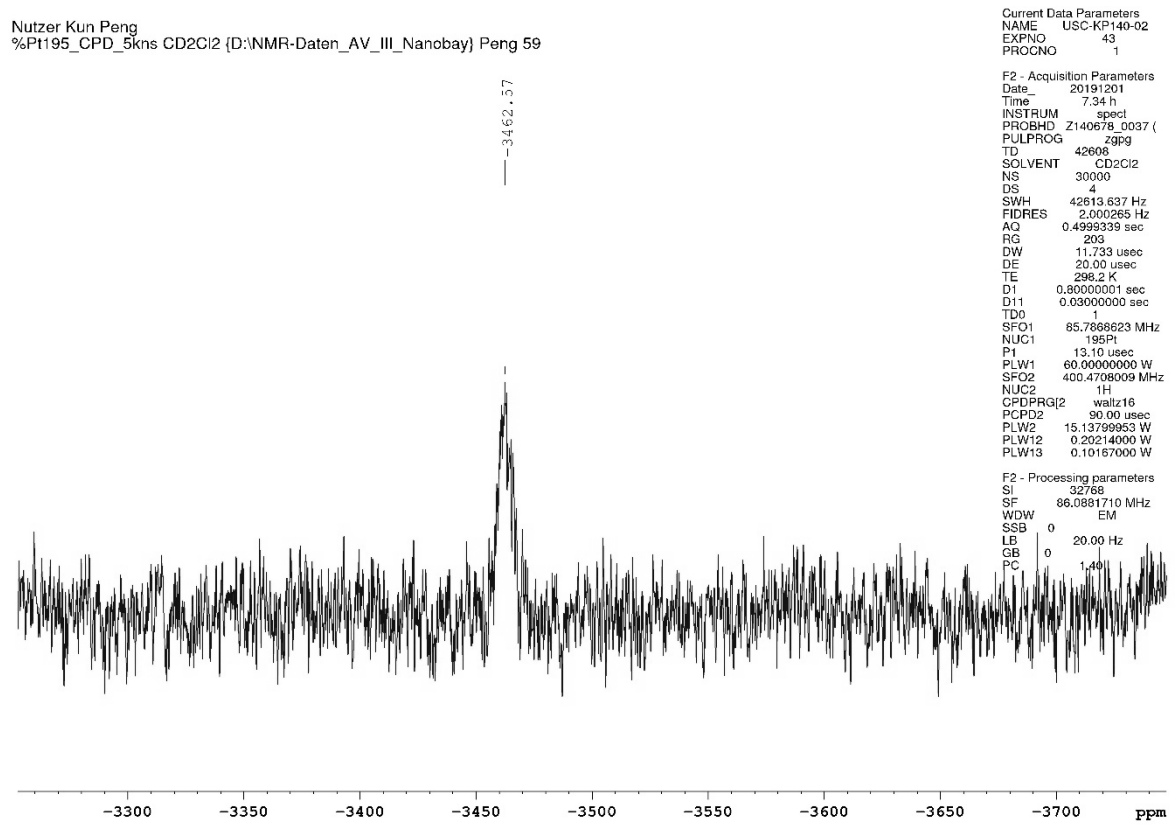
Nutzer Kun Peng
%Pt195_CPD_5kns CD2Cl2 {D:\NMR-Daten_AV_III_Nanobay} Peng 59
-3462.57
Current Data Parameters
NAME USC-KP140-02
EXPNO 43
PROCNO 1
F2 - Acquisition Parameters
Date_ 20191201
Time 7.34 h
INSTRUM spect
PROBHD Z140678_0037 (
PULPROG zgpg
TD 42608
SOLVENT CD2Cl2
NS 30000
DS 4
SWH 42613.637 Hz
FIDRES 2.000265 Hz
AQ 0.4999339 sec
RG 203
DW 11.733 usec
DE 20.00 usec
TE 296.2 K
D1 0.80000001 sec
D11 0.03000000 sec
TD0 1
SFO1 85.7868623 MHz
NUC1 195Pt
P1 13.10 usec
PLW1 60.00000000 W
SFO2 400.4708009 MHz
NUC2 1H
CPDPRG[2 waltz16
PCPD2 90.00 usec
PLW2 15.13799953 W
PLW12 0.20214000 W
PLW13 0.10167000 W
F2 - Processing parameters
SI 32768
SF 86.0881710 MHz
WDW EM
SSB 0
LB 20.00 Hz
GB 0
PC 1.40
-3300
-3350
-3400
-3450
-3500
-3550
-3600
-3650
-3700
ppm

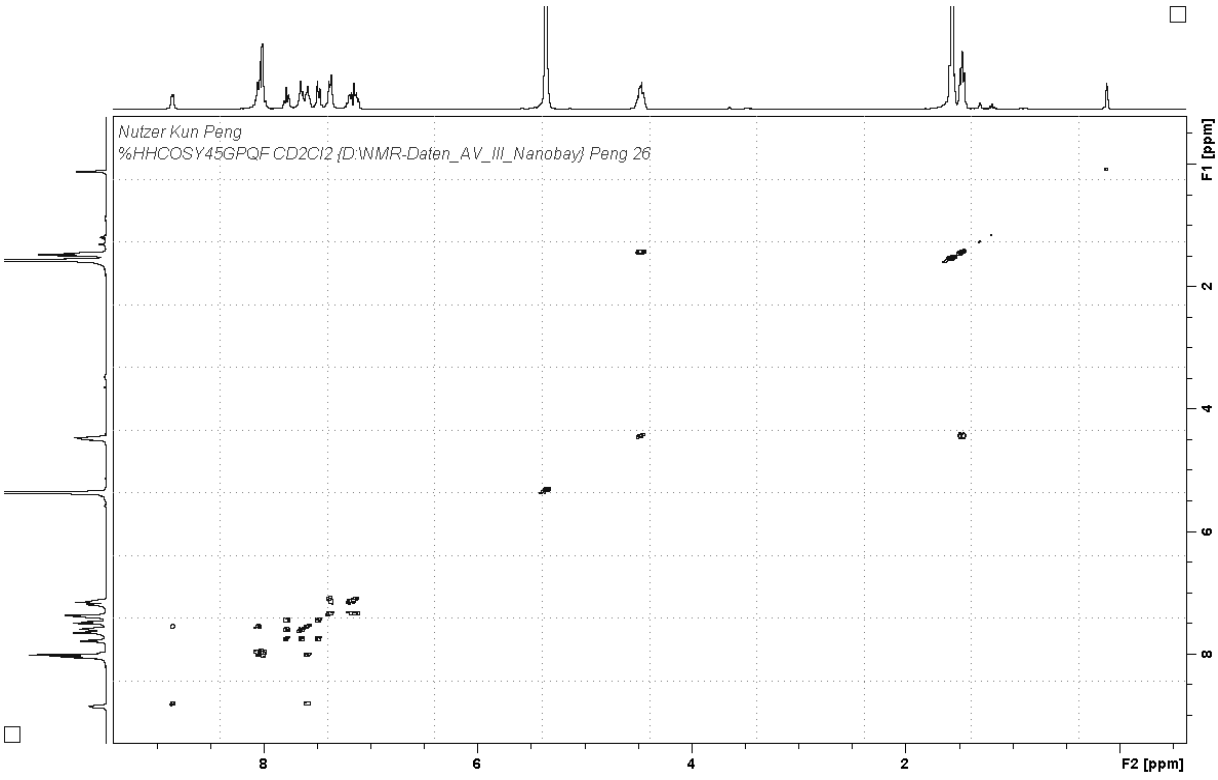
Nutzer Kun Peng
%HHCOSY45GPQF CD2Cl2 {D:\NMR-Daten_AV_III_Nanobay} Peng 26
F1 [ppm]
F2 [ppm]
2
4
6
8
8
6
4
2

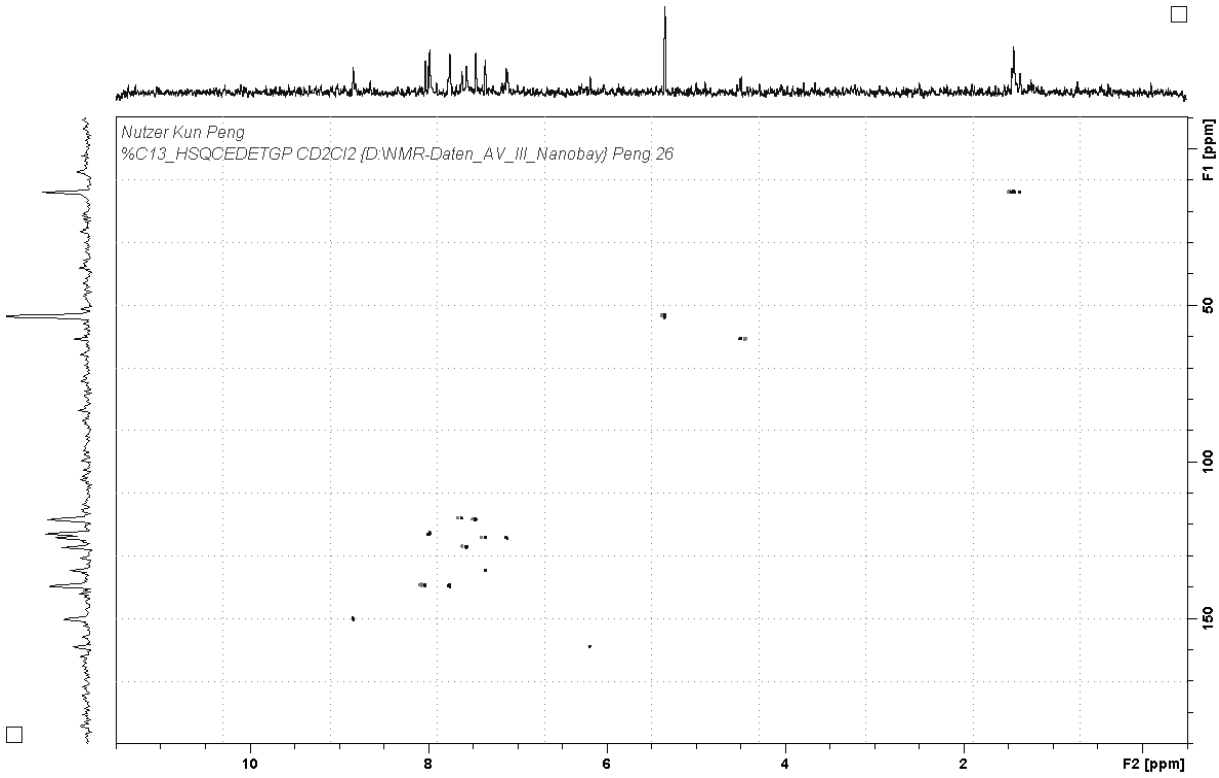
Nutzer Kun Peng
%C13_HSQCEDETGP CD2Cl2 {D:\NMR-Daten_AV_III_Nanobay} Peng 26
F1 [ppm]
50
100
150
10
8
6
4
2
F2 [ppm]

5.3.27 Synthesis of *(E)*-*N*-phenyl-2-(1-(pyridin-2-yl)ethylidene)hydrazine-carbothioamide

USC-KP043-01

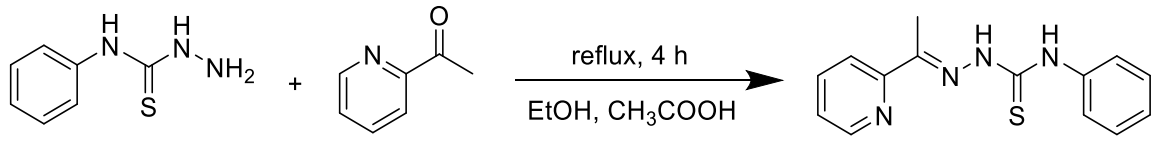

$C_7H_9N_3S$
167.23 g/mol

C_7H_7NO
121.14 g/mol

$C_{14}H_{14}N_4S$
270.35 g/mol

In a 250 mL flask, *N*-phenyl hydrazine carbothioamide (2.01 g, 12.0 mmol) was dissolved in ethanol (60 mL) at 60 °C to give a clear yellow solution. Then, 2-acetylpyridine (1.51 g, 12.5 mmol) in acetic acid (1 mL) was added and the mixture heated to reflux. After about 1 h, a light yellow solid started to precipitate. Heating was continued for another 3 h and then, the solution was cooled to room temperature. The resulting light yellow solid was filtered off, washed with ethanol (3 × 10 mL), and dried under vacuum for 1 d. Yield: 86% (2.80 g, 10.4 mmol). **IR** (ATR): $\tilde{\nu}$ = 3297 (m), 3240 (m), 3052 (w), 1514 (m), 1485 (m), 1466 (m), 1435 (m), 1360 (w), 1300 (w), 1263 (w), 1186 (w), 781 (w), 740 (w) cm^{-1}. **^{1}H NMR** (400.40 MHz, DMSO-d_6): δ = 10.68 (s, 1H, N*H*), 10.20 (s, 1H, N*H*-phenyl), 8.60 (ddd, 1H, $^3J_{H6,H5}$ = 4.8 Hz, $^4J_{H6,H4}$ = 1.6 Hz, $^5J_{H6,H3}$ = 0.9 Hz, py-H6), 8.54 (d, 1H, $^3J_{H3,H4}$ = 8.1 Hz, py-H3), 7.81 (dt, 1H, $^3J_{H4,H3/H5}$ = 7.8 Hz, $^4J_{H4,H6}$ = 1.6 Hz, py-H4), 7.58 (d, 2H, $^3J_{H2'/H6',H3'/H5'}$ = 7.5 Hz, phenyl-H2'/H6'), 7.41–7.37 (m, 3H, py-H5, phenyl-H3'/H5'), 7.23 (t, 1H, $^3J_{H4',H3'/H5'}$ = 7.4 Hz, phenyl-H4'), 2.48 (s, 3H, CH_3) ppm; **^{13}C NMR** (100.68 MHz, DMSO-d_6): δ = 177.26 (*C*=S), 154.52 (*C*=N), 149.18 (py-C2), 148.46 (py-C6), 139.14 (phenyl-C1'), 136.34 (py-C4), 128.11 (phenyl-C2'/C6'), 126.13 (phenyl-C3'/C5'), 125.54 (py-C5), 124.09 (py-C3), 121.23 (phenyl-C4'), 12.49 (*C*H_3) ppm. **Elemental analysis** (%) calcd. for $C_{14}H_{14}N_4S$: C 62.20, H 5.22, N 20.72, S 11.86; found (%): C 62.23, H 5.24, N 20.80, S 11.78.

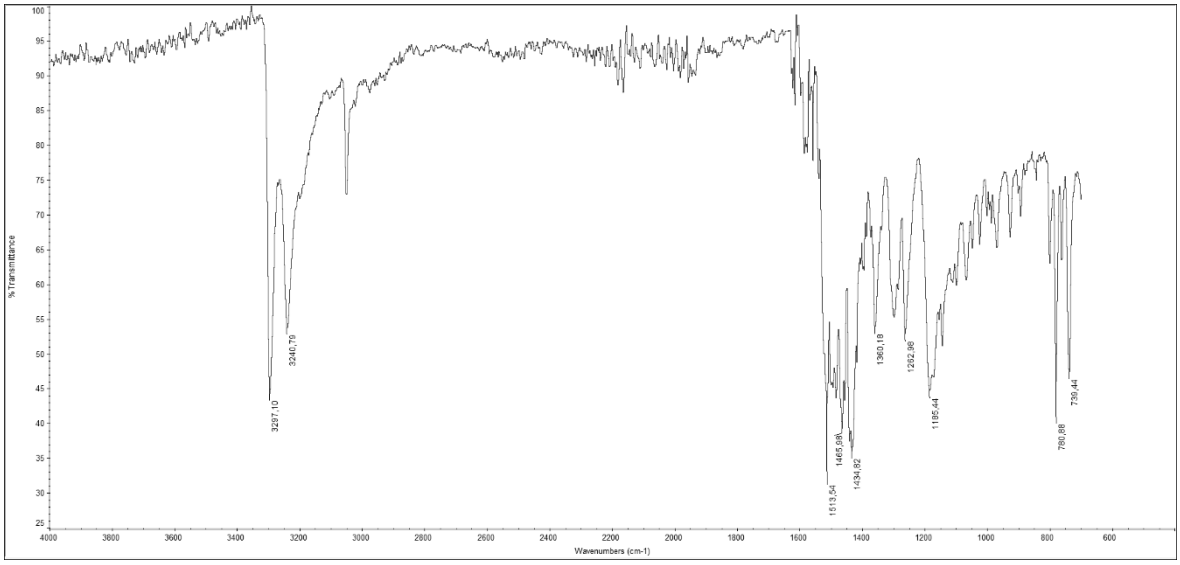
%Transmittance
Wavenumbers (cm-1)
3297,10
3240,79
1513,54
1465,98
1434,62
1360,18
1262,96
1195,44
780,88
739,44

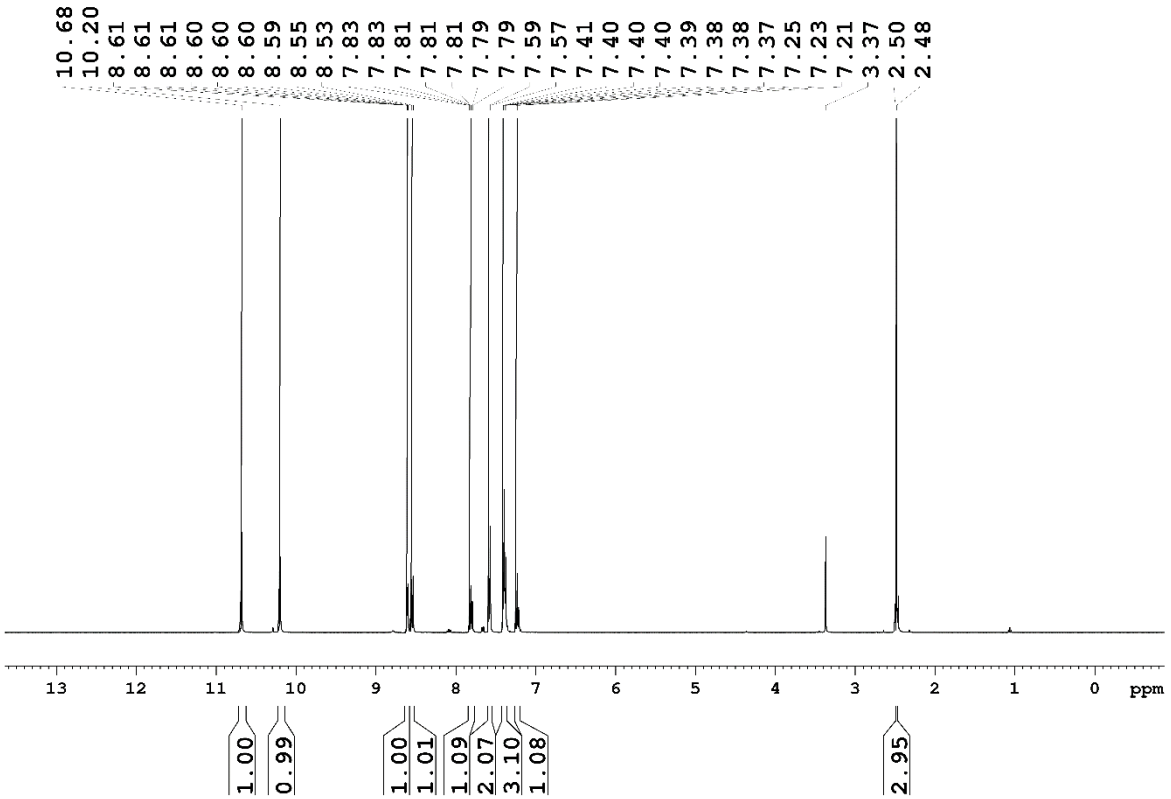
10.68
10.20
8.61
8.61
8.61
8.60
8.60
8.60
8.59
8.55
8.53
7.83
7.83
7.81
7.81
7.81
7.79
7.79
7.59
7.57
7.41
7.40
7.40
7.40
7.39
7.38
7.38
7.37
7.25
7.23
7.21
3.37
2.50
2.48
ppm
1.00
0.99
1.00
1.01
1.09
2.07
3.10
1.08
2.95

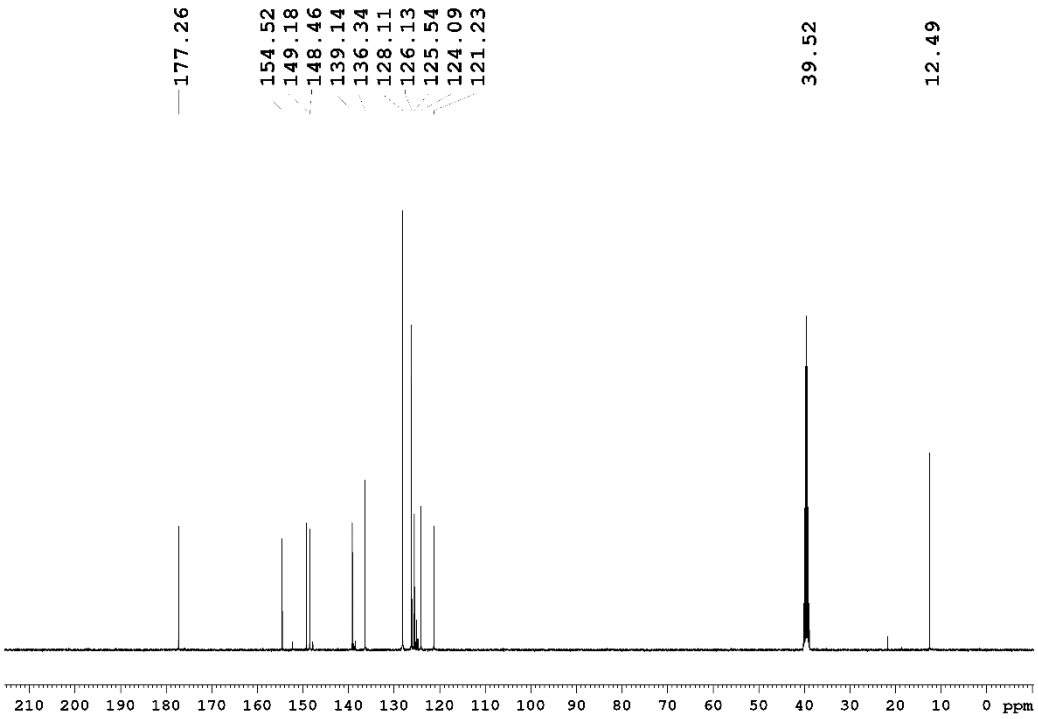
177.26
154.52
149.18
148.46
139.14
136.34
128.11
126.13
125.54
124.09
121.23
39.52
12.49
210 200 190 180 170 160 150 140 130 120 110 100 90 80 70 60 50 40 30 20 10 0 ppm

5.3.28 Synthesis of [PdCl(pht)]

USC-KP039-12

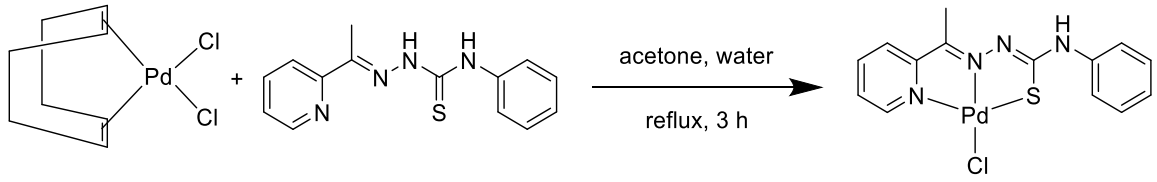

$C_8H_{12}Cl_2Pd$
285.51 g/mol

$C_{14}H_{14}N_4S$
270.35 g/mol

$C_{14}H_{13}ClN_4PdS$
411.22 g/mol

A mixture of [$PdCl_2$(cod)] (85 mg, 0.27 mmol) suspended in water (15 mL) and (*E*)-*N*-phenyl-2-(1-(pyridin-2-yl)ethylidene)hydrazine carbothioamide (82.6 mg, 0.31 mmol) dissolved in acetone (10 mL) was stirred under reflux for 3 h. Then, the solution was cooled to room temperature, the resulting yellow precipitate filtered off, washed with acetone (3 × 2 mL) and water (3 × 5 mL), and dried under vacuum for 1 d. Yield: quantitative (109 mg, 0.27 mmol). **IR** (ATR): $\tilde{\nu}$ = 3303 (s), 3062 (w), 1596 (m), 1559 (w), 1537 (m), 1501 (m), 1456 (m), 1433 (s), 1317 (m), 1252 (m), 1153 (m), 1069 (m), 771 (w), 748 (m) cm^{-1}. **^{1}H NMR** (500.13 MHz, DMSO-d_6): δ = 10.19 (s, 1H, N*H*-phenyl), 8.60 (ddd, 1H, $^3J_{H6,H5}$ = 5.3 Hz, $^4J_{H6,H4}$ = 1.6 Hz, $^5J_{H6,H3}$ = 0.6 Hz, py-H6), 8.20 (dt, 1H, $^3J_{H4,H3/H5}$ = 7.9 Hz, $^4J_{H4,H6}$ = 1.6 Hz, py-H4), 7.94 (d, 1H, $^3J_{H3,H4}$ = 7.6 Hz, py-H3), 7.68 (ddd, 1H, $^3J_{H5,H4}$ = 7.7 Hz, $^3J_{H5,H6}$ = 5.3 Hz, $^4J_{H5,H3}$ = 1.3 Hz, py-H5), 7.62 (d, 2H, $^3J_{H3'/H5',H2'/H6'}$ = 7.7 Hz, phenyl-H3'/H5'), 7.33 (t, $^3J_{H2'/H6',H3'/H5'}$ = 8.0 Hz, phenyl-H2'/H6'), 7.04 (t, $^3J_{H4',H3'/H5'}$ = 7.4 Hz, phenyl-H4'), 2.48 (s, 3H, CH_3) ppm; **^{13}C NMR** (125.76 MHz, DMSO-d_6): δ = 174.56 (*C*-S), 159.09 (*C*=N), 157.96 (py-C2), 147.91 (py-C6), 140.97 (phenyl-C1'), 140.28 (py-C4), 128.71 (phenyl-C3'/C5'), 126.72 (py-C5), 125.63 (py-C3), 123.15 (phenyl-C4'), 119.82 (phenyl-C2'/C6'), 13.87 (*C*H_3) ppm. **Elemental analysis** (%) calcd. for $C_{14}H_{13}ClN_4PdS$: C 40.89, H 3.19, N 13.62, S 7.80; found (%): C 40.97, H 3.19, N 13.56, S 7.71.

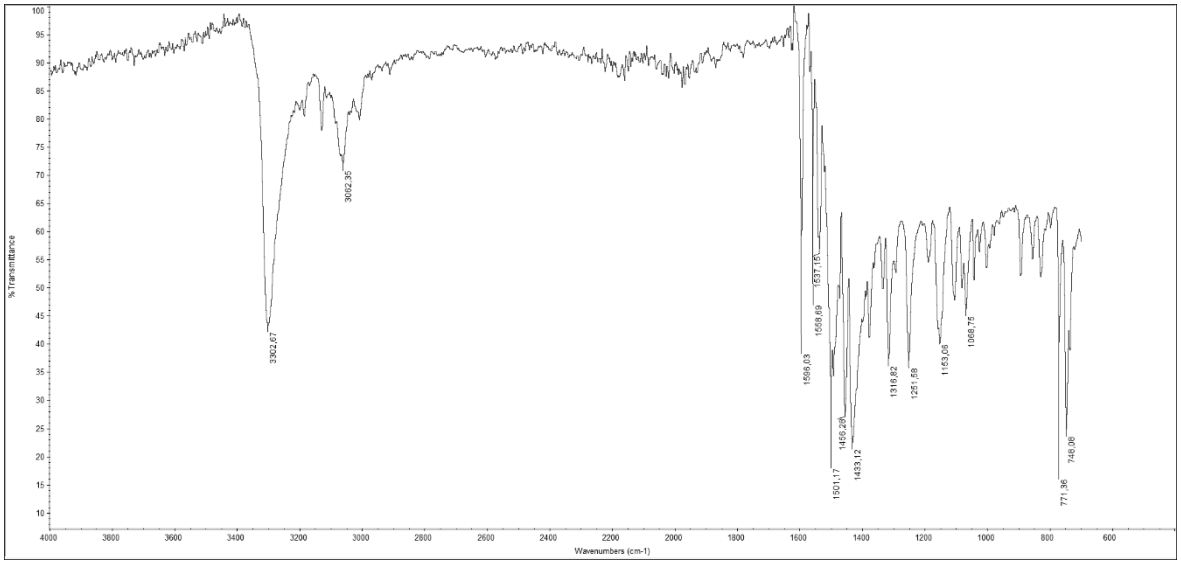
% Transmittance
Wavenumbers (cm-1)
3302,67
3062,35
1598,03
1558,89
1537,16
1501,17
1456,28
1433,12
1316,82
1251,58
1153,05
1068,75
771,36
748,06

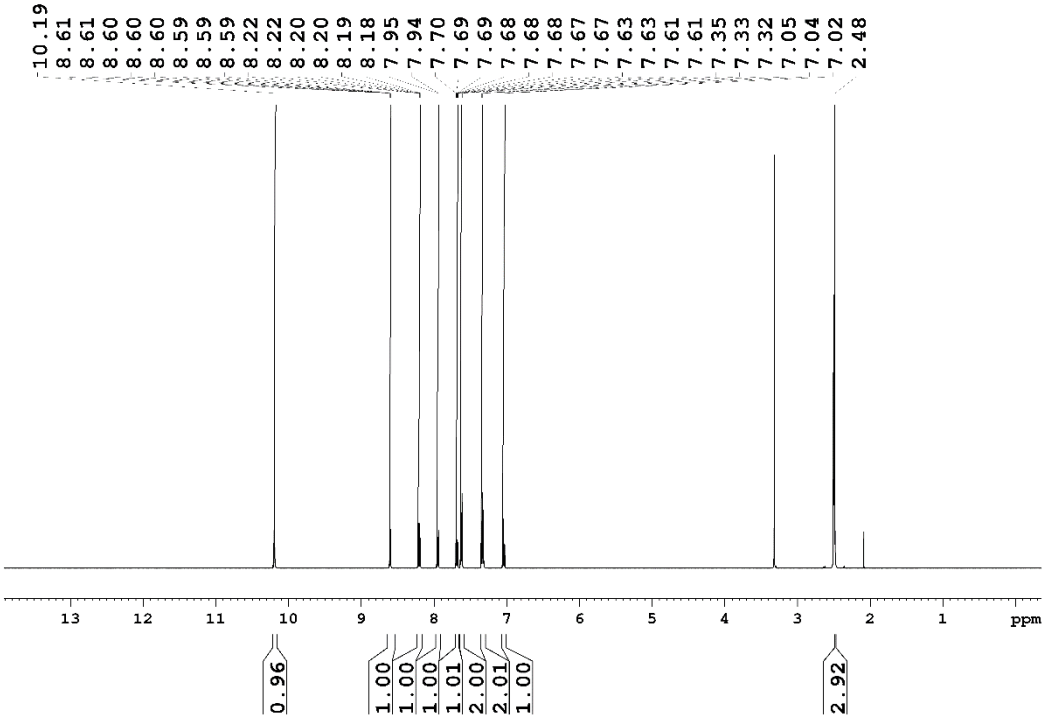
10.19
8.61
8.61
8.60
8.60
8.60
8.59
8.59
8.59
8.22
8.22
8.20
8.20
8.19
8.18
7.95
7.94
7.70
7.69
7.69
7.68
7.68
7.68
7.67
7.67
7.63
7.63
7.61
7.61
7.35
7.33
7.32
7.05
7.04
7.02
2.48
13
12
11
10
9
8
7
6
5
4
3
2
1
ppm
0.96
1.00
1.00
1.00
1.01
2.00
2.01
1.00
2.92

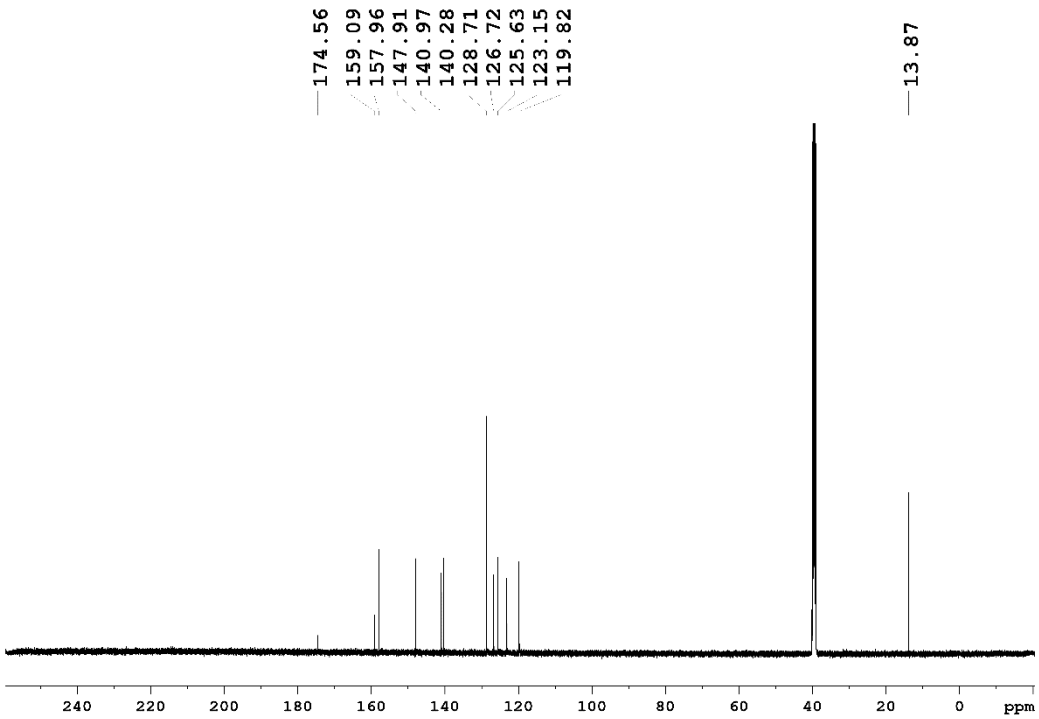
174.56
159.09
157.96
147.91
140.97
140.28
128.71
126.72
125.63
123.15
119.82
13.87
240
220
200
180
160
140
120
100
80
60
40
20
0
ppm

5.3.29 Synthesis of [PtCl(pht)]

USC-KP042-10

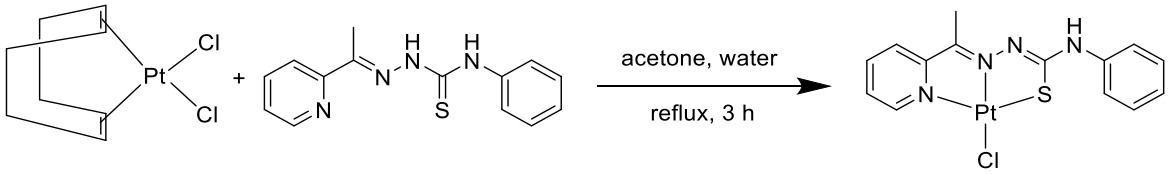

$C_8H_{12}Cl_2Pt$
374.16 g/mol

$C_{14}H_{14}N_4S$
270.35 g/mol

$C_{14}H_{13}ClN_4PtS$
499.88 g/mol

A mixture of [$PtCl_2$(cod)] (60 mg, 0.15 mmol) suspended in water (7 mL) and *(E)*-*N*-phenyl-2-(1-(pyridin-2-yl)ethylidene)hydrazine carbothioamide (45 mg, 0.17 mmol) dissolved in acetone (7 mL) was stirred under reflux for 3 h. Then, the solution was cooled to room temperature and the resulting red precipitate filtered off, washed with acetone (3 × 2 mL) and water (3 × 5 mL), and dried under vacuum for 1 d. Yield: 97% (72.2 mg, 0.14 mmol). **IR** (ATR): $\tilde{\nu}$ = 3332 (s), 3071 (w), 1598 (m), 1558 (w), 1541 (m), 1510 (m), 1493 (m), 1462 (s), 1435 (s), 1320 (w), 1250 (w), 1155 (m), 759 (w), 745 (m) cm^{-1}. **^{1}H NMR** (500.13 MHz, DMSO-d_6, ppm): δ = 10.29 (s, 1H, N*H*-phenyl), 8.83 (ddd, 1H, $^3J_{H6,H5}$ = 5.5 Hz, $^4J_{H6,H4}$ = 1.5 Hz, $^5J_{H6,H3}$ = 0.6 Hz, py-H6), 8.21 (dt, 1H, $^3J_{H4,H3/H5}$ = 7.9 Hz, $^4J_{H4,H6}$ = 1.6 Hz, py-H4), 7.88 (d, 1H, $^3J_{H3,H4}$ = 7.6 Hz, py-H3), 7.74 (ddd, 1H, $^3J_{H5,H4}$ = 7.7 Hz, $^3J_{H5,H6}$ = 5.5 Hz, $^4J_{H5,H3}$ = 1.3 Hz, py-H5), 7.63 (d, 2H, $^3J_{H3'/H5',H2'/H6'}$ = 7.7 Hz, phenyl-H3'/H5'), 7.35 (t, 2H, $^3J_{H2'/H6',H3'/H5'}$ = 8.0 Hz, phenyl-H2'/H6'), 7.04 (t, 1H, $^3J_{H4',H3'/H5'}$ = 7.4 Hz, phenyl-H4'), 2.45 (s, 3H, CH_3) ppm; **^{13}C NMR** (125.76 MHz, DMSO-d_6): δ = 177.67 (*C*-S), 159.22 (py-C2), 159.08 (*C*=N), 146.30 (py-C6), 140.67 (phenyl-C1'), 140.32 (py-C4), 128.66 (phenyl-C3'/C5'), 127.47 (py-C5), 126.21 (py-C3), 123.33 (phenyl-C4'), 120.10 (phenyl-C2'/C6'), 13.87 (*C*H_3) ppm; **^{195}Pt NMR** (107.51 MHz, DMSO-d_6): δ = -3165 ppm. **Elemental analysis** (%) calcd. for $C_{14}H_{13}ClN_4PtS$: C 33.64, H 2.62, N 11.21, S 6.41; found (%): C 33.82, H 2.70, N 11.26, S 6.36.

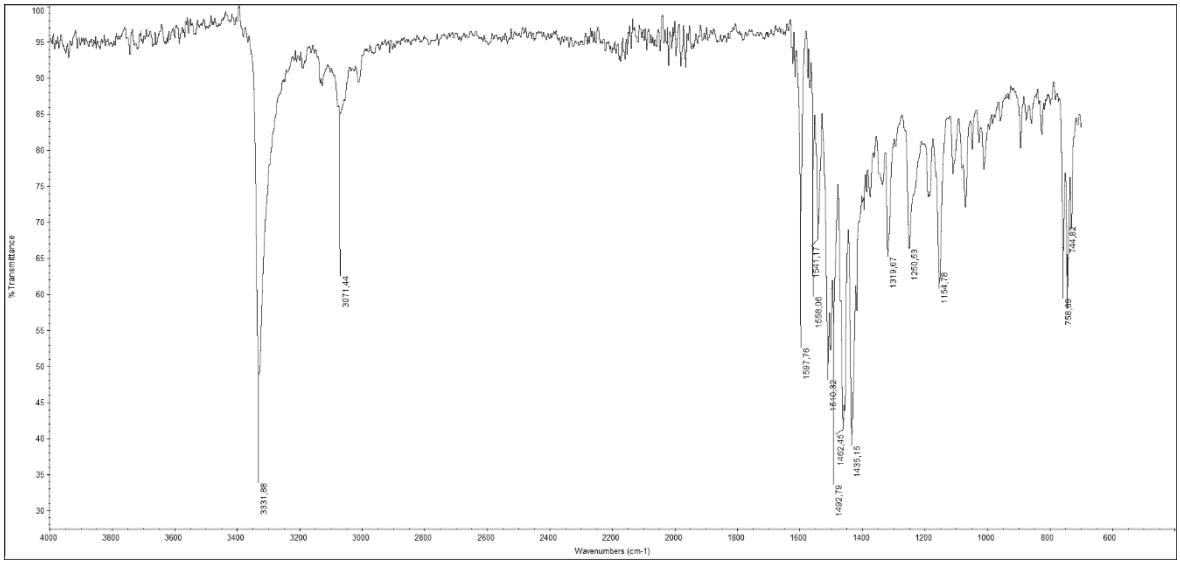
% Transmittance
Wavenumbers (cm-1)
3331.88
3071.44
1597.76
1541.17
1492.79
1435.15
1319.67
1250.23
1154.78
744.83

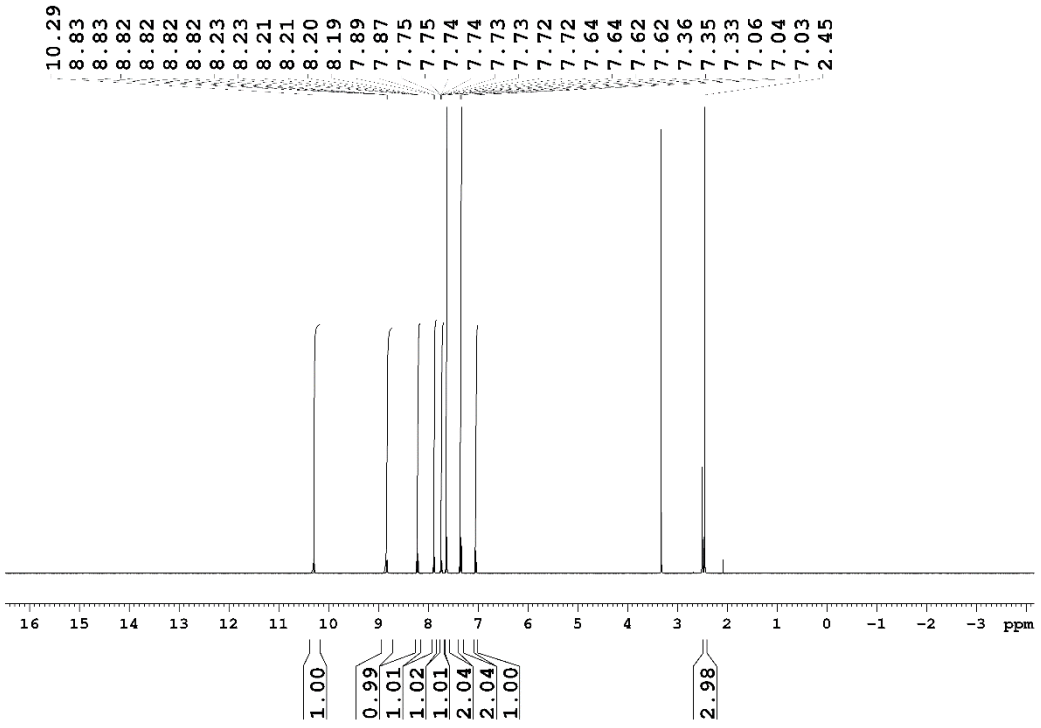
10.29
8.83
8.83
8.82
8.82
8.82
8.82
8.23
8.23
8.21
8.21
8.20
8.19
7.89
7.87
7.75
7.75
7.74
7.74
7.73
7.73
7.72
7.72
7.64
7.64
7.62
7.62
7.36
7.35
7.33
7.06
7.04
7.03
2.45
ppm
1.00
0.99
1.01
1.02
1.01
2.04
2.04
1.00
2.98

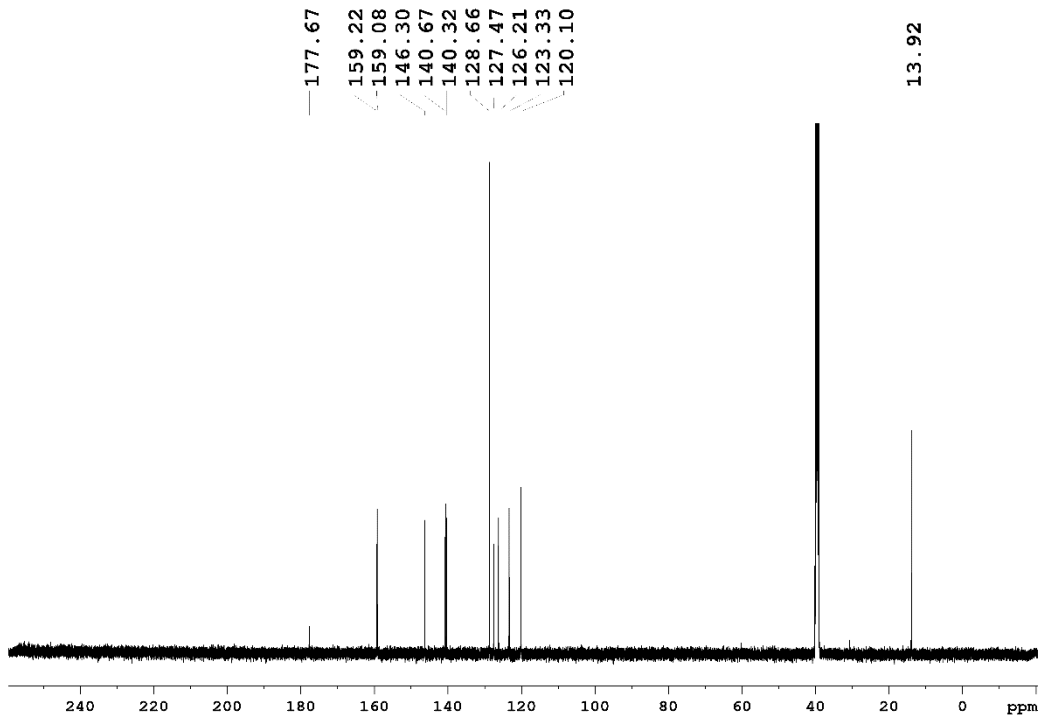
177.67
159.22
159.08
146.30
140.67
140.32
128.66
127.47
126.21
123.33
120.10
13.92
240
220
200
180
160
140
120
100
80
60
40
20
0
ppm

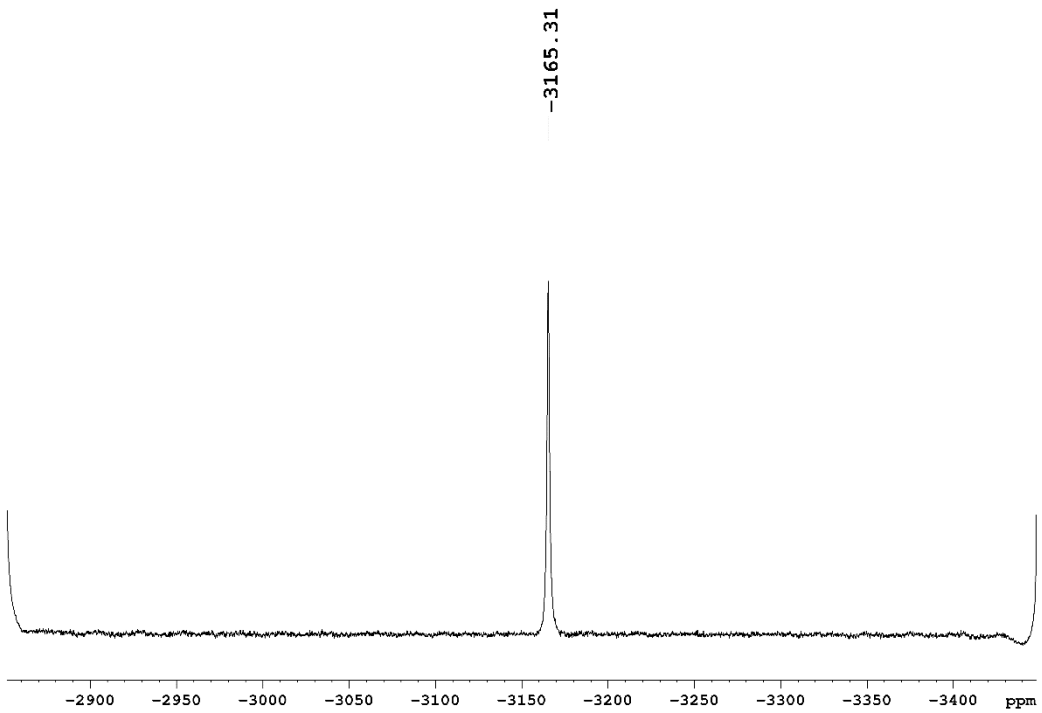
-3165.31
-2900
-2950
-3000
-3050
-3100
-3150
-3200
-3250
-3300
-3350
-3400
ppm

5.3.30 Synthesis of [Pd(N3)(pht)]

USC-KP041-15

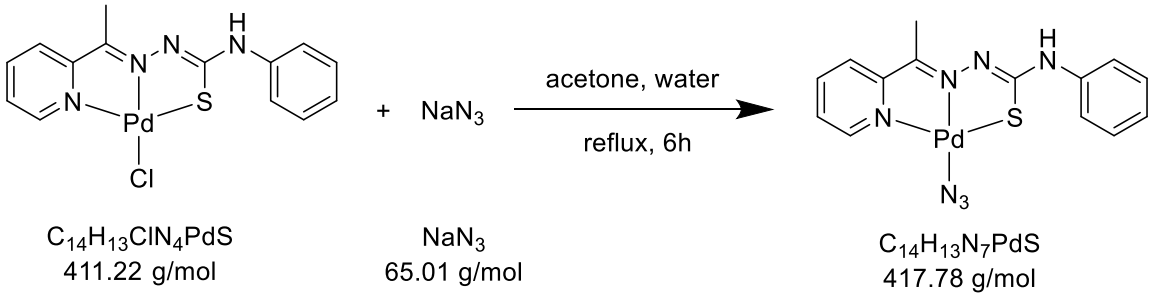

[PdCl(pht)] (120 mg, 0.29 mmol) was dissolved in acetone (80 mL) with heating. To the clear orange solution, sodium azide (325 mg, 5.00 mmol) in water (15 mL) was added and the mixture heated to reflux for 6 h. Then, the volume of the solution was reduced to about 20 mL, upon which a yellow precipitate formed, which was collected, washed with water (3 × 10 mL), and dried under vacuum for 1 d. Yield: 87% (106 mg, 0.25 mmol). **IR** (ATR): $\tilde{\nu}$ = 3271 (m), 3085 (w), 2047 (s), 1599 (m), 1550 (m), 1502 (m), 1457 (m), 1435 (m), 1317 (w), 1254 (m), 1156 (m), 1073 (w), 757 (m), 735 (w) cm^{-1}. **^{1}H NMR** (500.13 MHz, DMSO-d_6): δ = 10.20 (s, 1H, N*H*-phenyl), 8.23–8.21 (m, 1H, py-H6), 8.19 (dd, 1H, $^3J_{H4,H3/H5}$ = 7.9 Hz, $^4J_{H4,H6}$ = 1.7 Hz, py-H4), 7.93 (d, 1H, $^3J_{H3,H4}$ = 7.9 Hz, py-H3), 7.66 (ddd, 1H, $^3J_{H5,H4}$ = 7.7 Hz, $^3J_{H5,H6}$ = 5.3 Hz, $^4J_{H5,H3}$ = 1.2 Hz, py-H5), 7.61 (d, 2H, $^3J_{H3'/H5',H2'/H6'}$ = 7.7 Hz, phenyl-H3'/H5'), 7.33 (t, 2H, $^3J_{H2'/H6',H3'/H5'}$ = 8.0 Hz, phenyl-H2'/H6'), 7.04 (t, 1H, $^3J_{H4',H3'/H5'}$ = 7.4 Hz, phenyl-H4'), 2.45 (s, 3H, CH_3) ppm; **^{13}C NMR** (125.76 MHz, DMSO-d_6): δ = 172.68 (*C*-S), 159.30 (*C*=N), 157.57 (py-C2), 147.20 (py-C6), 141.09 (phenyl-C1'), 140.21 (py-C4), 128.72 (phenyl-C3'/C5'), 126.91 (py-C5), 125.57 (py-C3), 123.21 (phenyl-C4'), 119.89 (phenyl-C2'/C6'), 13.61 (*C*H_3) ppm. **Elemental analysis** (%) calcd. for $C_{14}H_{13}N_7PdS$: C 40.25, H 3.14, N 23.47, S 7.68; found (%): C 40.29, H 3.33, N 23.16, S 7.63.

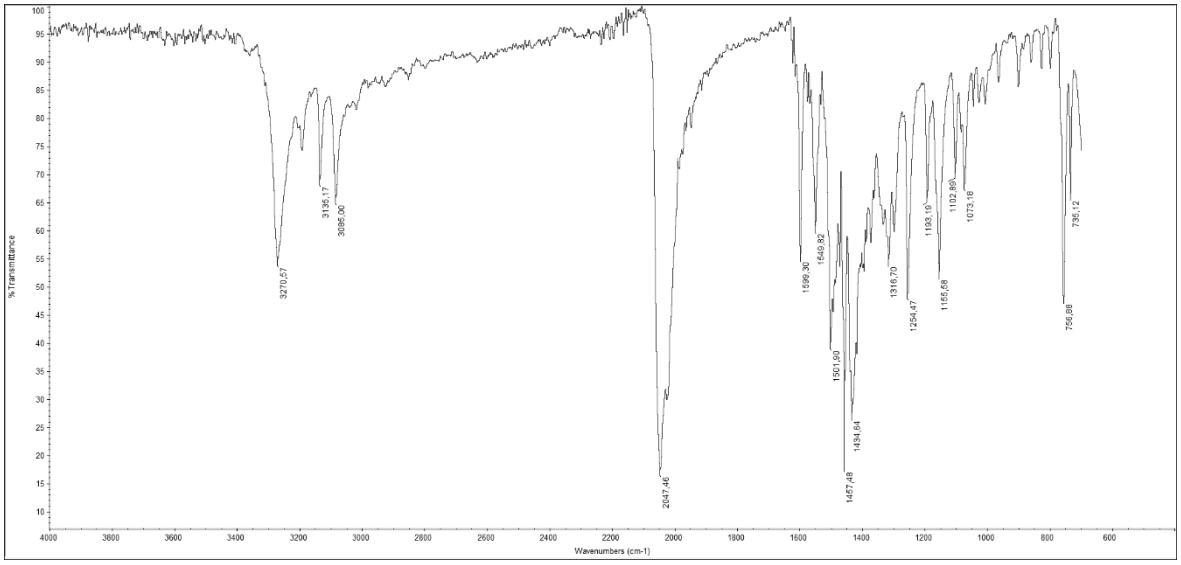
% Transmittance
Wavenumbers (cm-1)
3270,57
3136,17
3086,00
2047,46
1599,30
1540,82
1501,99
1457,48
1434,64
1316,70
1254,47
1193,19
1155,68
1102,85
1073,16
756,88
736,12

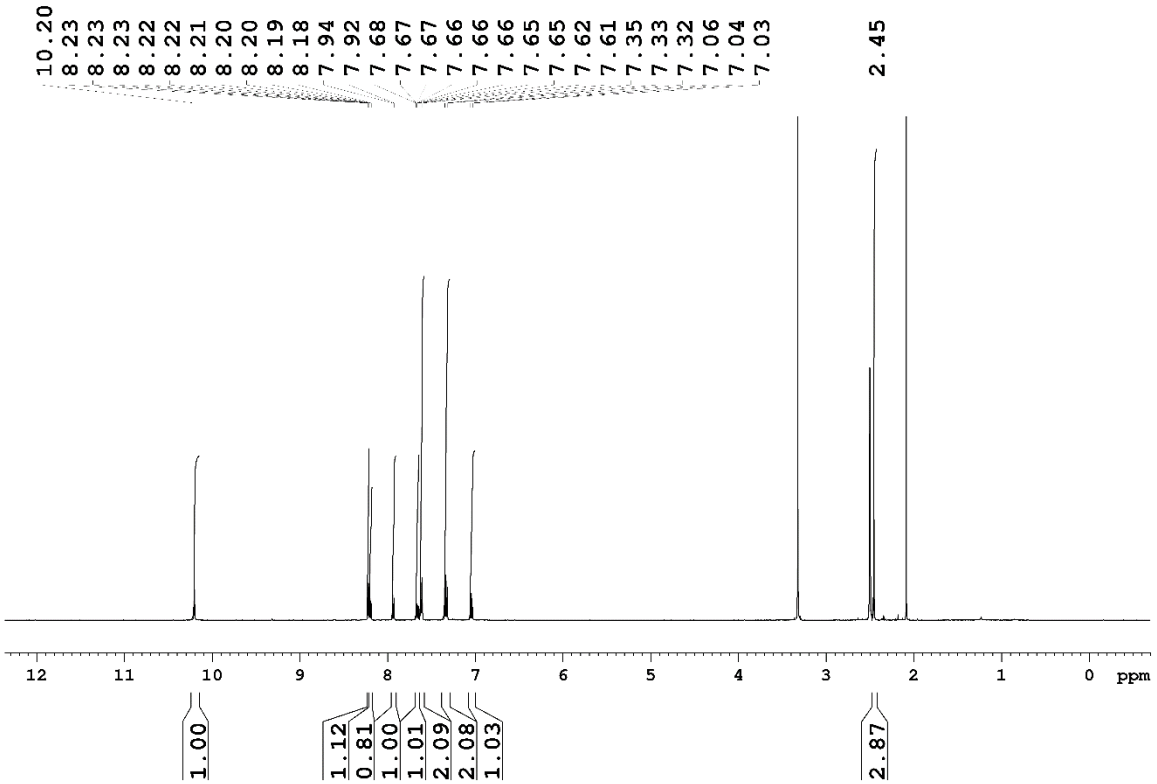
10.20
8.23
8.23
8.23
8.22
8.22
8.21
8.20
8.20
8.19
8.18
7.94
7.92
7.68
7.67
7.67
7.66
7.66
7.66
7.65
7.65
7.62
7.61
7.35
7.33
7.32
7.06
7.04
7.03
2.45
12
11
10
9
8
7
6
5
4
3
2
1
0
ppm
1.00
1.12
0.81
1.00
1.01
2.09
2.08
1.03
2.87

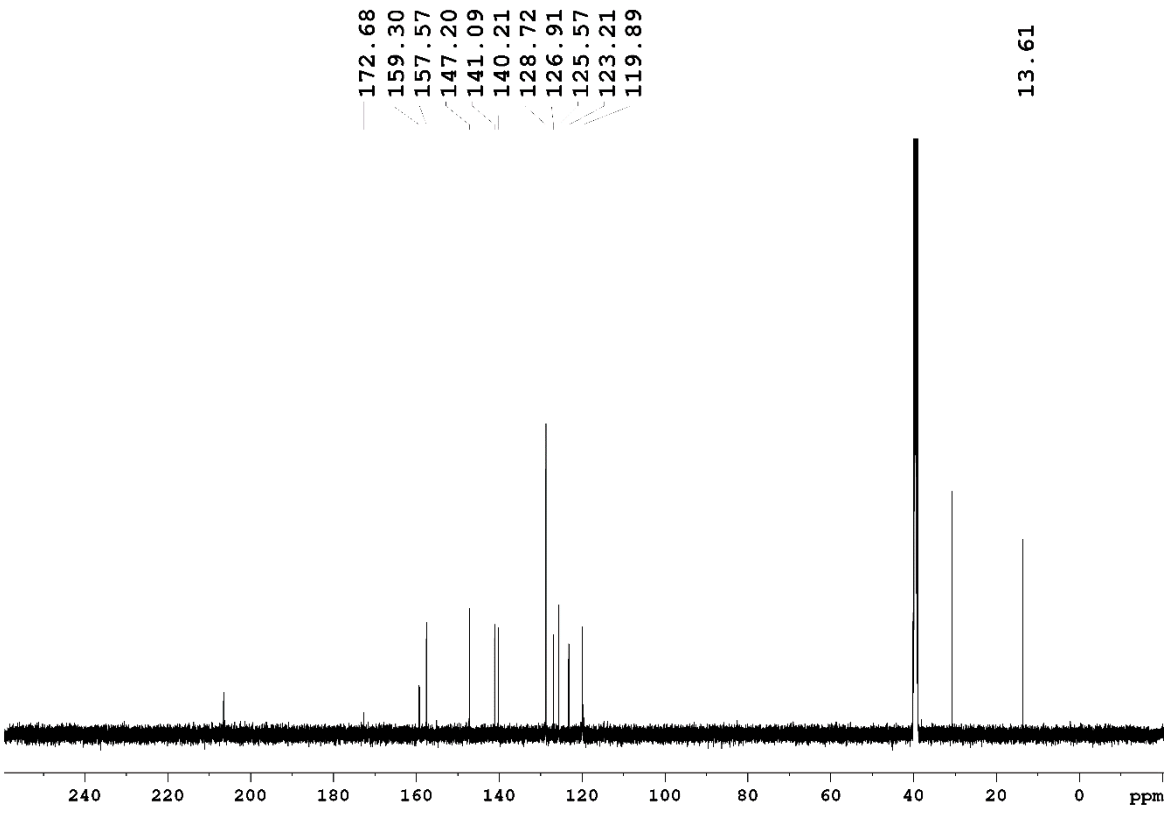
172.68
159.30
157.57
147.20
141.09
140.21
128.72
126.91
125.57
123.21
119.89
13.61
240
220
200
180
160
140
120
100
80
60
40
20
0
ppm

5.3.31 Synthesis of [Pt(N3)(pht)]

USC-KP044-10

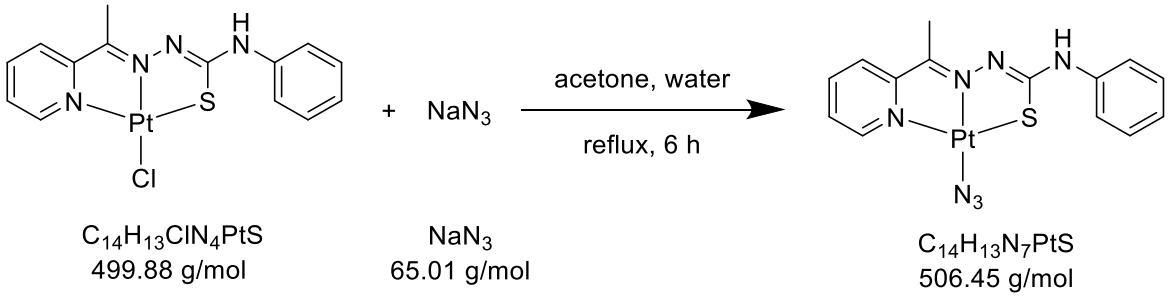

[PtCl(pht)] (80 mg, 0.16 mmol) was dissolved in acetone (40 mL) with heating. To the clear dark red solution, sodium azide (259 mg, 3.98 mmol) in water (10 mL) was added and the mixture heated to reflux for 6 h. The volume of resulting solution was reduced to about 15 mL, upon which a red precipitate formed, which was collected, washed with water (3 × 10 mL), and dried under vacuum for 1 d. Yield: 88% (72 mg, 0.14 mmol). **IR** (ATR): $\tilde{\nu}$ = 3279 (m), 3137 (w), 3086 (w), 2061 (s), 1600 (w), 1550 (w), 1493 (w), 1458 (m), 1434 (m), 1317 (w), 1252 (m), 1154 (m), 1073 (w), 755 (m), 735 (w) cm^{-1}. **^{1}H NMR** (500.13 MHz, DMSO-d_6): δ = 10.30 (s, 1H, N*H*-phenyl), 8.44 (ddd, 1H, $^{3}J_{H6,H5}$ = 5.4 Hz, $^{4}J_{H6,H4}$ = 1.5 Hz, $^{5}J_{H6,H3}$ = 0.7 Hz, py-H6), 8.21 (dt, 1H, $^{3}J_{H4,H3/H5}$ = 7.9 Hz, $^{4}J_{H4,H6}$ = 1.6 Hz, py-H4), 7.87 (d, 1H, $^{3}J_{H3,H4}$ = 8.0 Hz, py-H3), 7.69 (ddd, 1H, $^{3}J_{H5,H4}$ = 7.7 Hz, $^{3}J_{H5,H6}$ = 5.5 Hz, $^{4}J_{H5,H3}$ = 1.3 Hz, py-H5), 7.62 (d, 2H, $^{3}J_{H3'/H5',H2'/H6'}$ = 7.7 Hz, phenyl-H3'/H5'), 7.35 (t, 2H, $^{3}J_{H2'/H6',H3'/H5'}$ = 8.0 Hz, phenyl-H2'/H6'), 7.05 (t, 1H, $^{3}J_{H4',H3'/H5'}$ = 7.4 Hz, phenyl-H4'), 2.45 (s, 3H, CH_3) ppm; **^{13}C NMR** (125.76 MHz, DMSO-d_6): δ = 175.42 (*C*-S), 159.57 (*C*=N), 158.72 (py-C2), 146.02 (py-C6), 140.72 (phenyl-C1'), 140.24 (py-C4), 128.68 (phenyl-C3'/C5'), 127.65 (py-C5), 126.24 (py-C3), 123.39 (phenyl-C4'), 120.14 (phenyl-C2'/C6'), 13.64 (*C*H$_3$) ppm; **^{195}Pt NMR** (107.51 MHz, DMSO-d_6): δ = -3101 ppm. **Elemental analysis** (%) calcd. for $C_{14}H_{13}N_7PtS$: C 33.20, H 2.59, N 19.36, S 6.33; found (%): C 33.38, H 2.84, N 19.34, S 6.29.

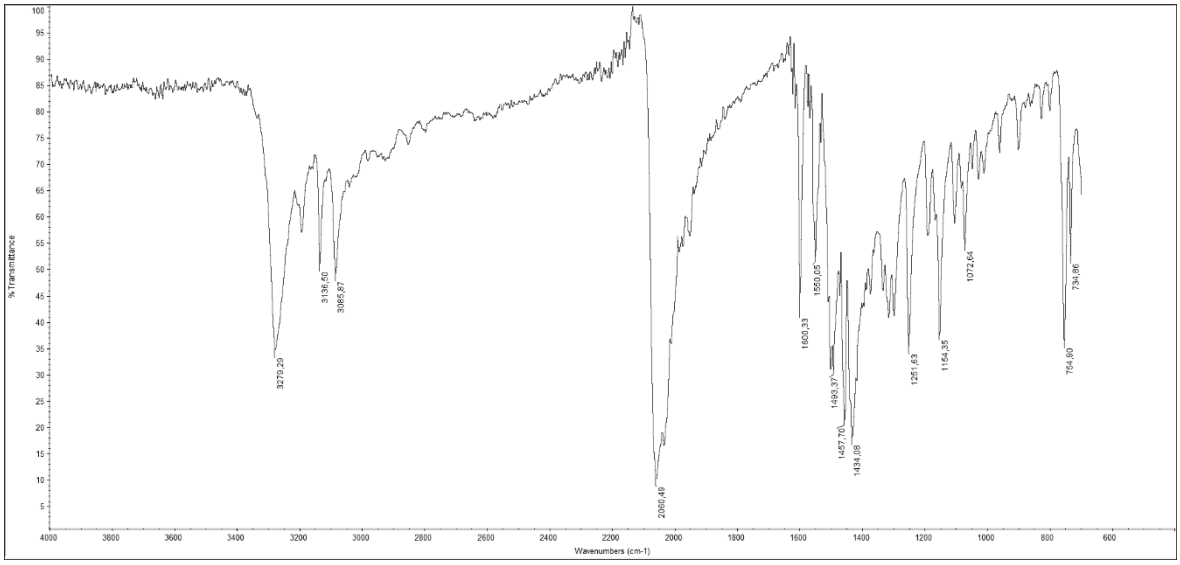
% Transmittance
Wavenumbers (cm-1)
3279,20
3136,50
3085,87
2060,49
1600,33
1559,05
1493,97
1457,70
1434,08
1251,63
1154,35
1072,64
754,80
734,86

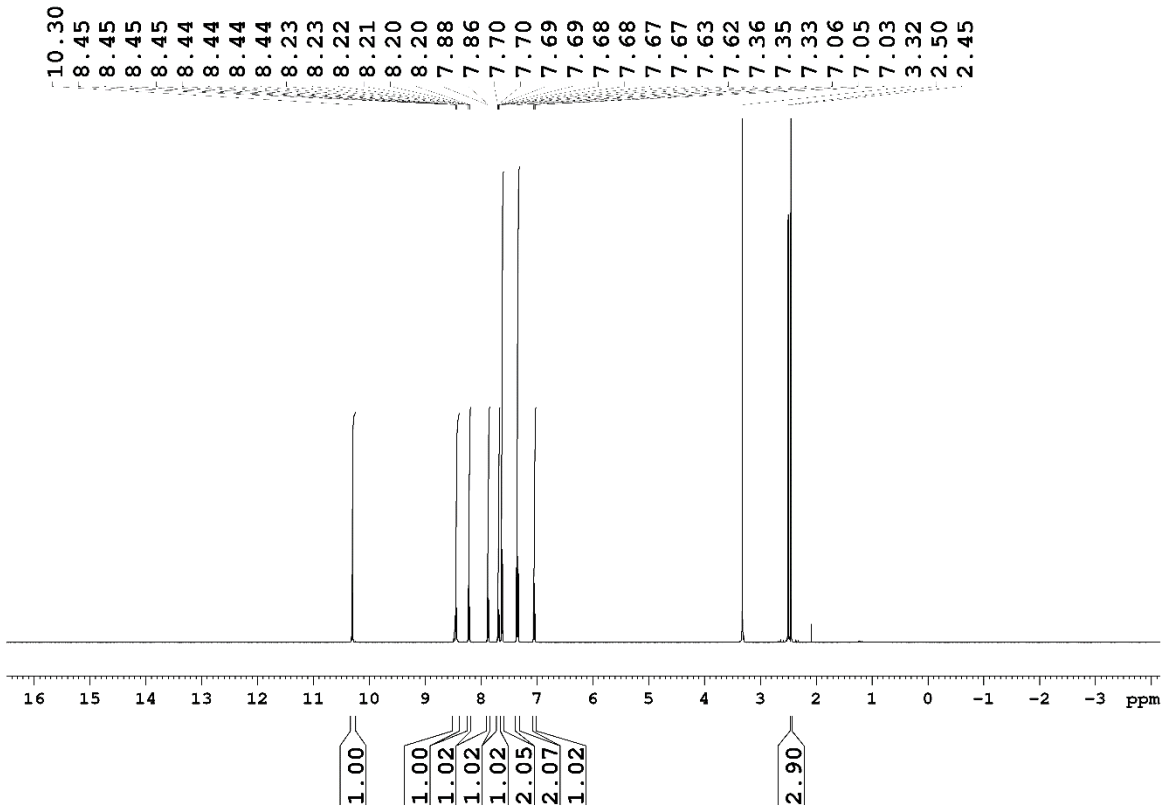
10.30
8.45
8.45
8.45
8.45
8.44
8.44
8.44
8.44
8.23
8.23
8.22
8.21
8.20
8.20
7.88
7.86
7.70
7.70
7.69
7.69
7.68
7.68
7.67
7.67
7.63
7.62
7.36
7.35
7.33
7.06
7.05
7.03
3.32
2.50
2.45
16 15 14 13 12 11 10 9 8 7 6 5 4 3 2 1 0 -1 -2 -3 ppm
1.00
1.00
1.02
1.02
1.02
2.05
2.07
1.02
2.90

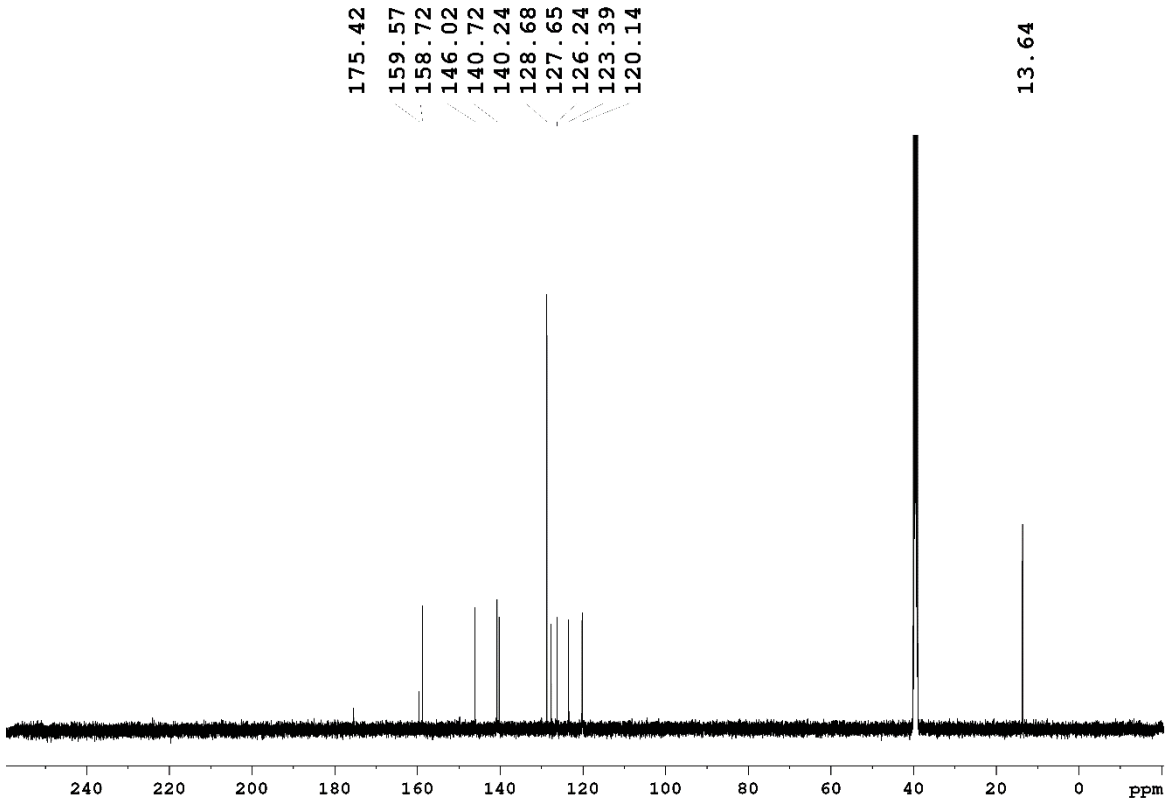
175.42
159.57
158.72
146.02
140.72
140.24
128.68
127.65
126.24
123.39
120.14
13.64
240
220
200
180
160
140
120
100
80
60
40
20
0
ppm

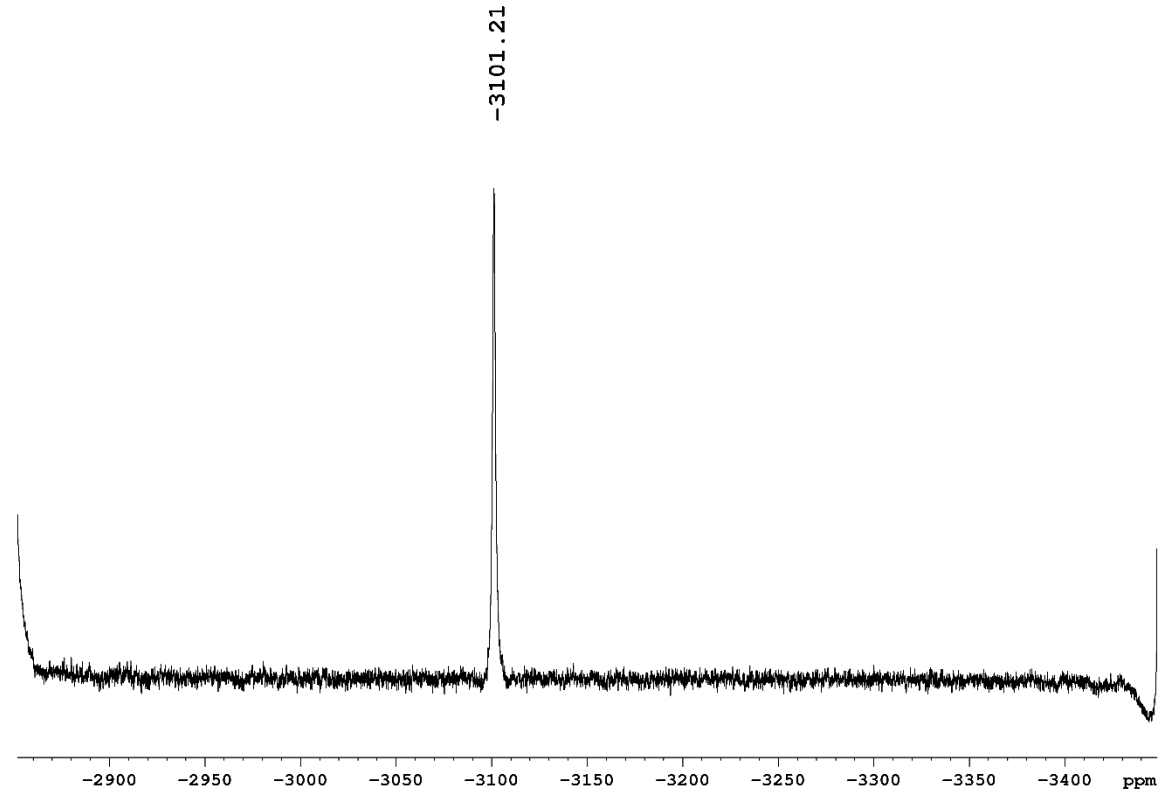
-3101.21
-2900
-2950
-3000
-3050
-3100
-3150
-3200
-3250
-3300
-3350
-3400
ppm

5.3.32 Synthesis of [Pd(pht)(triazolate^{CF3,COOEt})]

USC-KP040-33

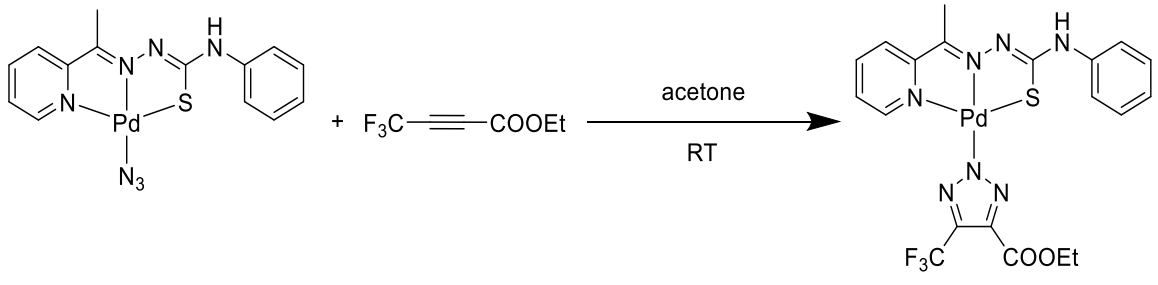

$C_{14}H_{13}N_7PdS$
417.79 g/mol

$C_6H_5F_3O_2$
166.10 g/mol

$C_{20}H_{18}F_3N_7O_2PdS$
583.89 g/mol

[Pd(N_3)(pht)] (35 mg, 0.08 mmol) was suspended in acetone (20 mL) in a large glass vial at room temperature. Then, 4,4,4-trifluoro-2-butynoic acid ethyl ester (30 µL, 38.1 mg, 0.23 mmol) was added and stirring was continued at room temperature until the solution became clear, which took about 3 h. The resulting clear dark orange solution was then evaporated to dryness. The orange solid thus obtained was washed with *n*-hexane (5 × 5 mL) and dried under vacuum for 1 d. Yield: 75% (37 mg, 0.06 mmol). **IR** (ATR): $\tilde{\nu}$ = 3333 (m), 1709 (s), 1601 (w), 1544 (w), 1510 (m), 1466 (s), 1438 (s), 1310 (m), 1191 (m), 1134 (s), 1060 (m), 763 (w), 746 (w) cm^{-1}. **^{1}H NMR** (500.13 MHz, DMSO-d_6): δ = 10.22 (s, 1H, N*H*-phenyl), 8.91 (dd, 1H, $^3J_{H6,H5}$ = 5.4 Hz, $^4J_{H6,H4}$ = 1.1 Hz, py-H6), 8.24 (dt, 1H, $^3J_{H4,H3/H5}$ = 7.9 Hz, $^4J_{H4,H6}$ = 1.6 Hz, py-H4), 8.00 (d, 1H, $^3J_{H3,H4}$ = 8.0 Hz, py-H3), 7.72 (ddd, 1H, $^3J_{H5,H4}$ = 7.7 Hz, $^3J_{H5,H6}$ = 5.5 Hz, $^4J_{H5,H3}$ = 1.3 Hz, py-H5), 7.60 (d, 2H, $^3J_{H3'/H5',H2'/H6'}$ = 7.8 Hz, phenyl-H3'/H5'), 7.33 (t, 2H, $^3J_{H2'/H6',H3'/H5'}$ = 7.7 Hz, phenyl-H2'/H6'), 7.05 (t, 1H, $^3J_{H4',H3'/H5'}$ = 7.4 Hz, phenyl-H4'), 4.31 (q, 2H, ^3J = 7.1 Hz, CH_2CH$_3$), 2.53 (s, 3H, CH_3), 1.30 (t, 3H, ^3J = 7.1 Hz, CH$_2$CH_3) ppm; **^{13}C NMR** (125.76 MHz, DMSO-d_6): δ = 172.89 (*C*-S), 160.69 (*C*=N), 159.70 (*C*OOEt), 157.76 (py-C2), 149.36 (py-C6), 141.30 (phenyl-C1'), 140.13 (py-C4), 137.88 (triazolate-C4), 136.64 (triazolate-C5), 128.77 (phenyl-C3'/C5'), 126.91 (py-C5), 125.98 (py-C3), 123.26 (phenyl-C4'), 121.41 (q, $^1J_{C,F}$ = 268.1 Hz, *C*F$_3$), 119.88 (phenyl-C2'/C6'), 60.74 (*C*H$_2$CH$_3$), 14.00 (*C*H$_3$), 13.99 (CH$_2$*C*H$_3$) ppm; **^{19}F NMR** (470.59 MHz, DMSO-d_6): δ = -58.58 (C*F*$_3$) ppm. **Elemental analysis** (%) calcd. for $C_{20}H_{18}F_3N_7O_2PdS$: C 41.14, H 3.11, N 16.79, S 5.49; found (%): C 41.23, H 3.09, N 16.21, S 5.43.

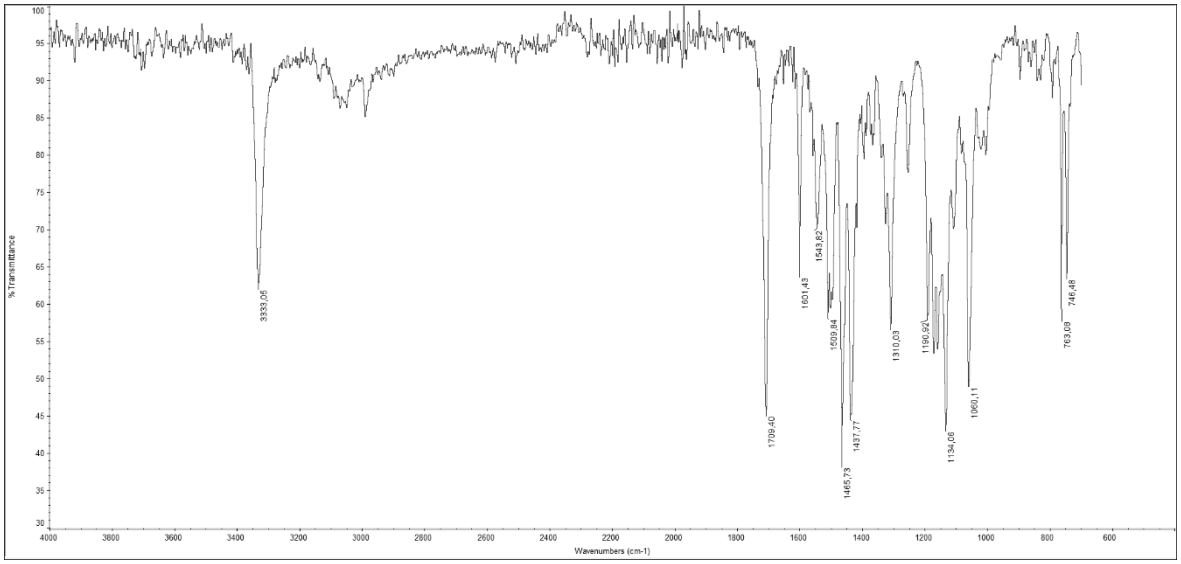
% Transmittance
Wavenumbers (cm-1)
3333,06
1709,40
1601,43
1543,82
1509,84
1497,77
1465,73
1310,03
1190,92
1134,06
1060,11
763,09
746,48

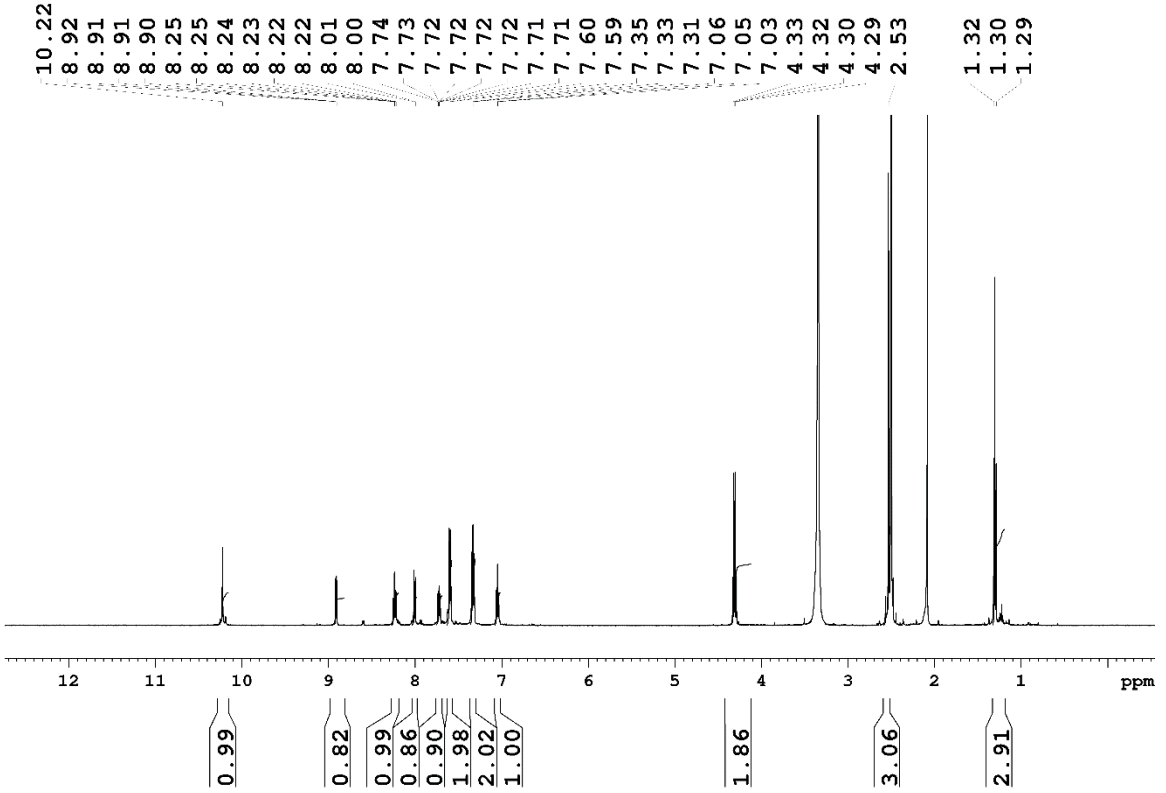
10.22
8.92
8.91
8.91
8.90
8.25
8.25
8.24
8.23
8.22
8.22
8.01
8.00
7.74
7.73
7.72
7.72
7.72
7.72
7.71
7.71
7.60
7.59
7.35
7.33
7.31
7.06
7.05
7.03
4.33
4.32
4.30
4.29
2.53
1.32
1.30
1.29
ppm
0.99
0.82
0.99
0.86
0.90
1.98
2.02
1.00
1.86
3.06
2.91

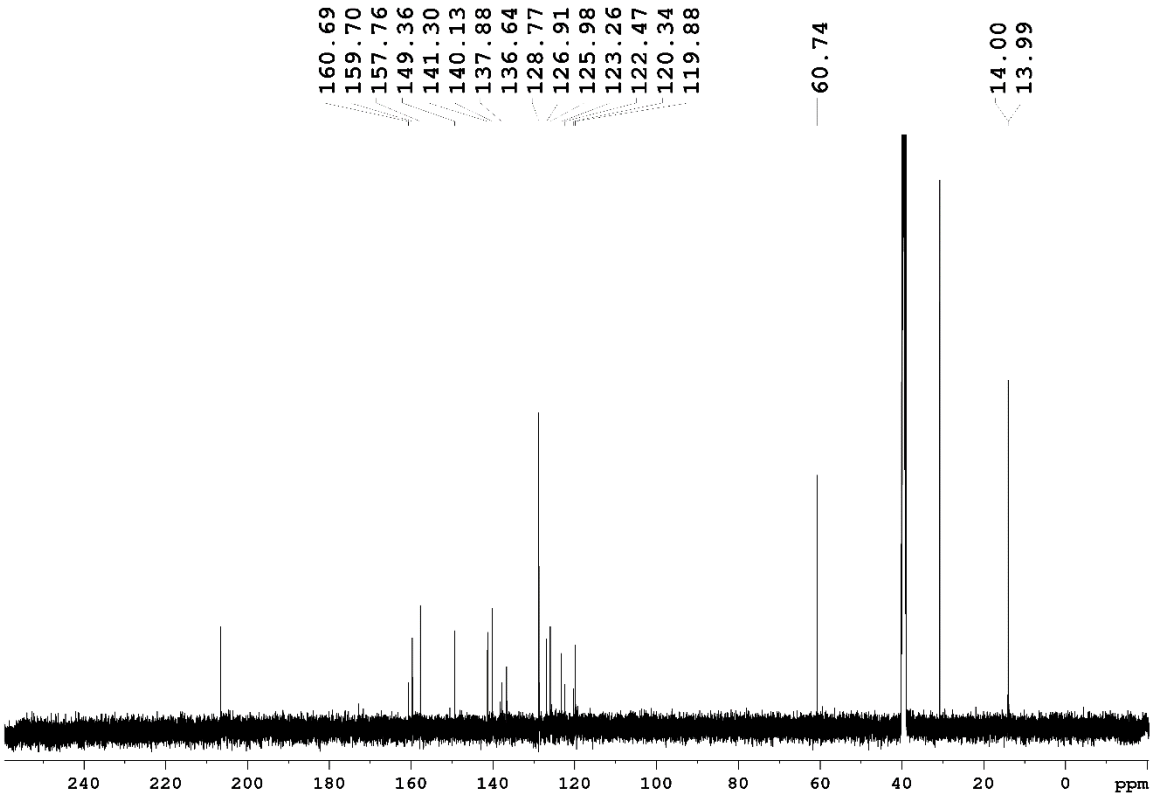
160.69
159.70
157.76
149.36
141.30
140.13
137.88
136.64
128.77
126.91
125.98
123.26
122.47
120.34
119.88
60.74
14.00
13.99
240
220
200
180
160
140
120
100
80
60
40
20
0
ppm

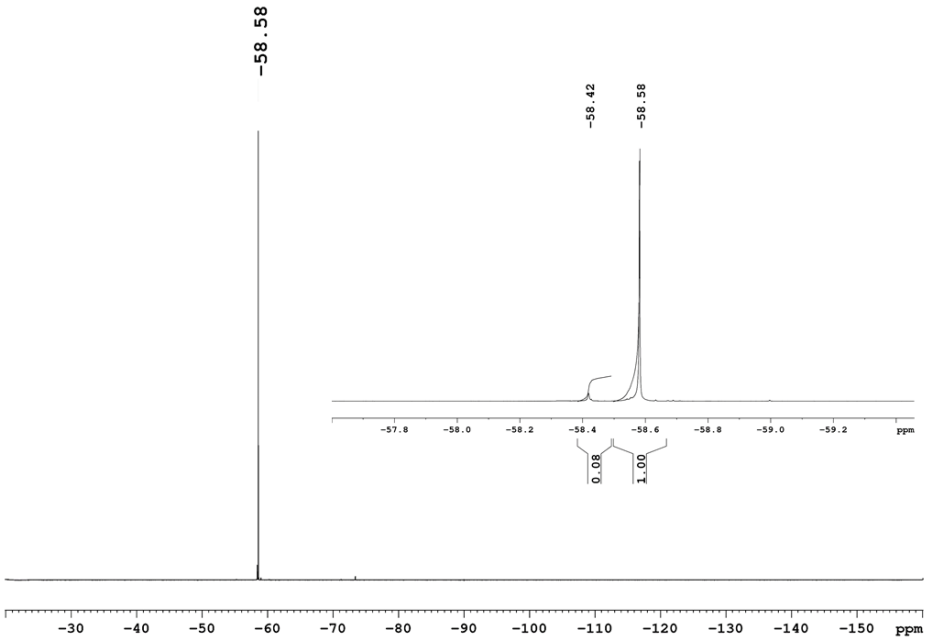
-58.58
-58.42
-58.58
-57.8
-58.0
-58.2
-58.4
-58.6
-58.8
-59.0
-59.2
ppm
0.08
1.00
-30
-40
-50
-60
-70
-80
-90
-100
-110
-120
-130
-140
-150
ppm

5.3.33 Synthesis of [Pt(pht)(triazolate^{CF3,COOEt})]

USC-KP045-17

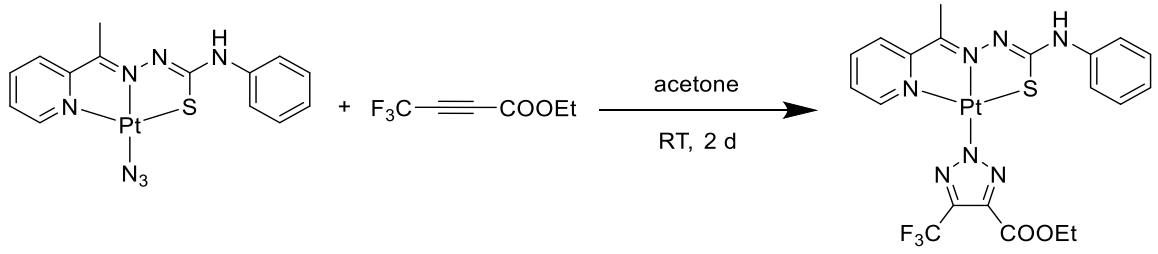

$C_{14}H_{13}N_7PtS$ 506.45 g/mol

$C_6H_5F_3O_2$ 166.10 g/mol

$C_{20}H_{18}F_3N_7O_2PtS$ 672.55 g/mol

[Pt(N_3)(pht)] (25 mg, 0.05 mmol) was suspended in acetone (10 mL) in a large glass vial at room temperature. Then, 4,4,4-trifluoro-2-butynoic acid ethyl ester (10 µL, 12.7 mg, 0.07 mmol) was added and stirring was continued at room temperature for 2 d. The resulting clear red solution was evaporated to dryness. The red solid obtained was washed with *n*-hexane (5 × 5 mL) and dried under vacuum for 1 d. Yield: 80% (25 mg, 0.04 mmol). **IR** (ATR): $\tilde{\nu}$ = 3336 (m), 1710 (s), 1546 (w), 1499 (m), 1467 (s), 1437 (s), 1311 (m), 1192 (m), 1135 (s), 1061 (s), 760 (w), 747 (m) cm^{-1}. **^{1}H NMR** (500.13 MHz, DMSO-d_6): δ = 10.30 (s, 1H, N*H*-phenyl), 9.21 (ddd, 1H, $^3J_{H6,H5}$ = 5.5 Hz, $^4J_{H6,H4}$ = 1.5 Hz, $^5J_{H6,H3}$ = 0.6 Hz, py-H6), 8.23 (dt, 1H, $^3J_{H4,H3/H5}$ = 7.9 Hz, $^4J_{H4,H6}$ = 1.6 Hz, py-H4), 7.92 (d, 1H, $^3J_{H3,H4}$ = 7.4 Hz, py-H3), 7.72 (ddd, 1H, $^3J_{H5,H4}$ = 7.7 Hz, $^3J_{H5,H6}$ = 5.6 Hz, $^4J_{H5,H3}$ = 1.3 Hz, py-H5), 7.60 (d, 2H, $^3J_{H3'/H5',H2'/H6'}$ = 7.7 Hz, phenyl-H3'/H5'), 7.34 (t, 2H, $^3J_{H2'/H6',H3'/H5'}$ = 8.0 Hz, phenyl-H2'/H6'), 7.05 (t, 1H, $^3J_{H4',H3'/H5'}$ = 7.4 Hz, phenyl-H4'), 4.32 (q, 2H, ^3J = 7.1 Hz, CH_2CH$_3$), 2.56 (s, 3H, CH_3), 1.31 (t, 3H, ^3J = 7.1 Hz, CH$_2$CH_3) ppm; **^{13}C NMR** (125.76 MHz, DMSO-d_6): δ = 175.24 (*C*-S), 161.21 (*C*=N), 159.42 (*C*OOEt), 158.72 (py-C2), 148.70 (py-C6), 140.85 (phenyl-C1'), 140.14 (py-C4), 138.17 (q, $^2J_{C,F}$ = 37.8 Hz, triazolate-C4), 136.74 (triazolate-C5), 128.67 (phenyl-C3'/C5'), 127.51 (py-C5), 126.53 (py-C3), 123.34 (phenyl-C4'), 121.14 (q, $^1J_{C,F}$ = 268.2 Hz, *C*F$_3$), 120.07 (phenyl-C2'/C6'), 61.80 (*C*H$_2$CH$_3$), 13.95 (*C*H$_3$), 13.76 (CH$_2$*C*H$_3$) ppm; **^{19}F NMR** (470.59 MHz, DMSO-d_6): δ = -58.71 (C*F*$_3$) ppm; **^{195}Pt NMR** (107.51 MHz, DMSO-d_6): δ = -3108 ppm. **Elemental analysis** (%) calcd. for $C_{20}H_{18}F_3N_7O_2PtS$: C 35.72, H 2.70, N 14.58, S 4.77; found (%): C 35.78, H 2.55, N 14.24, S 4.60.

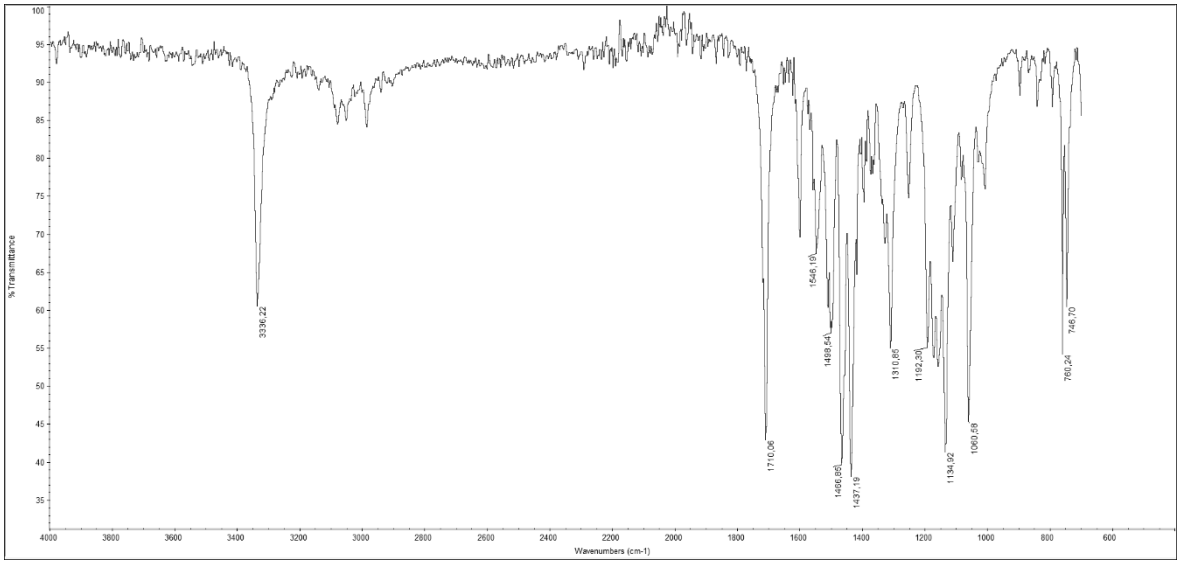
%Transmittance
Wavenumbers (cm-1)
3336,22
1710,06
1546,16
1468,64
1456,86
1437,19
1310,85
1192,30
1134,92
1060,59
760,24
746,70

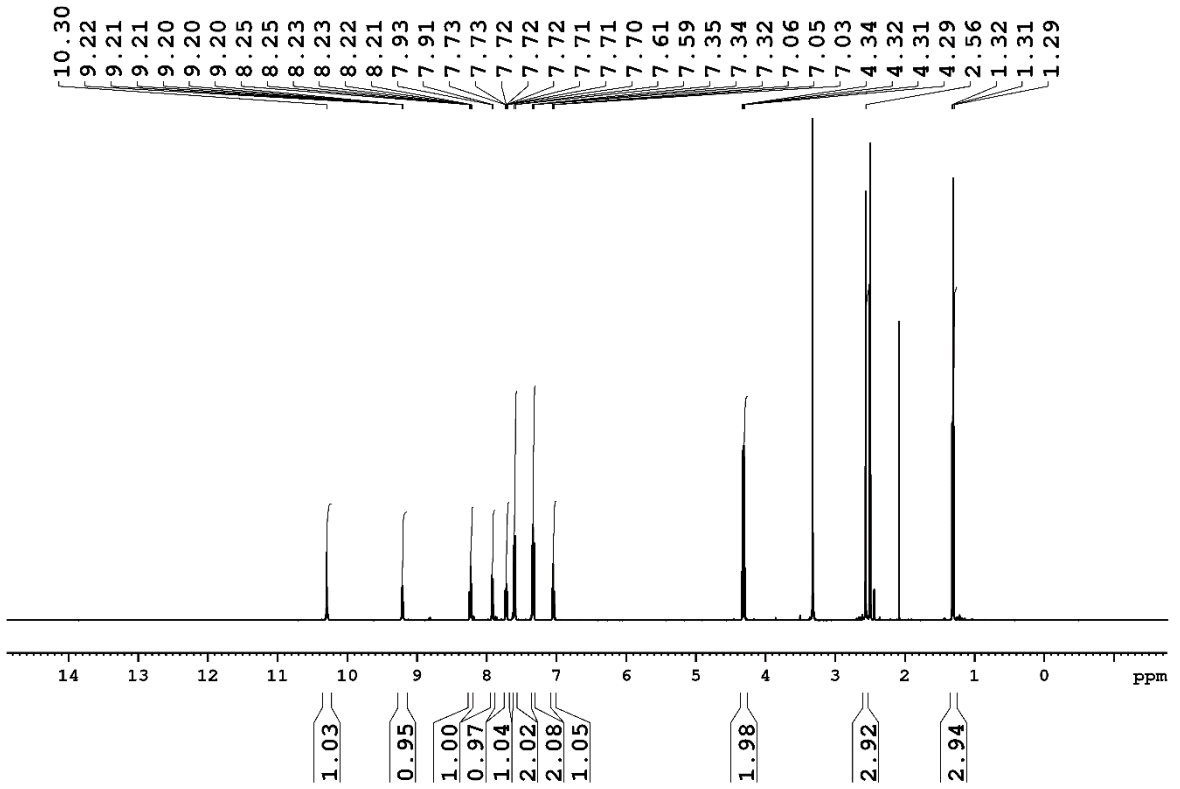
10.30
9.22
9.21
9.21
9.20
9.20
9.20
8.25
8.25
8.23
8.23
8.22
8.21
7.93
7.91
7.73
7.73
7.72
7.72
7.72
7.71
7.71
7.70
7.61
7.59
7.35
7.34
7.32
7.06
7.05
7.03
4.34
4.32
4.31
4.29
2.56
1.32
1.31
1.29
ppm
1.03
0.95
1.00
0.97
1.04
2.02
2.08
1.05
1.98
2.92
2.94

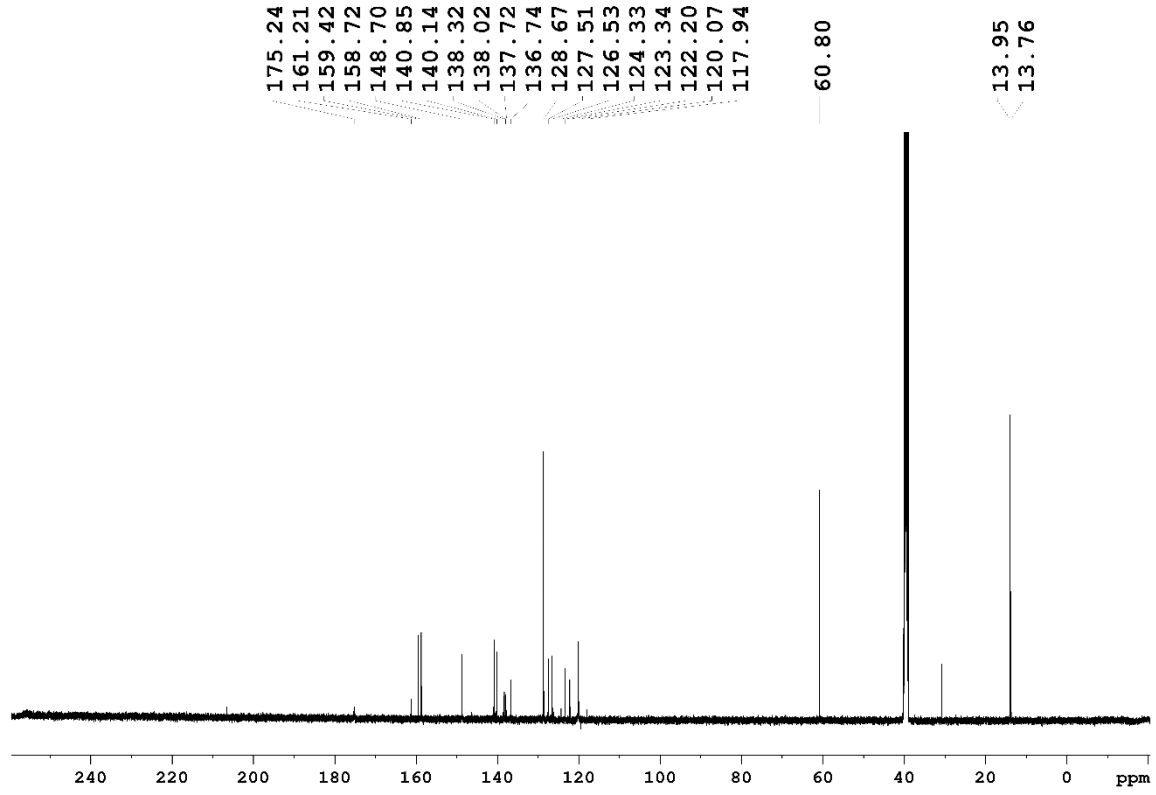
175.24
161.21
159.42
158.72
148.70
140.85
140.14
138.32
138.02
137.72
136.74
128.67
127.51
126.53
124.33
123.34
122.20
120.07
117.94
60.80
13.95
13.76
240
220
200
180
160
140
120
100
80
60
40
20
0
ppm

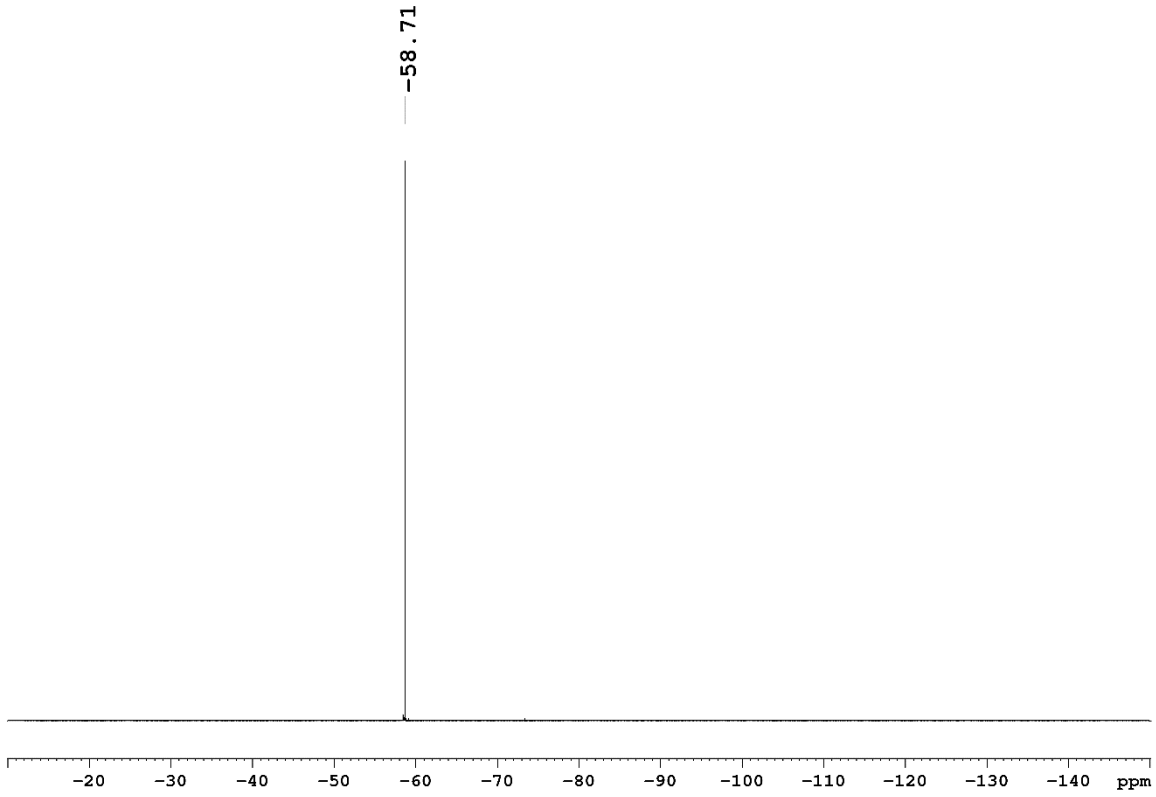
-58.71
-20
-30
-40
-50
-60
-70
-80
-90
-100
-110
-120
-130
-140
ppm

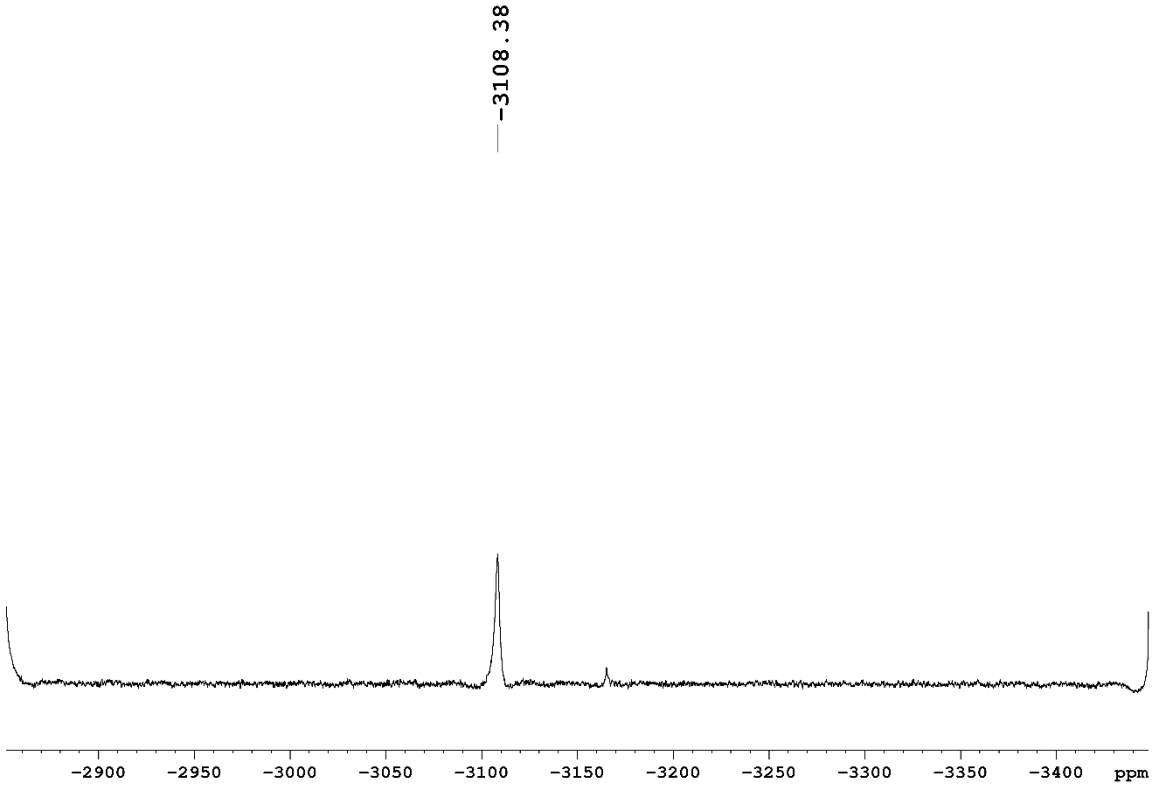
-3108.38
-2900
-2950
-3000
-3050
-3100
-3150
-3200
-3250
-3300
-3350
-3400
ppm

5.3.34 Synthesis of [Pd(pht)(triazolate^{COOCH3,COOCH3})]

USC-KP046-17

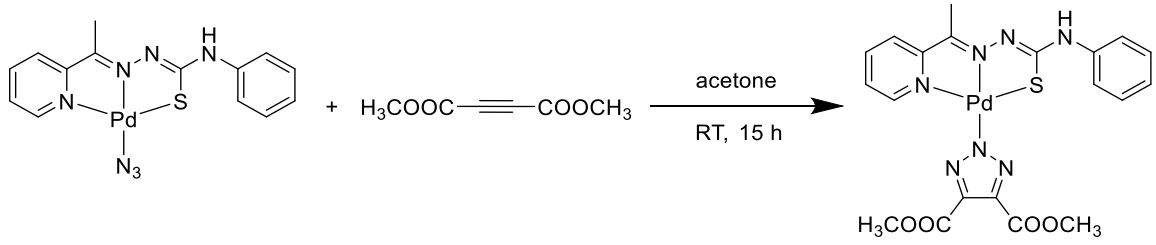

$C_{14}H_{13}N_7PdS$
417.78 g/mol

$C_6H_6O_4$
142.11 g/mol

$C_{20}H_{19}N_7O_4PdS$
559.89 g/mol

[Pd(N_3)(pht)] (40 mg, 0.10 mmol) was suspended in acetone (16 mL) in a large glass vial at room temperature. Then, dimethyl acetylenedicarboxylate (DMAD, 20 µL, 23.1 mg, 0.16 mmol) was added and stirring was continued at room temperature for 15 h. The resulting orange precipitate was filtered off, washed with *n*-hexane (5 × 5 mL), and dried under vacuum for 1 d. Yield: 70% (39 mg, 0.07 mmol). **IR** (ATR): $\tilde{\nu}$ = 3308 (m), 3092 (w), 1730 (m), 1709 (w), 1602 (w), 1553 (w), 1502 (m), 1460 (m), 1437 (s), 1396 (w), 1294 (m), 1159 (w), 1090 (m), 828 (w), 800 (w), 770 (w), 756 (w) cm^{-1}. **^{1}H NMR** (500.13 MHz, DMSO-d_6): δ = 10.18 (s, 1H, N*H*-phenyl), 8.91 (ddd, 1H, $^3J_{H6,H5}$ = 5.4 Hz, $^4J_{H6,H4}$ = 1.6 Hz, $^5J_{H6,H3}$ = 0.5 Hz, py-H6), 8.24 (dt, 1H, $^3J_{H4,H3/H5}$ = 7.9 Hz, $^4J_{H4,H6}$ = 1.6 Hz, py-H4), 7.97 (d, 1H, $^3J_{H3,H4}$ = 7.5 Hz, py-H3), 7.69 (ddd, 1H, $^3J_{H5,H4}$ = 7.7 Hz, $^3J_{H5,H6}$ = 5.4 Hz, $^4J_{H5,H3}$ = 1.3 Hz, py-H5), 7.58 (d, 2H, $^3J_{H3'/H5',H2'/H6'}$ = 7.7 Hz, phenyl-H3'/H5'), 7.32 (t, 2H, $^3J_{H2'/H6',H3'/H5'}$ = 8.0 Hz, phenyl-H2'/H6'), 7.04 (t, 1H, $^3J_{H4',H3'/H5'}$ = 7.4 Hz, phenyl-H4'), 3.81 (s, 6H, COOCH_3), 2.52 (s, 3H, CH_3) ppm; **^{13}C NMR** (125.76 MHz, DMSO-d_6): δ = 173.21 (*C*-S), 161.99 (*C*OOCH$_3$), 160.47 (*C*=N), 157.78 (py-C2), 149.47 (py-C6), 141.24 (phenyl-C1'), 140.17 (py-C4), 139.40 (triazolate-C4/C5), 128.80 (phenyl-C3'/C5'), 12.89 (py-C5), 125.92 (py-C3), 123.31 (phenyl-C4'), 120.04 (phenyl-C2'/C6'), 52.05 (COO*C*H$_3$), 14.01 (*C*H$_3$) ppm. **Elemental analysis** (%) calcd. for $C_{20}H_{19}N_7O_4PdS$: C 42.90, H 3.42, N 17.51, S 5.73; found (%): C 42.85, H 3.79, N 17.58, S 5.62.

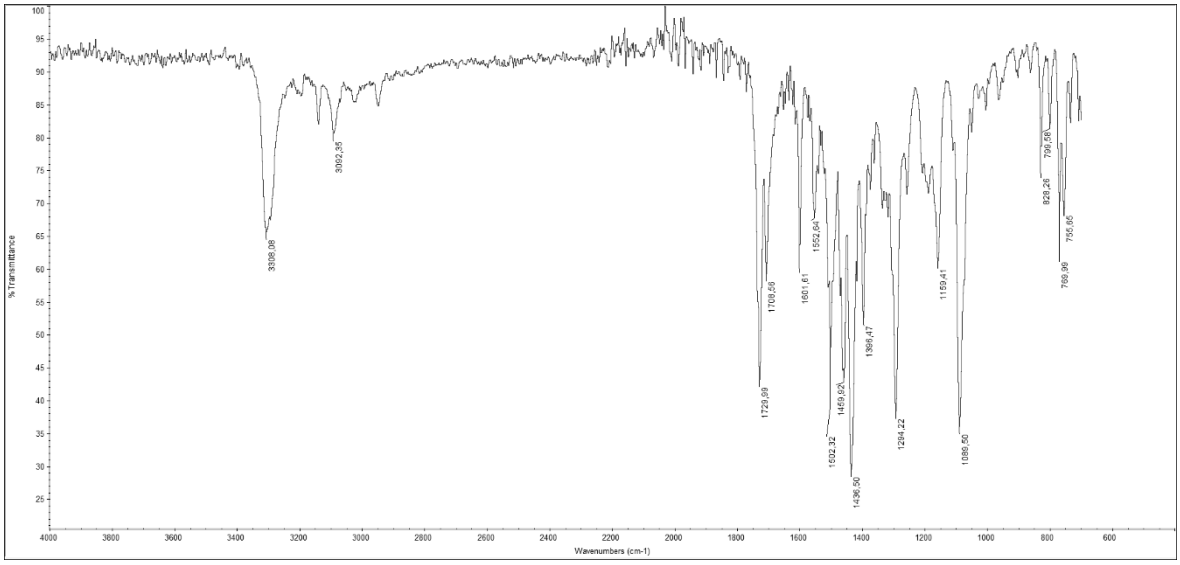
% Transmittance
Wavenumbers (cm-1)
3388,08
3062,35
1729,69
1708,58
1661,61
1552,64
1602,32
1459,60
1436,90
1366,47
1284,22
1159,41
1086,50
829,26
790,66
760,96
755,66

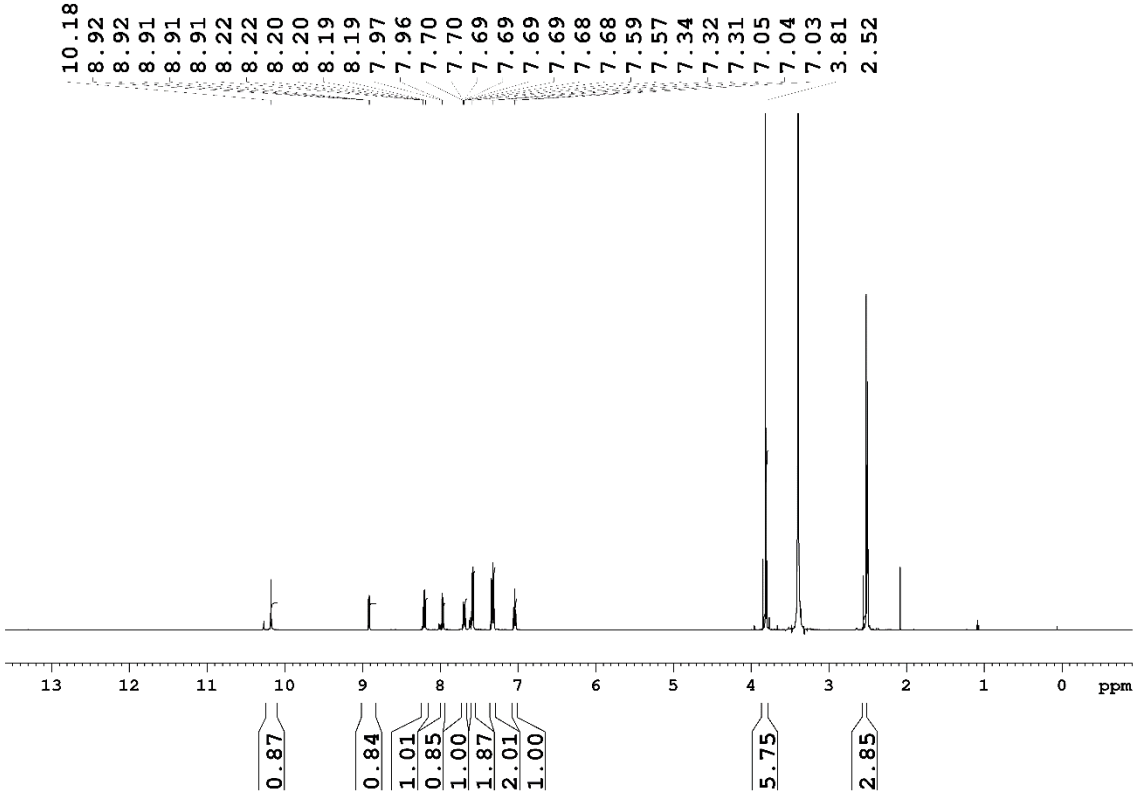
10.18
8.92
8.92
8.91
8.91
8.91
8.22
8.22
8.20
8.20
8.19
8.19
7.97
7.96
7.70
7.70
7.69
7.69
7.69
7.69
7.68
7.68
7.59
7.57
7.34
7.32
7.31
7.05
7.04
7.03
3.81
2.52
ppm
0.87
0.84
1.01
0.85
1.00
1.87
2.01
1.00
5.75
2.85

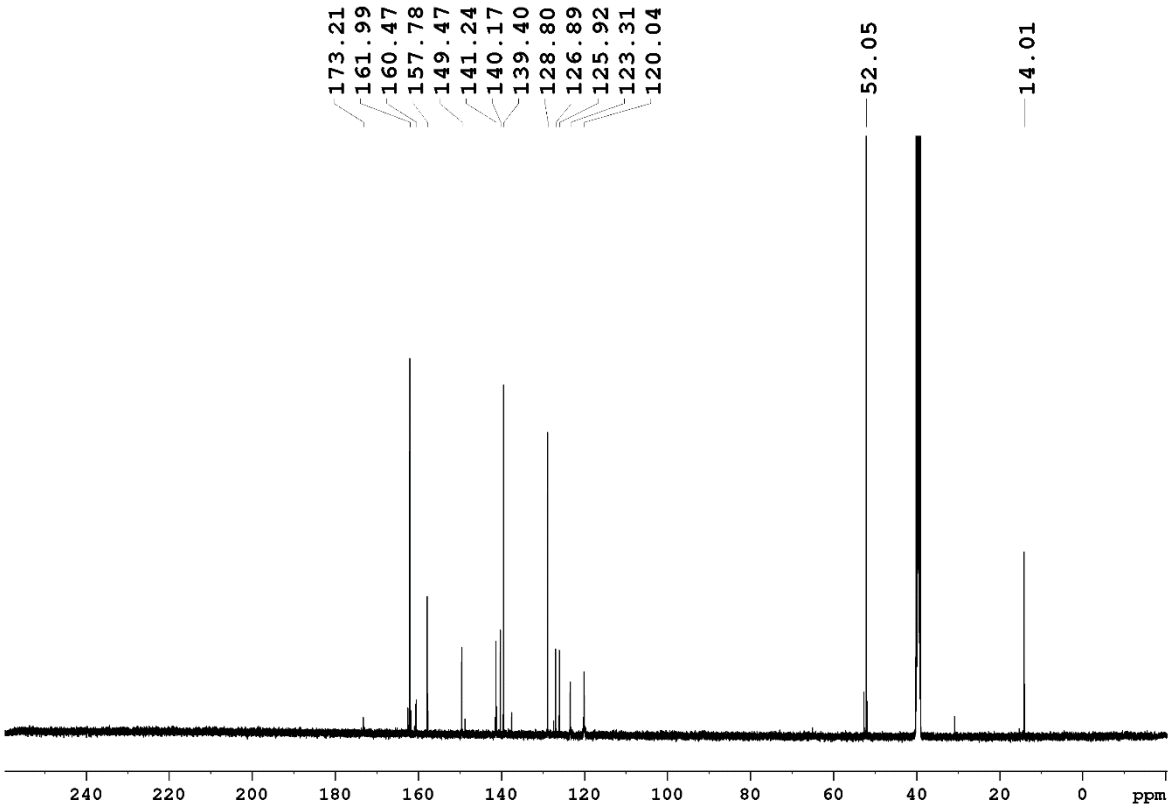
173.21
161.99
160.47
157.78
149.47
141.24
140.17
139.40
128.80
126.89
125.92
123.31
120.04
52.05
14.01
240
220
200
180
160
140
120
100
80
60
40
20
0
ppm

5.3.35 Synthesis of [Pt(pht)(triazolate^{COOCH3,COOCH3}-N^1)]

USC-KP047-20

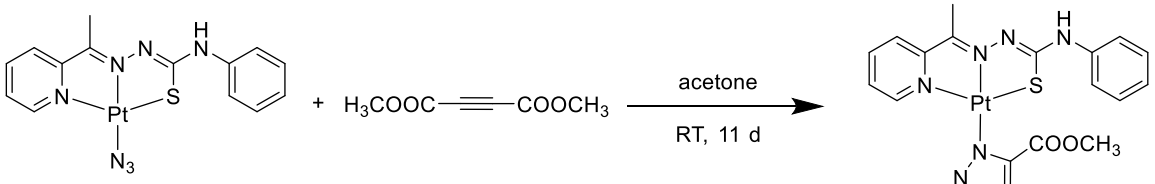

$C_{14}H_{13}N_7PtS$
506.45 g/mol

$C_6H_6O_4$
142.11 g/mol

$C_{20}H_{19}N_7O_4PtS$
648.56 g/mol

[Pt(N_3)(pht)] (30 mg, 0.06 mmol) was suspended in acetone (15 mL) in a large glass vial at room temperature. Then, dimethyl acetylenedicarboxylate (DMAD, 30 µL, 34.7 mg, 0.24 mmol) was added and stirring was continued at room temperature for 11 d. Then, the volume of solution was reduced to approx. 7 mL and the resulting orange precipitate filtered off, washed with *n*-hexane (3 × 5 mL), and dried under vacuum for 1 d. Yield: 60% (23 mg, 0.04 mmol). **IR** (ATR): $\tilde{\nu}$ = 3013 (w), 1730 (m), 1728 (m), 1560 (w), 1512 (w), 1461 (m), 1440 (s), 1322 (w), 1259 (w), 1202 (w), 1155 (m), 1154 (m), 1108 (w), 1037 (w), 758 (w) cm^{-1}. **^{1}H NMR** (400.40 MHz, DMSO-d_6): δ = 10.42 (s, 1H, N*H*-C_6H_5), 8.28 (t, 1H, $^3J_{H4,H3/H5}$ = 8.4 Hz, py-H4), 8.00–7.96 (m, 2H, py-H3, py-H6), 7.69–7.64 (m, 3H, py-H5, phenyl-H3'/H5'), 7.36 (t, 2H, $^3J_{H2'/H6',H3'/H5'}$ = 7.7 Hz, phenyl-H2'/H6'), 7.06 (t, 1H, $^3J_{H4',H3'/H5'}$ = 7.6 Hz, phenyl-H4'), 3.84 (s, 3H, triazolate-C5-COOC*H*$_3$), 3.80 (s, 3H, triazolate-C4-COOC*H*$_3$), 2.61 (s, 3H, C*H*$_3$) ppm. No ^{13}C and ^{195}Pt NMR spectra were recorded due to low solubility of the compound in all common solvents. **Elemental analysis** (%) calcd. for $C_{20}H_{19}N_7O_4PtS$: C 37.04, H 2.95, N 15.12, S 4.94; found (%): C 36.95, H 3.03, N 15.22, S 4.94.

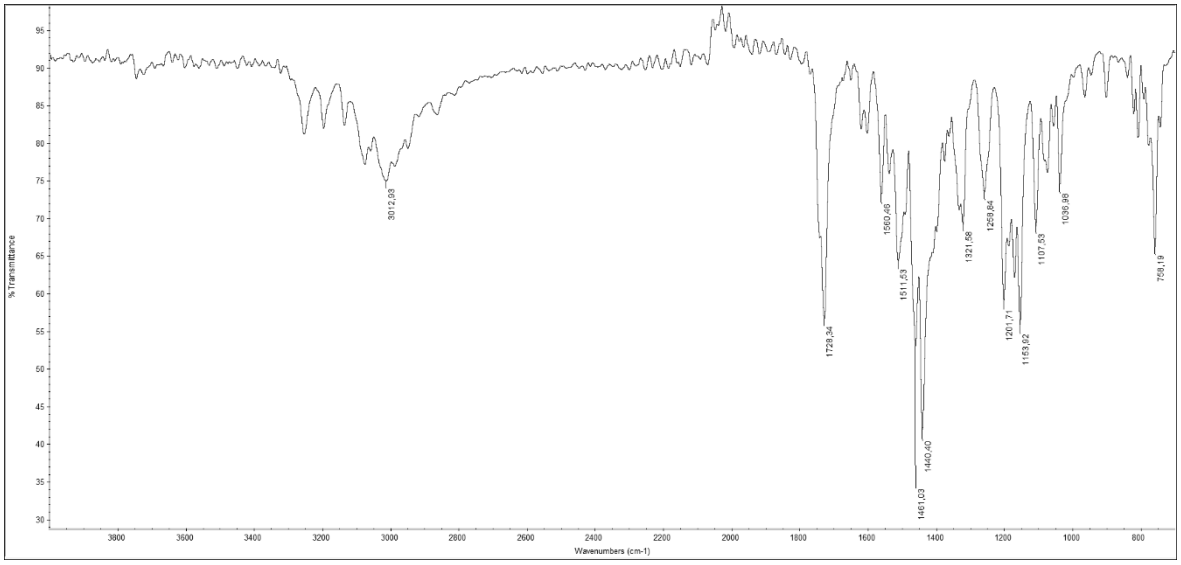
% Transmittance
Wavenumbers (cm-1)
3012,93
1729,34
1560,49
1511,53
1461,03
1440,40
1321,58
1259,84
1201,71
1163,62
1107,53
1036,98
759,19

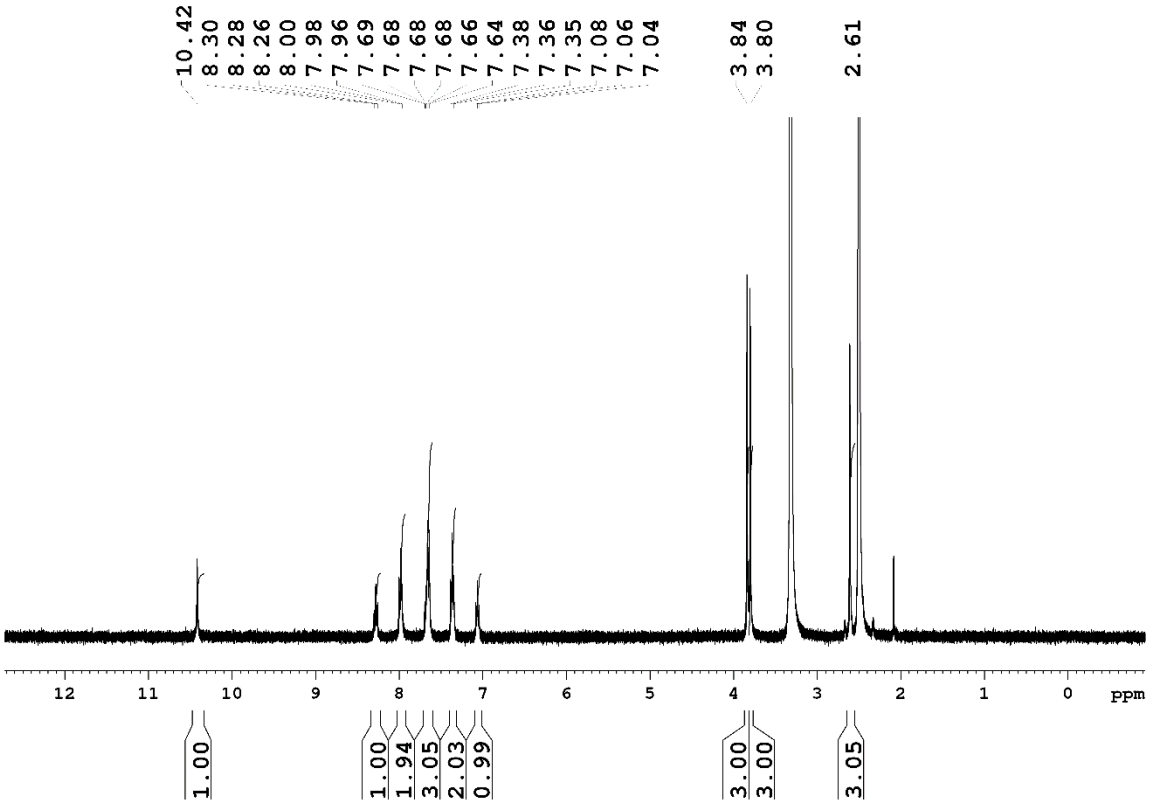
10.42
8.30
8.28
8.26
8.00
7.98
7.96
7.69
7.68
7.68
7.68
7.66
7.64
7.38
7.36
7.35
7.08
7.06
7.04
3.84
3.80
2.61
ppm
1.00
1.00
1.94
3.05
2.03
0.99
3.00
3.00
3.05

5.3.36 Synthesis of [Pt(pht)(triazolate^{COOCH3,COOCH3}-N^2)]

USC-KP060-01

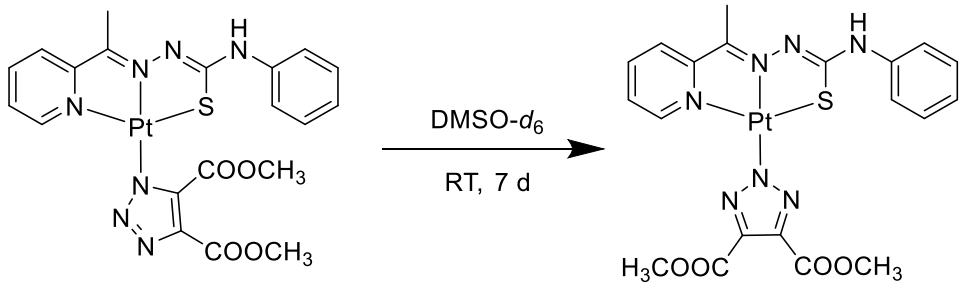

$C_{20}H_{19}N_7O_4PtS$
648.56 g/mol

$C_{20}H_{19}N_7O_4PtS$
648.56 g/mol

A suspension of [Pt(pht)(triazolate^{COOCH3,COOCH3}-N^1)] (approx. 10 mg) in DMSO-d_6 was kept in an NMR tube at room temperature for 7 d, during which time the light orange suspension turned into a clear dark red solution, which was identified as the N2-coordinated isomer by NMR spectroscopy. **^{1}H NMR** (500.13 MHz, DMSO-d_6): δ = 10.30 (s, 1H, N*H*-C_6H_5), 9.24 (ddd, 1H, $^3J_{H6,H5}$ = 5.6 Hz, $^4J_{H6,H4}$ = 1.5 Hz, $^5J_{H6,H3}$ = 0.6 Hz, py-H6), 8.25 (dt, 1H, $^3J_{H4,H3/H5}$ = 7.9 Hz, $^4J_{H4,H6}$ = 1.6 Hz, py-H4), 7.93 (d, 1H, $^3J_{H3,H4}$ = 7.4 Hz, py-H3), 7.75 (ddd, 1H, $^3J_{H5,H4}$ = 7.7 Hz, $^3J_{H5,H6}$ = 5.6 Hz, $^4J_{H5,H3}$ = 1.4 Hz, py-H5), 7.61 (d, 2H, $^3J_{H3'/H5',H2'/H6'}$ = 7.7 Hz, phenyl-H3'/H5'), 7.35 (t, 2H, $^3J_{H2'/H6',H3'/H5'}$ = 8.0 Hz, phenyl-H2'/H-6'), 7.06 (t, 1H, $^3J_{H4',H3'/H5'}$ = 7.4 Hz, phenyl-H4'), 3.83 (s, 6H, COOCH_3), 2.57 (s, 3H, CH_3) ppm; **^{13}C NMR** (125.76 MHz, DMSO-d_6): δ = 175.59 (*C*-S), 161.64 (*C*OOCH$_3$), 161.03 (*C*=N), 158.76 (py-C2), 148.76 (py-C6), 140.87 (phenyl-C1'), 140.15 (py-C4), 139.54 (triazolate-C4/C5), 128.71 (phenyl-C3'/C5'), 127.61 (py-C5), 126.52 (py-C3), 123.43 (phenyl-C4'), 120.25 (phenyl-C2'/C6'), 52.07 (COO*C*H$_3$), 13.76 (*C*H$_3$) ppm. **^{195}Pt NMR** (107.51 MHz, DMSO-d_6): δ = -3105 ppm.

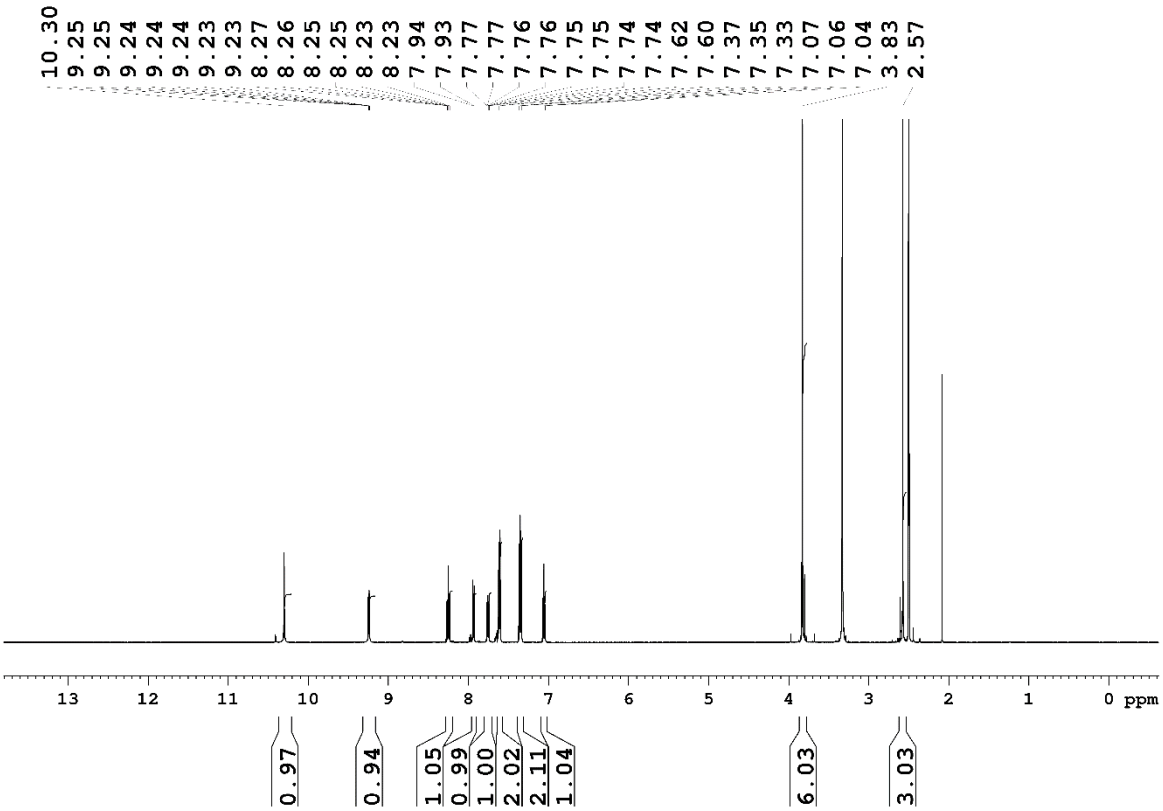
10.30
9.25
9.25
9.24
9.24
9.24
9.23
9.23
8.27
8.26
8.25
8.25
8.23
8.23
7.94
7.93
7.77
7.77
7.76
7.76
7.75
7.75
7.74
7.74
7.62
7.60
7.37
7.35
7.33
7.07
7.06
7.04
3.83
2.57
13 12 11 10 9 8 7 6 5 4 3 2 1 0 ppm
0.97
0.94
1.05
0.99
1.00
2.02
2.11
1.04
6.03
3.03

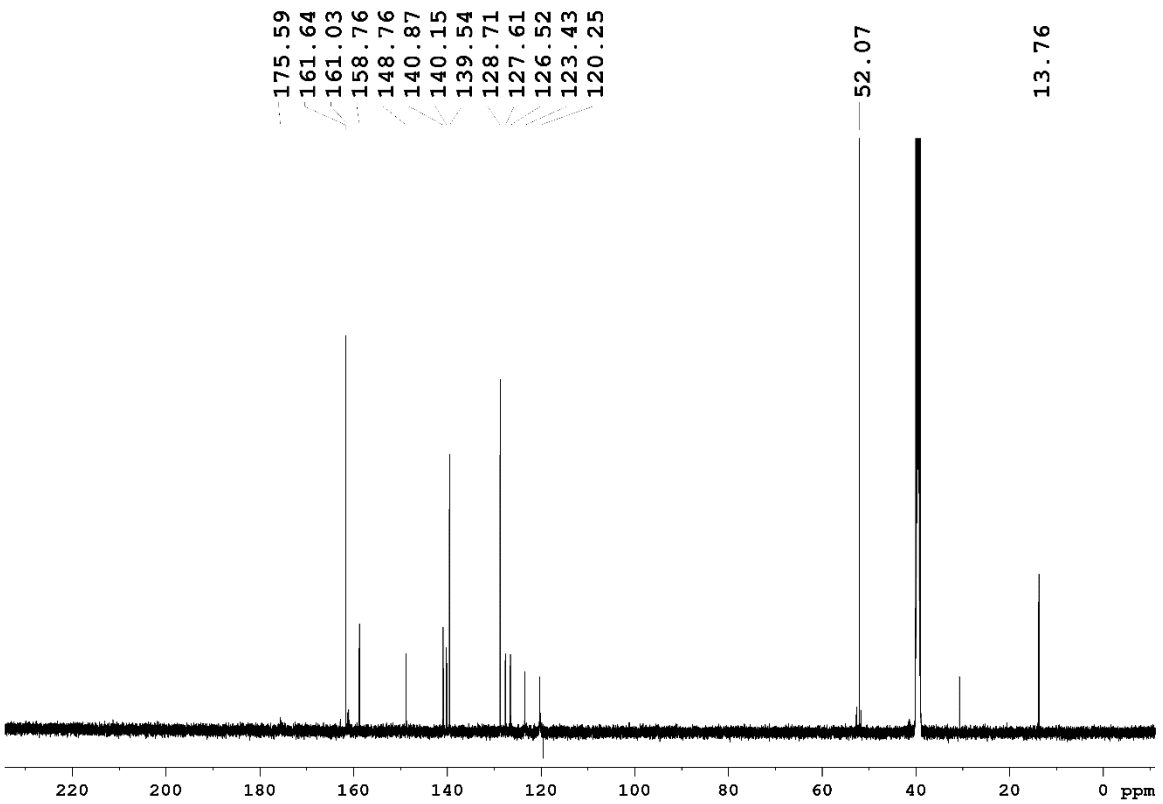
175.59
161.64
161.03
158.76
148.76
140.87
140.15
139.54
128.71
127.61
126.52
123.43
120.25
52.07
13.76
220 200 180 160 140 120 100 80 60 40 20 0 ppm

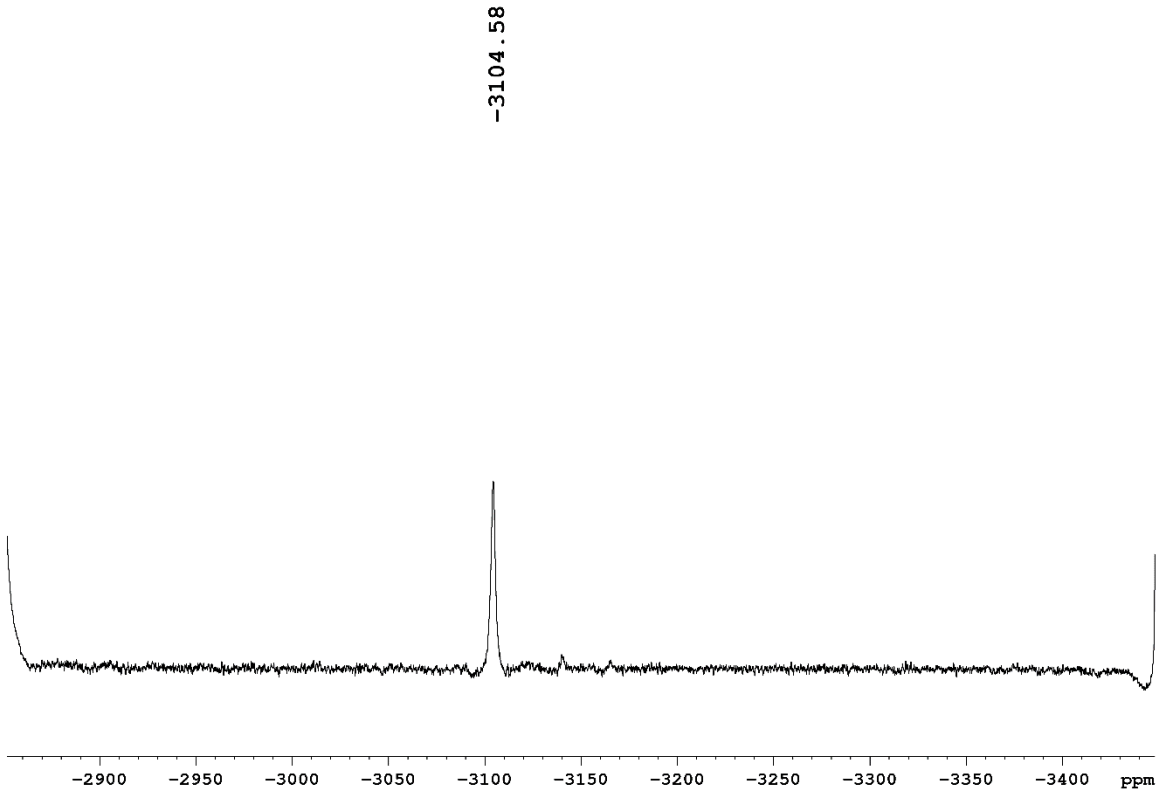
-3104.58
-2900
-2950
-3000
-3050
-3100
-3150
-3200
-3250
-3300
-3350
-3400
ppm

5.3.37 Synthesis of [Pd(pht)(triazolate^{COOEt,COOEt})]

USC-KP052-10

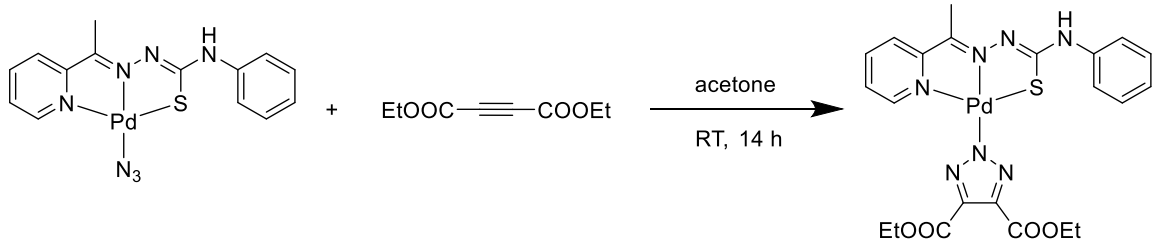

$C_{14}H_{13}N_7PdS$
417.78 g/mol

$C_8H_{10}O_4$
170.16 g/mol

$C_{22}H_{23}N_7O_4PdS$
587.95 g/mol

[Pd(N_3)(pht)] (12 mg, 28.7 µmol) was suspended in acetone (9 mL) in a large glass vial at room temperature. Then, diethyl acetylenedicarboxylate (24 µL, 25.5 mg, 150 µmol) was added and stirring continued at room temperature for 14 h. The resulting yellow precipitate was filtered off, washed with *n*-hexane (5 × 5 mL), and dried under vacuum for 1 d. Yield: 89% (15 mg, 25.5 µmol). **IR** (ATR): $\tilde{\nu}$ = 3303 (m), 1727 (s), 1602 (w), 1498 (m), 1461 (s), 1437 (s), 1293 (m), 1194 (w), 1155 (w), 1090 (s), 762 (w), 742 (w) cm^{-1}. **^{1}H NMR** (500.13 MHz, DMSO-d_6): δ = 10.23 (s, 1H, N*H*-phenyl), 8.92 (ddd, 1H, $^3J_{H6,H5}$ = 5.4 Hz, $^4J_{H6,H4}$ = 1.6 Hz, $^5J_{H6,H3}$ = 0.6 Hz, py-H6), 8.25 (dt, 1H, $^3J_{H4,H3/H5}$ = 7.9 Hz, $^4J_{H4,H6}$ = 1.6 Hz, py-H4), 8.02 (d, 1H, $^3J_{H3,H4}$ = 7.4 Hz, py-H3), 7.75 (ddd, 1H, $^3J_{H5,H4}$ = 7.7 Hz, $^3J_{H5,H6}$ = 5.4 Hz, $^4J_{H5,H3}$ = 1.3 Hz, py-H5), 7.62 (d, 2H, $^3J_{H3'/H5',H2'/H6'}$ = 7.7 Hz, phenyl-H3'/H5'), 7.35 (t, 2H, $^3J_{H2'/H6',H3'/H5'}$ = 8.0 Hz, phenyl-H2'/H-6'), 7.06 (t, 1H, $^3J_{H4',H3'/H5'}$ = 7.4 Hz, phenyl-H4'), 4.28 (q, 4H, ^3J = 7.1 Hz, COOC*H*$_2$CH$_3$), 2.54 (s, 3H, C*H*$_3$), 1.28 (t, 6H, ^3J = 7.1 Hz, COOCH$_2$C*H*$_3$) ppm; **^{13}C NMR** (100.68 MHz, DMSO-d_6): δ = 173.18 (*C*-S), 161.58 (*C*OOCH$_2$CH$_3$), 160.40 (*C*=N), 157.75 (py-C2), 149.39 (py-C6), 141.21 (phenyl-C1'), 140.14 (py-C4), 139.53 (triazolate-C4/C5), 128.73 (phenyl-C3'/C5'), 126.84 (py-C5), 125.88 (py-C3), 123.24 (phenyl-C4'), 119.96 (phenyl-C2'/C6'), 60.65 (*C*H$_2$CH$_3$), 14.03 (CH$_2$*C*H$_3$), 13.95 (*C*H$_3$) ppm. **Elemental analysis** (%) calcd. for $C_{22}H_{23}N_7O_4PdS$: C 44.94, H 3.94, N 16.68, S 5.45; found (%): C 44.80, H 4.01, N 16.57, S 5.37.

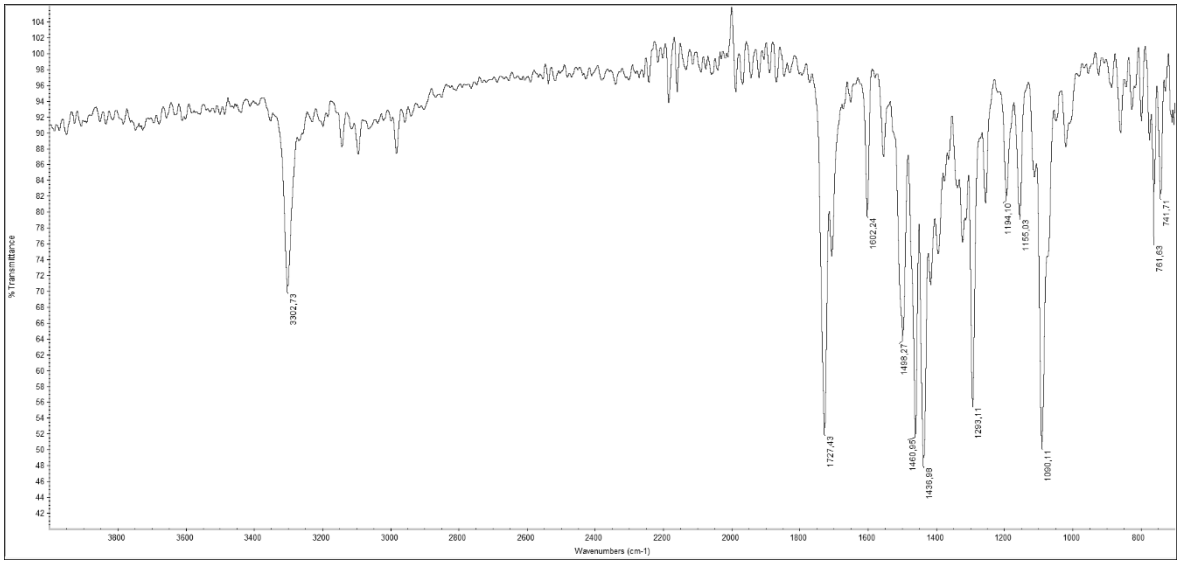
% Transmittance
Wavenumbers (cm-1)
3302,73
1727,43
1602,24
1498,27
1460,66
1436,68
1293,11
1194,10
1155,03
1060,11
761,63
741,71

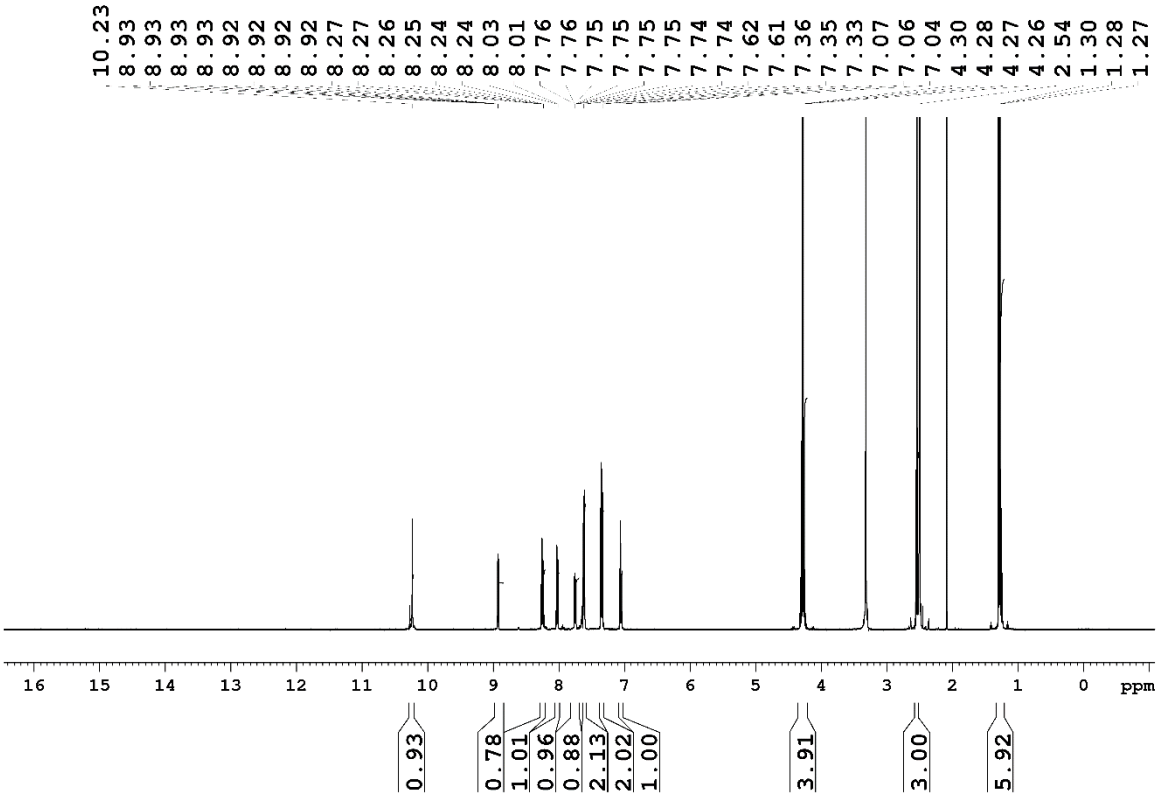
10.23
8.93
8.93
8.93
8.93
8.92
8.92
8.92
8.92
8.27
8.27
8.26
8.25
8.24
8.24
8.03
8.01
7.76
7.76
7.75
7.75
7.75
7.75
7.74
7.74
7.62
7.61
7.36
7.35
7.33
7.07
7.06
7.04
4.30
4.28
4.27
4.26
2.54
1.30
1.28
1.27
ppm
0.93
0.78
1.01
0.96
0.88
2.13
2.02
1.00
3.91
3.00
5.92

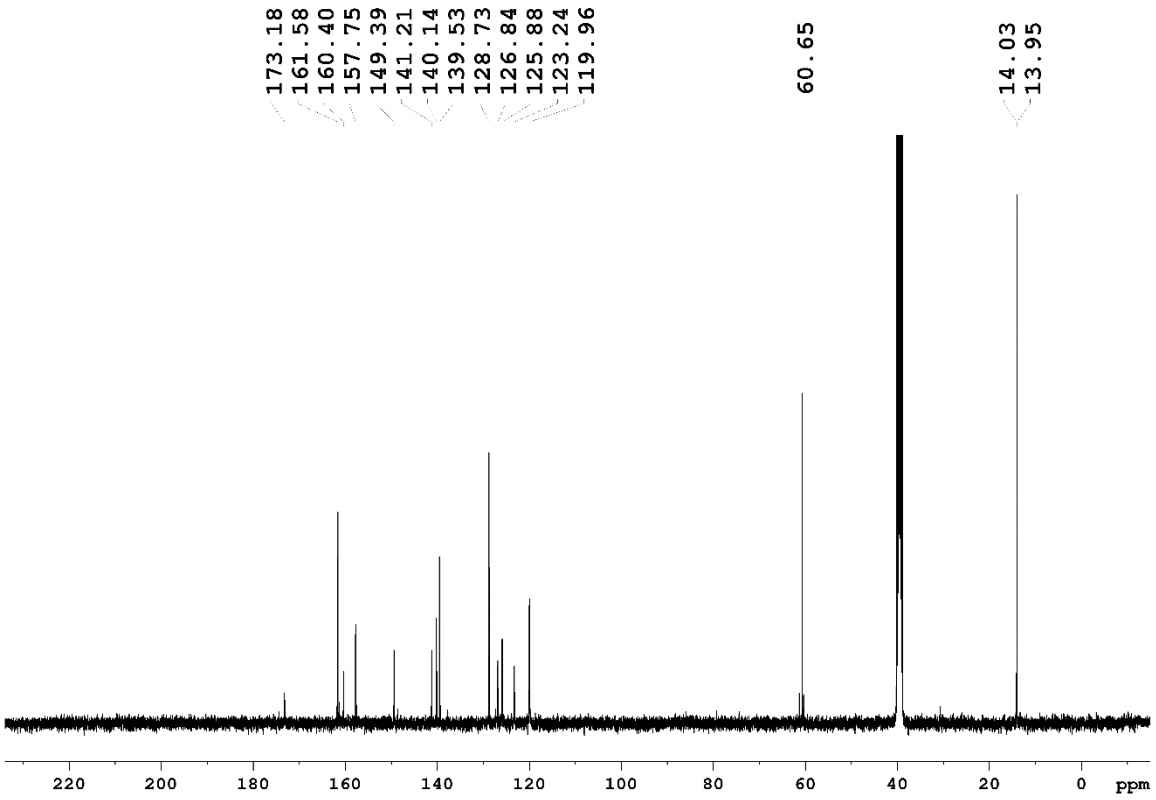
173.18
161.58
160.40
157.75
149.39
141.21
140.14
139.53
128.73
126.84
125.88
123.24
119.96
60.65
14.03
13.95
220
200
180
160
140
120
100
80
60
40
20
0
ppm

5.3.38 Synthesis of [Pt(pht)(triazolate^{COOEt,COOEt}-N^1)]

USC-KP053-03

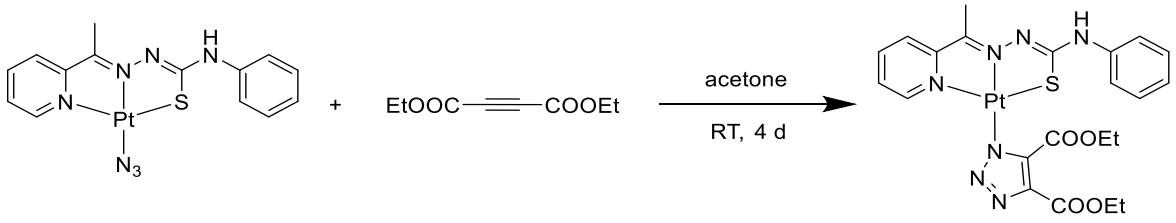

$C_{14}H_{13}N_7PtS$
506.45 g/mol

$C_8H_{10}O_4$
170.16 g/mol

$C_{22}H_{23}N_7O_4PtS$
676.61 g/mol

[Pt(N_3)(pht)] (20 mg, 39.5 µmol) was suspended in acetone (10 mL) in a large glass vial at room temperature. Then, diethyl acetylenedicarboxylate (40 µL, 42.5 mg, 250 µmol) was added and stirring continued at room temperature for 4 d. The resulting light red precipitate was filtered off, washed with *n*-hexane (5 × 5 mL), and dried under vacuum for 1 d. Yield: 11 mg (16.3 µmol, 41%). **IR** (ATR): $\tilde{\nu}$ = 3252 (w), 2987 (w), 1721 (s), 1605 (w), 1559 (w), 1503 (m), 1462 (m), 1440 (s), 1337 (w), 1259 (w), 1191 (m), 1156 (m), 1105 (w), 758 (m) cm^{-1}. **^{1}H NMR** (400.40 MHz, DMSO-d_6): δ = 10.39 (s, 1H, N*H*-phenyl), 8.27 (t, 1H, $^3J_{H4,H3/H5}$ = 7.6 Hz, py-H4), 7.98 (d, 1H, $^3J_{H3,H4}$ = 7.7 Hz, py-H3), 7.88 (d, 1H, $^3J_{H6,H5}$ = 5.4 Hz, py-H6), 7.68–7.64 (m, 3H, py-H5, phenyl-H3'/H5'), 7.36 (t, 2H, $^3J_{H2'/H6',H3'/H5'}$ = 7.9 Hz, phenyl-H2'/H6'), 7.06 (t, 1H, $^3J_{H4',H3'/H5'}$ = 7.2 Hz, phenyl-H4'), 4.32–4.24 (m, 4H, triazolate-C4-COOC*H*$_2$CH$_3$/triazolate-C5-COOC*H*$_2$CH$_3$), 2.61 (s, 3H, C*H*$_3$), 1.28–1.23 (m, 6H, triazolate-C4-COOC*H*$_3$/triazolate-C5-COOCH$_2$C*H*$_3$) ppm; **^{13}C NMR** (100.68 MHz, DMSO-d_6): δ = 162.30 (triazolate-C5-*C*OOCH$_2$CH$_3$), 160.79 (triazolate-C4-*C*OOCH$_2$CH$_3$), 158.48 (py-C2), 147.81 (py-C6), 141.00 (phenyl-C1'), 140.82 (py-C4), 128.71 (phenyl-C3'/C5'), 128.14 (py-C5), 126.70 (py-C3), 123.53 (phenyl-C4'), 120.22 (phenyl-C2'/C6'), 61.51 (triazolate-C5-COO*C*H$_2$CH$_3$), 60.31 (triazolate-C4-COO*C*H$_2$CH$_3$), 14.08 (triazolate-C5-COOCH$_2$*C*H$_3$), 13.90 (*C*H$_3$), 13.86 (triazolate-C4-COOCH$_2$*C*H$_3$) ppm. The C-S and C=N as well as triazolate-C4 and C5 carbon atom signals were not observed due to low solubility of the compound. Furthermore, no ^{195}Pt NMR could be recorded for this compound for the same reason. **Elemental analysis** (%) calcd. for $C_{22}H_{23}N_7O_4PtS$: C 39.05, H 3.43, N 14.49, S 4.74; found (%): C 39.03, H 3.51, N 14.63, S 4.63.

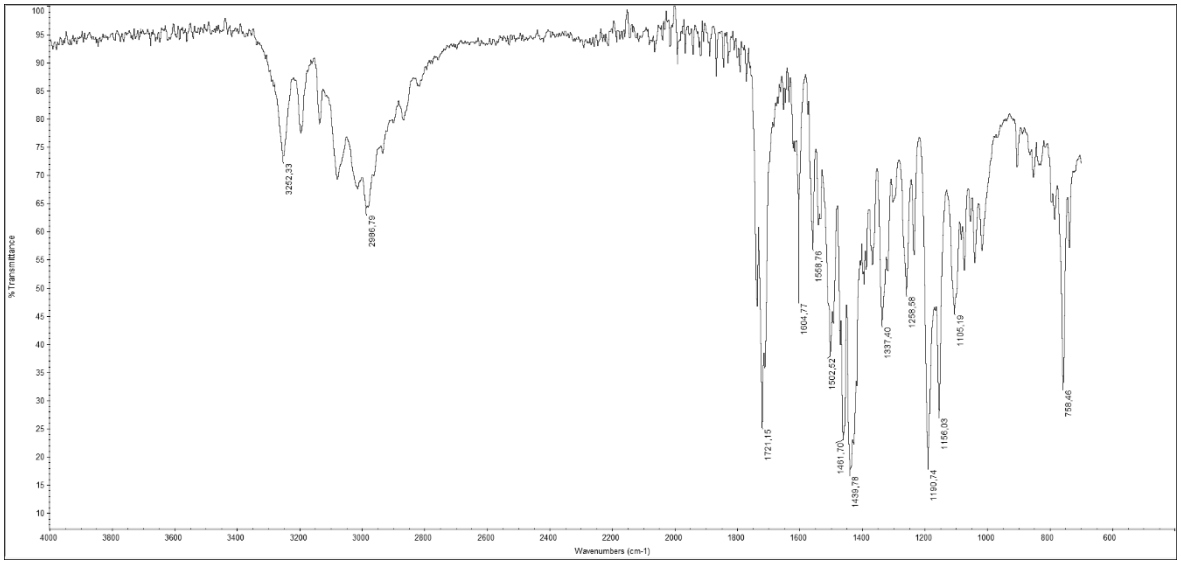
% Transmittance
Wavenumbers (cm-1)
3252.33
2896.79
1721.15
1604.77
1558.76
1502.62
1491.70
1439.78
1337.40
1258.98
1195.19
1190.74
1156.03
758.46

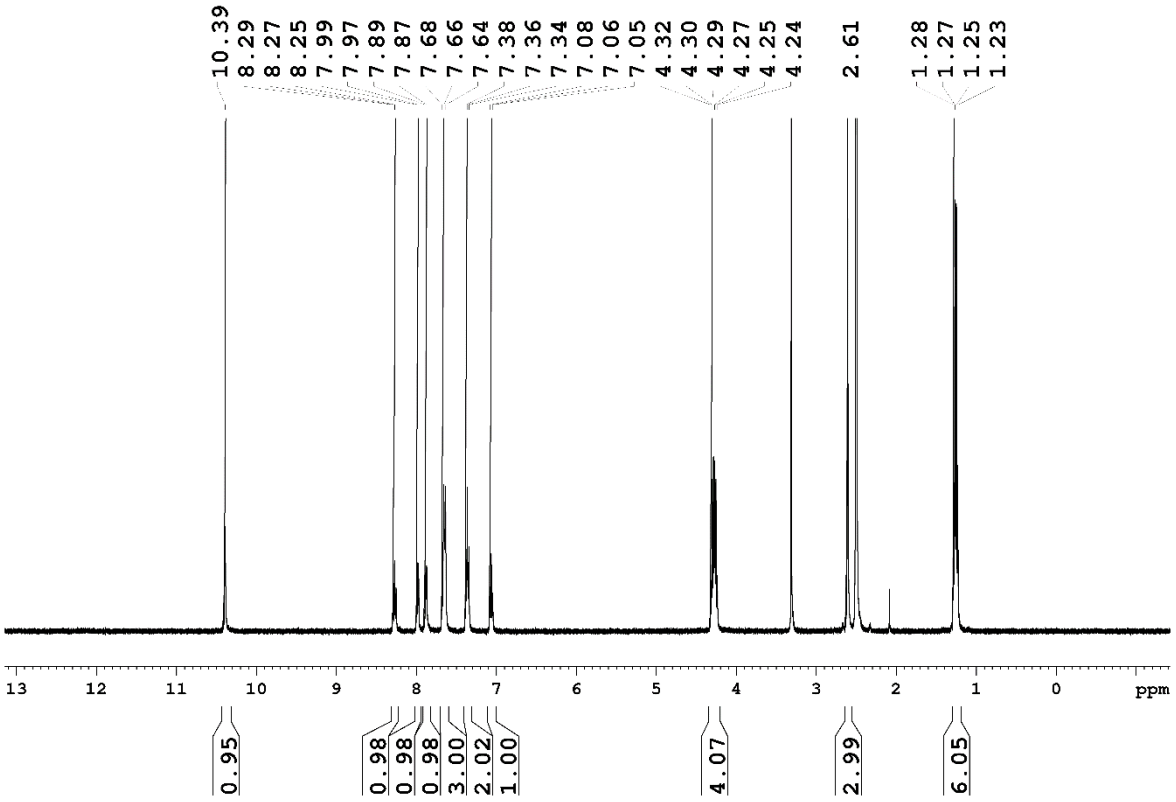
10.39
8.29
8.27
8.25
7.99
7.97
7.89
7.87
7.68
7.66
7.64
7.38
7.36
7.34
7.08
7.06
7.05
4.32
4.30
4.29
4.27
4.25
4.24
2.61
1.28
1.27
1.25
1.23
13
12
11
10
9
8
7
6
5
4
3
2
1
0
ppm
0.95
0.98
0.98
0.98
3.00
2.02
1.00
4.07
2.99
6.05

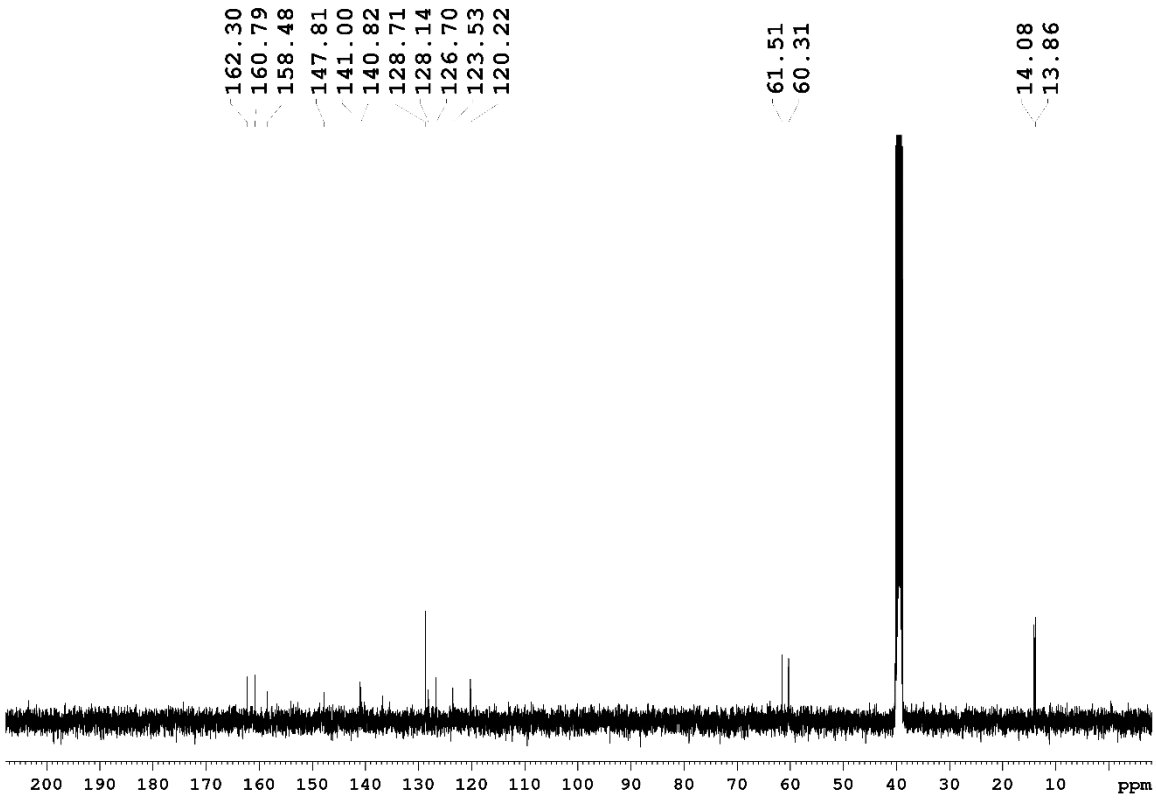
162.30
160.79
158.48
147.81
141.00
140.82
128.71
128.14
126.70
123.53
120.22
61.51
60.31
14.08
13.86
200 190 180 170 160 150 140 130 120 110 100 90 80 70 60 50 40 30 20 10 ppm

5.3.39 Synthesis of [Pt(pht)(triazolate^{COOEt,COOEt}-N^2)]

USC-KP061-01

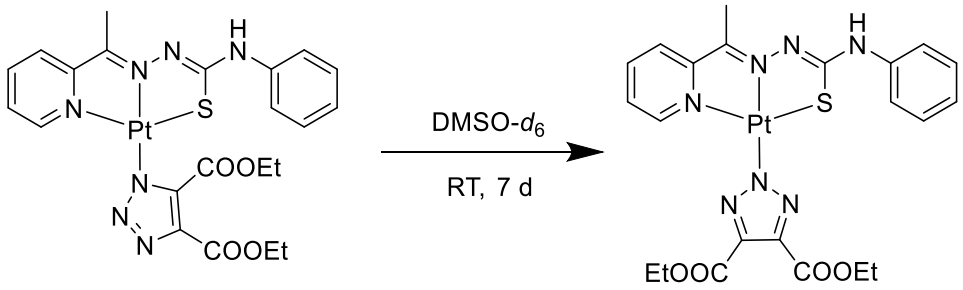

$C_{22}H_{23}N_7O_4PtS$
676.61 g/mol

$C_{22}H_{23}N_7O_4PtS$
676.61 g/mol

A suspension of [Pt(pht)(triazolate^{COOEt,COOEt}-N^1)] (approx. 10 mg) in DMSO-d_6 was kept in an NMR tube at room temperature for 7 d, during which time the light orange suspension changed into a clear dark red solution, which was identified as the N2 isomer by NMR spectroscopy. **^{1}H NMR** (500.13 MHz, DMSO-d_6): δ = 10.30 (s, 1H, N*H*-phenyl), 9.24 (ddd, 1H, $^3J_{H6,H5}$ = 5.5 Hz, $^4J_{H6,H4}$ = 1.5 Hz, $^5J_{H6,H3}$ = 0.6 Hz, py-H6), 8.24 (dt, 1H, $^3J_{H4,H3/H5}$ = 7.9 Hz, $^4J_{H4,H6}$ = 1.6 Hz, py-H4), 7.93 (d, 1H, $^3J_{H3,H4}$ = 7.4 Hz, py-H3), 7.74 (ddd, 1H, $^3J_{H5,H4}$ = 7.7 Hz, $^3J_{H5,H6}$ = 5.6 Hz, $^4J_{H5,H3}$ = 1.4 Hz, py-H5), 7.61 (d, 2H, $^3J_{H3'/H5',H2'/H6'}$ = 7.7 Hz, phenyl-H3'/H5'), 7.35 (t, 2H, $^3J_{H2'/H6',H3'/H5'}$ = 8.0 Hz, phenyl-H2'/H6'), 7.05 (t, 1H, $^3J_{H4',H3'/H5'}$ = 7.4 Hz, phenyl-H4'), 4.29 (q, 4H, ^3J = 7.1 Hz, COOC*H*$_2$CH$_3$), 2.58 (s, 3H, C*H*$_3$), 1.29 (t, 6H, ^3J = 7.1 Hz, COOCH$_2$C*H*$_3$) ppm; **^{13}C NMR** (125.76 MHz, DMSO-d_6): δ = 175.55 (*C*-S) 161.29 (*C*OOCH$_2$CH$_3$), 161.01 (*C*=N), 158.76 (py-C2), 148.72 (py-C6), 140.85 (phenyl-C1'), 140.16 (py-C4), 139.68 (triazolate-C4/C5), 128.68 (phenyl-C3'/C5'), 127.54 (py-C5), 126.51 (py-C3), 123.39 (phenyl-C4'), 120.22 (phenyl-C2'/C6'), 60.75 (*C*H$_2$CH$_3$), 14.02 (CH$_2$*C*H$_3$), 13.76 (*C*H$_3$) ppm; **^{195}Pt NMR** (107.51 MHz, DMSO-d_6): δ = -3104 ppm.

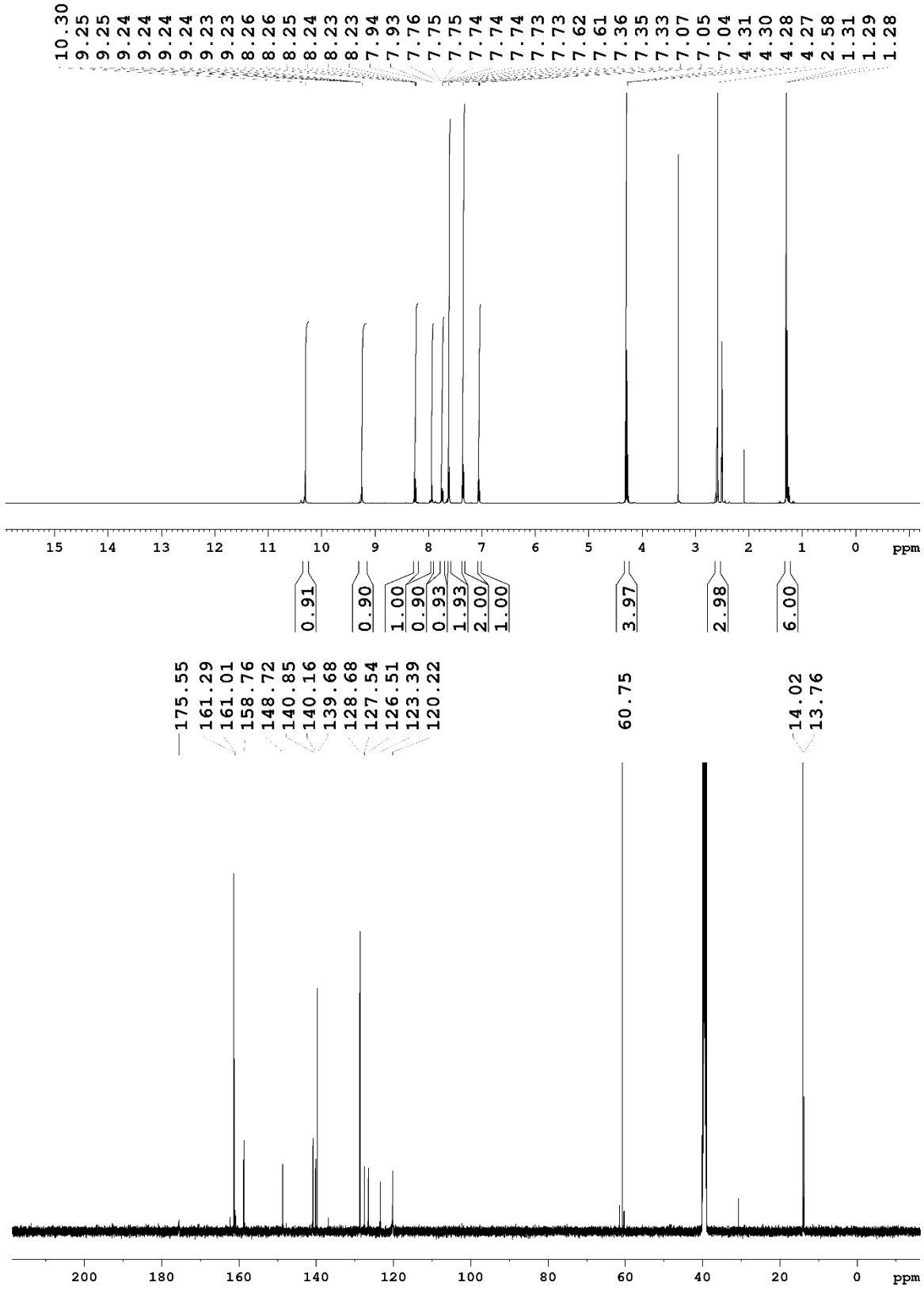
10.30
9.25
9.25
9.24
9.24
9.24
9.24
9.23
9.23
8.26
8.26
8.25
8.24
8.23
8.23
7.94
7.93
7.76
7.75
7.75
7.74
7.74
7.74
7.73
7.73
7.62
7.61
7.36
7.35
7.33
7.07
7.05
7.04
4.31
4.30
4.28
4.27
2.58
1.31
1.29
1.28
15 14 13 12 11 10 9 8 7 6 5 4 3 2 1 0 ppm
0.91
0.90
1.00
0.90
0.93
1.93
2.00
1.00
3.97
2.98
6.00
175.55
161.29
161.01
158.76
148.72
140.85
140.16
139.68
128.68
127.54
126.51
123.39
120.22
60.75
14.02
13.76
200 180 160 140 120 100 80 60 40 20 0 ppm

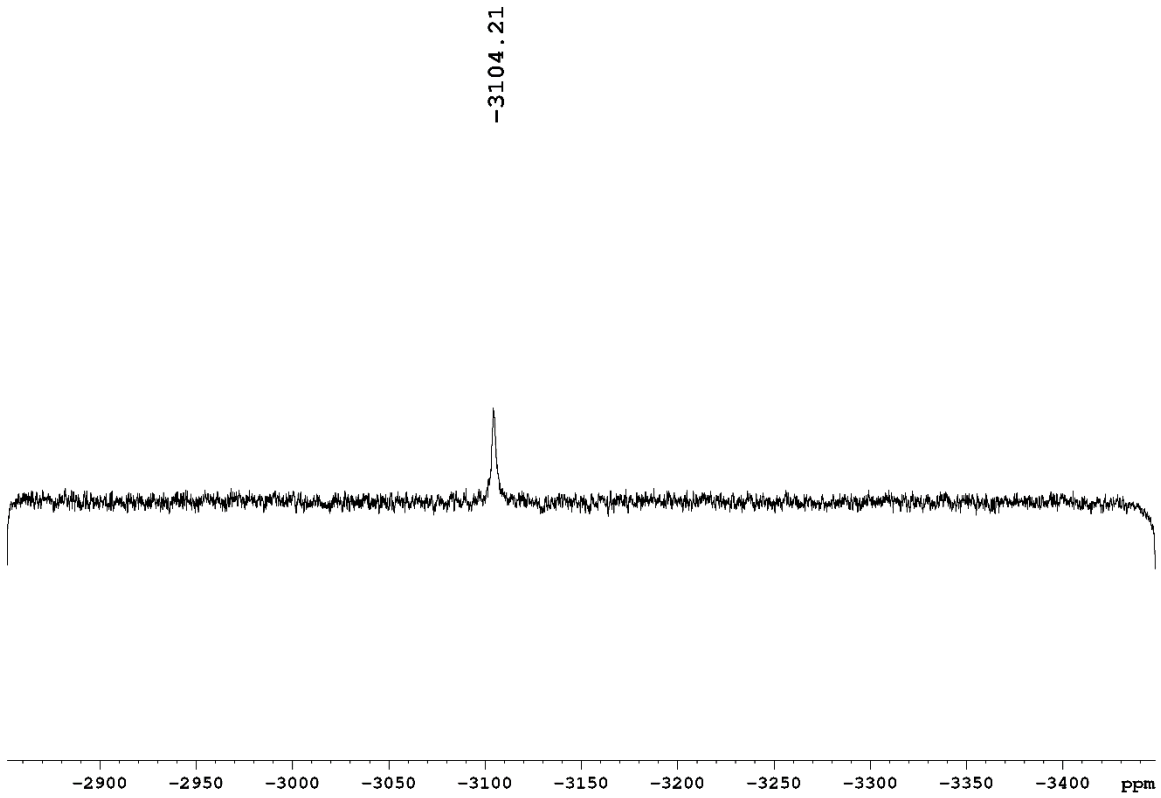
-3104.21
-2900
-2950
-3000
-3050
-3100
-3150
-3200
-3250
-3300
-3350
-3400
ppm

5.3.40 Synthesis of [Pd(pht)(triazolate^{COOCH2CH2OCH3,COOCH2CH2OCH3})]

USC-KP058-03

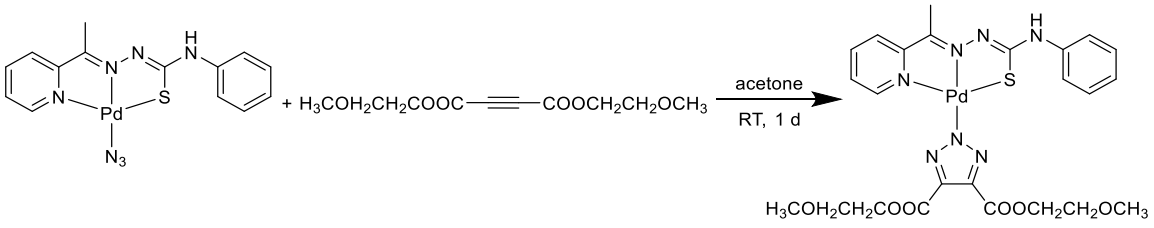

$[Pd(N_3)(pht)]$ (21 mg, 50.4 µmol) was suspended in acetone (10 mL) in a large glass vial at room temperature. Then, bis(2-methoxyethyl)but-2-ynedioate (11.0 µL, 12.9 mg, 56.0 µmol) was added and stirring continued at room temperature for 1 d. The resulting clear orange solution was evaporated to dryness,the orange solid thus obtained washed with diethyl ether (5 × 5 mL), and dried under vacuum for 1 d. Yield: 67% (22 mg, 34.0 µmol). **IR** (ATR): $\tilde{\nu}$ = 3340 (w), 2939 (w) 1727 (m), 1600 (w), 1502 (m), 1458 (m), 1435 (s), 1292 (w), 1188 (m), 1077 (m), 753 (w) cm^{-1}. **^{1}H NMR** (500.13 MHz, DMSO-d_6): δ = 10.19 (s, 1H, N*H*-phenyl), 8.90 (dd, 1H, $^3J_{H6,H5}$ = 5.4 Hz, $^4J_{H6,H4}$ = 1.2 Hz, py-H6), 8.21 (dt, 1H, $^3J_{H4,H3/H5}$ = 7.9 Hz, $^4J_{H4,H6}$ = 1.6 Hz, py-H4), 7.98 (d, 1H, $^3J_{H3,H4}$ = 7.7 Hz, py-H3), 7.67 (ddd, 1H, $^3J_{H5,H4}$ = 7.7 Hz, $^3J_{H5,H6}$ = 5.5 Hz, $^4J_{H5,H3}$ = 1.3 Hz, py-H5), 7.59 (d, 2H, $^3J_{H3'/H5',H2'/H6'}$ = 7.7 Hz, phenyl-H3'/H5'), 7.32 (t, 2H, $^3J_{H2'/H6',H3'/H5'}$ = 8.0 Hz, phenyl-H2'/H6'), 7.04 (t, 1H, $^3J_{H4',H3'/H5'}$ = 7.4 Hz, phenyl-H4'), 4.35 (t, 4H, ^3J = 4.7 Hz, OC*H*$_2$CH$_2$OCH$_3$), 3.62 (t, 4H, ^3J = 4.8 Hz, OCH$_2$C*H*$_2$OCH$_3$), 3.29 (s, 6H, OC*H*$_3$), 2.53 (s, 3H, C*H*$_3$) ppm; **^{13}C NMR** (125.76 MHz, DMSO-d_6): δ = 173.12 (*C*-S), 161.48 (*C*OOCH$_2$), 160.43 (*C*=N), 157.77 (py-C2), 149.36 (py-C6), 141.22 (phenyl-C1'), 140.14 (py-C4), 139.41 (triazolate-C4/C5), 128.73 (phenyl-C3'/C5'), 126.75 (py-C5), 125.90 (py-C3), 123.23 (phenyl-C4'), 119.97 (phenyl-C2'/C6'), 69.64 (O*C*H$_2$CH$_2$OCH$_3$), 63.81 (OCH$_2$*C*H$_2$OCH$_3$), 58.12 (O*C*H$_3$), 13.99 (*C*H$_3$) ppm. **Elemental analysis** (%) calcd. for $C_{24}H_{27}N_7O_6PdS$: C 44.48, H 4.20, N 15.13, S 4.95; found (%): C 44.20, H 4.35, N 14.69, S 4.92.

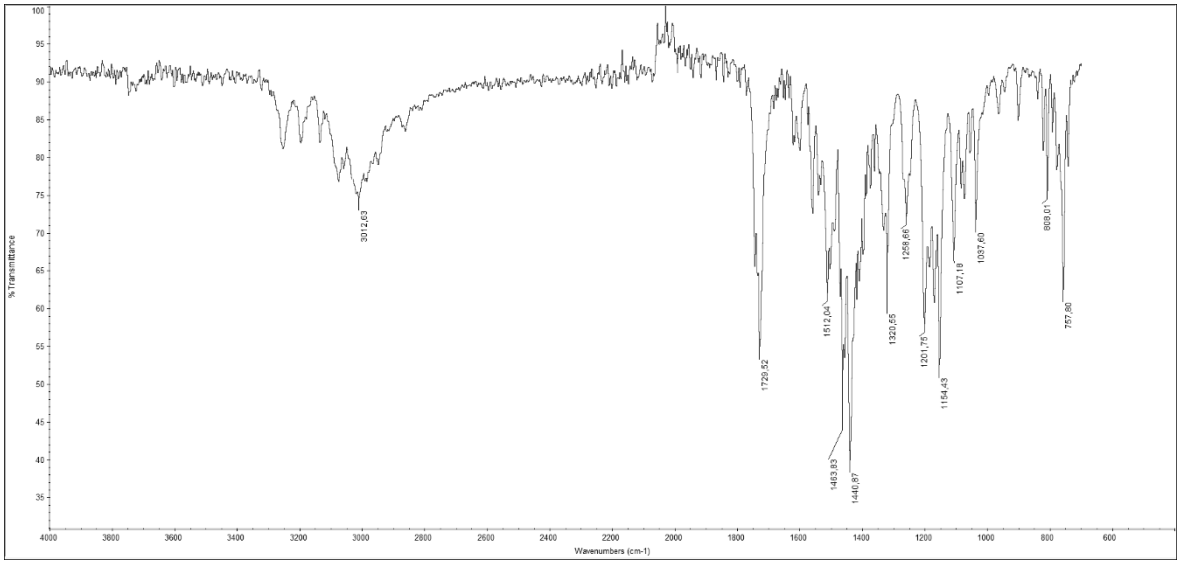
% Transmittance
Wavenumbers (cm-1)
3012.63
1720.52
1512.04
1463.83
1440.87
1320.65
1258.66
1201.75
1154.43
1107.19
1037.63
808.01
757.80

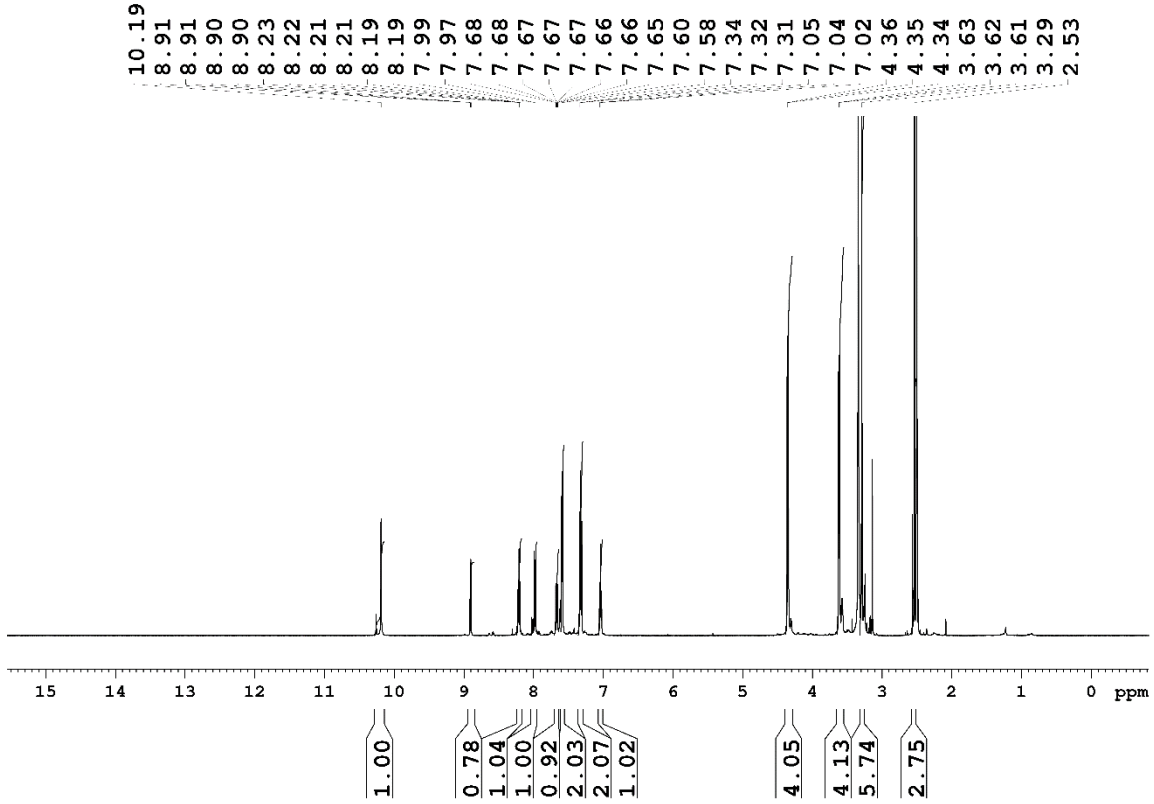
10.19
8.91
8.91
8.90
8.90
8.23
8.22
8.21
8.21
8.19
8.19
7.99
7.97
7.68
7.68
7.67
7.67
7.67
7.66
7.66
7.65
7.60
7.58
7.34
7.32
7.31
7.05
7.04
7.02
4.36
4.35
4.34
3.63
3.62
3.61
3.29
2.53
15 14 13 12 11 10 9 8 7 6 5 4 3 2 1 0 ppm
1.00
0.78
1.04
1.00
0.92
2.03
2.07
1.02
4.05
4.13
5.74
2.75

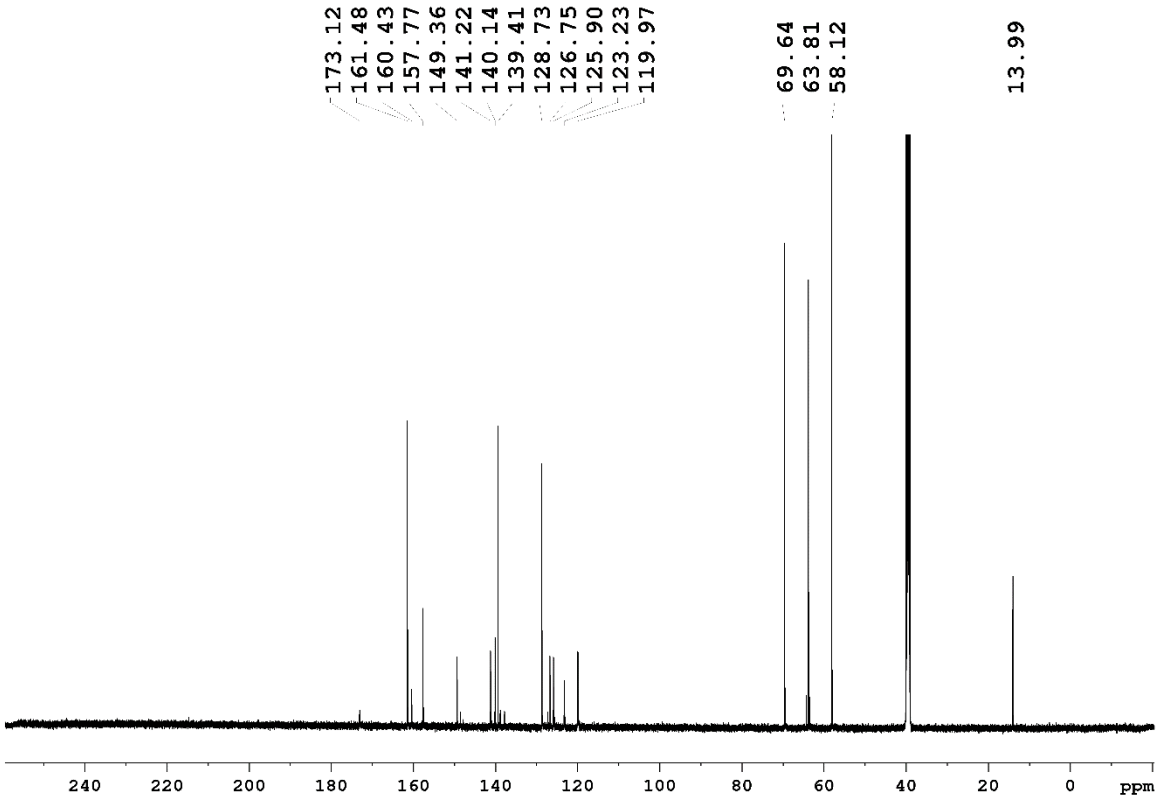
173.12
161.48
160.43
157.77
149.36
141.22
140.14
139.41
128.73
126.75
125.90
123.23
119.97
69.64
63.81
58.12
13.99
240
220
200
180
160
140
120
100
80
60
40
20
0
ppm

5.3.41 Synthesis of [Pt(pht)(triazolate^{COOCH2CH2OCH3,COOCH2CH2OCH3})]

USC-KP057-02

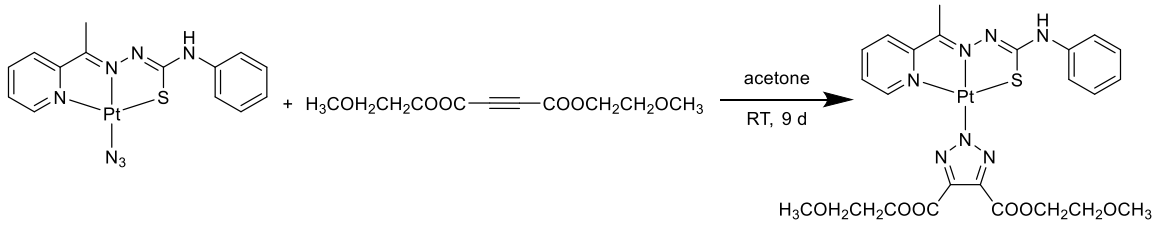

$C_{14}H_{13}N_7PtS$ 506.45 g/mol

$C_{10}H_{14}O_6$ 230.22 g/mol

$C_{24}H_{27}N_7O_6PtS$ 736.67 g/mol

[Pt(N_3)(pht)] (10 mg, 19.3 µmol) was suspended in acetone (8 mL) in a large glass vial at room temperature. Then, bis(2-methoxyethyl)but-2-ynedioate (4.4 µL, 5.1 mg, 22.3 µmol) was added and stirring continued at room temperature for 9 d, during which the reaction mixture slowly cleared up. The resulting clear red solution was evaporated to dryness and the red solid thus obtained washed with diethyl ether (5 × 5 mL) and dried under vacuum for 1 d. Yield: 63% (9 mg, 12.2 µmol). **IR** (ATR): $\tilde{\nu}$ = 3341 (w), 2947 (w), 1738 (m), 1599 (w), 1502 (m), 1463 (m), 1435 (s), 1294 (w), 1250 (w), 1191 (m), 1190 (m), 1078 (m), 1028 (m), 867 (w), 753 (m) cm^{-1}. **^{1}H NMR** (500.13 MHz, DMSO-d_6): δ = 10.30 (s, 1H, N*H*-phenyl), 9.22 (ddd, 1H, $^3J_{H6,H5}$ = 5.6 Hz, $^4J_{H6,H4}$ = 1.5 Hz, $^5J_{H6,H3}$ = 0.6 Hz, py-H6), 8.23 (dt, 1H, $^3J_{H4,H3/H5}$ = 7.9 Hz, $^4J_{H4,H6}$ = 1.6 Hz, py-H4), 7.92 (d, 1H, $^3J_{H3,H4}$ = 7.4 Hz, py-H3), 7.70 (ddd, 1H, $^3J_{H5,H4}$ = 7.6 Hz, $^3J_{H5,H6}$ = 5.6 Hz, $^4J_{H5,H3}$ = 1.4 Hz, py-H5), 7.61 (d, 2H, $^3J_{H3'/H5',H2'/H6'}$ = 7.7 Hz, phenyl-H3'/H5'), 7.34 (t, 2H, $^3J_{H2'/H6',H3'/H5'}$ = 8.0 Hz, phenyl-H2'/H6'), 7.05 (t, 1H, $^3J_{H4',H3'/H5'}$ = 7.4 Hz, phenyl-H4'), 4.36 (t, 4H, ^3J = 4.7 Hz, OC*H*$_2$CH$_2$OCH$_3$), 3.62 (t, 4H, ^3J = 4.7 Hz, OCH$_2$C*H*$_2$OCH$_3$), 3.30 (s, 6H, OC*H*$_3$), 2.58 (s, 3H, C*H*$_3$) ppm; **^{13}C NMR** (125.76 MHz, DMSO-d_6): δ = 175.52 (*C*-S) 161.20 (*C*OOCH$_2$), 161.06 (*C*=N), 158.79 (py-C2), 148.70 (py-C6), 140.88 (phenyl-C1'), 140.17 (py-C4), 139.58 (triazolate-C4/C5), 128.70 (phenyl-C3'/C5'), 127.48 (py-C5), 126.53 (py-C3), 123.42 (phenyl-C4'), 120.26 (phenyl-C2'/C6'), 69.62 (OC*H*$_2$C*H*$_2$OCH$_3$), 63.91 (OCH$_2$C*H*$_2$OCH$_3$), 58.13 (OC*H*$_3$), 13.79 (C*H*$_3$) ppm; **^{195}Pt NMR** (107.51 MHz, DMSO-d_6): δ = -3106 ppm. **Elemental analysis** (%) calcd. for $C_{24}H_{27}N_7O_6PtS$: C 39.13, H 3.69, N 13.31, S 4.35; found (%): C 38.94, H 3.66, N 12.93, S 4.24.

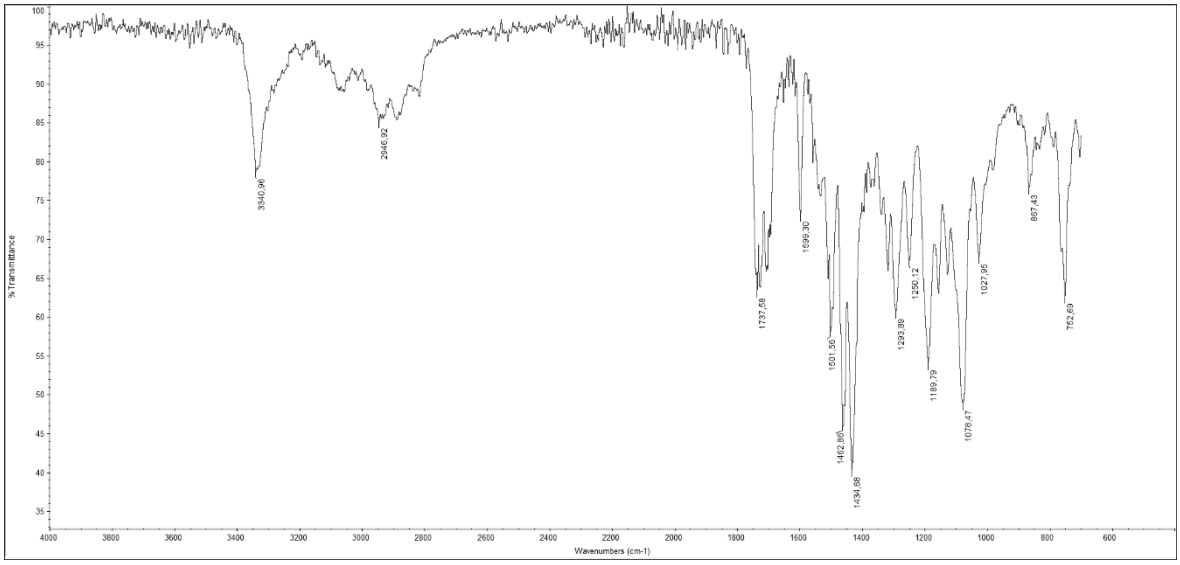
% Transmittance
Wavenumbers (cm-1)
3340.96
2946.92
1737.58
1699.30
1601.56
1462.86
1434.08
1293.86
1260.12
1189.79
1078.47
1027.96
867.43
762.69

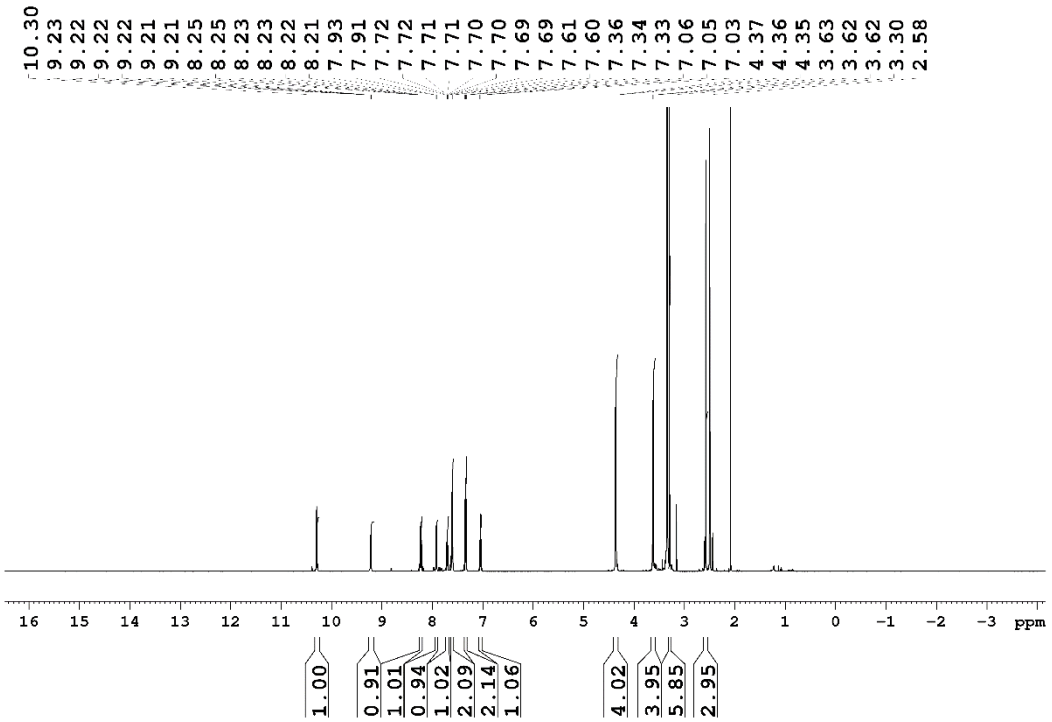
10.30
9.23
9.22
9.22
9.22
9.21
9.21
8.25
8.25
8.23
8.23
8.22
8.21
7.93
7.91
7.72
7.72
7.71
7.71
7.70
7.70
7.69
7.69
7.61
7.60
7.36
7.34
7.33
7.06
7.05
7.03
4.37
4.36
4.35
3.63
3.62
3.62
3.30
2.58
ppm
1.00
0.91
1.01
0.94
1.02
2.09
2.14
1.06
4.02
3.95
5.85
2.95

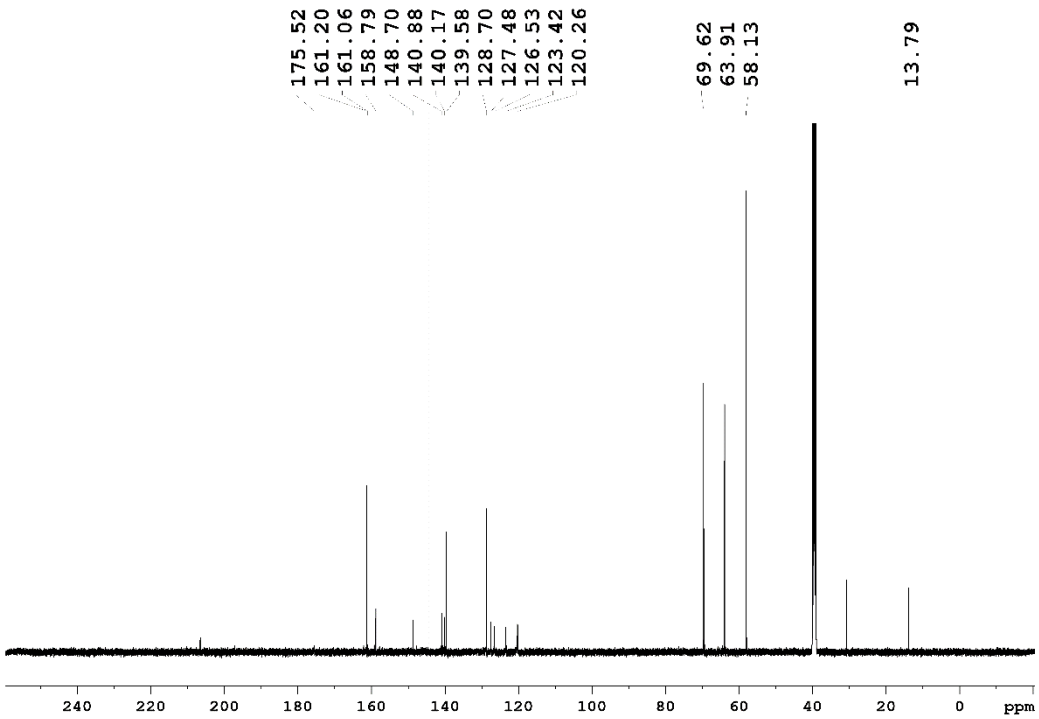
175.52
161.20
161.06
158.79
148.70
140.88
140.17
139.58
128.70
127.48
126.53
123.42
120.26
69.62
63.91
58.13
13.79
240
220
200
180
160
140
120
100
80
60
40
20
0
ppm

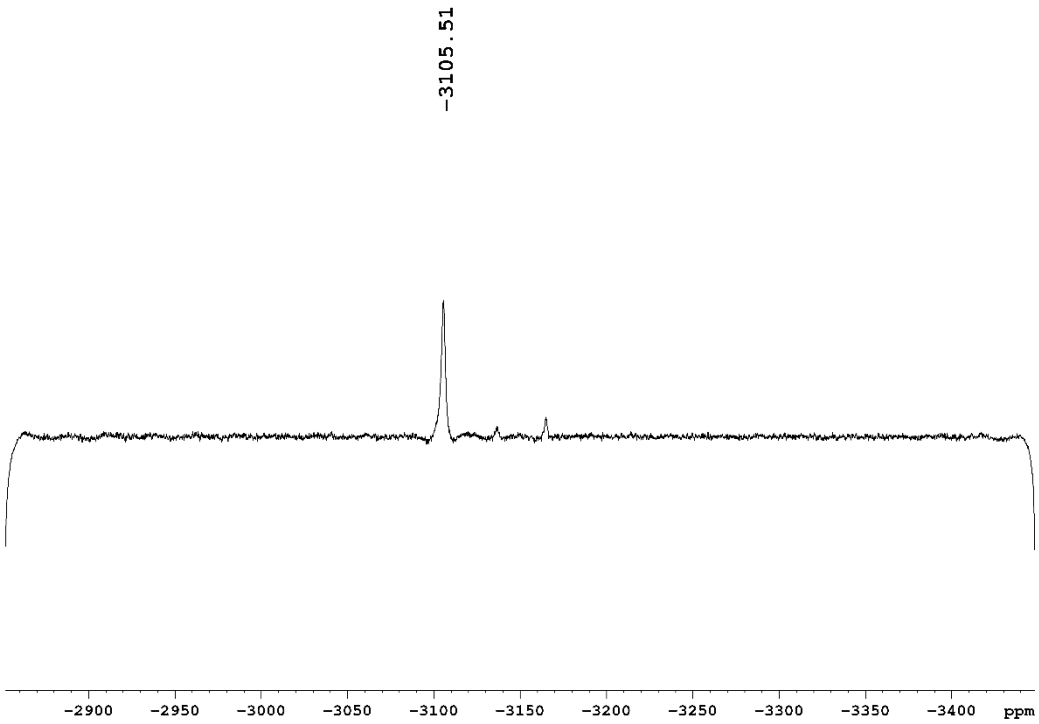
-3105.51
-2900
-2950
-3000
-3050
-3100
-3150
-3200
-3250
-3300
-3350
-3400
ppm

5.3.42 Synthesis of [Pt(pht)(dmso)]OTf

USC-KP110-01

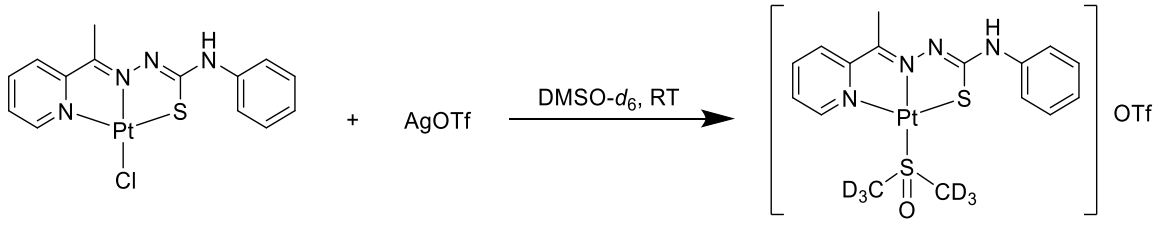

$C_{14}H_{13}ClN_4PtS$
499.88 g/mol

$CAgF_3O_3S$
256.93 g/mol

$C_{17}H_{13}D_6F_3N_4O_4PtS_3$
697.66 g/mol

[PtCl(pht)] (10 mg, 20 µmol) was mixed with DMSO-d_6 (600 µL) in an NMR tube to give a clear dark red solution. After recording a NMR spectrum, solid silver triflate (10.3 mg, 40 µmol) was added to immediately give a white precipitate, which was filtered off. The resulting brown filtrate was then analysed by NMR spectroscopy again. **^{1}H NMR** (400.47 MHz, DMSO-d_6): δ = 10.68 (s, 1H, N*H*-phenyl), 9.12 (d, 1H, $^3J_{H6,H5}$ = 4.8 Hz, py-H6), 8.38 (dt, 1H, $^3J_{H4,H3/H5}$ = 7.8 Hz, $^4J_{H4,H6}$ = 1.3 Hz, py-H4), 8.11 (d, 1H, $^3J_{H3,H4}$ = 7.5 Hz, py-H3), 7.89 (t, 1H, $^3J_{H5,H4/H6}$ = 6.6 Hz, py-H5), 7.62 (d, 2H, $^3J_{H3'/H5',H2'/H6'}$ = 8.0 Hz, phenyl-H3'/H5'), 7.39 (t, 2H, $^3J_{H2'/H6',H3'/H5'}$ = 7.9 Hz, phenyl-H2'/H6'), 7.11 (t, 1H, $^3J_{H4',H3'/H5'}$ = 7.4 Hz, phenyl-H4'), 2.69 (s, 3H, C*H*$_3$) ppm; **^{19}F NMR** (376.82 MHz, DMSO-d_6): δ = -77.74 (C*F*$_3$SO$_3^-$) ppm; **^{195}Pt NMR** (86.09 MHz, DMSO-d_6): δ = -3650 ppm. Similar NMR spectra were also obtained when the procedure described above was repeated using silver tetrafluoroborate instead of silver triflate.

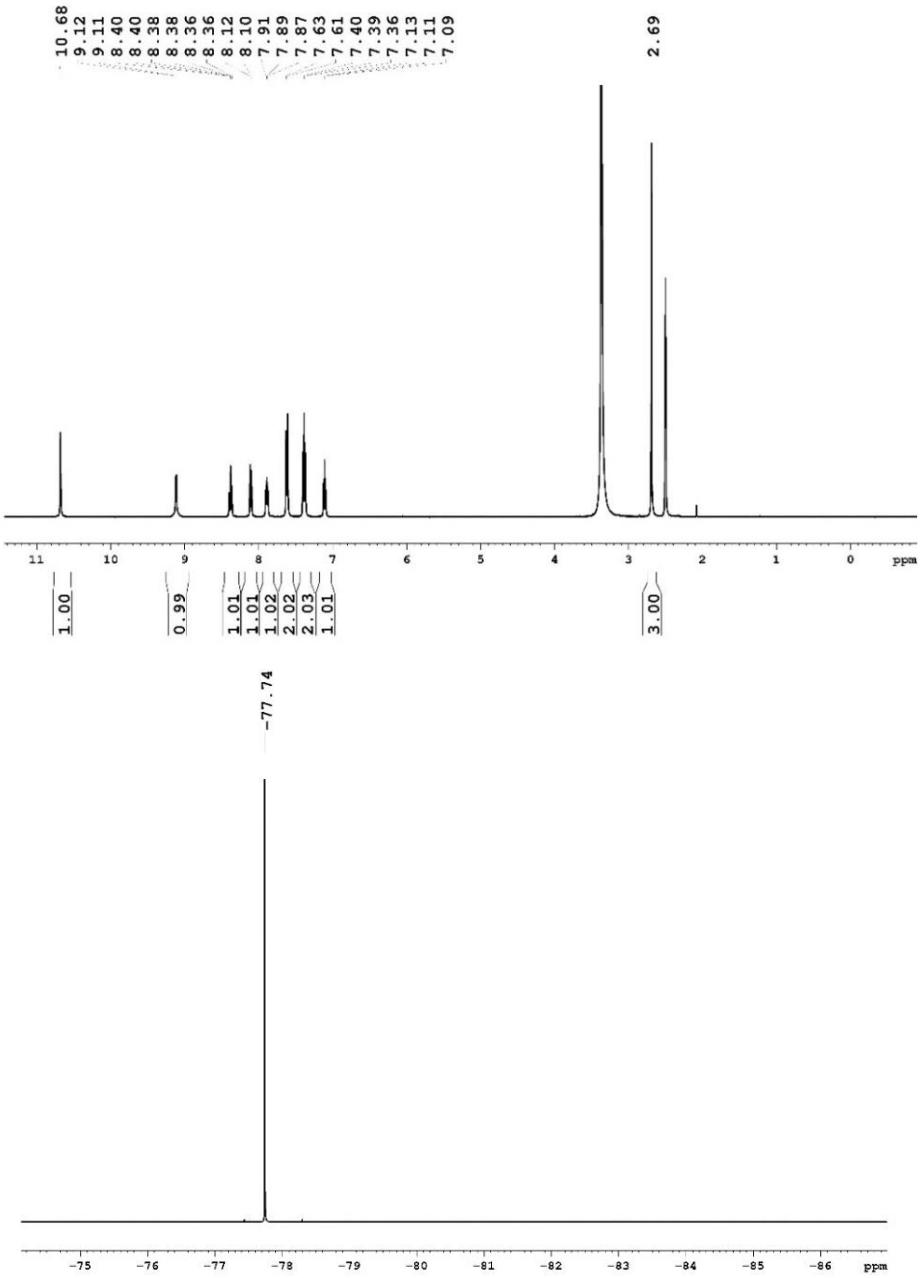
10.68
9.12
9.11
8.40
8.40
8.38
8.38
8.36
8.36
8.12
8.10
7.91
7.89
7.87
7.63
7.61
7.40
7.39
7.36
7.13
7.11
7.09
2.69
11
10
9
8
7
6
5
4
3
2
1
0
ppm
1.00
0.99
1.01
1.01
1.02
2.02
2.03
1.01
3.00
-77.74
-75
-76
-77
-78
-79
-80
-81
-82
-83
-84
-85
-86
ppm

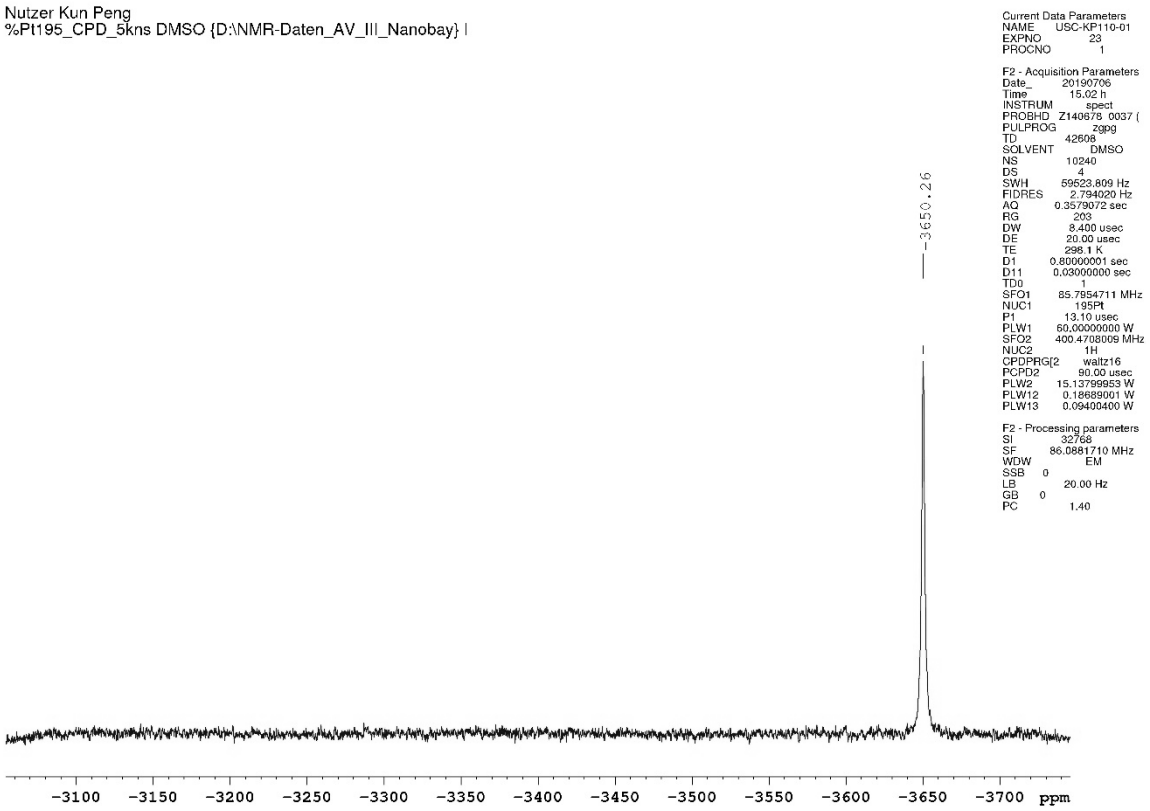
Nutzer Kun Peng
%Pt195_CPD_5kns DMSO {D:\NMR-Daten_AV_III_Nanobay} I
-3650.26
Current Data Parameters
NAME USC-KP110-01
EXPNO 23
PROCNO 1
F2 - Acquisition Parameters
Date_ 20190706
Time 15.02 h
INSTRUM spect
PROBHD Z140678_0037 (
PULPROG zgpg
TD 42608
SOLVENT DMSO
NS 10240
DS 4
SWH 59523.809 Hz
FIDRES 2.794020 Hz
AQ 0.3579072 sec
RG 203
DW 8.400 usec
DE 20.00 usec
TE 298.1 K
D1 0.80000001 sec
D11 0.03000000 sec
TD0 1
SFO1 85.7954711 MHz
NUC1 195Pt
P1 13.10 usec
PLW1 50.00000000 W
SFO2 400.4708009 MHz
NUC2 1H
CPDPRG[2 waltz16
PCPD2 90.00 usec
PLW2 15.13799953 W
PLW12 0.18689001 W
PLW13 0.09400400 W
F2 - Processing parameters
SI 32768
SF 86.0881710 MHz
WDW EM
SSB 0
LB 20.00 Hz
GB 0
PC 1.40
−3100 −3150 −3200 −3250 −3300 −3350 −3400 −3450 −3500 −3550 −3600 −3650 −3700 ppm

5.3.43 Synthesis of [Pt(bodipy)(triazolate^{COOCH3,COOCH3})(PEt$_3$)$_2$]

USC-KP066-07

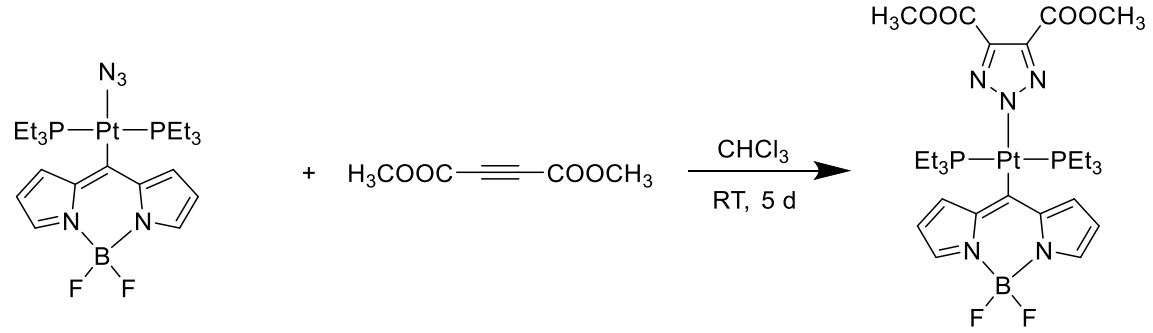

$C_{21}H_{36}BF_2N_5P_2Pt$
664.38 g/mol

$C_6H_6O_4$
142.11 g/mol

$C_{27}H_{42}BF_2N_5O_4P_2Pt$
806.49 g/mol

In a round-bottom flask, [Pt(bodipy)(N_3)(PEt_3)$_2$] (30 mg, 0.05 mmol) was dissolved in chloroform (5 mL) at room temperature to give a clear yellow solution. Then, dimethyl acetylenedicarboxylate (8.3 µL, 9.6 mg, 0.07 mmol) was added and stirring continued at room temperature for 5 d. The resulting clear light orange solution was evaporated to dryness. The dark brown solid thus obtained was dried under vacuum for 2 d to fully remove remaining alkyne and solvent. Yield: 80% (35 mg, 0.04 mmol). **IR** (ATR): $\tilde{\nu}$ = 2973 (w), 1725 (s), 1524 (m), 1406 (s), 1379 (s), 1176 (s), 1122 (s), 1057 (s), 901 (m), 868 (m), 731 (m) cm^{-1}. **^{1}H NMR** (400.47 MHz, $CDCl_3$): δ = 7.72 (s, 2H, H3/H5), 7.60 (d, 2H, $^3J_{H1,H2/H7,H6}$ = 3.1 Hz, H1/H7), 6.47 (m, 2H, H2/H6), 3.94 (s, 6H, COOC*H*$_3$), 1.46–1.42 (m, 12H, PC*H*$_2$CH$_3$), 1.04–0.96 (m, 18H, PCH$_2$C*H*$_3$) ppm; **^{11}B NMR** (128.49 MHz, $CDCl_3$): δ = 0.11 (t, $^1J_{B,F}$ = 30.1 Hz, *B*F$_2$) ppm; **^{13}C NMR** (100.70 MHz, $CDCl_3$): δ = 174.49 (s, C8), 162.93 (s, *C*OOCH$_3$), 142.75 (s, C8a/C7a), 140.65 (s, triazolate-C4/C5), 137.83 (s, C3/C5), 133.45 (s, C1/C7), 116.51 (s, C2/C6), 52.37 (s, COO*C*H$_3$), 14.08 (t, $^1J_{C,P}$ = $^2J_{C,Pt}$ = 16.8 Hz, P*C*H$_2$CH$_3$), 7.75 (s, PCH$_2$*C*H$_3$) ppm; **^{19}F NMR** (376.82 MHz, $CDCl_3$): δ = -146.60 (q, $^1J_{F,B}$ = 30.1 Hz, B*F*$_2$) ppm; **^{31}P NMR** (162.11 MHz, $CDCl_3$): δ = 10.98 (s, with satellites $^1J_{P,Pt}$ = 2511 Hz) ppm; **^{195}Pt NMR** (86.09 MHz, $CDCl_3$): δ = -4092 (t, $^1J_{Pt,P}$ = 2516 Hz) ppm. **Elemental analysis** (%) calcd. for $C_{27}H_{42}BF_2N_5O_4P_2Pt$: C 40.21, H 5.25, N 8.68; found (%): C 40.52, H 5.49, N 8.27.

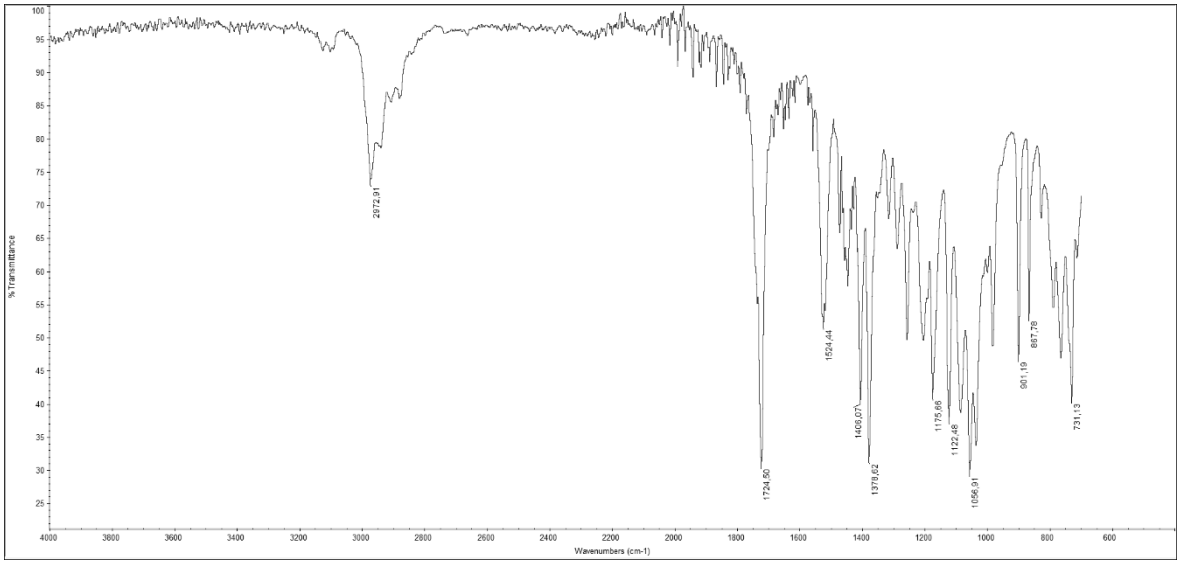
% Transmittance
Wavenumbers (cm-1)
2872,91
1724,50
1524,44
1469,07
1379,62
1175,66
1122,46
1056,91
961,19
867,78
731,13

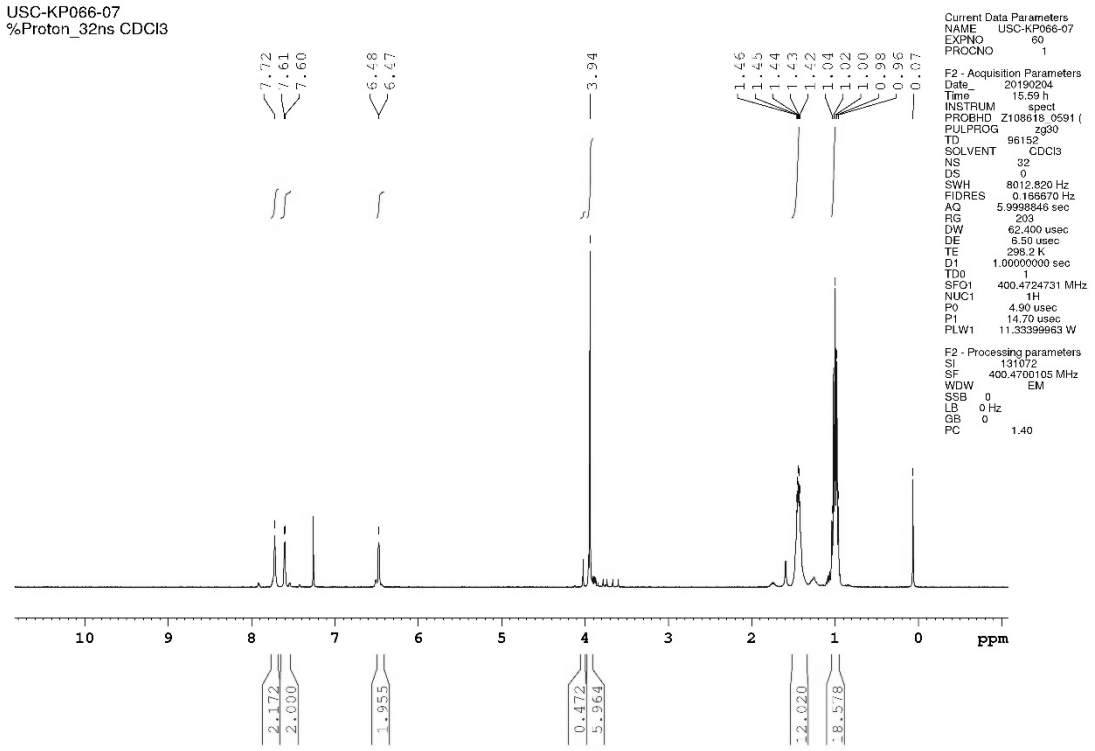
USC-KP066-07
%Proton_32ns CDCl3
7.72
7.61
7.60
6.48
6.47
3.94
1.46
1.45
1.44
1.43
1.42
1.04
1.02
1.00
0.98
0.96
0.07
Current Data Parameters
NAME USC-KP066-07
EXPNO 60
PROCNO 1
F2 - Acquisition Parameters
Date_ 20190204
Time 15.59 h
INSTRUM spect
PROBHD Z108618_0591 (
PULPROG zg30
TD 96152
SOLVENT CDCl3
NS 32
DS 0
SWH 8012.820 Hz
FIDRES 0.166670 Hz
AQ 5.9998846 sec
RG 203
DW 62.400 usec
DE 6.50 usec
TE 298.2 K
D1 1.00000000 sec
TD0 1
SFO1 400.4724731 MHz
NUC1 1H
P0 4.90 usec
P1 14.70 usec
PLW1 11.33399963 W
F2 - Processing parameters
SI 131072
SF 400.4700105 MHz
WDW EM
SSB 0
LB 0 Hz
GB 0
PC 1.40
10
9
8
7
6
5
4
3
2
1
0
ppm
2.172
2.000
1.955
0.472
5.964
2.020
8.578

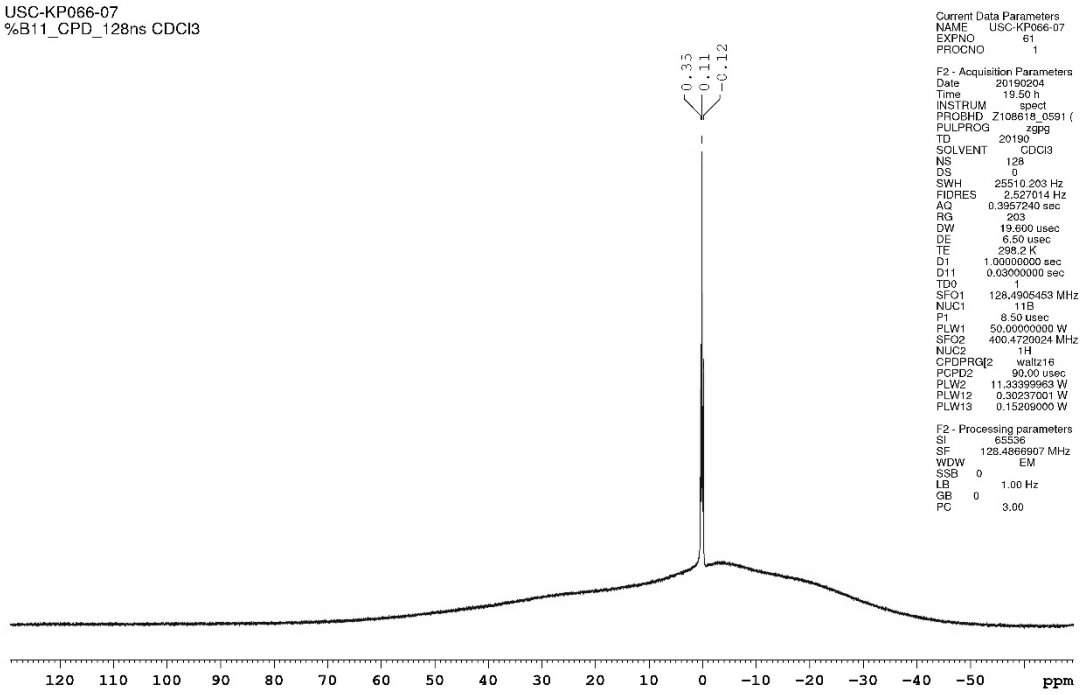
USC-KP066-07
%B11_CPD_128ns CDCl3
0.35
0.11
-0.12
Current Data Parameters
NAME USC-KP066-07
EXPNO 61
PROCNO 1
F2 - Acquisition Parameters
Date 20190204
Time 19.50 h
INSTRUM spect
PULPROG zgpg
TD 20190
SOLVENT CDCl3
NS 128
DS 0
SWH 25510.203 Hz
FIDRES 2.527014 Hz
AQ 0.3957240 sec
RG 203
DW 19.600 usec
DE 6.50 usec
TE 298.2 K
D1 1.00000000 sec
D11 0.03000000 sec
TD0 1
SFO1 128.4905453 MHz
NUC1 11B
P1 8.50 usec
PLW1 50.00000000 W
SFO2 400.4720024 MHz
NUC2 1H
CPDPRG[2 waltz16
PCPD2 90.00 usec
PLW2 11.33399963 W
PLW12 0.30237001 W
PLW13 0.15209000 W
F2 - Processing parameters
SI 65536
SF 128.4866907 MHz
WDW EM
SSB 0
LB 1.00 Hz
GB 0
PC 3.00
120 110 100 90 80 70 60 50 40 30 20 10 0 -10 -20 -30 -40 -50 ppm

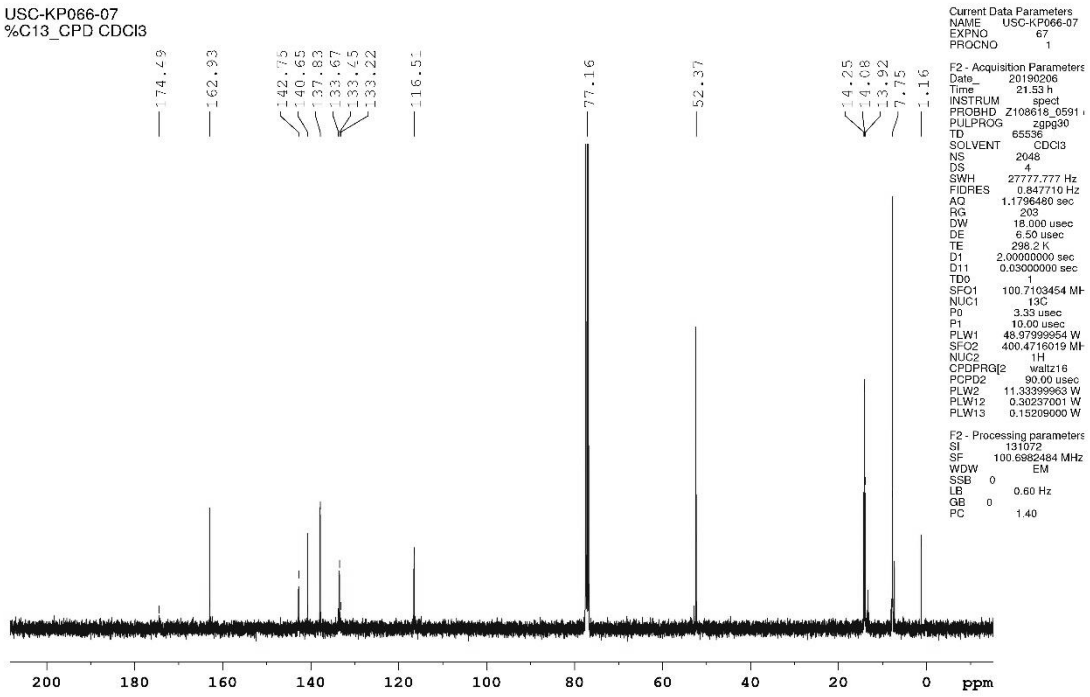
USC-KP066-07
%C13_CPD CDCl3
174.49
162.93
142.75
140.65
137.83
133.67
133.45
133.22
116.51
77.16
52.37
24.25
24.08
23.92
7.75
Current Data Parameters
NAME USC-KP066-07
EXPNO 67
PROCNO 1
F2 - Acquisition Parameters
Date_ 20190206
Time 21.53 h
INSTRUM spect
PULPROG zgpg30
TD 65536
SOLVENT CDCl3
NS 2048
DS 4
SWH 27777.777 Hz
FIDRES 0.847710 Hz
AQ 1.1796480 sec
RG 203
DW 18.000 usec
DE 6.50 usec
TE 298.2 K
D1 2.00000000 sec
D11 0.03000000 sec
TD0 1
SFO1 100.7103454 MH
NUC1 13C
P0 3.33 usec
P1 10.00 usec
PLW1 48.97999954 W
SFO2 400.4716019 MH
NUC2 1H
CPDPRG[2 waltz16
PCPD2 90.00 usec
PLW2 11.33399963 W
PLW12 0.30237001 W
PLW13 0.15209000 W
F2 - Processing parameters
SI 131072
SF 100.6982484 MHz
WDW EM
SSB 0
LB 0.60 Hz
GB 0
PC 1.40
200 180 160 140 120 100 80 60 40 20 0 ppm

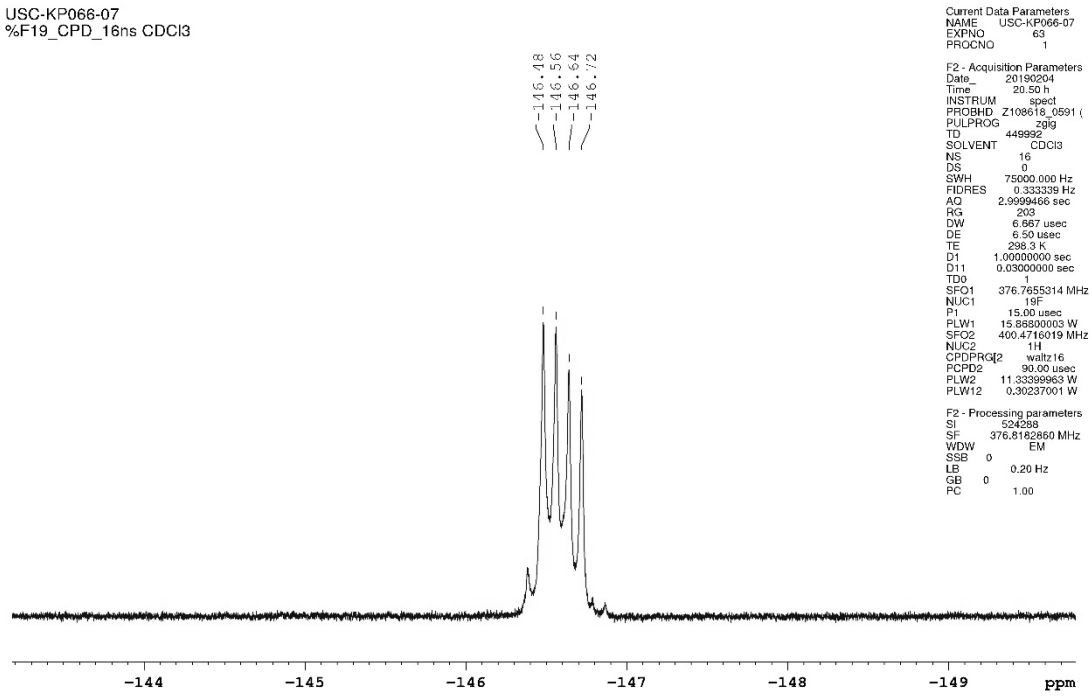
USC-KP066-07
%F19_CPD_16ns CDCl3
-146.48
-146.56
-146.64
-146.72
Current Data Parameters
NAME USC-KP066-07
EXPNO 63
PROCNO 1
F2 - Acquisition Parameters
Date_ 20190204
Time 20.50 h
INSTRUM spect
PROBHD Z108618_0591 (
PULPROG zg
TD 449992
SOLVENT CDCl3
NS 16
DS 0
SWH 75000.000 Hz
FIDRES 0.333339 Hz
AQ 2.9999466 sec
RG 203
DW 6.667 usec
DE 6.50 usec
TE 298.3 K
D1 1.00000000 sec
D11 0.03000000 sec
TD0 1
SFO1 376.7655314 MHz
NUC1 19F
P1 15.00 usec
PLW1 15.88800003 W
SFO2 400.4716019 MHz
NUC2 1H
CPDPRG[2 waltz16
PCPD2 90.00 usec
PLW2 11.33399963 W
PLW12 0.30237001 W
F2 - Processing parameters
SI 524288
SF 376.8182860 MHz
WDW EM
SSB 0
LB 0.20 Hz
GB 0
PC 1.00
-144
-145
-146
-147
-148
-149
ppm

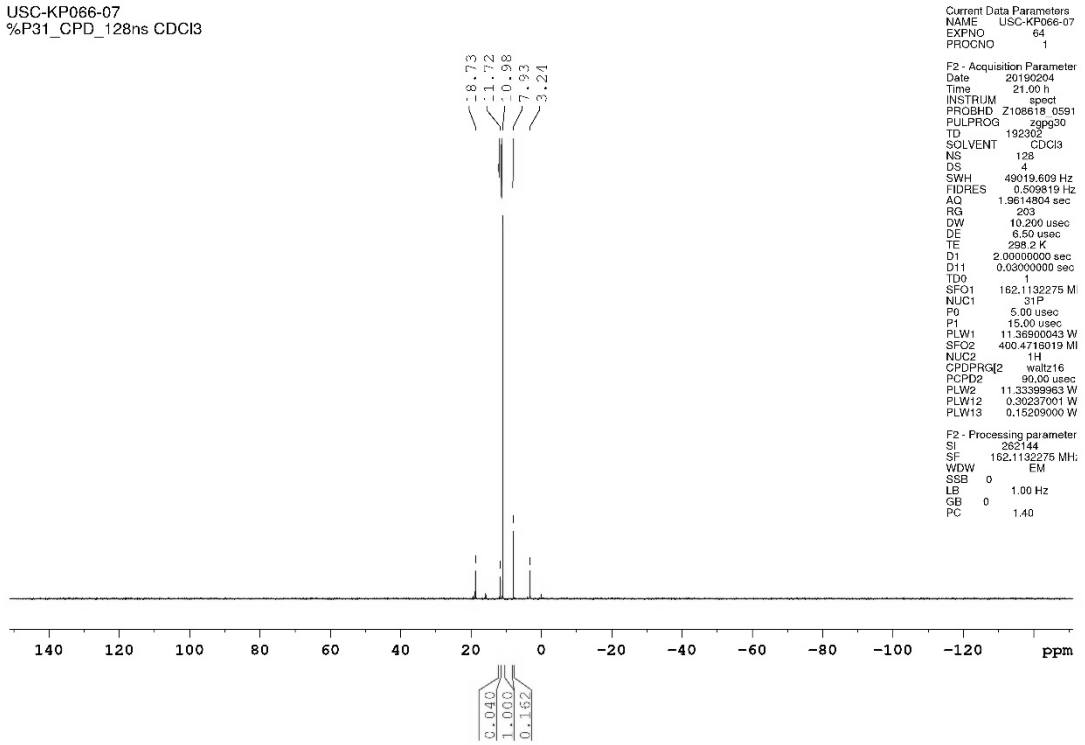
USC-KP066-07
%P31_CPD_128ns CDCl3
18.73
11.72
10.98
7.93
3.24
Current Data Parameters
NAME USC-KP066-07
EXPNO 64
PROCNO 1
F2 - Acquisition Parameter
Date 20190204
Time 21.00 h
INSTRUM spect
PROBHD Z108618_0591
PULPROG zgpg30
TD 192302
SOLVENT CDCl3
NS 128
DS 4
SWH 49019.609 Hz
FIDRES 0.509819 Hz
AQ 1.9614804 sec
RG 203
DW 10.200 usec
DE 6.50 usec
TE 298.2 K
D1 2.00000000 sec
D11 0.03000000 sec
TD0 1
SFO1 162.1132275 M
NUC1 31P
P0 5.00 usec
P1 15.00 usec
PLW1 11.36900043 W
SFO2 400.4716019 MI
NUC2 1H
CPDPRG[2 waltz16
PCPD2 90.00 usec
PLW2 11.33399963 W
PLW12 0.30237001 W
PLW13 0.15209000 W
F2 - Processing parameter
SI 262144
SF 162.1132275 MH
WDW EM
SSB 0
LB 1.00 Hz
GB 0
PC 1.40
140
120
100
80
60
40
20
0
-20
-40
-60
-80
-100
-120
ppm
0.040
1.000
0.162

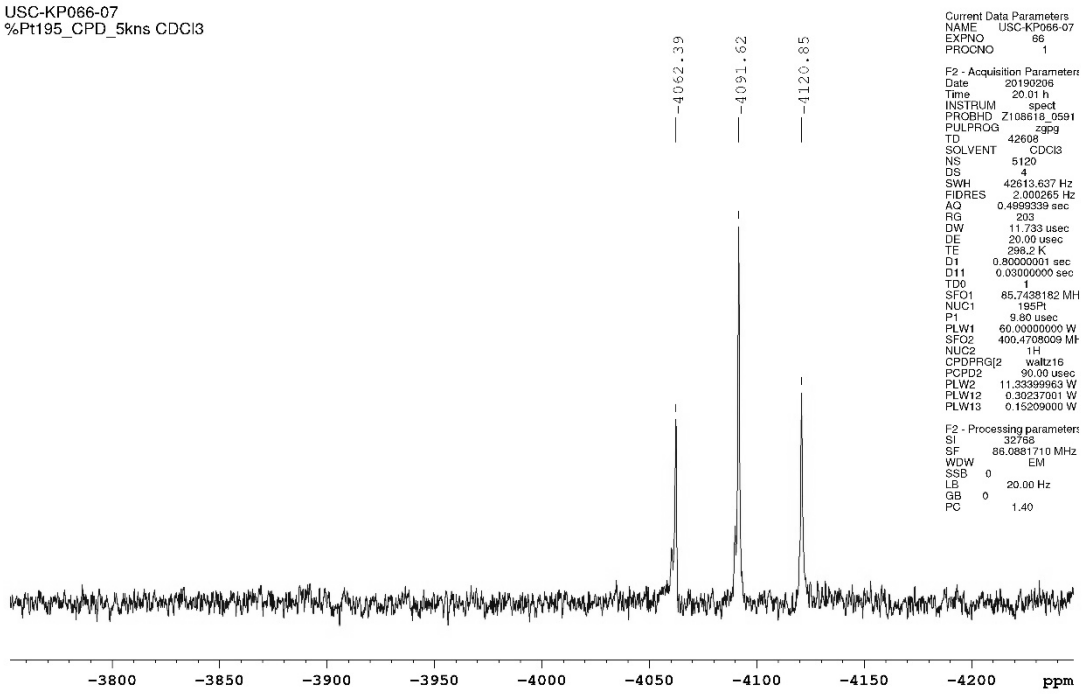
USC-KP066-07
%Pt195_CPD_5kns CDCl3
-4062.39
-4091.62
-4120.85
Current Data Parameters
NAME USC-KP066-07
EXPNO 66
PROCNO 1
F2 - Acquisition Parameters
Date 20190206
Time 20.01 h
INSTRUM spect
PROBHD Z108618_0591
PULPROG zgpg
TD 42608
SOLVENT CDCl3
NS 5120
DS 4
SWH 42613.637 Hz
FIDRES 2.000265 Hz
AQ 0.4999339 sec
RG 203
DW 11.733 usec
DE 20.00 usec
TE 298.2 K
D1 0.80000001 sec
D11 0.03000000 sec
TD0 1
SFO1 85.7438182 MH
NUC1 195Pt
P1 9.80 usec
PLW1 60.00000000 W
SFO2 400.4708009 MH
NUC2 1H
CPDPRG[2 waltz16
PCPD2 90.00 usec
PLW2 11.33399963 W
PLW12 0.30237001 W
PLW13 0.15209000 W
F2 - Processing parameters
SI 32768
SF 86.0881710 MHz
WDW EM
SSB 0
LB 20.00 Hz
GB 0
PC 1.40
-3800
-3850
-3900
-3950
-4000
-4050
-4100
-4150
-4200
ppm

5.3.44 Synthesis of [Pt(bodipy)(triazolate^{CF3,COOEt})(PEt_3)$_2$]

USC-KP067-07

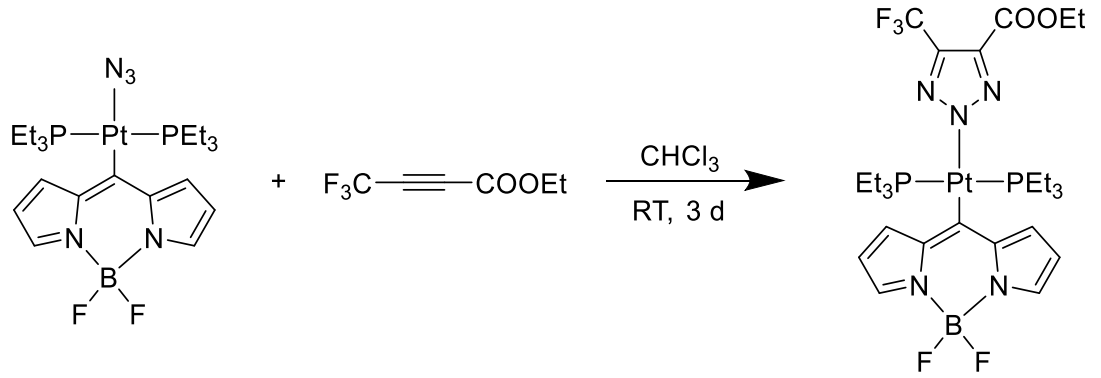

$C_{21}H_{36}BF_2N_5P_2Pt$ 664.38 g/mol

$C_6H_5F_3O_2$ 166.10 g/mol

$C_{27}H_{41}BF_5N_5O_2P_2Pt$ 830.48 g/mol

In a round-bottom flask, [Pt(bodipy)(N_3)(PEt_3)$_2$] (40 mg, 0.06 mmol) was dissolved in chloroform (10 mL) at room temperature to give a clear yellow solution. Then, 4,4,4-trifluoro-2-butynoic acid ethyl ester (11.8 µL, 14.99 mg, 0.09 mmol) was added and stirring continued at room temperature for 3 d. The resulting clear light orange solution was evaporated to dryness and the dark orange solid thus obtained dried under vacuum for 2 d to fully remove remaining alkyne and chloroform. Yield: 83% (41 mg, 0.05 mmol). **IR** (ATR): $\tilde{\nu}$ = 2974 (w), 1728 (m), 1524 (m), 1408 (m), 1377 (s), 1257 (m), 1121 (s), 1054 (s), 901 (m), 868 (m), 729 (m) cm^{-1}. **^{1}H NMR** (500.13 MHz, $CDCl_3$): δ = 7.73 (s, 2H, H3/H5), 7.59 (d, 2H, $^3J_{H1,H2/H7,H6}$ = 3.6 Hz, H1/H7), 6.49 (dd, 2H, $^3J_{H2,H1/H6,H7}$ = 3.9 Hz, $^3J_{H2,H3/H6,H5}$ = 2.0 Hz, H2/H6), 4.41 (q, 2H, ^3J = 7.1 Hz, COO*C*H_2CH$_3$), 1.45–1.39 (m, 15H, PC*H*$_2$CH$_3$+COOCH$_2$C*H*$_3$), 1.04–0.97 (m, 18H, PCH$_2$C*H*$_3$) ppm; **^{11}B NMR** (160.46 MHz, $CDCl_3$): δ = 0.12 (t, $^1J_{B,F}$ = 30.0 Hz, *B*F$_2$) ppm; **^{13}C NMR** (125.76 MHz, $CDCl_3$): δ = 173.98 (t, $^2J_{C,P}$ = 8.7 Hz, C8), 161.06 (s, *C*OOEt), 142.66 (s, C8a/C7a), 139.85 (q, $^2J_{C,F}$ = 38.2 Hz, triazolate-C4), 137.91 (s, C3/C5), 137.84 (s, triazolate-C5), 133.45 (s, C1/C7), 121.73 (q, $^1J_{C,F}$ = 268.4 Hz, *C*F$_3$), 116.59 (s, C2/C6), 61.23 (s, COO*C*H$_2$CH$_3$), 14.26–13.76 (m, P*C*H$_2$CH$_3$+COOCH$_2$*C*H$_3$,), 7.71 (s, PCH$_2$*C*H$_3$) ppm; **^{19}F NMR** (188.11 MHz, $CDCl_3$, ppm): δ = -59.83 (s, C*F*$_3$), -146.63 (q, $^1J_{F,B}$ = 29.9 Hz, B*F*$_2$) ppm; **^{31}P NMR** (202.46 MHz, $CDCl_3$): δ = 11.26 (s, with satellites $^1J_{P,Pt}$ = 2511 Hz) ppm; **^{195}Pt NMR** (107.51 MHz, $CDCl_3$): δ = -4093 (t, $^1J_{Pt,P}$ = 2511 Hz) ppm. **Elemental analysis** (%) calcd. for $C_{27}H_{41}BF_5N_5O_2P_2Pt$: C 39.05, H 4.98, N 8.43; found (%): C 39.38, H 5.08, N 8.08.

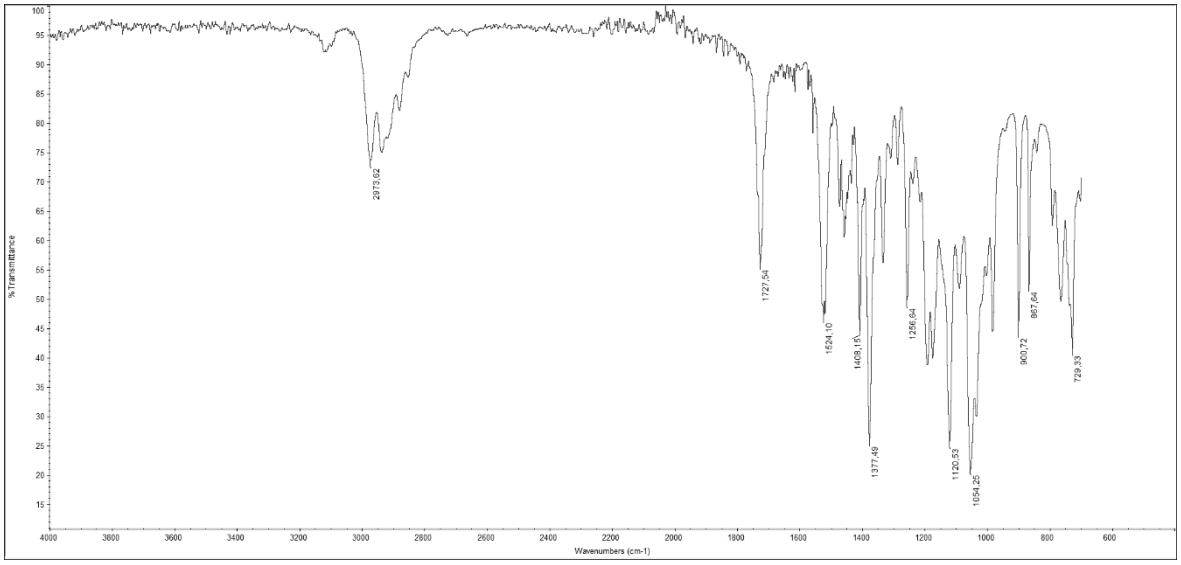
% transmittance
Wavenumbers (cm-1)
2973,62
1727,54
1524,10
1408,16
1377,49
1256,64
1120,53
1054,25
900,72
867,64
729,33

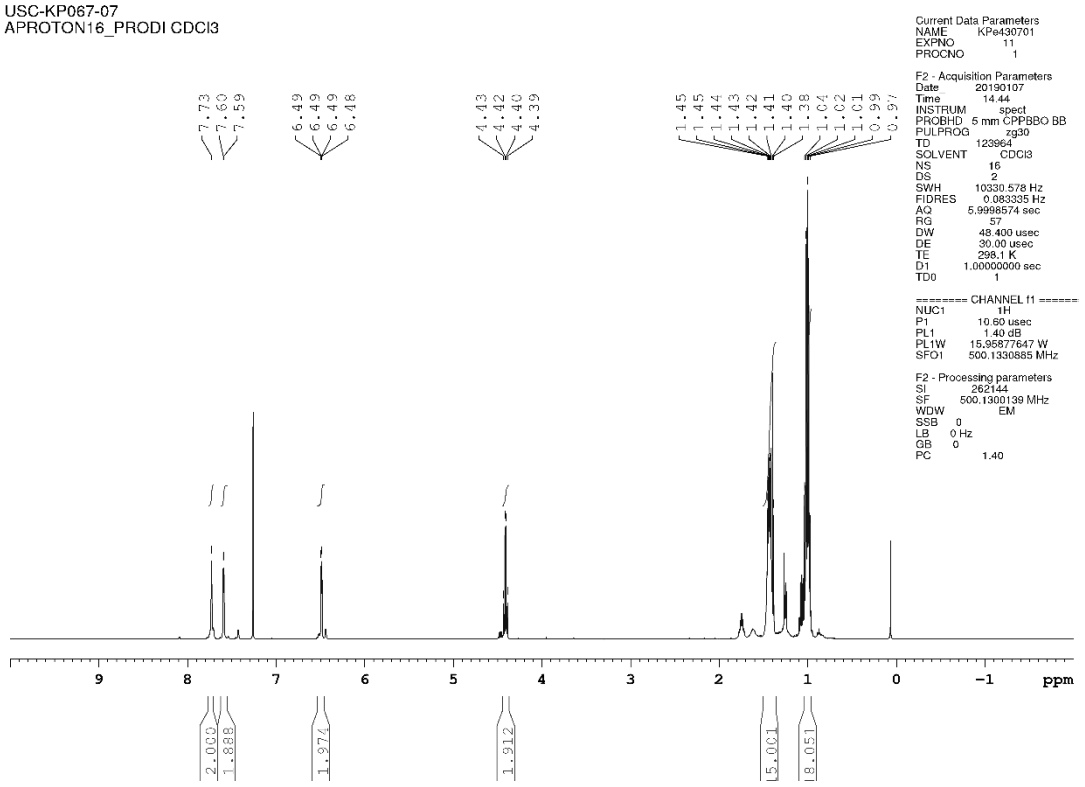
USC-KP067-07
APROTON16_PRODI CDCl3
Current Data Parameters
NAME KPe430701
EXPNO 11
PROCNO 1
F2 - Acquisition Parameters
Date 20190107
Time 14.44
INSTRUM spect
PROBHD 5 mm CPPBBO BB
PULPROG zg30
TD 123964
SOLVENT CDCl3
NS 16
DS 2
SWH 10330.578 Hz
FIDRES 0.083335 Hz
AQ 5.9998574 sec
RG 57
DW 48.400 usec
DE 30.00 usec
TE 298.1 K
D1 1.00000000 sec
TD0 1
======== CHANNEL f1 ======
NUC1 1H
P1 10.60 usec
PL1 1.40 dB
PL1W 15.95877647 W
SFO1 500.1330885 MHz
F2 - Processing parameters
SI 262144
SF 500.1300139 MHz
WDW EM
SSB 0
LB 0 Hz
GB 0
PC 1.40
7.73
7.60
7.59
6.49
6.49
6.49
6.48
4.43
4.42
4.40
4.39
1.45
1.45
1.44
1.43
1.42
1.41
1.40
1.38
1.04
1.02
1.01
0.99
0.97
ppm
2.003
1.888
1.974
1.912
5.001
8.051

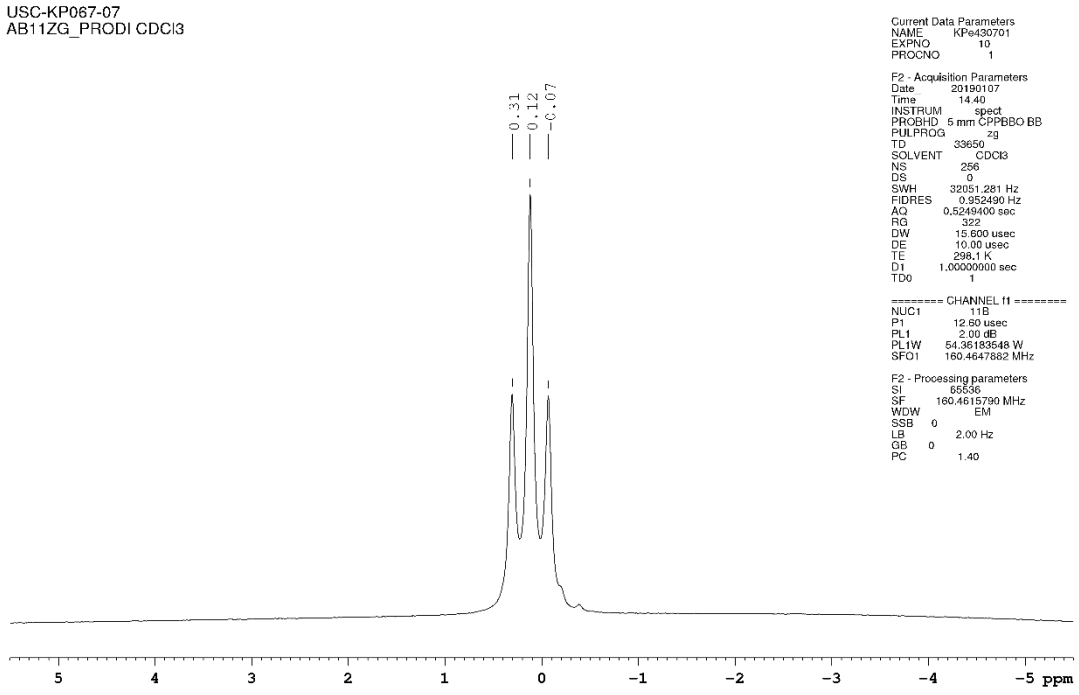
USC-KP067-07
AB11ZG_PRODI CDCl3
0.31
0.12
-0.07
5
4
3
2
1
0
-1
-2
-3
-4
-5 ppm
Current Data Parameters
NAME KPe430701
EXPNO 10
PROCNO 1
F2 - Acquisition Parameters
Date 20190107
Time 14.40
INSTRUM spect
PROBHD 5 mm CPPBBO BB
PULPROG zg
TD 33650
SOLVENT CDCl3
NS 256
DS 0
SWH 32051.281 Hz
FIDRES 0.952490 Hz
AQ 0.5249400 sec
RG 322
DW 15.600 usec
DE 10.00 usec
TE 298.1 K
D1 1.00000000 sec
TD0 1
======== CHANNEL f1 ========
NUC1 11B
P1 12.60 usec
PL1 2.00 dB
PL1W 54.36183648 W
SFO1 160.4647882 MHz
F2 - Processing parameters
SI 65536
SF 160.4615790 MHz
WDW EM
SSB 0
LB 2.00 Hz
GB 0
PC 1.40

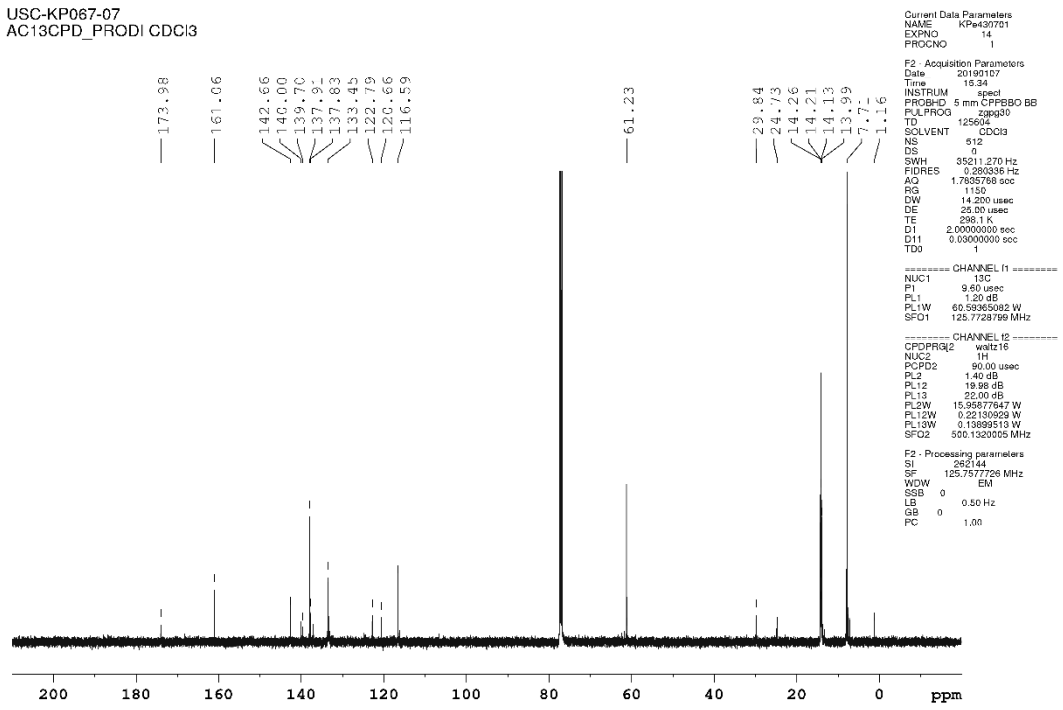
USC-KP067-07
AC13CPD_PRODI CDCl3
173.98
161.06
142.66
140.00
139.70
137.90
137.83
133.45
122.79
120.66
116.59
61.23
29.84
24.73
14.26
14.21
14.13
13.99
7.71
1.16
200
180
160
140
120
100
80
60
40
20
0
ppm
Current Data Parameters
NAME KPe430701
EXPNO 14
PROCNO 1
F2 - Acquisition Parameters
Date 20190107
Time 15.34
INSTRUM spect
PROBHD 5 mm CPPBBO BB
PULPROG zgpg30
TD 125604
SOLVENT CDCl3
NS 512
DS 0
SWH 35211.270 Hz
FIDRES 0.280336 Hz
AQ 1.7835768 sec
RG 1150
DW 14.200 usec
DE 25.00 usec
TE 298.1 K
D1 2.00000000 sec
D11 0.03000000 sec
TD0 1
======== CHANNEL f1 ========
NUC1 13C
P1 9.60 usec
PL1 1.20 dB
PL1W 60.59365082 W
SFO1 125.7728799 MHz
======== CHANNEL f2 ========
CPDPRG[2 waltz16
NUC2 1H
PCPD2 90.00 usec
PL2 1.40 dB
PL12 19.98 dB
PL13 22.00 dB
PL2W 15.95877647 W
PL12W 0.22130929 W
PL13W 0.13899513 W
SFO2 500.1320005 MHz
F2 - Processing parameters
SI 262144
SF 125.7577726 MHz
WDW EM
SSB 0
LB 0.50 Hz
GB 0
PC 1.00

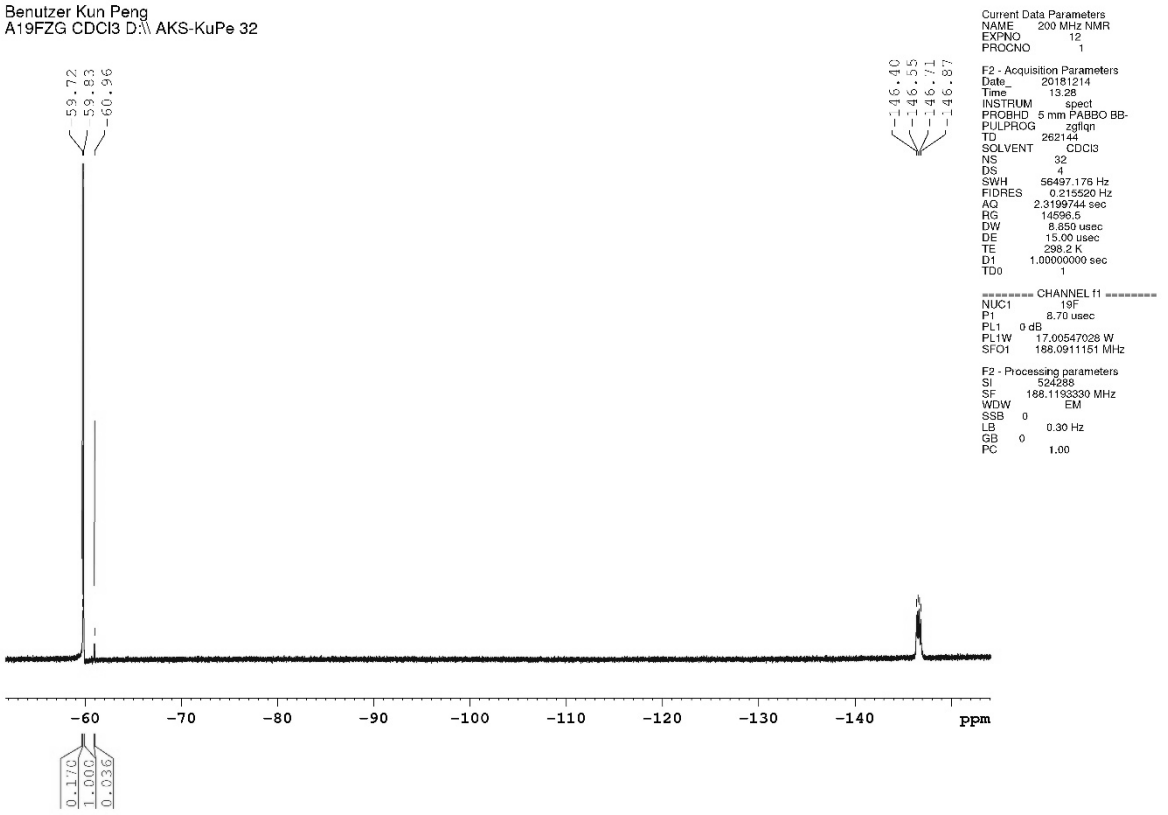
Benutzer Kun Peng
A19FZG CDCl3 D:\\ AKS-KuPe 32
-59.72
-59.83
-60.96
-146.40
-146.55
-146.71
-146.87
Current Data Parameters
NAME 200 MHz NMR
EXPNO 12
PROCNO 1
F2 - Acquisition Parameters
Date_ 20181214
Time 13.28
INSTRUM spect
PROBHD 5 mm PABBO BB-
PULPROG zgflqn
TD 262144
SOLVENT CDCl3
NS 32
DS 4
SWH 56497.176 Hz
FIDRES 0.215520 Hz
AQ 2.3199744 sec
RG 14596.5
DW 8.850 usec
DE 15.00 usec
TE 298.2 K
D1 1.00000000 sec
TD0 1
======== CHANNEL f1 ========
NUC1 19F
P1 8.70 usec
PL1 0 dB
PL1W 17.00547028 W
SFO1 188.0911151 MHz
F2 - Processing parameters
SI 524288
SF 188.1193330 MHz
WDW EM
SSB 0
LB 0.30 Hz
GB 0
PC 1.00
-60
-70
-80
-90
-100
-110
-120
-130
-140
ppm
0.170
1.000
0.036

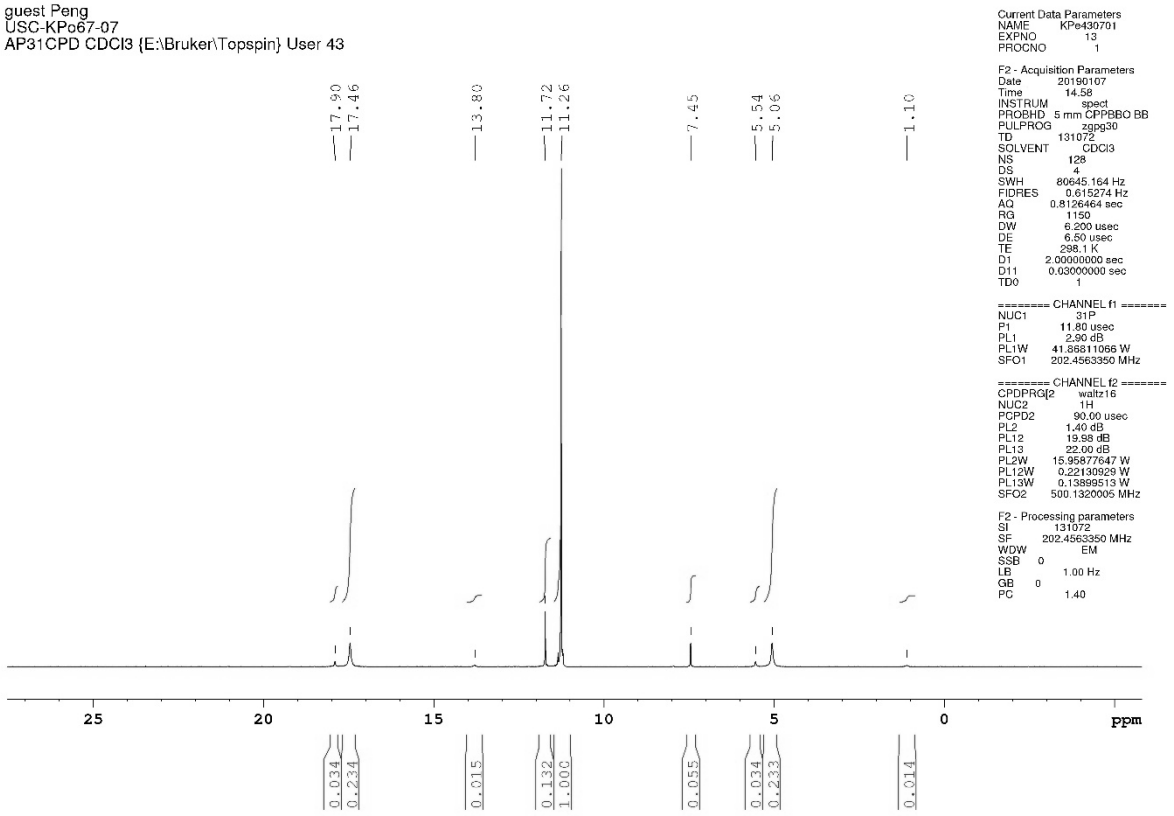
guest Peng
USC-KPo67-07
AP31CPD CDCl3 {E:\Bruker\Topspin} User 43
17.50
17.46
13.80
11.72
11.26
7.45
5.54
5.06
1.10
Current Data Parameters
NAME KPe430701
EXPNO 13
PROCNO 1
F2 - Acquisition Parameters
Date 20190107
Time 14.58
INSTRUM spect
PROBHD 5 mm CPPBBO BB
PULPROG zgpg30
TD 131072
SOLVENT CDCl3
NS 128
DS 4
SWH 80645.164 Hz
FIDRES 0.615274 Hz
AQ 0.8126464 sec
RG 1150
DW 6.200 usec
DE 6.50 usec
TE 298.1 K
D1 2.00000000 sec
D11 0.03000000 sec
TD0 1
======== CHANNEL f1 =======
NUC1 31P
P1 11.80 usec
PL1 2.90 dB
PL1W 41.86811066 W
SFO1 202.4563350 MHz
======== CHANNEL f2 =======
CPDPRG[2 waltz16
NUC2 1H
PCPD2 90.00 usec
PL2 1.40 dB
PL12 19.98 dB
PL13 22.00 dB
PL2W 15.95877647 W
PL12W 0.22130929 W
PL13W 0.13899513 W
SFO2 500.1320005 MHz
F2 - Processing parameters
SI 131072
SF 202.4563350 MHz
WDW EM
SSB 0
LB 1.00 Hz
GB 0
PC 1.40
25
20
15
10
5
0
ppm
0.034
0.234
0.015
0.132
1.000
0.055
0.034
0.233
0.014

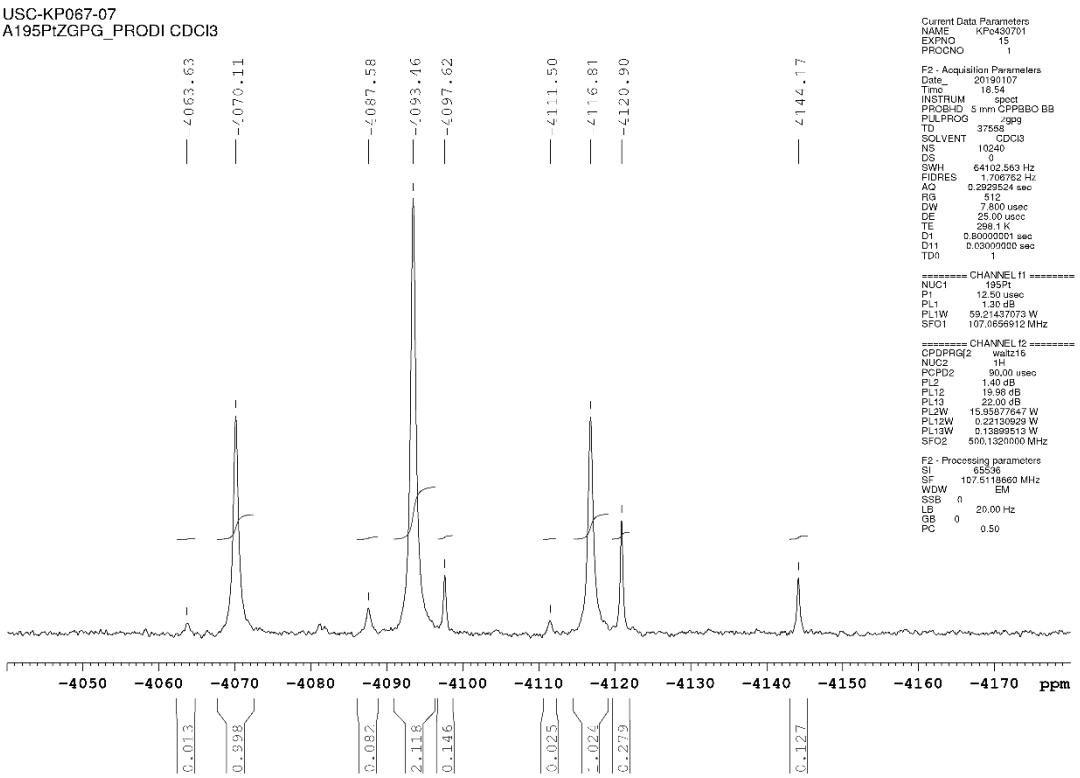
USC-KP067-07
A195PtZGPG_PRODI CDCl3
-4063.63
-4070.11
-4087.58
-4093.46
-4097.62
-4111.50
-4116.81
-4120.90
-4144.17
Current Data Parameters
NAME KPc430701
EXPNO 15
PROCNO 1
F2 - Acquisition Parameters
Date_ 20190107
Time 16.54
INSTRUM spect
PROBHD 5 mm CPPSBO BB
PULPROG zgpg
TD 37568
SOLVENT CDCl3
NS 10240
DS 0
SWH 64102.563 Hz
FIDRES 1.706762 Hz
AQ 0.2929524 sec
RG 512
DW 7.800 usec
DE 25.00 usec
TE 298.1 K
D1 0.80000001 sec
D11 0.03000000 sec
TD0 1
======== CHANNEL f1 ========
NUC1 195Pt
P1 12.50 usec
PL1 1.30 dB
PL1W 59.21437073 W
SFO1 107.0656912 MHz
======== CHANNEL f2 ========
CPDPRG[2 waltz16
NUC2 1H
PCPD2 90.00 usec
PL2 1.40 dB
PL12 19.98 dB
PL13 22.00 dB
PL2W 15.95877647 W
PL12W 0.22130929 W
PL13W 0.13889513 W
SFO2 500.1320000 MHz
F2 - Processing parameters
SI 65536
SF 107.5118660 MHz
WDW EM
SSB 0
LB 20.00 Hz
GB 0
PC 0.50
-4050
-4060
-4070
-4080
-4090
-4100
-4110
-4120
-4130
-4140
-4150
-4160
-4170
ppm
0.013
0.998
0.082
2.118
0.146
0.025
1.024
0.279
0.127

5.3.45 Synthesis of [AuCl(terpy)]C1$_2$·2H$_2$O

USC-KP015-01

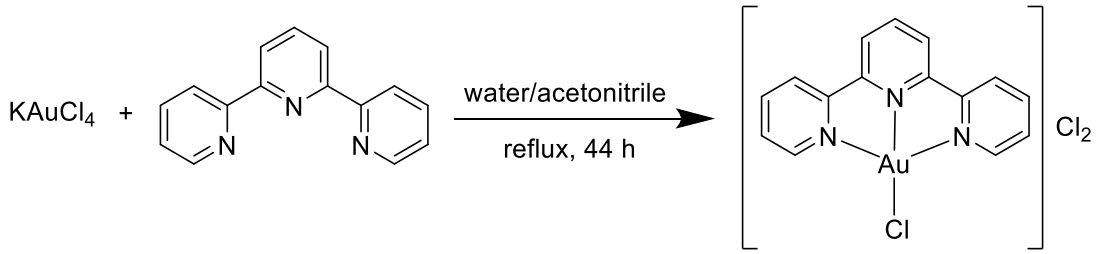

$AuCl_4K$ 377.86 g/mol

$C_{15}H_{11}N_3$ 233.27 g/mol

$C_{15}H_{11}AuCl_3N_3$ 536.59 g/mol

2,2':6',2''-Terpyridine (116 mg, 0.50 mmol) was dissolved in acetonitrile (15 mL) under nitrogen to give a clear colourless solution. Then, potassium tetrachloroaurate(III) (126 mg, 0.33 mmol) in water (15 mL) was added dropwise to the colourless solution. After stirring at room temperature for 1 h, the mixture was heated to reflux for 44 h. The resulting solution was cooled to room temperature and filtered. The filtrate was evaporated to dryness to obtain an amber solid, which was washed with acetone (10 mL) and dried under vacuum for 1 d. Yield: 85% (148 mg, 0.28 mmol). **IR** (ATR):: $\tilde{\nu}$ = 3374 (w), 1605 (s), 1467 (m), 1457 (s), 1349 (m), 1245 (m), 1036 (m), 769 (m), 753 (m) cm^{-1}; **^{1}H NMR** (199.93 MHz, DMSO-d_6): δ = 8.77 (ddd, 2H, $^3J_{H6,H5/H6",H5"}$ = 4.8 Hz, $^4J_{H6,H4/H6",H4"}$ = 1.6 Hz, $^5J_{H6,H3/H6",H3"}$ = 0.7 Hz, H6/H6"), 8.71 (d, 2H, $^3J_{H3,H4/H3",H4"}$ = 8.0 Hz, H3/H3"), 8.49 (d, 2H, $^3J_{H3'/H5',H4'}$ = 7.9 Hz, H3'/H5'), 8.20–8.08 (m, 3H, H4/H4'/H4"), 7.59 (ddd, 2H, $^3J_{H5,H4/H5",H4"}$ = 7.5 Hz, $^3J_{H5,H6/H5",H6"}$ = 4.9 Hz, $^4J_{H5,H3/H5",H3"}$ = 1.1 Hz, H5/H5"); **^{13}C NMR** (100.68 MHz, DMSO-d_6): δ = 153.87 (C2'/C6'), 153.82 (C2/C2"), 148.48 (C6/C6"), 138.94 (C4/C4"), 138.83 (C4'), 124.94 (C5/C5"), 121.45 (C3/C3", C3'/C5') ppm; **Elemental analysis** calcd. (%) for $C_{15}H_{11}AuCl_3N_3·(H_2O)_2$: C 31.46, H 2.64, N 7.34; found (%): C 31.11, H 2.64, N 7.30.

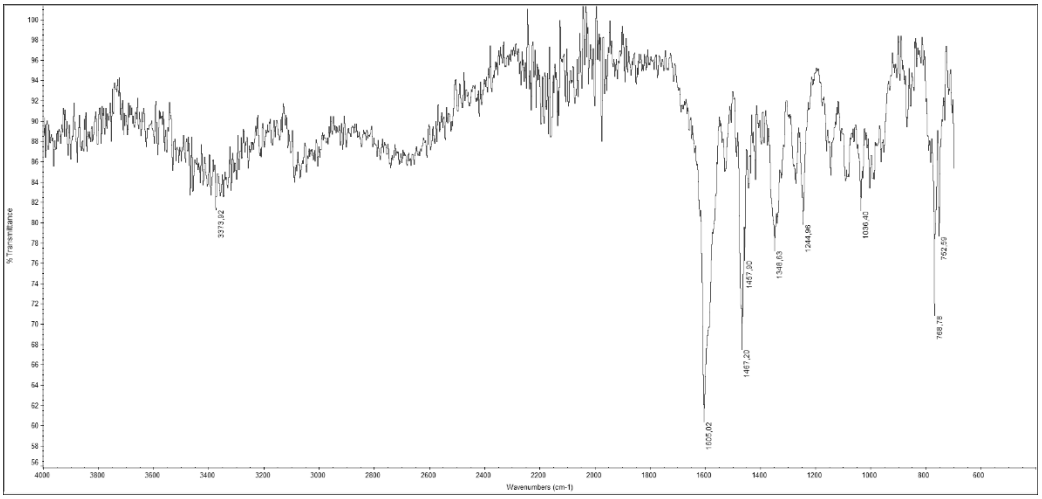
% Transmittance
Wavenumbers (cm-1)
3373.92
1605.92
1487.20
1457.90
1348.63
1244.96
1036.40
792.59
766.76

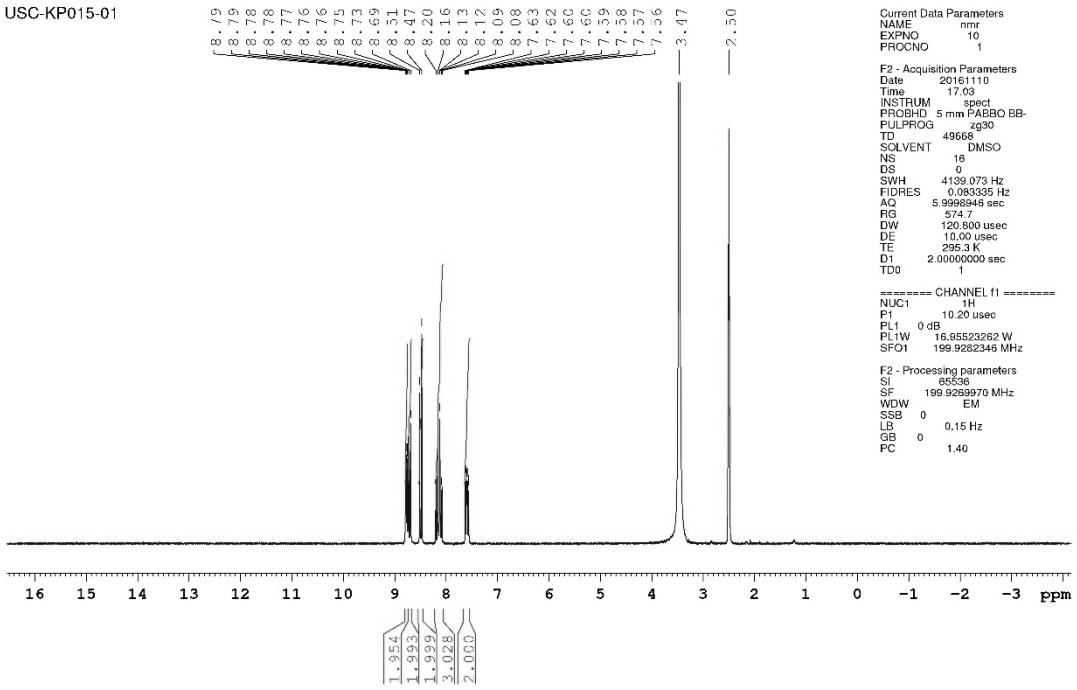
USC-KP015-01
8.79
8.79
8.78
8.78
8.77
8.76
8.76
8.75
8.73
8.69
8.51
8.47
8.20
8.16
8.13
8.12
8.09
8.08
7.63
7.62
7.60
7.60
7.59
7.58
7.57
7.56
3.47
2.50
Current Data Parameters
NAME nmr
EXPNO 10
PROCNO 1
F2 - Acquisition Parameters
Date 20161110
Time 17.03
INSTRUM spect
PROBHD 5 mm PABBO BB-
PULPROG zg30
TD 49668
SOLVENT DMSO
NS 16
DS 0
SWH 4139.073 Hz
FIDRES 0.083335 Hz
AQ 5.9998948 sec
RG 574.7
DW 120.800 usec
DE 10.00 usec
TE 295.3 K
D1 2.00000000 sec
TD0 1
======== CHANNEL f1 ========
NUC1 1H
P1 10.20 usec
PL1 0 dB
PL1W 16.95523262 W
SFO1 199.9282346 MHz
F2 - Processing parameters
SI 65536
SF 199.9269970 MHz
WDW EM
SSB 0
LB 0.15 Hz
GB 0
PC 1.40
16 15 14 13 12 11 10 9 8 7 6 5 4 3 2 1 0 −1 −2 −3 ppm
1.954
1.993
1.999
3.028
2.000

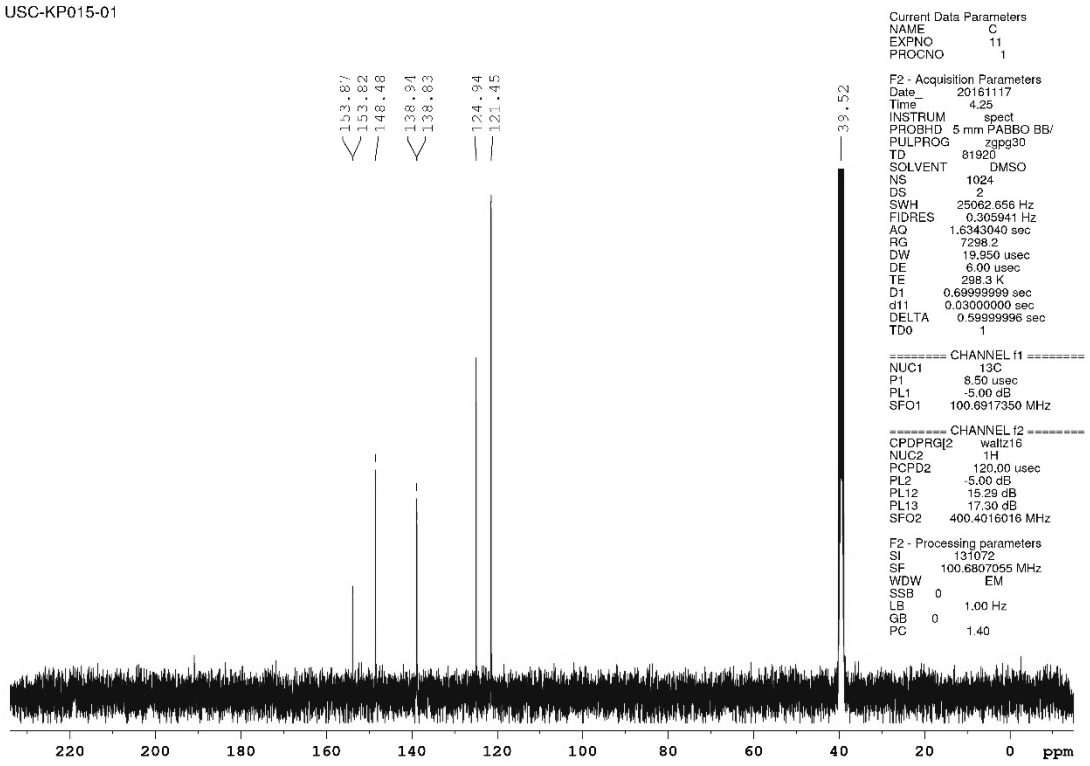
USC-KP015-01
153.87
153.82
148.48
138.94
138.83
124.94
121.45
39.52
Current Data Parameters
NAME C
EXPNO 11
PROCNO 1
F2 - Acquisition Parameters
Date_ 20161117
Time 4.25
INSTRUM spect
PROBHD 5 mm PABBO BB/
PULPROG zgpg30
TD 81920
SOLVENT DMSO
NS 1024
DS 2
SWH 25062.656 Hz
FIDRES 0.305941 Hz
AQ 1.6343040 sec
RG 7298.2
DW 19.950 usec
DE 6.00 usec
TE 298.3 K
D1 0.69999999 sec
d11 0.03000000 sec
DELTA 0.59999996 sec
TD0 1
======== CHANNEL f1 ========
NUC1 13C
P1 8.50 usec
PL1 -5.00 dB
SFO1 100.6917350 MHz
======== CHANNEL f2 ========
CPDPRG[2 waltz16
NUC2 1H
PCPD2 120.00 usec
PL2 -5.00 dB
PL12 15.29 dB
PL13 17.30 dB
SFO2 400.4016016 MHz
F2 - Processing parameters
SI 131072
SF 100.6807055 MHz
WDW EM
SSB 0
LB 1.00 Hz
GB 0
PC 1.40
220
200
180
160
140
120
100
80
60
40
20
0
ppm

5.3.46 Synthesis of [Au(N$_3$)$_3$(terpy)]

USC-KP016-33

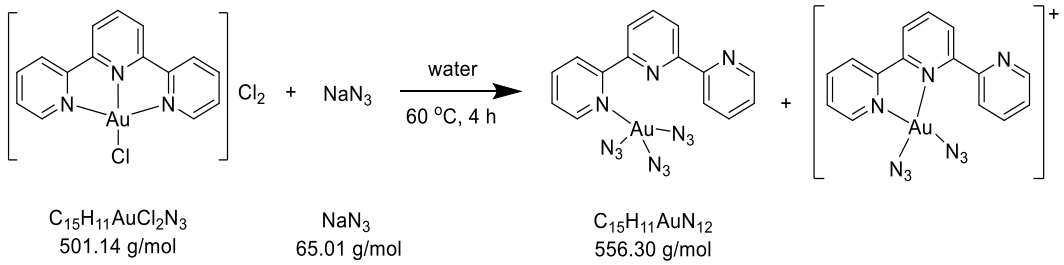

$C_{15}H_{11}AuCl_2N_3$ 501.14 g/mol

NaN_3 65.01 g/mol

$C_{15}H_{11}AuN_{12}$ 556.30 g/mol

[AuCl(terpy)]Cl$_2$ (50 mg, 0.09 mmol) was dissolved in water (10 mL) at 60 °C to give a clear yellow solution. Then, a solution of sodium azide (31 mg, 0.48 mmol) in water (2 mL) was added. The mixture was heated to 60 °C for 4 h, during which an orange solid precipitated. The solution was cooled to room temperature and the orange precipitate filtered off (*Caution: This material exploded when scratched with a metal spatula*). The solid was then washed with diethyl ether (5 × 2 mL) and dried under vacuum overnight. The resulting material was used for IR and NMR spectroscopy as well as elemental analysis. Orange block-like crystals suitable for X-ray structure analysis were obtained by slow diffusion of diethyl ether into a solution of the product in acetone. Yield: 56% (28 mg, 0.05 mmol). **IR** (ATR): $\tilde{\nu}$ = 3091 (w), 2014 (s), 1581 (m), 1423 (m), 1247 (m), 1162 (m), 766 (m), 750 (m) cm^{-1}; **^{1}H NMR** (500.13 MHz, acetone-d_6): major species: δ = 9.08 (m, 1H, H6), 8.75–8.70 (m, 3H, H3, H4, H6”), 8.55 (d, 2H, $^3J_{H3'/H5',H4'}$ = 7.8 Hz, H3’/H5’), 8.32–8.26 (m, 2H, H4’, H3”), 8.01 (dt, 1H, $^3J_{H4",H3"/H5"}$ = 7.7 Hz, $^4J_{H4", H6"}$ = 1.8 Hz, H4”), 7.82 (m, 1H, H5), 7.48 (ddd, 1H, $^3J_{H5",H4"}$ = 7.5 Hz, $^3J_{H5",H6"}$ = 4.7 Hz, $^4J_{H5",H3"}$ = 1.2 Hz, H5”) ppm; minor species: δ = 9.27 (dd, 1H, $^3J_{H6,H5}$ = 5.9 Hz, $^4J_{H6,H4}$ = 1.2 Hz, H6), 9.18 (s,1H, H6”), 9.16(dd, 1H, $^3J_{H3",H4"}$ =8.0 Hz, $^4J_{H3",H5"}$ = 1.4 Hz, H3”), 9.01 (dt, 1H, $^3J_{H4",H3"/H5"}$ = 7.9 Hz, $^4J_{H4",H6"}$ = 1.4 Hz, H4”), 8.51(ddd, 2H, $^3J_{H4,H5/H4',H5'}$ = 7.7 Hz, $^3J_{H4,H3/H4',H3'}$ = 6.0 Hz, $^4J_{H4,H6/H4',H6'}$ = 1.6 Hz, H4/H4’), 8.09 (t, 2H, $^3J_{H5,H4/H5',H4'}$ = 7.8 Hz, H5/H5’) ppm (the peaks for H3, H3’ and H5” were not observed due to overlap with the major species signals); **^{13}C NMR** (125.76 MHz, acetone-d_6): major species: δ = 156.50 (C6’), 156.09 (C2’), 155.01 (C2”), 151.16 (C2), 150.02 (C6”), 140.33 (C6), 139.01 (C4”), 138.15 (C4’), 132.24 (C4), 130.02 (C5”), 128.58 (C5’), 125.06 (C5), 124.83 (C3”), 121.78 (C3’), 121.70 (C3) ppm; minor species: δ = 150.95, 149.21, 148.36, 127.26 ppm (most signals not observed due to low abundancy); **Elemental Analysis** (%) calcd for $C_{15}H_{11}AuN_{12}$: C 32.39, H 1.99, N 30.21; found (%): C 31.50, H 2.12, N 30.08.

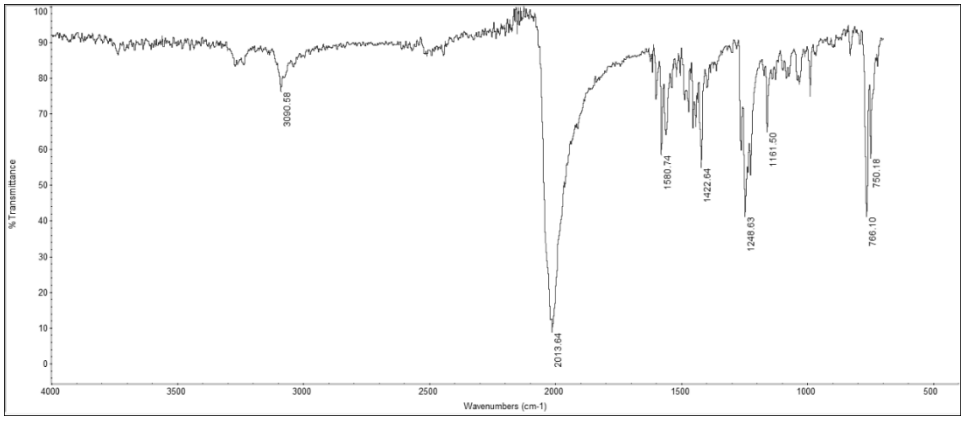
%Transmittance
Wavenumbers (cm-1)
3090.68
2013.64
1580.74
1422.64
1248.63
1161.50
766.10
750.18

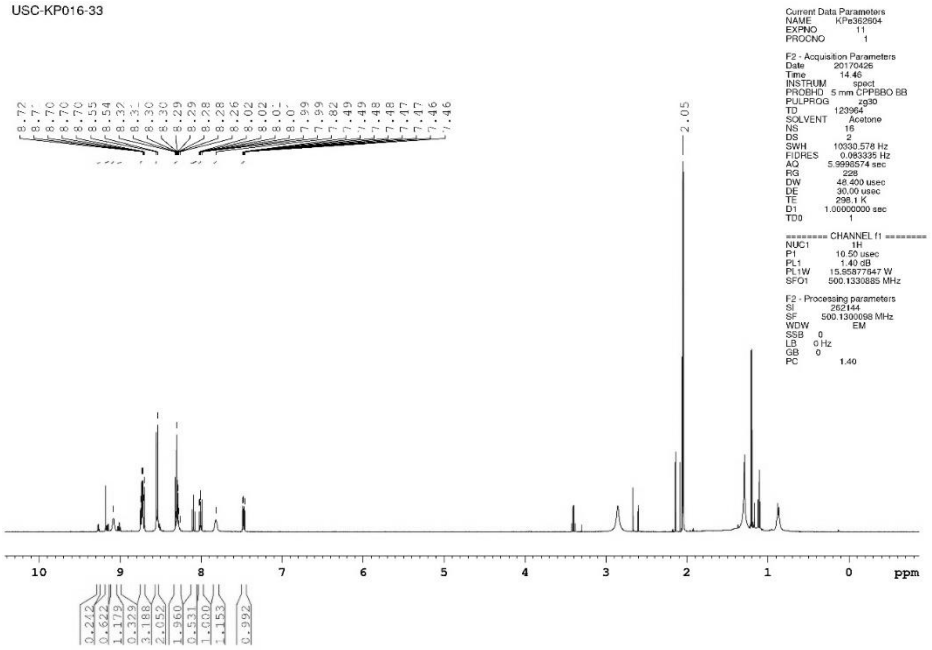
USC-KP016-33
2.05
ppm

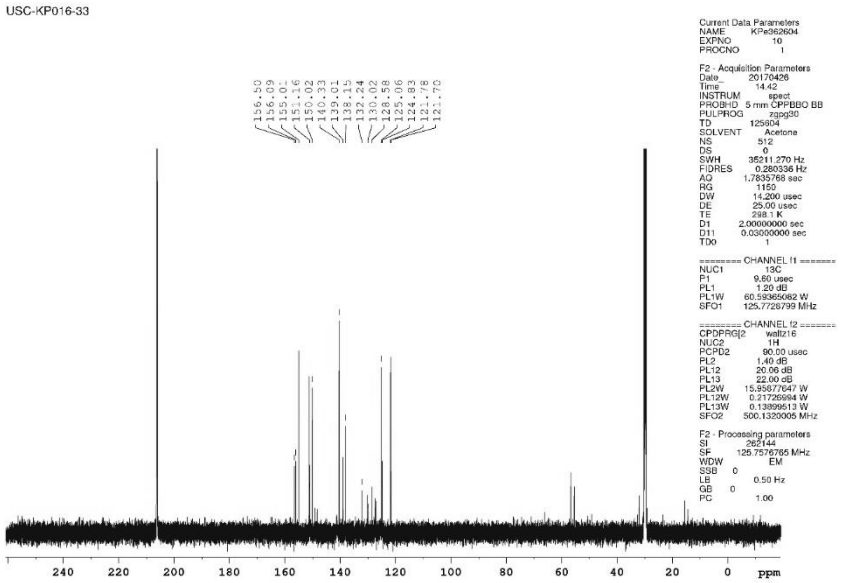
USC-KP016-33
ppm

Tab 5.1: Single-crystal X-ray diffraction data and structure refinement of complex **60**.

[Au(N$_3$)$_3$(terpy-**κ**^{1}-*N*^{1})]	**60**
Empirical formula	$C_{15}H_{11}AuN_{12}$
Formula weight (g·mol^{-1})	556.3
Temperature (K)	100(2)
Radiation, l (Å)	Mo_{Ka} 0.71073
Crystal system	Monoclinic
Space group	*C2/c*
Unit cell dimensions	
***a* (Å)**	16.174(7)
***b* (Å)**	10.772(5)
***c* (Å)**	19.565(8)
α (°)	90
β (°)	92.84(2)
γ (°)	90
Volume (Å^3)	3405(2)
Z	8
Calculated density (g·cm^{-3})	2.171
Crystal size (mm)	0.32 × 0.33 × 0.60
***F*(000)**	2112
Theta range for collection (°)	2.084–26.022
Reflections collected	19200
Unique reflections	3350
Parameters / restraints	253 / 0
Parameters / restraints	253 / 0
Goodness-of-fit on F^2	1.190
μ (mm^{-1})	8.674
***R*$_1$ [I>2σ(I)]**	0.0252
***w*R^2 (all data)**	0.0607
Maximum/minimum residual electron density (e·Å^{-3})	1.317 / –1.380
CCDC number	1918121

6 References

[1] I. Kostova, *Recent Pat. Anti-Cancer Drug Discovery* **2006,** *1*, 1-22.

[2] B. Rosenberg, L. Van Camp, T. Krigas, *Nature* **1965,** *205*, 698-699.

[3] N. Cutillas, A. Martinez, G. S. Yellol, V. Rodriguez, A. Zamora, M. Pedreno, A. Donaire, C. Janiak, J. Ruiz, *Inorg. Chem.* **2013,** *52*, 13529-13535.

[4] C. Santini, M. Pellei, V. Gandin, M. Porchia, F. Tisato, C. Marzano, *Chem. Rev.* **2014,** *114*, 815-862.

[5] B. Rosenberg, L. VanCamp, *Cancer Res.* **1970,** *30*, 1799-1802.

[6] I. Ali, W. A. Wani, K. Saleem, A. Haque, *Anti-Cancer Agents Med. Chem.* **2013,** *13*, 296-306.

[7] M. Pellei, G. G. Lobbia, C. Santini, R. Spagna, M. Camalli, D. Fedeli, G. Falcioni, *Dalton Trans.* **2004**, 2822-2828.

[8] J. Reedijk, *Proc. Natl. Acad. Sci. U. S. A.* **2003,** *100*, 3611-3616.

[9] R. C. Todd, S. J. Lippard, *Metallomics* **2009,** *1*, 280-291.

[10] M. A. Jakupec, M. Galanski, B. K. Keppler, *Rev. Physiol. Biochem. Pharmacol.* **2003,** *146*, 1-54.

[11] V. Pinzani, F. Bressolle, I. J. Haug, M. Galtier, J. P. Blayac, P. Balmes, *Cancer Chemother. Pharmacol.* **1994,** *35*, 1-9.

[12] C. Moncharmont, P. Auberdiac, A. Melis, S. Afqir, C. Pacaut, C. Chargari, Y. Merrouche, N. Magne, *Bull. Cancer* **2011,** *98*, 164-175.

[13] J. A. Gietema, H. J. Guchelaar, E. G. de Vries, P. Aulenbacher, D. T. Sleijfer, N. H. Mulder, *Anticancer Drug.* **1993,** *4*, 51-55.

[14] J. A. Gietema, G. J. Veldhuis, H. J. Guchelaar, P. H. Willemse, D. R. Uges, A. Cats, H. Boonstra, W. T. van der Graaf, D. T. Sleijfer, E. G. de Vries, N. H. Mukder, *Br. J. Cancer* **1995,** *71*, 1302-1307.

[15] J. J. Kavanagh, C. L. Edwards, R. S. Freedman, M. B. Finnegan, O. Balat, D. Tresukosol, K. Burk, S. Loechner, M. Hord, J. L. Franklin, et al., *Gynecol. Oncol.* **1995,** *58*, 106-109.

[16] M. Degardin, J. P. Armand, B. Chevallier, P. Cappelaere, M. A. Lentz, M. David, H. Roche, *Invest. New Drugs* **1995,** *13*, 253-255.

[17] J. Welink, E. Boven, J. B. Vermorken, H. E. Gall, W. J. van der Vijgh, *Clin. Cancer Res.* **1999,** *5*, 2349-2358.

[18] D. K. Kim, G. Kim, J. Gam, Y. B. Cho, H. T. Kim, J. H. Tai, K. H. Kim, W. S. Hong, J. G. Park, *J. Med. Chem.* **1994,** *37*, 1471-1485.

[19] D.-K. Kim, H.-T. Kim, J. H. Tai, Y.-B. Cho, T.-S. Kim, K. H. Kim, J.-G. Park, W.-S. Hong, *Cancer Chemother. Pharmacol.* **1995,** *37*, 1-6.

[20] N. Farrell, T. T. B. Ha, J.-P. Souchard, F. L. Wimmer, S. Cros, N. P. Johnson, *J. Med. Chem.* **1989,** *32*, 2240-2241.

[21] N. Farrell, L. R. Kelland, J. D. Roberts, M. Van Beusichem, *Cancer Res.* **1992,** *52*, 5065-5072.

[22] M. Van Beusichem, N. Farrell, *Inorg. Chem.* **1992,** *31*, 634-639.

[23] A. Maisonial, P. Serafin, M. Traikia, E. Debiton, V. Thery, D. J. Aitken, P. Lemoine, B. Viossat, A. Gautier, *Eur. J. Inorg. Chem.* **2008,** 298-305.

[24] J. Zhang, X. Wang, C. Tu, J. Lin, J. Ding, L. Lin, Z. Wang, C. He, C. Yan, X. You, Z. Guo, *J. Med. Chem.* **2003,** *46*, 3502-3507.

[25] N. J. Wheate, J. G. Collins, *Coord. Chem. Rev.* **2003,** *241*, 133-145.

[26] C. Manzotti, G. Pratesi, E. Menta, R. Di Domenico, E. Cavalletti, H. H. Fiebig, L. R. Kelland, N. Farrell, D. Polizzi, R. Supino, G. Pezzoni, F. Zunino, *Clin. Cancer Res.* **2000,** *6*, 2626-2634.

[27] Y. Zhao, W. He, P. Shi, J. Zhu, L. Qiu, L. Lin, Z. Guo, *Dalton Trans.* **2006**, 2617-2619.

[28] L. J. Teixeira, M. Seabra, E. Reis, M. T. da Cruz, M. C. de Lima, E. Pereira, M. A. Miranda, M. P. Marques, *J. Med. Chem.* **2004,** *47*, 2917-2925.

[29] C. M. Giandomenico, M. J. Abrams, B. A. Murrer, J. F. Vollano, M. I. Rheinheimer, S. B. Wyer, G. E. Bossard, J. D. Higgins, *Inorg. Chem.* **1995,** *34*, 1015-1021.

[30] M. D. Hall, T. W. Hambley, *Coord. Chem. Rev.* **2002,** *232*, 49-67.

[31] Y. R. Zheng, K. Suntharalingam, T. C. Johnstone, H. Yoo, W. Lin, J. G. Brooks, S. J. Lippard, *J. Am. Chem. Soc.* **2014,** *136*, 8790-8798.

[32] D. Gibson, *Dalton Trans.* **2016,** *45*, 12983-12991.

[33] K. D. Tutsch, R. Z. Arzoomanian, D. Alberti, M. B. Tombes, C. Feierabend, H. I. Robins, D. R. Spriggs, G. Wilding, *Invest. New Drugs* **1999,** *17*, 63-72.

[34] L. Pendyala, J. W. Cowens, G. B. Chheda, S. P. Dutta, P. J. Creaven, *Cancer Res.* **1988,** *48*, 3533-3536.

[35] A. Bhargava, U. N. Vaishampayan, *Expert Opin. Invest. Drugs.* **2009,** *18*, 1787-1797.

[36] T. C. Johnstone, K. Suntharalingam, S. J. Lippard, *Chem. Rev.* **2016,** *116*, 3436-3486.

[37] P. Bouchal, J. Jarkovsky, K. Hrazdilova, M. Dvorakova, I. Struharova, L. Hernychova, J. Damborsky, P. Sova, B. Vojtesek, *Proteome Sci.* **2011,** *9*, 68-76.

[38] M. J. Clarke, F. Zhu, D. R. Frasca, *Chem. Rev.* **1999,** *99*, 2511-2534.

[39] K. M. Hindi, M. J. Panzner, C. A. Tessier, C. L. Cannon, W. J. Youngs, *Chem. Rev.* **2009,** *109*, 3859-3884.

[40] B. K. Keppler, W. Rupp, *J. Cancer Res. Clin. Oncol.* **1986,** *111*, 166-168.

[41] P. V. Simpson, N. M. Desai, I. Casari, M. Massi, M. Falasca, *Future Med. Chem.* **2019,** *11*, 119-135.

[42] E. Alessio, G. Mestroni, A. Bergamo, G. Sava, *Curr. Top. Med. Chem.* **2004,** *4*, 1525-1535.

[43] S. E. H. Etaiw, A. S. Sultan, M. M. El-Bendary, *J. Organomet. Chem.* **2011,** *696*, 1668-1676.

[44] S. J. Berners-Price, C. K. Mirabelli, R. K. Johnson, M. R. Mattern, F. L. McCabe, L. F. Faucette, C. M. Sung, S. M. Mong, P. J. Sadler, S. T. Crooke, *Cancer Res.* **1986,** *46*, 5486-5493.

[45] S. J. Berners-Price, R. K. Johnson, A. J. Giovenella, L. F. Faucette, C. K. Mirabelli, P. J. Sadler, *J. Inorg. Biochem.* **1988,** *33*, 285-295.

[46] L. Messori, G. Marcon, *Met. Ions Biol. Syst.* **2004,** *42*, 385-424.

[47] G. Marcon, S. Carotti, M. Coronnello, L. Messori, E. Mini, P. Orioli, T. Mazzei, M. A. Cinellu, G. Minghetti, *J. Med. Chem.* **2002,** *45*, 1672-1677.

[48] P. Shi, Q. Jiang, Y. Zhao, Y. Zhang, J. Lin, L. Lin, J. Ding, Z. Guo, *J. Biol. Inorg. Chem.* **2006,** *11*, 745-752.

[49] S. Leijen, J. H. Beijnen, J. HM. Schellens, *Curr. Clin. Pharmacol.* **2010,** *5*, 186-191.

[50] L. M. Murrow, S. V. Garimella, T. L. Jones, N. J. Caplen, S. Lipkowitz, *Breast Cancer Res. Treat* **2010,** *122*, 347-357.

[51] G. J. Yang, H. J. Zhong, C. N. Ko, S. Y. Wong, K. Vellaisamy, M. Ye, D. L. Ma, C. H. Leung, *Chem. Commun.* **2018,** *54*, 2463-2466.

[52] H. C. Kolb, M. G. Finn, K. B. Sharpless, *Angew. Chem. Int. Ed.* **2001,** *40*, 2004-2021.

[53] R. Huisgen, Weberndo.V, *Experientia* **1961,** *17*, 566-566.

[54] R. Huisgen, *Angew. Chem. Int. Ed.* **1963,** *2*, 565-598.

[55] R. Huisgen, *Angew. Chem. Int. Ed.* **1963,** *2*, 633-645.

[56] V. V. Rostovtsev, L. G. Green, V. V. Fokin, K. B. Sharpless, *Angew. Chem. Int. Ed.* **2002,** *41*, 2596-2599.

[57] C. W. Tornøe, C. Christensen, M. Meldal, *J. Org. Chem.* **2002,** *67*, 3057-3064.

[58] N. J. Agard, J. A. Prescher, C. R. Bertozzi, *J. Am. Chem. Soc.* **2004,** *126*, 15046-15047.

[59] J. M. Baskin, J. A. Prescher, S. T. Laughlin, N. J. Agard, P. V. Chang, I. A. Miller, A. Lo, J. A. Codelli, C. R. Bertozzi, *Proc. Natl. Acad. Sci. U. S. A.* **2007,** *104*, 16793-16797.

[60] P. V. Chang, J. A. Prescher, E. M. Sletten, J. M. Baskin, I. A. Miller, N. J. Agard, A. Lo, C. R. Bertozzi, *Proc. Natl. Acad. Sci. U. S. A.* **2010,** *107*, 1821-1826.

[61] S. T. Laughlin, J. M. Baskin, S. L. Amacher, C. R. Bertozzi, *Science* **2008,** *320*, 664-667.

[62] W. Tang, M. L. Becker, *Chem. Soc. Rev.* **2014,** *43*, 7013-7039.

[63] R. van Geel, G. J. Pruijn, F. L. van Delft, W. C. Boelens, *Bioconjugate Chem.* **2012,** *23*, 392-398.

[64] T. S. Seo, Z. Li, H. Ruparel, J. Ju, *J. Org. Chem.* **2003,** *68*, 609-612.

[65] Z. M. Li, T. S. Seo, J. Y. Ju, *Tetrahedron Lett.* **2004,** *45*, 3143-3146.

[66] S. S. van Berkel, A. T. Dirks, M. F. Debets, F. L. van Delft, J. J. Cornelissen, R. J. Nolte, F. P. Rutjes, *ChemBioChem* **2007,** *8*, 1504-1508.

[67] A. B. Lowe, *Polym. Chem.* **2010,** *1*, 17-36.

[68] D. P. Nair, M. Podgorski, S. Chatani, T. Gong, W. X. Xi, C. R. Fenoli, C. N. Bowman, *Chem. Mater.* **2014,** *26*, 724-744.

[69] S. Ulrich, D. Boturyn, A. Marra, O. Renaudet, P. Dumy, *Chem. Eur. J.* **2014,** *20*, 34-41.

[70] E. Saxon, J. I. Armstrong, C. R. Bertozzi, *Org. Lett.* **2000,** *2*, 2141-2143.

[71] F. L. Lin, H. M. Hoyt, H. van Halbeek, R. G. Bergman, C. R. Bertozzi, *J. Am. Chem. Soc.* **2005,** *127*, 2686-2695.

[72] P. E. Dawson, S. B. Kent, *Annu. Rev. Biochem.* **2000,** *69*, 923-960.

[73] T. J. Del Castillo, S. Sarkar, K. A. Abboud, A. S. Veige, *Dalton Trans.* **2011,** *40*, 8140-8144.

[74] L. Birkofer, P. Wegner, *Chem. Ber.* **1966,** *99*, 2512-2517.

[75] H. Gorth, M. C. Henry, *J. Organomet. Chem.* **1967,** *9*, 117-123.

[76] T. Hitomi, S. Kozima, *J. Organomet. Chem.* **1977,** *127*, 273-280.

[77] N. Jagerovic, J. M. Barbe, M. Farnier, R. Guilard, *Dalton Trans.* **1988**, 2569-2571.

[78] R. Guilard, S. S. Gerges, A. Tabard, P. Richard, M. A. El Borai, C. Lecomte, *J. Am. Chem. Soc.* **1987,** *109*, 7228-7230.

[79] R. Guilard, N. Jagerovic, A. Tabard, P. Richard, L. Courthaudon, A. Louati, C. Lecomte, K. M. Kadish, *Inorg. Chem.* **1991,** *30*, 16-27.

[80] M. Herberhold, A. Goller, W. Milius, *Z. Anorg. Allg. Chem.* **2003,** *629*, 1162-1168.

[81] F. C. Liu, Y. L. Lin, P. S. Yang, G. H. Lee, S. M. Peng, *Organometallics* **2010,** *29*, 4282-4290.

[82] F.-C. Liu, J.-E. Liang, J.-Y. Jin, Y.-L. Lin, Y.-J. Chu, P.-S. Yang, G.-H. Lee, S.-M. Peng, *J. Organomet. Chem.* **2013,** *735*, 1-9.

[83] P. Schmid, M. Maier, H. Pfeiffer, A. Belz, L. Henry, A. Friedrich, F. Schonfeld, K. Edkins, U. Schatzschneider, *Dalton Trans.* **2017,** *46*, 13386-13396.

[84] T. M. Becker, J. A. Krause-Bauer, C. L. Homrighausen, M. Orchin, *Polyhedron* **1999,** *18*, 2563-2571.

[85] J. A. K. Bauer, T. M. Becker, M. Orchin, *J. Chem. Crystallogr.* **2004,** *34*, 843-849.

[86] L. Henry, C. Schneider, B. Mutzel, P. V. Simpson, C. Nagel, K. Fucke, U. Schatzschneider, *Chem. Commun.* **2014,** *50*, 15692-15695.

[87] P. V. Simpson, B. W. Skelton, P. Raiteri, M. Massi, *New J. Chem.* **2016,** *40*, 5797-5807.

[88] R. Guilard, I. Perrot, A. Tabard, P. Richard, C. Lecomte, Y. H. Liu, K. M. Kadish, *Inorg. Chem.* **1991,** *30*, 27-37.

[89] L. Busetto, F. Marchetti, S. Zacchini, V. Zanotti, *Inorg. Chim. Acta* **2005,** *358*, 1204-1216.

[90] K. S. Singh, K. A. Kreisel, G. P. A. Yap, M. R. Kollipara, *J. Organomet. Chem.* **2006,** *691*, 3509-3518.

[91] S. L. Nongbri, B. Therrien, K. M. Rao, *Inorg. Chim. Acta* **2011,** *376*, 428-436.

[92] S. L. Nongbri, B. Das, K. M. Rao, *J. Organomet. Chem.* **2009,** *694*, 3881-3891.

[93] K. Pachhunga, B. Therrien, M. R. Kollipara, *Inorg. Chim. Acta* **2008,** *361*, 3294-3300.

[94] C. W. Chang, G. H. Lee, *Organometallics* **2003,** *22*, 3107-3116.

[95] C. K. Chen, H. C. Tong, C. Y. C. Hsu, C. Y. Lee, Y. H. Fong, Y. S. Chuang, Y. H. Lo, Y. C. Lin, Y. Wang, *Organometallics* **2009,** *28*, 3358-3368.

[96] T. Cruchter, K. Harms, E. Meggers, *Chem. Eur. J.* **2013,** *19*, 16682-16689.

[97] T. Daniel, W. Knaup, M. Dziallas, H. Werner, *Chem. Ber.* **1993,** *126*, 1981-1993.

[98] K. Pachhunga, P. J. Carroll, K. M. Rao, *Inorg. Chim. Acta* **2008,** *361*, 2025-2031.

[99] T. Kemmerich, J. H. Nelson, N. E. Takach, H. Boebme, B. Jablonski, W. Beck, *Inorg. Chem.* **1982,** *21*, 1226-1232.

[100] H. Bing-tai, J. H. Nelson, E. B. Milosavljević, W. Beck, T. Kemmerich, *Inorg. Chim. Acta* **1987,** *133*, 267-274.

[101] E. Evangelio, N. P. Rath, L. M. Mirica, *Dalton Trans.* **2012,** *41*, 8010-8021.

[102] E. A. Giner, M. Gomez-Gallego, L. Casarrubios, M. C. de la Torre, C. Ramirez de Arellano, M. A. Sierra, *Inorg. Chem.* **2017,** *56*, 2801-2811.

[103] W. Rigby, P. M. Bailey, J. A. McCleverty, P. M. Maitlis, *Dalton Trans.* **1979**.

[104] S. M. de Salinas, J. Diez, M. P. Gamasa, E. Lastra, *ChemistrySelect* **2017,** *2*, 3172-3177.

[105] L. Waag-Hiersch, J. Mößeler, U. Schatzschneider, *Eur. J. Inorg. Chem.* **2017,** 3024-3029.

[106] J. Erbeund, W. Beck, *Chem. Ber.* **1983,** *116*, 3867-3876.

[107] P. H. Kreutzer, J. C. Weis, H. Bock, J. Erbe, W. Beck, *Chem. Ber.* **1983,** *116*, 2691-2707.

[108] I. Sánchez-Sordo, J. Díez, E. Lastra, M. P. Gamasa, *Organometallics* **2019,** *38*, 1168-1177.

[109] P. Paul, K. Nag, *Inorg. Chem.* **1987,** *26*, 2969-2974.

[110] P. Paul, S. Chakladar, K. Nag, *Inorg. Chim. Acta* **1990,** *170*, 27-35.

[111] W. Beck, K. Burger, W. P. Fehlhammer, *Chem. Ber.* **1971,** *104*, 1816-1825.

[112] L. Busetto, A. Palazzi, R. Ros, *Inorg. Chim. Acta* **1975,** *13*, 233-238.

[113] A. R. Powers, X. Yang, T. J. Del Castillo, I. Ghiviriga, K. A. Abboud, A. S. Veige, *Dalton Trans.* **2013,** *42*, 14963-14966.

[114] N. J. Farrer, G. Sharma, R. Sayers, E. Shaili, P. J. Sadler, *Dalton Trans.* **2018,** *47*, 10553-10560.

[115] A. P. Gaughan, K. S. Bowman, Z. Dori, *Inorg. Chem.* **1972,** *11*, 601-608.

[116] R. F. Ziolo, J. A. Thich, Z. Dori, *Inorg. Chem.* **1972,** *11*, 626-631.

[117] M. Trose, F. Nahra, D. B. Cordes, A. M. Z. Slawin, C. S. J. Cazin, *Chem. Commun.* **2019,** *55*, 12068-12071.

[118] D. V. Partyka, J. B. Updegraff, M. Zeller, A. D. Hunter, T. G. Gray, *Organometallics* **2007,** *26*, 183-186.

[119] T. J. Robilotto, N. Deligonul, J. B. Updegraff, 3rd, T. G. Gray, *Inorg. Chem.* **2013,** *52*, 9659-9668.

[120] A. R. Powers, I. Ghiviriga, K. A. Abboud, A. S. Veige, *Dalton Trans.* **2015,** *44*, 14747-14752.

[121] C. C. Beto, X. Yang, A. R. Powers, I. Ghiviriga, K. A. Abboud, A. S. Veige, *Polyhedron* **2016,** *108*, 87-92.

[122] X. Yang, S. Wang, I. Ghiviriga, K. A. Abboud, A. S. Veige, *Dalton Trans.* **2015,** *44*, 11437-11443.

[123] M. Howe-Grant, S. J. Lippard, *Biochemistry* **1979,** *18*, 5762-5769.

[124] S. D. Cummings, *Coord. Chem. Rev.* **2009,** *253*, 449-478.

[125] M. Howe-Grant, K. C. Wu, W. R. Bauer, S. J. Lippard, *Biochemistry* **1976,** *15*, 4339-4346.

[126] K. Jennette, J. Gill, J. Sadownick, S. Lippard, *J. Am. Chem. Soc.* **1976,** *98*, 6159-6168.

[127] J. A. Todd, P. Turner, E. J. Ziolkowski, L. M. Rendina, *Inorg. Chem.* **2005,** *44*, 6401-6408.

[128] D. L. Jameson, L. E. Guise, C. A. Bessel, K. Takeuchi, *Inorg. Synth.* **1998,** *32*, 46-50.

[129] H. B. Jonassen, J. H. Nelson, D. L. Schmitt, R. A. Henry, D. W. Moore, *Inorg. Chem.* **1970,** *9*, 2678-2681.

[130] R. Kieft, W. Peterson, G. Blundell, S. Horton, R. Henry, H. Jonassen, *Inorg. Chem.* **1976,** *15*, 1721-1722.

[131] D. A. Redfield, J. H. Nelson, R. A. Henry, D. W. Moore, H. B. Jonassen, *J. Am. Chem. Soc.* **1974,** *96*, 6298-6309.

[132] W. R. Ellis Jr, W. L. Purcell, *Inorg. Chem.* **1982,** *21*, 834-837.

[133] T. Kemmerich, J. H. Nelson, N. E. Takach, H. Boebme, B. Jablonski, W. Beck, *Inorg. Chem.* **1982,** *21*, 1226-1232.

[134] N. E. Takach, E. M. Holt, N. W. Alcock, R. A. Henry, J. H. Nelson, *J. Am. Chem. Soc.* **1980,** *102*, 2968-2979.

[135] S. Tabassum, S. Mathur, F. Arjmand, K. Mishra, K. Banerjee, *Metallomics* **2012,** *4*, 205-217.

[136] Q.-L. Zhang, J.-G. Liu, H. Chao, G.-Q. Xue, L.-N. Ji, *J. Inorg. Biochem.* **2001,** *83*, 49-55.

[137] B. J. Pages, D. L. Ang, E. P. Wright, J. R. Aldrich-Wright, *Dalton Trans.* **2015,** *44*, 3505-3526.

[138] A. Kellett, Z. Molphy, C. Slator, V. McKee, N. P. Farrell, *Chem. Soc. Rev.* **2019,** *48*, 971-988.

[139] N. Metzler-Nolte, U. Schatzschneider, Bioinorganic Chemistry: A Practical Course, Walter de Gruyter: **2009**.

[140] R. Loganathan, S. Ramakrishnan, M. Ganeshpandian, N. S. Bhuvanesh, M. Palaniandavar, A. Riyasdeen, M. A. Akbarsha, *Dalton Trans.* **2015,** *44*, 10210-10227.

[141] A. Klein, B. Rausch, A. Kaiser, N. Vogt, A. Krest, *J. Organomet. Chem.* **2014,** *774*, 86-93.

[142] C. R. Kowol, E. Reisner, I. Chiorescu, V. B. Arion, M. Galanski, D. V. Deubel, B. K. Keppler, *Inorg. Chem.* **2008,** *47*, 11032-11047.

[143] K. Peng, V. Mawamba, E. Schulz, M. Lohr, C. Hagemann, U. Schatzschneider, *Inorg. Chem.* **2019,** *58*, 11508-11521.

[144] V. Prachayasittikul, R. Pingaew, N. Anuwongcharoen, A. Worachartcheewan, C. Nantasenamat, S. Prachayasittikul, S. Ruchirawat, V. Prachayasittikul, *Springerplus* **2015,** *4*, 571.

[145] K. Peng, R. Einsele, P. Irmler, R. F. Winter, U. Schatzschneider, *Organometallics* **2020,** *39*, 1423-1430.

[146] P. Paul, K. Nag, *Inorg. Chem.* **1987,** *26*, 2969-2974.

[147] Ž. D. Bugarčić, J. Bogojeski, R. van Eldik, *Coord. Chem. Rev.* **2015,** *292*, 91-106.

[148] K. Peng, A. Friedrich, U. Schatzschneider, *Chem. Commun.* **2019,** *55*, 8142-8145.

[149] Z. Dori, R. F. Ziolo, *Chem. Rev.* **1973,** *73*, 247-254.

[150] F. Jensen, *J. Chem. Theory Comput.* **2010,** *6*, 2726-2735.

[151] G. R. Fulmer, A. J. M. Miller, N. H. Sherden, H. E. Gottlieb, A. Nudelman, B. M. Stoltz, J. E. Bercaw, K. I. Goldberg, *Organometallics* **2010,** *29*, 2176-2179.

[152] G. M. Sheldrick, *Acta Crystallogr. C* **2015,** *71*, 3-8.

[153] G. M. Sheldrick, *Acta Crystallogr. A* **2008,** *64*, 112-122.

[154] F. Neese, *WIREs: Comput. Mol. Sci.* **2012,** *2*, 73-78.

[155] F. Weigend, R. Ahlrichs, *Phys. Chem. Chem. Phys.* **2005,** *7*, 3297-3305.

Julius-Maximilians-
UNIVERSITÄT
WÜRZBURG

Selbstständigkeitserklärung

Hiermit erkläre ich an Eides statt, dass ich die Dissertation

„*iClick reactions as a modular access to palladium(II) and platinum(II) triazolato complexes: Trends in kinetics and biological activity* **“**

selbständig angefertigt und keine anderen als die von mir angegebenen Quellen und Hilfsmittel benutzt habe.

Ich erkläre außerdem, dass diese Arbeit weder in gleicher oder anderer Form bereits in einem anderen Prüfungsverfahren vorgelegen hat.

Ich habe früher außer den mit dem Zulassungsgesuch urkundlich vorgelegten Graden keine weiteren akademischen Grade erworben oder zu erwerben versucht.

Würzburg, den

Unterschrift
(Kun Peng)